Charles University

Faculty of Science

Department of Zoology

PhD study program: Zoology

Emmanuel Arriaga Varela, Msc.

Understanding the biodiversity boom in terrestrial hydrophilid beetles

-

Co stojí za evoluční explozí diverzity terestrických vodomilů?

DOCTORAL THESIS

Supervisor: Martin Fikáček

Prague, 2019

I declare that this thesis has not been submitted for the purpose of obtaining of the same or another academic degree earlier or at another institution. My involvement in the research presented in this thesis is expressed through the authorship order of the included publications and manuscripts. All literature sources I used when writing this thesis have been properly cited.

Prague, 2019 Emmanuel Arriaga Varela

Understanding the biodiversity boom in terrestrial hydrophilid beetles

Emmanuel Arriaga-Varela

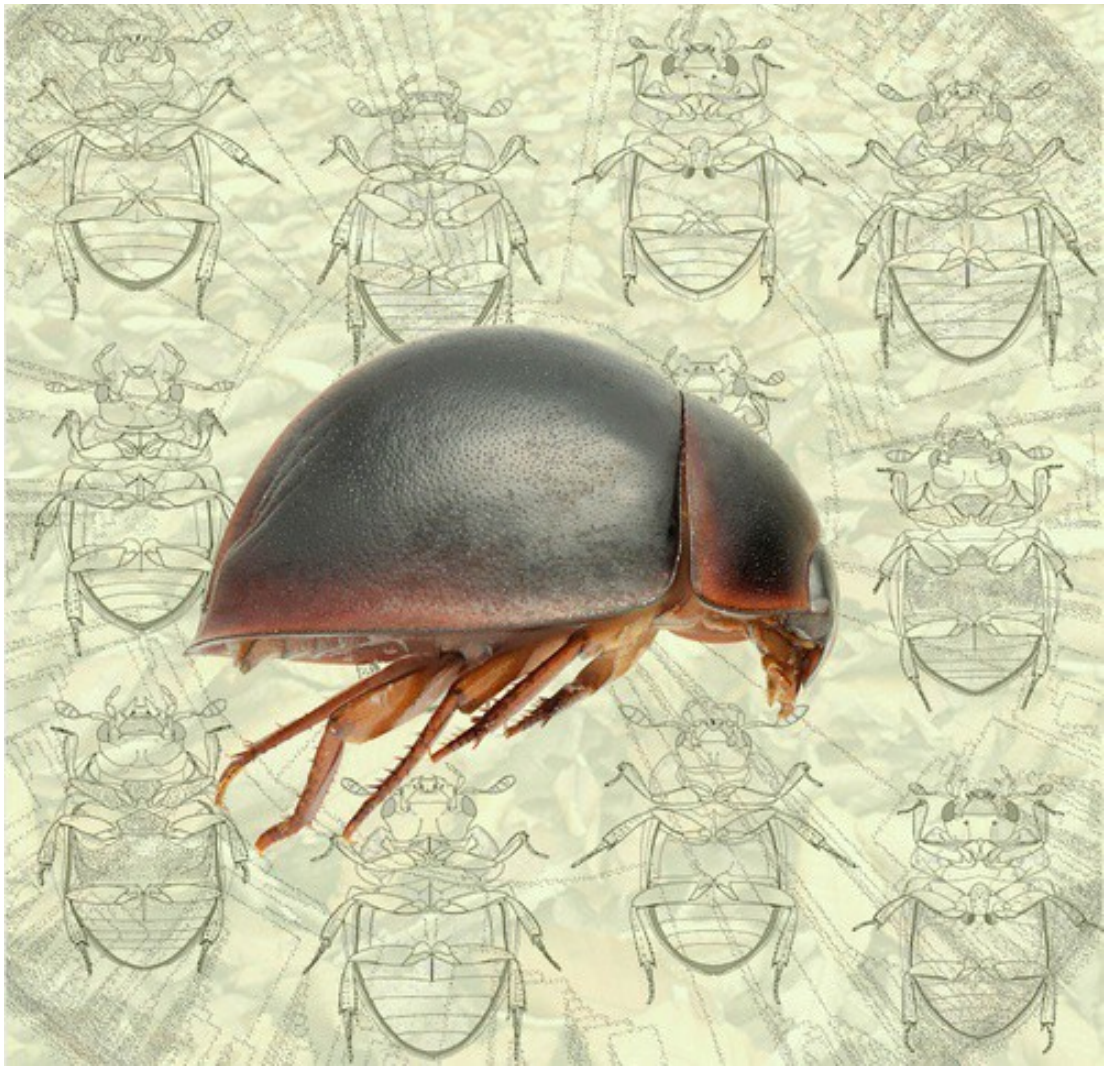

I dedicate this work to my family and to Ana, without whom this work would be unthinkable :)

CONTENTS

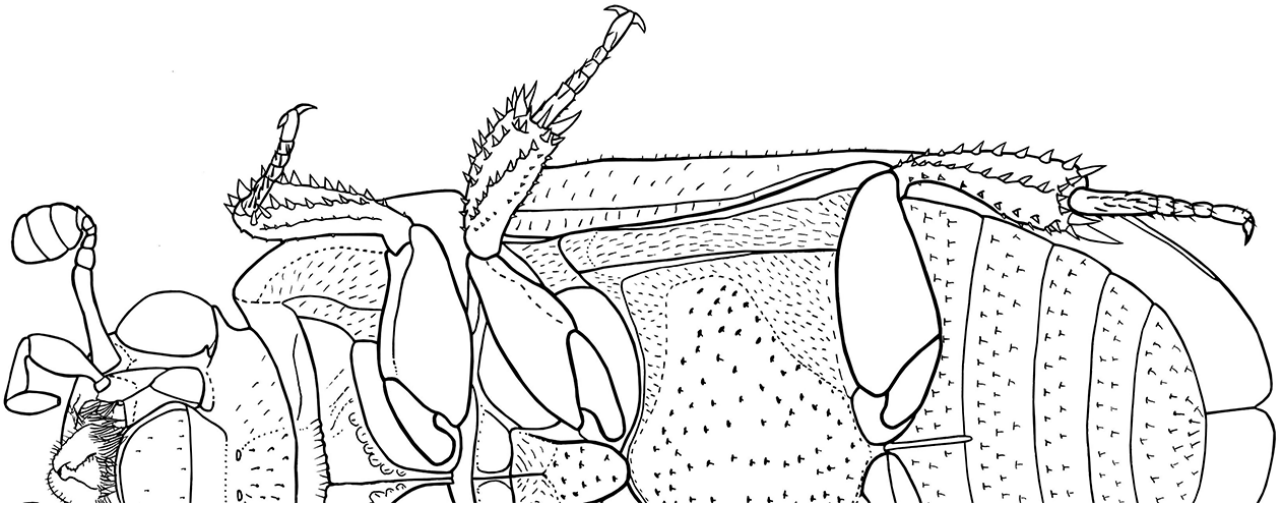

ACKNOWLEDGEMENTS

I want to thank Martin Fikáček for the confidence and all the support during the realization of this work. David Král, Jakub Prokop, Jiři Hájek, Lukaš Sekerka and all professors, colleagues, fellow students and staff of the Entomology sections of the Charles University and National Museum are kindly acknowledged for allowing me to be part of a exciting scientific enviroment. I am thankful to Matthias Seidel for all his help and support during this PhD. This work would be impossible without the effort of Alexei Solodovnikov (Natural History Museum of Denmark, University of Copenhagen and all the people involved in the BIG4 project. Thanks to Niklas Wahlberg and Hamid Ghanavi (Lund University) for their help during the secondment of EAV in Lund University, and Adam Brunke (Canadian National Collection of Insects, Arachnids and Nematodes), Lisa Carroll and Trevor Burt for their kindness during my secondment to the Canadian National Collection of Insects, Arachnids and Nematodes. Dominik Vondráček, Guntima Suwannapong, Andrés Ramírez Ponce, Jesús Cortés Aguilar and Fredy Alvarado for their help and support during field work. This work would not be possible without the collaboration of all my fellow coauthors. I kindly acknowledge them for allowing me to include our work as part of my PhD thesis.

This work was supported by the European Union's Horizon 2020 research and innovation programme under the Marie Skłodowska-Curie grant agreement No. 642241. My work at the Department of Zoology, Charles University, Prague was partly supported by grant SVV260434/2018.

ABSTRACT

The research contained in this thesis explores the phylogenetic systematics, taxonomy, evolution and biogeography of tribe Megasternini (Coleoptera: Hydrophilidae: Sphaeridiinae). Megasternines are an oustandingly diverse group of terrestrial water scavenger beetles with almost 600 described species and probably up to 1,000 species in total. Its species can be found in a wide array of habitats with abundant decaying material like humid leaf litter, dung, rotten cacti, beach wrack, flowers, etc. The specific and ecological diversity as well as their global distribution makes Megasternini an interesting model group for the understanding of processes underlying the diversification, biogeography and evolution of beetles. The scientific part of the thesis contains seven papers: three published, one accepted, one submitted and two manuscripts. **Chapters 1–4** are focused on the taxonomy of selected groups. These chapters aim to cover a variety of cases in terms of biogeography (the Greater Antilles, northern Neotropics, Africa and Southeast Asia), ecology (species associated with leaf litter, dung, flower and rotten cacti) and different taxonomic scenarios. One new extant genus and eight new extant species are described in these chapters. **Chapter 5** is a revision of all known hydrophilid fossils from Baltic amber. I used micro-CT technology in order to observe their morphology otherwise not accessible due to the suboptimal preservation of the specimens. Three new fossil species are described and their systematic relationships discussed. The identity of the only fossils specimen reported as belonging to Megasternini (*Cercyon* sp.) is corrected as a member of the family Phalacridae. The diversification and evolution of ecological preferences in family Hydrophilidae is investigated in **Chapter 6** on the basis of a comprehensive sampling of terrestrial representatives and incorporating the findings from **Chapter 5** for the divergence dating analyses. Megasternini tribe was found to have the most extended increase in diversification in the family. Diversification patterns in terrestrial hydrophilids are linked to their ability to transition between habitats. In **Chapter 7** I present a a phylogenetic analyses based on a multigene dataset obtained from an extensive sampling of tribe Megasternini. Our results support the division of Megasternini in two main clades: Oosternina new subtribe and Megasternina, These lineages are diagnosable based on the morphology of male terminalia. Our analyses on the historical biogrography indicate that the hypethermic conditions of the early Eocene allowed the intercontinental dispersion of megasternines in multiple and opposite directions. The climatic changes that ocurred during the Eocene seem to have had a differential effect on the diversification patterns in both subtribes.

ABSTRAKT

Výsledky obsažené v této disertační práci shrnují výzkum zaměřený na systematiku, taxonomii, evoluční historii a biogeografii tribu Megasternini (Coleoptera: Hydrophilidae: Sphaeridiinae), skupiny vodomilovitých brouků vyznačující se mimořádnou druhovou diverzitou 600 popsaných druhů a ca. 1000 druhů celkem. Zástupci této skupiny obývají široké spektrum habitatů bohatých na rozkládající se materiál, např. listovou hrabanku, mrtvé pletivo kaktusů, mořské řasy naplavené na pobřeží, květy atd. Vysoká druhová a ekologická diverzita a celosvětové rozšíření dělají z tribu Megasternini modelovou skupinu pro studium procesů ovlivňujících diverzifikaci, biogeografii a evoluci brouků, tj. nejúspěšnější skupiny živočichů. Vědecká část této práce obsahuje sedm studií: tři publikované články, jeden akceptovaný k tisku, jeden zaslaný do redakce a dva rukopisy. **Kapitoly 1-4** jsou zaměřeny na taxonomii vybraných skupin různého rozšíření (Velké Antily, severní neotropy, Afrika a JV Asie) a ekologie (druhy obývající hrabanku, rozkládající se kaktusy a květy). Je popsán jeden nový rod a osm nových druhů. **Kapitola 5** je revizí všech známých vodomilovitých brouků z baltského jantaru. Ke studiu suboptimálně zachovaných kusů, jejichž znaky nejsou dobře viditelné, jsem použil techniku microCT. Jsou popsány tři nové fosilní druhy a je diskutována jejich systematika. Jediná fosílie dříve řazená do tribu Megasternini (*Cercyon* sp.) je přeřazena do čeledi Phalacridae. Diverzifikace a evoluce ekologických preferencí vcelé čeledi Hydrophilidae je analyzována v **Kapitole 6** na základě representativního vzorku terestrických druhů a s využitím výsledků **Kapitoly 5** k nadatování fylogenetického stromu. Ukazuje, že v tribu Megasternini došlo k nejvyššímu nárůstu diverzifikační rychlosti v celé čeledi. Rozdíly v diverzifikační dynamice terestrických vodomilů jsou spojeny s jejich schopností osídlit nové biotopy. V **Kapitole 7** shrnuji výsledky fylogenetické multi-genové analýzy založené na reprezentativním vzorku tribu Megasternini. Ty ukazují, že tribus Megasternini se dělí na dva základní subtriby, Oosternina a Megasternina, jejichž zástupce je možné rozeznat i podle morfologie samčích terminálií. Analýza historické biogeografie ukazuje, že teplé klima na začátku eocénu umožnilo obousměrnou disperzi mezi kontinenty. Klimatické změny během eocénu měly pravděpodobně odlišný vliv na diverzifikační dynamiku v každém podtribu.

GENERAL INTRODUCTION

As the name of the family suggests, hydrophilid beetles love water, or at least humidity. More than 3,000 spp. have been described and classified in 6 subfamilies (Short and Fikaček 2014). While the "basal" subfamilies are found in aquatic environments, members of Cylominae and Sphaerdiinae have conquered a wide array of terrestrial habitats, especially stinky substrates with some degree of humidity. Tribe Megasternini (Sphaeridiinae) stands as the most diverse within these groups, with more than 566 spp. (and about 900 including non-described ones). It has been proved that its diversification rate is higher than in any other group within Hydrophilidae (Bloom et al. 2014). Nevertheless, the internal classification is in dire need of revision due to a likely high degree of morphological homoplasy. My PhD thesis is focused on proposing a phylogenetic hypothesis that serves as framework for its classification and deepens our understanding of the factors conducting the tempo and mode of its evolutionary history. The chapters of my thesis are aimed to answer the main questions on the evolution of the Megasternini: the 'HOW's - How many species? How do they look like? How do they live? How are they related?; the WHEN's - When did they originated? When did they start to diversify?; and the WHY's - Why are they more diverse than other hydrophilids? Why are they so difficult to classify? What is there to understand this biodiversity boom?

Explosions and metaphors

The expression “Biodiversity boom” brings to our mind an explosive burst of different forms of life radiating and evolving into different shapes and habits. It is a metaphor that depicts a scenario of a multitude of organisms diverging from a common point and reaching new positions in the multi-dimensional evolutionary landscape at a quick, disruptive tempo. Metaphors like this are heuristic tools used by scholars for centuries in the process of defining the patterns and process of nature according to relational schemes accessible to our minds. Metaphors affect the way we perceive the world, categorize experiences, and organize our thoughts (Casakin 2007). The use metaphors and analogies as a structuring device for our cognitive systems is as old as mankind (Lakoff 1993). It is common place for biologists to talk about 'mapping' the character on the tree, 'arms races' and 'red queens', ecological 'niches' and adaptive 'landscapes' (Olson et al. 2019). Such expressions signify the most economical way to talk about complex patterns and processes observed or inferred in nature.

Adaptive radiation is one of the key metaphors of evolutionary biology nowadays (Givnish 1997; Roff 2001) and has been around for more than one century (Osborn 1902). The term invokes a booming divergence of lifeforms and brings into biologists' heads the pictures of Darwin's finches in Galapagos (Grant & Grant 2008), fruit flies in Hawaii (Craddock 2000) and cichlid fishes in African lakes (Kocher 2004). Outstanding qualities of these examples circle around two main axes: accelerated speciation pace and its associated adaptive divergence. According to the basic introductiory definition by Schluter (2000): "Adaptative radiation is the evolution of ecological diversity within a rapidly multiplying lineage. It is the differentation of a single ancestor into an array of species that inhabit a variety of environments and that differ in traits used to exploit those environments. It includes the origin of new species and the evolution of ecological differences between them". In some occasions, the variable of increased diversification as a characteristic of a radiating lineage is substituted by an indicator such as the morphological disparity of a lineage (Jackman et al. 1997; Losos & Miles 2002; Ribera & Balke 2007).

Understanding the evolutionary processes underlying the diversification and ecological divergence that have shaped the biodiversity on the Earth throughout the time should take into account the complex and continuous nature of these phenomena. Although they are inherently challenging due to the large proportion of unknown diversity, the studies on the evolution of beetles, arguably the most successfull group of animals, offer a plethora of examples depicting different evolutionary scenarios. It is, therefore, crucial that systematic coleopterists build a research program that starts on the basis of alpha-taxonomy and discovery, and explores the complexity of patterns and process behind the asymmetrical diversity patterns and ecological divergence testing for the causal relations between them.

Beetles, an explosion of diversity

Coleoptera are the most diverse group of living organisms (Bouchard et al. 2009); arguably, they represent one of the biggest explosions of biodiversity in the planet, with approximately 360,000 species adapted to an outstanding variety of habitats. However, the view of Coleoptera as the most diverse order has been recently disputed in favour of parasitic wasps if the yet undescribed diversity is taken into account (Forbes et al. 2018). Beetles are a drastic example of asymmetrical specific and ecological diversity of a group when compared with its adelphotaxon. The sister group of Coleoptera is the obscure order Strepsiptera (Beutel et al. 2018), a group of small parasitoid insects with twisted wings, astonishing sexual dimorphism and adaptations to the parasitoid life, whose diversity only amounts to around 600 species (Pohl & Beutel 2008).

Coleoptera itself represents a strong candidate for the label of the most extended adaptive radiation on the planet. However, not all beetle lineages are as speciose or as ecologically diverse.

The evolution of beetles is full of examples of disparity in success and habits that are itself relevant model groups for exploring evolutionary processes.

The family Hydrophilidae is a example of a lineage nested in Coleoptera wich evolutionary history has been proven relevant in the study of radiation patterns. Hydrophilids are ancestrally aquatic (Bloom et al. 2014), however, they include the most successful case of the 'return to land'. Terrestrial hydrophilids have 'radiated' to a wide variety of habitats, habits and shapes that make the family an interesting case of study. This is why Hydrophilidae or their subgroups has been subject of studies aimed on the evolution of habitat preferences, diversification and biogeography (e.g. Bernhard et al 2006; Bloom et al. 2014; Song et al 2014; Pallarés et al 2017; Toussaint and Short 2018).

Megasternini, a explosive group of beetles?

The family Hydrophilidae is a group of beetles mostly found in aquatic environments of many kind. Although it has been shown that the ancestral condition for Hydrophilidae clade is an aquatic life style (Bloom et al. 2014; Song et al. 2014), approximately 150 million years ago, the common ancestor of subfamilies Cylominae and Sphaeridiinae returned to land (Toussaint & Short 2018). This proves wrong the persisting opinions that no aquatic insect lineage has 'returned to land' with success (Vršanský et al. 2019). Almost a half of species of Hydrophilidae are found in terrestrial enviroments (Bloom et al. 2014). The large majority of these species are part of the monophylum composed by subfamilies Cylominae + Sphaeridiinae.

The tribe Megasternini is a group deeply nested in the subfamily Sphaeridiinae. Along with its sister clade, Sphaeridiini, Megastenini is the most recently diverging tribe in the family. These lineages are estimated to have diverged between 130–110 Mya (Bloom et al. 2014; Toussaint & Short 2018). Besides being the most recent tribal lineages in the family, Megasternini is the most diverse one in terms of habitats colonized and total species. Approximately 566 megasternine species have been described (Short & Fikáček 2011), while the total number of species, including undescribed ones could reach up to 900. This estimation is based on recent taxonomic studies like those of Szczepański et al. (2018), Deler et al. (2014) and Arriaga-Varela et al. (2017) which found a high proportion of undescibed specis in relatively small tropical areas like the Greater Antilles or an elevation transsect in Papua New Guinea. The relatively young age of the clade is coupled with the high species diversity, a patterwhich has been proven a result of a increased diversification (Bloom et al. 2014).

In terms of ecology, Megasternini can be found in a wide array of habitats, the widest among water scavenger beetle lineages. Most of the megasternine species are associated with various kinds of decaying organic matter, like mammal dung (e.g., Smetana 1978, Ryndevich 2008, Ryndevich et

al. 2017, Arriaga-Varela et al. 2017, 2018), humid forest leaf-litter (e.g., Deler-Hernández et al. 2015; Fikáček et al. 2009; Fikáček and Short 2006) or rotten seaweed (e.g., Smetana 1978; Ryndevich 2001). The concept of Megasternini has changed over time. Before the first attempts of natural classification, two tribes were recognized for what is Megasternini today: Cercyonini and Megasternini (Horn, 1890). The concept of Cercyonini was historically used to accommodate small representatives of Sphaeridiinae with developed elytral epipleuron reaching at least elytral mid-length, combined with a not raised or demarcated central portion of the prosternum (Smetana 1978). In contrast, Megasternini accommodated species with reduced elytral epipleuron and broad raised medial portion of the prosternum. Both tribes included members of the current tribe Omicrini as well. The monophyly of the Megasternini combined with Cercyonini as well as the status of Sphaeridiini as its sister clade has been repeatedly recognized since the first phylogenetic analysis of Hydrophiloidea performed by Hansen (1991) on the basis of morphological characters. Therein, Cercyonini was synonymized under Megasternini, and the tribe was characterized by elytral punctures arranged in longitudinal series (not conspicuously in *Agna* Smetana, *Cercyodes* Broun and *Tectosternum* Balfour-Browne), compact antennal club, clypeus not deflexed laterally, sucking-disc in male maxilla (absent in *Agna* and *Pseudoosternum* Hansen) and well defined antennal grooves (absent or poorly defined in *Cycreon* Orchymont, *Cercyodes* and few other clades).
The first phylogenetic studies based on DNA sequences focused on the relationships among hydrophiloid families were performed by Bernhard et al. (2006, 2009). Megasternini was shown therein as sister to Sphaeridiini, but it was represented by a single terminal taxon, *Cercyon ustulatus* (Preyssler). The subsequent contribution by Song et al. (2014) involved only three megasternine taxa: *Cercyon ustulatus, Pachysternum stevensi* Orchymont, and *Cryptoplerum* sp. Fikáček (2010) and Fikáček & Short (2010b) performed the first partial phylogenetic analyses based on morphological characters in order to understand the relations of genera *Kanala* Balfour-Browne and *Cetiocyon* Hansen with the rest of the southern-hemisphere genera of Megasternini.

The internal classification of tribe Megasternini can been regarded as the most taxonomically complex task in the Hydrophilidae. Half of the diversity in the tribe is currently classified in the genus *Cercyon* Leach. It stands out as the most speciose genus in the tribe with more than 250 species (Short and Fikácek 2011), currently arranged in eight valid subgenera, and representing almost a third of the diversity in Megastenini. The genus is amalgamated by a diagnostic combination of characters. However, the morphological features vary greatly inside the genus and its subgenera (see Arriaga-Varela et al 2018). The relevance of the generic concept of *Cercyon* in the taxonomic history of Megasternini is well exemplified by 16 genus names in the tribe composed of a derivation, anagram or combination of the word *Cercyon*. Currently, 51 genera are recognized. The diversity of species and genera and the complexity of the patterns of morphological diversity

including potentially homoplastic characters makes Megasternini one of the most taxonomically complicated clades in the whole Hydrophiloidea superfamily. Although they are small to rarely medium-sized beetles of compact ovoid body, they show a great diversity in morphology. The classification is largely based on the shapes and proportions of the ventral parts of the thorax, specially the shape of the mesoventrite. As with the many derivates of *Cercyon*, the shape of the mesoventral elevation can tell us a lot about the morphological patterns in the group. The type genus of the tribe, *Megasternum* Mulsant, posses a very large pentagonal mesoventral plate, while in *Pachysternum* Motschulsky the plate is thick, squared in *Quadristernum* Balfour-Browne, vanishing in *Evanesternum* Arriaga-Varela et al..and egg shaped in *Oosternum* Sharp. As it happens with the many derivates of *Cercyon*, the genus *Oosternum*, second most diverse in the family, have had a significan ingluence in the taxonomy and nomenclature of the tribe, with genera like *Paroosternum* Scott, *Pseudoosternum* Hansen, *Sacosternum* Hansen or the anagram *Motonerus* Hansen.

This nomenclatural idiosyncracy found in the taxonomy of Megasternini is just a reflection of a complex pattern of morphological diversity where many apparently crucial characters for classification might be highly homoplasic. There is a undeniable need for an evolutionary framework for this group based on distinct lines of evidence, particularly molecular sequences, and on a comprehensive sampling of taxa. Only with such kind of hypothesis in hand, all the dimensions of the 'biodiversity boom' in this group can be understood. Somewhere between the purines and pyrimidines there is a signal that should shed light on the evolutionary processes that produced the amazing diversity that lies between *Cercyon oosternoides* Knisch and *Oosternum cercyonoides* Deler et al.

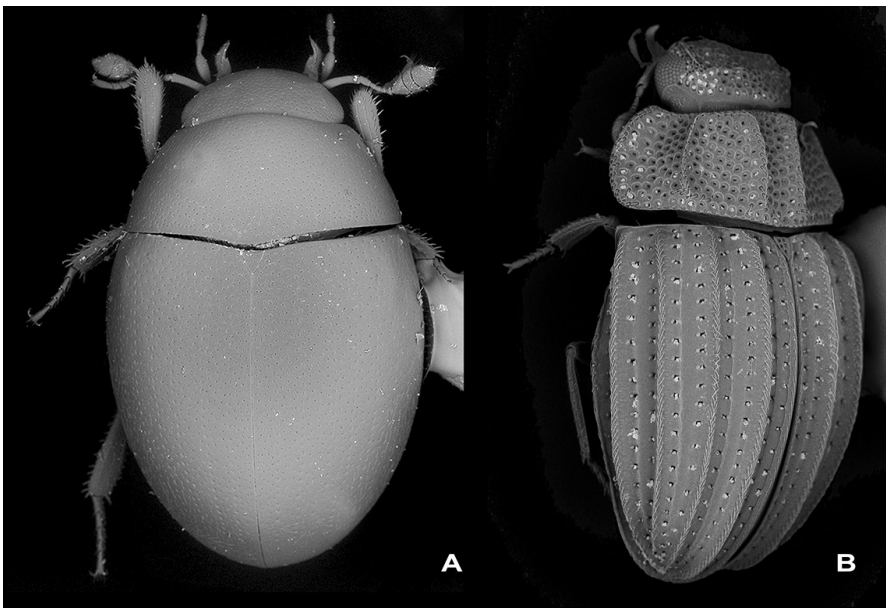

Figure 1. A – *Agna capillata* (LeConte) from USA; **B -** *Oosternum* ('*Pemelus*') sp. from Guatemala

Objectives of the thesis

The main objective of this thesis is to deepen our understanding of the evolution and diversity of tribe Megasternini on the basis of a phylogenetic hypothesis based on the genetic sequences of a comprehensive sample of megasternine taxa. Under this framework I aim to understand; (1) how the transitions between habitats are related to the diversification of the terrestrial water scavenger beetles (2) propose a hypothesis of systematic relationships within Megasternini upon which supraspecific classification can be based (3) understand the historical biogeography that shaped the diversity of the tribe. In parallel, I explored the taxonomy of selected extant groups that provide us with relevant information and insights into the diversity, ecology and distribution of megasternines. Also, I used innovative techniques in the study of extinct biodiversity in order to give precision to the temporal dimension of the evolution of hydrophlids in general and megasternines in particular.

Material and method

This study is aimed to perform an integrative approach for studying the biodiversity from a systematic point of view. The cornerstone of the different chapters of this contribution are the entomological specimens. The molecular phylogenetics section was made possible through the accessibility to freshly collected organisms provided by many colleagues and friends around the world. These specimens were kept in conditions that prevented the degradation of the genetic information. Additionally, I, along with the members of the Fikáček lab participated in entomological expeditions to different parts of the globe. This field work allowed us to obtain first-hand information on the natural history of many species and genera. It is my believe that any attempt to provide an evolutionary framework on the relationships between species needs to be in involved in a feedback relationship with taxonomy and nomenclature. It is for this reason that the work presented in my thesis relies heavily on the importance of a carefull examination of museum specimens. That includes the freshly collected specimens that were the basis for my DNA sequencing work as well as the historical specimens gathering dust in entomological collections for more than a century.

Additionally, my intention is to set this contribution on an open science framework that allows the free dissemination of all information available. For this reason I used different platforms that go from formal ones that allow the storage of large quantities of data such Zenodo (https://www.zenodo.org/) to ones that are more accessible and user-friendly as Flickr

(https://www.flickr.com/photos/142655814@N07/), a platform designed for the visualization of images of all kind.

Figure 2. A – DNA-grade collection in Fikáček lab; **B –** Winklers extractors doing their work during our trip to Mexico in 2016; **C –** Holotype of *Cercyon variegatus* Sharp

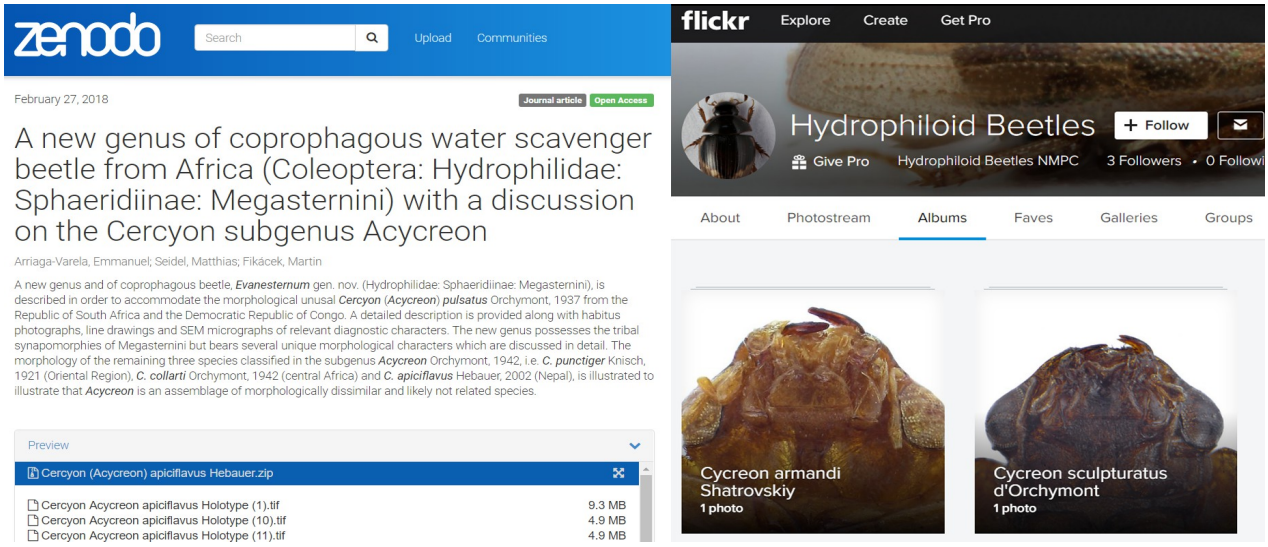

Figure 3. Examples of on-line platforms for the storage of data and dissemination of our results.

Structure of the thesis

The thesis is composed by seven chapters. **Chapters 1-4** are taxonomic revisions of selected groups. Basically any group in Megasternini is in need of taxonomical revision.
I aimed to cover as wide spectrum of diversity variables as possible, like geography, ecology and systematic position. The findings are particular examples of how detailed morphological comparative study of specimens may inform us about the diversity to be discovered. And that this

information is the cornerstone of biodiversity and evolutionary research. **Chapter 5** is focused on the temporal axis of the evolution of water scavenger beetles. I used Micro-CT tools to study all known specimens of the family from the Baltic amber. In **Chapter 6** I investigate the shifts between microhabitats and its relation to diversification patterns in the whole family with an emphasis on terrestrial clades Cylominae and Sphaeridiinae, including the extensively sampled Megasternini. Observations on the natural history from **Chapters 1-4** are included. The age of the divergences in the tree are calibrated incorporating the discoveries reported in **Chapter 5**. **Chapter 7** is the multigene phylogenetic analysis using at the moment the most comprehensive sampling of members of the Megasternini. The discoveries of the morphological diversity and distribution data from **Chapters 1-4** are included there. The divergence events on the tree are calibrated on the basis of results of **Chapter 6**. The resulting time tree is used to investigate main biogeographical patterns of the Megasternini as well as the pace of diversification of the lineage.

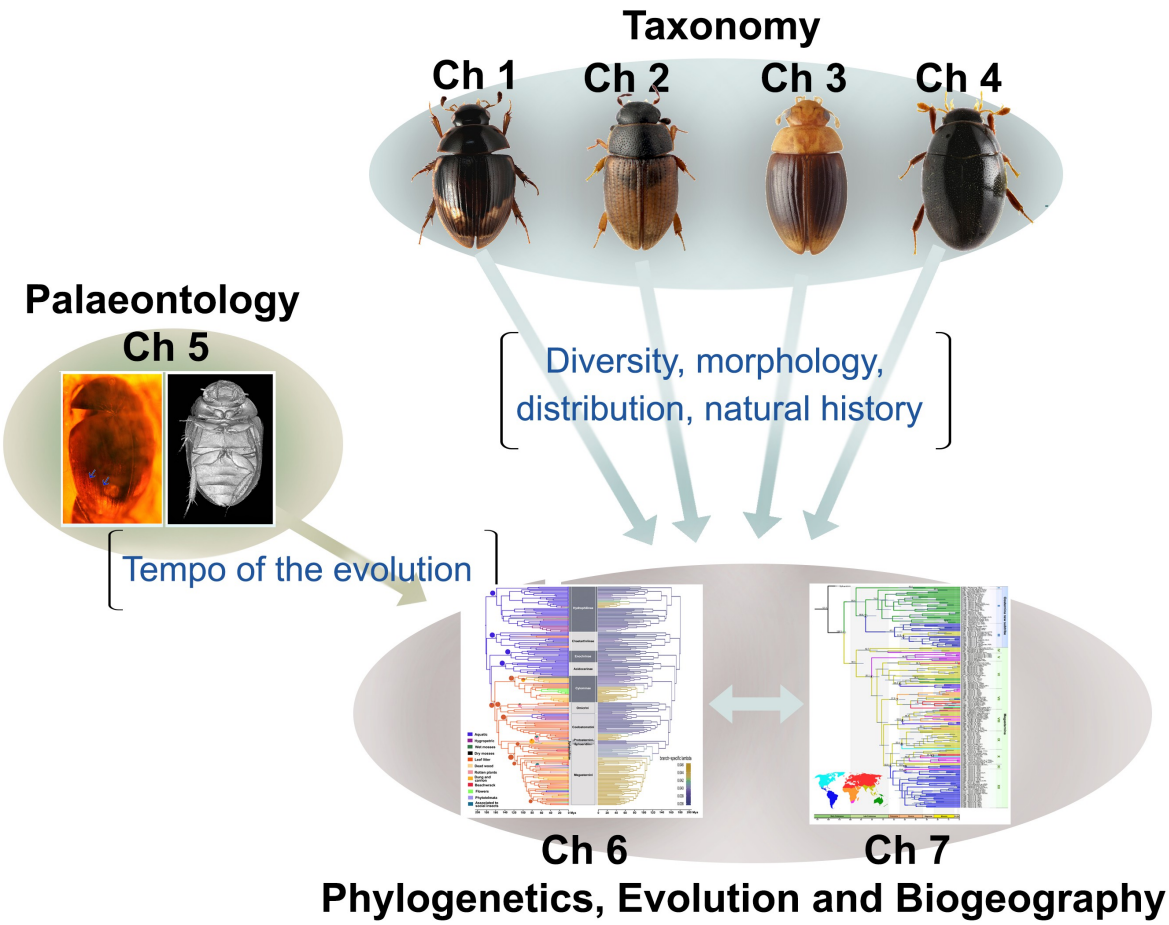

Figure 4. Scheme showing the interconections between the chapters of the present thesis.

Brief description of chapters

Chapter 1

Title: A review of the *Cercyon* Leach (Coleoptera, Hydrophilidae, Sphaeridiinae) of the Greater Antilles

Authors: Emmanuel Arriaga-Varela, Matthias Seidel, Albert Deler-Hernández, Victor Senderov and Martin Fikáček **(Published paper)**

Ten species were recognized, including five new ones endemic to a single island, four to La Hispaniola and one to Jamaica. Two intruduced species from the old world are recorded. Three of the new species from La Hispaniola are part of the *Cercyon gimmeli* species group, a lineage of coprophagous beetles whose adults can be distinguished through comparison of male genitalia and molecular markers such as mitochondrial cytochrome oxidase I. To complicate things, species of this group are partially sympatric and can be found in the same piece of excrement. Larvae of two species, *C. taino* sp. nov. (*C. gimmeli* group) and *C. insularis* Chevrolat were associated to adults using COI sequences. Descibed larvae shows previously unknown morphological features.

Figure 5. Graphical abstract of Chapter 1.

Citation:

Arriaga-Varela, E., Seidel, M., Deler-Hernández, A., Senderov, V. and Fikáček, M., 2017. A review of the Cercyon Leach (Coleoptera, Hydrophilidae, Sphaeridiinae) of the Greater Antilles. *ZooKeys*, (681), 39-93.

Chapter 2

Title: A new genus of coprophagous water scavenger beetle from Africa (Coleoptera, Hydrophilidae, Sphaeridiinae, Megasternini) with a discussion on the *Cercyon* subgenus *Acycreon*

Authors: Emmanuel Arriaga-Varela, Matthias Seidel and Martin Fikáček **(published paper)**

The morphology of the *Cercyon* (*Acycreon*) subgenus is reviewed. The particular morphological features of African coprophagous species *Cercyon* (*Acycreon*) *pulsatum* justifies the description of a new taxon, *Evanesternum* gen. nov., to accomodate it on the basis of unique mesosternum and genital segment. The subgenus Acycreon was raised for species with mesoventral plate declined anteriorly; comparison of remaining species in subgenus *Acycreon* suggest the taxon is very likely not monophyletic.

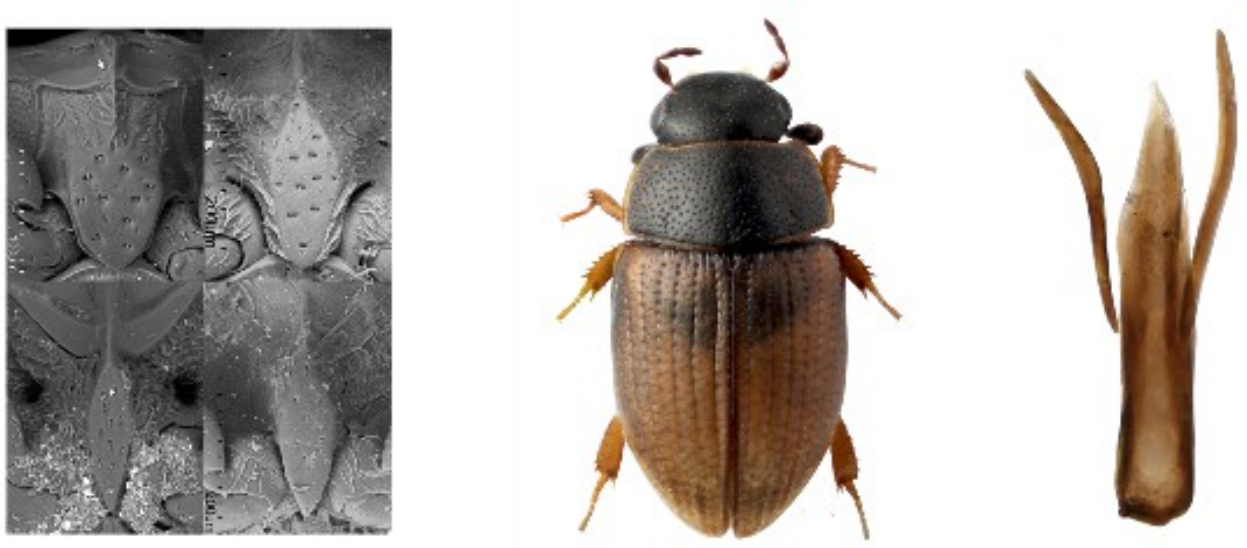

Figure 6. Graphical abstract of Chapter 2.

Citation:
Arriaga-Varela, E., Seidel, M. and Fikáček, M., 2018. A new genus of coprophagous water scavenger beetle from Africa (Coleoptera, Hydrophilidae, Sphaeridiinae, Megasternini) with a discussion on the *Cercyon* subgenus *Acycreon*. *African Invertebrates*, 59, 1-23.

Chapter 3

Title: Review of the flower-inhabiting water scavenger beetle genus *Cycreon* (Coleoptera, Hydrophilidae), with descriptions of new species and comments on its biology

Authors: Emmanuel Arriaga-Varela, Sin Yeng Wong, Alexander Kirejshuk, and Martin Fikáček **(published paper)**

Southeast Asian genus *Cycreon* was previously known from two historical specimens. We described two new species and one new subspecies based on abundant recently collected material mainly obtained during the survey of pollinators and visitor of Araceae inflorescences. Field observations and mid gut contents indicate that *Cycreon* specimens feed on organic material included pollen of the host plant and probably contribut to the pollination of a variety of species.

Figure 7. Graphical abstract of Chapter 3.

Citation:

Arriaga-Varela, E., Wong, S.Y., Kirejtshuk, A. and Fikácek, M., 2018. Review of the flower-inhabiting water scavenger beetle genus *Cycreon* (Coleoptera, Hydrophilidae), with descriptions of new species and comments on its biology. *Deutsche Entomologische Zeitschrift*, 65, 99-115.

Chapter 4

Title: Water scavenger beetles in rotten cacti: A review of *Agna* with the description of a new species from Mexico (Coleoptera: Hydrophilidae: Sphaeridiinae)

Authors: Emmanuel Arriaga-Varela, Jesús Cortés-Aguilar and Martin Fikáček **(Accepted paper in *Revista Mexicana de Biodiversidad*)**

The Rotten cacti specialist genus *Agna* Smetana is reviewed. Three species are recognized including a new one from central and southern Mexico. A summary of all known hydrophilids associated to decaying stems of family Cactaceae is presented, including new distribution records.

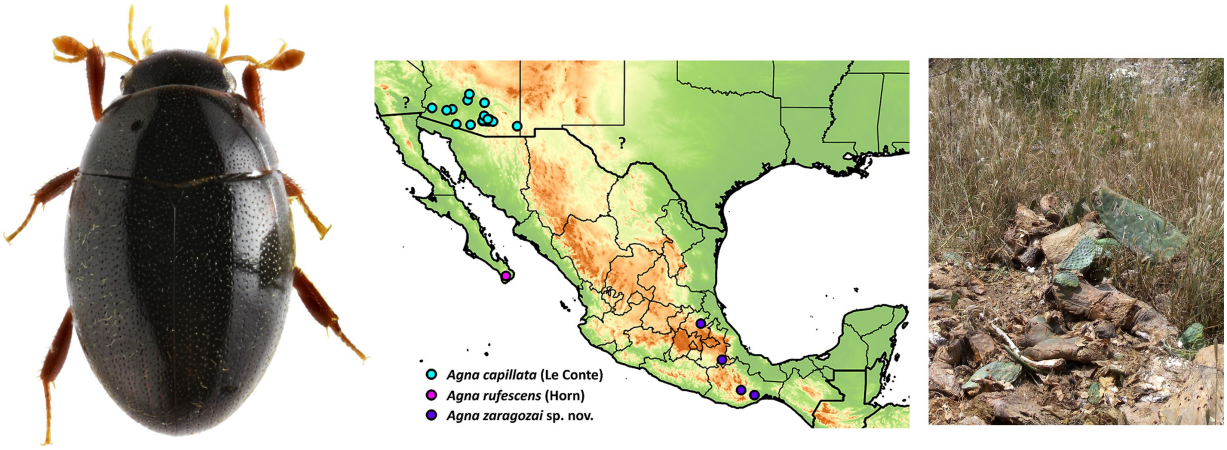

Figure 8. Graphical abstract of Chapter 4.

Chapter 5

Title: Micro-CT reveals hidden morphology and clarifies the phylogenetic position of Baltic amber water scavenger beetles (Coleoptera: Hydrophilidae)

Authors: Emmanuel Arriaga-Varela, Adam Brunke, Jennifer C. Girón, Karol Szawaryn, Jana Bruthansová and Martin Fikáček **(submitted to *Papers in Palaeontology*)**

All available hydrophid fossil embeded in amber from the Baltic region were scanned using micro-CT technology in order to examine their morphology. Micro-CT scans allowed us to see characters not visible under conventional tools in detail. Three species are described in genera *Crenitis, Anacaena* (Chaetarthrinae) and *Helochares* (Acidocerinae). Only known fossil Megasternine, *Cercyon* sp. (Kubisz 2002), was examined and we discovered it really belong in family Phalacridae.

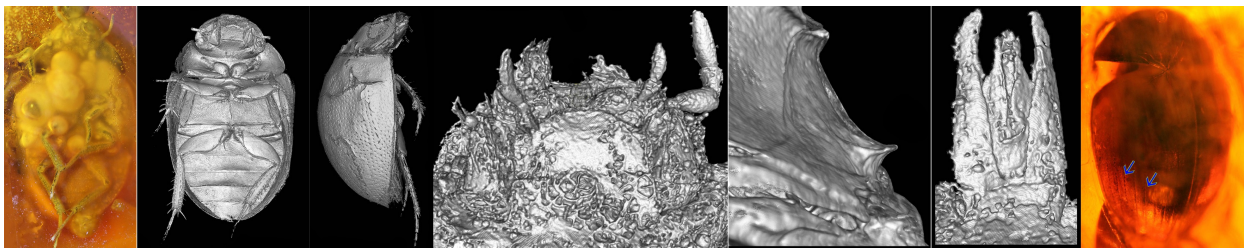

Figure 9. Graphical abstract of Chapter 5.

Chapter 6

Title: Phylogeny, habitat shifts and diversification of terrestrial water scavenger beetles (Hydrophiloidea: Hydrophilidae)

Authors: Emmanuel Arriaga-Varela, Vít Sýkora, Hamid Ghanavi, Matthias Seidel and Martin Fikáček **(manuscript)**

We assembled a multigene dataset of 236 hydrophilid taxa, including the most comprehensive sampling of terrestrial hydrophilids. The time tree was calibrated with a set of eight fossils including the changes and additions from Chapter 5. We reconstructed the ancestral states for the evolution of habitat preferences between 12 different options. Leaf litter was found to be the ancestral condition of the MRCA of the terrestrial clade (Cylominae + Sphaeridiinae) and for all of their main tribal lineages except the two with the least diversity, Sphaeridiini and Protosternini. The branch specific diversity was estimated. Megasternini was corroborated as showing the most extendend increase in diversification in the family. This increase is, however, more accentuated in the Cercyon group of genera. Additional shifts were found in particular lineages in Hydrophylinae (Limnoxenus), Cylominae (New Zealand genera *Cyloma, Adolopus* and *Rygmodus*) and Coelostomatini (Phaenonotum). These shifts can be explained by the colonization of insular environments that likely promoted their ecological and taxonomical diversification. The increase in diversification rate in Megasternini is likely linked to a wider array of colonized habitats.

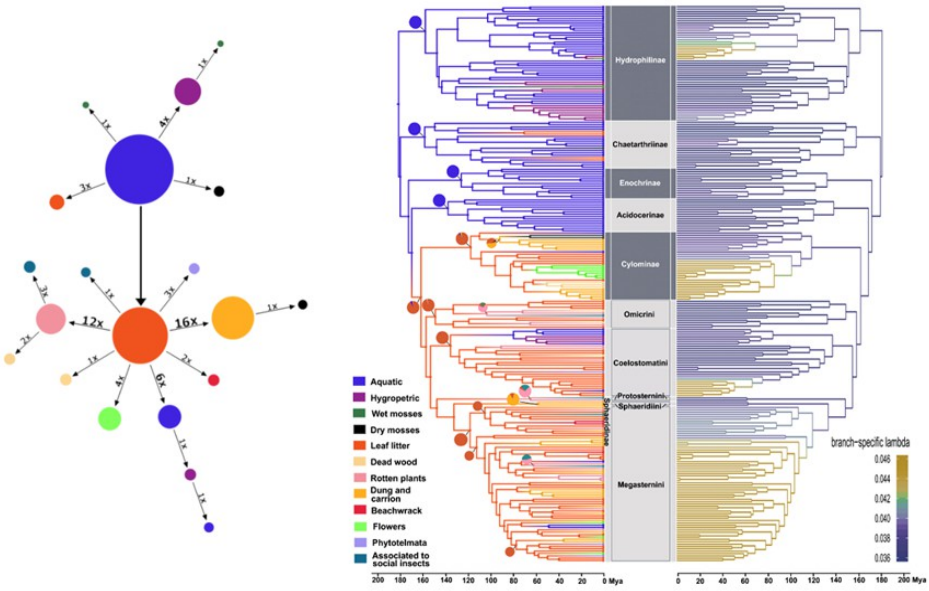

Figure 10. Graphical abstract of Chapter 6.

Chapter 7

Molecular phylogeny of terrestrial water scavenger beetle tribe Megasternini (Hydrophilidae: Sphaeridiinae) reveals repeated and bidirectional continental interchange during the Eocene

Authors: Emmanuel Arriaga-Varela and Martin Fikáček **(manuscript)**

The phylogenetic relationships of members of tribe Megasternini are investigated on the basis of a multigene dataset obtained from extensive taxonomic sampling. Our results support the division of Megasternini in two main clades: Oosternina new subtribe and Megasternina, These lineages are diagnosable based on the morphology of male terminalia. Twelve clades are recognized, nine in Megasternina and three in Oosternina, and their morphological patterns discussed. Our analyses on the historical biogrography indicate that the hypethermic conditions of the early Eocene allowed the intercontinental dispersion of megasternines in multiple and opposite directions. The climatic changes that ocurred during the Eocene seem to have had a differential effect on the diversification patterns in both subtribes.

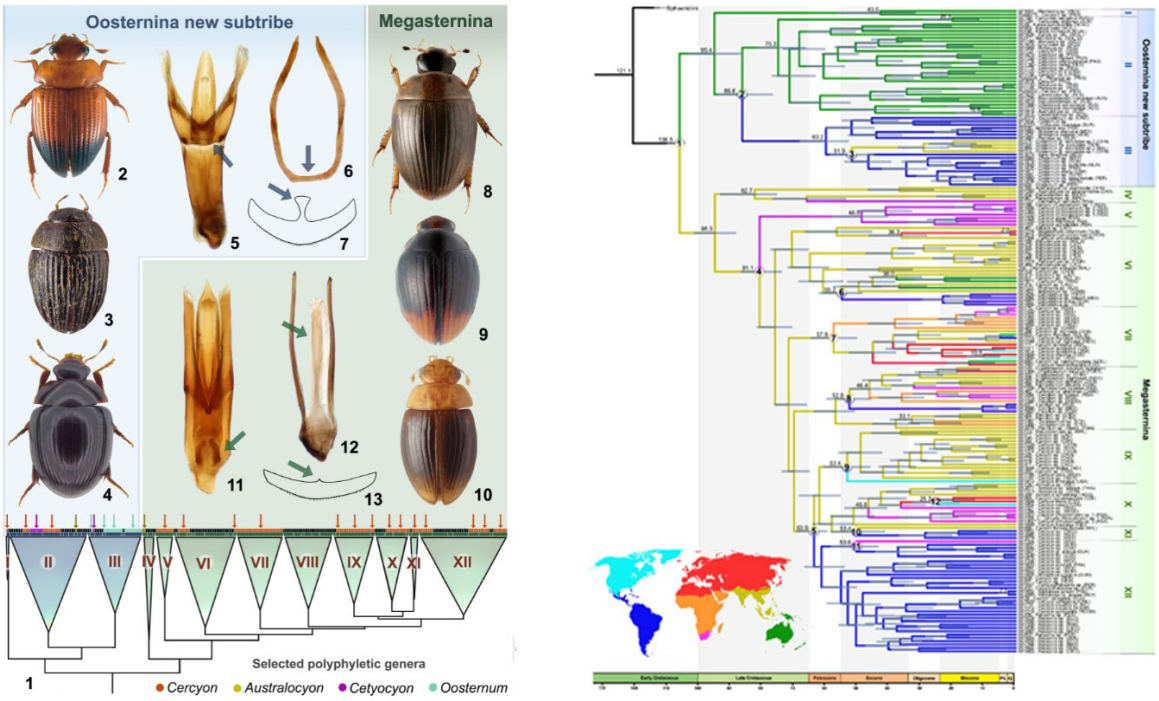

Figure 11. Graphical abstract of Chapter 7.

Results and discussion

How many megasternine species are there? How do they look? Where and how do they live?
Chapters 1 to 4 of my thesis unveil new data and insights into basic aspects of the diversity of the group. Regarding the question of the number of species, there are two main parts of this question. The first one is the number of described species: based on the most updated catalogue (Short & Fikáček 2010) and subsequent additions, there are 566 species described. The second one, and probably more open to discussion, is the total number of species including undescribed ones. My results and other recent contributions (e.g.Szczepański et al. 2018, Deler et al. 2014) and personal observations suggest that previous estimations on this regard, particularly those by Bloom et al (2014) on a total number of 870 species, may be underestimated. Relatively limited areas in tropical zones of the globe, such as La Hispaniola or central New Guinea, can harbor a significant number of previously unknown species. Our personal observations suggest that the large part of the diversity is still not completely explored in tropical areas. Examples of this are *Cercyon/ Platycyon/ Merosoma* species from New Guinea or species of *Pelosoma* or *Cercyon* clades in the Neotropics. My estimate is that the concept of Megasternini as the hydrophilid lineage with the most underestimated number of species is correct.

Parallely, *Pelosoma* and *Cercyon* Neotropical lineages surely contain a large quantity of ecological particularities that are still to be fully understood. (see Chapter 4 for comments on *Pelosoma* species associated to rotten stems of succulent plants in arid zones of the northernmost Neotropics). Our results on Chapter 3 show that lineages of Megasternini such *Cycreon* are tightly associated to a diversity of inflorescences of araceaen plants and that they may be involved in their pollination. On the other hand, Chapter 2 provide a clear evidence of the morphological diversity inside of the largest genus *Cercyon* at the moment not reflected in formal classification, resulting in polyphyletic arrangements. Information like that presented in the taxonomical papers of this thesis, focused on reviewing taxa from different parts of the globe associated to different habitats, is the fundament of evolutionary analyses like the one in Chapter 6 about the pattern of habitat transitions of hydrophilid beetles.

Why is Megasternini so diverse? Are they the result of adaptive radiation?
Megasternini, being a comparatively recent lineage deeply nested within Hydrophilidae, is a definite example of asymmetry in terms of diversification. This is especially noticeable when compared to the number of species, 42, in its sister lineage, Sphaeridiini (Fikáček and Kropáček 2015). The only genus in Sphaeridiini is almost exclusively found feeding on animal excrements. On the other hand, the common ancestor of Megasternini was reconstructed as present in leaf litter.

Our reconstruction of the shifts between habitats showed that leaf litter is a pivotal habitat from which organisms transition to other 'more specialized' ones, like rotten stems of bamboo or cacti, aroid inflorescences, beachwrack, mammal excrements, rotting fungi, association with social insects, among others. This pattern was previously found for the whole Staphyliniformia as well (McKenna et al. 2015).

While leaf litter is the most common habitat, megasternines have colonized the widest spectrum of habitats for any hydrophilid group. The ecological disparity of members of the Megasternini is coupled with a complex pattern of morphological evolution that have led to the evolution of homoplastic characters previously considered diagnostic at genus level. A striking example of this is *Cercyon,* which representatives are found in more than ten places in the tree. This apparent morphological plasticity is crystalized in the relatively fast modification of the morphology that can be associated to adaptation to particular life styles. One example of this is the genus *Chimaerocyon*, a outstandingly modified megasternine associated to *Pheidole* ants (Fikáček et al. 2013) that was recover in the phylogeny as nested in a group of typically-looking megasternines currently assigned to the genus *Cercyon*.

My results on the reconstruction of the historical biogeography of the tribe show how the concomitance of climatic fluctuations and shifting land mass configuration shaped the diversity and distribution of Megasternini. Megasternines were able to reach new geographical areas in different times and directions. These processes were accentuated during the hyperthemal conditions of the Palaeocene-Eocene transition that allowed the existence of a boreotropical biome that interconnected the land masses of the northern hemisphere (Brunke et al 2017; Garrouste and Nel 2019; Zachos et al. 2001). Given their ancestral geographical ranges, the members of subtribe Megasternina were able to exploit this interconectivity and disperse to new continents more frequently than those of Oosternina, which are, with the exception of the clade III (*Oosternum* group *sensu novo*), restricted to Oceania. When the Eocene climatic optimum reached its end, the cooling of the climate pushed the boreotropical biomes to the equator and caused their fragmentation which very likely promoted the speciation. The results of the divergence through time analyses suggested that these processed resulted in different patterns of diversification in which Megasternina benefited more than the more geographically restricted Oosternina.

The increased diversification and the ecological disparity seen in Megasternini would point out to the assignment of the label 'adaptative radioation' on the tribe. However, the study of evolutionary phenomena is more intrincate than following a research program aimed to assign categorical labels like 'adaptive radiation' upon the patterns and process observed in nature. Recent views on the complex nature of the evolutionary radiations (or 'bursts' of diversification) have

expanded the pantheon of labels to encompass explanations of climatological or geographical nature, as well as differential extinction rates (Simões et al. 2017).

Megasternines are a clear example of how the outstanding diversification of a group could be a result of not only the adaptation to new environments but to a complex interrelation of geographical, climatic, develomental and macrovelutionary processes acting in an intrincate manner at different times and scales. Understanding such complex processes should not be constrained to by assigning of set of labels. Evolutionary radiations are not to be regarded as a processes essentially different from evolution itself. The study of evolutionary phenomena should aim to consider variables as continua in which setting of arbitrary tresholds is artifactual and ultimately counterproductive (Olson and Arroyo 2009). Concepts and metaphors in biology need to be constantly reviewed and updated or left behind if deemed necessary (Olson et al 2019). This applies to ideas from 'adaptive radiation' to the 'generic concept of *Cercyon'*.

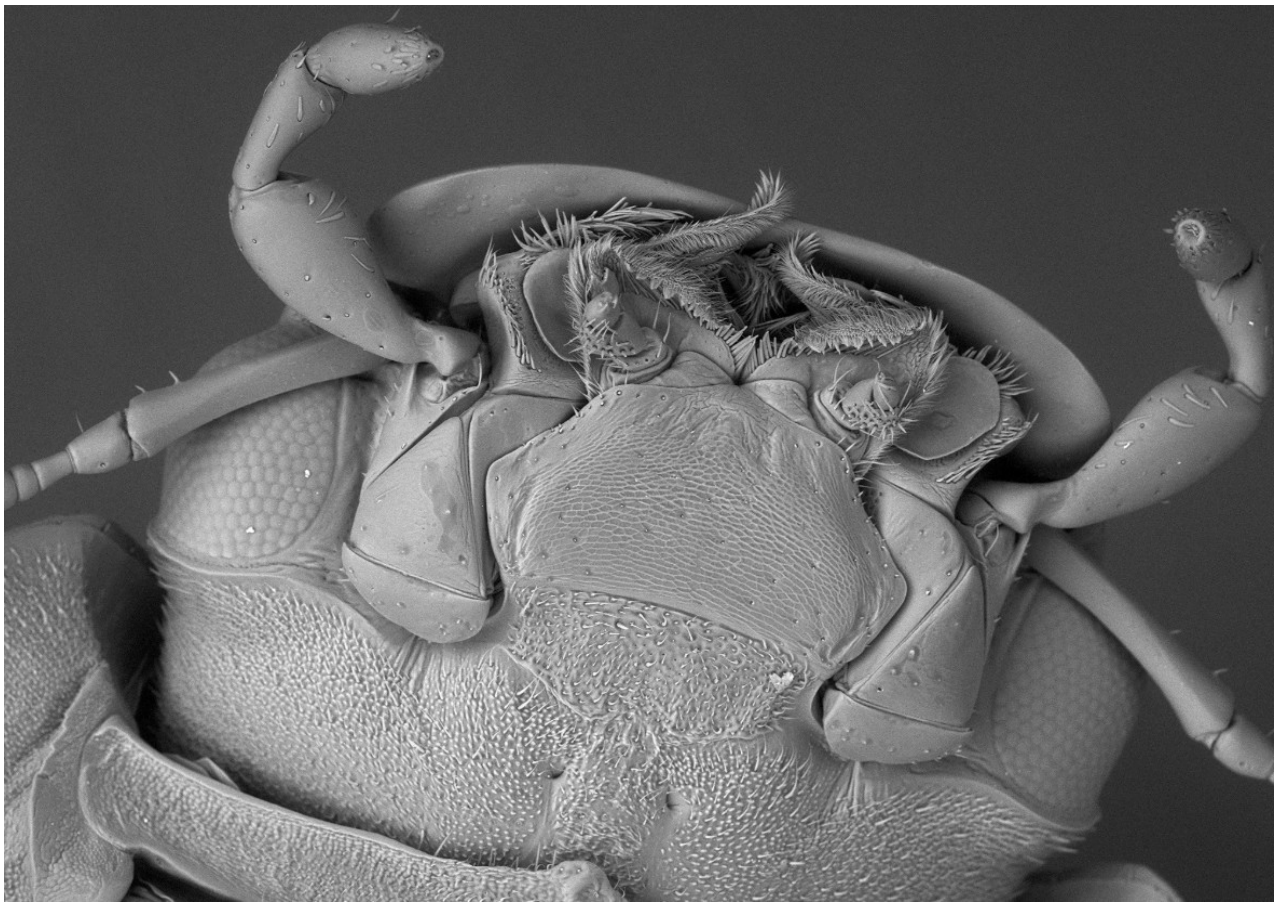

Figure 12. Ventral view of head of *Cercyon aphodioides* d'Orchymont from South Africa

References

Arriaga-Varela, E., Seidel, M., Deler-Hernández, A., Senderov, V. and Fikáček, M., 2017. A review of the *Cercyon* Leach (Coleoptera, Hydrophilidae, Sphaeridiinae) of the Greater Antilles. *ZooKeys*, (681), 39.

Arriaga-Varela, E., Seidel, M. and Fikáček, M., 2018. A new genus of coprophagous water scavenger beetle from Africa (Coleoptera, Hydrophilidae, Sphaeridiinae, Megasternini) with a discussion on the *Cercyon* subgenus *Acycreon*. *African Invertebrates*, 59, 1-23.

Bernhard, D., Schmidt, C., Korte, A., Fritzsch, G. and Beutel, R.G., 2006. From terrestrial to aquatic habitats and back again—molecular insights into the evolution and phylogeny of Hydrophiloidea (Coleoptera) using multigene analyses. *Zoologica Scripta*, 35(6), 597–606.

Bloom, D., Fikáček, M. and Short, A.E.Z. 2014. Clade age and diversification rate variation explain disparity in species richness among water scavenger beetle (Hydrophilidae) lineages. *PLoS ONE* 9(6), e98430.

Bouchard, P., Grebennikov, V.V., Smith, A.B. and Douglas, H., 2009. Biodiversity of Coleoptera. *Insect biodiversity: science and society*, pp.265-301.

Brunke, A.J., Chatzimanolis, S., Metscher, B.D., Wolf-Schwenninger, K. and Solodovnikov, A. 2017. Dispersal of thermophilic beetles across the intercontinental Arctic forest belt during the early Eocene. *Scientific Reports*, 7(1), 12972.

Casakin, H. P. (2007). Factors of metaphors in design problem-solving: Implications for design creativity. *International Journal of Design*, 1(2), 21-33.

Craddock, E. M. 2000. Speciation processes in the adaptive radiation of Hawaiian plants and animals. *Evolutionary biology* (pp. 1-53). Springer.

Deler-Hernández, A., Cala-Riquelme, F. and Fikácek, M., 2014. A review of the genus *Oosternum* Sharp of the West Indies (Coleoptera: Hydrophilidae: Sphaeridiinae). *Deutsche Entomologische*

Zeitschrift, 61, 43-63.

Fikáček, M. 2010. Hydrophilidae: The genus *Kanala* Balfour-Browne (Coleoptera). In: Jäch, M.A. and Balke, M. (Eds.). *Water Beetles of New Caledonia, Vol. 1. Monographs of Coleoptera,* 3, 365–394.

Fikáček, M. and Kropáček, D., 2015. A new species of *Sphaeridium* from northeastern India and Myanmar (Coleoptera: Hydrophilidae: Sphaeridiinae). *Acta Entomologica Musei Nationalis Pragae,* 55(2), 673-680.

Fikáček, M. and Short, A.E.Z. 2006. A revision of the Neotropical genus *Motonerus* Hansen (Coleoptera: Hydrophilidae: Sphaeridiinae). *Zootaxa*, 1268, 1–38.

Fikáček, M. and Short, A.E., 2010. Taxonomic revision and phylogeny of the genus *Cetiocyon* and its discovery in the Neotropical region (Insecta: Coleoptera: Hydrophilidae). Arthropod Systematics & Phylogeny , 68(3), 309– 329.

Fikáček, M.., Maruyama, M., Vondráček, D. and Short, A.E. 2013. *Chimaerocyon* gen. nov., a morphologically aberrant myrmecophilous genus of water scavenger beetle (Coleoptera: Hydrophilidae: Sphaeridiinae). *Zootaxa*, 3716(2), 277-288.

Forbes, A.A., Bagley, R.K., Beer, M.A., Hippee, A.C. and Widmayer, H.A., 2018. Quantifying the unquantifiable: why Hymenoptera, not Coleoptera, is the most speciose animal order. *BMC Ecology*, 18(1), 1-21.

Garrouste, R. and Nel, A., 2019. Alaskan Palaeogene insects: a challenge for a better knowledge of the Beringian ‘route’ (Odonata: Aeshnidae, Dysagrionidae). *Journal of Systematic Palaeontology*, 1-8.

Givnish, T.J. 1997. Adaptive radiation and molecular systematics: issues and approaches. In: Givnish, T.J., Sytsma, K,J. eds; *Molecular Evolution and Adaptive Radiation*. 1–54, Cambridge University Press.

Grant, P. R. and Grant R. B. 2008. *How and why species multiply. The radiation of Darwin's finches Princteon,* Princeton University Press.

Hansen, M. 1991. The Hydrophiloid Beetles. Phylogeny, Classification and a Revision of the Genera (Coleoptera, Hydrophiloidea). *Biologiske Skrifter, Det Kongelige Danske Videnskabernes Selskab*, 40, 1-368.

Horn GH .1890. A revision of the Sphaeridiini inhabiting boreal America. *Transactions of the American Entomological Society*, 17 (3), 279–314, pl. 9.

Lakoff, G. 1993. The contemporary theory of metaphor. In A. Ortony (Ed.), *Metaphor and thought*, 202-251. Cambridge University Press.

Mckenna, D.D., Farrell, B.D., Caterino, M.S., Farnum, C.W., Hawks, D.C., Maddison, D.R., Seago, A.E., Short, A.E., Newton, A.F. and Thayer, M.K. 2015. Phylogeny and evolution of S taphyliniformia and S carabaeiformia: forest litter as a stepping stone for diversification of nonphytophagous beetles. *Systematic Entomology*, 40(1), 35-60.

Kocher, T.D. 2004. Adaptive evolution and explosive speciation: the cichlid fish model. *Nature Reviews Genetics*. 5, 288–298.

Heath T.A., Hedtke S.M. and Hillis D.M. 2008. Taxon sampling and the accuracy of phylogenetic analyses, *Journal of Systematics and Evolution,* 46, 239-257

Jackman, T. 1997. Phylogenetic studies of convergent adaptive radiations in Caribbean Anolis lizards. *Molecular evolution and adaptive radiation*, 535-557.

Losos, J.B. and Miles, D.B., 2002. Testing the hypothesis that a clade has adaptively radiated: iguanid lizard clades as a case study. *The American Naturalist*, 160(2), 147-157.

Ribera, I. and Balke, M. 2007. Recognition of a species-poor, geographically restricted but morphologically diverse Cape lineage of diving beetles (Coleoptera: Dytiscidae: Hyphydrini). *Journal of Niogeography*, 34(7), 1220-1232.

Olson, M.E. and Arroyo-Santos, A., 2009. Thinking in continua: beyond the “adaptive radiation” metaphor. *BioEssays*, 31(12), 1337-1346.

Olson, M.E., Arroyo-Santos, A. and Vergara-Silva, F., 2019. A user's guide to metaphors in ecology and evolution. *Trends in Ecology & Evolution,* published online.

Pallarés, S., Arribas, P., Bilton, D.T., Millán, A., Velasco, J. and Ribera, I., 2017. The chicken or the egg? Adaptation to desiccation and salinity tolerance in a lineage of water beetles. *Molecular Ecology*, 26(20), 5614-5628.

Pohl, H. and Beutel, R.G. 2008. The evolution of Strepsiptera (Hexapoda). *Zoology*, 111(4), 318-338.

Roff, D., 2001. Adaptive radiation: does the evidence support the theory?. *Journal of Evolutionary Biology*, 14(3), 521-522.

Ryndevich, S.K. 2001. On identification of species of the *Cercyon dux* group (Coleoptera: Hydrophilidae). *Zoosystematica Rossica,* 10(1), 79–83.

Ryndevich, S.K, 2008. Review of species of the genus *Cercyon* Leach, 1817 of Russia and adjacent regions. IV. The subgenera *Paracycreon* Orchymont, 1924 and *Dicyrtocercyon* Ganglbauer, 1904 (Coleoptera: Hydrophilidae). *Zoosystematica Rossica,* 17(2), 89–97.

Ryndevich, S.K., Jia, F. and Fikáček, M. 2017. A review of the Asian species of the *Cercyon unipunctatus* group (Coleoptera: Hydrophilidae: Sphaeridiinae). *Acta Entomologica Musei Nationalis Pragae*, 57(2), 535-576.

Schluter, D., 2000. *The ecology of adaptive radiation*. OUP Oxford.

Short, A.E. and Fikáček, M. 2011. World catalogue of the Hydrophiloidea (Coleoptera): additions and corrections II (2006–2010). *Acta Entomologica Musei Nationalis Pragae*, 51(1), 83-122.

Simões, M., Breitkreuz, L., Alvarado, M., Baca, S., Cooper, J.C., Heins, L., Herzog, K. and Lieberman, B.S. 2016. The evolving theory of evolutionary radiations. *Trends in Ecology & Evolution*, 31(1), 27-34.

Smetana, A., 1978. Revision of the subfamily Sphaeridiinae of America north of Mexico (Coleoptera: Hydrophilidae). *The Memoirs of the Entomological Society of Canada*, 110(S105), 1-

292.

Song, K.Q., Xue, H.J., Beutel, R.G., Bai, M., Bian, D.J., Liu, J., Ruan, Y.Y., Li, W.Z., Jia, F.L. and Yang, X.K. 2014. Habitat-dependent diversification and parallel molecular evolution: Water scavenger beetles as a case study. *Current Zoology*, 60(5), 561-570.

Szczepański, W.T., Vondráček, D., Seidel, M., Wardhaugh, C. and Fikáček, M., 2018. High diversity of *Cetiocyon* beetles (Coleoptera: Hydrophilidae) along an elevational gradient on Mt. Wilhelm, New Guinea, with new records from the Bird's Head Peninsula. *Arthropod Systematics and Phylogeny,* 76, 323-347.

Toussaint, E.F., and Short, A.E. 2018. Transoceanic Stepping–stones between Cretaceous waterfalls? The enigmatic biogeography of pantropical Oocyclus cascade beetles. *Molecular Phylogenetics and Evolution,* 127, 416-428.

Vršanský, P., Sendi, H., Aristov, D., Bechly, G., Müller, P., Ellenberger, S., Azar, D., Ueda, K., Barna, P. and Garcia, T., 2019. Ancient roaches further exemplify 'no land return' in aquatic insects. *Gondwana Research*, 68, 22-33.

Zachos, J., Pagani, M., Sloan, L., Thomas, E. and Billups, K. 2001. Trends, rhythms, and aberrations in global climate 65 Ma to present. *Science*, 292(5517), 686-693.

Chapter 1

A review of the *Cercyon* Leach (Coleoptera, Hydrophilidae, Sphaeridiinae) of the Greater Antilles

Arriaga-Varela, E., Seidel, M., Deler-Hernández, A., Senderov, V. and Fikáček, M., 2017. A review of the Cercyon Leach (Coleoptera, Hydrophilidae, Sphaeridiinae) of the Greater Antilles. *ZooKeys*, (681), 39-93.

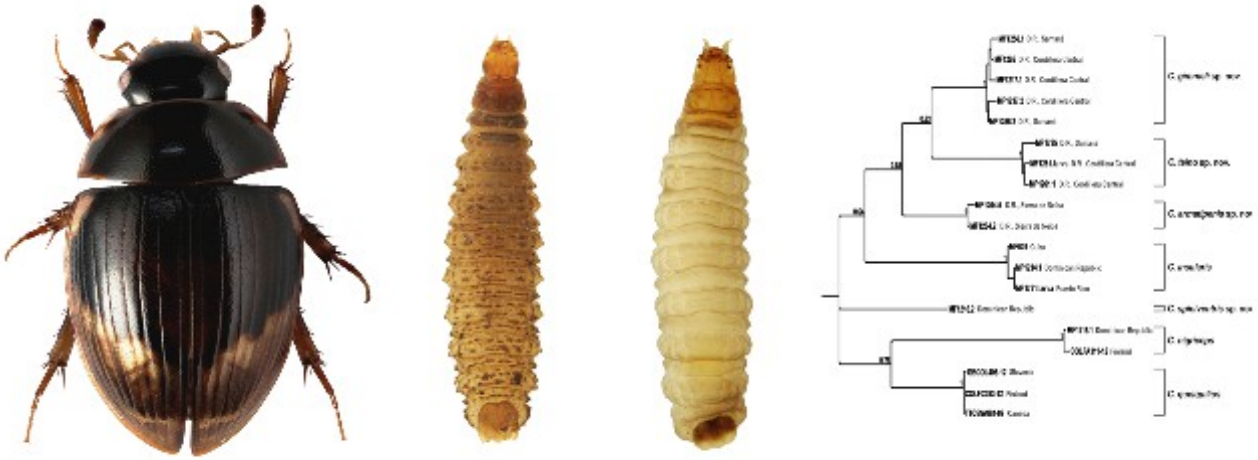

ZooKeys 681: 39–93 (2017)
doi: 10.3897/zookeys.681.12522
http://zookeys.pensoft.net

RESEARCH ARTICLE

A peer-reviewed open-access journal
ZooKeys
Launched to accelerate biodiversity research

A review of the *Cercyon* Leach (Coleoptera, Hydrophilidae, Sphaeridiinae) of the Greater Antilles

Emmanuel Arriaga-Varela[1,2], Matthias Seidel[1,2], Albert Deler-Hernández[1], Viktor Senderov[3,4], Martin Fikáček[1,2]

1 *Department of Zoology, Faculty of Science, Charles University, Prague, Viničná 7, CZ-128 44 Praha 2, Czech Republic* **2** *Department of Entomology, National Museum, Cirkusová 1, CZ-193 00 Praha, Czech Republic* **3** *Pensoft Publishers, Prof. Georgi Zlatarski Street 12, 1700 Sofia, Bulgaria* **4** *Institute of Biodiversity and Ecosystems Research, Bulgarian Academy of Sciences, 1113 Sofia, Bulgaria*

Corresponding author: *Emmanuel Arriaga-Varela* (arriagavarelae@natur.cuni.cz)

Academic editor: *M. Michat* | Received 3 March 2017 | Accepted 21 May 2017 | Published 21 June 2017

http://zoobank.org/439764EC-BA05-4D8A-815A-FC48E5D57FE4

Citation: Arriaga-Varela E, Seidel M, Deler-Hernández A, Senderov V, Fikáček M (2017) A review of the *Cercyon* Leach (Coleoptera, Hydrophilidae, Sphaeridiinae) of the Greater Antilles. ZooKeys 681: 39–93. https://doi.org/10.3897/zookeys.681.12522

Abstract

The representatives of the genus *Cercyon* Leach occurring in the Greater Antilles are reviewed. Ten species are recorded, of which five are described here as new: *C. gimmeli* **sp. n.** (Dominican Republic), *C. armatipenis* **sp. n.** (Dominican Republic), *C. taino* **sp. n.** (Dominican Republic), *C. sklodowskae* **sp. n.** (Jamaica) and *C. spiniventris* **sp. n.** (Dominican Republic). Diagnoses and detailed distributional data are also provided for *C. floridanus* Horn, 1890 (distributed in southeastern United States of America and Cayman Islands), *C. insularis* Chevrolat, 1863 (endemic to the Antilles), *C. praetextatus* (Say, 1825) (widely distributed in the New World incl. Greater Antilles), *C. quisquilius* (Linnaeus, 1761) (an adventive species of Paleartic origin) and *C. nigriceps* (Marshall, 1802) (an adventive species probably of Oriental origin). *Cercyon armatipenis*, *C. gimmeli*, *C. taino* form a group of closely related species only distinguishable by male genitalia and DNA sequences. A key to the Great Antillean *Cercyon* is provided and important diagnostic characters are illustrated. The larvae of *C. insularis* and *C. taino* were associated with adults using COI barcode sequences, illustrated and diagnosed. Full occurrence data, additional images and COI barcode sequences were submitted to open access on-line depositories in an effort to provide access to complete data.

Keywords

Megasternini, morphology, taxonomy, new species, Caribbean, COI, DNA barcode, larva, biodiversity informatics

Introduction

Until very recently, water scavenger beetles (Hydrophilidae) from the Greater Antilles in the Caribbean Region were largely neglected and systematic or faunistic studies were scarce. For instance, 46 of 56 hydrophilid species recorded from Cuba were described in the 18th and 19th centuries (Peck 2005). Nevertheless, recent taxonomic studies have brought to light many new species and new country records in this region e.g. in genera *Berosus* Leach (Deler-Hernández et al. 2013a), *Enochrus* Thomson (Deler-Hernández and Delgado 2010; Short 2005), *Oosternum* Sharp (Deler-Hernández et al. 2014), *Phaenonotum* Sharp (Deler-Hernández et al. 2013b) and *Tropisternus* Solier (Spangler and Short 2008). However, many other groups still await a comprehensive treatment, which includes *Cercyon*, the most speciose genus within the subfamily Sphaeridiinae. As with most members of the subfamily, *Cercyon* species have predominantly terrestrial habits, and are frequently associated with decaying plant material and feces. Approximately 260 species have been described from all zoogeographical zones (Short and Fikáček 2011), of which 24 have been recorded from Central and South America (Hansen 1999; Fikáček 2006). The number of described species seems highly underestimated in the Neotropical Region, due to the lack of recent taxonomic work. The most comprehensive identification resource for Central American fauna still remains the iconic *Biologia Centrali-Americana* (Sharp 1882, 1887). The situation is also aggravated by the presence of introduced Old World synanthropic species, which are difficult to recognize and are sometimes confused with native species (Fikáček 2009).

Six species of *Cercyon* have been recorded from the Greater Antilles: the Cuban-endemic *C. insularis* Chevrolat whose identity has remained unclear (Hansen 1999; Peck 2005), two species widely distributed in the New World (*Cercyon variegatus* Sharp, *Cercyon praetextatus* (Say); Leng and Mutchler 1917; Smetana 1984; Fikáček 2009), one species native to southeastern United States of America (*Cercyon floridanus* Horn; Thomas et al. 2013) and two widely distributed adventive species (*Cercyon nigriceps* Marsham, *Cercyon quisquilius* (Linnaeus); Leng and Mutchler 1917; Fikáček 2009). Our recent field work and examination of museum material revealed that additional species occur in the area, which provided the impetus for this study. In order to provide a review that will constitute a reliable reference for future studies on the genus *Cercyon* and the tribe Megasternini, we complemented the traditional taxonomic account with COI sequences (i.e., "DNA barcodes"), complete occurrence data, and full set of high-resolution photographs, all deposited in online freely available platforms.

Material and methods

Examined specimens and depositories. A total of 848 specimens of *Cercyon* from the Greater Antilles were examined, including the type specimens of *Cercyon insularis* Chevrolat and *C. variegatus* Sharp. Label data are only reproduced verbatim for type specimens; each individual label is separated by double slash "//"; notes on the label data or

additional information are written between square brackets [ ]. All holotypes are marked with red label bearing the following text: "HOLOTYPE, *Cercyon* [name of the species] sp. n., Arriaga-Varela, Seidel, Deler-Hernández and Fikáček des. 2016". All paratype specimens are marked by yellow label bearing the following text: "PARATYPE, *Cercyon* [name of the species] sp. n., Arriaga-Varela, Seidel, Deler-Hernández and Fikáček des. 2016". A georeferenced dataset of the studied specimens is available as Excel spreadsheet in Suppl. material 1. The file only includes specimens identified to species. The distribution maps (Figs 15–16) were constructed from the GPS data extracted from the Excel spreadsheet and mapped using the R script (see Suppl. material 4).

The examined specimens are deposited in the following collections:

BCPC	Bruno Clarkson private collection, Rio de Janeiro, Brazil;
BMNH	Natural History Museum, London, United Kingdom (M.V.L. Barclay);
CMN	Canadian Museum of Nature, Ottawa, Canada (R. Anderson, F. Génier);
CNC	Canadian National Collection of Insects, Arachnids and Nematodes, Ottawa, Canada (P. Bouchard);
CNIN	Colección Nacional de Insectos, Instituto de Biología, Universidad Nacional Autónoma México, Mexico City, Mexico (S. Zaragoza);
FSCA	Florida State Collection of Arthropods, Gainesville, USA (P. Skelley);
HNHM	Hungarian National History Museum, Budapest, Hungary (O. Merkl, G. Szél);
MNHNSD	Museo Nacional de Historia Natural, Santo Domingo, Dominican Republic (C. Suriel);
MNHN	Muséum National d'Histoire Naturelle, Paris, France (A. Mantilleri);
NHMW	Naturhistorisches Museum, Wien, Austria (M. A. Jäch);
NMPC	National Museum, Prague, Czech Republic (M. Fikáček);
SBNM	Santa Barbara Museum of Natural History, Santa Barbara, USA (M. L. Gimmel);
SBPC	Stewart Peck Personal Collection, Ottawa, Canada;
UPRM	University of Puerto Rico, Mayagüez, Puerto Rico (A. Segarra);
ZMUC	Zoological Museum, Natural History Museum of Denmark, Copenhagen, Denmark (A. Solodovnikov).

Morphological studies. Specimens were dissected, with genitalia embedded in a drop of alcohol-soluble Euparal resin on a piece of glass glued to a small piece of cardboard attached below the respective specimen. All species are diagnosed and illustrated, and new species are described in detail.

Habitus photographs were taken using a Canon D-550 digital camera with attached Canon MP-E65mm f/2.8 1–5 macro lens. Pictures of genitalia were taken using a Canon D1100 digital camera attached to an Olympus BX41 compound microscope; pictures of different focus were combined in Helicon Focus software. Scanning electron micrographs were taken using Hitachi S-3700N environmental electron microscope at the Department of Paleontology, National Museum in Prague. Pictures used for plates

were adapted in Adobe Photoshop CS6. All original pictures including additional views not presented in this paper are published and freely available on Flickr in order to serve for further morphological studies.

DNA barcoding. Most of the examined specimens were collected during recent expeditions to Cuba, Dominican Republic and Puerto Rico. Samples were preserved in 96% ethanol and stored at -20 °C. DNA was extracted from complete specimens using a QiaGen Blood and Tissue DNA extraction kit following the manufacturer's instructions. The highly variable 5' region of the mitochondrial cytochrome c oxidase subunit I gene (COI) was amplified using LCO1490 (5'-GGTCAACAAATCATAAAGATATTGG-3') and HCO2198 (5'-TAAACTTCAGGGTGACCAAAAAATCA-3') primers (Folmer et al. 1994). Each 10 µl PCR reaction contained 6.7 µl H_2O, 0.4 µl of $MgCl_2$ (25 mM), 0.2 µl of dNTPs (10 mM), 0.3 µl of each forward and reverse primer (10 µM), 0.1 µl of Taq polymerase (5 u/µl), 1.0 µl of 10x Taq buffer, and 1.0 µl of DNA template. The PCR conditions consisted of 3 min at 94 °C + 35 cycles of 30 s at 94 °C, 45 s at 48 °C and 1 min at 72 °C + 8 min at 72 °C. 5 µl of each PCR product were purified by adding 0.5µl (20 u) Exonuclease I (Exo1) and 1µl (1 u) Thermosensitive Alkaline Phosphatase (FastAP) (Thermo Fisher Scientific) and incubating the mixture for 15 min at 37°C, followed by 15 min at 80°C. The Sanger sequencing was performed by BIOCEV (Vestec, Czech Republic) on a capillary DNA sequencer. Sequences were edited with Geneious 9.1.4. We did not attempt DNA extraction and sequencing of old museum specimens, which is why we only provide sequences for six of the ten species occurring in Greater Antilles.

Analyses of molecular data. In order to identify the larvae collected along with adult specimens, a maximum likelihood analysis of obtained COI sequences was performed. We combined the newly generated sequences of freshly collected adults and larvae, and combined them with additional sequences of two introduced species (*C. quisquilius* and *C. nigriceps* from Europe and Canada) from the Barcode of Life Data Systems (BOLD; http://www.boldsystems.org). Sequences were aligned using the ClustalW algorythm in Geneious 9.1.4. The final alignment had a length of 610 bp and was tested for the best nucleotide substitution model using MEGA7 (Kumar et al. 2016). A phylogenetic analysis using the maximum likelihood algorythm and 1000 bootstrap replicates was performed in the same software.

Open access to complete data

This taxonomic paper includes only a part of the data accumulated in the course of our study. Part of the primary data (e.g., unedited photographs, the complete set of unedited SEM micrographs, DNA sequences, spreadsheet-fomatted species distribution data) are not included here. To make all primary data accessible, we deposited them to open access on-line depositories as specified below. For more details about biodiversity data publishing, see e.g. the policies and guidelines implemented for Pensoft Publishers (Penev et al. 2011).

Complete primary data. Complete primary data were submitted as a .zip file to the Zenodo depository (https://zenodo.org/) under the doi 10.5281/zenodo.580260.

Species distribution data. The distribution data on all specimens examined are presented in unstructured text format directly in the paper. The conversion of these data into a structured, computable format (as XML, so called parsing) is difficult, and no algorithm exists for parsing occurrence records (see Sautter and Böhm 2014 for the analogous problem of parsing literature references).

The text-formatted distribution data published here are, however, based on a structured Excel spreadsheet following the Darwin Core (henceforth DwC) format for biodiversity data described by Wieczorek et al (2012). DwC defines how the data should be structured (i.e. which columns may be included in the table, how they should be called and which part of the data they should include). In some cases DwC also specifies the format of the entries (e.g., how date should be formatted). Details are available through the website of the Biodiversity Information Standards (TWDG; http://rs.tdwg.org/dwc/terms/). Being a formal biodiversity standard, DwC is nowadays used by a wide spectrum of on-line biodiversity portals, e.g. by the Global Biodiversity Information Facility (GBIF), Encyclopedia of Life, and the Atlas of Living Australia. This is the reason why we selected it. The Excel file is attached here as Suppl. material 1, it is included in the .zip file submitted to Zenodo, and was used for the GBIF submission.

The Publication of distribution data to GBIF is possible through the institution or organization, which is a member or partner of GBIF (direct submissions from individual users are not possible) using the Integrated Publishing Toolkit (IPT). IPT allows to upload the distribution data from the DwC-formatted Excel spreadsheet, specify the metadata about the dataset, and publish the data to the GBIF portal. We submitted our data through Pensoft as an organization associated with GBIF using the Pensoft IPT Data Hosting Centre (http://ipt.pensoft.net/).

DNA data and voucher information. The cytochrome oxidase I barcode sequences and the data about the voucher specimens were submitted to the Barcode of Life Data Systems (BOLD; http://www.boldsystems.org/) using the user web interface available after registration. The submission requires first the submission of the specimen data using the Excel-based spreadsheet following the Specimen Data Submission Protocol (http://www.boldsystems.org/index.php/resources/handbook?chapter=3_submissions.html&section=data_submissions). To prevent the re-typing of the specimen data again, we wrote an R script converting the data from DwC to the format required for BOLD submissions (see Suppl. material 3). Once specimen data are submitted, all other information (voucher photos, DNA sequences, DNA trace files) can be submitted, using the identification code (SampleID) to connect the data to the respective voucher specimen. We submitted the sequences under Process ID GANTC001-16 and GANTC002-17 to GANTC015-17 in BOLD.

Original photo-documentation. The original photo-documentation includes the unedited high-resolution versions of photos and SEM micrographs that we used in this

publication, plus many photos and SEM micrographs that were taken for comparative purposes but are not published here. We submitted all these files to Zenodo as a part of the .zip file containing all our primary data. Since the images are not easy to see in this way, we also submitted all photos to Flickr photo hosting service where they can be easily displayed; they are available at https://www.flickr.com/photos/142655814@N07/collections/72157678126129411/.

Taxonomy

Cercyon Leach, 1817

Cercyon Leach, 1817: 95. - Type species: *Dermestes melanocephalus* Linnaeus (designated by Thomson 1859: 19).

Diagnosis. *Cercyon* can be distinguished from other hydrophilid genera occurring in the Greater Antilles by the following combination of characters: antenna with compact club; prothorax with conspicuous antennal groove not reaching pronotal margin; medial part of prosternum not demarcated from lateral parts; metaventrite without arcuate lines in anterolateral corners; mesoventral plate fusiform, narrowing anteriorly and posteriorly, touching anterior margin of metaventrite in one point.

Cercyon species are very similar to the members of *Pelosoma*, a Neotropical genus that is recorded from the Lesser Antilles; *Pelosoma* differs from *Cercyon* by the mesoventral plate widely contacting the metaventrite (it only narrowly contacts it in *Cercyon*). Small species of *Cercyon* may resemble the members of *Oosternum*, which can be easily distinguished from *Cercyon* by possessing a metaventrite with an arcuate ridge delimiting its anterolateral corner, and in some species also by elevated median part of the prosternum.

Key to the Greater Antilles species of *Cercyon*

1 Small species, body length 1.0–2.1 mm. Metaventrite with complete femoral lines (Fig. 13d)..... ***Cercyon nigriceps* (Marsham)**

– Larger species, body length 2.3–4.1 mm. Metaventrite without femoral lines (Figs 7d, 8g, 9c, h, 10g, 11g, 12g, 13b, f)..... **2**

2 Mesoventral plate very wide, 1.9× as long as wide (Fig. 7d). Mesoventral plate and pentagonal raised part of the metaventrite with large, deep, semicircular punctures (Fig. 7d) ..... ***Cercyon floridanus* Horn**

– Mesoventral plate moderately to very narrow, 3.3–5.9× as long as wide (Figs 8f, 9c, h, 10f, 11f, 12f, 13b, e). Mesoventral plate and pentagonal raised part of the metaventrite with small and shallow punctures (Figs 8g, 9c, h, 10g, 11g, 12g, 13b, f)..... **3**

3 Mesoventral plate wide, 3.3× as long as wide (Fig. 13a). Dorsal coloration black, with large yellow spot at elytral apex; lateral margin of elytra narrowly

yellow, the yellow stripe not widened in humeral area (Fig. 2g–i)..... ..... ***Cercyon praetextatus* (Say)**

– Mesoventral plate narrow, 5.7–6.3× as long as wide as long as wide (Figs 8f, 9c, h, 10g, 11g, 12g, 13e). Dorsal coloration variable, if elytra is black with a large yellowish spot at apex, then the yellow coloration at the lateral margin of elytra expands to humeral area..... **4**

4 Metaventrite with raised pentagonal area markedly wide at midlength, 0.6× as long as wide (Fig. 13f) ..... ***Cercyon quisquilius* (Linnaeus)**

– Metaventrite with raised pentagonal area rather narrow at midlength, 0.9–1.2× as long as wide (Figs 8g, 9c, h, 10g, 11g) **5**

5 Dorsal surface of head black, with reddish-brown spot(s) at vertex. Pronotum (Fig. 4a) yellowish to dark reddish, with a large median spot and smaller spot on each side, often fused together into one large tri-lobate spot. Elytra brown with black humeral spots extending to anterior margin and suture. Prosternum with median ridge not projected ventrally at anterior margin (Fig. 12c)..... ..... ***Cercyon insularis* Chevrolat**

– Dorsal surface of head including vertex black, anterolateral margins of clypeus yellowish. Pronotum either black with yellowish to reddish lateral margins (Figs 1a–i, g, 2a–c), or uniformly light brown (Fig. 3a–i). Elytra either more or less uniformly brown, or black with yellowish to reddish lateral and apical parts..... **6**

6 Pronotum uniformly light brown, elytra more or less uniformly greyish-brown (Fig. 3a). First abdominal ventrite of females (Fig. 11h) with longitudinal carina prolonged into an acute spiniform setose process; longitudinal carina of male first abdominal ventrite not projected. Raised area of metaventrite comparatively wide, 0.8× as long as wide (Fig. 11g)..... ..... ***Cercyon spiniventris* sp. n.**

– Pronotum and elytra black with pale contrasting markings (Figs 1a, c, d, f, g, i, 2a, c): pronotum black with creamy-white or reddish lateral margins; elytra black with creamy-white to reddish humeral spot, lateral margins and apical third. First abdominal ventrite of both sexes not projecting beyond posterior margin (Figs 8h, 10h). Raised area of metaventrite rather narrow, 1.1–1.2× longer than wide (Figs 8g, 9c, h)..... **7**

7 Prosternum with median ridge forming a small rounded to weakly pointed process (Fig. 10c). Raised median area of metaventrite reaching anterior margin of metaventrite (Fig. 10g). Anterior margin of mentum emarginate medially (Fig. 10a). Apex of fifth abdominal ventrite with a triangular bulged projection in females (Fig. 10i), not modified in males. Jamaica .... ***Cercyon sklodowskae* sp. n.**

– Prosternum with median ridge forming a large rounded knob (Figs 8c, 9g). Raised median area of metaventrite not reaching anterior margin of metaventrite (Figs 8g, 9c, h). Anterior margin of mentum not emarginate medially

(Figs 8a, 9a, h). Apex of fifth abdominal ventrite rounded in both sexes. Hispaniola..... ***Cercyon gimmeli* species group**...**8**

8 Median lobe strongly acuminate at apex (Fig. 5f–g); parameres distinctly shorter than phallobase (Fig. 5e) ..... ***Cercyon taino* sp. n.**

– Median lobe blunt at apex (Fig. 5c, k); parameres as long as or longer than phallobase (Fig. 5a, i) **9**

9 Median lobe wide basally, narrowing apically, with large gonopore and many spines in apical fifth (Fig. 5j–k); parameres ca. as long as phallobase (Fig. 5i).... ..... ***C. armatipenis* sp. n.**

– Median lobe narrowly parallel–sided, with indistinct gonopore and without spines at apex (Fig. 5b–c); parameres distinctly longer than phallobase (Fig. 5a) ..... ***C. gimmeli* sp. n.**

Species treatments

Cercyon gimmeli species group

This species group is composed of three very closely related species endemic to the island of Hispaniola. Specimens are indistinguishable on the basis of external morphology and can be only told apart by examination of male genitalia. At least in one locality, two species of this group were collected syntopically. For this reason, we refrain from using female specimens as paratypes unless the specimen was associated with males by DNA barcode, and female specimens are not listed in the text below neither in the DarwinCore spreadsheet submitted to GBIF for that reason. Below, we provide a diagnosis allowing to separate all species of the species group from other *Cercyon* species. Further on, we describe *Cercyon gimmeli* sp. n. in full, and provide only comparative diagnoses for the other two species, *C. armatipenis* sp. n. and *C. taino* sp. n.

Diagnosis of the *Cercyon gimmeli* species group. Members of the species group can be differentiated from other Greater-Antillean *Cercyon* by the following combination of characters: size 2.8–3.5 mm; dorsal surface of head black, with yellowish anterolateral margins of clypeus; pronotum black with sharply defined creamy-white areas at lateral margins; elytra black, with large, pale, rather sharply defined spot in posterior third of both elytra (Fig. 1); anterior margin of mentum not emarginated (Figs 8a, 9a, f); medial ridge of prosternum anteriorly forming a rounded knob (Figs 8c, 9g); mesoventral plate narrow, ca. 5.7× as long as wide (Figs 8f, 9c, h); metaventrite (Figs 8g, 9c, h) without femoral lines, with narrow raised pentagonal area, 1.1× as long as wide; first abdominal ventrite without spine-like process in both sexes (Fig. 8h); metatibia slightly bent outwards; apex of fifth abdominal ventrite without an apical triangularly bulged projection in both sexes (Fig. 8i).

By the dorsal coloration, the species of *C. gimmeli* group could be confused with *C. praetextatus* (Say), *C. floridanus* Horn and *C. sklodowskae* sp. n. However, they can be easily distinguished from from *C. praetextatus* and *C. floridanus* Horn by the distinctly

narrower mesoventral plate (compare Fig. 8f with Figs 7d and 13a) and yellow coloration of lateral part of elytra expanding to humeral area at elytral base, and from *C. sklodowskae* sp. n. by the bare median portion of mesoventrite not reaching anteriorly, bulged projection of the prosternum, metatibia slightly bent outwards, anterior margin of mentum not emarginated, and females without a triangularly bulging projection at apex of the fifth ventrite.

Distribution. The species group is endemic to Hispaniola and seems widespread on the island. No records are known from Haiti, likely due to collecting bias.

***Cercyon gimmeli* sp. n.**
http://zoobank.org/DDB83C0C-AAF4-4BE7-BD49-E86443ADD650
Figures 1a–c, 5a–d, 8a–i, 15a

DNA barcodes. GANTC002-17 to GANTC006-17

BIN ID. BOLD:ADF7790.

Figures on Flickr. www.flickr.com/photos/142655814@N07/albums/72157-671425298360

Type locality. Dominican Republic, Samaná Province, Monumento Natural Salto, El Limón 2.8 km SSW of El Limón, 19°16.56'S 69°26.47'W, 160 m a.s.l.

Type material. Holotype (male): "DOMINICAN REP.: Samaná, MN Salto El Limón 2.8 km SSW of El Limón; 19°16.56'S 69°26.47'W; 160 m; 2.ix.2014, Deler, Fikáček, Gimmel. DR29a // secondary vegetation and tiny remnants of forest among coffee plantations and pastures: in horse excrement" (NMPC) [DNA extract: MF1256.1]. **Paratypes: DOMINICAN REPUBLIC: Samaná:** same label data as the holotype (1 males, 1 female: NMPC; 1 male: BCPC; 1 male: CNC; 1 male: CNIN; 1 male: SBNM) [DNA extract: MF1256.2 in NMPC]. **La Vega:** "DOMINICAN REP.: La Vega, PN A. Bermúdez, 8 km W of Manabao, 19°4.05'N, 70°51.98'W, 1140 m, 22–26.viii.2014, Deler, Fikáček, Gimmel DR16 // montane broad-leaf forest: in cow and horse excrement" (2 males: NMPC). "DOMINICAN REPUBLIC: Pr. La Vega La Cienaga de Manabao, Park Hdqt, 3-5-VII-1999, 3000 ft, R.E. Woodruff, blacklight" (1 male: FSCA). **Monseñor Nouel:** "DOMINICAN REP.: Msñ. Nouel, PN La Humeadora; 11.6km SSW, of Piedra Blanca; 18°44.92'N, 70°21.63'W; 636 m; 8.ix.2014, Deler, Fikáček, Gimmel DR41 // in horse excrement in moist broad-leaf forest in a valley of a small stony stream" (14 males, 2 females: NMPC; 1 male: BMNH; 1 male: CMN; 2 males: MNHNSD; 1 male: NHMW; 3 males: SBNM) [DNA extracts of both females: MF1217.1, MF1217.2 in NMPC]. **Barahona:** "DOMINICAN REP.: Prov. Barahona. nr. Filipinas, Larimar Mine: 26-VI/7-VII-1992: Woodruff & Skelley, flight trap" (2 males: FSCA; 2 males: NMPC). "DOMINICAN REP.: Prov. Barahona. nr. Filipinas, Larimar Mine: 26-VI/7-VII-1992: Woodruff, Skelley, Skillman. dung trap" (10 males: FSCA; 4 males: NMPC). "DOMINICAN REP.: Prov. Barahona. nr. Filipinas, Larimar Mine: 20-VII/26-VI-1992: Woodruff & Skelley, human dung" (7 males: FSCA). "DOMINICAN REP.: Prov. Barahona. nr. Filipinas, Larimar Mine:

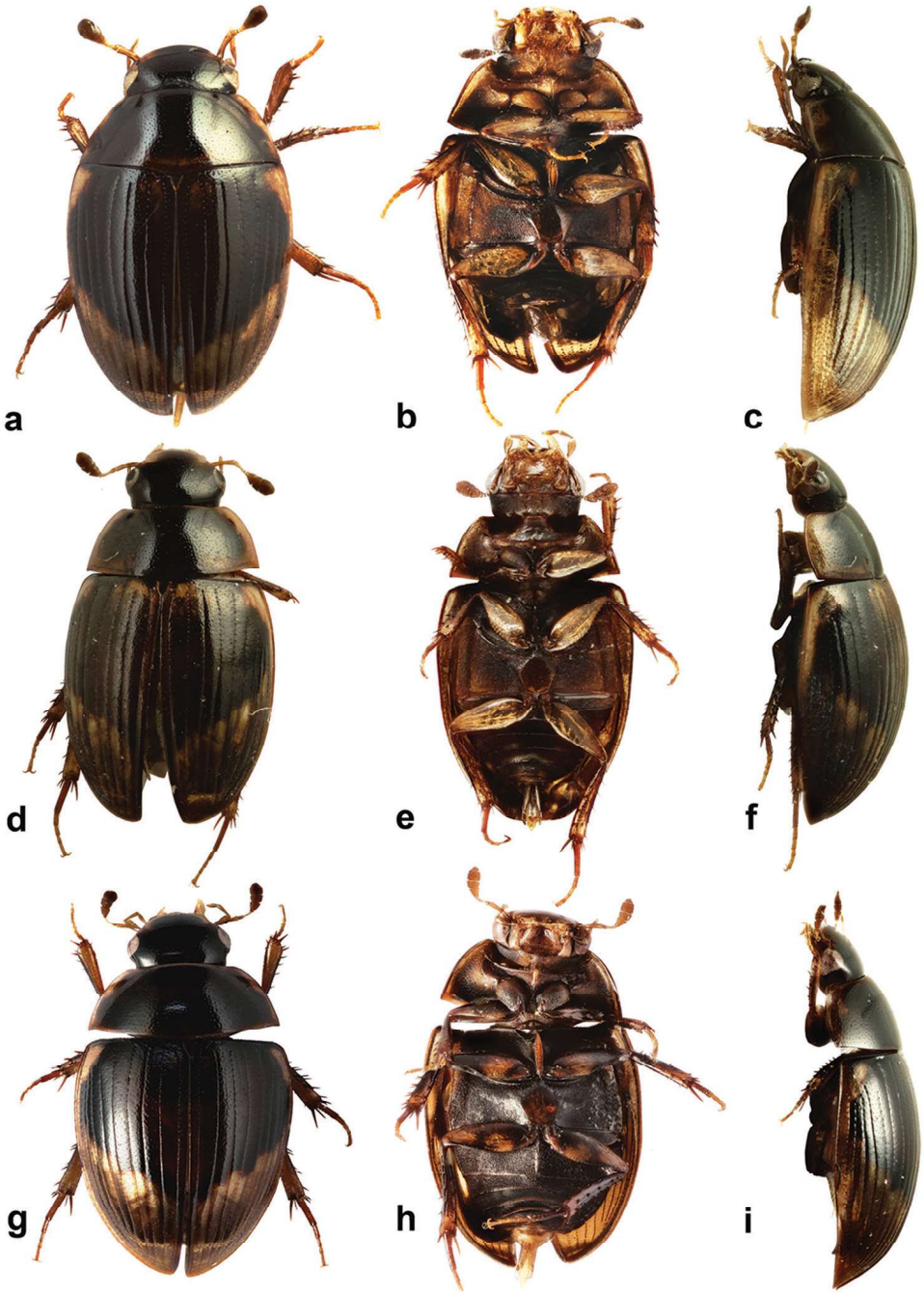

Figure 1. *Cercyon* spp. n. **a–c** *Cercyon gimmeli* sp. n. **d–f** *Cercyon armatipenis* sp. n. **g–i** *Cercyon taino* sp. n. **a, d, g** dorsal habitus **b, e, h** ventral habitus **c, f, i** lateral habitus.

26-VI/7-VII-1992: Woodruff, Skelley & Skillman, at light" (5 males: FSCA). "DOMINICAN REP.: Prov. Barahona. nr. Filipinas, Larimar Mine: 20-VII/26-VI-1992: Woodruff & Skelley, at day" (2 males: FSCA). DOMINICAN REP.: Prov. Barahona. nr. Filipinas, Larimar Mine: 20-VII/26-VI-1992: Woodruff & Skelley, at light" (5 males: FSCA). "DOMINICAN REP.: Prov. Barahona. nr. Filipinas, Larimar Mine: 26-VI/7-VII-1992: Woodruff & Skelley, rat carrion" (1 male: FSCA). "DOMINICAN REP.: Prov. Barahona. nr. Filipinas, Larimar Mine: 26-VI/7-VII-1992: Skelley, day catch, beating" (1 male: FSCA).

Diagnosis. Externally identical with other members of the *Cercyon gimmeli* species group, it may be only distinguished from them by the morphology of the aedeagus (Fig. 5a–d): parameres longer than the phallobase; median lobe without spines, narrowly parallel-sided, with rounded apex.

Description. *Body.* (Fig. 1a–c) 2.8–3.5 mm long (length of holotype: 3.25 mm); long oval, 1.8–1.9× as long as wide, widest at basal fourth of elytra; moderately convex, 3.2× as long as high, (height of holotype: 1.05 mm). *Coloration.* Dorsal surface of head black, clypeus with widely yellowish anterolateral margins. Antennae and ventral surface of head, including mouthparts, brown, antennal club dark-brown. Pronotum black, with a wide, rather sharply defined creamy-white area along lateral margins, broader at anterior half. Prosternum and hypomeron brown, gradually turning black in posterior half. Elytra dark brown to black, with large, pale, rather sharply defined apical spot covering posterior quarter of elytral interval 1, and gradually larger portion on subsequent intervals up to posterior three–quarters of interval 9; two lateralmost intervals completely pale; apical area slightly darker (yellowish brown) posteriorly, with bright yellowish stripe or spots at least along its anterior border; basal portion of elytra with a pair of pale elongated dots at sides of scutellar shield. Ventral surface of mesothorax blackish to pitchy black. Metepisternum brown. Metaventrite brown with dusk anteromedial part. Abdomen brown, ventrites sometimes with dusky marks on anterior margin. Legs yellow to brown ventrally, dorsally with black markings on femora.

Head. Clypeus with rather sparse and shallow punctation consisting of crescent-shaped setiferous punctures intermixed with denser, smaller and rather transverse non–setiferous punctures; interstices without microsculpture. Anterior margin of clypeus with a narrow bead. Frontoclypeal suture conspicuous as a zone without punctuation, vanished in middle. Frons with punctation similar to that on clypeus, punctures of same shape all over, slightly sparser on sides; interstices without microsculpture. Eyes rather small; interocular distance about 6× the width of one eye in dorsal view. Labrum membranous, nearly completely concealed under clypeus, only with narrowly exposed sinuate anterior margin. Mentum (Fig. 8a) subtrapezoid, widest at posterior fourth, about 2.1× wider than long, 1.3× wider at widest part than at anterior margin, concave in anterior half, with a shallow transverse impression anteromesally; surface glabrous, punctures rather small and shallow, almost vanishing anteromessally, interstices without microsculpture. Antenna with 9 antennomeres, scapus ca. 1.7× as long antennomeres 2–6 combined; antennal club moderately elongate, about twice as long as wide, about as 1.1× as long as scapus; antennomere 9 acuminate at apex.

Prothorax. Pronotum transverse, widest at base 2.1–2.2× wider than long; 1.8× wider at base than between anterior angles, 1.8× wider than head including eyes, as convex as elytra in lateral view. Punctation moderately dense and shallow, consisting of crescent-shaped setiferous punctures intermixed with denser, smaller and rather transverse non–setiferous punctures; punctures slightly feebler on sides. Prosternum (Fig. 8b) strongly tectiform medially, medial ridge thickened in anterior half, forming a large rounded knob in lateral view (Fig. 8c). Antennal grooves distinct, with lateral margin curved, slightly feebler anteriorly.

Pterothorax. Scutellar shield 1.1× as long as wide, sparsely punctured. Elytra widest at anterior fifth, 2.55–2.85× as long as pronotum, 1.25–1.35× as wide as pronotum; surface glabrous (Fig. 8d), with 10 series of punctures; series 6, 8 and 9 not reaching elytral base, serial punctures getting slightly larger laterally; intervals moderately convex; punctation of interval 1 and odd intervals composed of crescent-shaped setiferous punctures intermixed with denser, smaller and rather transverse non–setiferous punctures; even intervals with non-setiferous punctures only; all interstices without microsculpture. Humeral bulge indistinct. Mesoventral plate (Fig. 8f) narrowly elongate, ca. 5.7× as long as wide, widest at midlength, gradually and symmetrically narrowing posteriad and anteriad to pointed apices, posterior tip slightly overlapping over anterior portion of metaventrite; surface with few sparsely arranged coarse punctures. Metaventrite with narrow median raised pentagonal area (Fig. 8g), 1.1× as long as wide at widest portion, glabrous, weakly and sparsely punctuate, punctures with fine setae at least along margins of elevation, with bare area not reaching anterior margin; femoral lines absent; lateral parts of metaventrite densely covered by short pubescence.

Legs. Femora with sparse rather shallow punctures ventrally, interstices with weak microsculpture at bases, consisting of longitudinal lines; tibial grooves distinct. Tibiae with rather large lateral spines. Metatibiae moderately narrow and elongate, slightly bent outwards, 0.3–0.4× as long as elytra, 5.3× as long as wide. Metatarsus long, 0.9× as long as metatiba, with few short but rather stout setae ventrally.

Abdomen with five ventrites, first abdominal ventrite about as long as second and third ventrites combined, with distinct median longitudinal carina (Fig. 8h) narrowing posteriad, not projecting posteriorly in both sexes; fifth ventrite (Fig. 8i) with acuminate and very weakly bulged apex in both sexes.

Male genitalia. Median projection of sternite 9 (Fig. 5d) very narrow, shorter than lateral struts, without subapical setae. Aedeagus: Phallobase (Fig. 5a) distinctly shorter than parameres, asymmetrically narrowing basally, base widely rounded. Parameres narrow throughout, slightly widened apically, subsinuate on outer face near apex, apex pointed, with a couple of setae. Median lobe (Fig. 5b) narrow throughout, indistinctly narrowing apically; apex (Fig. 5c) rounded with finely truncate tip, gonopore moderately large, situated subapically; basal portion with dorsal plate narrow and simply bifid basally. Median projection of sternite 9 (Fig. 5a) very narrow, shorter than lateral struts, without subapical setae.

Variability. In some specimens the pale spots at sides of the scutellar shield are longer, almost reaching the second fourth of elytral length.

Etymology. We are pleased to dedicate this species to Matthew L. Gimmel (Santa Barbara Museum of Natural History), who participated in the expedition to the Dominican Republic and collected part of the type series of this species.

Distribution. Dominican Republic: Barahona, La Vega, Monseñor Nouel, Samaná (Fig. 14a).

Biology. All specimens were collected in in broad-leaf tropical forests and coffee plantations and pastures, mainly on cow and horse dung, but also on human dung, rat carrion, at black-light or at day by beating.

***Cercyon armatipenis* sp. n.**

http://zoobank.org/B937F9C3-3948-4256-8879-37EF7A6ACCBC

Figures 1d–f, 5i–l, 9a–d, 15a

DNA barcodes. GANTC013-17, GANTC014-17

BIN ID. BOLD:ADF5573

Figures on Flickr. www.flickr.com/photos/142655814@N07/albums/72157676345486243

Type locality. Dominican Republic, Independencia Province, Parque Nacional Sierra de Neiba, 11.3 km NW of La Descubierta, 18°39.81'N, 71°46.17'W, 1650 m a.s.l.

Type material. Holotype (male): "DOMINICAN R.: Independencia, PN Sierra de Neiba, 11.3 km NW of La Descubierta; 1650 m, 18°39.81'N, 71°46.17'W; 18.viii.2014, Deler, Gimmel DR13 // disturbed montane cloud forest with many ferns and mosses: in cow excrement" (NMPC). **Paratypes: DOMINICAN REPUBLIC: Independencia:** same label data as the holotype (2 males: NMPC; 1 male: BMNH; 1 male: SBNM) [DNA extractions MF1264.5, MF1264.6 in NMPC].

Diagnosis. Externally identical with other members of the *Cercyon gimmeli* species group, it may be only distinguished from them by the morphology of the aedeagus (Fig. 5i–l): parameres as long as phallobase; median lobe moderately wide basally, narrowing apicad, with spines in apical fifth, apex finely truncate.

Description. *Measurements.* (Fig. 1d–f) 3.0–3.7 mm long (length of holotype: 3.45 mm); 1.8–1.9× as long as wide, 3.2× as long as high (height of holotype: 1.15 mm).

Conforming to the description of *C. gimmeli*, with the following differences: *Pterothorax.* Punctation of even intervals consisting of small non-setiferous punctures, but here and there with infrequent crescent-shaped larger setiferous punctures; only lateralmost elytral interval completely pale.

Male genitalia. Median projection of sternite 9 (Fig. 5l) moderately wide, slightly widening apically, with few subapical setae. Phallobase (Fig. 5i) as long as parameres, asymmetrically narrowing basally, base narrowly rounded. Parameres wide basally,

gradually narrowing towards apex, sinuate on outer face near apex, apex rounded, with 3 apical and few subapical setae. Median lobe (Fig. 5j) wide basally, gradually narrowing towards apex; (Fig. 5k) apex finely truncate, with numerous backward-directed spines on dorsal and lateral surfaces; gonopore large, subapical; basal portion with dorsal plate simply bifid.

Etymology. The species name is derived from Latin words *armatus* (armed) and *penis* (penis), in reference to the diagnostic character of this species, i.e. the apex of the median lobe armed by small spines.

Distribution. Dominican Republic: Independencia (Fig. 15a).

Biology. Specimens were collected in cow dung in a cloud forest.

***Cercyon taino* sp. n.**
http://zoobank.org/7EEF52BE-5EAE-412C-AE23-DD1AB8CA8C1A
Figures 1g–i, 5e–h, 9f–i, 15b

DNA barcodes. GANTC007-17 to GANTC009-17

BIN ID. BOLD:ADF5574

Figures in Flickr. www.flickr.com/photos/142655814@N07/albums/72157-671656199632

Type locality. Dominican Republic, Samaná Province, dam 2.5 km N of Samaná, 58 m a.s.l., 19°13.70'N, 69°19.85'W.

Type material. Holotype (male): "DOMINICAN REP.: Samaná, dam 2.5 km N of Samaná, 19°13.70'N, 69°19.85'W; 58 m, 5.ix.2014, Deler, Fikáček, Gimmel DR35 // in older cow excrements dampered by recent rains at the grassy bank of a reservoir" (NMPC) [DNA extract: MF1735]. **Paratypes: DOMINICAN REPUBLIC: La Vega:** "DOMINICAN REP.: La Vega, PN Valle Nuevo, Salto Aguas Blancas; 18°50.60'N, 70°40.68'W; 1655 m; 25.viii.2014, Deler, Fikáček, Gimmel DR21 // Sifting of moist leaf litter in small remnants of montane forest in a small ravine with a spring and on slopes just above the small river" (5 males: NMPC); "DOMINICAN REP.: La Vega, PN A. Bermúdez, 10.3 km W of Manabao, 19°4.37'N, 70°53.26'W, 1270 m, 26.viii.2014, M. Fikáček lgt. (DR22) (2 males: NMPC). **Independencia:** "DOMINICAN R.: Independencia, PN Sierra de Neiba, 11.3 km NW of La Descubierta; 1650 m, 18°39.81'N, 71°46.17'W; 18.viii.2014, Deler, Gimmel DR13 // disturbed montane cloud forest with many ferns and mosses: in cow excrement" (1 male: NMPC; 1 male: BMNH; 1 male: SBNM) [DNA extract: MF 1264.1 in NMPC].

Diagnosis. Externally identical with other members of the *Cercyon gimmeli* species group, it may be only distinguished from them by the morphology of the aedeagus (Fig. 5e–g): parameres shorter than phallobase; median lobe without spines, narrowly parallel–sided, pointed at apex.

Description. *Measurements.* (Fig. 1g–i) 2.8–3.5 mm long (length of holotype: 3.35 mm); 1.8–1.9× as long as wide, 3.2× as long as high (height of holotype: 1.10 mm).

Conforming with description of *C. gimmeli*, with the following differences: *Pterothorax*. Punctation of even intervals consisting of small non-setiferous punctures, but here and there with infrequent crescent-shaped larger setiferous punctures; only lateralmost elytral interval completely pale.

Male genitalia. Median projection of sternite 9 (Fig. 5h) moderately wide, slightly widening apically, with few subapical setae. Phallobase (Fig. 5e) longer than parameres, asymmetrically narrowing basally, base widely rounded. Parameres narrow throughout, slightly narrowing towards apex, weakly sinuate on outer face near apex, apex rounded, with one apical and one subapical seta. Median lobe (Fig. 5f) narrowly parallel-sided throughout, apically narrowing into pointed apex (Fig. 5g), apex without spines, gonopore minute, subapical; basal portion with dorsal plate simply bifid.

Etymology. The new species is named after the indigenous Taíno people inhabiting the Greater Antilles including Hispaniola before and at the time of the arrival of Europeans.

Distribution. Dominican Republic (Samaná, La Vega, Independencia) (Fig. 15b).

Biology. Examined specimens and the associated larvae (see below) were collected from leaf litter of montane forests and from cow dung.

***Cercyon sklodowskae* sp. n.**
http://zoobank.org/6679B59D-E7CE-4D95-8894-12C6084607A4
Figures 2a–c, 5m–p, 10a–l, 15c

Figures in Flickr. www.flickr.com/photos/142655814@N07/albums/72157669507211493

Type locality. Jamaica, Saint Thomas Parish, Corn Puss Gap, 6.44 km N of Bath. 640 m a.s.l.

Type material. Holotype (male): "JAM., St. Thomas, Corn Puu Gap [sic!, = Corn Puss Gap], 2100', 4mi. N, Bath, 3-8.VIII.1974, S. Peck, dung" (CNC). **Paratypes: JAMAICA: St. Thomas:** same data as the holotype (1 female: CNC; 1 female: NMPC); "JAM., St. Thomas, Corn Puss Gap, 2100", 4mi. N, Bath, 3.viii.74, S. Peck, DT16-20" (1 male: CNC); "JAM., St. Thomas P. Portland Gap, 5500',17.XII.72-1.I.73, S&J Peck, cloud for., dung&carrion tr." (1 male, 1 female: CNC); "JAM., St. Thomas P., Portland Gap, 17.XII.72-1.II.73, S & J Peck (1 female: CNC); "JAM., St. Thomas, below Port. Gap, 1-5.VIII.1974, 4500", S. Peck, dung trap 12" (1 female: CNC).

Diagnosis. *Cercyon sklodowskae* sp. n. can be easily differentiated from other Greater-Antilles *Cercyon* species by the following combination of characters: body size 3.1–3.5 mm; dorsal surface of head black with yellowish anterolateral margins of clypeus; pronotum black with sharply defined yellowish areas at lateral margins (Fig. 2c); elytra (Fig. 2a) black, with large apical spot covering posterior third; medial ridge of prosternum anteriorly forming a small rounded to weakly pointed projection (Fig. 10c); mesoventral plate (Fig. 10f) narrow, ca. 5.8× as long as wide; metaventrite (Fig. 10g) without femoral lines, with narrow raised pentagonal area, 1.2× as long as wide;

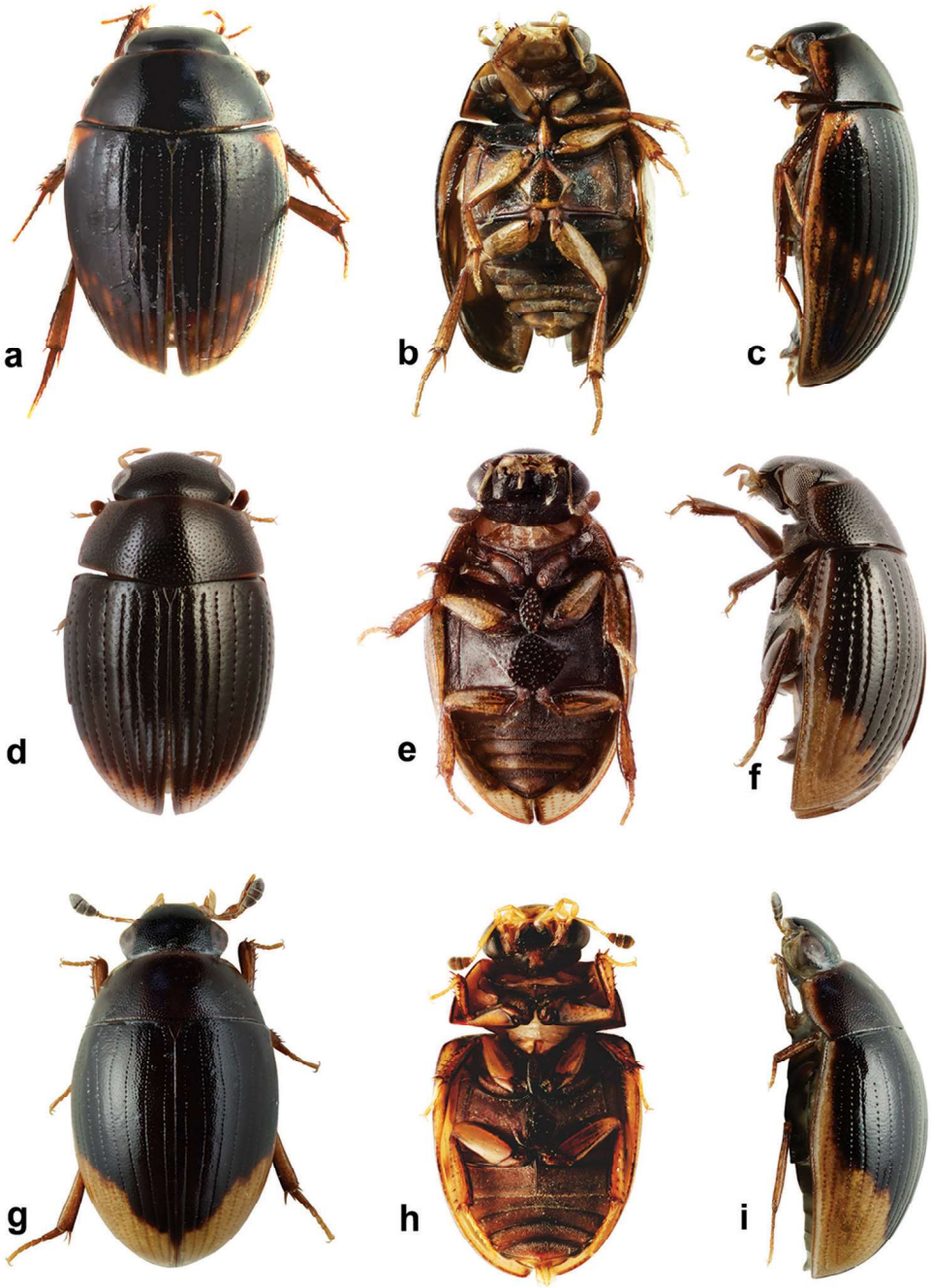

Figure 2. *Cercyon* spp. **a–c** *Cercyon sklodowskae* sp. n. **d–f** *Cercyon floridanus* Horn **g–i** *Cercyon praetextatus* Say **a, d, g** dorsal habitus **b, e, h** ventral habitus **c, f, i** lateral habitus.

first abdominal ventrite without spiniform process in both sexes (Fig. 10h); apex of fifth abdominal ventrite with a triangular projection in females (Fig. 10i); aedeagus with very short parameres (Fig. 5m), median lobe (Fig. 5o) covered with spines in apical third.

C. sklodowskae may be confused with *C. praetextatus* (Say) and *Cercyon floridanus* Horn and the members of *C. gimmeli* species group. It can be distinguished from *C. praetextatus* and *C. floridanus* by the head with widely yellowish clypeal margin and yellow coloration of elytra expanded basally (clypeus black and basal part of elytra only narrowly yellow in *C. praetextatus* and *C. floridanus*) and by much narrower mesoventral plate (5.8× as long as wide in *C. sklodowskae*, 1.9× as long as wide in *C. floridanus* and 3.3× in *C. praetextatus*). It differs from members of *C. gimmeli* group by the mesoventral plate reaching anterior part of metaventrite (not reaching anterior margin in *C. gimmeli* group), only a small rounded process of median prosternal ridge (large rounded knob in *C. gimmeli* group), straight metatibia (slightly curved outside in *C. gimmeli* group), and last abdominal ventrite in females forming a triangular projection (without projection in *C. gimmeli* group). It differs from all these species by the morphology of male genitalia; by the apically spinose median lobe it resembles *C. armatipenis*, but differs from it by parameres much shorter than phallobase.

Description. *Body.* (Fig. 2a–c) 3.10–3.45 mm long (length of holotype: 3.29 mm); long oval, 1.8–1.9× as long as wide, widest at basal fourth of elytra; moderately convex, 2.8–3.0× as long as high, (height of holotype: 1.1 mm). *Coloration*. Dorsal surface of head blackish to pitchy black, clypeus with wide rather sharply defined yellowish area along anterolateral margins, slightly broader at sides. Ventral surface of head dark brown, almost black on sides. Antennae, mentum and mouthparts dark brown. Pronotum blackish to pitchy black, with narrowly brownish lateral margins, broader at anterolateral corners (Fig. 2c). Prosternum and hypomeron black, with darker anterolateral margins. Elytron (Fig. 2a) black, with large, pale, rather sharply defined apical spot covering posterior quarter of elytral interval 1 and gradually larger portion on subsequent intervals up to posterior three–quarters on interval 9, lateralmost interval completely yellowish to dark brown; apical spot slightly darker (yellowish-brown) posteriorly, with lighter brown spots at least along its anterior border. Ventral surface of mesothorax (Fig. 2b) blackish to pitchy black. Metepisternum dark brown. Metaventrite black with darker anteromedial part and anterior margins. Abdomen black, posteromedial margins and anterolateral corners of ventrites darker. Legs dark brown.

Head. Clypeus with moderately dense and shallow punctation consisting of crescent-shaped punctures intermixed with denser, slightly smaller and rather transverse punctures; interstices without microsculpture. Anterior margin of clypeus with a narrow bead. Frontoclypeal suture conspicuous as a zone without punctation, vanishing mesally. Frons with punctation similar to that on clypeus, punctures sparser on sides;

interstices without microsculpture. Eyes rather small; interocular distance about 6× the width of one eye in dorsal view. Labrum membranous, nearly completely concealed under clypeus, only with narrowly exposed sinuate anterior margin. Mentum (Fig. 10a) subtrapezoid, widest at posterior fourth, about 2.1× wider than long, 1.4× wider at widest part than at anterior margin, concave in anterior half, strongly emarginated anteromesally; surface glabrous, punctures rather small, shallow and sparse, almost vanishing anteromesally, interstices without microsculpture. Antenna with 9 antennomeres, scapus ca. 1.9× as long antennomeres 2–6 combined; antennal club moderately elongate, about twice as long as wide, about as 1.2× as long as scapus; antennomere 9 acuminate at apex.

Prothorax. Pronotum transverse, widest at base 2.1–2.2× wider than long; 1.6–1.7× wider at base than between front angles, 1.7× wider than head including eyes, as convex as the elytra in lateral view. Punctation (Fig. 10b) moderately dense and shallow, consisting of crescent-shaped punctures intermixed with denser, slightly smaller and rather transverse punctures; punctures slightly feebler on sides. Prosternum strongly tectiform medially, medial ridge (Fig. 10c) weakly thickened anteriad, forming a small rounded to slightly pointed process. Antennal grooves distinct, with lateral margin curved, slightly feebler anteriad.

Pterothorax. Scutellar shield 1.25× as long as wide, sparsely punctured. Elytra widest at anterior fifth, 2.7–3.0× as long as pronotum, 1.2× as wide as pronotum, surface (Fig. 10d) glabrous, with 10 series of punctures; series 6, 8 and 9 not reaching elytral base, serial punctures of same size in all series; intervals moderately convex; interval punctation composed by crescent-shaped punctures intermixed with denser, slightly smaller and rather transverse punctures in all intervals. Humeral bulge indistinct. Mesoventral plate (Fig. 10f) narrowly elongate, ca. 5.8× as long as wide, widest in anterior two-fifths, more strongly narrowing towards anterior apex which is pointed, posterior tip rounded, slightly overlapping over anterior portion of metaventrite; surface with a few sparse coarse punctures. Metaventrite (Fig. 10g) with narrow raised pentagonal area, 1.2× longer than wide, glabrous, weakly and sparsely punctuate, punctures with fine setae at least along margins of the elevation; bare elevated area reaching anterior margin of metaventrite; punctures absent at two slightly elongate areas in the center; femoral lines absent; lateral parts of metaventrite densely covered by short pubescence.

Legs. Femora with sparse rather shallow punctures ventrally, interstices with weak microsculpture consisting of longitudinal lines; tibial grooves distinct. Tibiae with rather small lateral spines. Metatibiae moderately narrow and elongate, straight, 0.3–0.4× as long as elytra, 5.3× as long as wide. Metatarsus long, 0.9× as long as metatibia, with short rather stout setae ventrally.

Abdomen. With five ventrites, first abdominal ventrite (Fig. 10h) about as long as the second and third ventrites combined, with distinct median longitudinal carina narrowing posteriad, not projecting posteriorly in both sexes; fifth ventrite with acuminate apex, weakly bulged in males and with a triangularly bulged apical projection in females (Fig. 10i).

Genitalia. Sternite 9 (Fig. 5p) asymmetrical basally, median process narrow, ca. as long as lateral struts, acuminate at apex, without subapical setae. Phallobase (Fig. 5m) almost twice as long as parameres, asymmetrically narrowing at base, base narrowly rounded and hooked. Parameres continuously narrowing apically, apex pointed, with two minute setae. Median lobe (Fig. 5n) widest in apical third, slightly narrowing towards base, continuously narrowing in apical third; apex (Fig. 5o) acuminate with rounded tip, apical part with numerous spines directed backwards; gonopore moderately large, subapical; basal portion with dorsal plate narrow and simply bifid basally.

Etymology. We dedicate this species to the eminent physicist and chemist Marie Skłodowska-Curie, on whose honor the Marie Skłodowska-Curie actions program of the European Union, funding this research, is named.

Distribution. Jamaica: Saint Thomas (Fig. 15b).

Biology. The specimens were collected on dung and using dung and carrion-baited traps in cloud forests.

Cercyon floridanus Horn, 1890

Figures 2d–f, 7a–d, 16a

Cercyon floridanus Horn, 1890: 303.
Cercyon floridanuus Smetana (Thomas et al. 2013: 33 *lapsus calami*)

Figures in Flickr. www.flickr.com/photos/142655814@N07/albums/72157676249-653654

Type locality. Florida (without specific locality).

Greater Antillean specimens studied. CAYMAN ISLANDS: Grand Cayman: blacklight trap, vi.1992, leg. blacklight trap (1 male; FSCA), blacklight trap, vi.1992, lgt. P. Fitzgerald (1: FSCA); Queen Elizabeth Botanic Garden, blacklight trap, 28.v.2009, leg. Thomas, Turnbow & Ball (1: FSCA); Georgetown, blacklight, 30.iii.1973. E.J. Gerberg (1: FSCA).

Published Greater Antillean records. GRAND CAYMAN: 3 km W Colliers, 19°21'N, 81°07'W (Thomas et al. 2013).

Diagnosis. Body size 2.35–2.70 mm; dorsal surface of head (Fig. 2d) completely black, pronotum black sometimes with undefined piceous areas at lateral margins; elytra black (Figs 2d, f), with large rather sharply-defined yellowish to reddish-yellow lateroapical areas reaching apex lateralmost interval, medial ridge of prosternum anteriorly very weakly projected ventrally; mesoventral plate (Fig. 7d) very wide, ca. 1.9× as long as wide; metaventrite (Fig. 7d) without femoral lines, with broad raised pentagonal area (about 0.67× as long as wide) with large, deep and semicircular punctures; first abdominal ventrite without spiniform process in both sexes; apex of fifth ventrite without triangularly bulged projection at apex in both sexes; aedeagus (Fig. 7a) with parameres slightly shorter than phallobase, sinuately widened and bearing long setae at

apex; median lobe widest at midlegth, narrowing to very finely truncate apex, without spines. For complete description see Smetana (1978).

Cercyon floridanus is part of the *C. tristis* group according to Smetana (1978) It resembles members of the *C. gimmeli* species group, *C. sklodowskae* sp. n. and *C. praetextatus.* Besides of the features of the aedeagus (Fig. 7a–c), it can be easily distinguished from them by the distinctly by the smallersize (2.35–2.70 mm), wider mesoventral plate (1.9× as long as wide in *C. floridanus*, 3.3–5.8× as long as wide in the other species). Besides that, females of *C. floridanus* lack the triangular projection on the apex of the fifth abdominal ventrite (present in *C. sklodowskae*), has a very small process of mid-prosternal ridge (large in *C. gimmeli* species group), and almost straight metatibia (curved in *C. gimmeli* species group).

Distribution. *Cercyon floridanus* is distributed in the southeastern USA, mainly in Florida, but rare records are also known from Georgia, Louisiana and Mississippi (Smetana 1978). In the Greater Antilles it is only known from Cayman Islands, from where it was first reported by Thomas et al. (2013) under the name "*C. floridanuus* Smetana" (Fig. 16a).

***Cercyon praetextatus* (Say, 1825)**
Figures 2g–i, 6a–d, 13a–b, 15c

Sphaeridium praetextatum Say, 1825: 190.
Cercyon praetextatum (Say): Melsheimer, 1853: 37.
For complete synonymy see Smetana (1978: 84) and Hansen (1999: 286).

Figures in Flickr. www.flickr.com/photos/142655814@N07/albums/72157669492-876764

Type locality. USA, "Cambridge" (based on neotype designated by Smetana 1978).

Greater Antillean specimens studied. CUBA: Santiago de Cuba: Dos Caminos, farm field, MV lights, 20.18043°N, 75.77806°W, 165 m, 23.iii.2013, leg. A. Smith & A. Deler-Hernández (1 spec.: NMPC). **Cienfuegos**: Cumanayagua municipality, JBC [= Jardín Botánico de Cienfuegos], Soledad, 22°7'18.44"N, 80°19'35.26"W, 3.x.2012, leg. A. Deler-Hernández (1 spec.: NMPC). **CAYMAN ISLANDS: Grand Cayman:** black-light trap, 17.v.1992, leg. P. Fitzgerald (1 spec.: FSCA). **DOMINICAN REPUBLIC: La Vega Prov.:** Jarabacoa, 440 m a.s.l., riverside, UV light, 24.vii.-2.viii.1995, leg. S. & J. Peck (3 spec.: CMN). La Ciénega de Manabao, Park Headquarters, 915 m a.s.l. black-light, 3-5.vii.1999, leg. R.E. Woodruff (1 spec.: FSCA).

Published Greater Antillean records. CUBA: Habana Province: Laguna de Ariguanabo (Spangler 1981). **JAMAICA:** without precise locality (Smetana 1978).

Diagnosis. Body size 2.7–4.1 mm; dorsal surface of head (Fig. 2g) black, with a pair of small reddish-brown spots on vertex, sometimes fused to one spot; pronotum black with sharply defined yellowish to reddish areas at anterolateral corners, some-

times extending to complete lateral margins; elytra black, with large sharply-defined yellowish to reddish-yellow lateroapical area reaching about apical fourth, laterally reaching elytral base in lateralmost interval, yellow spot not extended to humeral area basally; medial ridge of prosternum anteriorly forming a small rounded to slightly pointed process; mesoventral plate (Fig. 13a) wide, ca. 3.3× as long as wide; metaventrite (Fig. 13b) without femoral lines, with narrow raised pentagonal area (ca. as long as wide); first abdominal ventrite without spiniform process in both sexes; apex of fifth ventrite without triangularly bulged projection at apex in both sexes; aedeagus (Fig. 6a–c) with parameres almost twice as long as phallobase, sinuately widened and bearing long setae at apex; median lobe widest at midlegth, narrowing to pointed apex, without spines. For complete description see Smetana (1978).

This species was assigned to the *C. marinus* group according to Smetana (1978). By the coloration of pronotum and elytra (Fig. 2g, i), *C. praetextatus* may be confused with members of the *C. gimmeli* species group and with *C. sklodowskae* sp. n. Besides of the features of the aedeagus (Fig. 6a–c), it can be easily distinguished from them by the distinctly wider mesoventral plate (3.3× as long as wide in *C. praetextatus*, 5.7–5.8× as long as wide in the other species) and the yellow stripe along lateral margin of elytra not expanding basally. Besides of that, females of *C. praetextatus* lack the triangular projection on the apex of the fifth abdominal ventrite (present in *C. sklodowskae*), has a very small process of mid-prosternal ridge (large in *C. gimmeli* species group), and almost straight metatibia (curved in *C. gimmeli* species group).

Distribution. *Cercyon praetextatus* is widely distributed in North America (southern Canada, USA, Mexico; Smetana 1978; Ryndevich 2004) and reaches to Central America (Guatemala, Costa Rica; Smetana 1978) and to the Caribbean (Cayman Islands, Cuba, Dominican Republic, Jamaica, Smetana 1978, Spangler 1981, this paper); it has also been introduced to Argentina (Fikáček 2009). We report it here from Dominican Republic (La Vega Province) and the Cayman Islands for the first time (Fig. 15c).

Biology. This species seems to prefer wet environments, living primarily on many kind of organic debris, like decomposing plant remnants, carrion and dung (Smetana 1978). In Cuba and the Dominican Republic this species has been attracted to light.

***Cercyon spiniventris* sp. n.**
http://zoobank.org/B172C05C-D9C0-4863-AF24-EB754A45BFC6
Figures 3a–c, 6e–h, 11a–i, 16a

DNA barcode. GANTC010-17

BIN ID. BOLD:ADF5572

Figures in Flickr: www.flickr.com/photos/142655814@N07/albums/7215767-1689463811

Type locality. Dominican Republic, Monseñor Nouel Province, Parque Nacional La Humeadora; 11.6 km SSW of Piedra Blanca, 636 m a.s.l., 18°44.92'N, 70°21.63'W.

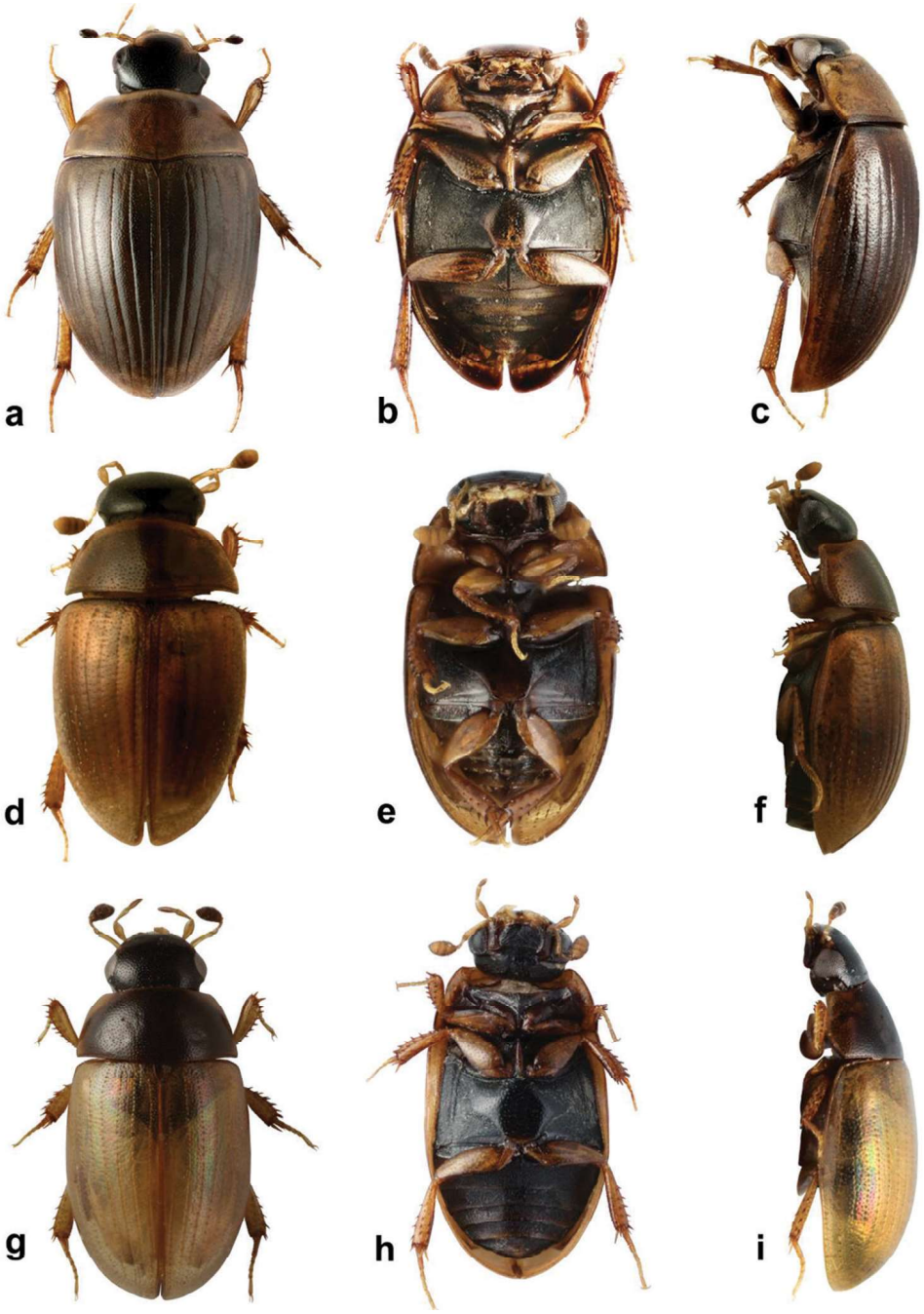

Figure 3. *Cercyon* spp. **a–c** *Cercyon spiniventris* sp. n. **d–f** *Cercyon nigriceps* Marsham **g–i** *Cercyon quisquilius* Linnaeus **a, d, g** dorsal habitus **b, e, h** ventral habitus **c, f, i** lateral habitus.

Type material. Holotype (male): "DOMINICAN REP.: Msñ. Nouel, PN La Humeadora; 11.6km SSW, of Piedra Blanca; 18°44.92'N, 70°21.63'W; 636 m; 8.ix.2014, Deler, Fikáček, Gimmel DR41 // in horse excrement in moist broad-leaf forest in a valley of a small stony stream" (NMPC) [DNA extract: MF1216.1]. **Paratypes**: **DOMINICAN REPUBLIC: Barahona:** "DOMINICAN REP.: Prov. Barahona. nr. Filipinas, Larimar Mine: 26-VI/7-VII-1992: Woodruff, Skelley, Skillman. dung trap (1 males: FSCA). "DOMINICAN REP.: Prov. Barahona. nr. Filipinas, Larimar Mine: 26-VI/7-VII-1992: Woodruff & Skelley, rat carrion" (2 females: FSCA). **Monseñor Nouel:** same data as the holotype (7 males, 3 females, 12 spec.: NMPC; 2 males: BCPC; 2 males: BMNH; 2 males: CNC; 3 males: CNIN; 3 males: NHMW; 4 males, 1 female: SBNM; 3 males: SBP; 2 ZMUC). **Duarte:** "DOMINICAN REP.: Duarte. 9.1 km SW of El Factor, slope above La Factoria; 19°15.30'N, 69°56.52'W; 255 m; 4.ix.2014. Deler, Fikáček, Gimmel DR32 // area with cocoa plantations and small remnants of forests at very steep slopes: in horse excrement" (2 males: NMPC). **Independencia:** "DOMINICAN R.: Independencia, PN Sierra de Neiba, 11.3 km NW of La Descubierta; 1650 m, 18°39.81'N, 71°46.17'W; 18.viii.2014, Deler,Gimmel DR13 // disturbed montane cloud forest with many ferns and mosses: in cow excrement" (2 males, 4 females, 1 spec.: NMPC). **La Vega:** "DOMINICAN REP.: La Vega, PN A. Bermúdez, 8 km W of Manabao, 19°4.05'N, 70°51.98'W, 1140 m, 22-26. viii.2014, Deler, Fikáček, Gimmel DR16 // montane broad-leaf forest: in cow and horse excrement" (12 males, 15 females: NMPC; 1 male: BMNH; 1 male: CNIN; 2 males: FSCA; 1 male: MNHNSD; 3 males, 2 females: SBNM) [DNA extraction of one male: MF1753 in NMPC]; "DOM. REP; La Vega Prov., 10km NE Jarabacoa, Hotel Montana, forest, 18.VII-4.VIII.95, 550m, FIT, S.+J. Peck, 95-30" (2 females: CMN); "DOM. REP; La Vega Prov., PN. A. Bermudez, Cienaga, 19.VII-2.VIII.95, 1000m, trop.evgrn.for., FIT, S.+J. Peck, 95-32" (2 females: CMN); "DOM. REP; La Vega Prov., PN. A. Bermudez, Cienaga, 19.VII-2.VIII.95, 1020m, trop.evgrn.for., FIT, S.+J. Peck, 95-34" (1 male: CMN); "DOM. REP; La Vega Prov., PN. A. Bermudez, Cienaga, 21.-24.VII.95, 1000m, for. carrion trap, S.+J. Peck, 95-38" (1 female: CMN). **Samaná:** "DOMINICAN REP.: Samaná, MN Salto El Limón 2.8 km SSW of El Limón; 19°16.56'S 69°26.47'W; 160 m; 2.ix.2014, Deler, Fikáček, Gimmel. DR29a // secondary vegetation and tiny remnants of forest among coffee plantations and pastures: in horse excrement" (3 males, 3 females: NMPC).

Diagnosis. Body size 3.4–4.1 mm; dorsal surface of head black with yellowish anterolateral margins of clypeus (Fig. 3a); pronotum homogeneously light brown, elytra greyish-brown; medial ridge of prosternum anteriorly with a small rounded process (Fig. 11c); mesoventral plate narrow, ca. 5.9× as long as wide; metaventrite (Fig. 11f) without femoral lines; raised pentagonal area of metaventrite moderately wide, 0.9× as long as wide; first abdominal ventrite with an spiniform process in females (Fig. 11h), without process in males; apex of fifth abdominal ventrite without apical triangular projection in both sexes (Fig. 11i); aedeagus with parameres about as long as phallobase (Fig. 6e), median lobe narrowly parallel-sided, acute at apex, without spines.

Cercyon spiniventris somewhat resembles *C. nigriceps* by the dorsal coloration pattern (predominantly black head and rather homogeneously brown pronotum and elytra); it can be easily distinguished from *C. nigriceps* by much larger body size (3.4–4.1 mm in *C. spiniventris*, 1.0–2.1 mm in *C. nigriceps*) and by the lack of femoral lines on the metaventrite (present in *C. nigriceps*). *Cercyon spiniventris* is unique among Caribbean *Cercyon* species by a presence of a long spiniform process in the first abdominal ventrite of females.

Description. *Body* (Fig. 3a–c). 3.4–4.0 mm long (length of holotype: 3.5 mm); moderately short-oval, 1.8–1.9× as long as wide, widest at basal fourth of elytra; moderately convex, 2.9–3.0× as long as high (height of holotype: 1.15 mm). *Coloration.* Dorsal surface of head blackish to pitchy black, clypeus with wide rather sharply defined yellowish area along anterolateral margins, broader at sides. Antennae and ventral surface of head black, mentum with posterior half yellowish brown, mouthparts and antenna yellowish brown, antennal club dark-brown. Pronotum light brown. Prosternum yellowish-brown with posterior half black, hypomeron brown with large black marks on posterior third, and close to the yellowish-brown lateral margins. Elytra dark greyish-brown, with lateral and anterior margins, apex and epipleura slightly paler. Ventral surface of mesothorax blackish to pitch-black, with procoxal rests and mesoventral plate brown. Metepisternum black. Metaventrite black with paler raised anteromedial part. Abdomen black, posteromedial margins and anterolateral corners of ventrites brownish. Legs brown, femora dorsally black.

Head. Clypeus with dense and moderately deep punctation consisting of crescent-shaped setiferous punctures intermixed with denser, smaller and rather transverse non-setiferous punctures; interstices without microsculpture. Anterior margin of clypeus with a narrow bead. Frontoclypeal suture conspicuous as a zone without punctuation, vanished mesally. Frons with punctation similar to that on clypeus, punctures of same shape all over; interstices without microsculpture. Eyes rather small; interocular distance about 5.4× the width of one eye in dorsal view. Labrum membranous, nearly completely concealed under clypeus, only with narrowly exposed sinuate anterior margin. Mentum (Fig. 11a) subtrapezoid, widest at posterior fourth, about 2× wider than long, 1.5× wider at widest part than at anterior margin, weakly concave in anterior half; surface glabrous, punctures large and deep, becoming coarser anteromesally, interstices on anterior half with transverse depressions near each puncture. Antenna with 9 antennomeres, scapus ca. 1.8× as long as antennomeres 2–6 combined; antennal club moderately elongate, about twice as long as wide, about as 1.2× as long as scapus; antennomere 9 acuminate at apex.

Prothorax. Pronotum transverse, widest at base 2.1–2.3× wider than long; 1.7× wider at base than between anterior angles, 1.8× wider than head including eyes, as convex as elytra in lateral view. Punctation rather dense and moderately deep, consisting of crescent-shaped setiferous punctures intermixed with denser, smaller and rather transverse non-setiferous punctures; punctures slightly feebler on sides. Prosternum (Fig. 11b–c) strongly tectiform medially, medial ridge very weakly thickened ante-

riad, forming a small rounded process. Antennal grooves distinct, with lateral margin curved, feebler anteriad.

Pterothorax. Scutellar shield about as long as wide, moderately densely punctured. Elytra widest at anterior fifth, 2.7–2.9× as long as pronotum, 1.1–1.2× as wide as pronotum, surface (Fig. 10d) glabrous, with 10 series of punctures; series 6, 8 and 9 not reaching elytral base, serial punctures of same size in all series; intervals moderately convex; interval punctation composed of crescent-shaped setiferous punctures intermixed with denser, smaller and rather tranverse non-setiferous punctures; setiferous punctures present on all intervals; interstices without microsculpture. Humeral bulge indistinct. Mesoventral plate (Fig. 11f) narrowly elongate, ca. 5.9× as long as wide, widest at midlength, gradually and symmetrically narrowing to pointed apices, posterior tip slightly overlapping over anterior part of metaventrite; surface with coarse punctures. Metaventrite (Fig. 11g) without femoral lines, raised pentagonal area wide, 0.8× as long as wide at widest portion, glabrous, rather weakly and sparsely punctate, punctures with fine setae at least along margins of elevation, punctures absent at two slightly elongate areas in the center, bare area not reaching anterior margin of metaventrite mesally; lateral parts of metaventrite densely covered by short pubescence.

Legs. Femora with sparse rather shallow punctures ventrally, interstices with weak granulose microsculpture; tibial grooves distinct. Tibiae with moderately large lateral spines. Metatibiae moderately narrow and elongate, slightly bent outwards, 0.4× as long as elytra, 6.0× as long as wide. Metatarsus moderately long, 0.7–0.8× as long as metatibia, with short rather stout setae ventrally.

Abdomen with five ventrites, first abdominal ventrite longer than second and third ventrites combined, with long setae in medial third, median longitudinal carina present, slightly narrowing posteriad, not projecting posteriorly in males, projecting posteriad as a short spine in females (Fig. 11h); ventrite 5 with acuminate apex in both sexes.

Genitalia. Median projection of sternite 9 (Fig. 6h) rounded apically, without subapical setae, median portion narrowing posteriorly, shorter than lateral struts. Phallobase (Fig. 6e) about as long as parameres, asymmetrically narrowing basally, base acuminate and slightly hooked. Parameres weakly narrowing apically, subsinuate near apex, apex pointed apically. Median lobe (Fig. 6f) narrow, parallel-sided throughout, apex acuminate, gonopore moderately large, situated subapically; basal portion with dorsal horseshoe-shaped plate, base bifid. throughout, apex acuminate, gonopore moderately large, situated subapically; basal portion with dorsal horseshoe-shaped plate, base bifid.

Etymology. The name of this species is derived from Latin words *spina* (spine) and *venter* (underside), in reference to the spine-like process on the first abdominal ventrite of females.

Distribution. Dominican Republic: Duarte, Independencia, La Vega, Monseñor Nouel, Samaná (Fig. 16a).

Bionomics. Most of the specimens were collected in cow and horse dung in tropical forest and surrounding pastures.

***Cercyon nigriceps* (Marsham, 1802)**
Figures 3d–f, 6i–k, 13c–d

Dermestes nigriceps Marsham, 1802: 72.
Cercyon nigriceps Stephens (1829: 151).
= *Dermestes atricapillus* Marsham, 1802: 72 (synonymized by Gemminger and Harold 1868: 498; precedence of *C. nigriceps* over *C. atricapillus* determined by Stephens 1939: 97, see also Hansen 1999: 284).
= *Sphaeridium centrimaculatum* Sturm, 1807: 23 (synonymized by Gemminger and Harold 1868: 498).
= *Cercyon striatus* Sharp, 1882: 108 (synonymized by Fikáček 2009: 354).
= *Cercyon panamensis* Hansen, 1999: 286 (replacement name of *C. striatus* Sharp; synonymized by Fikáček 2009: 354).
For complete synonymy see Smetana (1978) and Hansen (1999).

DNA barcode. GANTC015-17
BIN ID. BOLD:AAO0116
Figures in Flick. www.flickr.com/photos/142655814@N07/albums/72157671-425572500
Type locality. "Britannia" [= Great Britain, without specified locality].
Specimens examined. CAYMAN ISLANDS: Cayman Brac: black-light trap, 06.vi.2008, lgt. R.H. Turnbow & B.K. Dozier (3 spec.: FSCA); Agricultural Exp. Sta. S. Of Songbird Dr., black-light trap, 04.vii.2013, leg. M.C. Thomas (3 spec.: FSCA); **CUBA: Cienfuegos:** Cumanayagua municipality, 22°7'18.44"N, 80°19'35.26"W, 722 m, 21.v.2013 (1 spec.: NMPC). **Guantánamo:** El Yunque, 0.5-1.0 km W of Campismo Popular, 20°20.1'N, 74°33.6'W, 40–50 m. 10.vi.2012, leg. Deler-Hernández & Fikáček (MF01) (8 spec.: NMPC). **Holguín:** Mayarí municipality, Feltón, 20°43'7.92"N, 75°37'59.19"W, 23.iii.2013, leg. Deler-Hernández (28: NMPC). **Santiago de Cuba:** El Vivero, 1.6 km E of Dos Caminos, 20°10.8'N, 75°46.4'W, 150 m, 20-21.vi.2012, leg. Deler-Hernández & Fikáček (MF18) (54 spec.: NMPC) [DNA extract: MF604]; San Luis Municipality, Dos Caminos, 20°10'57.82"N, 75°46'40.84"W, leg. Deler-Hernández (16 spec.: NMPC). **Artemisa:** Cañon de Santa Cruz, Río de Santa Cruz, 22°45'1.29"N 83°08'56.36"W, 199 m a.s.l., 16.vii.2016, leg. A. Deler-Hernández (8 spec.: NMPC) [DNA extraction: MF1750]. **DOMINICAN REPUBLIC: Samaná:** Samaná, dam 2.5 km N of Samaná, in older cow excrements dampered by recent rains at the grassy bank of a reservoir, 19°13.70'N, 69°19.85'W, 58 m a.s.l., 5.ix.2014, leg. Deler, Fikáček & Gimmel (DR35) (3 spec.: NMPC); MN Salto El Limón 2.8 km SSW of El Limón, secondary vegetation and tiny remnants of forests among coffee plantations and pastures, cow excrements, 19°16.56'N, 69°26.47'W, 2.ix.2014, leg. Deler-Hernández, Fikáček & Gimmel (DR29a) (1 spec.: NMPC). **La Altagracia:** Nisibon, Black-light trap, 03.v.1978, lgt. R.E. Woodruff & G.B. Fairchild (2 spec.: FSCA); **La Vega:** 7.0 km W of Manabao, side of a stony stream in a valley with scattered houses and plantations surrounded by montane forest, in cow excrement, 19°04.56'N, 70°51.46'W, 1185 m

a.s.l., 23.viii.2014, leg. Deler-Hernández, Fikáček & Gimmel (1 spec.: NMPC). **Monseñor Nouel:** PN La Humeadora; 11.6 km SSW, of Piedra Blanca, in horse excrement in moist broad-leaf forest in a valley of a small stony stream, 18°44.92'N, 70°21.63'W, 636 m a.s.l., 8.ix.2014, leg. Deler, Fikáček & Gimmel (DR41) (2 spec.: NMPC). **Monte Cristi:** 8.2 km. N Villa Elisa, 01.vi.1994, leg. R. Turnbow (1 spec.: FSCA). **San Pedro de Macoris:** Juan Dolio, at light, 10.-18.xii.2005, leg. Fencl (15 spec.: NMPC). **HAITI: Artibonite:** Montrouis, black-light trap, 05.vii.1977, leg. J.H. Frank (2 spec.: FSCA). **PUERTO RICO: Naguabo:** El Yunque National Forest (southern part), 3.45 km N of Río Blanco at road PR191, in horse excrements on exposed small pasture on the slope of El Yunque massive, 18°14.8'N, 65°47.9'W, 170 m a.s.l., 24.vi.2016, leg. Deler-Hernández, Fikáček & Seidel (PR2a) (17 spec. NMPC) [DNA extraction of one specimen: MF1732]; El Yunque National Forest (southern part), 4.9 km N iof Río Blanco, margin of the rainforest in an area with many flowering *Etlingera elatior* plants, FIT, 18°15.8'N, 65°47.3'W, 495 m a.s.l., 24.vi.-2.vii.2016, leg. Fikáček & Seidel (PR11)(1 spec.: NMPC). **Arecibo:** small settlement in Bosque Estatal Río Abajo, small settlement in the middle of the lowland forest, horse excrement, 18°19.7'N, 66°42.1'W, 340 m a.s.l., 27.vi.2016, leg. Deler-Hernández, Fikáček & Seidel (PR15) (13 spec.: NMPC). **Cabo Rojo:** Boquerón, black light, 18°13.11'N, 67°10.96'W, 5-6.x.2011, leg. A. Segarra (7 spec.: UPRM). **Rio Grande:** El Verde Biological Station, at light, 26.v.1994, leg. R. Turnbow (2 spec.: FSCA). **Lesser Antilles: ANTIGUA:** Christian valley, blacklight trap, 19.viii.1991, leg. FAO insect survey (1 spec.: SBP); same locality and collector, 26.vii.1991 (1 spec.: SBP); same locality and collector, 29.x.1991 (3 spec.: SBP); same locality and collector, 14.-15.ix.1991 (1 spec.: SBP). **GRENADA:** St. Andrew, Mirabeu Agriculture Lab, light trap, 9.iv.1990, leg. J. Telesford (1 spec.: SBP). **SAINT LUCIA:** Vieux Fort, horse dung sifting, 13°43.9'N 60°53.9'W, 3 m a.s.l., 12.vii.2007, S & J. Peck (07-60) (2 spec.: SBP); Mon Repos, Fox Grove lnn, UV light, 13°51.8'N, 60°54.4'W, 90 m a.s.l., 8.-18.vii.2007, leg. S. & J. Peck (07-50) (1 spec.: SBP). Soufriere, Rechette Pt. 11.VII.1980, leg. L.S. Mahunka (59 spec.: HNHM). **SAINT VINCENT & THE GRENADINES: St. Vincent:** Emerald Valley Hotel E of Layou, horse dung, 13°12.0'N, 61°14.8'W, 20 m a.s.l., 24.viii.2006, S. & J. Peck (06-120) (3 spec.: SBP); same locality, UV light at forest edge, 27.-29.viii.2006, leg. S. & J. Peck (06-123) (1 spec.: SBP). **Union Island:** Chatham Bay, Water Rock Reserve, UV traps in tall forest, 12°36.18'N, 61°26.59'W, 125 m a.s.l.,16.viii.2009, leg. S. Peck (09-64) (2 spec.: SBP); Campbell Miss Irene Reserve, high canopy thorn forest, 12°35.44'N, 61°27.34'W, 85 m a.s.l., 18.viii.2009, leg. S. Peck (09-66) (1 spec.: SBP).

Published records from the Caribbean. CUBA: Matanzas: Cárdenas (as *C. centrimaculatum*, Gundlach 1891); without precise locality (as *C. centrimaculatum*, de la Sagra 1857). **JAMAICA:** without precise locality (Leng and Mutchler 1917). **Trelawny:** Good Hope; Duncans (Fikáček 2009). **DOMINICAN REPUBLIC: Pedernales**: 4 km W of Oviedo (Fikáček 2009). **GUADELOUPE:** without precise locality (Leng and Mutchler 1914); Peck et al. 2014). **MONTSERRAT:** without precise locality (Peck et al. 2014).

Diagnosis. Body size 1.0–2.1 mm; dorsal surface of head black; pronotum (Fig. 3d) reddish brown, rarely with a vaguely darker central area; elytra uniformly reddish-

brown, rarely with a vaguely darker central area; mesoventral plate (Fig. 13c) narrow, ca. 6× as long as wide; metaventrite (Fig. 13d) with complete femoral lines; first abdominal ventrite without spiniform process of both sexes; apex of fifth ventrite without a triangularly bulged projection in both sexes; aedeagus with parameres twice as long as phallobase (Fig. 6i), median lobe (Fig. 6j) continuously acuminate, with long narrowly acute apex, without spines.

This species was assigned to *C. nigriceps* group (= *C. atricapillus* group) by Smetana (1978). *Cercyon nigriceps* can be distinguished from other species in the region by its small size and the presence of complete femoral lines on the metaventrite. It may be confused with representatives of the genus *Oosternum* by the small body size and coloration, but differs from them by presence of femoral lines (absent in *Oosternum*), absence of anterolateral ridge on mesoventrite (present in all *Oosternum*) and by very narrow mesoventral plate (1.7–2.8× as long as wide in *Oosternum*, see Deler-Hernández et al. 2014).

Distribution. This is an adventive species currently distributed in all zoogeographical regions. In Greater Antilles widespread in all islands: Cayman Islands, Cuba (Artemisa, Cienfuegos, Guantánamo, Holguín, Matanzas, Santiago de Cuba; Gundlach 1891), Dominican Republic (La Altagracias, La Vega, Monte Cristi, Samaná, San Pedro de Macoris; this paper), Haiti (Artibonite, this paper), Jamaica (Trelawny; Fikáček 2009) and Puerto Rico (Naguabo, Arecibo, Cabo Rojo). It is also widespread in the Lesser Antilles (Antigua, Grenada, Saint Lucia, Saint Vincent and the Grenadines; this paper) (Fig. 16b). Based on the record by de la Sagra (1857), the species was introduced to the Greater Antilles no later than the first half of the 19th century.

Biology. A terrestrial species collected in cow and horse dung and in decaying plant matter (e.g., compost piles). It is also frequently collected at light.

***Cercyon quisquilius* (Linnaeus, 1761)**
Figures 3g–i, 6l–n, 13e–f, 15c

Scarabaeus quisquilius Linnaeus, 1761: 138.
Cercyon quisquilium Stephens (1829: 153).
For complete synonymy see Smetana (1978) and Hansen (1999).

Figures in Flickr. www.flickr.com/photos/142655814@N07/albums/72157671688128241

Type locality. "Suecia" [= Sweden, without specified locality].

Specimens examined. CUBA: Holguín: Mayarí Municipality, Feltón, Vuelta Larga, permanent lagoon, 23.iii.2013, leg. A. Deler-Hernández (2 spec.: NMPC) [DNA extraction: MF1599].

Published records. JAMAICA: without precise locality (Leng and Mutchler 1917).

Diagnosis. Body size 2.4–3.2 mm; dorsal surface of head completely black; pronotum (Figs 3g, i) black with vaguely defined yellowish to brownish lateral margins,

broader in anterolateral corners; scutellar shield black; elytra yellow to brownish-yellow; mesoventral plate (Fig. 13e) narrow, ca. 6.3× as long as wide; metaventrite (Fig. 13f) without femoral lines, with raised pentagonal area very wide, 0.6× as long as wide in widest part; first abdominal ventrite without spiniform process in both sexes; apex of fifth abdominal ventrite without triangularly bulged projection; aedeagus with parameres ca. 0.75× as long as phallobase, narrowing towards slightly lobate apex; median lobe fusiform, without spines.

Cercyon quisquilius was assigned to *C. unipunctatus* group according to Smetana (1978). This species can be only confused with *C. nigriceps* in Greater Antilles. It may be distingushed from it by the coloration of the pronotum (blackish with diffuse yellowish areas on lateral margins in *C. quisquilius*, almost homogeneously piceous to reddish brown and similar to elytral coloration in *C. nigriceps*), larger body size (2.4–3.2 mm in *C. quisquilius*, 1.0–2.1 mm in *C. nigriceps*), and by metaventrite without femoral lines and with wide raised median part (with femoral lines and narrower median part in *C. nigriceps*).

Distribution. *Cercyon quisquilius* is a species native to the Palearctic Region, but currently introduced to the Nearctic, Neotropical and Australian Regions (Smetana 1978; Hansen 1999; Fikáček 2009). We are providing the first precise records of this species from the Caribbean based of specimens from Cuba (Holguín province) (Fig. 15c).

Cercyon insularis Chevrolat, 1863

Figures 4a–i, 12 a–i, 16c

Cercyon insulare Chevrolat, 1863: 208.
Cercyon insulare Gundlach (1891: 50, redescription).

DNA barcodes. GANTC001-16, GANTC011-17, GANTC012-17

BIN ID. BOLD:ADC9388.

Figures in Flickr. www.flickr.com/photos/142655814@N07/albums/7215766-9492393134

Type locality. Cuba: Havana.

Type material. Holotype (unsexed specimen): "Havana, D. Poey // Cercyon insulare, Chev Cuba, [illegible] // TYPE [red label]" (MNHN).

Additional material examined. CUBA: Camagüey: Sierra de Cubitas municipality, Limones-Tuabaquey, 21°35'52.10"N, 77°47'17.62"W, 16.v.2013, leg. R. Anderson (1 spec.: NMPC). **Guantánamo:** El Yunque, 3.2 km SW of campismo popular, at right tributary of Duabe river, secondary evergreen forest, cow excrement, 20°19'N, 74°34'W, 150 m a.s.l., 13.vi.2012, leg. Deler-Hernández & Fikáček (MF09) (7 spec.: NMPC); El Yunque, ca. 1.4 km W of campismo popular, cocoa plantations shaded by palms, cow excrement, 20°20.2'N, 74°33.7'W, 60-150 m a.s.l., 11.vi.2012, Deler-Hernández & Fikáček (MF03) (16 spec.: NMPC). **Santiago de Cuba:** El Vivero, 1.6 km E of Dos Caminos, cow excrements on pasture, 20°10.8'N,

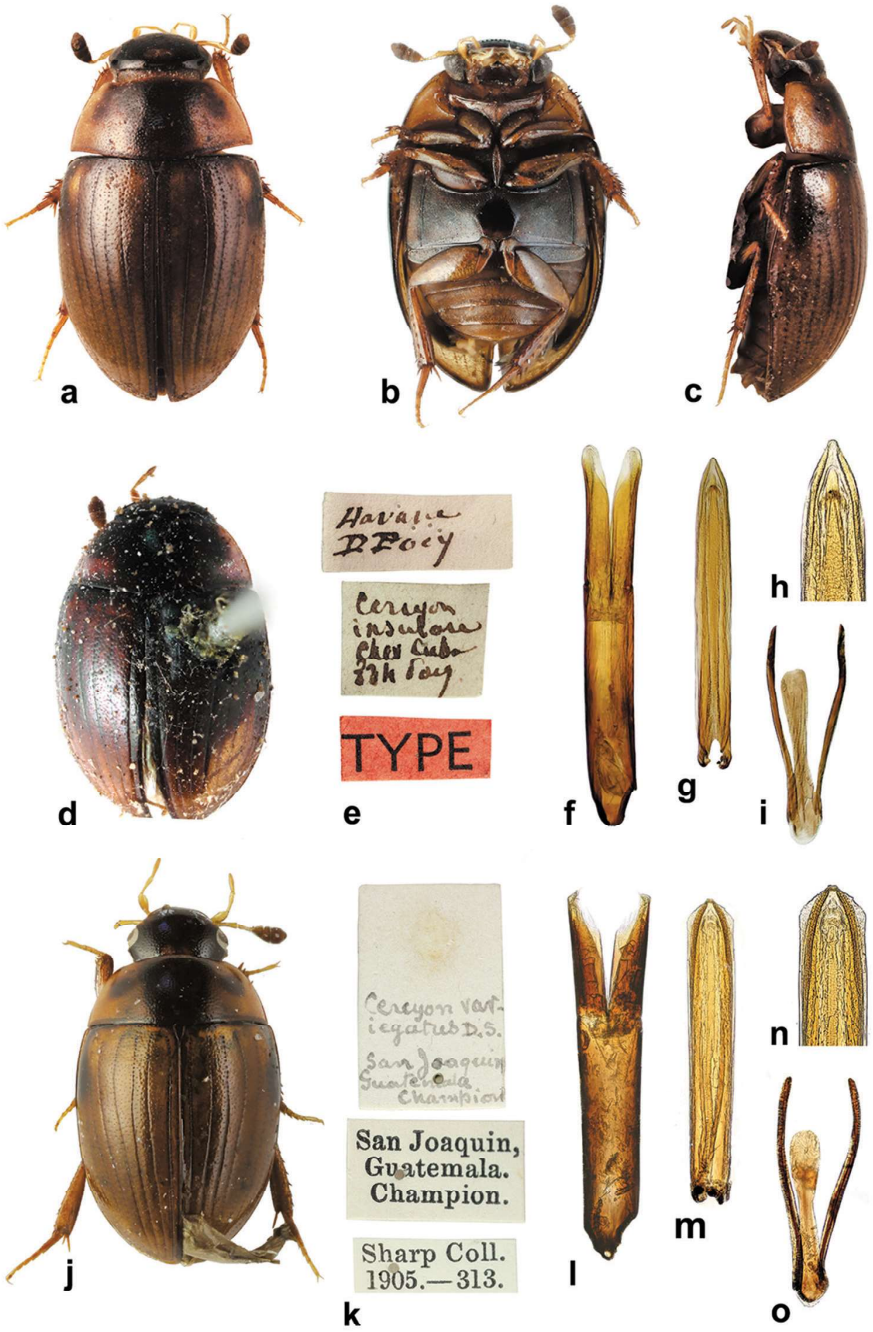

Figure 4. *Cercyon insularis* Chevrolat and *C. variegatus* Sharp. **a–i** *C. insularis*: **a–c** dorsal, ventral and lateral habitus of the non-type specimen from Cuba **d** habitus of the holotype **e** labels of the holotype **f–i** male genitalia of non-type specimen from Dominican Republic. **j–o** lectotype of *C. variegatus*: **j** dorsal habitus **k** labels **l–o** male genitalia. Genital parts illustrated: **f, l** tegmen of aedeagus **g, m** median lobe of aedeagus **h, n** detail of apex of median lobe; **i, o** 9th sternite.

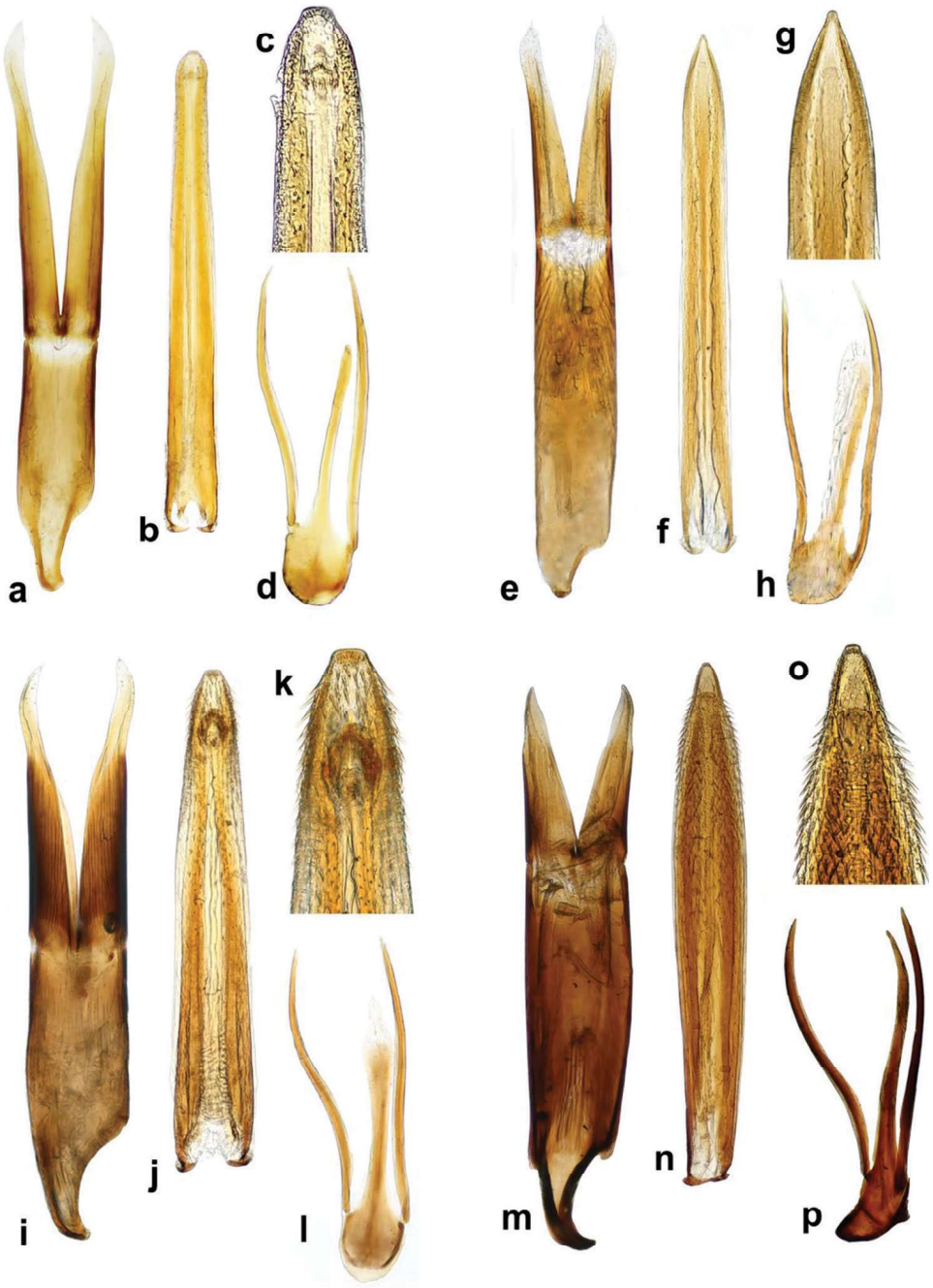

Figure 5. *Cercyon* spp. n. genitalia **a–d** *Cercyon gimmeli* sp. n. **e–h** *Cercyon taino* sp. n. **i–l** *Cercyon armatipenis* sp. n. **m–p** *Cercyon sklodowskae* sp. n. **a, e, i, m** tegmen of aedeagus **b, f, j, n** median lobe of aedeagus **c, g, k, o** 9th sternite.

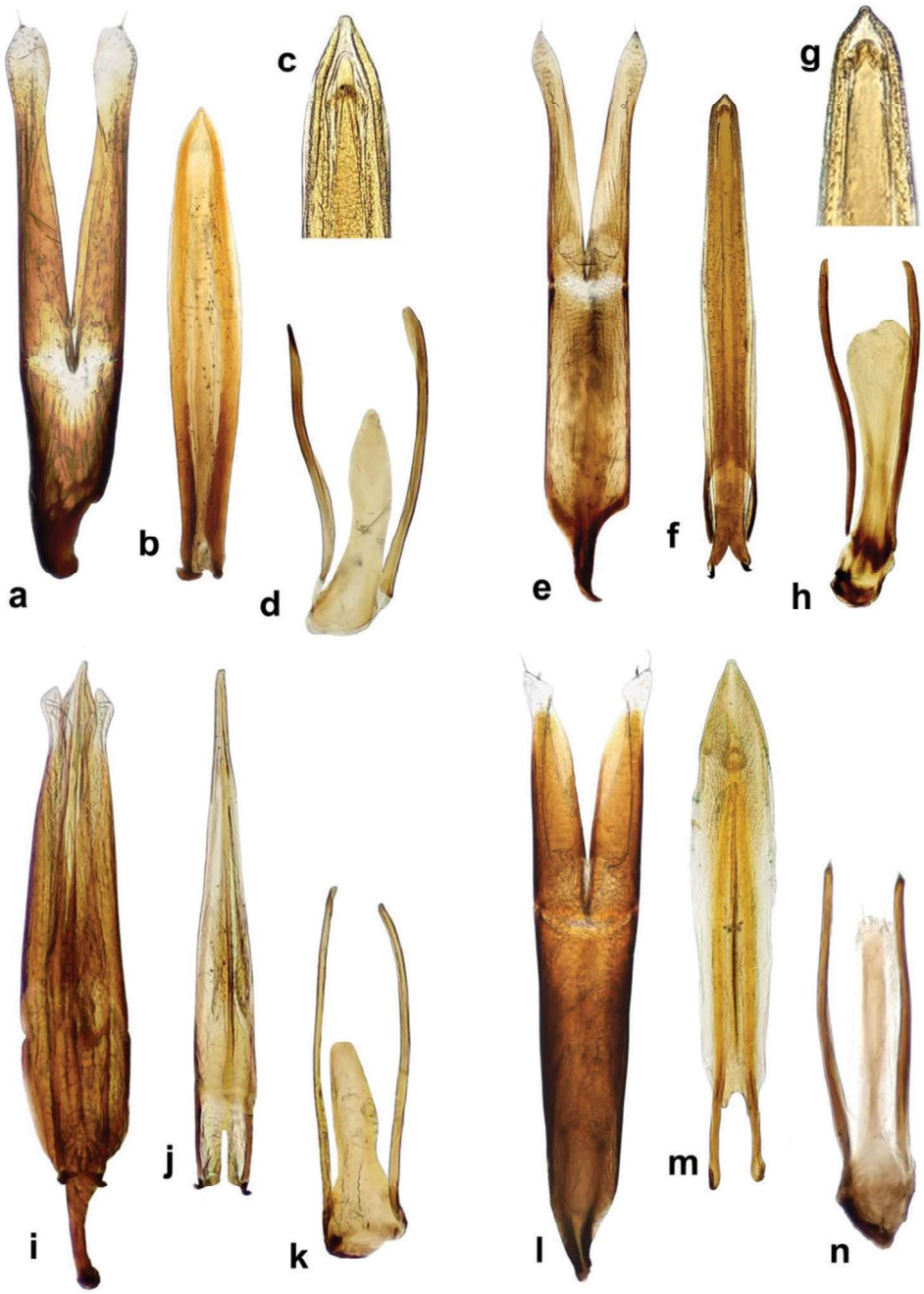

Figure 6. *Cercyon* spp. n. genitalia **a–d** *Cercyon praetextatus* Say **e–h** *Cercyon spiniventris* sp. n. **i–k** *Cercyon nigriceps* Marsham **l–n** *Cercyon quisquilius* Linnaeus **a, e, i, l** tegmen of aedeagus **b, f, j, m** median lobe of aedeagus **c, g** 9th sternite.

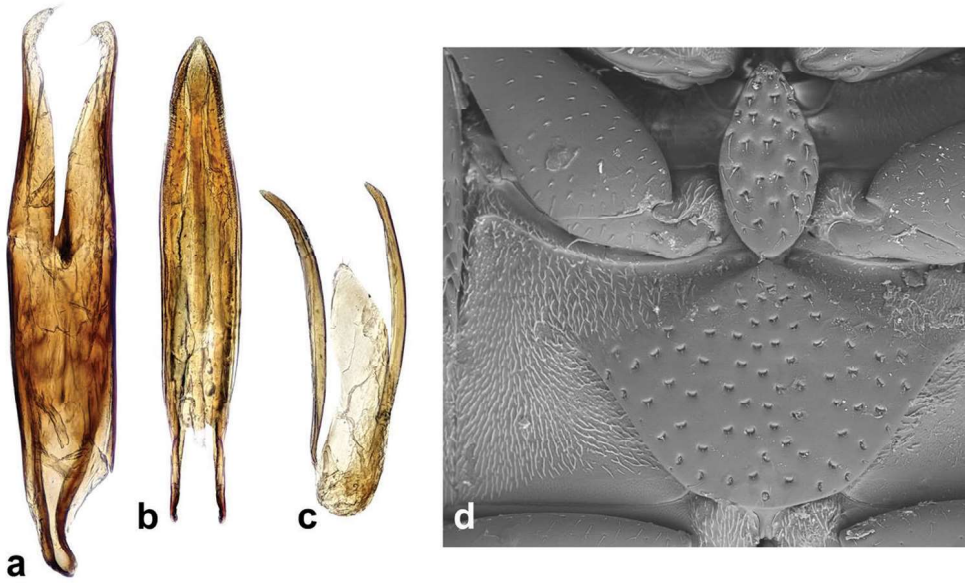

Figure 7. *Cercyon floridanus* Horn **a** tegmen of aedeagus **b** median lobe of aedeagus **c** 9th sternite **d** ventral view of pterothorax.

75°46.4'W, 150 m, 20-21.vi.2012, leg. Deler-Hernández & Fikáček (MF18) (1 spec.: NMPC); San Luis Municipality, Dos Caminos, 20°10'57.82"N, 75°46'40.84"W, 3.x.2012, leg. Deler-Hernández (12 spec.: NMPC). **Granma:** PN Turquino, around La Platica, 20°0.7'N, 76°53.4'W, 880 m, 25–26.vi.2012, leg. Deler-Hernández & Fikáček (MF24) (12 spec.: NMPC); PN Turquino, on the trail up to 0.5 km S of La Platica, 20°0.5'N, 76°53.3'W, 920 m, 23–27.vi.2012, leg. Deler-Hernández & Fikáček (MF20) (2 spec.: NMPC); PN Turquino, La Siguapa, ca. 1.5 km SE of La Platica, sifting leaf litter in evergreen forest, 20°0.2'N, 76°52.8'W, 1290 m, 25.vi.2012, leg. F. Cala-Riquelme (MF25) (1 spec.: NMPC) [DNA extract at NMPC] (1: NMPC). **Artemisa:** Cañon de Santa Cruz, Río de Santa Cruz, 22°45'1.29"N 83°08'56.36"W, 199 m a.s.l., 16.vii.2016, leg. A. Deler-Hernández (1 spec.: NMPC) [DNA extraction: MF1749]. **DOMINICAN REPUBLIC: La Vega:** 7.0 km W of Manabao, side of a stony stream in a valley with scattered houses and plantations surrounded by montane forest, in cow excrements, 19°4.56'N, 70°51.46'W, 1185 m a.s.l., 23.viii.2014, leg. Deler-Hernández, Fikáček & Gimmel (DR18) (3 spec.: NMPC); at S margin of Manabao, 19°3.85'N, 70°47.61'W, 912 m a.s.l., 27.viii.2014, leg. Deler-Hernández & Fikáček (DR23) (3 spec.: NMPC). **Samaná:** MN Salto El Limón 2.8 km SSW of El Limón, secondary vegetation and tiny remnants of forests among coffee plantations and pastures, cow excrements, 19°16.56'N, 69°26.47'W, 2.ix.2014, leg. Deler-Hernández, Fikáček & Gimmel (DR29a) (16 spec.: NMPC). **Monseñor Nouel:** PN La Humeadora; 11.6 km SSW, of Piedra Blanca, in horse excrement in moist broad-leaf forest in a valley of a small stony stream, 18°44.92'N, 70°21.63'W, 636 m a.s.l., 8.ix.2014, leg. Deler, Fikáček & Gimmel (DR41) (4 spec.: NMPC) [DNA

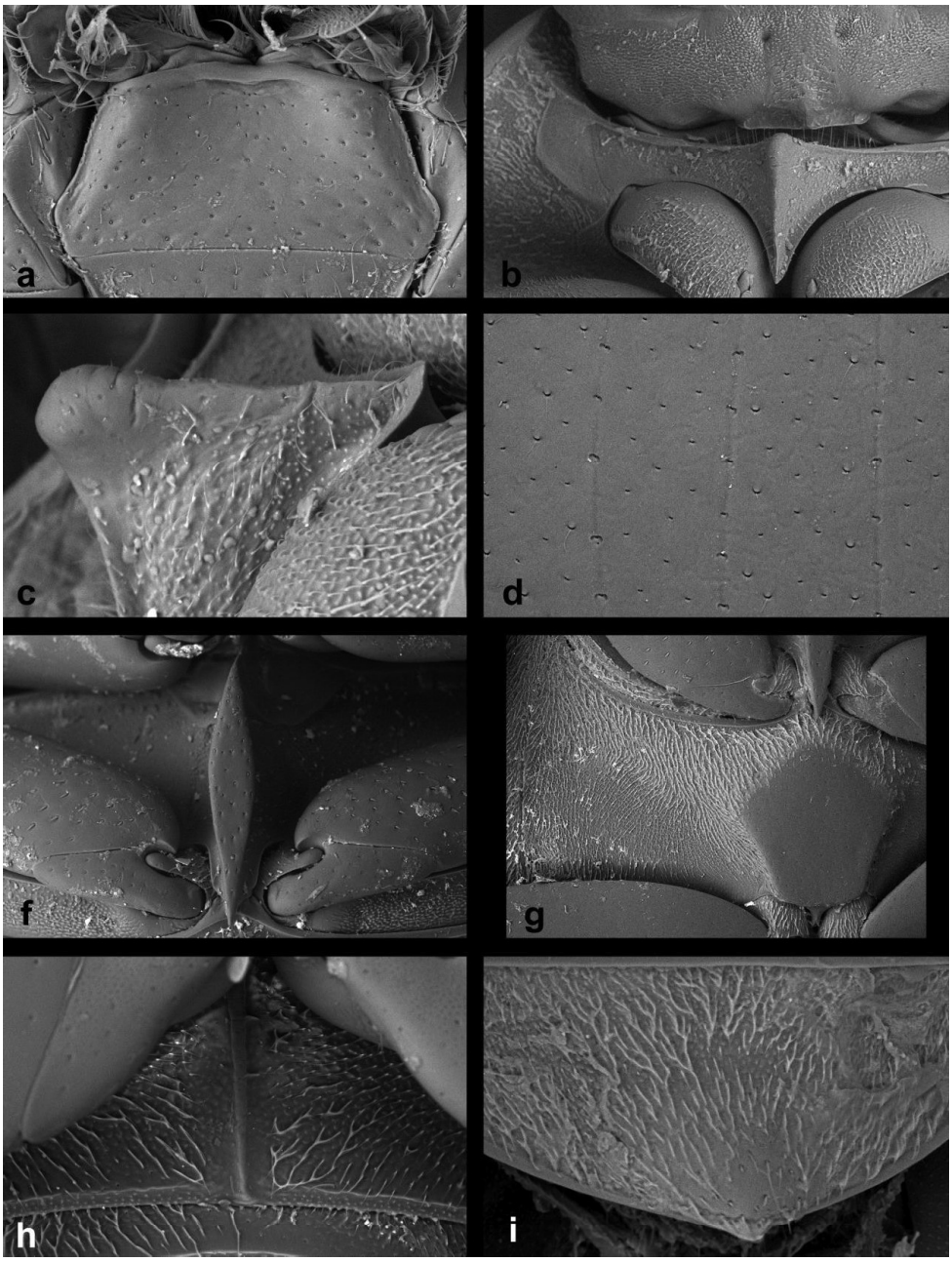

Figure 8. *Cercyon gimmeli* sp. n. **a** mentum **b** prosternum **c** lateral view of median ridge of prosternum **d** detail of elytral surface **f** mesoventral plate **g** metaventrite **h** median ridge of first abdominal ventrite **i** fifth abdominal ventrite.

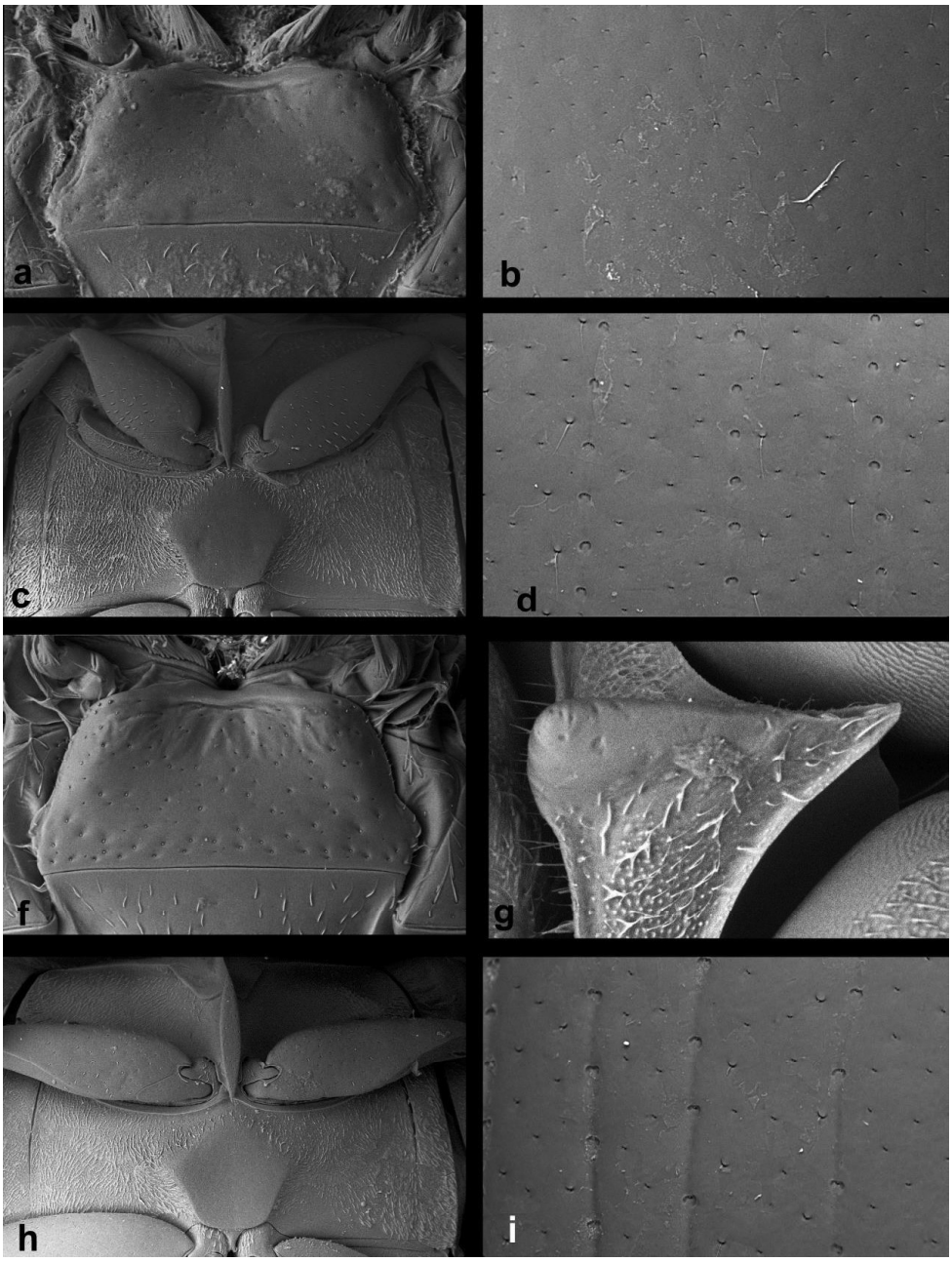

Figure 9. *Cercyon* spp. n. **a–d** *Cercyon armatipenis* sp. n. **f–i** *Cercyon taino* sp. n. **a, f** mentum **b** detail of pronotal surface **c, h** ventral view of pterothorax **d, i** detail of elytral surface **g** lateral view of median ridge of prosternum.

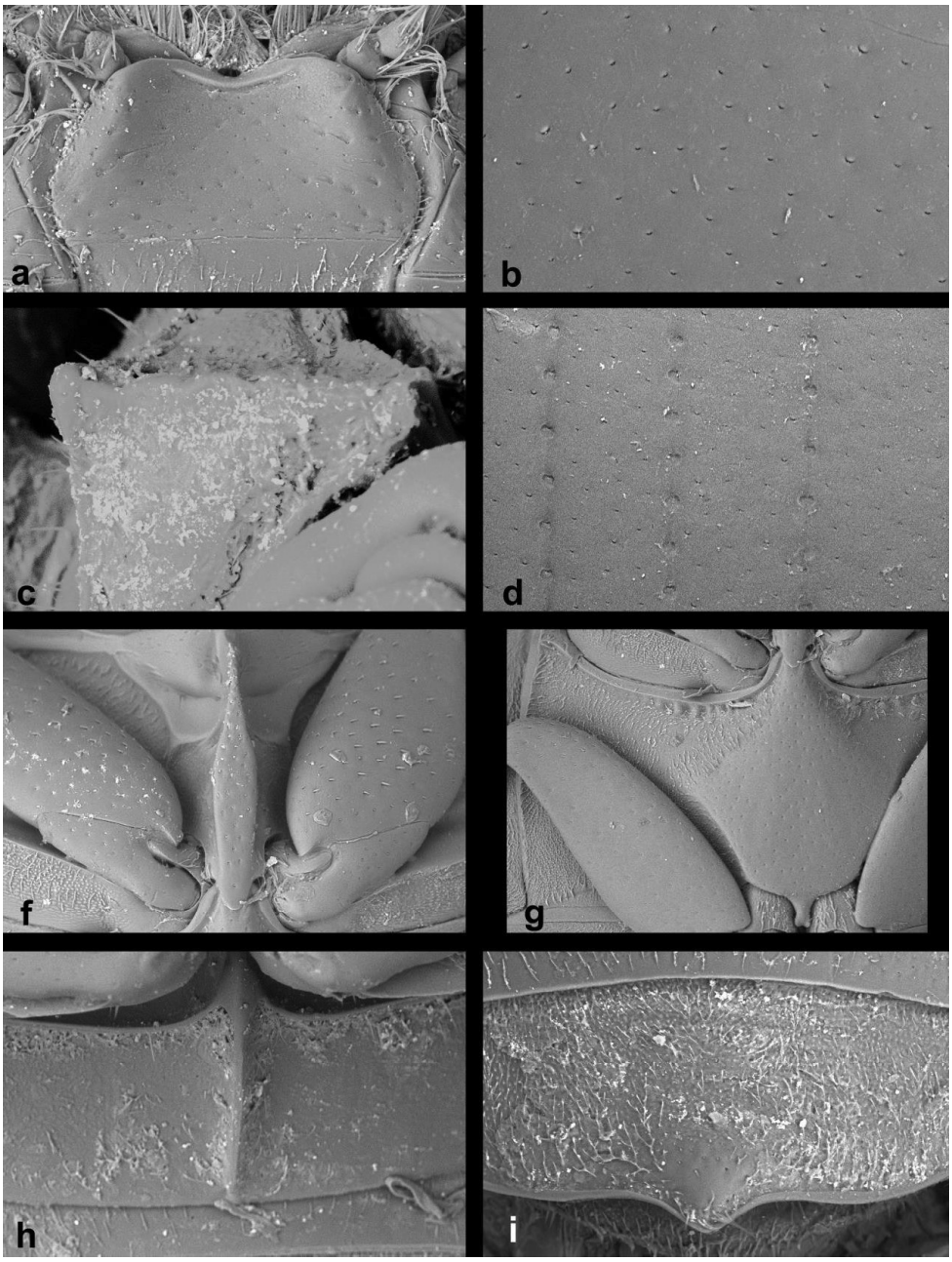

Figure 10. *Cercyon sklodowskae* sp. n. **a** mentum **b** detail of pronotal surface **c** lateral view of median ridge of prosternum **d** detail of elytral surface **f** mesoventral plate **g** metaventrite **h** median ridge of first abdominal ventrite **i** female fifth abdominal ventrite.

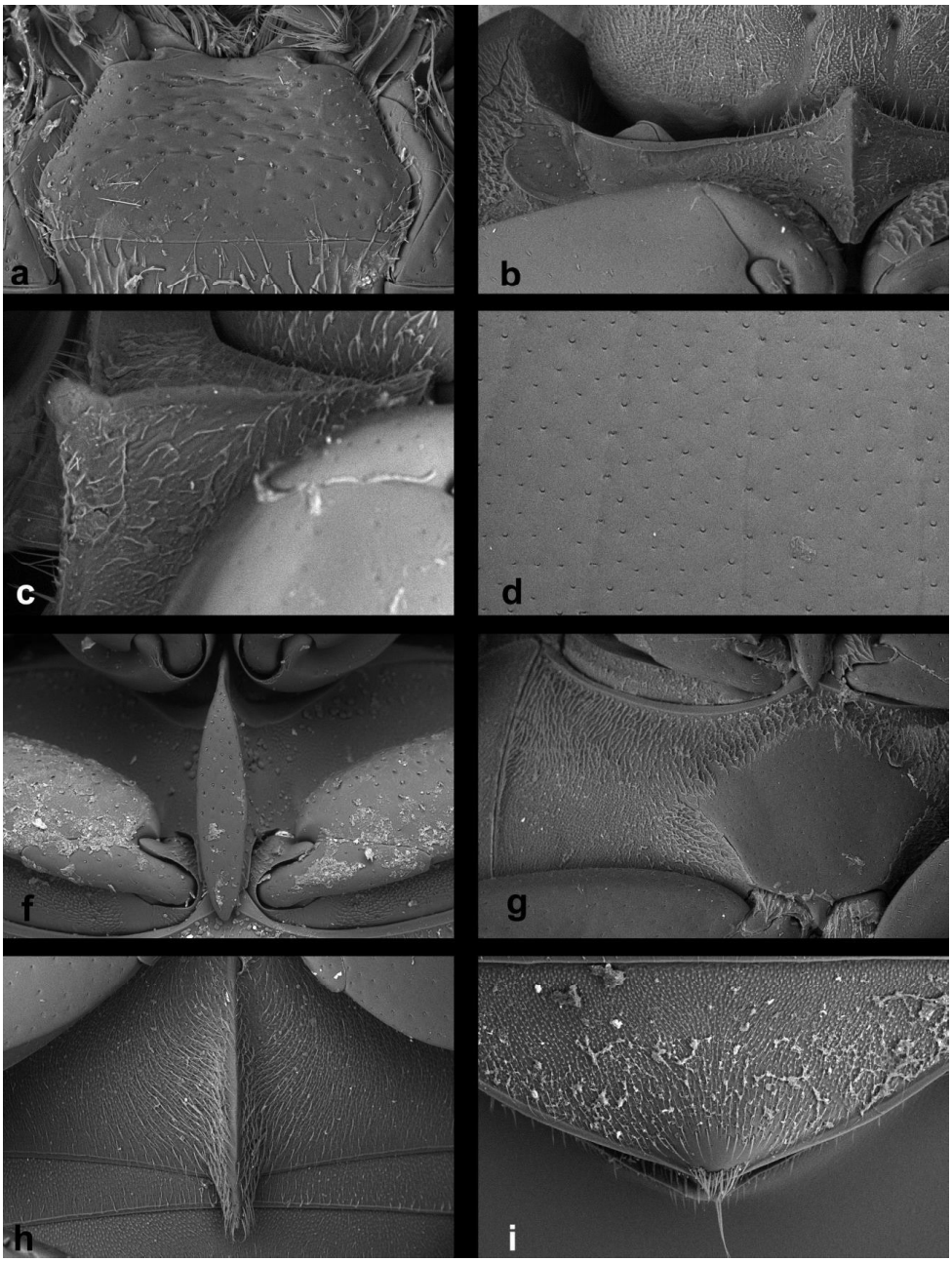

Figure 11. *Cercyon spiniventris* sp. n. **a** mentum **b** prosternum **c** lateral view of median ridge of prosternum **d** detail of elytral surface **f** mesoventral plate **g** metaventrite **h** median ridge of female first abdominal ventrite **i** fifth abdominal ventrite.

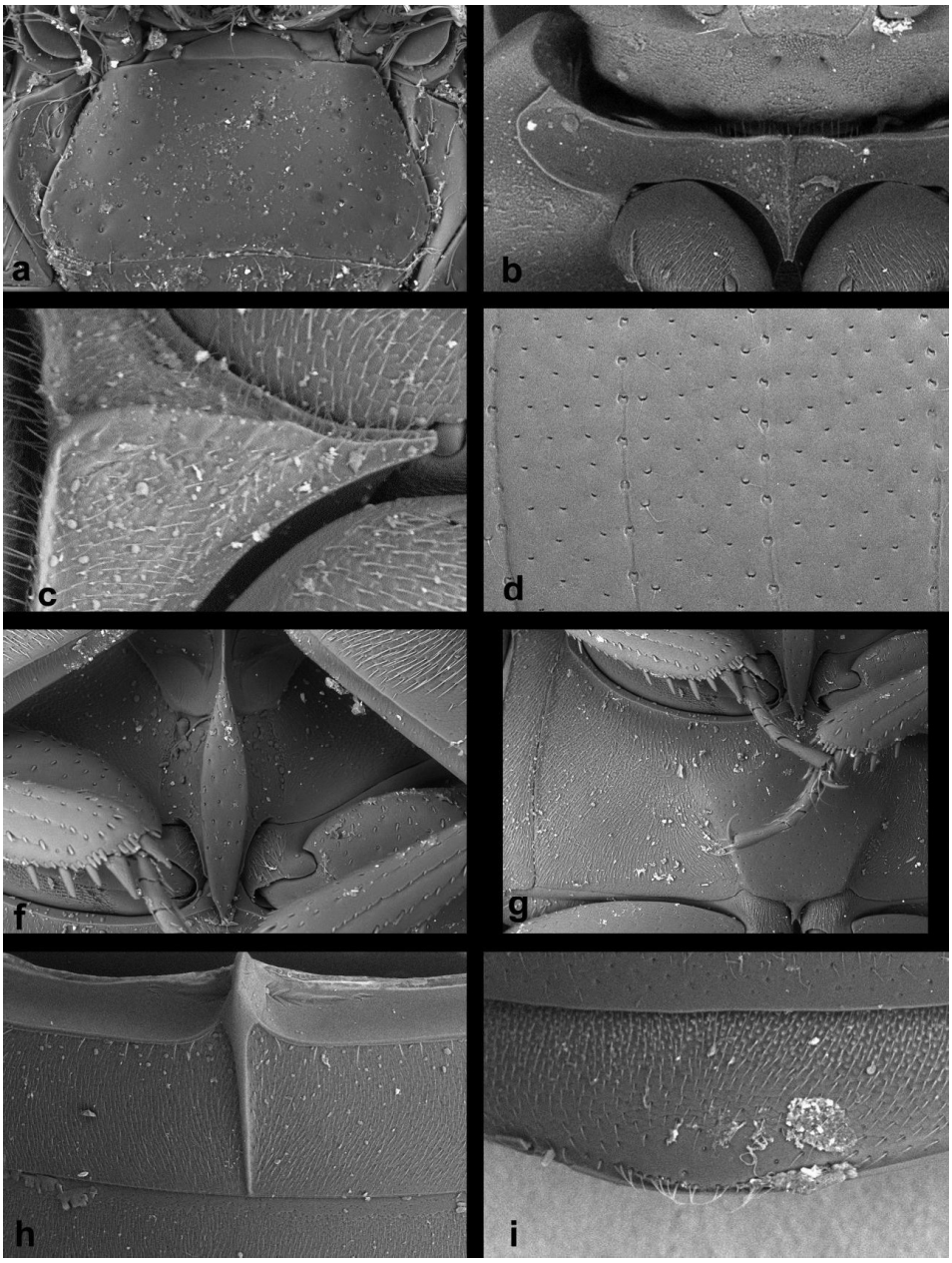

Figure 12. *Cercyon insularis* Chevrolat **a** mentum **b** prosternum **c** lateral view of median ridge of prosternum **d** detail of elytral surface **f** mesoventral plate **g** metaventrite **h** median ridge of female first abdominal ventrite **i** fifth abdominal ventrite.

extracts: MF1214.1, MF1214.2]. **PUERTO RICO: Naguabo:** El Yunque National Forest (southern part), 3.45 km N of Río Blanco at road PR191, in horse excrements on exposed small pasture on the slope of El Yunque massive, 18°14.8'N, 65°47.9'W,

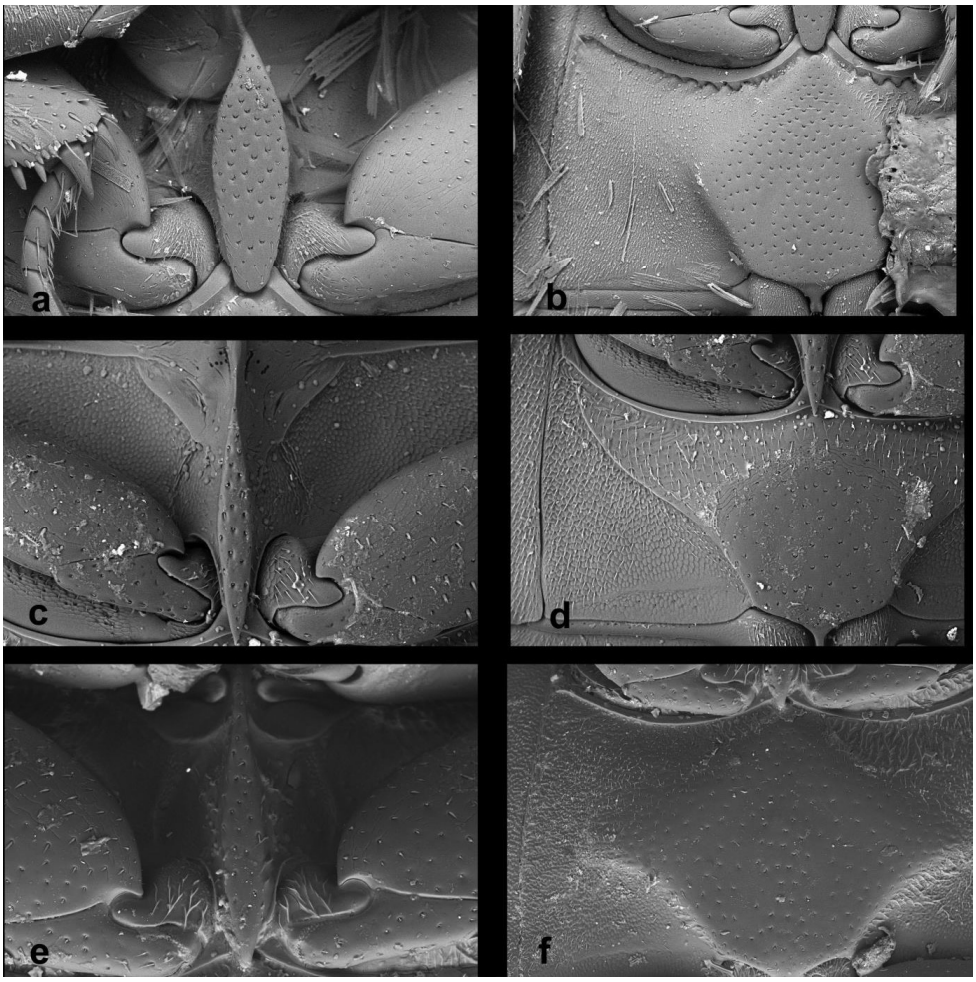

Figure 13. *Cercyon* spp. **a–b** *Cercyon praetextatus* Say **c–d** *Cercyon nigriceps* Marsham **e–f** *Cercyon quisquilius* Linnaeus **a, c, e** mesoventral plate **b, d, f** metaventrite.

170 m a.s.l., 24.vi.2016, leg. Deler-Hernández, Fikáček & Seidel (PR2a) (19 spec.: NMPC) [DNA extraction: MF1731]; El Yunque National Forest (southern part), 4.9 km N iof Río Blanco, margin of the rainforest in an area with many flowering *Etlingera elatior* plants, FIT, 18°15.8'N, 65°47.3'W, 495 m a.s.l., 24.vi.–2.vii.2016, leg. Fikáček & Seidel (PR11) (3 spec.: NMPC). **Arecibo: s**mall settlement in Bosque Estatal Río Abajo, in the middle of the lowland forest, horse excrement, 18°19.7'N, 66°42.1'W, 340 m a.s.l., 27.vi.2016, leg. Deler-Hernández, Fikáček & Seidel (PR15) (1 spec.: NMPC). **Lesser Antilles: DOMINICA:** Springfield Estate, mature secondary forest, FIT, 15°20.796'N, 61°22.142'W, 30.v.-16.vi.2004, S. & J. Peck (04-86) (3 spec.: SBP). **GRENADA:** Grand Etang Forest Reserve, FIT in rainforest, 12°04.846'N 61°42.333'W, 360 m a.s.l., leg. S. Peck (10-61) (2 spec.: SBP); Grand Etang Forest Reserve, FIT in rainforest, 12°04.162'N 61°42.162'W, 400 m a.s.l.,

leg. S. Peck (10-63) (2 spec.: SBP); St. Andrew, Mirabeu Agriculture Lab, light trap, 19.iv.1990, leg. J. Telesford (2 spec.: SBP). **SAINT LUCIA:** Mon Repos, 6.5 km W Fox Grove Inn, submontane forest, carrion traps, 13°52.5'N, 60°56.4'W, 300 m a.s.l., leg. S. & J. Peck (0759) (2 spec.: SBP).

Published records (as *C. variegatus*). JAMAICA: without precise locality (Smetana 1978). **PUERTO RICO:** without precise locality (Smetana 1978). **DOMINICA:** without precise locality (Leng and Mutchler 1917; Peck 2006).

Diagnosis. Body size 2.4–3.4 mm; dorsal surface of head (Fig. 4a) black with a pair of small pale spots on vertex (sometimes fused in one central spot), pronotum yellowish to dark reddish-brown with a large blackish central spot and two small round blackish spots at sides (sometimes obscured); elytra yellowish with black humeral spot, in dark specimens whole elytral base and suture darkened; medial ridge of prosternum not projected ventrally (Fig. 12c); mesoventral plate narrow, 5.8× as long as wide (Fig. 12f); metaventrite (Fig. 12g) without femoral lines, with raised pentagonal area as long as wide; first abdominal ventrite without spine-like process in both sexes (Fig. 12h); apex of fifth abdominal ventrite (Fig. 12i) without apical projection in both sexes; aedeagus narrow, parameres 0.7× as long as phallobase (Fig. 4f), rounded at apex; median lobe (Fig. 4g) subparallel throughout except for acuminate apex, without subapical spines.

Redescription. *Body.* (Fig. 4a–d) 2.4–3.4 mm long (length of holotype: 2.8 mm); moderately elongate oval, 1.7–1.8× as long as wide, widest at basal fifth of elytra; moderately convex, 2.6–2.8× as long as high (height of holotype: 1.0 mm). *Coloration*. Dorsal surface of head black with a pair of small rufotestaceous spots on vertex. Antennal scape and flagellum and ventral surface of head including mouthparts light-brown, antennal club and mentum dark brown. Pronotum yellowish to dark reddish-brown, with a large blackish central spot and two small round blackish spots at its sides, sometimes connected with central spot. Prosternum yellowish to light brown, hypomeron slightly darkened. Elytra with elongate blackish spot posterior to humeri, elytral base and suture darkened, elytral epipleura uniformly pale. Ventral surface of mesothorax blackish. Metepisternum brown. Metaventrite blackish, darker at medial elevation. Abdomen yellowish to reddish-brown. Legs yellowish to light brown.

Head. Clypeus with moderately dense and shallow punctation consisting of small transverse punctures; interstices without microsculpture. Anterior margin of clypeus with narrow bead. Frontoclypeal suture conspicuous as a zone without punctuation, vanished mesally. Frons with punctation similar to that on clypeus, punctures sparser on sides; interstices without microsculpture. Eyes rather small, interocular distance about 6× the width of one eye in dorsal view. Labrum membranous, nearly completely concealed under clypeus, only with narrowly exposed sinuate anterior margin. Mentum (Fig. 12a) subtrapezoid, widest at posterior fourth, about 2× wider than long, 1.5× wider at widest part than at anterior margin, strongly concave in anterior half, anterior margin not emarginate; surface almost glabrous, punctures small, shallow and

sparse, almost vanishing anteromesally, interstices without microsculpture. Antenna with 9 antennomeres, scapus ca. 1.8× as long antennomeres 2–6 combined; antennal club moderately elongate, about twice as long as wide, as long as scapus; antennomere 9 acuminate at apex.

Prothorax. Pronotum transverse, widest at base 2.1–2.2× wider than long; 1.7–1.8× wider at base than between front angles, 1.8× wider than head including eyes, as convex as pronotum in lateral view. Punctation rather dense and moderately deep, consisting of crescent-shaped punctures intermixed with denser, slightly smaller and rather transverse punctures; punctures slightly feebler on sides. Prosternum (Fig. 12b) strongly tectiform medially, median ridge (Fig. 12c) with the same width throughout, anterior apex not projecting ventrally. Antennal grooves distinct, with lateral margin curved.

Pterothorax. Scutellar shield 1.2× as long as wide, sparsely punctured. Elytra widest at anterior fifth, 1.0–1.1× longer than wide, 2.6–2.8× as long as pronotum, 1.2–1.3× as wide as pronotum, surface glabrous, with 10 series of punctures; series 6, 8 and 9 not reaching anterior margin, surface glabrous (Fig. 12d), serial punctures getting slightly smaller lateraly; intervals moderately convex; punctation on interval 1 and odd intervals composed of crescent-shaped setiferous punctures, close to striae denser and intermixed with smaller, transverse non-setiferous punctures; even intervals with non-setiferous punctures only; all interstices without microsculpture. Humeral bulge indistinct. Mesoventral plate (Fig. 12f) narrowly elongate, ca. 5.8× as long as wide, widest at midlength, symmetrically narrowing to both apices, anterior apex pointed, posterior apex rounded, posterior tip slightly overlapping over anterior portion of metaventrite; surface with few sparse punctures. Metaventrite (Fig. 12g) with raised pentagonal area ca. as wide as long, weakly, sparsely, uniformly punctated, without visible setae, bare part not reaching anterior margin of metaventrite; femoral lines absent; lateral parts of metaventrite densely covered by short pubescence.

Legs. Femora with sparse shallow punctures ventrally, interstices with weak microsculpture consisting of longitudinal lines; tibial grooves distinct. Tibiae with rather small lateral spines. Metatibiae moderately broad and long, straight, 0.33× as long as elytra, 5× as long as wide. Metatarsus long, 0.86–0.89× as long as metatibia, with just a few short rather stout setae ventrally.

Abdomen with five ventrites, first abdominal ventrite (Fig. 12h) about as long as the second and third ventrites together, with distinct median longitudinal carina narrowing posteriad, not projecting posteriorly in both sexes; fifth ventrite with acuminate apex and weakly bulged in both sexes (Fig. 12i).

Male genitalia. Median projection of sternite 9 (Fig. 4i) rounded apically, with a pair of subapical setae, base symmetrical. Phallobase (Fig. 4f) almost 1.4× longer than parameres, narrow, parallel sided, base widely rounded, manubrium indistinct. Parameres nearly of the same width in basal 3/4, divergent near apex, rounded and weakly narrowing apically. Median lobe (Fig. 4g) narrow and subparallel throughout, pointed at apex (Fig. 4h), gonopore moderately large, basal portion of median lobe with dorsal plate narrow and simply bifid basally.

Variability. The general dorsal coloration of the pronotum and elytra varies from yellow to dark reddish-brown. In dark specimens, lateral pronotal spots join the large central spot, and the whole anterior part of elytra and the elytral suture are distinctly darkened, with pale areas maintained in humeral area and at sides of scutellar shield. In pale specimens, the lateral pronotal spots are rather small and sometimes very vague and indistinct, and the elytra are completely yellow except base, sutural interval and the posthumeral dark spots.

Distribution. *Cercyon insularis* seems to be widely distributed across Greater and Lesser Antilles, here we are recording it from Cuba, Dominican Republic, Puerto Rico, Grenada, Saint Lucia and Dominica. It seems that all records of *C. variegatus* from the Caribbean (Jamaica, Puerto Rico: Smetana 1978; Dominica: Peck 2006) actually concern *C. insularis*, as we failed to find the true *C. variegatus* in the material examined. For that reason we consider *C. insularis* to occur in Jamaica, although we did not examine any specimens from Jamaica ourselves.

Bionomics. Most of the specimens were collected in cow and horse dung on pastures, in coffee plantations and in tropical forests; few were collected using flight intercept traps.

Discussion. Chevrolat (1863) described *C. insularis* based on a single specimen from Cuba collected by D. F. Poëy and deposited in Chevrolat's collection. On our request to loan this specimen, we received a single specimen standing under the name *C. insularis* in the Chevrolat collection, corresponding well with the original description and marked as a type. In contrast to the data mentioned by Chevrolat (1863), the specimen also bears a label indicating Habana as the place of its origin. Since there is no reason to doubt the type identity of this specimen, we correct the type locality of *C. insularis* to Habana, in agreement with the label data of the holotype.

Cercyon insularis was only briefly mentioned once by Gundlach (1891) and its type was not reexamined, therefore its identity remained unclear. Our inspection of the type revealed it corresponds by coloration with what was recorded from the Caribbean as *Cercyon variegatus* Sharp, 1882, by Smetana (1978), Hansen (1999) and Peck (2006). In order to determine the identity of the species present in the Caribbean we studied the lectotype of *C. variegatus* (Fig. 4j–o, deposited in BMNH) and compared it to the type of *C. insularis* and additional recently collected material from Cuba. Based on this comparison, it became clear that Cuban specimens are not conspecific with *C. variegatus*, but belong to a different species indistinguishable from it by external morphology: all dissected Cuban specimens were conspecific, differed from *C. variegatus* by genital morphology, and no other species of the same external coloration was found. We hence consider the Cuban specimens conspecific with the type specimen of *C. insularis*, even though it cannot be dissected because of its poor condition. Both median lobe (Fig. 4g) as well as phallobase and parameres (Fig. 4f) are narrower in *C. insularis* than in *C. variegatus*. The apices of parameres are rounded in *C. insularis*, while they are more acuminate in *C. variegatus* (Fig. 4l). Moreover, the apex of the median lobe of *C. variegatus* has a small flank on each side (Fig. 4n) (Full set of pictures of the lectotype of *C. variegatus* in www.flickr.com/photos/142655814@N07/albums/72157676248390724).

Cercyon insularis and *C. variegatus* belong to a species complex corresponding to the *C. variegatus* group of Smetana (1978), distributed from the southern USA to Argentina; the species within this complex can be only distinguished by the morphology of the male genitalia (Arriaga-Varela and Fikáček, pers. observation). Only two species of this species complex have been formally described (*C. variegatus* and *C. insularis*) and the group requires a detailed revision. The species recorded from Suriname as "*Cercyon rishwani*" by Makhan (2004) also belongs to this species complex based on color pattern of the pronotum and the general shape of the aedeagus, but a more detailed comparison with *C. insularis* and *C. variegatus* is impossible based on the description and illustrations provided. "*Cercyon rishwani* Makhan, 2004" is moreover considered a *nomen nudum* (see Short and Hebauer, 2006 for details).

Larval morphology

***Cercyon taino* sp. n.**
Figure 14a–f

Material examined. DOMINICAN REPUBLIC: La Vega: PN Valle Nuevo, Salto Aguas Blancas, sifting of moist leaf litter in small remnants of montane forest in a small ravine with a spring and on slopes just above the small river, 18°50.60'N, 70°40.68'W, 1655 m a.s.l., 25.viii.2014, leg. Deler, Fikáček & Gimmel (DR21) (2 larvae associated with adults: NMPC; DNA extraction of one larva: MF1261.L).

Larval diagnosis. Head capsule (Fig. 14e) longer than wide; cuticle with polygonal microsculpture; head capsule with two "lenses" (anteriorly and posterior of the eye spot) on each side, lateral part of head capsule without apparent group of setae ca. at midlength; clypeolabrum uniformly arcuate at the right side from the setiferous emargination. Metanotum (Fig. 14a) with wide and strongly sclerotized transverse tergite. Legs (Fig. 14d) reduced into two-segmented vestiges. Membranous parts of thorax and abdomen (Fig. 14a–c) covered by long blackish cuticular projections. Abdominal segments acutely lobate laterally, abdominal segments 1-7 each with three transverse rows of low tubercles. Tergite on 8th abdominal segment (Fig. 14f) ca. as long as wide, deeply sinuate on anterior margin, with three slightly acute lobes on posterior margin.

***Cercyon insularis* Chevrolat**
Figure 14g–l

Material examined. PUERTO RICO: Naguabo: El Yunque National Forest, (southern part), 3.45 km N of Río Blanco at road PR191, in horse excrements on exposed small pasture on the slope of El Yunque massive, 18°14.8'N, 65°47.9'W, 170 m

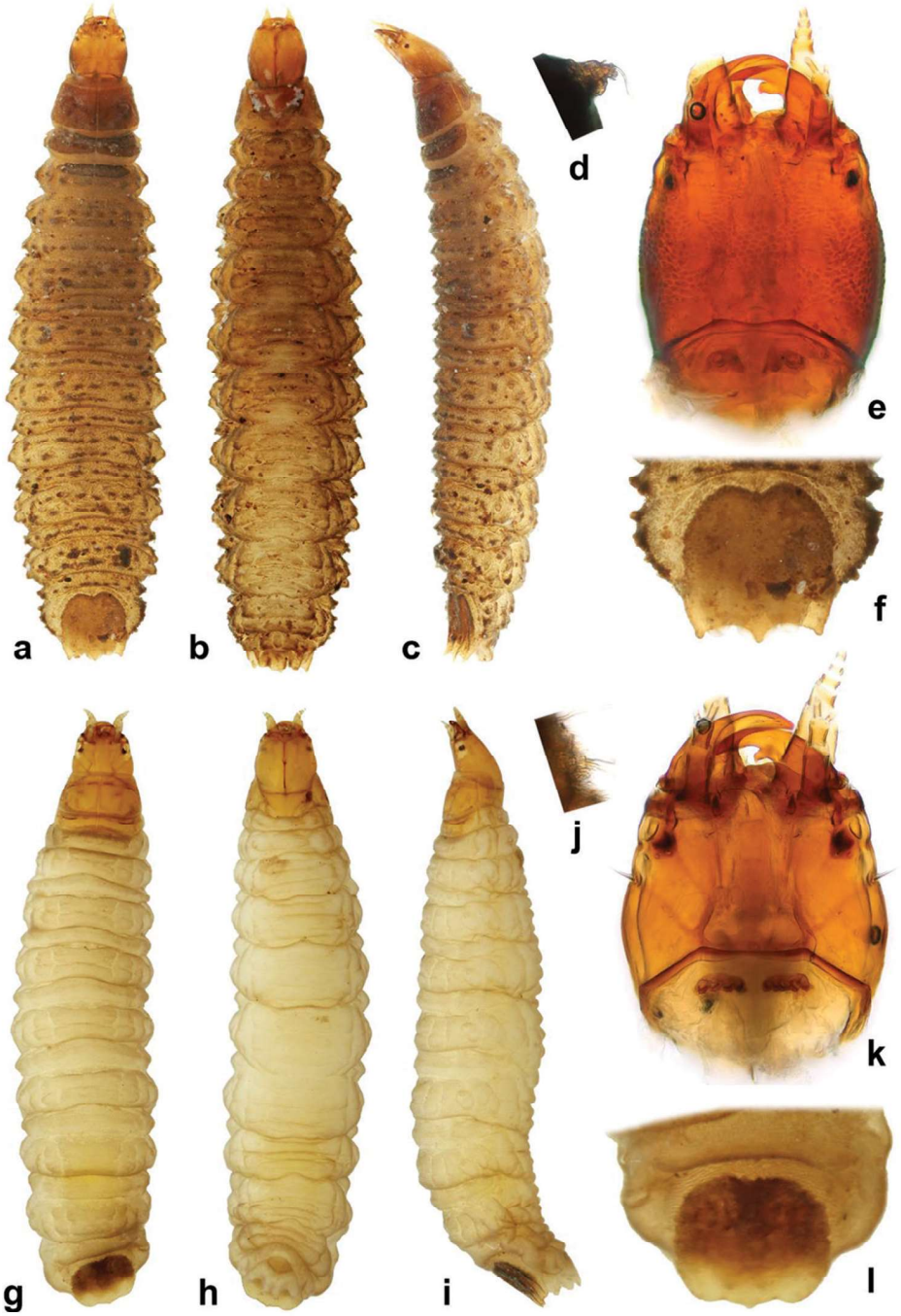

Figure 14. *Cercyon* spp. larval morphology **e–f** *Cercyon taino* sp. n. **g–l** *Cercyon insularis* Chevrolat **a, g** dorsal habitus **b, h** ventral habitus **c, i** lateral habitus **d, j** front leg **e, k** dorsal view of head **f, l** tergite on 8th abdominal segment.

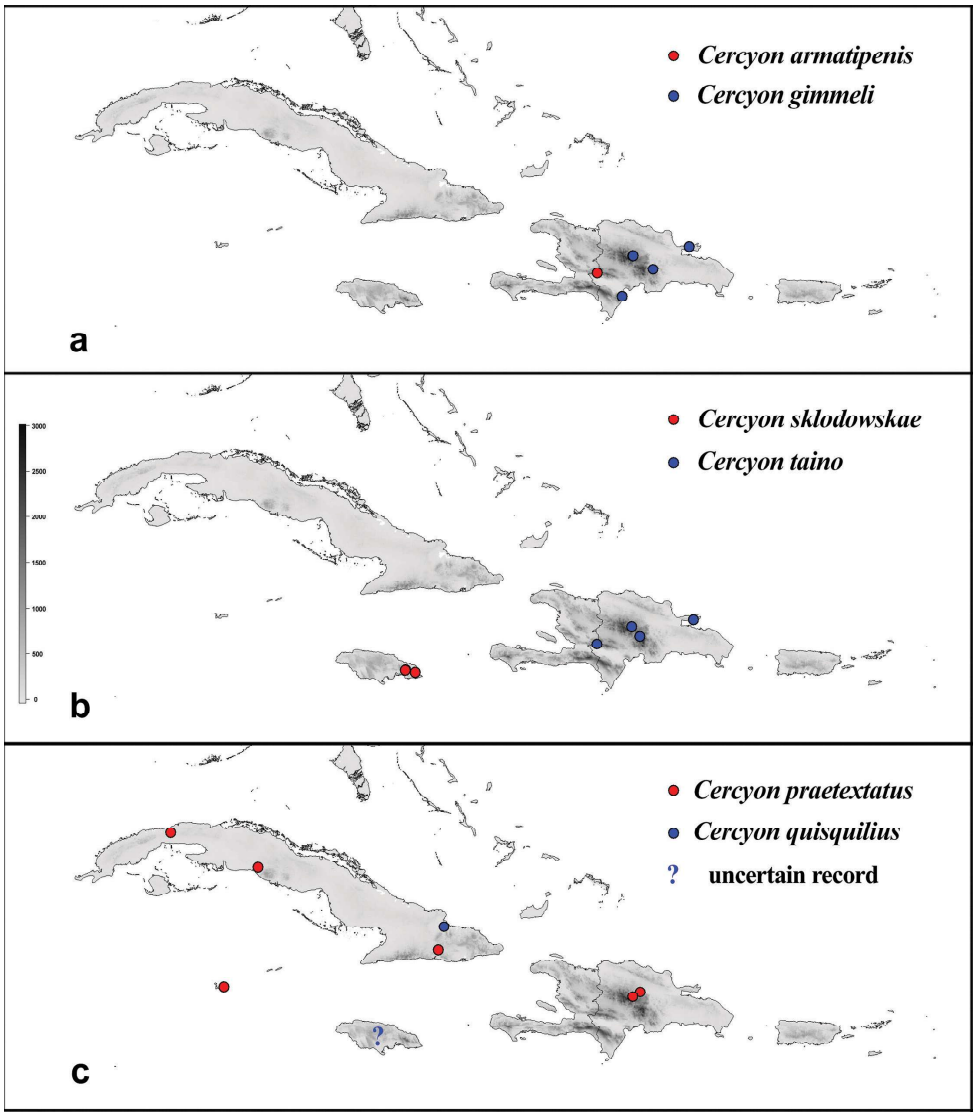

Figure 15. *Cercyon* spp. distribution maps. **a** *Cercyon armatipenis* sp. n. (●) *Cercyon gimmeli* sp. n. (●) **b** *Cercyon sklodowskae* sp. n. (●) *Cercyon taino* sp. n. (●) **c** *Cercyon praetextatus* Say (●) *Cercyon quisquilius* Linnaeus (●).

a.s.l., 24.vi.2016, leg. Deler-Hernández, Fikáček & Seidel (PR2a) (2 larvae associated with adults: NMPC; DNA extraction of one larva: MF1731.L)

Larval diagnosis. Head capsule (Fig. 14k) ca. as long as wide; cuticle smooth, without distinct miscrosculpture; head capsule with two "lenses" (anteriorly and posterior of the eye spot) on each side, lateral part of head capsule with apparent group of setae (PA12-14 *sensu* Fikáček et al. 2008) ca. at midlength; clypeolabrum angulate at the

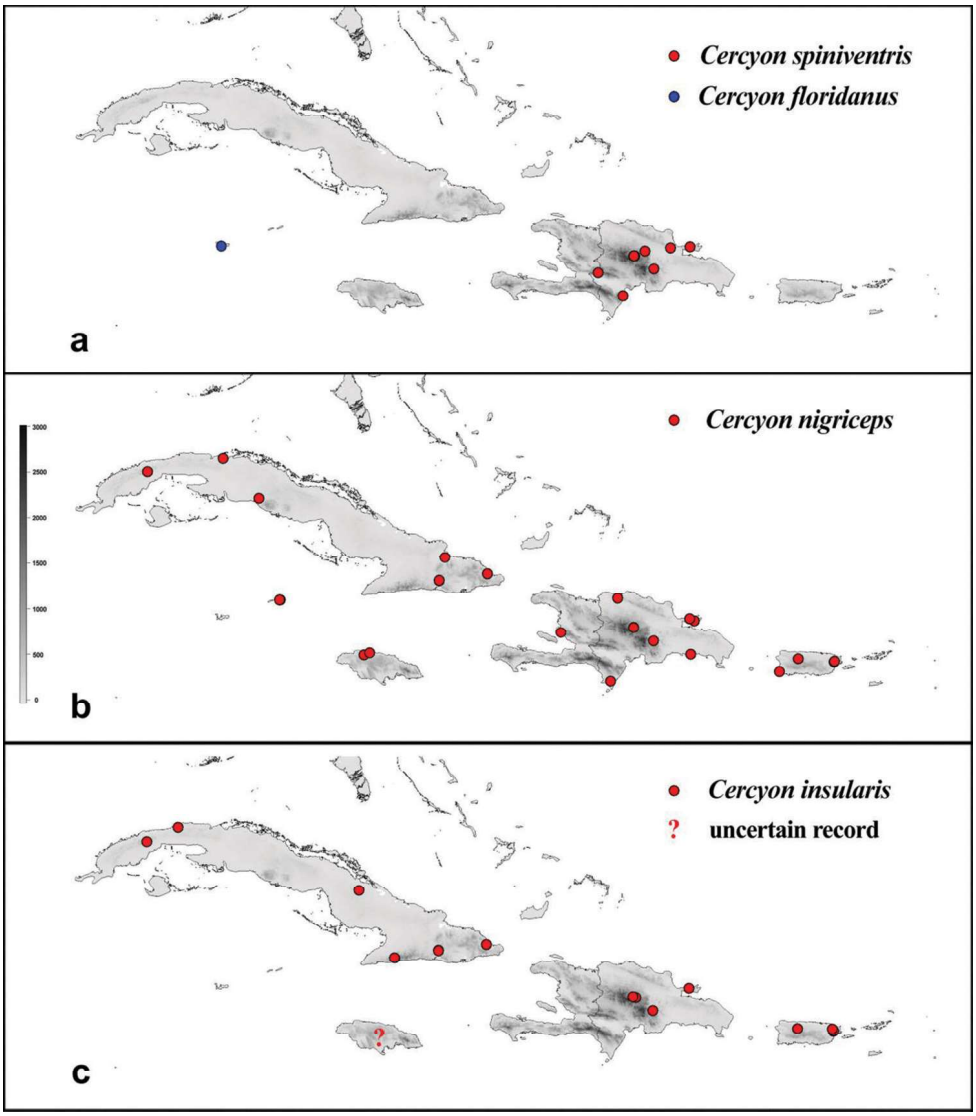

Figure 16. *Cercyon* spp. distribution map. **a** *Cercyon spiniventris* sp. n. (●) *Cercyon floridanus* Horn (●) **b** *Cercyon nigriceps* Marsham (●) **c** *Cercyon praetextatus* Say (●) *Cercyon insularis* Chevrolat (●).

right side from the setiferous emargination. Metanotum (Fig. 14g) with very narrow and weakly sclerotized transverse tergite. Legs (Fig. 14g) reduced into one-segmented setiferous tubercle. Membranous parts of thorax and abdomen covered by extremely short and dense whitish microtrichia. Abdominal segments (Fig. 14g–i) without lateral lobes, smooth (i.e. without transverse rows of tubercles) dorsally. Tergite on 8th abdominal segment (Fig. 14l) wider than long, shallowly sinuate on anterior margin, weakly sinuate on posterior margin.

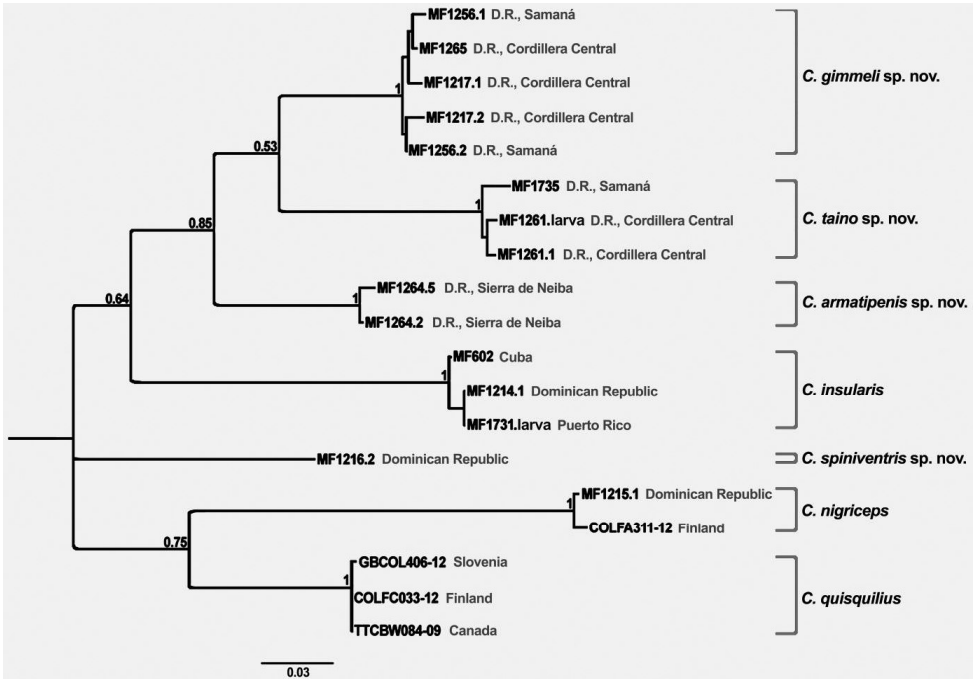

Figure 17. Maximum likelihood tree 1000 bootstrap replicates resulting from the phylogenetic analysis of DNA barcode of 19 specimens of *Cercyon* spp. Newly sequenced Caribbean specimens have the MF codes, other sequences are adopted from BOLD database.

Analysis of molecular data

Partial COI sequences of the 19 *Cercyon* specimens sampled resulted in a 610 bp alignment. JModelTest (Darriba et al. 2012) determined the GTR+I+G model as best nucleotide substitution model. The resulting maximum likelihood tree revealed 7 clades corresponding to the species as defined by morphological characters (Fig. 17). The statistical support for all species clades containing multiple specimens was high (bootstrap 100%), whereas the backbone of the phylogeny was poorly supported (bootstrap 53–85%), corresponding to the fact that we used a single marker with high substitution rate with limited information content for interspecific phylogeny, especially when introduced (and hence likely not closely related) species were included in the analysis. However, we recovered the *C. gimmeli* species complex as a well-supported monophyletic group, containing three well separated lineages (corresponding to the species as delimited by genital morphology) with mean interspecific distances 9–10 %. Sequenced females of the *C. gimmeli* species complex, morphologically not identifiable to species, were all unambiguously associated with male specimens and included as paratypes. *Cercyon insularis*, *C. spiniventris* and the introduced species were also revealed as well separated lineages in our analysis. The intraspecific genetic distances were low in all species for which multiple specimens were included, ranging between 0.0 to 1.4 %.

Larval specimens were unambiguously assigned to co-occuring adults in both cases (larva MF1261.L to *C. taino*, larva MF1731.L to *C. insularis*). The only sequenced specimen of *C. nigriceps* from Puerto Rico is genetically very similar to that of Finland (genetic distance 0.6 %) (See supplementary material 2).

Discussion

Faunal composition of *Cercyon* in the Greater Antilles. Our revision raises the number of *Cercyon* species from six to 10, and shows that the composition of the fauna largely differs from the original ideas: (1) five species, i.e. half of the fauna, are probably single-island endemics (four species in Hispaniola, one in Jamaica) and one additional species (*C. insularis*) seems to be a widespread Caribbean endemic not occurring in the mainland Americas; (2) only two species occurring in the Greater Antilles (*C. praetextatus* and *C. floridanus*) are native to the American continent, of which *C. floridanus* is moreover limited only to Cayman islands and does not occur in the four main islands of Greater Antilles; (3) two introduced Old World species (*C. nigriceps* and *C. quisquilius*) occur in the Greater Antilles, both of which are nowadays also widespread in the American continent (Smetana 1978; Fikáček 2009). The widespread continental *Cercyon variegatus* which was originally recorded from Jamaica and Puerto Rico by Smetana (1978) does not occur in the Caribbean Region at all, and is replaced there by morphologically very similar and likely closely related *C. insularis*.

The comparison of the original ideas about the *Cercyon* fauna and its real composition corresponds to the situation found in many other groups of minute arthropods, which were recently studied in the Greater Antilles. These studies frequently discover higher numbers of single-island endemics than expected, and reveal that some widespread continental species recorded from the Caribbean are in fact endemic species closely related but not identical to the continental ones (e.g., Dziki et al. 2015; Agnarsson et al. 2016).

The probable single-island endemics discovered during this study are distributed in Hispaniola (four species) and Jamaica (one species) only. No new species were discovered in Cuba and Puerto Rico, despite our collecting effort in both islands. Our field work in Puerto Rico was rather short and did not cover all mountain regions. Therefore, we cannot exclude additional discoveries in the island. On the other hand, our sampling effort was highest in Cuba, with intensive field work performed in 2010–2016. Hence we consider the discovery of a new endemic species in Cuba less likely. This puts in contrast Cuba, i.e. the largest Greater Antillean island, with no endemic species, with the smaller Hispaniola, hosting at least four single-island endemics. Moreover, the discovery of *C. armatipenis* sp. n. in a single locality in Sierra de Neiba at the Dominican-Haitian border indicates that additional species may be expected in this species complex in the western part of the island (i.e. Haiti) which was not sampled so far. In the same manner, there is a chance that the only species so far known exclusively from the Lesser Antilles, *Cercyon cribratus* Castelnau (1840), described from Guade-

loupe island, could be present in the Greater Antilles. However, we were not able to find any specimen fitting its description in the examined material.

Both the extremely similar morphology and results of the analysis of the COI sequences imply that the *C. gimmeli* species complex forms a monophyletic clade endemic to Hispaniola. The fact that all species of the complex occur sympatrically and no clear geographic pattern can be observed in their ranges suggests that the radiation of this group in Hispaniola may be a result of subdivision of Hispaniola in smaller paleoislands during the Oligocene to Middle Miocene followed by range expansion when the paleoislands got interconnected more recently (Iturralde-Vinent and MacPhee 1999; Iturralde-Vinent 2006; Matos-Maravi et al. 2014). The group would be hence a good model for a further more detailed biogeographic study.

Novel morphological characters. Morphological studies of the Greater-Antillean *Cercyon* revealed some characters of adults relevant to species discrimination and identification, but not used before: the presence/absence and shape of the projection of the anterior part of the prosternal medial ridge, and the sexually dimorphic characters of abdominal ventrites found in *C. spiniventris* and *C. sklodowskae*. Females of *C. spiniventris* are characterized by a spine-like process on the first abdominal ventrite (absent in males), which has not been recorded in any other *Cercyon* species so far, but is present in females of the Australian megasternine genus *Cercyodes* Broun (Hansen 1990). Females of *C. sklodowskae* are characterized by modified shape of the fifth abdominal ventrite (compared to simple one in males). We have observed the variation of the shape of the fifth ventrite also in some other *Cercyon* species (without checking their sex). Hence the sexual dimophism in this character may be more widespread than expected.

Interesting discoveries were also made by a brief examination of the larvae of *C. insularis* and *C. taino*. Both larvae are surprisingly quite different from each other, differing especially in the head proportions, extent of leg reduction, shape of the tergite of 8th abdominal segment, and surface vestiture membranous parts of thorax and abdomen. In all these characters, *C. insularis* is more similar to other *Cercyon* larvae described in the literature (*C. quisquilius* and *C. praetextatus*: Archangelsky 2016; *C. melanocephalus* and *C. haemorrhoidalis*: De Marzo 2000; *C. unipunctatus*, *C. pygmaeus* and *C. lateralis*: Schulte 1985). When examining the larval head of both *C. insularis* and *C. taino*, we found two circular areas of thickened transparent cuticle, one situated just in front of the ocular spot and another one just behind it (the areas are also visible as paler spots in lateral view of the head). We suppose that these areas of thickened cuticle may function as lenses. This character was never studied in sphaeridiine larvae and the only information about the ocular region available in the literature concerns the presence and shape of the pigmented "ocular spots": in larval Megasternini one spot is present, interpreted as an aggregation of all six stemmata or three anterior stemmata only (Hansen and Richardson 1998; Archangelsky 1999). Additional studies are needed to understand the function of this structure and its distribution in the Megasternini and Sphaeridiinae. One lens is present on each side of the head capsule of the larvae of *C. praetextatus* and the unidentified Japanese larvae of *Cercyon* (M. Archangelsky and Y. Minoshima, pers. comm. 2016), and two lenses (one before and one behind

the pigmented spot) are present on each side of the head of larval *Sphaeridium*, i.e. the sister-group to the tribe Megasternini (M. Archangelsky, pers. comm.).

The novel characters mentioned above of both adults and larvae are useful for diagnostic purposes, but can also have phylogenetic signal which will help to corroborate the results of the ongoing phylogenetic study of the tribe Megasternini. The differences found between the larvae of *C. insularis* and *C. taino* and the differences in the number of lenses between different megasternine taxa show that larval morphology of the Megasternini is not that uniform as previously believed, and is in need of more studies.

Subgeneric assignment of the Greater Antilles *Cercyon* species. All species treated in this paper fall into the concept of *Cercyon* sensu stricto. However, we refrain from assigning them to any subgenus since the systematics of the genus *Cercyon* and allies is currently under study, and previous studies have shown that *Cercyon* in the current concept may be a polyphyletic assemblage of species (e.g. Short and Fikáček 2013). Newly discovered characters of adults and larvae discussed above also indicate that *Cercyon* is much more morphologically heterogeneous than expected, which corresponds to its supposed polyphyly.

Author contribution

ADH, MF and MS performed the field work; EAV and MF accumulated additional museum material; EAV performed the majority of morphological studies, prepared the first draft and photodocumentation; EAV and MS did the molecular work, analysis of the data and prepared the data for submissions to BOLD; VS, MF and EAV prepared the datasets, wrote and tested the scripts, and submitted the data to BOLD, GBIF and Flickr; all authors commented drafts of the paper at different stages and helped with completing the manuscript for submission.

Acknowledgments

We greatly appreciate the help of all the curators who allowed us to work on the specimens held in their collections. Matthew L. Gimmel (Santa Barbara Museum of Natural History) in sincerely ackowledged for their contribution during the fieldwork performed in the Dominican Republic. This work was supported by the European Union's Horizon 2020 research and innovation program under the Marie Skłodowska-Curie grant agreement No. 642241 to M. Seidel and E. Arriaga-Varela, and the Ministry of Culture of the Czech Republic (DKRVO 2017/14, National Museum, 00023272) to Martin Fikáček. The work of the first three authors at the Department of Zoology, Charles University in Prague was partly supported by grant SVV 260 434 /2017. The Synthesys project. http://www.synthesys.info/ funded the stay of EA-V at the HNHM under the grant No. HU-TAF-6176.

References

Agnarsson I, LeQuier SM, Kuntner M, Cheng RC, Coddington JA, Binford G (2016) Phylogeography of a good Caribbean disperser: *Argiope argentata* (Aranea, Araneidae) and a new 'cryptic' species from Cuba. ZooKeys 625: 25–44. https://doi.org/10.3897/zookeys.625.8729

Archangelsky M (1999) Adaptations of immature stages of Sphaeridiinae (Staphyliniformia, Hydrophiloidea: Hydrophilidae and state of knowledge of preimaginal Hydrophilidae. Coleopterist Bulletin 53(1): 64–79.

Archangelsky M (2016) Chaetotaxy and larval morphometry of *Cercyon praetextatus* (Say) and *C. quisquilius* (Linnaeus) (Coleoptera: Hydrophilidae: Sphaeridiinae) and their phylogenetic implications. Arthropod Systematics & Phylogeny 74(2): 177–193.

Castelnau FLL de (1840) Histoire naturelle des Animaux articulés. Annelides, Crustaces, Arachnides, Myriapodes et Insectes. Histoire natlurelle des Insectes Coléoptères, Vol. 2. (Necrophages-Trimères). P. Dumenil, Paris, 565 pp.

Chevrolat A (1863) Coleopteres de l'lle de Cuba. Notes, synonymieset descriptionsd'especesnouvell es. Families des Cicindeietes, Carabiques, Dytiscides, Gyrinides et Palpicornes. Annales de la Societe entomologique de France (4)3: 183–210.

Darriba D, Taboada GL, Doallo R, Posada D (2012) jModelTest 2: more models, new heuristics and parallel computing. Nature methods (9): 772–772. http://dx.doi.org/10.1038/nmeth.2109

DeMarzo L (2000) Larve di coleotteri in detriti vegetali di origine agricola: lineamenti morfologici e presenza stagionale (Polyphaga: 20 famiglie). Entomologica (Bari) 34: 65-131.

Deler-Hernández A, Delgado JA (2010) Primer registro de *Enochrus* (*Lumetus*) *hamiltoni* (Horn, 1890) para Cuba (Coleoptera: Hydrophilidae) con datos sobre su hábitat. Revista de la Sociedad Colombiana de Entomología 36(2): 338–339.

Deler-Hernández A, Fikáček M, Cala-Riquelme F (2013a) A review of the genus *Berosus* Leach of Cuba (Coleoptera: Hydrophilidae). Zookeys 273: 73–106. https://doi.org/10.3897/zookeys.273.4591

Deler-Hernández A, Cala-Riquelme F, Fikáček M (2013b) Description of a new species of *Phaenonotum* from eastern Cuba (Coleoptera: Hydrophilidae: Sphaeridiinae). Acta Entomologica Musei Nationalis Pragae 53(2): 615–622.

Deler-Hernández A, Cala-Riquelme F, Fikáček M (2014) A review of the genus *Oosternum* Sharp of the West Indies (Coleoptera: Hydrophilidae: Sphaeridiinae). Deutsche Entomologische Zeitschrift 61: 43–63. https://doi.org/10.3897/dez.61.7566

Dziki A, Binford GJ, Coddington JA, Agnarsson I (2015) *Spintharus flavidus* in the Caribbean – a 30 million year biogeographical history of a 'widespread species'. PeerJ 3:e1422. https://doi.org/10.7717/peerj.1422

Fikáček M, Archangelsky M, Torres PM (2008) Primary chaetotaxy of the larval head capsule and head appendages of the Hydrophilidae (Insecta: Coleoptera) based on larvae of the genus *Hydrobius* Leach. Zootaxa 1874, 16–34.

Fikáček M (2009) Occurrence of introduced species of the genus *Cercyon* (Coleoptera: Hydrophilidae) in the Neotropical Region Revista de la Sociedad Entomológica Argentina 68(3-4): 351–357.

Gundlach J (1891) Constribucion a la entomología Cubana. Tomo III. A. Alvarez Comp., Habana, 404 pp.

Hansen M (1990) Australian Sphaeridiinae (Coleoptera: Hydrophilidae): A Taxonomic Outline with Descriptions of New Genera and Species. Invertebrate Taxonomy 4: 317–395. https://doi.org/10.1071/IT9900317

Hansen M (1999) World Catalogue of Insects 2: Hydrophiloidea (Coleoptera). Apollo Books, Stenstrup, 416 pp.

Hansen M, Richardson BA (1998) A new species of *Omicrus* Sharp (Coleoptera: Hydrophilidae) from Puerto Rico and its larva, the first known larva of Omicrini. Systematic Entomology 23: 1–8. https://doi.org/10.1046/j.1365-3113.1998.00036.x

Iturralde-Vinent MA (2006) Meso-Cenozoic Caribbean paleogeography: implications for the historical biogeography of the region. International Geology Review 48(9): 791–827. https://doi.org/10.2747/0020-6814.48.9.791

Iturralde-Vinent MA, MacPhee RDE (1999) Paleogeography of the Caribbean region: implications for Cenozoic biogeography. American Museum of Natural History Bulletin 238: 1–95.

Kumar S, Stecher G, Tamura K (2016) MEGA7: Molecular Evolutionary Genetics Analysis version 7.0 for bigger datasets. Molecular Biology and Evolution 33: 1870–1874. https://doi.org/10.1093/molbev/msw054

Leach WE (1817) The zoological miscellany. Vol. 3., R. P. Nodder, London. 151 pp, 121–150 pl.

Leng CW, Mutchler AJ (1914) A preliminary list of the Coleoptera of the West Indies as recorded to Jan. 1, 1914. Bulletin of the American Museum of Natural History 33(30): 391–493.

Leng CW, Mutchler AJ (1917) Supplement to preliminary list of the Coleoptera of the West Indies. Bulletin of the American Museum of Natural History 37: 191–220.

Makhan D (2004) Hydrochidae of the World, Dryopidae and Hydrophilidae (Coleoptera). Calodema 2: 11–26.

Matos-Maravi P, Águila RN, Peña C, Miller JY, Sourakov A, Wahlberg N (2014) Causes of endemic radiation in the Caribbean: evidence from the historical biogeography and diversification of the butterfly genus Calisto (Nymphalidae: Satyrinae: Satyrini). BMC Evolutionary Biology 14: 199. https://doi.org/10.1186/s12862-014-0199-7

Peck SB (2005) A checklist of the beetles of Cuba with data on distribution and bionomics (Insecta: Coleoptera). Arthropods of Florida and Neighbouring Land Areas 18: 1–241.

Peck SB (2006) The beetle fauna of Dominica, Lesser Antilles (Insecta: Coleoptera): diversity and distribution. Insecta Mundi 20: 165–209.

Peck SB, Thomas MC, Turnbow RH, Jr. (2014) The diversity and distributions of the beetles (Insecta: Coleoptera) of the Guadeloupe Archipelago (Grande-Terre, Basse-Terre, La Désirade, Marie-Galante, Les Saintes, and Petite-Terre), Lesser Antilles. Insecta Mundi 0352: 1–156.

Penev L, Mietchen D, Chavan V, Hagedorn G, Remsen D, Smoth V, Shotton D (2011) Pensoft data publishing policies and guidelines for biodiversity data. http://pensoft.net/J_FILES/Pensoft_Data_Publishing_Policies_and_Guidelines.pdf

de la Sagra R (1857) Historia física, política y natural de la isla de Cuba. Segunda parte. Historia Natural. Tomo VII. Crustaceos, aragnides é insectos. Arthus Bertrand, Paris, 371 pp.

Ryndevich SK (2004) New data on the distribution of American Hydrophilidae (Coleoptera). Latissimus, 18: 11–13.

Sautter G, Böhm K (2014) Improved bibliographic reference parsing based on repeated patterns. International Journal on Digital Libraries, 14(1–2): 59–80. https://doi.org/10.1007/s00799-014-0110-6

Schulte F (1985) Eidonomie, Ethökologie und Larvalsystematic dungbewohnender Cercyon-Species (Coleoptera: Hydrophilidae). Entomologia Generalis 11(1/2): 47–55. https://doi.org/10.1127/entom.gen/11/1985/47

Sharp D (1882) Insecta: Coleoptera. Vol. 1. Part 2 (Haliplidae, Dytiscidae, Gyrinidae, Hydrophilidae, Heteroceridae, Parnidae, Georissidae, Cyathoceridae, Staphylinidae). In: Godman FC, Salvin O (Eds) Biologia Centrali-Americana. Volume 16. Taylor & Francis, London, i–xv + 1–144.

Short AEZ (2005) Two new species of *Enochrus* Thomson, subgenus *Hugoscottia* Knisch, from Costa Rica and Mexico (Coleoptera: Hydrophilidae). Zootaxa 865: 1–7. https://doi.org/10.11646/zootaxa.865.1.1

Short AEZ, Fikáček M (2011) World catalogue of the Hydrophiloidea (Coleoptera): additions and corrections II (2006–2010). Acta Entomologica Musei Nationalis Pragae 51(1): 83–122.

Short AEZ, Fikáček M (2013) Molecular phylogeny, evolution and classification of the Hydrophilidae (Coleoptera). Systematic Entomology 38(4): 723–752. https://doi.org/10.1111/syen.12024

Short AEZ, Hebauer F (2006) World Catalogue of Hydrophiloidea – additions and corrections, 1 (1999–2005) (Coleoptera). Koleopterologische Rundschau 46: 315–359.

Smetana A (1978) Revision of the subfamily Sphaeridiinae of America north of Mexico (Coleoptera: Hydrophilidae). Memoirs of the Entomological Society of Canada 105: 1–292. https://doi.org/10.4039/entm110105fv

Spangler PJ (1981) Supplement to the aquatic and semiaquatic Coleoptera of Cuba collected by the biospeleological expeditions to Cuba by the Academies of Science of Cuba and Romania. Résultats des Expéditions Biospéologiques CubanoRoumaines à Cuba 3: 145–171.

Spangler PJ, Short AEZ (2008) Three new species of Neotropical Tropisternus Solier (Coleoptera: Hydrophilidae). Zootaxa 1917: 65–68.

Thomas MC, Turnbow RH Jr, Steiner W (2013) An annotated checklist of the Coleoptera (Insecta) of the Cayman Islands. Insecta Mundi 280: 1–56.

Thomson CG (1859) Skandinaviens Coleoptera. Vol. 1. Berlingska Boktryckeriet, Lund, 290 pp.

Wieczorek J, Bloom D, Guralnick R, Blum S, Döring M, Giovanni R, Robertson T, Vierglais D (2012) Darwin Core: An evolving community-developed biodiversity data standard. PLoS ONE, 7(1): e29715. https://doi.org/10.1371/journal.pone.0029715

Supplementary material 1

Darwin Core formatted distribution data

Authors: Emmanuel Arriaga-Varela, Matthias Seidel, Albert Deler-Hernández, Viktor Senderov, Martin Fikáček

Data type: species distribution

Explanation note: The Excel file includes all fields (columns) defined by the DarwinCore (DwC) format relevant to our data (headers highlighted in green) and ordered in a customized way (order of columns is not important, columns are identified by their header names that need to remain unchanged). We added a few fields (columns), which are not present in DwC, to include additional information needed in our case (about specimens in a DNA-tissue collection, DNA extracts done, and DNA barcodes), or to make the data input more convenient (two separate columns for starting and ending event dates, from which the date range in DwC format is formed and saved in the eventDate field); headers of all additional fields are marked in grey in Suppl. material 1.

Link: https://doi.org/10.3897/zookeys.681.12522.suppl1

Supplementary material 2

Genetic distances within and between species of Caribbean *Cercyon*

Authors: Emmanuel Arriaga-Varela, Matthias Seidel, Albert Deler-Hernández, Viktor Senderov, Martin Fikáček

Data type: molecular data

Explanation note: Mean genetic distances based on barcode CO1 sequences within (in grey fields) and between species (in white fields) calculated using the Maximum Composite Likelihood model as implemented in MEGA7. Standard error estimates (in square brackets) obtained by bootstraping (1000 replicates).@.

Link: https://doi.org/10.3897/zookeys.681.12522.suppl2

Supplementary material 3

DwC2BOLD script

Authors: Emmanuel Arriaga-Varela, Matthias Seidel, Albert Deler-Hernández, Viktor Senderov, Martin Fikáček

Data type: script

Explanation note: We used this script to automatically transform the DwC-formatted specimen data into the format required for the submission of specimen data to BOLD. The script uses the Barcode field (column) in our DwC spreadsheet to filter out the specimens that were barcoded and that need to be submitted to BOLD (notice that the Barcode field was added by us and is not a part of the DwC format!). Due to the slightly different data format used in DwC and BOLD, it is not possible to convert all information automatically, and the resulting BOLD-formatted data should be checked before submission. The script displays alerts for fields in which a mismatch between DwC and BOLD is possible. The script is available in Suppl. material 3 as a zip archive containing an R script, a PDF rendering and an HTML rendering.

Link: https://doi.org/10.3897/zookeys.681.12522.suppl3

Supplementary material 4

DwC2Map script

Authors: Emmanuel Arriaga-Varela, Matthias Seidel, Albert Deler-Hernández, Viktor Senderov, Martin Fikáček

Data type: script

Explanation note: The script reads the decimal GPS data from our DwC Excel file and creates a dataframe with all observations for each species. In the next step it allows to construct the maps of the area from freely available on-line data and map the occurrences of thes species on these maps. The maps in Figs 15–16 were generated using this script. The script is available in Suppl. material 4 as a zip archive containing an R script, a PDF rendering and an HTML rendering.

Link: https://doi.org/10.3897/zookeys.681.12522.suppl4

Chapter 2

A new genus of coprophagous water scavenger beetle from Africa (Coleoptera, Hydrophilidae, Sphaeridiinae, Megasternini) with a discussion on the *Cercyon* subgenus *Acycreon*

Arriaga-Varela, E., Seidel, M. and Fikáček, M., 2018. A new genus of coprophagous water scavenger beetle from Africa (Coleoptera, Hydrophilidae, Sphaeridiinae, Megasternini) with a discussion on the *Cercyon* subgenus *Acycreon*. *African Invertebrates*, 59, 1-23.

African Invertebrates 59(1): 1–23 (2018)
doi: 10.3897/AfrInvertebr.59.14621
http://africaninvertebrates.pensoft.net

RESEARCH ARTICLE

African Invertebrates
A journal of biodiversity research

A new genus of coprophagous water scavenger beetle from Africa (Coleoptera, Hydrophilidae, Sphaeridiinae, Megasternini) with a discussion on the *Cercyon* subgenus *Acycreon*

Emmanuel Arriaga-Varela[1,2], Matthias Seidel[1,2], Martin Fikáček[2,1]

1 *Department of Zoology, Faculty of Science, Charles University, Viničná 7, CZ-128 44 Praha 2, Czech Republic* **2** *Department of Entomology, National Museum, Cirkusová 1, CZ-193 00 Praha 9, Czech Republic*

Corresponding author: *Emmanuel Arriaga-Varela* (arriagavarelae@natur.cuni.cz)

Academic editor: *Y. Mutafchiev* | Received 20 June 2017 | Accepted 22 December 2017 | Published 11 January 2018

http://zoobank.org/3269C8DF-93AB-4B41-B19E-32CC863760E7

Citation: Arriaga-Varela E, Seidel M, Fikáček M (2018) A new genus of coprophagous water scavenger beetle from Africa (Coleoptera, Hydrophilidae, Sphaeridiinae, Megasternini) with a discussion on the *Cercyon* subgenus *Acycreon*. African Invertebrates 59(1): 1–23. https://doi.org/10.3897/AfrInvertebr.59.14621

Abstract

A new genus of coprophagous beetle, *Evanesternum* **gen. n.** (Hydrophilidae: Sphaeridiinae: Megasternini), is described in order to accommodate *Cercyon* (*Acycreon*) *pulsatus* d'Orchymont, 1937 from the Republic of South Africa and the Democratic Republic of Congo. A detailed description is provided along with habitus photographs, line drawings and SEM micrographs of relevant diagnostic characters. The new genus possesses the tribal synapomorphies of Megasternini but bears several unique morphological characters which are discussed in detail. The morphology of the remaining three species classified in the subgenus *Acycreon* d'Orchymont, 1942 (i.e. *C. punctiger* Knisch, 1921, *C. collarti* d'Orchymont, 1942 and *C. apiciflavus* Hebauer, 2002), is illustrated in order to provide evidence that *Acycreon* is an assemblage of morphologically dissimilar and likely not related species. An identification key to the Megasternini genera and subgenera known from the Republic of South Africa is presented.

Keywords

Cercyon, *Acycreon*, Afrotropical region, Republic of South Africa, Cape region, Democratic Republic of Congo, dung, morphology, new genus, new combination, subgenus, taxonomy

Introduction

Water scavenger beetles (Hydrophilidae) are mainly known as species associated with a wide variety of aquatic habitats; the majority of the species (ca. 65%) inhabit aquatic and semi-aquatic environments (Short and Fikáček 2011, Bloom et al. 2014). Aquatic species form the vast majority of the subfamilies Hydrophilinae, Chaetarthriinae, Enochrinae and Acidocerinae (Short and Fikáček 2013). However, more than a third of known hydrophilid beetles, mostly belonging to the subfamilies Cylominae and Sphaeridiinae, have colonised terrestrial habitats, typically those with large amounts of decaying organic matter (e.g. tropical forest leaf litter and rotten plant debris). Several groups are also associated with vertebrate dung (usually excrement from large herbivorous mammals) and many taxa are exclusively coprophagous. Dung provides an abundant and rich source of nutrients to a wide range of arthropods, with beetles being amongst them, along with Diptera, the most conspicuous and diverse. Hydrophilids, together with scarabs, are amongst the most important coprophagous beetles (Holter 2004).

The African continent is well known for its abundance of large mammal species, which in turn serve as a source of dung to be exploited. The diversity and abundance of large mammals (especially herbivores) likely promoted the diversification of beetle groups like scarab dung beetles and terrestrial hydrophilids of the subfamily Sphaeridiinae, which are both abundant and diverse in Africa (Davis and Scholtz 2001; Hebauer 2006). The tribe Megasternini is the most diverse group of hydrophilid beetles associated with terrestrial environments, comprising moreover the vast majority of obligatory coprophagous hydrophilid species. Seventeen genera are known to occur in Africa, of which *Cercyon* Leach, 1817, *Pachysternum* Motschulsky, 1863 and *Cryptopleurum* Mulsant, 1844 are especially species-rich. Nine small genera are endemic for the Afrotropical region: *Cercillum* Knisch, 1921 (Central and Southern Africa), *Cyrtonion* Hansen, 1989 (Central Africa), *Delimetrium* Hansen, 1999 (Republic of South Africa), *Parastromus* Balfour-Browne, 1948 (Central and Southern Africa), *Pelocyon* Balfour-Browne, 1950 (Central and Southern Africa), *Pseucyon* d'Orchymont, 1948 (Ethiopia), *Quadristernum* Balfour-Browne, 1950 (Rwanda-Burundi), *Acaryon* Hebauer, 2003 (Madagascar) and *Colerus* Hansen, 1999 (Madagascar). All of these are rare in collections and poorly known. They have rarely been mentioned after their description (Balfour-Browne 1948, 1950; Knisch 1921; d'Orchymont 1948) or have been described very recently (Hansen 1999b, Hebauer 2003) and few of them (*Colerus, Quadristernum*) are known only from one or a few specimens.

During the recent field work in the Cape region of the Republic of South Africa, the authors discovered a morphologically aberrant tiny representative of the Megasternini which represents an undescribed genus. The review of previously known South African species revealed that the species is already described, but misclassified as part of the subgenus *Acycreon* d'Orchymont, 1942 of the genus *Cercyon*. In this paper, the generic assignment of this species is re-evaluated, a new genus described for it, the morphology of the remaining species assigned at the moment to *Cercyon* (*Acycreon*) is reviewed and the taxonomic composition of this subgenus is discussed.

Materials and methods

This study is based on the specimens deposited in the following entomological collections:

MNRJ Museu Nacional, UFRJ, Rio de Janeiro, Brazil (B. Clarkson, M. L. Monné);
BMNH Natural History Museum, London, United Kingdom (M.V.L. Barclay);
CNIN Colección Nacional de Insectos, Instituto de Biología, Universidad Nacional Autónoma de México, Mexico City, Mexico (S. Zaragoza-Caballero);
FSCA Florida State Collection of Arthropods, Gainesville, USA (P. Skelley);
KMNH Kitakyushu Museum of Natural History and Human History, Kitakyushu, Japan (Y. Minioshima);
NHMW Naturhistorisches Museum, Wien (M. Jäch);
NMPC National Museum, Prague, Czech Republic (M. Fikáček);
RBINS Royal Belgian Institute of Natural Sciences, Brussels, Belgium (P. Limbourg);
SANC South African National Collection of Insects, Pretoria, Republic of South Africa (R. Staals);
SMNS Staatliches Museum für Naturkunde, Stuttgart, Germany (W. Schawaller);
TMSA Ditsong National Museum of Natural History, Pretoria, Republic of South Africa (formerly Transvaal Museum) (R. Muller);
ZMUC Zoological Museum, Natural History Museum of Denmark (A. Solodovnikov).

During the field work, about 15 kg of relatively fresh horse and cow dung was collected in a thick 60 litre plastic bag. The bag was closed and an air buffer was left above the excrement. The bottom of the bag was perforated with 1 cm holes using a knife. This bag was enclosed in another intact bag and hung above the ground in a shaded area. The beetles accumulated overnight in the second bag and were collected in 96% ethanol, without needing to check the excrement by hand.

Part of the specimens examined was dissected, with genitalia embedded in a drop of ethanol-soluble Euparal resin on a small piece of glass glued to cardboard attached below the respective specimen.

Habitus photographs were taken using a Canon D-550 digital camera with attached Canon MP-E65 mm f/2.8 1–5 macro lens. Pictures of genitalia were taken using a Canon D1100 digital camera attached to an Olympus BX41 compound microscope; pictures of different focus were combined in Helicon Focus software. Scanning electron micrographs were taken using Hitachi S-3700N environmental electron microscope at the Department of Paleontology, National Museum in Prague. Pictures used for plates were adapted in Adobe Photoshop CS6. All original pictures including additional views, not presented in this paper, are published and freely available on Flickr (https://www.flickr.com/photos/142655814@N07/sets/72157681650620964) and submitted to Zenodo repository (https://zenodo.org/) under https://doi.org/10.5281/zenodo.806765.

Results

***Evanesternum* gen. n.**
http://zoobank.org/20A0E313-3427-4049-89DF-0B80D8AEDCEE

Diagnosis. *Evanesternum* gen. n. can be distinguished from other members of the Megasternini by the following combination of characters: dorsal surface of head and protonum covered by granulose-reticulate microsculpture (Fig. 4d–e); anterior margin of mentum rounded (Figs 2b, 4b); gena with strong ridge parallel to posterior margin of eye (Fig. 4a); pronotum with broadly and deeply sulcate lateral margins (Fig. 4e); antennal grooves present, small, not reaching lateral margins of pronotum (Fig. 4c); middle portion of prosternum faintly demarcated from antennal grooves by a group of oblique wrinkled sulci (Fig. 4c); mesoventral plate broad, elliptical at base but abruptly vanished in anterior half (Fig. 4g); metaventrite without anterolateral arcuate lines and femoral lines, with very large median raised elevated area almost reaching lateral margins (Figs 3, 4h); male sternite 9 with lateral struts only reaching to half the length of the median projection (Fig. 1f).

Description. Body small, elongate-oval, weakly convex.

Head. Clypeus with anterior margin with fine bead-like protuberance, anteromedian margin straight medially, anterolateral corners rounded, antennal bases exposed (Fig. 4a); frontoclypeal suture distinct laterally, reduced medially; transverse ridges absent. Median portion of frons and clypeus not elevated above remaining surface. Whole dorsal surface with coarse transverse, moderately dense punctation, punctures bearing fine decumbent setae. Area between punctures with granulose-reticulate microsculpture (Fig. 4d). Eyes small, situated on lateral angular portions of head, with dorsal portion smaller than ventral one, separated by 6.8–7.5× the width of one eye in dorsal view, posterior margin with an additional ridge present along the posterior margin of eye, arising from its dorsolateral portion and reaching ca. half-way between eye and maxillary articulation ventrally (Fig. 4a). Labrum ca. 0.4× as wide as head, membranous, largely retracted under clypeus, weakly bisinuate on anterior margin, sparsely pubescent dorsally, setae longer on lateral portions (Fig. 2a). Mandible with apex simple, strongly curved, with external margin slightly crenulate in anterior half; prostheca with anterior third lobed and covered by thicker setae (Fig. 2c). Maxilla of male with sucking disc on galea; maxillary palps with basal palpomere minute, palpomere 2 large, widened apically, 1.2× as long as palpomere 3, palpomere 3 about as long as palpomere 4, slightly widening apicad, palpomere 4 fusiform, without digitiform sensilla (Fig. 2d). Mentum (Figs 2b, 4b) transverse, ca. 1.7× wider than long, lateral margins with few sparse setae, anterior margin rounded; labial palps trimerous, basal palpomere quadrate, palpomere 2 as long as and narrower than the basal one, with sparse long setae, terminal palpomere narrow, twice as long as the basal one. Submentum with few setiferous punctures, gular sutures vaguely developed, rather widely separated from each other, tentorial pits small, transverse. Antenna (Fig. 4a) with 9 antennomeres; scape long, cylindri-

cal, slightly curved medially; pedicel short, bulbous basally; antennomeres 3–5 short, subequal in length, antennomere 5 widened distad; cupule slightly asymmetrical, slightly shorter than antennomere 5; antennomeres 7–9 forming a weakly elongate pubescent club 1.3× longer than wide, antennomere 7 shortest, antennomeres 8–9 subequal in length, antennomere 9 round at apex; special sensorial antennal fields absent. Genal ridge absent.

Prothorax. Pronotum transverse, moderately convex, about as wide as bases of both elytra combined; lateral margins broadly sulcate; punctation uniform, consisting of coarse transverse punctures, bearing very small setae; punctures deeper and more rounded laterally. Prosternum (Fig. 4c) narrowly longitudinally carinate medially, weakly tectiform; prosternal process elongate, almost reaching posterior margin of procoxae, not bifurcate; prosternal portion anterior of procoxae moderately wide, with two or three oblique faintly defined wrinkled sulci on each side at mid-width. Procoxal cavities large, open posteriorly. Notosternal suture very short. Antennal grooves present, small, vaguely defined posteriad. (Fig. 3).

Mesothorax. Mesoventrite completely fused with an episternum; anterior collar of mesothorax narrow. Median portion of mesoventrite elevated as a mesoventral plate slightly overlapping anterior margin of metaventrite; plate well defined posteriorly as a broad, semi-elliptical tablet abruptly vanished in anterior half leaving only a narrow median ridge. Grooves for reception of procoxae well defined by a conspicuous carina, short, transverse (Fig. 4g). Mesepimeron very narrow, widening laterad. Mesocoxal cavities moderately narrowly separated. Scutellar shield small, semi-elliptical, 1.7× as long as wide. Elytra (Fig. 1a, b) weakly convex, narrowly explanate laterally, each elytron bearing 10 series, series 1–9 consisting of setiferous punctures as large as interval punctures but surrounded by a foveolate depression; punctures in series situated in longitudinal impressed sulci; series 1–4 and 9 reaching apex, series 5 and 8 enclosing series 6–7 subapically, series 10 reduced both anteriorly and posteriorly; epipleuron horizontal, weakly gradually narrowing posteriad, accentuating about half the length of metaventrite, vanishing shortly after the posterior margin of the metaventrite, bearing sparse short setae (Fig. 3).

Metathorax. Metaventrite (Fig. 4h) with anterior rim narrow, widening on anterolateral corners; mesal elevate area flat and very wide, almost reaching lateral margins; anterior and posterolateral corners distinctly rugose, with short setae. Femoral lines and anterolateral ridges absent. Metanepisternum ca. 5× as long as wide, with anterior oblique ridge, metepimeron with minute ventral portion. Metafurca well developed. Metathoracic wings well developed, with transverse vein r4 arising from basal portion of radial cell, RP rather long, reaching ca. halfway to wing base, basal cubito-anal cell small, closed, wedge cell absent, transverse vein mp-cua joining to MP_{3+4}+CuA_{1+2}; anal lobe not defined.

Legs. Procoxae large, subglobular, slightly transverse, with few setae, junction with trochanter; meso- and metacoxae broad, transverse. Tronchatero-femoral junction straight. Femora flattened, with small setae; profemur without impressed parts; metafemur just slightly longer than mesofemur (Fig. 3). Tibiae short, triangular, flat-

tened, with broad and relatively long lateral spines and mesal spines. Tarsi pentamerous, with moderately long tarsomeres (Fig. 3), each tarsomere with few stiff setae ventrally and a few fine setae dorsally; metatarsomere 1 slightly longer than tarsomere 2 and 3 together, tarsomeres 2–4 becoming continuously shorter, tarsomere 5 slightly shorter than tarsomere 1. Claws simple, arcuate; empodium bisetose.

Abdomen with five ventrites. Ventrite 1 with moderately high, broad median carina, briefly extending beyond posterior margin (Fig. 4i). Ventrites 2–5 without mesal carinae. Male sternite IX with tongue-like median projection with acute anterior margin and subtruncate posterior margin, lateral struts reaching half of the length of the median projection (Fig. 1f). Aedeagus (Fig. 1c–e) simple, median lobe subparallel-sided, phallobase long, symmetrical, with manubrium slightly asymmetrical; parameres simple. Female genitalia corresponding to that of *Kanala* (see Fikáček 2010).

Etymology. The generic name is derived from *evanescere* (Latin, "to vanish") and *sternum* (Greek, "chest") which refers to the anteriorly vanishing mesoventral plate. The gender is neutrum.

Type and only species. *Evanesternum pulsatum* (d'Orchymont, 1937), comb. n.

***Evanesternum pulsatum* (d'Orchymont, 1937), comb. n.**
Figs 1–5

Basionym: *Cercyon pulsatus* d'Orchymont, 1937: 248.

Figures on Flickr. https://www.flickr.com/photos/142655814@N07/albums/72157-681650620964

Material examined. Paratype: 'Afrika-Natal, Pietermaritzburg, Fort Napier 1919. Eing. Nr.36. 1926 // Comparé au type: + collze + : 1.55 × 0.82 m // A. d'Orchymont det. *Cercyon* s. str. *pulsatus* paratype // Paratype' (1: RBINS); Voucher specimens**:** Republic of South Africa, Western Cape: 'R. SOUTH AFRICA: W. Cape 6.3 km W Suurbraak; Summerset Getaway Farm at river-bank; 34°0.01'S 20°35.18'E; 110 m a.s.l.; 28.xi–2.xii.2015; Arriaga, Fikáček, Seidel & Vondráček lgt. RSA30a / in cow and horse dung in a farmland' (85 specimens: BCPC, BMNH, CNIN, FSCA, KMNH, NHMW, NMPC, SANC, TMSA, ZMUC); Eastern Cape: 'South Africa: Eastern Cape, Amathole District, Nxuba l.m. road to Fort Fordyce Nat Res. ex Excrement, 4–6.i.2015, 32.6906°S, 26.5031°E, P. Šípek & P. Malec' (1 male: NMPC) [DNA voucher MF1243]. Democratic Republic of Congo 'Congo Belge: Eala, V.1935, n°527 Sour excréments d'elephant, J. Ghesquière' (1 male: RBINS); 'Forêt de Kawa, 23.IV.29, A. Collart // A. d'Orchymont *Cercyon pulsatus*' (3: RBINS).

Description. *Body.* (Figs 1a–b, 3) 1.22–1.65 mm long; long oval, 1.9–2.0× as long as wide, widest at basal fourth of elytra; moderately convex, 3.0–3.1× as long as high. Integument dull, very weakly shining. Colouration of elytra light-brown, with mouthparts and legs dark reddish-brown and ventral surfaces black. Vestiture composed of minute decumbent setae.

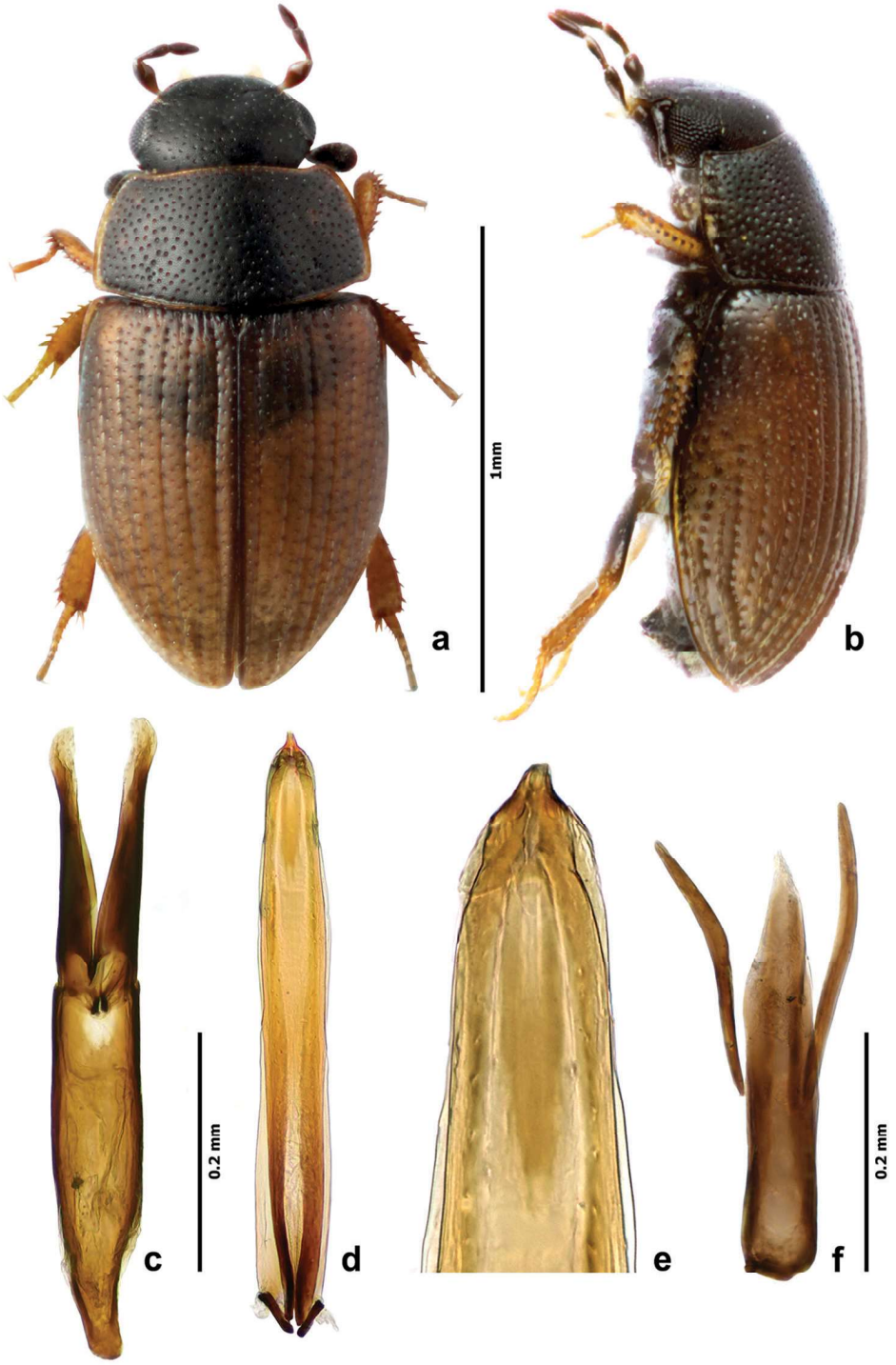

Figure 1. *Evanesternum pulsatum* (d'Orchymont) **a** dorsal habitus **b** lateral habitus **c** tegmen of aedeagus **d** median lobe of aedeagus **e** detail of apex of median lobe **f** 9th sternite.

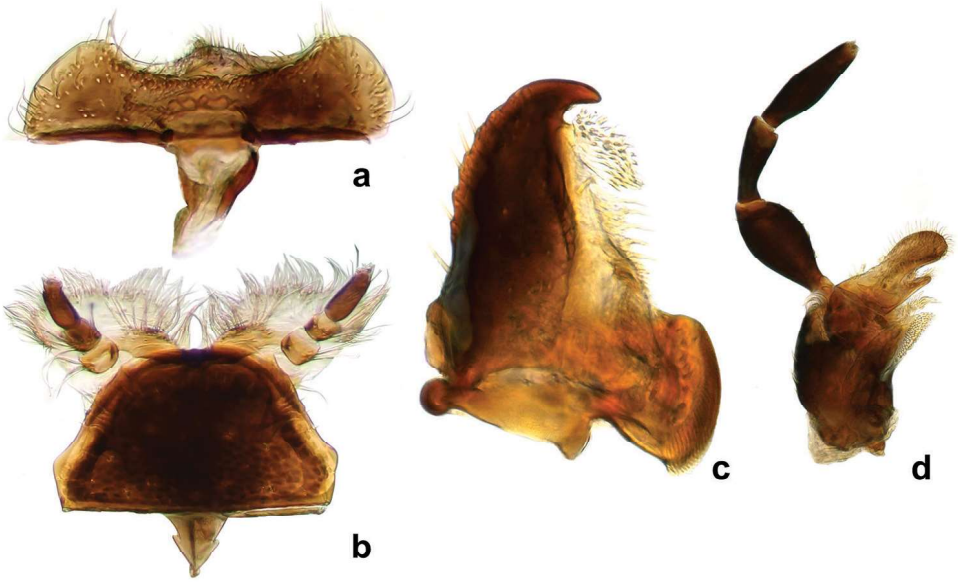

Figure 2. *Evanesternum pulsatum* (d'Orchymont) mouthparts **a** labrum **b** labium **c** mandible **d** maxilla.

Prothorax. Pronotum transverse, widest at base 1.9× wider than long; 1.45–1.50× wider at base than between anterior angles, 1.8× wider than head including eyes, as convex as elytra in lateral view. Prosternum weakly tectiform medially with anterior margin not thickened or projected ventrally (Fig. 4c). Antennal grooves distinct, weakly curved, open posteriorly (Fig. 3).

Mesothorax. Scutellar shield about 1.7× as long as wide, moderately densely punctured. Elytra widest at anterior fifth, 2.55–2.64× as long as pronotum, 1.1× as wide as pronotum, punctation composed of crescent-shaped setiferous punctures, larger on the longitudinal series; setiferous punctures present on all intervals (Fig. 4f). Surface between punctures micropunctate. Humeral bulge indistinct. Mesoventral plate semi-elliptical, abruptly vanished in anterior half leaving only a narrow median ridge (Fig. 4g).

Metathorax. Metaventrite (Fig. 4h) with raised area very wide, almost reaching lateral margins, about 1.5× as wide as long, rather roughly punctate, punctures transverse, resembling those on dorsal surfaces, with very small fine setae, surface finely squamose.

Legs. Tibiae robust, with moderately large spines. Metatibiae flattened and short, straight, 0.26–0.28× as long as elytron, 2.9-3.2× as long as wide (Fig. 3). Metatarsi moderately long, 0.85-0.90× as long as metatibiae, with short and stout setae ventrally.

Abdomen with five ventrites. Ventrite 1 with median longitudinal carina present, slightly narrowing posteriad, briefly projecting posteriorly in both sexes (Fig. 4i); ventrite 5 with rounded apex in both sexes, with a group of longer setae on apex.

Genitalia. Median projection of sternite 9 (Fig. 1f) subtruncate apically, without subapical setae, median portion narrowing posteriorly, with posterior end distinctly acute, lateral struts joined at mid length of the median projection. Phallobase (Fig. 1c)

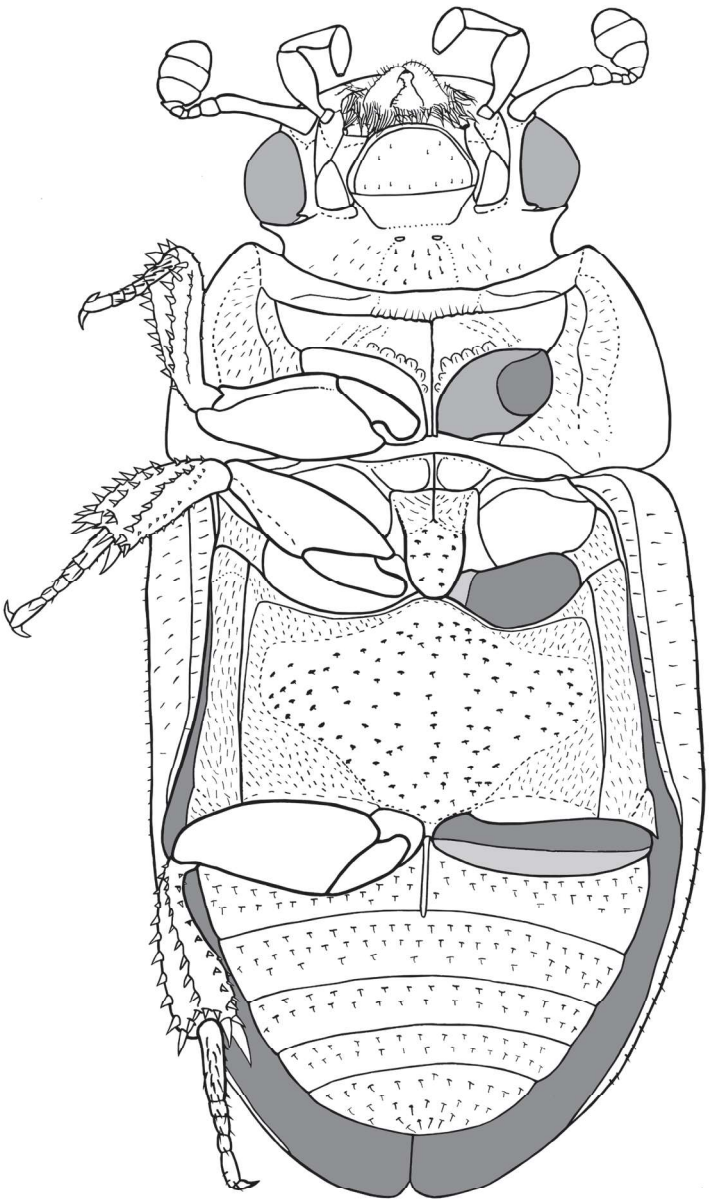

Figure 3. *Evanesternum pulsatum* (d'Orchymont) scheme of ventral morphology.

slightly longer than parameres, asymmetrically narrowing basally, base slightly curved. Parameres weakly narrowing apically, subsinuate and briefly widened near apex. Median lobe (Fig. 1d) narrow, parallel-sided throughout, apex acuminate, with small parallel apical projection, gonopore moderately large, situated subapically.

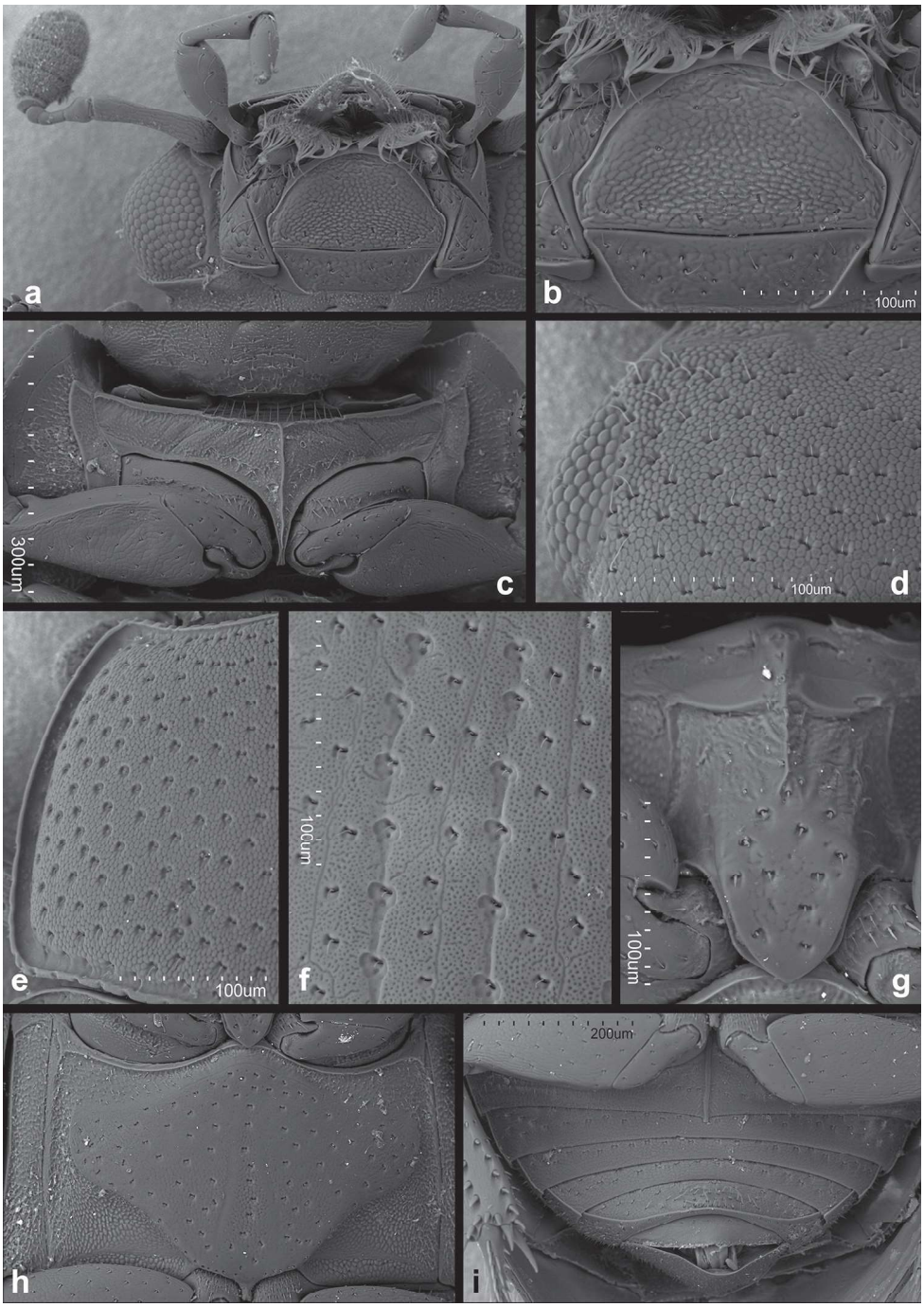

Figure 4. *Evanesternum pulsatum* (d'Orchymont) **a** ventral view of head **b** labium **c** prosternum **d** detail of head surface **e** detail of pronotal surface and lateral margin **f** detail of elytral surface **g** mesoventral plate **h** metaventrite **i** ventral view of abdomen.

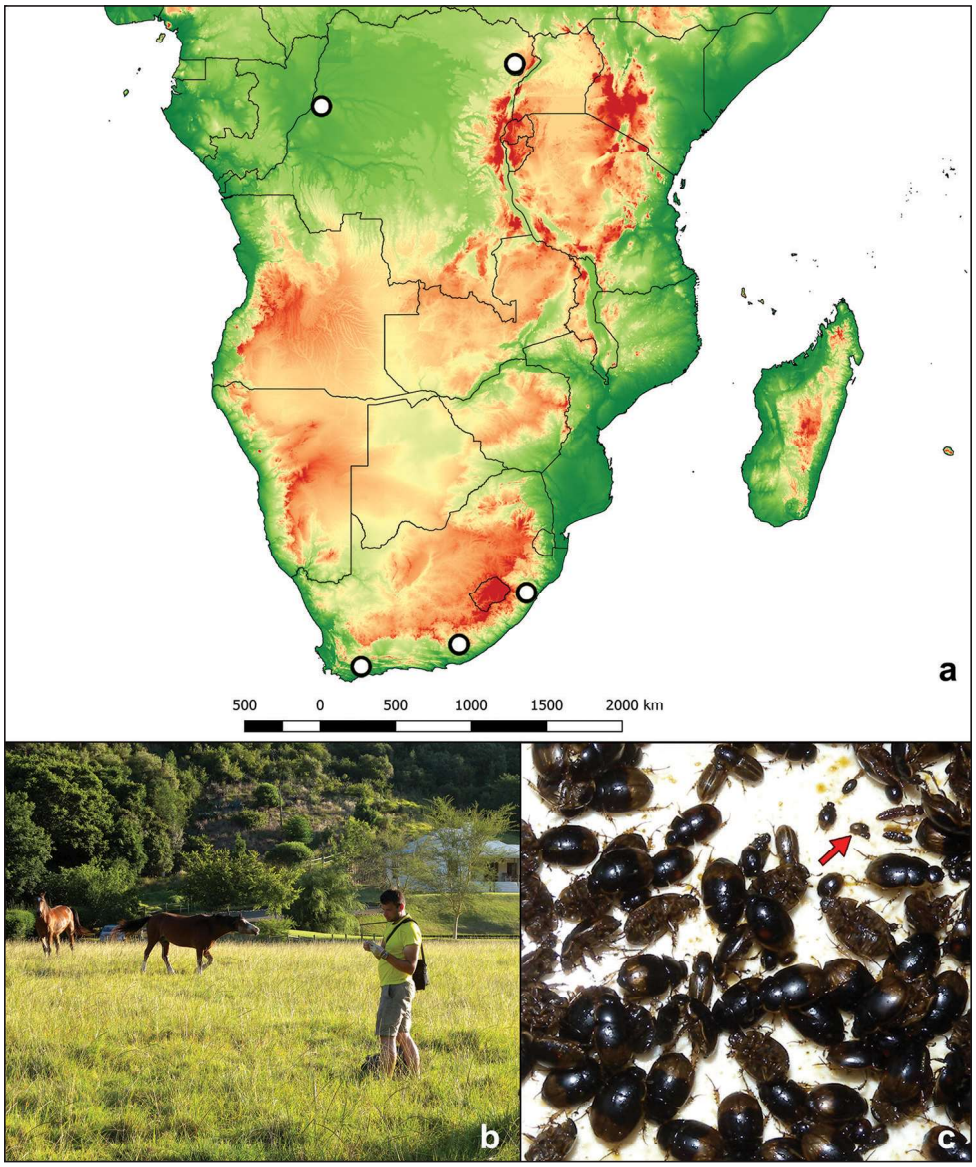

Figure 5. *Evanesternum pulsatum* (d'Orchymont) **a** distribution map **b** habitat collecting locality: Summerset Getaway Farm, Western Cape, Republic of South Africa **c** beetles collected from dung in Summerset Getaway Farm, Western Cape, Republic of South Africa. Red arrow is indicating an *Evanesternum pulsatum* (d'Orchymont) specimen.

Distribution. Known from southern Africa (Republic of South Africa: Eastern Cape, Western Cape, KwaZulu-Natal) and central Africa (Democratic Republic of Congo) (Fig. 5a).

Biology. Recently collected specimens from Western Cape were extracted from cow and horse dung in a small farm close to a river (Fig. 5b). Other hydrophilids from the same dung collected in abundance were *Sphaeridium caffrum* Castelnau, *S. abbreviatum* Boheman, *Pachysternum capense* (Mulsant) and three small *Cercyon* species (one belonging to the *Cercyon nigriceps* group and other two unidentified species). Other specimens examined were collected in unspecified type of dung while specimens from the Democratic Republic of Congo were collected from elephant excrement.

Key to the Megasternini genera and subgenera known from the Republic of South Africa

The key includes the genera recorded from the Republic of South Africa by Hansen (1999a) and Hebauer (2006). Due to unclear limits of *Cercyon* and *Parastromus*, the subgenera of *Cercyon* recorded from RSA are also included into the key to allow the identification of as many species as possible.

1 Prosternum with very large and deep antennal grooves reaching the lateral prothoracic margin **2**

– Antennal grooves either smaller, not reaching lateral prothoracic margin, or totally absent **3**

2 Mesoventral plate about as wide as long. Mentum at most slightly wider than long ..... ***Pachysternum***

– Mesoventral plate distinctly wider than long. Mentum much wider than long ..... ***Cryptopleurum***

3 Mesoventral plate truncate posteriorly, widely contacting metaventrite **4**

– Mesoventral plate acuminate or rounded posteriorly, at most narrowly overlapping the anterior margin of metaventrite, or contacting it in a single point **6**

4 Metaventrite without distinct femoral lines reaching its anterolateral corners ... . ***Pelosoma***

– Metaventrite with very distinct femoral lines, which reach its anterolateral corners **5**

5 Median portion of prosternum in form of an elevated plate, delimited from lateral portions by strong ridges ..... ***Pelocyon***

– Median portion of prosternum roof-like, not elevated as a whole and not delimited from lateral parts by strong ridges ..... ***Delimetrium***

6 Mesoventral plate widely rounded posteriorly, vanishing and indistinctly defined in anterior half. Median bare portion of metaventrite very wide, nearly reaching lateral margins. Male sternite 9 with lateral struts attached ca. at midlength ..... ***Evanesternum* gen. n.**

– Mesoventral plate pointed or rounded posteriorly with distinctly defined anterior part, or very narrow (lamellar). Median bare portion of metaventrite

never extended nearly to the lateral margins of metaventrite, at most moderately widened subanteriorly (in *Parastromus*). Male sternite 9 with lateral struts attached basally or subbasally 7

7 Mesoventral elevation in form of a well-defined plate of variable length and width **8**

– Mesoventral elevation in form of a longitudinal keel only... ***Cercyon* (*Paracycreon*)**

8 Anterolateral corners of metaventrite delimited from mesal portion by arcuate ridge ..... ***Cercyon* (*Arcocercyon*)**

– Anterolateral corners of metaventrite without such ridge **9**

9 Femoral lines of the metaventrite present, very distinct, reaching anterolateral corners of metaventrite ..... ***Cercyon* (s. str.)** (part: *C. nigriceps* group)

– Metaventrite without complete femoral lines; if remnants of them seem to be present posteriorly, they never reach anterolateral corners of metaventrite. 10

10 Pronotum very strongly convex, more convex than elytra in lateral view, very coarsely punctured ..... ***Parastromus***

– Pronotum not more convex than elytra in lateral view. Punctation of pronotum fine to moderately coarse ..... ***Cercyon* (s.str)** (part)

Cercyon (*Acycreon*) Orchymont, 1942

Acycreon Orchymont, 1942: 3.

Type species. *Cercyon punctiger* Knisch, 1921 (by original designation).

Cercyon (*Acycreon*) *punctiger* Knisch, 1921

Figs 6a–c, 7

Figures on Flickr. https://www.flickr.com/photos/142655814@N07/albums/72157690290894065

Material examined. Voucher specimens: 'Fort de Kock (Sumatra) 920 M., 1925, leg. E. Jacobson // Knisch det. 1925 *punctigerum* // A. d'Orchymont det. *Cercyon punctigerus* Knisch' (5: RBINS); 'Sumatra, D.E. Museum // Knisch det. 1925 *punctigerum*' (1: RBINS); 'Insel Sumbawa // Knisch det. 1925 *punctigerum* // Latcho, Tonkin, de Cooman // A. d'Orchymont det. *Cercyon punctigerum* Knisch' (1: RBINS); 'Pagsanjan, Luzon // A. d'Orchymont det. *Cercyon punctigerum* Knisch' (1: RBINS). 'India mer., Tamil Nadu, Nilgiri Hills, 15km SE of Kotagiri, Kunchappanai, 76°56'E 11°22'N; 900 m a.s.l.; 17–28.ix.1993, D. Boukal & Z. Kejval legt. // *Cercyon* (*Acycreon*) *punctiger* Knisch det. M. Fikáček 2012' (1: NMPC).

Re-description. 2.0–2.5 mm long, 1.8–1.9× as long as wide, 2.9–3.0× as long as high. Integument shining (Fig. 6a). Colouration reddish-brown with pale palpi. Eyes without thickened ridge at posterior margin (Fig. 7a.). Mentum subtrapezoid, with anterior mar-

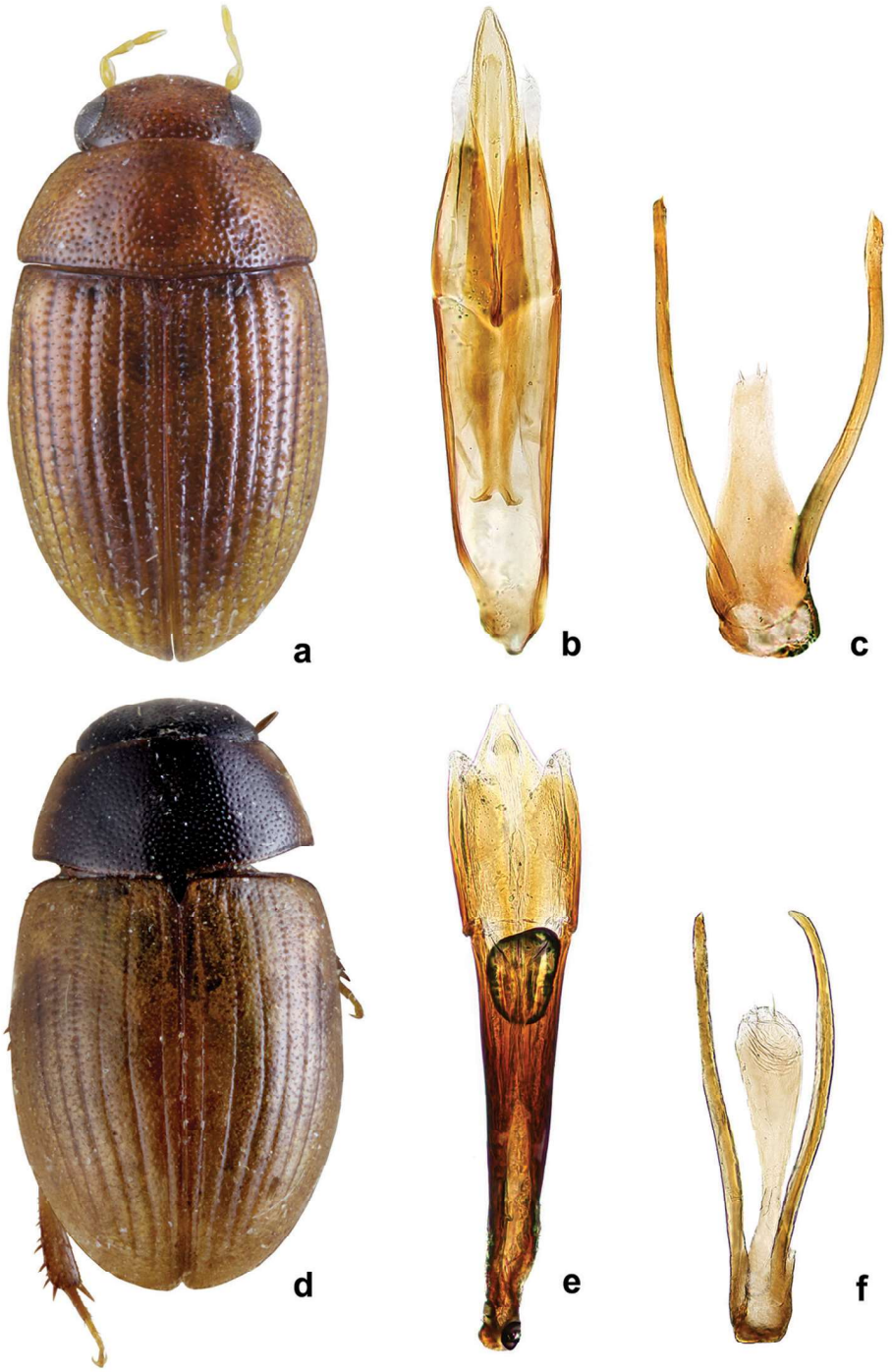

Figure 6. *Cercyon (Acycreon)* spp. **a–c** *Cercyon (Acycreon) punctiger* Knisch: **a** dorsal habitus **b** aedeagus **c** 9th sternite **d–f** *Cercyon (Acycreon) collarti* d'Orchymont paratype: **d** dorsal habitus **e** aedeagus **f** 9th sternite.

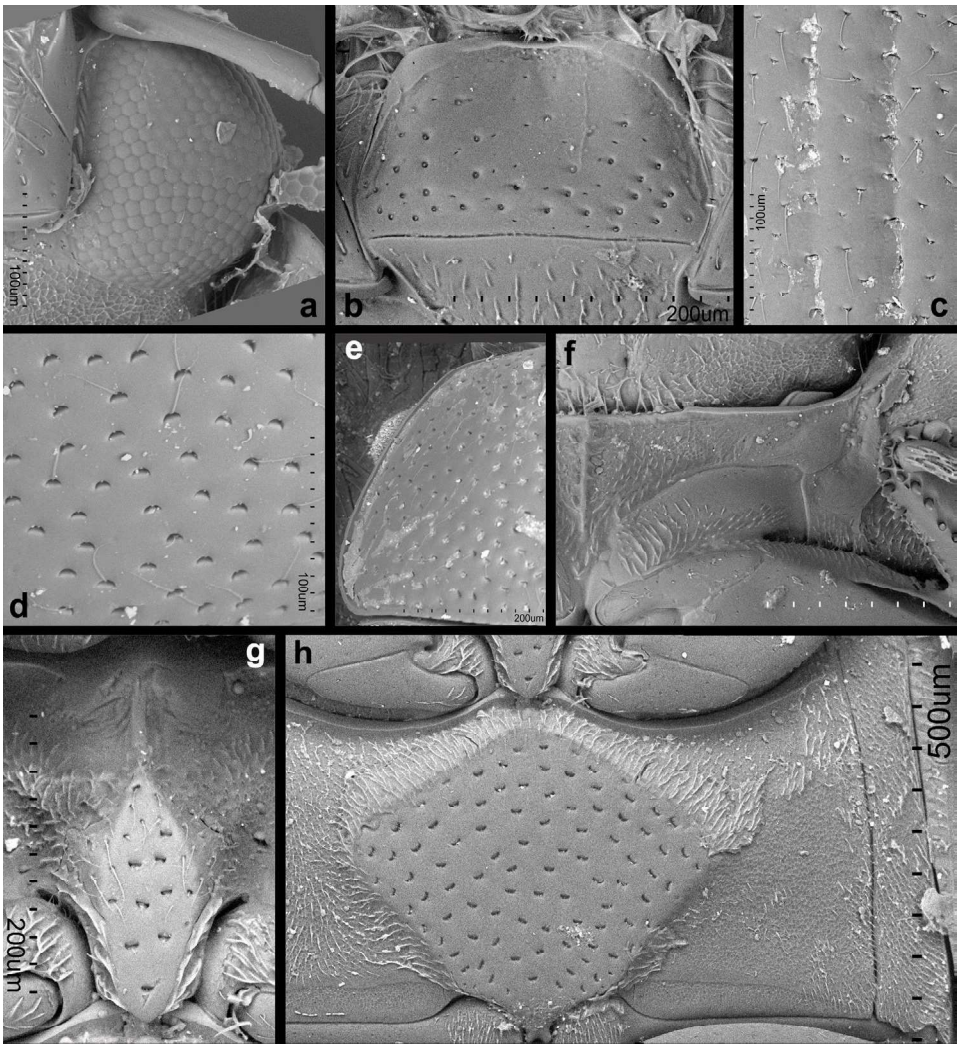

Figure 7. *Cercyon* (*Acycreon*) *punctiger* Knisch **a** ventral view of eye **b** labium **c** detail of elytral surface **d** detail of head surface **e** detail of pronotal surface and lateral margin **f** prosternum **g** mesoventral plate **h** metaventrite.

gin almost straight-lined (Fig. 7b). Pronotum with lateral margins moderately impressed (Fig. 7e). Pronotum and elytra deeply punctate without conspicuous microsculpture (Fig. 7c–d). Mesoventral elevation fusiform, short, not reaching anterior margin, procoxal rests not defined by transversal carinae (Fig. 7f). Raised portion of metaventrite about as long as wide, distinctly deeply punctate (Fig. 7h). Median lobe of aedeagus with parameres moderately broad, phallobase about 1.3× as long as parameres (Fig. 6b). Sternite 9 with median projection strongly narrowing anteriorly, lateral struts almost reaching base (Fig. 6c).

Distribution. Widespread Oriental species, recorded from Nepal, India, Sri Lanka, Vietnam, Singapore and Indonesia (Hansen 1999, Hebauer 2002).

***Cercyon* (*Acycreon*) *collarti* d'Orchymont, 1942**
Figs 6d–f, 8

Figures on Flickr. https://www.flickr.com/photos/142655814@N07/albums/72157689748012194

Material examined. Paratypes: 'Elisabethville, II-1940 // H.J. Brédo // Paratype' (2 males, 2 females, 6 unsexed: RBINS)

Re-description. 2.0–2.4 mm long, 1.9× as long as wide, 2.8–2.9× as long as high. Integument shining (Fig. 6d). Colouration of antennae, palpi, lateral margins of pronotum and elytra and legs yellowish-brown, with head, pronotal disc, prosternum, meso- and metaventrite and abdomen black. Eyes without thickened ridge at posterior margin (Fig. 8a) Mentum subtrapezoid, with anterior margin almost straight-lined (Fig. 8b). Pronotum with lateral margins narrowly and weakly impressed. Pronotum and elytra moderately punctate without conspicuous microsculpture (Fig. 8c–d). Mesoventral elevation fusiform, short, not reaching anterior margin, procoxal rests not defined by transversal carinae (Fig. 8f). Raised portion of metaventrite about as long as wide, moderately deeply punctate (Fig. 8g). Median lobe of aedeagus with parameres broad, short, phallobase about twice as long as parameres (Fig. 6e). Sternite 9 with median projection widening anteriorly, lateral struts reaching base (Fig. 6f).

Distribution. Only known from the Democratic Republic of Congo.

***Cercyon* (*Acycreon*) *apiciflavus* Hebauer, 2002**
Fig. 9

Figures on Flickr. https://www.flickr.com/photos/142655814@N07/albums/72157687839829212

Material examined. Holotype: 412 Sankhua Sabha Distr., Arun Valley betw. Mure and Hurure, mixed broad-leaved forest, 2050-2150 m a.s.l., 9-17 June 88, Martens & Schawaller // NEPAL-Expeditionen Jochen Martens // HOLOTYPUS *Cercyon apiciflavus* sp. n. det. Hebauer (1 female, SMNS).

Redescription. 1.8 mm long, 1.4× as long as wide, 2.4× as long as high. Integument shining (Fig. 9a). Colouration of head, pronotum, ventral surfaces and legs dark reddish-brown with pale palpi and antennae, elytra black with apex testaceous. Eyes without thickened ridge at posterior margin. Mentum subtrapezoid, with anterior margin straight-lined (Fig. 9b). Pronotum with lateral margins narrowly impressed (Fig. 9e). Pronotum and elytra deeply punctate without conspicuous microsculpture (Figs 9d–e). Mesoventral elevation fusiform, short, not reaching anterior margin, procoxal rests defined by oblique carinae, with a deep setose pore on each side of the mesoventral elevation (Fig. 9g). Raised portion of metaventrite about as long as wide, distinctly deeply punctate (Fig. 9h).

Distribution. Only known from the type locality in Nepal.

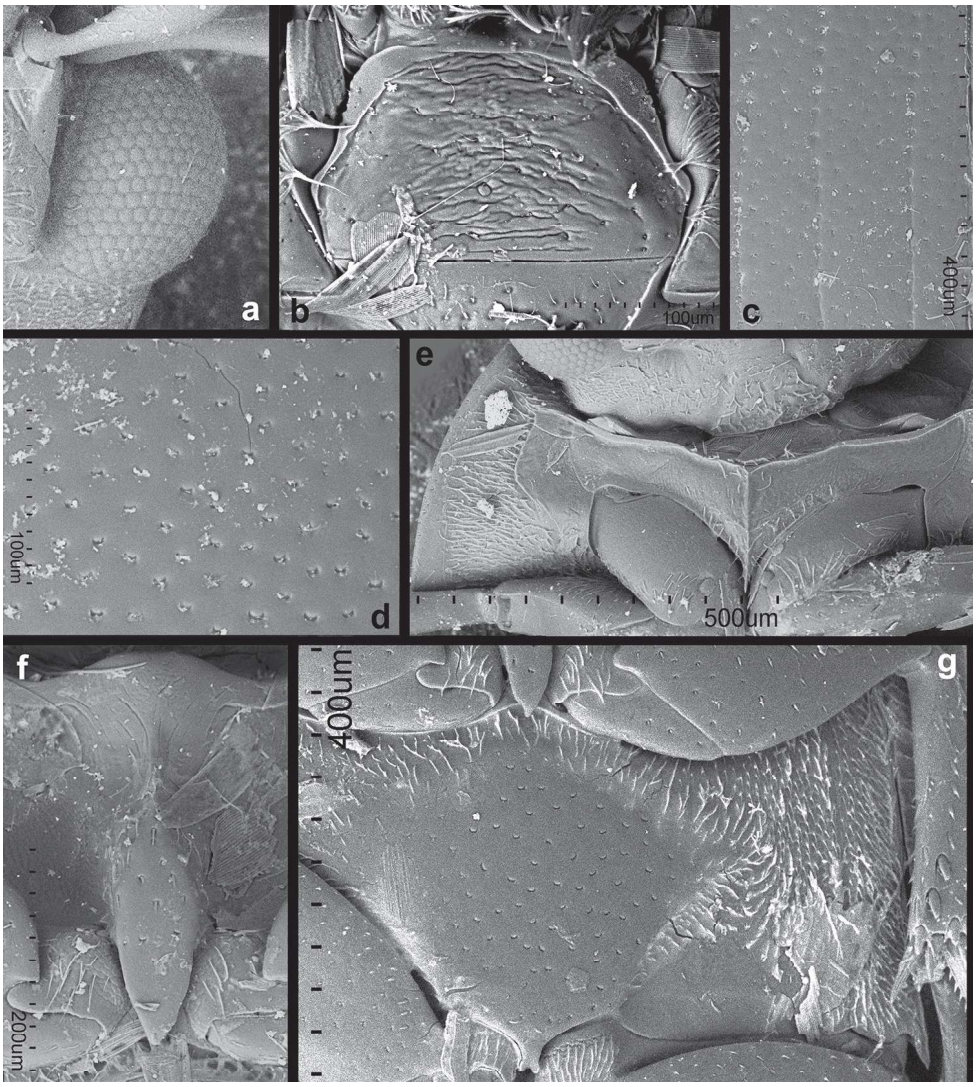

Figure 8. *Cercyon* (*Acycreon*) *collarti* d'Orchymont **a** ventral view of eye **b** labium **c** detail of elytral surface **d** detail of head surface **e** prosternum **f** mesoventral plate **g** metaventrite.

Comments. The species differs from the remaining two *Acycreon* species in the rather globular and widely rounded body. In these aspects, as well as in the morphology of the ventral parts of thorax, it is very similar to several undescribed species from the Chinese provinces, Yunnan and Sichuan (S. Ryndevich, in prep.). The deep, rounded setose pores on the mesoventrite on the side of the central elevation have not been recorded in any other *Cercyon* species and, along with the other morphological features of this species, suggest its distant relation to the type species of *Acycreon* subgenus.

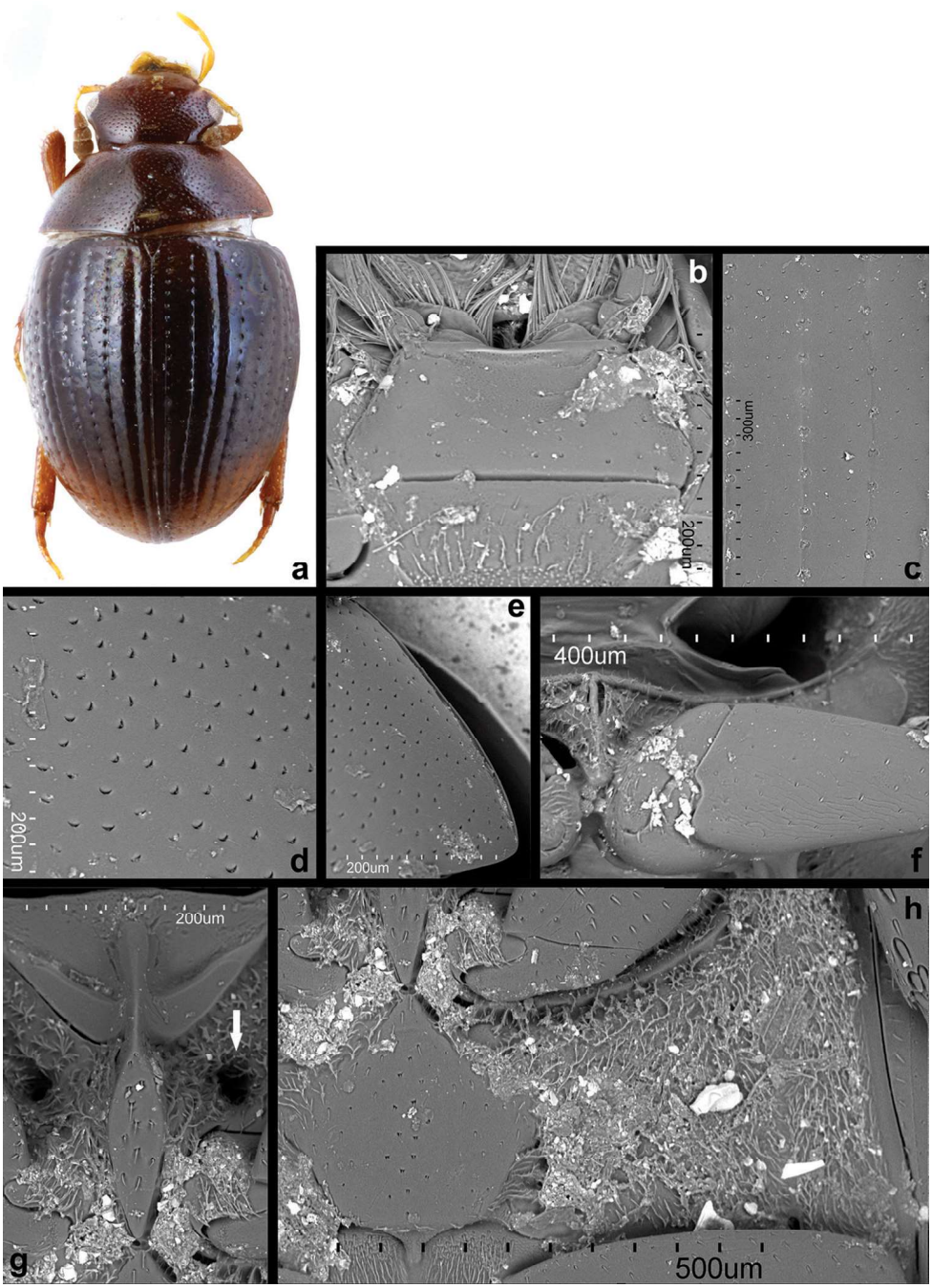

Figure 9. *Cercyon* (*Acycreon*) *apiciflavus* Hebauer **a** dorsal habitus **b** labium **c** detail of elytral surface **d** detail of head surface **e** detail of pronotal surface and lateral margin **f** prosternum **g** mesoventral plate (arrow pointing to the setose pore) **h** metaventrite.

Discussion

Cercyon is the largest genus of the tribe Megasternini, comprising over 260 described species (Short and Fikáček 2011). Eleven subgenera are considered valid at the moment: *Cercyon* (s.str.) Leach, 1897, *Acycreon* d'Orchymont, 1942, *Clinocercyon* d'Orchymont, 1942, *Oedocercyon* d'Orchymont, 1942, *Paracycreon* d'Orchymont, 1942, *Dicyrtocercyon* Ganglbauer, 1904, *Prostercyon* Smetana, 1978, *Paracercyon* Seidlitz, 1888, *Arcocercyon* Hebauer, 2003, *Conocercyon* Hebauer, 2003 and *Himalcercyon* Hebauer, 2002 (Hansen 1999a, Short and Hebauer 2006) and five more were proposed by previous authors but later synonymised with *Cercyon* s. str. (Hansen 1999a). *Acycreon* was described by d'Orchymont (1942) as a subgenus of *Cercyon* characterised by the median part of the mesoventrite not forming a complete plate-like elevation (mesoventral plate), as in most *Cercyon* subgenera, but an elongated protuberance which is carinate anteriorly and wider posteriorly (in contrast to completely carinate in the subgenus *Paracycreon* d'Orchymont, 1942, the only other subgenus without plate-like mesoventral elevation). Based on these characteristics, d'Orchymont (1942) included two species into the subgenus: the Oriental *C. punctiger* Knisch, 1921 (as type species) and the central African *C. collarti* d'Orchymont, 1942. Later, Hansen (1999) assigned *Cercyon pulsatus* (here transferred to *Evanesternum* gen. n.) in *Acycreon*, likely based on the fact that this species was mentioned as a species with 'some affinity' to *C. punctiger* in the original description. Hebauer (2002) largely followed d'Orchymont (1942) in the diagnosis of *Acycreon*, only adding that the mesoventral elevation is at least 'partly table-shaped beneath [= posteriorly]'. With some doubts, he assigned the Nepalese *C. apiciflavus* Hebauer, 2002 into *Acycreon*, indicating that it "passes over from the subgenus *Cercyon* to *Acycreon*" on the morphology of the median part of the mesoventrite. By using this concept, *Acycreon* hence contained four species (two African and two Oriental) sharing the unique morphology of the mesoventral elevation.

Evanesternum pulsatum comb. n. differs from *C. punctiger* (type species of *Acycreon*) and the other two species in the following characters: (1) male 9th sternite with lateral struts attached ca. at midlength (Fig. 1f) (basally or sub-basally in *C. punctiger* and *C. collarti* (Fig. 6c, f), not known for *C. apiciflavus*); (2) rugose-reticulate dorsal integument of head and pronotum (Fig. 4d–e) (without any microsculpture in *Acycreon* (Figs 7c–d, 8c–d); (3) medial raised part of metaventrite nearly reaching lateral margin (Fig. 4h) (present only mesally and not reaching laterally in *Acycreon* (Figs 7h, 8g, 9h); (4) thickened ridge running along posterior ventral margin of eye (Fig. 4a) (without such ridge in *Acycreon* (Figs 7a, 8a); (5) procoxal rests of mesoventrite defined by sharp transverse ridges (Fig. 4g) (in *Acycreon* without such ridges (Figs 7g, 8f) or with oblique ridges (Fig. 9g)); (6) pronotum deeply impressed along lateral margin (Fig. 4e) (at most weakly impressed in *Acycreon*; *Evanesternum pulsatum* comb. n. was mentioned by d'Orchymont (1942) as having the lateral portion of the pronotum similar to that of *C. punctiger*, but the margin is much deeper and broader in *Evanesternum* (compare Fig. 3h with Figs 7e and 9e). The above-mentioned morphological differences between *Evanesternum pulsatum* comb. n. and the members of *Acycreon* are substantial and it is

believed that *E. pulsatum* is not congeneric with them. *Evanesternum* gen. n. may, at first sight, resemble the small-bodied African megasternine genera *Delimetrium*, *Pelocyon* and *Pseucyon* or the smaller-sized species of the genus *Cercyon* (e.g. *C. minax* Balfour-Browne). The simple prosternum (i.e. not elevated medially) easily distinguishes it from all these genera except *Cercyon*. *Evanesternum* would be keyed out as*Cercyon* in the key to genera by Hansen (1991), which remains to date the most comprehensive resource for identification of Megasternini. The new genus has all the diagnostic characters of Megasternini: antenna with compact club, maxilla of male with sucking disc on galea; prosternum with antennal grooves, first abdominal ventrite carinate medially. However, it can be distinguished from *Cercyon* (as well as other megasternine genera) by the following combination of characters: (1) the mesoventral plate well-defined only posteriorly, not properly demarcated anteriorly (always well-demarcated as a complete plate in *Cercyon*); (2) mesal bare portion of metaventrite extending far laterally, covering the majority of the metaventral surface (always confined to median portion of metaventrite in *Cercyon*); (3) pronotum with deep groove along the lateral margin (absent in *Cercyon*); and (4) the morphology of male sternite 9 with very short lateral struts attaching at mid-length of the medial sclerite (lateral struts long and attaching basally in *Cercyon* and all genera of the *Cercyon*-group of genera). The morphology of the male terminalia and surrounding structures (sternite 9, articulation of the median lobe and parameres) seems to be phylogenetically informative in Megasternini, corresponding to the clades recognised by molecular phylogenetic analyses (Short and Fikáček 2013, Arriaga-Varela unpubl. data). Hence, the very unusual morphology of male sternite 9 of *Evanesternum* may indicate its rather isolated position in the *Cercyon*-group of the Megasternini. Preliminary analyses of molecular data (Arriaga-Varela, in prep.) seem to support this hypothesis.

Despite the mesal portion of prosternum being flat in *Evanesternum*, it bears a very faint demarcation of the mesal part with respect to the lateral parts by irregular diagonal sulci. These sulci 'define' the mesal portion which can be also inferred from the differences in the sculpture on the posterior margin and from the long setae present on the anterior margin. The prosternum as found in *Evanesternum* may possibly represent an intermediate condition between the flat prosternum (as present, for example, in *Cercyon*) and the mesally demarcated and elevated one (as present in genera *Cryptopleurum, Cyrtonion, Delimetrium*, *Pachysternum, Pelocyon* and *Pseucyon* in Africa) or a highly reduced version of a mesally demarcated prosternum.

Of the valid subgenera, *Cercyon* s. str. contains the largest number of species (slightly over 200) which are morphologically very diverse, indicating that the subgenus is likely to be an artificial assemblage of species rather than a monophyletic group. The remaining ten subgenera were created to accommodate some morphologically aberrant *Cercyon* species. They contain many less species and since they were mostly defined by some unique characters of the meso- or metaventrite, they more likely represent monophyletic groups. Still, the delimitation of some of them is unstable, resulting in frequent changes in subgeneric assignments of some species. This confusion concerns especially the subgenera *Clinocercyon* d'Orchymont, 1942 defined by the oblique, rath-

er than horizontal epipleura, which contains a very diverse assemblage of species from the Old World, with some species repeatedly moved in and in and out (e.g. Ryndevich 2007) and *Conocercyon* Hebauer, 2003 defined by a shape of the postcoxal ridge of the metaventrite (originally described for a few species from Madagascar and Seychelles, with two eastern Palaearctic species assigned to it later: Hebauer 2003, Ryndevich 2007, Hoshina 2008). Three subgenera, *Himalcercyon* Hebauer, 2002, *Oedocercyon* d'Orchymont, 1942 and *Prostercyon* Smetana, 1978, are monotypic (containing only one species). The results of this review of the subgenus *Acycreon* corresponds to the situation observed in these subgenera, i.e. it seems that the subgenus is defined by a single (and moreover weakly defined) character which picks up superficially similar but likely not closely related species. It is however surprising that this problem also concerns *Acycreon*, i.e. one of the smallest subgenera of *Cercyon* and clearly indicates that even the small subgenera need to be carefully tested for monophyly in future molecular phylogenetic studies.

After the transfer of *C. pulsatus* to *Evanesternum*, *Acycreon* contains three species, *C.* (*A.*) *punctiger*, *C.* (*A.*) *collarti* and *C.* (*A.*) *apiciflavus*. The mesoventrite of all of them forms a well-defined fusiform plate with a well-marked acute anterior tip, the plate being however rather short, ca. half as long as the length of the mesoventrite. The similarity of all three species hence concerns the relative length of the mesoventral plate, rather than the absence of the plate-like elevation mentioned by previous authors. In all other aspects, the *Acycreon* species are not very similar to each other in terms of external and genital morphology (compare Figs 6a–f, 7a–h, 8a–g) which indicates that they are likely not closely related and potentially not forming a monophyletic group. The distribution of the species (Oriental region versus tropical Africa) is also congruent with this view. Hence, even after excluding *C. pulsatus*, *Acycreon* consists of quite dissimilar species and may still be an artificial rather than natural assemblage. The concept of *Acycreon* needs to follow the morphology of its type species (*C. punctiger*) and can be only adapted after the phylogenetic position of that species has been resolved.

Acknowledgments

The curators of the collections where the studied material is deposited is gratefully acknowledged. We are also grateful to Dominik Vondráček (National Museum, Prague) for his collaboration during the expedition to Western Cape province in 2015, to Petr Šípek (Charles University, Prague) for the donation of the specimen from Eastern Cape, to Prof. Enzo Perisinotto (Nelson Mandela Metropolitan University) and Jiří Šmíd (National Museum, Prague) for his help with the logistics of our field trip and to the authorities of CapeNature for providing access to protected areas under their control. This work was supported by the European Union's Horizon 2020 research and innovation programme under the Marie Skłodowska-Curie grant agreement No. 642241 to M. Seidel and E. Arriaga-Varela and by the Ministry of Culture of the Czech Republic (DKRVO 2017/14, National Museum, 00023272) to Martin Fikáček. The

work of the first two authors at the Department of Zoology, Charles University, Prague was partly supported by grant SVV 260 434 /2017. Finally, we are thankful to the reviewers and the subject editor for their comments that helped us to improve the final version of the manuscript.

References

Balfour-Browne J (1948) New East African Palpicornia. Annals and Magazine of Natural History (11)14: 817–833.

Balfour-Browne J (1950) Palpicornia. Exploration du Parc National Albert. Mission G. F. de Witte (1933–35) 63: 1–84.

Bloom D, Fikáček M, Short AEZ (2014) Clade age and diversification rate variation explain disparity in species richness among water scavenger beetle (Hydrophilidae) lineages. PLoS ONE 9(6): e98430. https://doi.org/10.1371/journal.pone.0098430

Davis ALV, Scholtz CH (2001) Historical vs. ecological factors influencing global patterns of scarabaeine dung beetle diversity. Diversity and Distributions 7: 161–174. https://doi.org/10.1111/j.1472-4642.2001.00102.x

Fikáček M (2010) Hydrophilidae: The genus *Kanala* Balfour-Browne (Coleoptera). In: Jäch MA, Balke M (Eds) Water Beetles of New Caledonia, Vol. 1. Monographs of Coleoptera 3: 365–394.

Hansen M (1991) The hydrophiloid beetles: phylogeny, classification and a revision of the genera (Coleoptera, Hydrophiloidea). Biologiske Skrifter 40: 1–368.

Hansen M (1999a) World Catalogue of Insects 2: Hydrophiloidea (Coleoptera). Apollo Books, Stenstrup, 416 pp.

Hansen M (1999b) Fifteen new genera of Hydrophilidae (Coleoptera), with remarks on the generic classification of the family. Entomologica Scandinavica 30: 121–172. https://doi.org/10.1163/187631200X00228

Hebauer F (2002) Hydrophilidae of Northern India and Southern Himalaya (Coleoptera: Hydrophilidae). Acta Coleopterologica 18(1): 2–72.

Hebauer F (2003) Review of the Malgassic *Cercyon*, with description of new species and a new genus (Coleoptera: Hydrophilidae). Acta Coleopterologica 19(2): 5–26.

Hebauer F (2006) Checklist of the Hydrophiloidea of Africa and adjacent archipelagos (Coleoptera: Epimetopidae, Georissidae, Helophoridae, Hydrochidae, Hydrophilidae, Spercheidae). Entomologische Zeitschrift 116: 19–36.

Holter P (2004) Dung feeding in hydrophilid, geotrupid and scarabaeid beetles: Examples of parallel evolution. European Journal of Entomology 101: 365–372. https://doi.org/10.14411/eje.2004.051

Hoshina H (2008) A new species of the genus *Cercyon* (Coleoptera: Hydrophilidae) from the Fukui Pref., Japan. Memoirs of the Research and Education Center for Regional Environment, University of Fukui 15: 1–7.

Knisch A (1921) Die exotischen Hydrophiliden des Deutschen Entomologischen Museums (Col.). Archiv für Naturgeschichte 85(1919), A(8): 55–88.

d'Orchymont A (1937) Contribution à l'étude des Palpicornia IX. Bulletin et Annales de la Société Entomologique de Belgique 77: 213-255.

d'Orchymont A (1942) Palpicornia (Coleoptera). Notes diverses et espèces nouvelles. III. Bulletin du Musée Royal d'Histoire Naturelle de Belgique 18(26): 1–20.

d'Orchymont A (1948) Report on the Palpicornia (Coleoptera), Mr. Omer-Cooper's Investigation of the Abyssinian Fresh Waters (Hugh Scott Expedition). Proceedings of the Zoological Society of London 117(1947–48): 716–741.

Ryndevich S (2007) Review of species of genus *Cercyon* Leach, 1817 of Russia and adjacent regions. III. Subgenera *Clinocercyon* Orchymont, 1942 and *Conocercyon* Hebauer, 2003 (Coleoptera: Hydrophilidae). Zoosystematica Rossica 15(2006): 315–320.

Short AEZ, Hebauer F (2006) World catalogue of Hydrophiloidea – additions and corrections, 1 (1999-2005) (Coleoptera). Koleopterologische Rundschau 76: 315–359.

Short AEZ, Fikáček M (2011) World catalogue of the Hydrophiloidea (Coleoptera): additions and corrections II (2006-2010). Acta Entomologica Musei Nationalis Pragae 51(1): 83–122.

Short AEZ, Fikáček M (2013) Molecular phylogeny, evolution and classification of the Hydrophilidae. Systematic Entomology 38(4): 723–752. https://doi.org/10.1111/syen.12024

Chapter 3

Review of the flower-inhabiting water scavenger beetle genus *Cycreon* (Coleoptera, Hydrophilidae), with descriptions of new species and comments on its biology

Arriaga-Varela, E., Wong, S.Y., Kirejtshuk, A. and Fikácek, M., 2018. Review of the flower-inhabiting water scavenger beetle genus *Cycreon* (Coleoptera, Hydrophilidae), with descriptions of new species and comments on its biology. *Deutsche Entomologische Zeitschrift*, 65, 99-115.

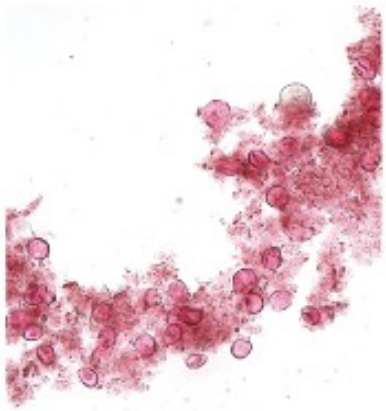

Dtsch. Entomol. Z. 65 (1) 2018, 99–115 | DOI 10.3897/dez.65.26261

PENSOFT

museum für naturkunde

Review of the flower-inhabiting water scavenger beetle genus *Cycreon* (Coleoptera, Hydrophilidae), with descriptions of new species and comments on its biology

Emmanuel Arriaga-Varela[1,2], Sin Yeng Wong[3,4,5], Alexander Kirejtshuk[6,7], Martin Fikáček[2,1]

1 *Department of Zoology, Faculty of Science, Charles University, Viničná 7, CZ-128 44 Praha 2, Czech Republic*
2 *Department of Entomology, National Museum, Cirkusová 1740, CZ-193 00 Praha, Czech Republic*
3 *Faculty of Resource Science & Technology, Universiti Malaysia Sarawak, 94300 Kota Samarahan, Sarawak, Malaysia*
4 *Harvard University Herbaria, 22 Divinity Avenue, Cambridge, MA 02138, USA*
5 *Ludwig-Maximilians-Universität München, Department Biologie I, Systematische Botanik und Mykologie, Menzinger Straße 67, 80638 München, Germany*
6 *Zoological Institute, Russian Academy of Sciences, Universitetskaya emb., 1, 199034 St. Petersburg, Russia*
7 *CNRS UMR 7205, Muséum national d'histoire naturelle, CP 50, Entomologie 45, rue Buffon, F-75005 Paris, France*

http://zoobank.org/4B756F25-162F-4FDA-BE04-60F397663847

Corresponding author: *Martin Fikáček* (mfikacek@gmail.com)

Received 28 April 2018
Accepted 6 June 2018
Published 12 June 2018

Academic editor:
James Liebherr

Key Words

Sphaeridiinae
Megasternini
flower visitor
Araceae
Schismatoglottideae
new species
Malay Peninsula
Borneo
Oriental Region
pollination

Abstract

The hydrophilid genus *Cycreon* Orchymont, 1919, previously known from two historical specimens only, is reviewed based on the numerous material collected recently from the inflorescences of various Araceae species in the Malay Peninsula and Borneo. Four species are recognized in the genus: *C. sculpturatus* Orchymont, 1919 from Sumatra, *C. armandi* Shatrovskiy, 2017 from Singapore, *C. adolescens* **sp. n.** from peninsular Malaysia, and *C. floricola* **sp. n.** with two subspecies, the nominotypical one from Peninsular Malaysia, and *C. floricola borneanus* **subsp. n.** from Borneo. All species are very similar, differing only by the pronotal punctation, shape of the clypeus and the mentum, and the form of the median lobe of the aedeagus. Specimens of *C. floricola* **sp. n.** and *C. adolescens* **sp. n.** were collected from inflorescences of various genera of the family Araceae. The field observations and analysis of mid gut contents indicates that they feed on organic material on internal organs of the inflorescences, including the pollen of the host plant. They were also observed to carry a large amount of pollen and are likely pollinators of their host species of Araceae.

Introduction

Among the water scavenger beetles (Polyphaga: Hydrophiloidea: Hydrophilidae), the members of the tribe Megasternini stand out in terms of species and morphological diversity, faster speciation rate and the wide array of microenvironments inhabited (Bloom et al. 2014; Fikáček et al. 2009, 2012). Most of the megasternine species are associated with various kinds of decaying organic matter, like mammal dung (e.g., Smetana 1978, Ryndevich 2008, Ryndevich et al. 2017, Arriaga-Varela et al. 2017, 2018), humid forest leaf-litter (e.g., Deler-Hernández et

al. 2015; Fikáček et al. 2009; Fikáček and Short 2006) or rotten seaweed (e.g., Smetana 1978; Ryndevich 2001). In contrast to this general pattern, few genera are known to inhabit the interior of various inflorescences: the Neotropical *Pelosoma* Mulsant has been collected inside *Heliconia* flowers (Archangelsky 1997), and the Neotropical *Nitidulodes* Sharp and Oriental *Cycreon* Orchymont, 1919 were recently reported to be associated to Araceae flowers (Bloom et al. 2014; Low et al. 2016; Hoe and Wong 2016; Hoe et al. 2018). However, very little is known about the biology and the systematics of these genera.

Only two specimens of *Cycreon* are known so far in the literature, representing two different species. The genus was described by d'Orchymont (1919) with *Cycreon sculpturatus* d'Orchymont, 1919 as the only species, based on a single female specimen collected in Palembang, Sumatra without any detailed collecting data. An additional male specimen from Singapore was later examined by d'Orchymont and labeled as '*Cycreon emarginatus* sp. n., however, whether is it not the male of *C. sculpturatus*', but never published. Both specimens were moreover on loan from d'Orchymont collection when M. Hansen was preparing a generic review of the hydrophiloid beetles (Hansen 1991). Shatrovskiy (2017) examined both these specimens and described the second specimen, male from Singapore, as *Cycreon armandi*.

Extensive sampling of insects associated with inflorescences of Malayan aroid plants was performed recently by Low et al. (2014, 2016), Hoe and Wong (2016) and Hoe et al. (2018) in order to study their pollination biology, and Takizawa (2010) in order to study the association of species of *Chaloenus* Westwood, 1861 (Chrysomelidae) with these inflorescences. As a result, a high number of *Cycreon* specimens from both Peninsular Malaysia and Borneo was accumulated. In this study, we use this material to redescribe and illustrate the genus *Cycreon* in detail, to revise the systematics of the genus, and to sum up the available data on the biology of the genus.

Material and methods

Examined specimens and depositories. A total of 1444 specimens of *Cycreon* were examined. Label data are reproduced verbatim; notes on the label data or additional information are written between square brackets []. List of examined specimens is available in DarwinCore-formatted spreadsheet file at Zenodo repository (https://doi.org/10.5281/zenodo.1258208). This file was also used to prepare the distribution map using QGIS software and freely available GLOBE altitude data and DIVA-GIS country borders data. The authors did not examine holotypes of *C. sculpturatus* and *C. armandi* as these are not accessible for the examination, and adopted the information about them from Shatrovskiy (2017). In addition, A. Shatrovskiy kindly provided a new photograph of ventral view of the head of *C. sculpturatus* used to illustrate the shape of the mentum of this species (Fig. 5P).

The examined specimens are deposited in the following collections:

BMNH Natural History Museum, London, United Kingdom (M.V.L. Barclay);
EIHU Hokkaido University Museum, Sapporo, Japan (M. Ôhara);
IBTP BORNEENSIS Collection, Institute for Tropical Biology and Conservation, Universiti Malaysia Sabah (P. Jimbau);
IRSNB Institute Royal des Sciences Naturelles de Belgique, Brussels, Belgium (P. Limbourg);
KMNH Kitakyushu Museum of Natural History and Human History, Kitakyushu, Japan (Y. Minoshima);
NHMW Naturhistorisches Museum, Wien, Austria (M. A. Jäch);
NMPC National Museum, Prague, Czech Republic (M. Fikáček);
SRBC Sergey Ryndevich collection, Baranovichy, Belarus;
ZIN Zoological Institute of the Russian Academy of Science, St. Petersburg, Russia (A.G. Kirejtshuk);
ZMHB Museum für Naturkunde der Humboldt-Universität, Berlin, Germany (J. Frisch, B. Jäger);
ZMUC Zoological Museum, Natural History Museum of Denmark (A.Yu. Solodovnikov).

Morphological studies. Specimens were dissected, with genitalia embedded in a drop of alcohol-soluble Euparal resin on a piece of glass glued to a small piece of cardboard attached below the respective specimen. Habitus photographs were taken using a Canon D-550 digital camera with attached Canon MP-E65mm f/2.8 1–5 macro lens. Pictures of genitalia were taken using a Canon D1100 digital camera attached to an Olympus BX41 compound microscope; combined pictures were were made with Helicon Focus software. Scanning electron micrographs were taken using Hitachi S-3700N environmental electron microscope at the Department of Paleontology, National Museum in Prague. Pictures used for plates were adapted in Adobe Photoshop CS6. All original pictures including additional views not presented in this paper are included in the dataset submitted to the Zenodo archive under doi 10.5281/zenodo.1258208.

All known species of *Cycreon* are very similar and share most structural characters. We therefore provide a generic description which includes shared morphological features, while the species descriptions are restricted mostly to species-specific characters.

Taxonomy

Cycreon Orchymont, 1919

Cycreon Orchymont, 1919: 119.

Types species. *Cycreon sculpturatus* Orchymont, 1919 (by original designation).

Diagnosis. (1) antennal grooves on prosternum small and marked by a weak ridge close to the lateral margins of prosternum (Fig. 2C–D); (2) mentum deeply excised anteromesally (Figs 1J, 2B, 5B, E, H, L, P) ; (3) mesoventral medial elevation reduced to a narrow carina (Fig. 2E–F); (4) grooves for reception of procoxae absent (Fig. 2E–F); (5) metaventrite without abdominal lines or demarcated anterolateral angles (Fig. 2E), (6) abdominal ventrite 1 not carinate medially (Fig. 2G); (7) aedeagus with the median lobe not fused to the bases of parameres, reaching into the phallobase; (8) median portion of male sternite 9 tongue-like (Fig. 3D, H, M).

Note. Orchymont (1919) mentioned the absence of antennal grooves, which were supposed by Hansen (1991) who did not have the chance to study specimens of this genus. Shatrovskiy (2017) revealed that antennal grooves are present although very small, and weakly marked by a faint ridge.

Differential diagnosis. *Cycreon* is distinct among Megasternini in lacking the median carina of abdominal ventrite 1 (Fig. 2G); in this character it only corresponds to the Megasternini genera *Pyretus* Balfour-Browne and *Acaryon* Hebauer. From *Pyretus*, *Cycreon* is easily diagnosed by the narrowly laminate elevation (in contrast to widely pentagonal and widely contacting metaventrite in *Pyretus*), simply carinate median portion of prosternum (forming an elevated prosternal plate in *Pyretus*), and small antennal grooves (antennal grooves are large and reaching lateral pronotal margin in *Pyretus*). The genus *Acaryon* from Madagascar is similar to *Cycreon* in many characters, including the relatively large eyes, simply carinate prosternum, antennal grooves not reaching pronotal margin, narrowly carinate elevation on mesoventrite, metaventrite without additional ridges, and dorsal punctation (with semicircular to circular punctures in *Cycreon*, and circular setiferous punctures intermixed with usual punctation in *Acaryon*). However, *Cycreon* can be distinguished from *Acaryon* by the shape of the mentum (deeply emarginate anteromedially in *Cycreon*, weakly sinuate on anterior margin in *Acycreon*), presence of the grooves for reception of procoxae at sides of the mesoventral elevation (absent in *Cycreon*, present in *Acaryon*) and the dorsal colouration (unicoloured or bicoloured in *Cycreon*, unicoloured yellow with dark central pronotal spot in *Acaryon*).

Description. Body (Fig. 1A–D) 2.2–3.4 mm long, elongate-oval, weakly convex. Colouration more or less reddish-brown, pronotum and underside usually somewhat paler (yellowish-brown), elytra usually darker.

Head. Clypeus with anterior margin with very fine bead, anteromedian margin slightly to strongly emarginate medially (Figs 1E, 5A, D, G, K, O), anterolateral angles rounded, antennal bases exposed; frontoclypeal suture distinct laterally, reduced in medial third; transverse ridges absent. Median portion of frons and clypeus not elevated above remaining surface. Dorsal surface glabrous, with dense punctation composed of shallow circular impressions (incomplete in some species), with a small puncture at anterior margin; interstices between punctures without visible microsculpture (Fig. 4A, D, G). Eyes moderately large, with dorsally visible portion slightly smaller than ventral one, separated by 4.9–5.5× the width of one eye in dorsal view. Labrum (Fig. 1I) ca. 0.4× as wide as head, membranous, largely retracted under clypeus, very weakly bisinuate at anterior margin, moderately densely pubescent dorsally, setae becoming longer on lateral portions. Mandible (Fig. 1F–H) with apex deeply bifid (teeth may be partially abraded in some specimens; compare Fig. 1F, G), curved; its external margin very weekly crenulate at basal half; prostheca with anterior third covered by long thin setae, distal group of these setae facing ventrally and proximal group of them facing mesally (Fig. 1H); mola with fine lamellae having poriferous structure. Maxilla of male with sucking disc on galea (Fig. 2B); maxillary palps with basal palpomere minute, palpomere 2 large, widened at apical half, 1.2× as long as palpomere 3, palpomere 3 slightly shorter than palpomere 4, slightly widening apicad, palpomere 4 fusiform, without digitiform sensilla. Mentum (Figs 1J, 2B, 5B, E, H, L, P) transverse, about twice as wide as long, lateral margins with few sparse setae, anterior margin very deeply emarginate; labial palps trimerous, palpomere 1 transverse, palpomere 2 subequal in width but slightly longer than palpomere 1 and with few long setae, palpomere 3 narrow, slightly longer than palpomere 2. Submentum with moderately dense setiferous punctures, gular sutures vaguely developed, rather widely separated from each other, tentorial pits small, almost rounded. Antenna with 9 antennomeres; scape (antennomere 1) long, cylindrical, constricted medially; pedicel (antennomere 2) rather short, bulbous basally; antennomeres 3–5 short, subequal in length, antennomere 5 much wider than preceding ones; cupule slightly asymmetrical, as long as antennomere 5; antennomeres 7–9 forming an elongate pubescent club (2.2× longer than wide), antennomeres 7–8 subequal in length, antennomere 9 slightly longer, roundly subacuminate at apex; sensorial antennal fields absent. Genal ridge absent.

Prothorax. Pronotum transverse, moderately convex, about as wide as bases of elytra combined; lateral margins minutely bordered; anterior and posterior angles rounded (Fig. 1E); punctation dense, composed of shallow circular impressions with one small puncture at posterior margin, circular impression sometimes incomplete (Fig. 4B, E, H). Prosternum (Fig. 2C) weakly raised medially, with faint longitudinal carina; prosternal process short, almost reaching midlenght of procoxal cavities, not bifurcate; precoxal part short. Procoxal cavities large, open posteriorly. Notosternal suture distinct. Antennal grooves present, very short, vaguely defined by thin ridge parallel to lateral notosternal suture, vanishing posteriad (Fig. 2C–D).

Mesothorax. Mesoventrite completely fused with anepisternum; anterior collar of mesothorax narrow. Median portion of mesoventrite simply tectiform, elevation forming a ridge shortly overlapping anterior margin of metaventrite. Grooves for reception of procoxae absent

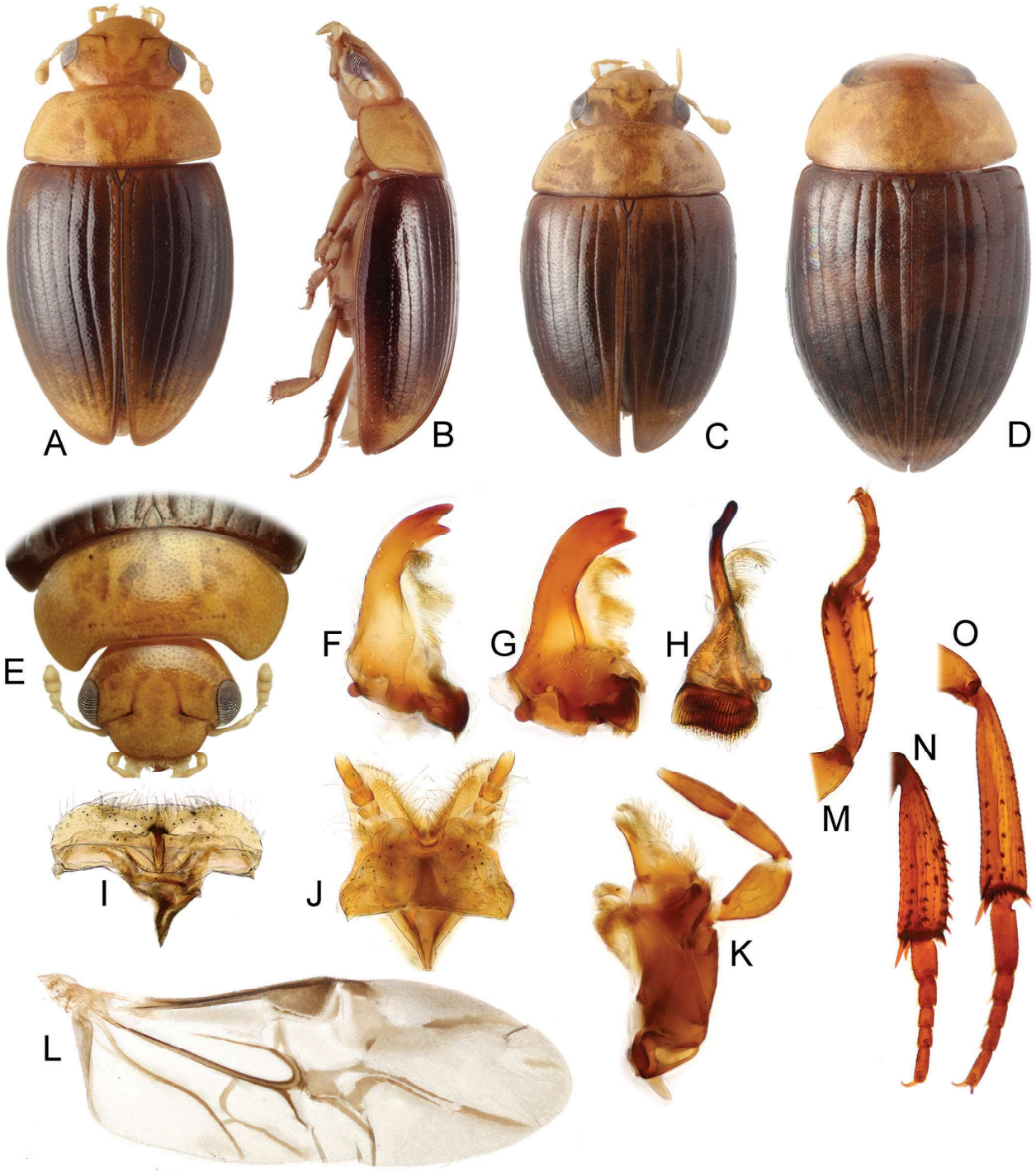

Figure 1. Habitus and morphology of *Cycreon* species. **A–D –** general habitus: **A–B –** *C. floricola floricola* ssp. n. (**A –** dorsal; **B –** lateral); **C –** *C. floricola borneanus* ssp. n., dorsal; **D –** *C. adolescens* sp. n., dorsal. **E–O –** morphology of *C. floricola floricola* ssp. n.: **E –** head and pronotum dorsally. **F–K –** mouthparts (**F –** mandible with unabraded apex; **G –** mandible with abraded apex; **H –** mandible, mesal view; **I –** labium; **J –** labrum; **K –** maxilla. **L –** metathoracic wing. **M–O –** tibiae and tarsi (**M –** prothoracic leg; **N –** mesothoracic leg; **O –** metathoracic leg).

(Fig. 2E–F). Mesepimeron moderately narrow, very weakly widening laterad. Mesocoxal cavities narrowly separated. Scutellar shield small, triangular, 1.1× as long as wide. Elytra weakly convex, weakly bordered laterally, each elytron bearing 10 series, series 1–9 consisting of foveate impressions (punctures) with a setiferous puncture on anterior margin (Fig. 4C, F, I); serial punctures situated in longitudinal sulci; series 1–4 and 9 reaching apex, series 5 and 8 enclosing series 6–7 subapically, series 9 and 10 fainter, series 10 reduced both anteriorly and posteriorly; epipleuron almost horizontal, gradually narrowing posteriad, vanishing behind level of posterior margin of metaventrite, bearing moderately dense short setae (Fig. 2E).

Metathorax. Metaventrite (Fig. 2E) with postcoxal line closely following posterior edge of mesocoxa and slightly deviating only in anterolateral angles; mesal elevate area flat and pentagonal, rather narrow, about as long as wide; lateral portions densely covered with short setae. Femoral lines and anterolateral ridges absent. Metanepisternum ca. 4.5× as long as wide, with anterior oblique ridge, metepimeron with minute ventral portion. Metafurca well developed. Hind wings (Fig. 1L) well developed, with transverse vein r4 arising from basal portion of radial cell, RP rather long, reaching ca. halfway to wing base, basal cubito-anal cell small, closed; wedge cell absent; transverse vein mp-cua joining to MP_{3+4}+CuA_{1+2}; anal lobe not defined.

Legs. Procoxae large, subglobular, transverse, with long setae, junction with trochanter; meso- and metacoxae wide, transverse. Tronchatero-femoral junction straight. Femora flattened, comparatively long, with very short setae; profemur without impressed parts; metafemur 1.1× as long as mesofemur (Fig. 1M–O). Tibiae rather long, triangular, flattened, straight or curved, especially on external margin, with short lateral and mesal spines. Tarsi pentamerous (Fig. 1N–O), tarsomeres densely covered by short stiff setae; metatarsomere 1 longer than metatarsomere 2 and 3 combined, metatarsomeres 2–4 continuously getting shorter, metatarsomere 5 about 0.4× than metatarsomere 1. Claws simple, arcuate; empodium bisetose.

Abdomen with five ventrites. Ventrite 1 without median carina (Fig. 1G), about as long as ventrites 2–4 together. Male sternite IX with tongue-like median projection with round to roundly acuminate anterior margin and rounded posterior margin, lateral struts almost reaching base of median projection (Fig. 3D, H, M). Aedeagus (Fig. 3A, E, J–K) simple; median lobe subparallel-sided to moderately sinuate, in *C. floricola* sp. n. enlarged basally and connected to phallobase by strong muscles; phallobase short, symmetrical to slightly asymmetrical, manubrium present, short; parameres simple. Female genitalia as in *Kanala* (see Fikáček 2010).

Key to the species of *Cycreon*

1 Clypeus strongly emarginated mesally (Figs 5K, O) 2
– Clypeus very weakly emarginated mesally (Figs 5A, D, G) 3
2 Pronotum with dense, completely ring-like impressions (punctures) (Fig. 5C); meso- and metatibiae straight (Fig. 5R) .... *C sculpturatus* d'Orchymont, 1919
– Pronotum with moderately dense, half-moon shaped impressions (punctures) (Fig. 5M); meso- and metatibiae curved (Fig. 5S) ..... *C. armandi* Shatrovskiy, 2017
3 Pronotum with completely circular impressions (punctures). Mentum less transverse, 1.7× as long as wide (5B), with anteromedial emargination reaching 1/5 of length, and with many ring-like impressions (punctures) in posterior half. Aedeagus with parameres about as long as phallobase; median lobe wide, bluntly pointed at apex (Fig. 3I–J) ..... *C. adolescens* sp. n.
– Pronotum with completely ciruclar or semicircular impressions (punctures). Mentum more transverse, 2.0× as long as wide (Figs 5E, H), with anteromedial emargination reaching 1/3 of length, and with few ring-like impressions (punctures) in posterior half. Aedeagus with parameres longer than phallobase; median lobe abruptly narrowed into a long acute tip at apex (Figs 3A–H). *C. floricola* sp. n. 4
4 Pronotum with incomplete ring-like impressions (punctures) only (Figs 4H, 5I) ..... *C. floricola floricola* spp. n.
– Pronotum with all or vast majority of impressions (punctures) in shape of complete rings (Figs 4E, 5F) .... *C. floricola borneanus* ssp. n.

Species accounts

***Cycreon sculpturatus* Orchymont, 1919**

Fig. 5O–R

Cycreon sculpturatus Orchymont, 1919: 121.
Cycreon sculpturatus: Shatrovskiy (2017: 589, redescription).

Type locality. Indonesia: South Sumatra: Palembang [ca. 2.9861°S, 104.7555°E].

Material examined. None (information adopted from Shatrovskiy 2017).

Diagnosis. *Cycreon sculpturatus* can be distinguished from other species of the genus by the deeply incised clypeus, pronotum densely covered with complete ring-like impressions (punctures) and straight meso- and metatibiae.

Addition to description. Body 2.6 mm long; colouration light reddish-brown, with slightly darker head and elytra; clypeus about 2.5× as wide as long, with anterior margin conspicuously emarginate medially (Fig. 5O); frons and clypeus with punctation composed of complete circular impressions (punctures); mentum (Fig. 5P) subtrapezoid, widest at posterior fifth, about 2.0× wider than long, anteromedian emargination reaching about 0.2× the mentum length; pronotum with dense and moderately deep punctation consisting of complete circular impressions with a small setiferous puncture in posterior part (Fig. 5Q), punctation of approximately same diameter and density all over pronotum; meso- and metatibiae straight (Fig. 5R); male genitalia unknown (because male remains unknown for this species).

Distribution. Only know by a single female specimen from the type locality (Indonesia, Sumatra, Palembang) (Fig. 7).

Remark. According to Shatrovskiy (2017) the proportions of the clypeus were given as 4× as long as wide, however, the picture in the paper (Shatrovskiy 2017: 591) shows that the ratio is about 2.5×.

Cycreon armandi Shatrovskiy, 2017

Figs 3K–M, 5K–M

Cycreon armandi Shatrovskiy, 2017: 589.

Type locality. Singapore.

Material examined. None (information adopted from Shatrovskiy 2017).

Diagnosis. *Cycreon armandi* can be distinguished from other known species by the deeply incised clypeus, the semicircular impressions (punctures) on the pronotum, and the curved meso- and metatibae.

Addition to description. Body 3.3 mm long; colouration completely light reddish-brown; clypeus about 2× as wide as long, anterior margin of clypeus strongly emarginate medially (Fig. 5K); frons and clypeus with small and not so closely disposed punctures; mentum (Fig. 5L) subtrapezoid, widest at posterior fifth, about 1.8× wider than long, with a deep anteromedian emargination reaching beyond the anterior fourth of length; pronotum with dense and shallow, punctation consisting of small setiferous half-moon shaped punctures (Fig. 5M); meso- and metatibiae curved (Fig. 5S); median projection of sternite 9 rounded apically (Fig. 3M); aedeagus (Fig. 3L) with phallobase 0.6× as long as parameres, almost symmetrical, manubrium narrow and very; parameres continuously narrowing towards apex; median lobe moderately wide (Fig. 3K), slightly constricted in apical fourth; apex acuminate, triagular.

Distribution. Only known from the type locality in Singapore (Fig. 7).

Remarks. According to Shatrovskiy (2017) the proportions of the clypeus are given as 3× as long as wide, however, the picture in the paper (Shatrovskiy 2017: 591) shows that the ratio is closer to 2.0×.

Cycreon adolescens sp. n.

http://zoobank.org/C6503E49-3440-4820-B671-D35E579D6247

Figs 1D, 3I–J, 4J, 5A–C

Type locality. Malaysia, Pahang, Genting Highland [ca. 3.4233°N, 101.7930°E].

Type material. Holotype (male, teneral specimen): "Malaysia, PAHANG / Genting Highland / 24.X.2012 / H. Takizawa" (IBTP). **Paratypes: MALAYSIA: Pahang:** [same data as holotype] (2 females: NMPC, KMNH).

Additional material examined. MALAYSIA: Pahang: Cameron Highlands, Tanah Rata, Robinson Waterfall [ca. 4.461778°N 101.38803°E], in flowers of Araceae, 15.iii.2015, H. Takizawa lgt. (5 females: EIHE, KMNH, NMPC).

Diagnosis. This species is most similar to *Cycreon floricola borneanus* ssp. n. in the very weakly emarginate anterior margin of the clypeus and pronotal punctation consisting of circular punctures, and straight meso- and metatibiae. It differs from the latter in the structure of the male genitalia (relatively longer phallobase and widely pointed apex of the median lobe) and by the less transverse mentum (1.7× wider than long), with many ring-like impressions in posterior half.

Description. *Measurements.* 2.4–3.0 mm long (length of holotype: 2.8 mm), 1.7× as long as wide, widest at basal fifth of elytra; weakly convex, 3.3–3.5× as long as high (height of holotype: 0.82 mm). *Colouration.* Light brown with slightly darker elytra (Fig. 1D).

Head. Clypeus about 2.4× as long as wide, with anterior margin of clypeus margin very weakly emarginate medially. Frons and clypeus with punctation composed of complete circular impressions (punctures) with a small setiferous puncture on anterior margin (Fig. 4A). Interocular distance about 5.5× the width of one eye in dorsal view. Mentum (Figs 4J, 5B) subtrapezoid, widest at posterior fifth, about 1.7× wider than long, with a moderately pronounced emargination reaching about the anterior fifth of mentum length; lateral angles weakly marked; surface with few sparse, moderately long setae in anterolateral angles, posterior half glabrous, punctures moderately large and deep, vanishing mesally, 11–13 punctures close to posterolateral angles with ring-like impressions (punctures).

Prothorax. Pronotum transverse, widest at base 2.2× wider than long; 1.6× wider at base than between anterior angles, 1.7× wider than head including eyes. Punctation dense and shallow, consisting of circular impressions with one small setiferous puncture on posterior margin (Fig. 4B), punctation of approximately same diameter and density all over pronotum.

Pterothorax. Elytra widest at anterior fifth, 1.1–1.2× as long as wide, 2.9–3.0× as long as pronotum, 1.2–1.3× as wide as pronotum. Punctation on intervals composed of semicircular impressions with a setiferous puncture on posterior margin (Fig. 4C). *Legs.* Metatibiae wide and flattened, weakly curved on external margin, 0.35× as long as elytra, 5.0× as long as wide.

Male genitalia (Fig. 3I–J). Phallobase about 1.1× as long as parameres, slightly asymmetrical, manubrium slightly hooked, widely rounded. Parameres continuously narrowing apically, external margins straight, apex rounded. Median lobe wide throughout, apex triangularly acuminate, gonopore rather small, situated subapically. Median projection of sternite 9 not examined.

Etymology. The species name reflects the teneral condition of the holotype (from Latin *adolescens* = growing up, maturing).

Distribution. The species is only known two localities in Pahang province, Malaysia.

Biology. No details about collecting circumstrances are available for type specimens; additional specimens from Tanah Rata were collected from inflorescences of Araceae (H. Takizawa, pers. comm. 2018).

Cycreon floricola sp. n.

http://zoobank.org/16453A2C-31B9-425C-998E-88D0836C8DE7

Figs 1A–C, E-O, 2, 3A–D, E–H, 4G–I, 5D–F, G–I, 6A–B

Description. *Measurements.* 2.2–3.4 mm long (length of holotype: 2.9 mm), 1.8–2.0× as long as wide, widest

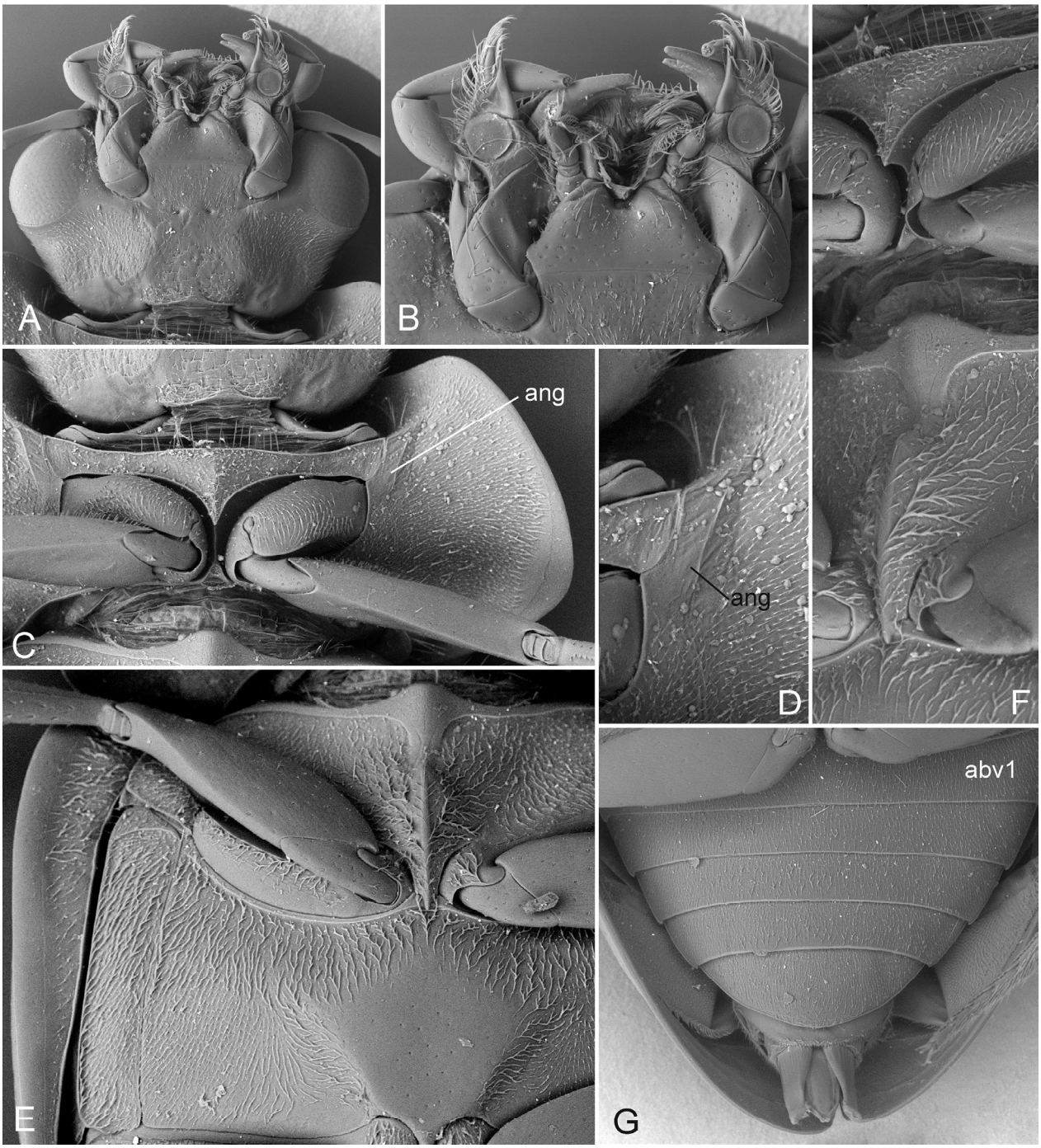

Figure 2. External morphology of *Cycreon floricola floricola* ssp. n. **A–** head, ventral view; **B –** detail of male mouthparts in ventral view; **C –** prothorax in ventral view; **D –** detail of the antennal groove; **E –** meso- and metaventrite; **F –** prosternum and mesoventral elevation in ventrolateral view; **G –** abdominal ventrites. Abbreviations: abv1 – abdominal ventrite 1; ang – antennal grooves.

at basal fifth of elytra; weakly convex, 3.1–3.4× as long as high (height of holotype: 0.9 mm). *Colouration.* Light brown with darker elytra (Figs 1A–C).

Head. Clypeus about 2.5× as wide as long, with anterior margin of clypeus margin very weakly emarginate medially. Frons and clypeus with punctation composed of complete circular impressions (punctures) with one small setiferous puncture on anterior margin (Figs 4G, D). Interocular distance about 4.9–5.2× width of one eye in dorsal view. Mentum (Figs 1J, 2B, 4K, 5E,H) subtrapezoid, widest at posterior fifth, about 2.1× as wide as long, with deep emargination reaching beyond anterior third of mentum length; surface with sparse, moderately long setae in anterior half, posterior half glabrous, punctures moderately large and deep, becoming smaller mesally, with 2–3 punctures with ring-like impressions close to posterolateral angles.

Prothorax. Pronotum transverse, widest at base, 2.2× as wide as long; 1.5–1.6× wider at base than at anterior

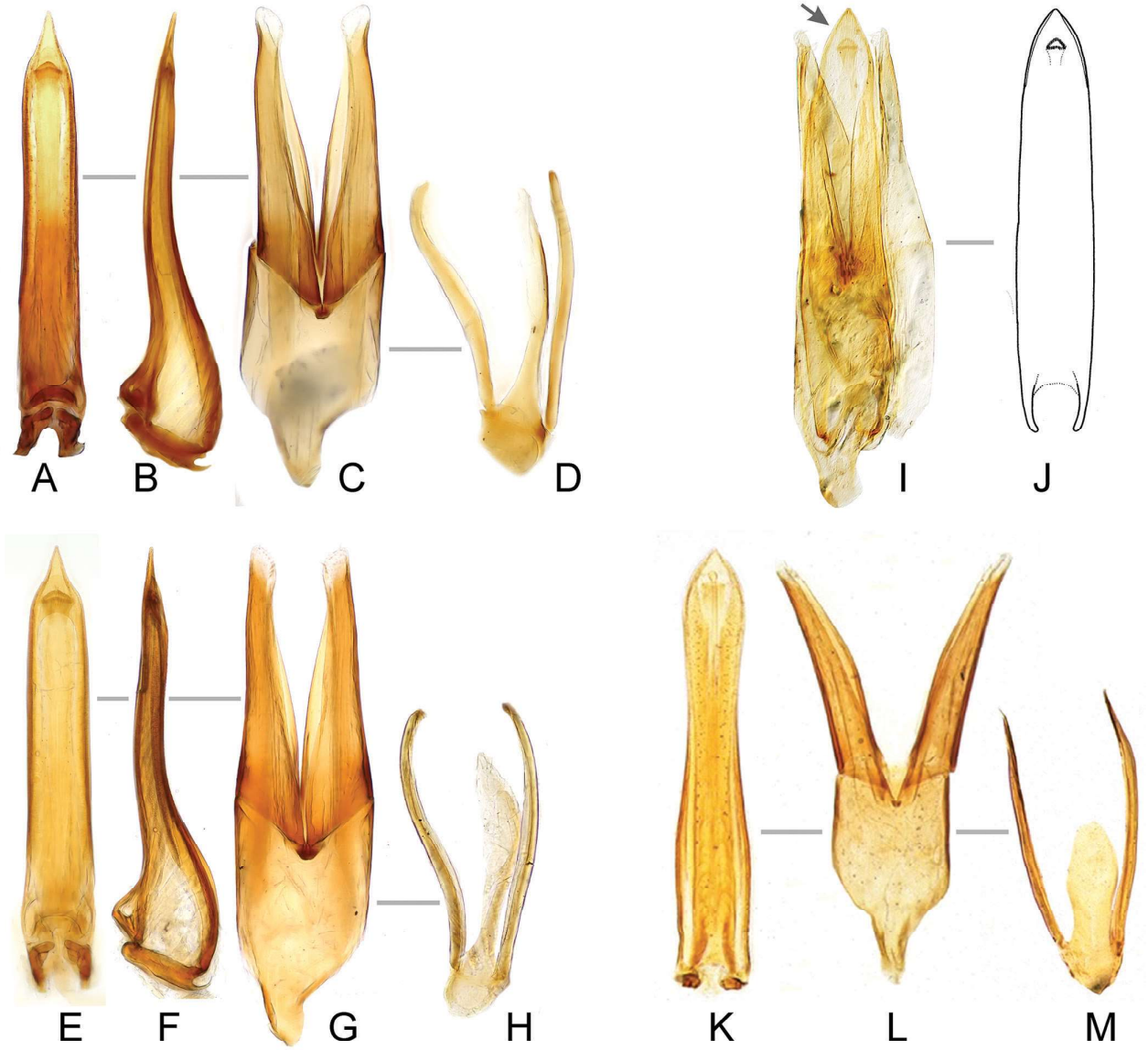

Figure 3. Male genitalia of *Cycreon* species (except *C. sculpturatus* for which male remains unknown). **A–D** – *C. floricola floricola* ssp. n., holotype; **E–H** – *C. floricola borneanus* ssp. n., holotype; **I–J** – *C. adolescens* sp. n., holotype; **K–M** – *C. armandi* Shatrovskiy, 2017, holotype. **A, E, K** – median lobe; **B, F** – median lobe in lateral view; **C, G, L** – tegmen; **D, H, M** – sternite 9; **I** – whole aedeagus; **J** – reconstructed shaped of the median lobe. **K–M** adapted from Shatrovskiy (2017).

angles, 1.6× as wide as head including eyes. Punctation dense and shallow, consisting of semicircular to complete ring-like impressions with a small setiferous puncture on posterior margin (Figs 4E, H, 5F, I), punctation approximately same in size and density all over pronotum.

Pterothorax. Elytra widest at anterior fifth, 1.1–1.2× as long as wide, 2.9–3.0× as long as pronotum, 1.1× as wide as pronotum. Punctation on intervals composed of semicircular impressions with setiferous puncture on posterior margin (Fig. 4F, I).

Legs. Metatibiae wide and flattened, very weakly curved, 0.35× as long as elytra, 4.8× as long as wide.

Male genitalia. Median projection of sternite 9 (Fig. 3D, H) rounded apically, with few short subapical setae, shorter than lateral struts. Phallobase (Fig. 3C, G) about 0.8× as long as parameres, asymmetrically narrowing towards base, manubrium acuminate and slightly hooked, with apex rounded. Parameres continuously narrowing from base to apex, but slightly widened at apex; external margins bisinuate; apex obliquely acuminate. Median lobe moderately wide (Fig. 3A–B, E–F), almost parallel-sided throughout, apex acuminate, with very acute tip, expanded basally and bent dorsally on lateral view, gonopore large, situated subapically.

Etymology. The species name reflects the association of this species with flowers, it consists of *flori-* (from Latin *flos, floris* = flower) and *-cola* (from Latin *incola* = inhabitant).

Comment. This species is composed of two phenotypically distinguishable forms which are geographically exclusive and are here descibed as subspecies. Morphological differences are mainly restricted to punctation on the pro-

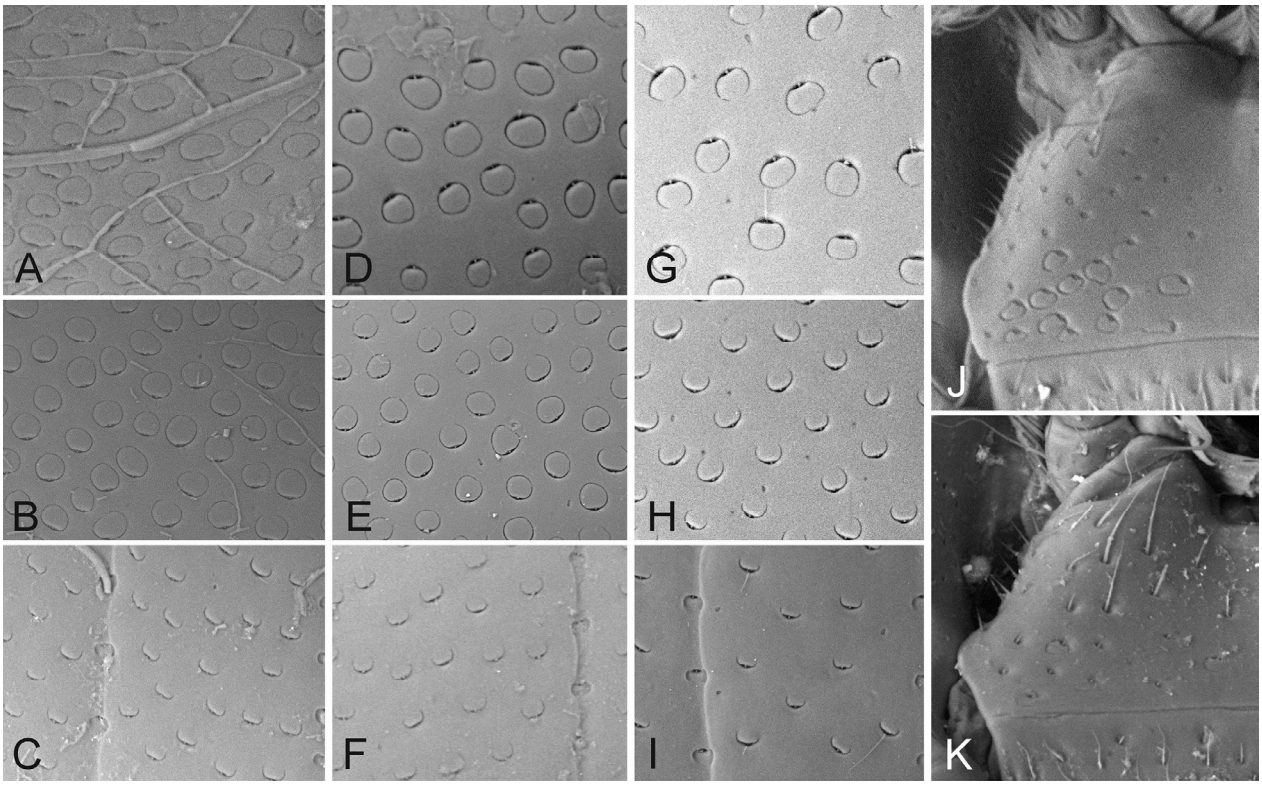

Figure 4. Surface sculptures of *Cycreon* species. **A–C, J –** *C. adolescens* sp. n., holotype; **D–F –** *C. floricola borneanus* ssp. n., paratype; **G–I, K –** *C. floricola floricola* ssp. n., paratype from the type locality. **A, D, G –** head punctation; **B, E, H –** pronotum punctation; **C, F, I –** elytral punctation; **J–K –** punctation of mentum.

notum, which consists exclusively of incomplete ring-like impressions in the mainland form (*C. f. floricola* ssp. n.), and exclusively or mainly of the completely ring-like forms in the specimens from Borneo (*C. f. borneanus* ssp. n.).

Cycreon floricola floricola ssp. n.

http://zoobank.org/953D42A0-7C3B-47BD-A2E5-26CB0ACAB588
Figs 1A–B,E–O, 2, 3A–D, 4G–I, K, 5G–I

Type locality. Malaysia, Kelantan, Guala Musang prov., Kuala Koh district, Taman Negara, 700 m from the entrance, 96 m a.s.l., 4°52.333′N 102°26.872′E.

Type material. Holotype (male: ZIN): "MALAYSIA: Kelantan AR-4332 / Guala Musang prov., Kuala Koh / distr., Taman Negara, 700 m / from entrance, 4°52.333′N / 102°26.872′E, 96m, 11.i.2014 / *Schismatoglottis* sp. HY Chen". **Paratypes: MALAYSIA: Johor:** Endau-Rompin N.P., NERC to Visitor Complex, Stream 1, 80 m, 2°25′12.8 ′ ″N 103°15′41.33″ E, flowering *Kiewia ridleyi*, 22.x.2008, Ooi Im Hin lgt. (AR-2602) (1: ZIN); Kota Tinggi, Hutan Simpan Panti, starting point of the trail to mount Panti, 14 m, 1°48.595′N 103°51.099′E, flowering *Schismatoglottis*, 4.xii.2013, Hoe Yin Chen lgt. (AR-4322) (21: ZIN, NMPC, IBTP); [same locality, except] 16 m, flowering *Schismatoglottis*, 4.xii.2013, Hoe Yin Chen lgt. (AR-4326) (11: ZIN); Kota Tinggi, Hutan Simpan Panti, starting point of the trail to mount Panti, 16 m, 01°48.565'N 103°51.104'E, flowering *Schismatoglottis*, 04.xii.2013, Hoe Yin Chen lgt. (AR-4328) (4: ZIN, NMPC); Kota Tinggi, Hutan Simpan Panti, Starting point of the trail to mount Panti, 16 m, 01°48.565'N 103°51.104'E, flowering *Schismatoglottis*, 13.xii.2013, Hoe Yin Chen lgt. (AR-4328) (6: ZIN, NMPC); **Kelantan:** Gua Musang, Kuala Koh, Taman Negara, 700 m away from the entrance gate (outside the park), 96 m, 4°52.333′N 102°26.872′E, flowering *Schismatoglottis*, 11.x.2014, Hoe Yin Chen lgt. (AR-4332) (237: ZIN, NMPC, IBTP, KMNH, EIHE, NHMW, BMNH, SRBC).

Diagnosis. This subspecies is very similar to *Cycreon floricola borneanus* ssp. n. with which it shares most of the external characters including genital morphology. *Cycreon floricola floricola* can be distinguished by the pronotal punctation consisting exclusively of the incomplete ring-like punctures. The dorsal coloration of the is slightly more contrasting in most specimens of *C. floricola floricola* than in representatives of *C. f. borneanus* ssp. n., with the pronotum darker compared to the elytra.

Description. *Measurements.* 2.4–3.2 mm long (length of holotype: 2.7 mm), 1.9–2.0× as long as wide, widest at basal fifth of elytra; weakly convex, 3.2–3.4× as long as high (height of holotype: 2.7 mm). *Colouration.* Pale yellowish-brown with dark-brown elytra (Fig. 1A–B).

Pronotum 2.2× wider than long; 1.6× wider at base than between anterior angles, with punctation dense and shallow, consisting of semicircular impressions (punctures) with a small setiferous puncture on posterior margin.

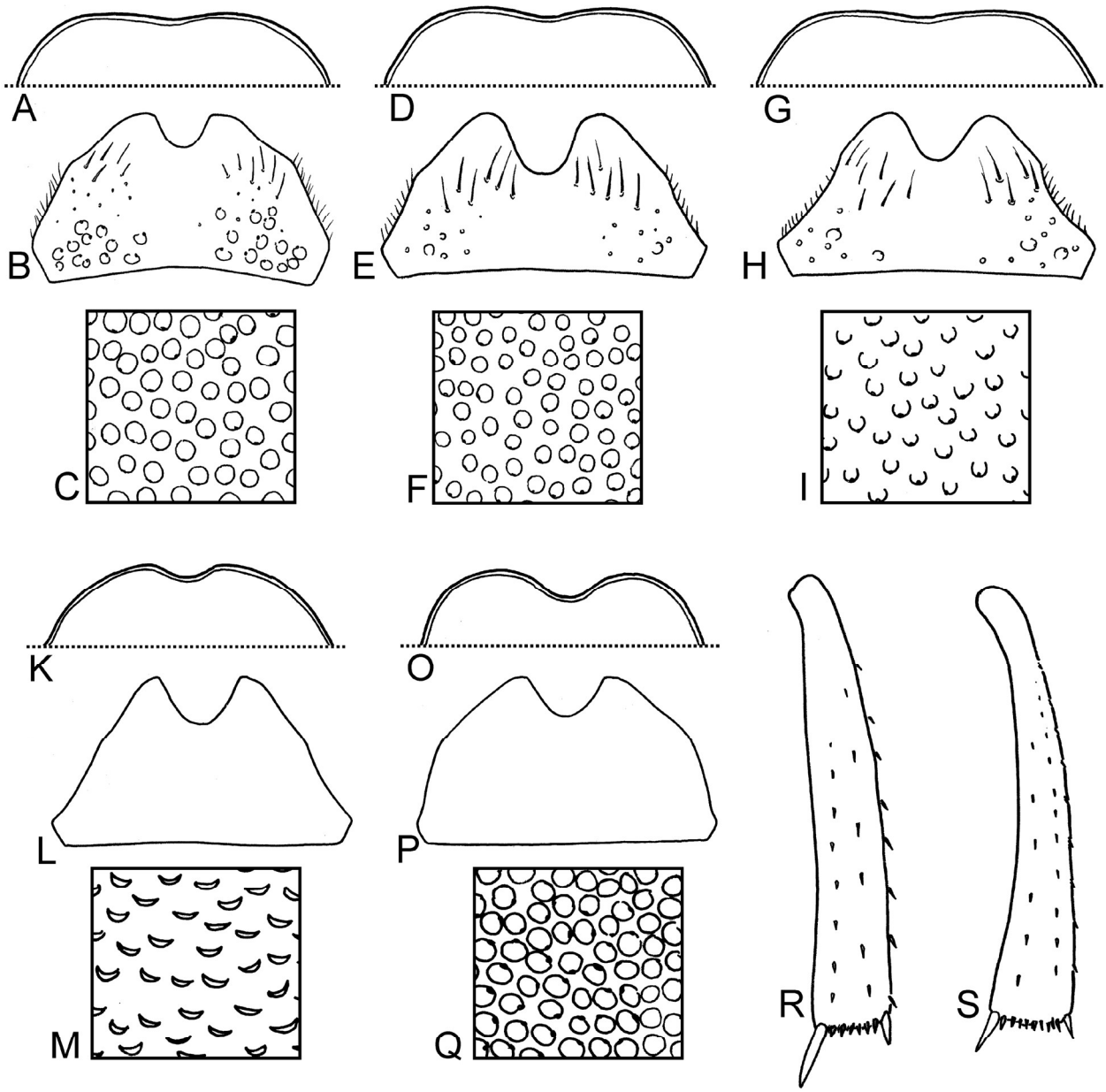

Figure 5. Diagnostic characters of known *Cycreon* species. **A–C** – *C. adolescens* sp. n.; **D–F** – *C. floricola borneanus* ssp. n.; **G–I** – *C. floricola floricola* ssp. n.; **K–L, S** – *C. armandi*; **O–R** – *C. sculpturatus*. **A, D, G, K, O** – anterior margin of clypeus; **B, E, H, L, P** – mentum (superficial sculpture omitted in **L** and **P**); **C, F, I, M, Q** – pronotal punctation; **R–S** – metatibia. **K, M–S** redrawn from Shatrovskiy (2017), **L** based on a photo provided by A. Shatrovskiy (pers. comm., 2017).

Punctation approximately same in size and density all over pronotum.

Elytra widest at anterior fifth, 1.1–1.2× as long as wide, 2.9–3.0× as long as pronotum, 1.1× as wide as pronotum. Punctation on intervals composed of semicircular impressions with one setiferous puncture on posterior margin.

Distribution. The subspecies is known from two regions in Peninsular Malaysia, in provinces of Johor and Kelantan.

Biology. Many specimens of *C. floricola floricola* were collected inside of inflorescences of *Schismatoglottis* species and *Kiewia ridleyi* (Low et al. 2018) (both Araceae).

Cycreon floricola borneanus ssp. n.

http://zoobank.org/ADFC83BC-973B-4A18-AE6F-B906027D49A1
Figs 1C, 3E–H, 5D–F, 6A–B

Type locality. Malaysia, Sabah, Tawau, Lahad Datu, Tawau Hills National Park, Kebun Botani, 305 m a.s.l., 4°23′59.4″N 117°53′17.2″E.

Type material. Holotype (male: ZIN): "MALAYSIA: Sabah AR-2659 / Tawau, Lahad Datu, Tawau Hills / NP, Kebun Botani, 305m / 04°23′59.4N 117°53′17.2E / *Schistamoglottis calyptrata* group, / 8.vii.2016, Wong Sin Yeng, / P. C. Boyce & Zaiety binti Thomas". **Paratypes: INDONESIA**: **Kalimantan Barat:** Bengkayang

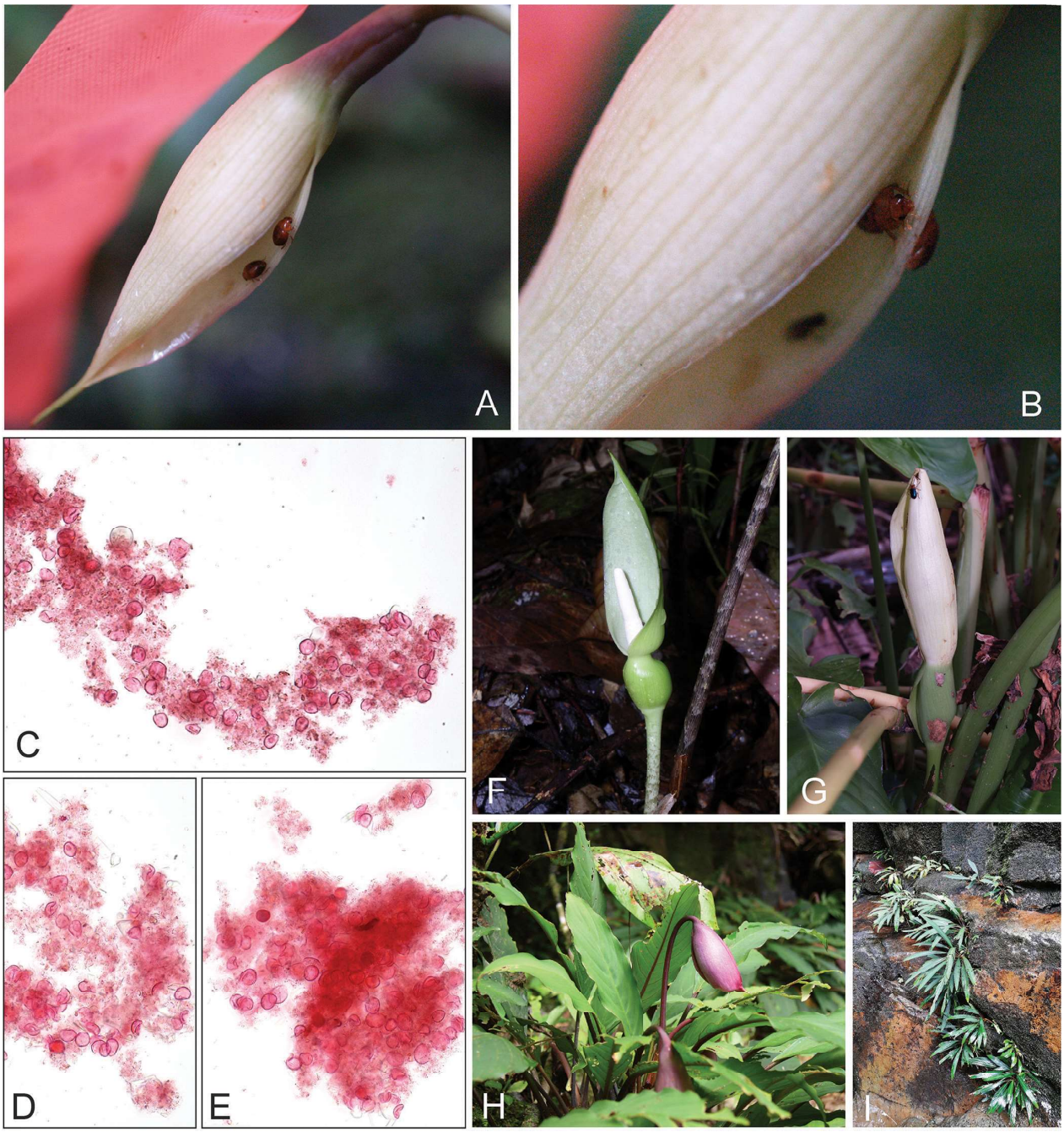

Figure 6. Biology of *Cycreon floricola* sp. n. **A–B –** alive specimens of *C. floricola borneanus* in the inflorescence of *Schottarum sarikeense* at Sebankoi Recreational Park, Betong, Roban, Sarawak in January 2010 (photo by S.-Y. Wong). **C–E –** safranine-dyed gut content of *C. floricola borneanus* collected from *Schismatoglottis calyptrata* complex in Tawau Hills, Kebun Botani on 8th July 2016 (collecting event AR-2659). **F–I –** examples of aroid plants on which the species were collected (**F –** *Alocasia longiloba*; **G –** *Schismatoglottis giamensis*; **H–I –** *Ooia glans*).

Pajintan, Ayer Terjun Sibohe, 80 m, 0°51'55.8"N 109°2'25.1"E, flowering *Schismatoglottis modesta*, 2.ix.2017, Wong & Boyce lgt. (AR-2812) (39: NMPC, ZIN). **Kalimantan Selantan:** 'S.O. Borneo / Grabowsky S. V.' (1: ZMNH); Kendangan, 15.5.1882, Grabowsky S. V. [ca.: S 2.592552°, E 115.028244°] (5: ZMNH). **MALAYSIA: Sabah:** Tawau, Lahad Datu, Tawau Hills NP, HQ Area, 304 m, 4°23′51.2"N 117°53′25.1"E, flowering *Alocasia longiloba* complex, 6.vii.2016, Wong Sin Yeng & P.C.Boyce lgt. (AL-315) (1: ZIN); [same locality] flowering *Schismatoglottis calyptrata* complex, 7. vii.2016, Wong Sin Yeng & P.C.Boyce lgt. (AR-2641) (101: ZIN, NMPC, IBTP, KMNH, NHMW); Tawau, Lahad Datu, Tawau Hills NP, Air Terjun Bukit Gelas, 315 m, 4°24′48.4"N 117°53′29.3"E, flowering *Gamogyne loi*, 6.vii.2016, Wong Sin Yeng & P.C.Boyce lgt. (AR-2638) (12: ZIN, NMPC); Tawau, Lahad Datu, Tawau Hills NP, Trail to Bukit Gelas, 319 m, 4°24′37.0"N

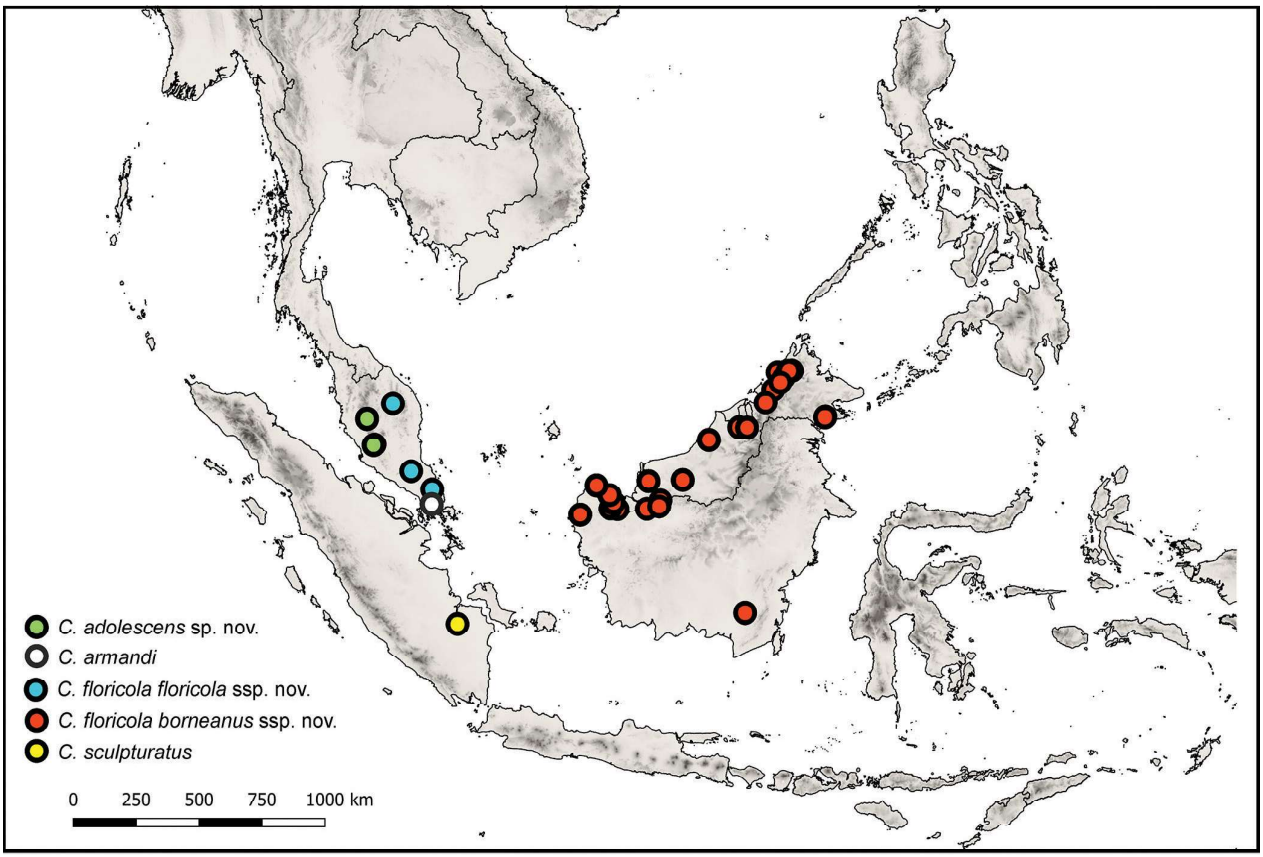

Figure 7. Known distribution of *Cycreon* species.

117°53′38.8”E, flowering *Homalomena hanneae* complex, 6.vii.2016, Wong Sin Yeng & P.C.Boyce lgt. (AR-2636) (18: ZIN, NMPC); [same locality] flowering *Schismatoglottis calyptrata* complex, 7.vii.2016, Wong Sin Yeng & P.C.Boyce lgt. (AR-2652) (36: ZIN, NMPC); Tawau, Lahad Datu, Tawau Hills NP, Kebun Botani, 305 m, 04°23′59.4″N 117°53′17.2″E, flowering *Schismatoglottis calyptrata* complex, 8.vii.2016, Wong Sin Yeng, P.C.Boyce & Zaiety binti Thomas lgt. (AR-2659) (116: ZIN, NMPC, IBTP, KMNH, NHMW, BMNH); Kg. Moyog, Jln. Tambunan, Penampang, 12.xii.2009, H. Takizawa lgt [ca. N 5.888455°, E 116.235335°] (11: EIHE, KMNH, NMPC, IBTP); [same locality and collector] 30.x.2008 (7: EIHE, KMNH); [same locality and collector,] 13.ix.2008 (7: EIHE, KMNH, IBTP); Poring park, Ranau, 19–20.ix.2008, H. Takizawa lgt [ca. N 6.047067°, E 116.703231°] (7: EIHE, KMNH, IBTP); [same locality and collector] 25–26.ix.2008 (5: EIHE, KMNH. IBTP); [same locality and collector] 8–9.i.2010 (7: EIHE, KMNH, IBTP); [same locality and collector] 11.xii.2008 (3: EIHE, KMNH); [same locality and collector] 27.v.2010 (1: EIHE); [same locality and collector] 25.ii.2009 (2: KMNH); [same locality and collector] 10.vii.2008 (1: EIHE); [same locality and collector] 12. iii.2009 (1: KMNH); [same locality and collector] 29. viii.2013 (1: KMNH); [same locality and collector] 12. iii.2009 (1: KMNH); [same locality and collector] 4–5. iv.2008 (3: KMNH, IBTP); [same locality and collector] 7.x.2012 (2: KMNH); Kg. Kiapad, Inanam, Kota Kinabalu, 7.ix.2008, H. Takizawa lgt [ca. N 5.988388°, E 116,190333°] (16: KMNH, EIHE, IBTP, NMPC); [same locality and collector] 2.i.2010 (3: KMNH, EIHE); [same locality and collector] 10.xi.2012 (16: KMNH, EIHE, IBTP, NMPC); [same locality and collector] 6.xii.2008 (18: KMNH, EIHE, IBTP, NMPC); [same locality and collector] 6.iv.2013 (7: KMNH, EIHE, IBTP); [same locality and collector] 5.vii.2008 (22: KMNH, EIHE, IBTP, NMPC); [same locality and collector] 4.x.2008 (3: KMNH); [same locality and collector] 7.xi.2009 (1: KMNH); Ulu Senagang subts., Keningau, 31.i.-2.ii.2011, H. Takizawa lgt. [ca. N 5.362946°, E 116.028679°] (14: KMNH, EIHE, IBTP); [same locality and collector] 24–26.vii.2010 (2: KMNH); Kinabalu PHQ, Ranau, 17–19. iii.2008, H. Takizawa lgt. [ca. N 6.021639°, E 116.542751°] (1: EIHE); Kinabalu Park, HQ, Ranau, 5.iii.2010, H. Takizawa lgt. [ca. N 6.021639°, E 116.542751°] (3: EIHE, KMNH); [same locality and collector] 14.iii.2012 (1: KMNH); [same locality and collector] 8.vii.2010 (2: KMNH); [same locality and collector] 23–25.iii.2010 (1: EIHE); [same locality and collector] 27–28.v.2008 (2: KMNH); [same locality and collector] 13–14.v.2010 (1: EIHE); [same locality and collector] 23–25.viii.2008 (2: KMNH); [same locality and collector] 23–25.vii.2008 (1: KMNH); [same locality and collector] 1.ii.2010 (1: KMNH); [same locality and collector] 23–24.ix.2008 (1: KMNH); [same locality

and collector] 17–19.x.2008 (1: KMNH); Muaya waterfall, Sipitang, 6–9.iii.2009, H. Takizawa lgt. [ca. N 4.903889°, E 115.760278°] (8: EIHE, KMNH, IBTP); Mahua waterfall, Crocker R. P., Tambunan, 26.vii.2011, H. Takizawa lgt [ca. N 5.797627°, E 116.408377°] (1: NMPC); Gn. Bombalai, Tawau Hills park, Tawau, 17. vi.2010, H. Takizawa lgt [ca. N 4.386858°, E 117.879748°] (4: EIHE, KMNH); Pk. Bundu Tuhan Kundasang, Ranau, 6.iii.2010, H. Takizawa lgt. [ca. N 5.996602°, E 116.528987°] (1: NMPC); Mesilau headgate, Kundasang, Ranau, 25.ii.2009, H. Takizawa lgt. [ca. N 6.044605°, E 116.596306°] (1: KMNH); Malangan, Kg. Tikolod, Tambunan, 12–14.iii.2010, H. Takizawa lgt. [ca. N 5.626763°, E 116.286933°] (1: EIHE); Pantai Barat, Kota Kinabalu, Inanam, Kionsom, Kionsom Waterfall, 230 m, 05 57 24.0N 116 12 25.3E, flowering *Schismatoglottis corneri*, 18.iv.2014, Wong Sin Yeng & P.C.Boyce lgt. (AR-4683) (7: ZIN, NMPC). **Sarawak:** Serian, Pichin, between Sugun Karang and Tahang Sipukam, Sungai Kakas, 48 m, 1°06′09.7″N 110°28′11.8″E, flowering *Schismatoglottis bulbifera*, 28.vi.2014, Ooi Im Hin & Jeland ak Kisai lgt. (AR-4832) (1: ZIN); Kuching, Padawan, Puncak Borneo, Jungle Trail, 890 m, 1°07′33.5″N 110°12′57.4″E, flowering *Ooia glans*, 15.ix.2014, Wong Sin Yeng & P.C.Boyce lgt. (AR-93) (92: ZIN, NMPC, IBTP, KMNH, NHMW); Kuching, Padawan, Puncak Borneo, Sungai Semangas, 472 m, 1°08′26.6″N 110°13′36.1″E, flowering *Ooia glans*, 16.ix.2014, Wong Sin Yeng & P.C.Boyce lgt. (AR-4979) (29: ZIN, NMPC, KMNH); Kuching, Matang, Kubah N.P., Sungai Bungen, 230 m, 1°36′30.9″N 110°11′35.0″E, flowering *Ooia glans*, 28.vii.2007, P.C.Boyce, Wong Sin Yeng & S.Maclean lgt. (AR-2118) (27: ZIN, NMPC, IBTP); [same locality] flowering *Schismatoglottis mayoana*, 28.vii.2007, Wong & Maclean lgt. (AR-2122) (1: ZIN); Kuching, Matang, Kubah N.P., Waterfall Trail, 190 m, 1°35′40.2″N 110°10′45.9″E, flowering *Ooia glans*, 28.vii.2007, P.C.Boyce, Wong Sin Yeng & S.Maclean lgt. (AR-2117) (10: ZIN, NMPC); Sri Aman, Lubok Antu, Sungai Engkari, Nanga Segerak, Sungai Serjanggut, 332 m, 1°24′46.5″N 112°00′18.5″E, flowering *Ooia* sp., 17.iii.2015, Wong Sin Yeng, P.C. Boyce & Bada ak Chendai lgt. (AR-5169) (11: ZIN, NMPC); Sri Aman, Lubok Antu, Engkilili, Tempat Rekreasi Sungai Raya, Sungai Raya, 13 m, 1°06′49.2″N 111°30′56.8″E, flowering *Schismatoglottis calyptrata* complex, 9. xii.2005, P.C.Boyce, Jeland ak Kisai, Jipom ak Tisai & Mael ak Late lgt. (AR-1632) (38: ZIN, NMPC, IBTP, KMNH); Sri Aman, Lubok Antu, Sungai Sepipit, 108 m, 1°11′54.9″N 111°57′29.4″E, flowering *Schismatoglottis petradoxa*, 27.vii.2014, Wong Sin Yeng & P.C.Boyce lgt. (AR-4894) (1: ZIN); Kuching, Siburan, Kampung, Giam, Sugun Jawan, 70 m, 1°19′20.7″N 110°16′21.4″E, flowering *Schismatoglottis giamensis*, 20.vi.2009, P.C.Boyce & Wong Sin Yeng lgt. (AR-2549) (56: ZIN, NMPC, IBTP, KMNH); Kuching, Siburan, Kampung Sikog, Air Terjun Baan Gong, 70 m, 1°20′16.1″N 110°20′09.6″E, flowering *Schismatoglottis baangongensis*, 26.vii.2009, P.C.Boyce & Wong Sin Yeng lgt. (AR-2588) (63: ZIN, NMPC, IBTP, KMNH); Miri, Marudi, Long Lama, Mulu N.P., Trail to Deer Cave, 60 m, 4°02′23.8″N 114°48′54.6″E, flowering *Phymatarum borneense*, 5.viii.2006, P.C.Boyce, Wong Sin Yeng, Jeland ak Kisai & Mael ak Litis lgt. (AR-1931) (23: ZIN, NMPC); Miri, Marudi, Long Lama, Mulu N.P., Trail to Deer Cave, 60 m, 4°02′02.0″N 114°49′00.0″E, flowering *Schismatoglottis muluensis*, 6.viii.2006, P.C.Boyce, Wong Sin Yeng, Jeland ak Kisai & Mael ak Litis lgt. (AR-1941) (110: ZIN, NMPC, IBTP, KMNH, NHMW); Kuching, Siburan, Kampung Giam, Air Terjun Giam, 37 m, 01°19’11.2”N 110°16’11.4”E, flowering *Homalomena giamensis*, 07.ii.2016, P.C.Boyce, Jeland ak Kisai & Wong Sin Yen lgt. (AR-1691) (13: ZIN, NMPC); Kampung, Sungai Temaga, trail to Gunung Pueh, 82 m, 01°46’58.6”N 109°43’06.6”E, flowering *Schismatoglottis*, 23.iii.2014, Wong Sin Yeng & P.C.Boyce lgt. (AR-4651) (1: ZIN); Kuching, Siburan, Air Terjun Baan Gong, 70 m, 01°20′16.1″N 110°20′09.6″E, flowering *Homalomena borneensis*, 26.vii.2009, P.C.Boyce & Wong Sin Yeng lgt. (AR-2575) (11: ZIN, NMPC); Kuching, Siburan, Sugun Jawan, 50 m, 01°19’16.1”N 110°16’16.7”E, flowering *Homalomena gastrofructa*, 09.vi.2009, P.C.Boyce & Wong Sin Yeng lgt. (AR-2559) (5: ZIN, NMPC); Miri, Niah N.P., Beside road margin, outside of the main entrance, 13 m, 03°49.598’N 113°45.683’E/03°49.577’N 113°45.710’E, flowering *Schismatoglottis*, 30.iii.2014, Hoe Yin Chen lgt. (AR-4665) (2: ZIN); Kuching, Sematan, Sungai Temaga, trail to Gunung Pueh, 82 m, 01°46’58.6”N 109°43’06.6”E, flowering *Homalomena caput-gorgonis*, 23.iii.2014, Wong Sin Yeng & P.C.Boyce lgt. (AR-4659) (2: ZIN); Kuching, Kampung Sebat Dayak, Air Terjun Sebat, 70 m, 01°48’05.6”N 109°43’09.6”E, flowering *Piptospatha elongata*, 21.iii.2014, Wong Sin Yeng & P.C.Boyce lgt. (AR-4367) (1: ZIN); Betong, Roban, Sebankoi, Taman Rekreasi Sebankoi, 154 m, 01°57′27.4″N 111°26′04.6″E, flowering *Homalomena ibanorum*, 05.xii.2005, P.C.Boyce, Jeland ak Kisai, Jepom ak Tisai, Mael ak Late & Wong Sin Yeng lgt. (AR-1538) (7: ZIN, NMPC); Kuching, Matang, Maha Mariamman Temple, trail to Indian Temple, 350 m, 01°35’25.7”N 110°13’12.8”E, flowering *Homalomena matangae*, 04.iii.2014, P.C.Boyce & Jeland ak Kisai lgt. (AR-230) (7: ZIN, NMPC); Kuching, Bau, Krokong, Gua Peri-peri, 30 m, 01°22’51.9”N 110°07’09.3”E, flowering *Schismatoglottis*, 09.v.2009, P.C.Boyce & Wong Sin Yeng lgt. (AR-2445) (2: ZIN); Kuching, Bau, Gua Angin, 45 m, 01°24’54.8”N 110°08’08.2”E, flowering *Schismatoglottis*, 21.vi.2005, P.C.Boyce & Jeland ak Kisai lgt. (AR-1240) (8: ZIN, NMPC); Roban, Sebankoi, Taman Rekreasi Sebankoi, Site 1, 154 m, 01°57’27.4”N 111°26’04.6”E, flowering *Schismatoglottis sarikeense*, 07.ii.2010, Low Shook Ling lgt. (AR-3001) (4: ZIN); Kuching, Siburan, Kampung Sikog, Air Tejun Baan Gong, 70 m, 01°20′16.1″N 110°20′09.6″E, flowering *Homalomena baangongensis*, 26.vi.2009, P.C.Boyce &

Wong Sin Yeng lgt. (AR-2574) (44: ZIN, NMPC, IBTP, KMNH); Kuching, Matang, Kubah N.P. Sungai Bungen, 230 m, 01°36′30.9″N 110°11′35.0″E, flowering *Ooia glans*, Ooi Im Hin lgt. (AR-2339) (2: ZIN); Kuching, Bau, Gua Angin, 45 m, 01°24'54.8"N 110°08'08.2"E, flowering *Schismatoglottis*, 21.vi.2005, P.C.Boyce & Jeland ak Kisai lgt. (AR-1240) (24: ZIN, NMPC). Miri, Miri, Marudi Long Lama, Mulu National Park, DC limestone, before Kenyalang trail junction, 65 m, 4°02'29.4"N 114°48'44.3"E, flowering *Schismatoglottis muluensis*, 25.xii.2017, SY Wang team lgt. (SK01) (38: NMPC); [same locality] DC limestone, before 2nd shelter, flowering *Schismatoglottis colocasioideae*, 27.xii.2017 (SK03) (11: NMPC); [same locality and host plant] 30.xii.2017 (SK07) (11: NMPC); [same locality] DC limestone, before Kenyalang trail junction, flowering *Schismatoglottis muluensis*, 1.i.2018 (SK10) (11: NMPC); [same locality] DC limestone, near Deer water cave, flowering *Schismatoglottis muluensis*, 1.i.2018 (SK11) (33: NMPC, IBTP); [same locality] DC limestone, canopy trail, flowering *Schismatoglottis colocasioideae*, 7.i.2018 (SK12) (13: NMPC); [same locality] BT right, flowering *Schismatoglottis serratodentata*, 8.i.2018 (SK13) (2: NMPC); [same locality and host plant] 23.i.2018 (SK17) (1: NMPC); [same locality] DC limestone, near Deer water cave, flowering *Schismatoglottis pellucida*, 30.i.2018 (SK18) (3: NMPC); [same locality] flowering *Schismatoglottis multinervia*, 31.i.2018 (SK19) (4: NMPC); [same locality and host plant] 3.ii.2018 (SK21) (3: NMPC); Kapit, Taman Rekreasi Sebabai, 84 m, 1°56'37.5"N 112°54'24.8"E, flowering *Ooia havilandii*, 22.ix.2017, Wong & Boyce lgt. (AR-3635) (23: NMPC, ZIN): Sarikei Bayong, Ulu Sarikei, Lubok Lemba, Rymah Nyuka, 55 m, 1°53'41.3"N 111°30'11.5"E, flowering *Ooia secta*, 3.vi.2017, Wong & Boyce lgt. (AR-2756) (1: NMPC); Kuching Lundu, Gunung Gading NP, waterfall 1, 200 m, 1°41'28.3"N 109°50'43.6"E, flowering *Homalomena*, 27.v.2017, Wong & Boyce lgt. (AR-2757) (3: NMPC); Sarikei Bayong, Ulu Sarikei, Lubok Lemba, Rymah Nyuka, 55 m, 1°53'41.3"N 111°30'11.5"E, flowering *Schismatoglottis erumpens* complex, 3.vi.2017, Wong & Boyce lgt. (AR-2753) (4: NMPC).

Diagnosis. This species is very similar to *Cycreon floricola floricola* with which it shares most external characters and genital morphology. *Cycreon floricola borneanus* ssp. n. can be distinguished from *C. floricola floricola* by the shape of the pronotal punctation consisting only or largely of complete ring-like punctures. The dorsal coloration of *C. floricola borneanus* sp. n. is usually more uniform, with elytral colouration not much darker than pronotal one.

Description. *Measurements.* 2.2–3.4 mm long (length of holotype: 2.9 mm), 1.8–1.9× as long as wide, widest at basal fifth of elytra; weakly convex, 3.1–3.3× as long as high (height of holotype: 2.8 mm). *Colouration.* Pale brown with weakly darker elytra (Fig. 1C).

Pronotum 2.2× wider than long; 1.5× wider at base than between anterior angles, 1.6× wider than head including eyes. Punctation dense and shallow, consisting of complete ring-like impressions with one small setiferous puncture on posterior margin (Figs 4E, 5F), punctation of approximately same in size and density all over pronotum.

Elytra widest at anterior fifth, 1.1–1.2× as long as wide, 2.9–3.0× as long as pronotum, 1.1× as wide as pronotum. Punctation on intervals composed of semicircular impressions with one setiferous puncture on posterior margin (Fig. 4F).

Variation. In most specimens examined from Borneo, the pronotal punctation consists exclusively of completely ring-like punctures. However, in few localities on the north-western coast of Borneo the punctation of 5-20% of specimens shows a mixture of complete and incomplete rings. In the absence of genetic data, we are unable to analyze this variation in detail, and hence temporarily treat even these specimens as *C. floricola borneanus*.

Etymology. The name of this species is derived from Borneo, the historical name of island where all the known specimens of this subspecies were collected.

Distribution. The species seems to be widespread in Borneo, it is recorded from Indonesia: Kalimantan Barat and Kalimantan Selantan and Malaysia: Sabah, Sarawak (Fig. 7)

Biology. This subspecies has been collected in inflorescences of a number of plant species belonging to the Araceae family. It was collected in high numbers in flowers of the genus *Schismatoglottis*: *S. calyptrata*, *S. colocasioideae*, *S. erumpens* complex, S. *giamensis* (Fig. 6G), *S. mayoana*, *S. modesta*, *S. muluensis*, *S. multinervia, S. pellucida*, *S. petradoxa* and *S. serratodentata.* It has been also collected in numbers close to one hundred specimens in an inflorescence of *Ooia glans* (Figs 6H–I) and *O. havilandii.* Other known records of host plants include *Alocasia longiloba* complex (Fig. 6F), *Gamogyne loi*, several species of *Homalomena* (this paper) *Phymatarum borneense* and *Schottarum sarikeense* (Fig. 6A–B) (Low et al. 2016). According to H. Takizawa (pers. comm. 2017), *C. borneanus* can be found in aggregations in a wide range of aroid inflorescences from lowlands to montane areas (ca. between 100–1500 m a.s.l), mainly in flowers on small open places like trail sides in or near well-preserved primary or secondary forests, or along small streams.

Biology of *Cycreon*

All specimens of both subspecies of *C. floricola* have been collected in inflorescences of various Araceae genera, often in high numbers, indicating their tight association with this microhabitat. The fact that there were only two specimens of the genus known up to now likely correspond with the biology of *Cycreon* beetles, since no study of flower-inhabiting beetles associated with Araceae in the Malaysian Peninsula and Sunda islands was performed previously.

Low et al. (2016) studied the biology of insects associated with inflorescences of Araceae in Borneo and demonstrated that *Cycreon floricola borneanus* specimens

are only present in the upper part of the inflorescences of *Phymatarum borneense* and *Schottarum sarikeense*, never in the pistillate zone (= bottom), and that they are not attracted by the smell of the inflorescences, unlike the co-occurring *Chaloenus* beetles (Chrysomelidae) and *Colocasiomyia* flies (Drosophilidae). Observations of few specimens covered by pollen grains were reported, but only *Colocasiomia* flies were considered as pollinators. Subsequent investigations of the pollination biology of the *Schismatoglottis calyptrata* complex (Hoe et al. 2018) revealed that *Cycreon floricola borneanus* visited all the investigated species except *Schismatoglottis calyptrata* and *S. laxipistillata*, but their abundance differed based on host plant species: they were very abundant in *S. giamensis, S. caesia and S. muluensis*, but present in single or few specimens only in *S. pseudoniahensis*, *S. pantiensis*, *S. adducta*, and *S. roh*. *Cycreon* beetles were observed to feed on the exudations from the interpistillar staminodes, mated on the pistillate zone and remained inside the lower spathe chamber. They were also revealed as the most effective pollen carriers, carrying 6–15 times more pollen than *Colocasiomyia* flies and hence considered as secondary pollinators (*Colocasiomyia* flies were 4–6 times more abundant and are hence considered as main pollinators). No hydrophilid larvae were found in the inflorescences, indicating that they may live in different microhabitat.

Mouthparts of *Cycreon* (Fig. 1F–K) are unusual when compared to other members of the tribe Megasternini examined so far, differing from them in three aspects: (1) structure of the mandible with two large teeth on the apex (Fig. 1F–G), (2) excision of the clypeus (varying from weak to very deep, depending of the species; Fig. 5), and (3) shape of the mentum, with deep anterior excision (Figs 1J, 2B, 5). The mandibles of other Megasternini examined so far bear simple apex (e.g., Fikáček 2010, Arriaga-Varela et al. 2018), while those of *Cycreon* have the apex deeply bifid and with two large teeth. When the mandible is examined in mesal view (Fig. 1H), both apical teeth are situated on sides of straight edge, and they become strongly abraded in some specimens (Fig. 1G). This may indicate that mandibular apex is used for processing of some hard/solid material, possibly for scraping organic material from internal parts of the aracean inflorescences, in agreement with the above observations by Hoe et al. (2018). The inspection of the gut contents of *Cycreon floricola borneanus* (Fig. 6C–E) revealed that the midgut contains two components, both stained by safranine dye: (1) pollen grains of the respective plant species and (2) the heterogeneous organic matter which cannot be further identified; it does not seem to be just remains of crushed pollen grains, as no partially crushed pollen grains or remains of their exine were found (safranine stains various organic compounds including cellulose, lignine, glucosamines and cell nuclei, and does not allow detailed identification of this component - it may represent organic detritus scraped by the beetles from interior of the inflorescence). The presence of this unspecified organic matter in the intestines indicates that *Cycreon* beetles are not specialized pollen feeders, but the presence of pollen grains in the midgut content confirms that pollen is part of the diet and may be possibly digested. When compared to specialized pollen-feeding New Zealand genus *Rygmodus* (Hydrophilidae: Cyclominae) analyzed by Minoshima et al. (2018), important differences in mandible morphology can be found, confirming that *Cycreon* is not specialized pollen feeder: (1) mandibular apex is simple and spoon-like in *Rygmodus*, whereas strongly bifid in *Cycreon*, (2) mola is simply tuberculate in *Rygmodus* (a supposed adaptation to disrupt the pollen exina by grinding), but bears poriferous lamellae in *Cycreon* and all other hydrophilids examined. Unlike in *Cycreon*, the midgut of *Rygmodus* contains nearly exclusively pollen grains, with very little fine organic matter (see Minoshima et al. 2018: fig 4).

The excised clypeus and anterior margin of mentum is unusual in the Megasternini. Excised mentum is only known in the Central American genus *Nitidulodes*, which is also associated with aroid inflorescences (Hansen 1991, Bloom et al. 2015). Excised clypeus is only present in *Cycreon*. Moreover, the strong variation of mentum and clypeus shape between different species of *Cycreon* is also unusual within Megasternini. Usually these characters are very similar in congeneric species and differ at most between genera. We suppose that this interspecific variation in *Cycreon* may indicate species-specific food and host-plant preferences. The data by Hoe et al. (2018) indicate some kind of specificity in host plants, which would be in agreement with this assumption. For example, various genera and species of Schismatoglottideae were sampled in Mulu National Park (Malaysia, Sarawak) from December 2017 to February 2018, but *Cycreon* beetles were only found in sampled species of *Schismatoglottis* (beetles were present in all sampled plants), whereas not a single specimen was found in inflorescences of *Anadendrum, Aglaonema, Alocasia, Bucephalandra* and *Lasia.* Additionally, the material collected from various inflorescences of the single aroid tribe Schismatoglottideae by Low et al. (2014, 2016), Hoe & Wong (2016) and Hoe et al. (2018) includes two very closely related subspecies only (*Cycreon floricola floricola* and *C. floricola borneanus*), despite consisting of more than 1000 specimens; not a single specimen of another *Cycreon* species was collected even in peninsular Malaysia, despite the sampled localities were close to those of two other species (*C. armandi* and *C. adolescens*). We suppose this may be caused by the focus on a single narrow group of host plants, and is congruent with the expected species-specific host preferences in *Cycreon* beetles.

Discussion

Interactions of *Cycreon* with aroid inflorescences can be interpreted as an initial stage of development of cantharophyly, i.e. interrelations between beetles and plant reproductive organs, in which only adult are associated with flowers (e.g., Kirejtshuk 1994, 1997). This type of inter-

relations is particularly possible in cases when blossoming period ends by decaying of part of flowers with fungal and microbial infection (Teichert et al. 2012). On the other hand, species of *Chaloenus* beetles (Chrysomelidae: Alticini) co-occurring with *Cycreon* may represents another type of interrelations with plants, connected with a secondary transition of adults from leaf-feeding to flower-feeding. Besides, one sample collected from *Leucocasia giganteum* in peninsular Malaysia included representatives of *Aethina* Erichson (Coleoptera: Nitidulidae: Nitidulinae); some species of the genus are known to be associated with fungi, others to feed on inflorescences (Kirejtshuk 1986). Few examined samples also included few staphylinids, possibly as occasional visitors of decaying aroid inflorescences.

Acknowledgements

We are indebted to H. Takizawa and Y. N. Minoshima (Japan) for providing us with the material from their collections. This work was supported by the European Union's Horizon 2020 research and innovation programme under the Marie Skłodowska-Curie grant agreement No. 642241 to EAV, and by the Ministry of Culture of the Czech Republic (DKRVO 2018/13, National Museum, 00023272) to MF. The work of EAV at the Department of Zoology, Charles University, Prague was partly supported by grant SVV260434/2018. WSY acknowledges the funding from the Ministry of Education of Malaysia through Vote No. NRGS/1089/ 47 2013-(03). The study of AGK was performed in the frames of the state research project AAAA-A17-117030310210-3 and partly supported by the programme of the Presidium of the Russian Academy of Sciences "Evolution of organic world. Significance and influence of planetary processes" and the Russian Foundation of Basic Research (grant No. 18-04-00243–a).

References

Archangelsky M (1997) Studies on the biology, ekology and systematice of the immature stages of New World Hydrophiloidea (Coleoptera: Staphyliniformia). Bulletin of the Ohio Biological Survey, New Series 12(1): 1–207.

Arriaga-Varela E, Seidel M, Deler-Hernández A, Senderov V, Fikáček M (2017) A review of the *Cercyon* Leach (Coleoptera, Hydrophilidae, Sphaeridiinae) of the Greater Antilles. ZooKeys 681: 39–93. https://doi.org/10.3897/zookeys.681.12522

Arriaga-Varela E, Seidel M, Fikáček M (2018) A new genus of coprophagous water scavenger beetle from Africa (Coleoptera, Hydrophilidae, Sphaeridiinae, Megasternini) with a discussion on the *Cercyon* subgenus *Acycreon*. African Invertebrates 59(1): 1–23. https://doi.org/10.3897/AfrInvertebr.59.14621

Bloom D, Fikáček M, Short AEZ (2014) Clade age and diversification rate variation explain disparity in species richness among water scavenger beetle (Hydrophilidae) lineages. PLoS ONE 9(6): e98430. https://doi.org/10.1371/journal.pone.0098430

Fikáček M (2010) Hydrophilidae: The genus Kanala Balfour-Browne (Coleoptera). In: Jäch MA, Balke M (Eds) Water Beetles of New Caledonia, volume 1. Monographs of Coleoptera 3: 365–394.

Fikáček M, Short, AEZ (2006) A revision of the Neotropical genus *Motonerus* Hansen (Coleoptera: Hydrophilidae: Sphaeridiinae). Zootaxa 1268: 1–38.

Fikáček M, Hebauer F, Hansen M (2009) Taxonomic revision of New World species of the genus *Oosternum* Sharp (Coleoptera: Hydrophilidae: Sphaeridiinae). I. Definition of species groups and revision of the *Oosternum aequinoctiale* group. Zootaxa 2054: 1–37.

Fikáček M, Jia FL, Prokin A (2012) A review of the Asian species of the genus *Pachysternum* (Coleoptera: Hydrophilidae: Sphaeridiinae). Zootaxa 3219: 1–53.

Hansen M (1991) The Hydrophiloid beetles: phylogeny, classification and a revision of the genera (Coleoptera, Hydrophiloidea). Kongelige Danske videnskabernes selskab, Copenhagen, 367 pp.

Hoe YC, Wong SY (2016) Floral biology of *Schismatoglottis baangongensis* (Araceae: Schismatoglottideae) in West Sarawak, Borneo. Plant Systematics and Evolution 302: 1239–1252. https://doi.org/10.1007/s00606-016-1329-z

Hoe YC, Wong SY, Gibernau M (2018) Diversity of pollination ecology in the *Schismatoglottis Calyptrata* Complex Clade (Araceae). Plant Biology. doi:10.1111/plb.12687

Kirejtshuk AG (1986) Revision of the genus Aethina Er. (Coleoptera, Nitidulidae) of the fauna of the Oriental and Palaearctic Regions. Proceedings of the Zioological Institute of Academy of Sciences of USSR 140: 44–82. [In Russian]

Kirejtshuk AG (1994) System, evolution of the way of life, and phylogeny of the order Coleoptera. I. Entomological Review 73(2): 266–288 (in Russian). [English translation: 1995, 74: 12–31]

Kirejtshuk AG (1997) On the evolution of anthophilous Nitidulidae (Coleoptera) in tropical and subtropical regions. Bonner Zoologische Beitrage 47(1–2): 111–134.

Low SL, Wong SY, Boyce PC (2014) *Schottarum* (Schismatoglottideae: Araceae) substantiated based on combined nuclear and plastid DNA sequences. Plant Systematics and Evolution 300: 607–617. https://doi.org/10.1007/s00606-013-0906-7

Low SL, Wong SY, Ooi IH, Hesse M, Städler Y, Schönenberger J, Boyce PC (2016) Floral diversity and pollination strategies of three rheophytic Schismatoglottideae (Araceae). Plant Biology 18(1): 84–97. https://doi.org/10.1111/plb.12320

Low SL, Wong SY, Boyce PC (2018). Naming the chaos: generic redelimitation in Schismatoglottideae (Araceae). Webbia 72: 1–100. https://doi.org/10.1080/00837792.2017.1409940

Minoshima YN, Seidel M, Wood JR, Leschen RAB, Gunter NL, Fikáček M (2018) Morphology and biology of the flower-visiting water scavenger beetle genus Rygmodus (Coleoptera: Hydrophilidae). Entomological Science. https://doi.org/10.1111/ens.12316

Orchymont A (1919) Contribution a l'étude des sous-familles des Sphaeridiinae et des Hydrophilinae (Col. Hydrophilidae). Annales de Société Entomologique de France 88 : 105–168.

Ryndevich SK (2001) On identification of species of the Cercyon dux group (Coleoptera: Hydrophilidae). Zoosystematica Rossica 10(1): 79–83.

Ryndevich SK (2008) Review of species of the genus *Cercyon* Leach, 1817 of Russia and adjacent regions. IV. The subgenera *Paracycreon* Orchymont, 1924 and *Dicyrtocercyon* Ganglbauer, 1904 (Coleoptera: Hydrophilidae). Zoosystematica Rossica 17(2): 89–97.

Ryndevich SK, Jia FL, Fikáček M (2017) A review of the Asian species of the Cercyon unipunctatus group (Coleoptera: Hydrophilidae: Sphaeridiinae). Acta Entomologica Musei Nationalis Pragae 57(2): 535–576. https://doi.org/10.1515/aemnp-2017-0089

Shatrovskiy A (2017) A new species of *Cycreon* d'Orchymont, 1919 from Singapore (Coleoptera: Hydrophilidae: Megasternini). Zootaxa 4217 (3): 588–592. https://doi.org/10.11646/zootaxa.4317.3.11

Short AEZ, Fikáček M (2011) World catalogue of the Hydrophiloidea (Coleoptera): additions and corrections II (2006–2010). Acta Entomologica Musei Nationalis Pragae 51: 83–122.

Short AEZ, Fikáček M (2013) Molecular phylogeny, evolution and classification of the Hydrophilidae (Coleoptera). Systematic Entomology 38: 723–752. https://doi.org/10.1111/syen.12024

Smetana A (1978) Revision of the subfamily Sphaeridiinae of America north of Mexico (Coleoptera: Hydrophilidae). Memoirs of Entomological Society of Canada 105: 1–292. https://doi.org/10.4039/entm110105fv

Takizawa H (2010) Revisional notes on the genus *Chaloenus* Westfood (Coleoptera: Chrysomelidae). In: Mohammed HJ, Ipor I, Meekiong K, Sapuan KA, Ampeng A (Eds) Lanjak Entimau Wildlife Sanctuary 'Hidden Jewel of Sarawak'. Proceedings of the Seminar: Lanjak Entimau Scientific Expeditions. Academy of Sciences Malaysia, 347–355.

Teichert H, Dötterl S, Framec D, Kirejtshuk A, Gottsberger G (2012) A novel pollination mode, saprocantharophily, in Duguetia cadaverica (Annonaceae): A stinkhorn (Phallales) flower mimic. Flora (Morphology, Distribution, Functional Ecology of Plants) 207(7): 522–529. https://doi.org/10.1016/j.flora.2012.06.013

Supplementary material 1

List of known specimens of Cycreon in DarwinCore format

Authors: Emmanuel Arriaga-Varela, Sin Yeng Wong, Alexander Kirejtshuk, Martin Fikáček

Data type: occurence

Link: https://doi.org/10.3897/dez.65.26261.suppl1

Chapter 4

Water scavenger beetles in rotten cacti: A review of *Agna* with the description of a new species from Mexico (Coleoptera: Hydrophilidae: Sphaeridiinae)

Arriaga-Varela, E., Cortés-Aguilar, J. and Fikácek, M. (Accepted). Water scavenger beetles in rotten cacti: A review of *Agna* with the description of a new species from Mexico (Coleoptera: Hydrophilidae: Sphaeridiinae). *Revista Mexicana de Biodiversidad.*

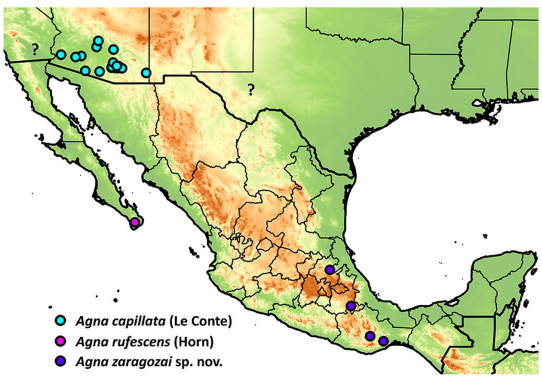

Water scavenger beetles in rotten cacti: A review of *Agna* with the description of a new species from Mexico (Coleoptera: Hydrophilidae: Sphaeridiinae)

Escarabajos hidrofílidos en cactus podridos: Una revisión de *Agna* con la descripción de una especie nueva de México (Coleoptera: Hydrophilidae: Sphaeridiinae)

Emmanuel Arriaga-Varela[a,b]*, Jesús Cortés-Aguilar[c], Martin Fikáček[b,a]

[a] *Department of Zoology, Faculty of Science, Charles University, Viničná 7, CZ-128 44 Praha 2, Czech Republic*

[b] *Department of Entomology, National Museum, Cirkusová 1740, CZ-193 00 Praha, Czech Republic*

[c] *Comisión Nacional Forestal. Periférico Poniente 5360, Zapopan, Mexico*

* corresponding author: arriagavarelae@natur.cuni.cz (E. Arriaga-Varela)

Abstract

The terrestrial hydrophilid genus , *Agna* Smetana (tribe Megasternini), specialized on rotten cacti, is reviewed,redescribed and illustrated. Known species are diagnosed and a new one, *A. zaragozai* sp. nov. is described from central Mexico (Hidalgo, Puebla and Oaxaca) and its molecular barcode is provided. Other species of Hydrophilidae known to be collected in cacti are listed and commented. *Dactylosternum cacti* (LeConte) (Coelostomatini) is recorded for the first time from Mexico and *Cryptopleurum impressum* Sharp (Megasternini) is recorded for the first time from the Mexican states of Jalisco and San Luis Potosí.

Keywords. Saprophilous, Neotropical, Neartic, arid, semiarid, Hydrophiloidea. barcode of life

Resumen

Se revisa el género terrestre de Hydrophylidae, *Agna* Smetana (tribu Megasternini), especializado en cactus podridos. El género es redescrito e ilustrado. Las especies conocidas son diagnosticadas y una nueva, *A. zaragozai* sp. nov., de Hidalgo, Puebla y Oaxaca es descrita. Otras especies de Hydrophilidae con registros de colecta en cactus podridos son listadas y comentadas. *Dactylosternum cacti* (LeConte) (tribu Coelostomatini) es registrada por primera vez en México y *Cryptopleurum impressum* Sharp (Megasternini) se registra por primera vez para los estados mexicanos de Jalisco y San Luis Potosí.

Keywords. Saprófilo, Neotropical, Neártico, árida, semiárida, Hydrophiloidea. Código de barras de la vida

Introduction

Cacti are a predominant component of arid and semi-arid landscapes in the New World. Their modified stems allow them to perform photosynthesis and store humidity in environments where moisture is usually a limited resource. For this reason, cacti in process of necrosis represent a great opportunity for the reincorporation of humidity back into the ecosystem, providing, for a brief period, the chance for the sustainment of a wide variety of invertebrates from different guilds (Ferro et al., 2013). Water scavenger beetles (Coleoptera: Hydrophiloidea: Hydrophilidae) are typically associated to a variety of water bodies (Hansen, 1991). Nevertheless, members of Sphaeridiinae, the most derived and probably most speciose subfamily in Hydrophilidae (Hansen, 1991, Short & Fikáček, 2013) are primarily found outside of water, almost wherever there is organic material in process of decomposition with enough content of humidity. Among the most common microenvironments where sphaeridiines can be collected are, for example, mammal excrements (Archangelsky, 1997; Sowig et al., 1997; Arriaga-Varela et al., 2018a), humid leaf litter (Fikáček & Short, 2006), inflorescences of Araceae and Heliconiaceae (Arriaga-Varela et al., 2018b) and debris accumulated by social insects in or near their nests (Spangler, 1962; Fikáček *et al.,* 2013). Few sphaeridiine representatives have colonized arid zones and are associated to necrotic tissues of succulent plants. Among the New World hydrophilids associated to rotten cacti we can find representatives of four genera: *Dactylosternum* Wollaston, 1854, *Cryptopleurum* Mulsant, 1844, *Pelosoma* Mulsant, 1844 and *Agna* Smetana, 1978.

Agna stands as the only sphaeridiine genus presumably strictly associated to necrotic tissue of succulent plants, mainly Cactaceae (Smetana, 1978). Its two closely similar Nearctic species where classified as members of *Pelosoma* until Smetana (1978) revealed that they differ from the latter by few crucial characters, namely the elevated middle portion of the prosternum, absence of male maxillary suckers and the concave metaventrite in males. Based on these differences, Smetana (1978) transfered both species into a new genus, *Agna* Smetana, 1978. In this paper we review the genus, redescribe its morphology and describe a new species collected in the semi-arid zones of Hidalgo, Oaxaca and Puebla states, Mexico. Additionally, we summarize the known data about the other New World Sphaeridiinae which have been found in rotten cacti.

Materials and methods

Morphologial studies. Acronyms for the collections where the examined specimens are deposited:

BMNH	Natural History Museum, London, United Kingdom (M.V. L. Barclay);
CAS	California Academy of Science, San Francisco, United States of America (D. Kavanaugh, V. Lee);
CNIN	Colección Nacional de Insectos, Instituto de Biología, Universidad Nacional Autónoma de México, Mexico City, Mexico (S. Zaragoza-Caballero);
CZUG	Colección Entomológica del Centro de Estudios en Zoología, Universidad de Guadalajara, Zapopan, Mexico (J. L. Navarrete-Heredia);
FMNH	Field Museum of Natural History, Chicago, United States of America (C. Maier, A. F. Newton, M. Thayer).
FSCA	Florida State Collection of Arthropods, Gainesville, USA (P. Skelley);
NHMW	Naturhistorisches Museum, Wien, Austria (M. A. Jäch);
NMPC	National Museum, Prague, Czech Republic (M. Fikáček).

Specimens were dissected, with genitalia embedded in a drop of alcohol-soluble Euparal resin on a piece of glass glued to a small piece of cardboard attached below the respective specimen. Habitus photographs were taken using a Canon D-550 digital camera with attached Canon MP-E65mm f/2.8 1–5 macro lens. Pictures of genitalia were taken using a Canon D1100 digital camera attached to an Olympus BX41 compound microscope; pictures of different focus were combined in Helicon Focus software. Scanning electron micrographs were taken using Hitachi S-3700N environmental electron microscope at the Department of Paleontology, National Museum in Prague. Pictures used for plates were adapted in Adobe Photoshop CS6. Distribution map, based on the examined material and records given by Smetana (1978), was prepared using QGIS software and freely available GLOBE altitude data and DIVA-GIS country borders data. All original pictures including additional views not presented in this paper are included in the dataset submitted to the Zenodo archive under doi: 10.5281/zenodo.1473568.

DNA barcoding. DNA was extracted from the holotype of the new species of *Agna* collected in a recent expedition in Mexico using a Qiagen Blood and Tissue DNA extraction kit following the manufacturer's instructions. The highly variable 5’ region of the mitochondrial cytochrome c oxidase subunit I gene (COI) was amplified using LCO1490 (5'GGTCAACAAATCATAAAGATATTGG-3') and HCO2198 (5'TAAACTTCAGGGTGACCAAAAAATCA-3') primers (Folmer et al. 1994). Each 10 µl PCR

reaction contained 6.7 µl H2O, 0.4 µl of MgCl2 (25 mM), 0.2 µl of dNTPs (10 mM), 0.3 µl of each forward and reverse primer (10 µM), 0.1 µl of Taq polymerase (5 u/µl), 1.0 µl of 10x Taq buffer, and 1.0 µl of DNA template. The PCR conditions consisted of 3 min at 94 °C + 35 cycles of 30 s at 94 °C, 45 s at 48 °C and 1 min at 72 °C + 8 min at 72 °C. 5 µl of each PCR product were purified by adding 0.5µl (20 u) Exonuclease I (Exo1) and 1µl (1 u) Thermosensitive Alkaline Phosphatase (FastAP) (Thermo Fisher Scientific) and incubating the mixture for 15 min at 37°C, followed by 15 min at 80°C. Sanger sequencing was performed by Macrogen Europe (Amsterdam, Netherlands) on a capillary DNA sequencer.

Taxonomy.

***Agna* Smetana, 1978**

Agna Smetana, 1978: 173 (type species: *Cercyon capillatum* LeConte, 1855, by original designation).

Diagnosis. Agna can be differentiated from other megasternines by the following characters: maxilla of both sexes without sucking disc (figs. 2d, 3b); prosternum strongly raised medialy, with a strong median carina, raised part clearly demarcated from the from lateral portions of prosternum (fig. 3d); mesoventral plate hexagonal, slightly longer than broad, posterior margin broadly connected with metaventrite (figs. 2g, 3g-i); male sternite IX horse-shoe shaped, without sclerotized median process (fig. 1i).

Differential diagnosis. Before the establishment of *Agna*, its species where classified as members of *Pelosoma*. Smetana (1978) distinguished *Agna* from *Pelosoma* (see above for diagnostic characters), but supposed them to be closely related on the basis of the mesoventral plate broadly connected to the metaventrite. The male sternite IX assignes *Agna* to the *Oosternum* group of genera (‘Gondwanan genera’ sensu Fikáček 2010 and Fikáček & Short 2010), in contrast to *Pelosoma,* that bears a tongue-like male sternite IX and is a part of the *Cercyon* group of genera. This phylogenetic placement is corroborated by molecular data (Arriaga-Varela, in prep.), therefore *Agna* and *Pelosoma* are not closely related as previously hypothesized. Whitin the *Oosternum* group of genera, *Agna* resembles some representatives *Oosternum* by the form of the prosternal plate and the mesoventral elevation (e.g. some undescribed Neotropical species of the *O. sahlbergi* group). It can be, however, very easily distinguished from all *Oosternum* by the absence of the ridge demarcating anterolateral portion of the metaventrite and by the elytra without impressed elytral striae. Among the genera without that ridge, *Agna* is superficially similar to the Neotropical species

of the genus *Australocyon* which also bear widely triangular to pentagonal mesoventral plate and smooth elytra with elytral series not impressed; it can be diagnosed from *Australocyon* by the prosternal elevation demarcated by a simple lateral ridge (rather than double V-shaped ridge as in *Australocyon*) and by the grooves for reception of the procoxae (procoxal rests) distinctly demarcated posteriorly and not reaching mesocoxal cavities (not demarcated posteriorly and reaching mesocoxae in *Australocyon*).

Description. Head. Anterior margin of clypeus with very fine bead, not emarginate medially, anterolateral corners rounded; antennal bases exposed; frontoclypeal suture distinct laterally, absent in medial third; transverse ridges absent. Median portion of frons and clypeus not elevated above remaining surface. Whole dorsal surface with relatively coarse setiferous punctures; setae fine and decumbent (fig. 3a); area between punctures without visible microsculpture. Eyes small, situated on lateral angular portions of head (fig. 3a), with dorsally-visible portion slightly smaller than ventral one, separated by 6–7× the width of one eye in dorsal view. Labrum ca. 0.4× as wide as head, membranous, largely retracted under clypeus, markedly bisinuate on anterior margin, with moderately dense pubescence dorsally, setae almost of same lenght all over (fig. 2b). Mandible with apex simple, curved, with external margin simple; prostheca with anterior half covered by long thin setae (fig. 2c). Maxilla of male without sucking disc on galea (fig. 2d); maxillary palps with basal palpomere minute, palpomere 2 large, widened at apical half, 1.8× as long as palpomere 3, palpomere 3 slightly widened apicad, palpomere 4 fusiform, 1.5× as long as palpomere 3, without digitiform sensilla. Mentum (figs 2e) transverse, more than twice as wide as long, lateral margins with few sparse setae, anterior margin emarginate; labial palps trimerous, basal palpomere transverse, palpomere 2 as wide as the basal one, ca. 1.4× as long as wide, terminal palpomere very narrow, elongate, almost as long as the previous ca. 2.4× as long as wide. Submentum with moderately dense setiferous punctures, gular sutures vaguely developed, rather widely separated from each other, tentorial pits small, shallow. Antenna (fig. 2a) with 9 antennomeres; scape long, cylindrical, constricted medially; pedicel rather short, narrowing apically; antennomeres 3–5 short, subequal in length, continuously widening apically; cupule weakly asymmetrical and long then antennomere 5; antennomeres 7–9 forming elongate pubescent club (ca. 3× longer than wide), antennomere 7 ca. 1.3× as long as 8, antennomere 9 1.5× longer than the previous one, acuminate at apex; special sensorial antennal fields absent. Genal ridge absent. *Prothorax.* Pronotum transverse, moderately convex, nearly as wide as bases of both elytra combined; lateral margins very minutely beaded; punctation dense, composed of comparatively large setiferous punctures. Prosternum (figs 2f, 3d) strongly raised medially, with strong median carina; raised part clearly demarcated from lateral portions of prosternum by a simple oblique ridge; prosternal process short,

almost reaching half of lenght of procoxal cavities, weakly bifurcate; prosternal portion anterior of procoxae very narrow. Procoxal cavities large, open posteriorly. Notosternal suture very short. Antennal grooves present, very small, defined laterally by a faint ridge parallel to lateral prosternal margin, vanishing posteriad. *Mesothorax.* Mesoventrite completely fused with anepisternum; anterior collar of mesothorax narrow (fig. 2g). Median portion of mesoventrite elevated forming a subpentagonal elongated plate, slightly longer than wide, posterior margin broadly connected with intercoxal portion of metaventrite, not overlaping it (figs. 3g–i). Grooves for reception of procoxae well defined posteriorly by a conspicuous carina, short, transverse (figs. 3i). Mesepimeron moderately narrow, very weakly widening laterad. Mesocoxal cavities broadly separated. Scutellar shield small, triangular, 1.2× as long as wide (fig. 2h). Elytra moderately convex, weakly bordered laterally, each elytron with 10 conspicuous series (fig. 2k) not situated in a impressed sulci (Fig. 3f), or without series, only bearing irregular ground punctation (fig. 3e), if present, the series consist of foveate impressions with a setiferous puncture on anterior margin, punctures diameter 1-2 × the diameter of punctures in the interstices, series 1 and 9 reaching apex, enclosing series 2–8 subapically, series 10 reduced both anteriorly and posteriorly; elytral series visible in all species in microscopic slides as composed of dots of more transparent cuticle (figs. 2k-l); epipleuron oblique, gradually narrowing posteriad to mid-length of elytra, very gradually narrowing more posteriorly, vanishing shortly after the posterior margin of metaventrite, bearing sparse short setae. *Metathorax.* Metaventrite (fig. 2g) rather homogeneously and densely covered by comparatively long setae (figs. 3g–i), anterior margin with narrow rim, weakly widening towards intercoxal process; mesal elevate area vaguely pentagonal, rather narrow, about as long as wide, concave in males, slightly convex in females. Femoral lines and anterolateral ridges absent. Metanepisternum ca. 6 × as long as wide, with anterior oblique ridge, metepimeron with minute ventral portion. Metafurca well developed. Metathoracic wings well developed, with transverse vein r4 arising from basal portion of radial cell, RP rather long, reaching ca. halfway to wing base, basal cubito-anal cell small, closed; wedge cell absent, transverse vein mp-cua joining to MP_{3+4}+CuA_{1+2}; anal lobe not defined. *Legs.* Procoxae large, subglobular, transverse, with long setae; meso- and metacoxae broad, transverse. Tronchatero-femoral junction straight. Femora flattened, comparatively short, with very short setae; profemur without impressed parts; metafemur 1.1 × as long as mesofemur (fig. 2j). Tibiae rather short, triangular, flattened, straight on external margin, weakly convex on internal margin, with short lateral and mesal spines. Tarsi pentamerous, with moderately long tarsomeres (fig. 2j), tarsomeres sparsely covered with short stiff setae; metatarsomere 1 to tarsomeres 2-3 together, tarsomeres 2–4 gradually getting shorter, tarsomere 5 almost as long as tarsomere 1. Claws simple, arcuate. *Abdomen* with five ventrites (fig. 2i). Ventrite 1 about as long as ventrites 2–3 combined, with median carina getting slightly narrower posteriad. Male sternite IX horse-shoe shaped, without

sclerotized median process, apophyses narrow (fig. 1i). Aedeagus (figs. 1g-h, j-k) simple, median lobe weakly sinuate, phallobase very short, symmetrical, without projected manubrium; parameres simple, sinuate. Female genitalia corresponding to that of *Kanala* (see Fikáček, 2010).

Key to the species of *Agna* Smetana

1.- Elytra with 10 longitudinal series of punctures visible in dorsal view (fig. 3f); males with raised area of metaventrite deeply concave at anterior 3/5 (fig. 3i).....2

- Elytra without visible longitudinal series of punctures in dorsal view (fig. 3e); males with raised area of metaventrite weakly concave at anterior 1/3 (fig. 3g).....***Agna zaragozai* sp. nov.**

2.- Body color predominantly black (figs. 1d-f); prosternum with median portion projected anteriorly USA: California, Arizona, Texas.....***Agna capillata* (LeConte)**

- Body color predominantly brown; prosternum with median portion not projected anteriorly. Mexico: Baja California Sur.....***Agna rufescens* (Horn)**

***Agna zaragozai* sp. nov.**

(figs. 1d–f, 1j–k; 2l; 3a–e, 3g–h, 4g)

DNA barcode:

BIN ID BOLD:

Type locality. Mexico: Hidalgo, Mezquititlán, 20°31.8'N 98°38.5'W.

Type material. Holotype: male: **MEXICO: Hidalgo:** 4.5 km SSW of Cacalomé on rd.105; 20°25.0'N 98°41.3'W; 1785 m; 13.ix.2016; Arriaga, Cortés, Fikáček & Seidel lgt. (2016-MX20) in rotten stems of *Stenocereus* cacti (partly fermented) (CNIN). **Paratypes. MEXICO: Puebla:** Tehuacan, Pue. ca. 5500ft. Alt. VII:6:41 // Col. By H. Dybas (2 males, 1 female: FMNH, 1 male: NMPC); **Oaxaca:** Mexico: Oaxaca, 5 mi W Tequilistlán [Tequisistlán], 1100 ft, viii.23-ix-5.73 // on rotting cacti, columnar/*Opuntia*, A. Newton (1 male: FMNH); Mexico: Oaxaca, 2.1 mi NW Totolapam [Totolapa], 3500 ft, x.6.1973 // on rotting cacti, columnar/*Opuntia*, A. Newton (2 females: FMNH).

Diagnosis. This species can be distinguished from the other two congeners by the elytra without conspicuous series of punctures (fig. 3e) (present in the other known species); metaventrite of males with median raised part just weakly concave anteriorly (fig. 3g) (distinctly concave at anterior 3/5 in *A. capillata*); the aedeagus is just slightly sinuate at base (lateral margins slightly more sinuose with basal half briefly broadened in *A. capillata* (fig. 1k).

Description. Body (figs 1d–f). 2.4–2.9 mm long; moderately long-oval, 2.0× as long as wide, widest at basal fourth of elytra; moderately convex, 2.6× as long as high. *Coloration.* dark-brown to piceous black with legs and mouthparts dark reddish-brown, antennae tanned-yellow. *Head.* Frons and clypeus with deep and large round punctures intermixed with few slightly transverse ones; interstices without microsculpture. Eyes small; interocular distance about 6.5× the width of one eye in dorsal view. Mentum (fig. 3b) subhexagonal, widest at posterior third, about 2.2× wider than long, 1.4× wider at widest part than at anterior margin, almost completely flat; surface glabrous, with few sparse small punctures, surface rugged. Antenna with scapus ca. 1.5× as long as antennomeres 2–6 combined; antennal club moderately elongate, about twice as long as wide, about 1.2× as long as scapus; antennomere 9 acuminate at apex. *Prothorax.* Pronotum transverse, widest at base 1.9–2.0× wider than long; 1.6–1.7× wider at base than between anterior angles, 1.7× wider than head including eyes, as convex as elytra in lateral view. Punctuation dense and comparatively deep, consisting of rounded setiferous punctures intermixed with denser, smaller and rather transverse non-setiferous punctures (fig. 3c). Elevated median portion of prosternum 1.4 wider than long, with anteriorly projecting anterior margin. *Pterothorax.* Elytra widest at anterior fourth, 1.2× as long as wide, 2.5–2.6× as long as pronotum, 1.1× as wide as pronotum. Surface (fig. 3c) shortly pubescent; interstices without microsculpture. Mesoventral plate deeply punctuate, 1.3–1.6× as long as wide (fig. 3g). Metaventrite with raised area vaguely pentagonal, about as long as wide, pubescent, slightly more sparsely punctate than lateral areas, slightly convex in females, weakly concave at center in anterior 1/3 in males (figs. 3g–h); lateral parts of metaventrite covered by short pubescence. Hind wings present. *Legs.* Metafemora with setiferous punctures shallow. Metatibiae 0.3× as long as elytra. Metatarsi 0.8× as long as metatibia. *Male genitalia.* Sternite 9 subtruncate apically, without median projection, Phallobase (fig.1j) very short. Parameres long, almost 9 × as long as phallobase, narrowing towards apical 3/4, then weakly broadening towards apex, apex slightly hooked. Median lobe (fig. 1k) narrow, almost parallel-sided in basal half, slightly constricted in apical 3/4, apex acuminate, gonopore moderately large, situated subapically; basal portion truncate.

Etymology. We dedicate this species to Santiago Zaragoza-Caballero (Instituto de Biología, UNAM) as a homage to his work on Mexican Coleoptera.

Distribution. Mexico: Hidalgo, Puebla, Oaxaca.

Biology. Specimens have been collected in decaying parts of *Opuntia* and *Steneocereus* spp. cacti (fig. 4d).

***Agna capillata* (LeConte)**

(figs. 1a–c, 1g–i, 2a–k, 3a–e, 3g–h, 4g)

Cercyon capillatum LeConte, 1855: 374.

Pelosoma capillatum; Horn, 1890: 306.

Agna capillata; Smetana, 1978: 174.

Type locality. United States of America, California, San Diego (based on lectotype designation by Smetana (1978)).

Type material. Not examined. We have studied a series of specimens compared with the lectotype by A. Smetana (see Material examined below).

Material examined. USA: Arizona: Phoenix, Ari. / Liebeck Collection / *Agna capillata* Smetana det. 1975 (1 male, NMPC); Arizona, Pimo Co. (10 mi. E), 11.Viii.1968 /Saguaro W. Setter leg. (1 female, NMPC); Arizona: Santa Catalina foot hills, Feb. 25 1968, K. Stephen leg (1 male, FSCA); Arizona; Pinal Co. Tortolita Mts. Cottonwood Cyn., Dec. 14 1969, K. Stephen leg. (1 female, FSCA); Arizona: Yuma Kofa Game Reserve, 17-IV-76, Karls Stephan (1 female, FSCA).

Diagnosis. This species can be distinguished from *A. zaragozai* by the elytra with conspicuous series of punctures (fig. 3f); metaventrite of males with median raised distinctly concave at anterior 3/5 (fig. 3i) (weakly concave at anterior 1/3 in *A. zaragozai*); the median lobe with slightly sinuate lateral margins, being briefly broadened at basal half (fig.1h) (lateral margins subparallel in *A. zaragozai* (fig. 1k)). *Agna capillata* is similar to the holotype of *A. rufescens* in the presence of elytral series. However, it can be distinguished by the body predominantly black (reddish-brown in *A, rufescens* holotype) and anterior part of prosternal elevation slightly projecting anteriorly (straight on anterior margin in *A. rufescens*).

Description. Body (figs. 1a–c). 2.4–2.7 mm long; moderately long-oval, 2.0× as long as wide, widest at basal fourth of elytra; moderately convex, 2.4× as long as high. *Coloration.* dark-brown to piceous black with legs and mouth parts dark reddish-brown, antennae tanned-yellow. *Head.* Frons and clypeus with deep and large punctures, punctuation composed of rounded and

transverse impressions; interstices without microsculpture. Eyes small; interocular distance about 6.0× the width of one eye in dorsal view. Mentum subhexagonal, widest at posterior third, about 2.2× wider than long, 1.4× wider at widest part than at anterior margin, almost completely flat; surface glabrous, with few sparse small punctures, surface rugged. Antenna with scape ca. 1.5× as long as antennomeres 2–6 combined; antennal club moderately elongate, about twice as long as wide, about as 1.2× as long as scape; antennomere 9 acuminate at apex. *Prothorax.* Pronotum transverse, widest at base 2.0–2.2× wider than long; 1.6–1.7× wider at base than between anterior angles, 1.7× wider than head including eyes, as convex as elytra in lateral view. Punctation dense and comparatively deep, consisting of rounded setiferous punctures intermixed with denser, smaller and rather transverse non-setiferous ones. Elevated median portion of prosternum 1.4 wider than long, with anteriorly projecting anterior margin. *Pterothorax*. Elytra widest at anterior fourth, 1.3–1.4× as long as wide, 2.6–2.9× as long as pronotum, 1.1–1.2× as wide as pronotum. Surface glabrous, with 10 series of punctures; serial punctures of same size in all series, their diameter almost twice as that of punctures on intervals; interval punctation composed of rounded setiferous punctures on all intervals; interstices without microsculpture. Mesoventral plate deeply punctuate, 1.2–1.4× as long as wide (fig. 3i). Metaventrite with raised area vaguely pentagonal, about as long as wide, pubescent, almost as densely punctuate as lateral areas, slightly convex in females, strongly concave at center in anterior 4/5 in males; lateral parts of metaventrite covered by short pubescence. Hind wings present. *Legs.* Metafemora with setiferous punctures rather deep. Metatibiae 0.3–0.4× as long as elytra. Metatarsi 0.7× as long as metatibia. *Male genitalia.* Sternite 9 (fig. 1i) subtruncate apically, without median projection. Phallobase (fig. 1g) very short. Parameres long, almost 9 × as long as phallobase, narrowing towards apical 3/4, then weakly broadening towards apex, apex slightly hooked. Median lobe (fig. 1h) narrow, almost parallel-sided in basal 1/4, then margins sinuated, slightly broadened close to half length, weakly constricted in apical 3/4, apex acuminate, gonopore moderately large, situated subapically; basal portion truncate.

Distribution. United States of America: Arizona, California, Texas (fig. 4g). It is highly likely that the distribution of this species extends to Northwest Mexico.

Biology. This species is commonly found in large rotting cacti like saguaro (*Carnegiea gigantea*), fishhook barrel cactus (*Ferocactus wilizeni*) and occasionally in *Agave* sp. plants (Ferro et al., 2013). It has been reported to be attracted to UV lights (Smetana, 1978).

***Agna rufescens* (Horn)**

Cercyon rufescens Horn, 1895: 233.

Pelosoma rufescens; Leech, 1948: 457.

Agna rufescens; Smetana, 1978: 174.

Type locality. Mexico: Baja California Sur, Sierra de San Lazaro.

Type material.. Holotype examined: unsexed, (likely a female as apices of cerci are apparently visible) (CAS): Sierra / San Lazaro // Horn / Type // HOLOTYPE // rufescens // California Academy / of Sciences / Type No. 7. The holotype was examined by M. Fikáček in 2005.

Type material. Just the holotype was examined.

Diagnosis. The holotype of *A. rufescences* is very similar to the examined specimens of *A. capillata*, and we found only the following differences: body is much paler in general coloration (thought this may be caused by a possible teneral condition of the), body is slightly smaller than in the known specimens of the other two species, median elevated portion of prosternum is not projecting anteriad.

Redescription. Body 2.1 mm long; moderately long-oval, 1.7× as long as wide; moderately convex. *Coloration* reddish, elytral apices slightly paler. *Head.* Frons and clypeus with moderately deep and large punctures; interstices without microsculpture. Eyes small; interocular distance about 5.0× the width of one eye in dorsal view. Mentum subhexagonal, widest at posterior third, about 2.3× wider than long; surface glabrous, with moderately dense small punctures, surface with distinct rugged microsculpture. *Prothorax.* Pronotum transverse, widest at base 2.0× wider than long, as convex as elytra in lateral view. Punctation dense and comparatively deep, consisting of rounded setiferous punctures, smaller intermixed punctures not observed. Elevated median portion of prosternum 1.7 wider than long, without anteriorly projecting anterior margin. *Pterothorax.* Elytral surface glabrous, with 10 series of punctures clearly visible in dorsal view; serial punctures of same size in all series, their diameter only slightly larger than punctures on intervals; interval punctation composed of rounded setiferous punctures on all intervals; interstices without microsculpture. Mesoventral plate deeply and densely punctate, 1.3× as long as wide. Metaventrite with raised area vaguely pentagonal; lateral parts of metaventrite covered by short pubescence.

Comments. Since no other specimens are available from the Baja California peninsula, and taking into account the isolated geographic position of the type locality (fig. 4g), we are treating here *A. rufescens* as a species separate from *A. capillata*. The examination of additional specimens from the Baja California peninsula is needed in order to confirm the status of this species.

Distribution. Mexico: Baja California Sur.

Other Hydrophilidae occurring in rotten cacti

***Dactylosternum cacti* (LeConte)**

(fig. 4a)

Cyclonotum cacti LeConte, 1855: 373.

Dactylosternum cacti Horn, 1890: 284.

Type locality. United States of America: California, San Diego (based on lectotype designation by Smetana 1978).

Distribution. United States of America: Arizona, California; Guatemala: El Progreso; Mexico: Hidalgo (NEW COUNTRY RECORD).

Material examined. **MEXICO: Hidalgo:** 4.5 km SSW of Cacalomé on rd.105; 20°25.0'N 98°41.3'W; 1785 m; 13.ix.2016; Arriaga, Cortés, Fikáček & Seidel lgt. (2016-MX20) in rotten stems of *Stenocereus* cacti (partly fermented) (38: NMPC; 3: BMNH; 3: NHMW; 3: CNIN, 2: CZUG).

Comments. Dactylosternum is a worldwide genus with 62 described species (Hansen, 1999). Most species can be collected in decaying plant material, as rotten banana stems, rotten palm trunks etc. *Dactylosternum cacti* was described from southwestern USA, and as the name suggest it is almost exclusively collected on rotten cacti. Type locality of the species is the same as that of *Agna capillata* (LeConte): San Diego, California. Besides southern California, this species is known from Arizona, and was also recorded from Guatemala (El Progreso) by Archangelsky (1997), (see Archangelsy et al. 2016) (identification of the Guatemalan specimens was confirmed by examination of male genitalia, Archangelsky, pers. comm). The presence of the species in Mexico is hence not surprising and was also expected by Smetana (1978). Here we confirm that the species occurs in Mexico.

Cryptopleurum impressum Sharp

(fig. 4b)

Cryptopleurum impressum Sharp, 1882: 115.

Cryptopleurum cerei Schwarz, 1899: 8.

Type locality. Mexico: Veracruz, Córdoba (based on lectotype designation by Smetana 1978).

Material examined. **MEXICO: Veracruz:** 1.7 mi of Teocelo, 3700ft, 23-24.vii.1973, berselate dead grass pile, A. Newton (21: NMPC; 30: FMNH); **Jalisco:** Puerto los Mazos, 10 mi. SW Autlán 4400 ft, 25.ix.1973, refuse deposit *Atta mexicana*, A. Newton (12: NMPC; 50: FMNH); **San Luis Potosí:** 15 mi. N Tamazunchale, 500 ft, 26.vi.1973, ex refuse deposit *Atta mexicana*, A. Newton (7: NMPC; 15: FMNH); **Oaxaca:** 9 mi. NE Oaxaca, Km 9.5 Mex 175, 6100 ft, 25.viii.1973, refuse deposit *Atta mexicana*, A. Newton [larvae vial #20] (3: NMPC; 10: FMNH).

Comments. *Cryptopleurum* is a globally distributed genus with 24 described species, seven of which are distributed in the New World, either as native species or accidentally introduced through human activities (Hansen, 1999). In USA, *Cryptopleurum impressum* is commonly found in decaying large cacti of the genus *Cereus* and other rotten cacti (Smetana, 1978). In Mexico, it has been most commonly found associated with refuse piles of *Atta* ants (Hinton & Ancona, 1934; this paper). In Mexico, *C. impressum* has been reported from Baja California, México, Morelos, Oaxaca, Veracruz (Arce-Pérez & Morón, 2011). Here we record its presence from Jalisco and San Luis Potosí states from the first time. Most likely this species is more widely distributed in Mexico than presently known.

Distribution. Mexico: Baja California, México, Morelos, Jalisco, Oaxaca, San Luis Potosí, Veracruz; United States of America: Arizona.

***Pelosoma* sp.**

(fig. 4c)

Material examined. 1 male,. 5 spec. (NMPC): **MEXICO: Hidalgo:** Mezquititlán, river bank at the bridge 20°31.8'N 98°38.5'W; 1350 m; 16-17.ix.2016; Arriaga, Cortés, Fikáček & Seidel lgt. 016-MX2 // in pile of decaying parts of *Opuntia ficus-indica.*

Comment. Pelosoma is a New World genus currently including 17 described species. Nonetheless, our observation indicate that the diversity is highly understimate. Specimens of this genus are commonly found in flowers or rotten tissue of platns. In humid tropical forests they are collected in interior parts of inflorescences of families Araceae and Heliconiaceae or other Zingiberales, or in rotten parts of these plants, like stems and bases of leaves, or in leaf litter. In seasonally dry or semi-arid zones they have been found in rotten succulent plants. We collected few specimens of this genus in a pile of rotting cladodes of *Opuntia ficus-indica* cactus in an area with xerophytic vegetation (Fig. 4f). Comparison of the specimens with the descriptions and illustrations of species known from USA and Central America (Sharp, 1882; Smetana, 1978) suggests that they represent an undescribed species. Additional observations are needed to reveal whether this species occurs specifically in rotten cactus tissues, or if it may inhabit a wider spectrum of microhabitats. A

diffetent unidentified species of *Pelosoma* was collected by one of us (JCA) in rotten *Agave valencia* (Asparagaceae), a succulent plant species of a diferent family than Cactaceae, in the ecotone of tropical dry forest and a seasonally dry *Quercus* forest, in El Coamil, Mascota, in the state of Jalisco, Mexico.

Acknowledgements

This work was supported by the European Union's Horizon 2020 research and innovation programme under the Marie Skłodowska-Curie grant agreement No. 642241 to EAV, and by the Ministry of Culture of the Czech Republic (DKRVO 2018/13, National Museum, 00023272) to MF. The work of EAV at the Department of Zoology, Charles University, Prague was partly supported by grant SVV260434/2018. We thank Matthias Seidel (Charles University, Prague) for his help in the collecting of the holotype of *Agna zaragozai* sp. nov.. The curators of the entomological collections where the material is deposited are kindly acknowledged.

References

Arce- Pérez, R. & Morón, M. A. (2011), Sinopsis de los Hydrophiloidea de México (Coleoptera: Hydrophilidae, Helophoridae, Epimetopidae, Georissidae e Hydrochidae), con una clave para la identificación de los géneros. *Revista Mexicana de Biodiversidad*, 82 (2), 491–514.

Archangelsky, M. (1997). Studies on the biology, ecology & systematics of the immature stages of New World Hydrophiloidea (Coleoptera: Staphyliniformia). *Bulletin of the Ohio Biological Survey (New Series),* 12 (1), ix+207.

Archangelsky, M., Rodriguez G. & Torres P. L. M. (2016). Primary chaetotaxy and larval morphometry of *Phaenonotum exstriatum* and *Dactylosternum cacti* (Coleoptera: Hydrophilidae). *Acta Entomologica Musei Nationalis Pragae,* 56, 167–193

Arriaga-Varela, E., Seidel, M. & Fikáček, M. (2018a). A new genus of coprophagous water scavenger beetle from Africa (Coleoptera, Hydrophilidae, Sphaeridiinae, Megasternini) with a discussion on the *Cercyon* subgenus *Acycreon*. *African Invertebrates,* 59(1), 1–23. https://doi.org/10.3897/AfrInvertebr.59.14621

Arriaga-Varela, E., Wong, S.Y., Kirejtshuk. A. & Fikáček, M. (2018b). Review of the flower-inhabiting water scavenger beetle genus *Cycreon* (Coleoptera, Hydrophilidae), with descriptions of new species and comments on its biology. *Deutsche Entomologische Zeitschrift,* 65(1), 99–115. https://doi.org/10.3897/dez.65.26261

Ferro, M. L., Nguyen, N. H., Tishechkin, A. K., Park J. S., Bayless, V. & Carlton C.E. (2013). Coleoptera collected from rotting fishhook barrel cacti (*Ferocactus wislizeni* (Engelm.) Britton and Rose), with a review of nearctic Coleoptera associated with succulent necrosis. *The Coleopterists Bulletin*, 67(4), 419–443.

Fikáček, M. (2010). Hydrophilidae: The genus *Kanala* Balfour-Browne (Coleoptera). In: M.A. Jäch, & M. Balke, (Eds.) *Water Beetles of New Caledonia, Vol. 1. Monographs of Coleoptera 3*, 365–394.

Fikáček, M. & Short, A. E. Z. (2006). A revision of the Neotropical genus *Motonerus* Hansen (Coleoptera: Hydrophilidae: Sphaeridiinae). *Zootaxa*, 1268, 1–38.

Fikáček, M. & Short, A. E. Z. (2010). A revision of the Neotropical genus *Sacosternum* Hansen (Coleoptera: Hydrophilidae: Sphaeridiinae). *Zootaxa,* 2538, 1–37.

Fikáček, M., Maruyama, M., Vondráček, D. & Short, A. E. Z. (2013). *Chimaerocyon* gen. nov., a morphologically aberrant myrmecophilous genus of water scavenger beetle (Coleoptera: Hydrophilidae: Sphaeridiinae). *Zootaxa*, 3716, 277–288.

Folmer, O., Black, M., Hoeh, W., Lutz, R. & Vrijenhoek, R. (1994). DNA primers for amplification of mitochondrial cytochrome c oxidase subunit I from diverse metazoan invertebrates. *Molecular Marine Biology and Biotechnology,* 3, 294–299.

Hansen, M. (1991). The hydrophiloid beetles: phylogeny, classification and a revision of the genera (Coleoptera, Hydrophiloidea). *Biologiske Skrifter,* 40, 1–368.

Hansen, M. (1999). *World Catalogue of Insects 2: Hydrophiloidea (Coleoptera)*. Apollo Books, Stenstrup, 416 pp.

Hinton, H. E. & Ancona, H. L. (1934). Fauna de coleópteros en nidos de hormigas (*Atta*), en México y Centro América. *Anales del Instituto de Biología, Universidad Nacional Autónoma de México*, 5, 243-248.

Horn, G. H. (1895). Coleoptera of Baja California. (Supplement I.). *Proceedings of the California Academy of Sciences,* (2) 5, 225–259, pl. XX.

LeConte, J. L. (1855). Synopsis of the Hydrophilidæ of the United States. -*Proceedings of the Academy of natural Sciences of Philadelphia,* 7, 356–375.

Sharp, D. (1882). Insecta: Coleoptera. Vol. 1. Part 2 (Haliplidae, Dytiscidae, Gyrinidae, Hydrophilidae, Heteroceridae, Parnidae, Georissidae, Cyathoceridae, Staphylinidae). In: Godman, F. C. & Salvin, O.(Eds) Biologia Centrali-Americana. Volume 16. Taylor & Francis, London, i–xv + 1–144.

Short, A. E. Z. & Fikáček, M. (2013). Molecular Phylogeny, Evolution, and Classification of the Hydrophilidae (Coleoptera). *Systematic Entomology*, 38, 723–752.

Smetana, A. (1978). Revision of the subfamily Sphaeridiinae of America north of Mexico (Coleoptera: Hydrophilidae). *Memoirs of the Entomological Society of Canada,* 105, 1–292.

Sowig, P., Himmelsbach, R. & Himmelsbach, W. (1997). Predator-prey relationships between insect larvae: growth of *Sphaeridium* larvae (Coleoptera: Hydrophilidae) under time constraints through predation on *Musca autumnalis* maggots (Diptera: Muscidae). *Canadian Journal of Zoology,* 75, 2069–2076.

Spangler, P. J. (1962). A new species of the genus *Oosternum* and a key to the U. S. species (Coleoptera: Hydrophilidae). *Proceedings of the Biological Society of Washington*, 75, 97–100.

Figure captions

Figure 1. *Agna* spp. habitus and genitalia; A-C, G-I, *A. capillata* (LeConte); D-F, J-K, *A. zaragozai* sp. nov. A, dorsal habitus. White arrow pointing to series of punctation. Scale bar 1mm; B, ventral habitus; C, lateral habitus; D, dorsal habitus. Scale bar 1mm; E, ventral habitus; F, lateral habitus; G, tegmen of aedeagus; H, median lobe of aedeagus; I sternite IX; J, tegmen of aedeagus; K, median lobe of aedeagus.

Figure 2. *Agna* spp. general morphology; A-K, *A. capillata* (LeConte); L, *A. zaragozai* sp. nov. A, ventral view of head; B, labrum; C, mandible; D, maxila; E, labium; F, ventral view of prothorax; G, meso- and metathoracic ventrites; H, scutellum; I, abdominal ventrites; J, hind leg; K, elytron in dorsal view; L, elytron in ventral view.

Figure 3. *Agna* spp. SEM micrographs; A-E, G-H, *A. zaragozai* sp. nov.; F, I, *A.capillata* (LeConte). A, dorsal surface of head; B, ventral view of mouthparts; C, dorsal surface of pronotum; D; prosternum, E, dorsal surface of elytron in horizontal position; F, dorsal surface of elytron in horizontal position; G, meso- and metaventrites of male; H, meso- and metaventrites of female; I, meso- and metaventrites of male.

Figure 4. A-C, dorsal habiti of rotten-cacti associated hydrophilids; A, *Dactylosternum cacti* (Le Conte), length: 6.6 mm; B, *Cryptopleurum impressum* Sharp, length: 1.6 mm; C, Pelosoma sp., length: 2.6 mm; D-F, habitats of rotten-cacti associated hydrophilids; D, collecting *Agna zaragozai* sp. nov. and *Dactylosternum cacti* in rotten *Stenocereus* in Mezquititlán, Hidalgo; E, *Dactylosternum cacti* in rotten *Stenocereus*; F, locality at the river bank in Mezquititlán, Hidalgo were *Pelosoma* sp. specimens were collected in a pile of rotten *Opuntia ficus-indica* (indicated by red arrow); G, map with known distribution of *Agna* species, cyan circles: *A. capillata* (Le Conte), interrogation marks: imprecise localities of *A. capillata*; purple circle: *A. rufescens* (Horn), blue circles: *A. zaragozai* sp. nov.

Figure 1. *Agna* spp. habitus and genitalia; A-C, G-I, *A. capillata* (LeConte); D-F, J-K, *A. zaragozai* sp. nov. A, dorsal habitus. White arrow pointing to series of punctation. Scale bar 1mm; B, ventral habitus; C, lateral habitus; D, dorsal habitus. Scale bar 1mm; E, ventral habitus; F, lateral habitus; G, tegmen of aedeagus; H, median lobe of aedeagus; I sternite IX; J, tegmen of aedeagus; K, median lobe of aedeagus.

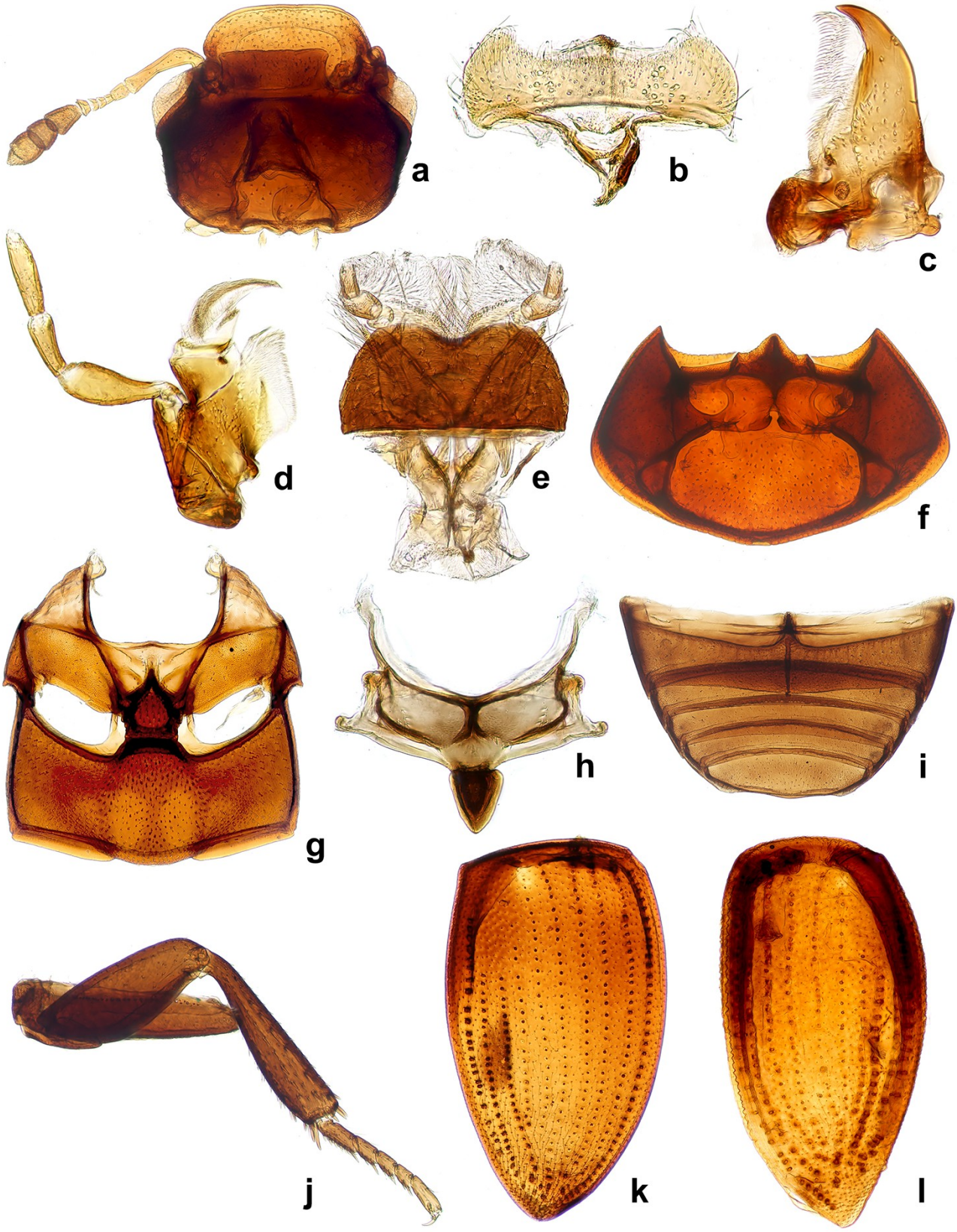

Figure 2. *Agna* spp. general morphology; A-K, *A. capillata* (LeConte); L, *A. zaragozai* sp. nov. A, ventral view of head; B, labrum; C, mandible; D, maxila; E, labium; F, ventral view of prothorax; G, meso- and metathoracic ventrites; H, scutellum; I, abdominal ventrites; J, hind leg; K, elytron in dorsal view; L, elytron in ventral view.

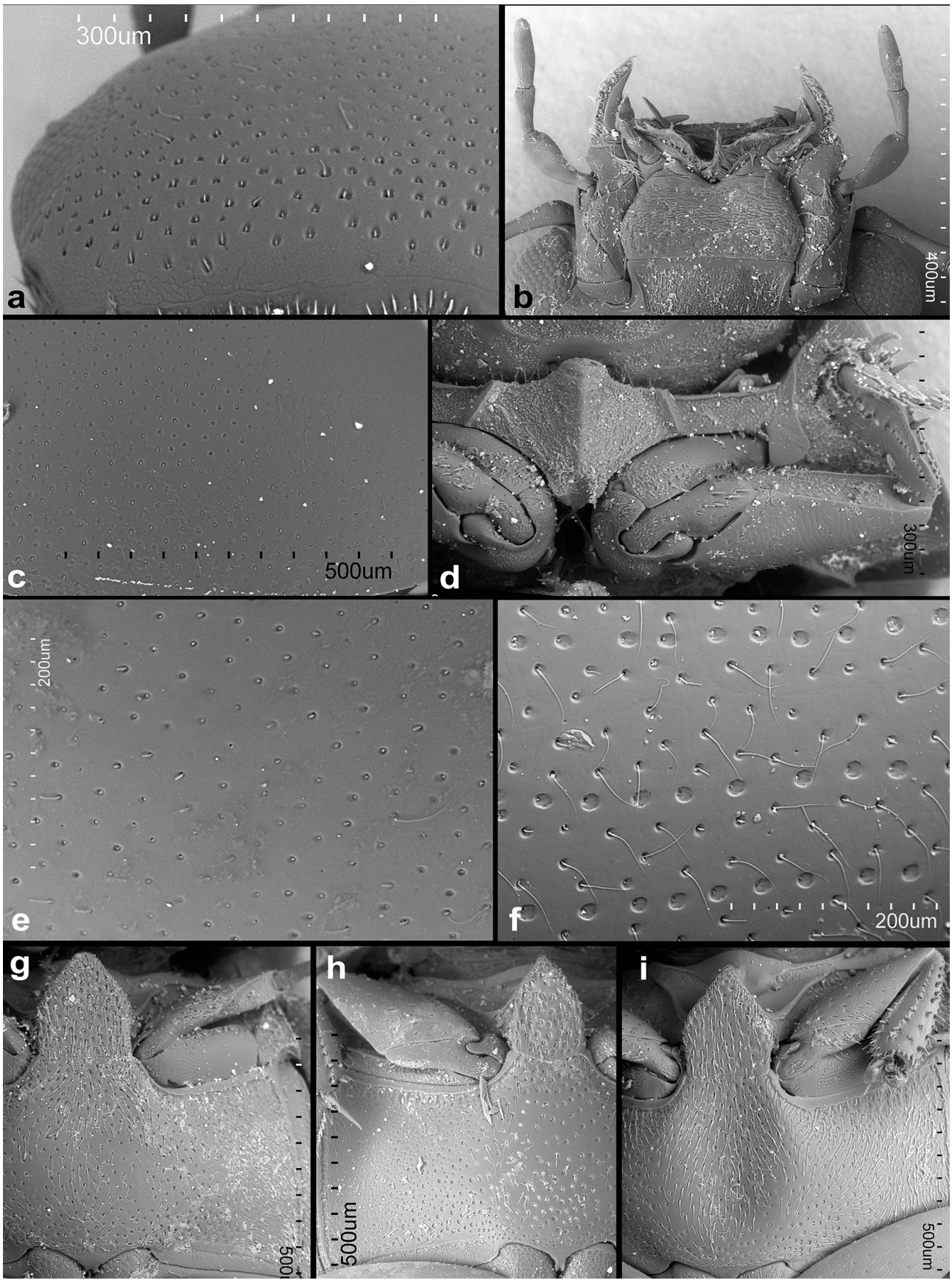

Figure 3. *Agna* spp. SEM micrographs; A-E, G-H, *A. zaragozai* sp. nov.; F, I, *A.capillata* (LeConte). A, dorsal surface of head; B, ventral view of mouthparts; C, dorsal surface of pronotum; D; prosternum, E, dorsal surface of elytron in horizontal position; F, dorsal surface of elytron in horizontal position; G, meso- and metaventrites of male; H, meso- and metaventrites of female; I, meso- and metaventrites of male.

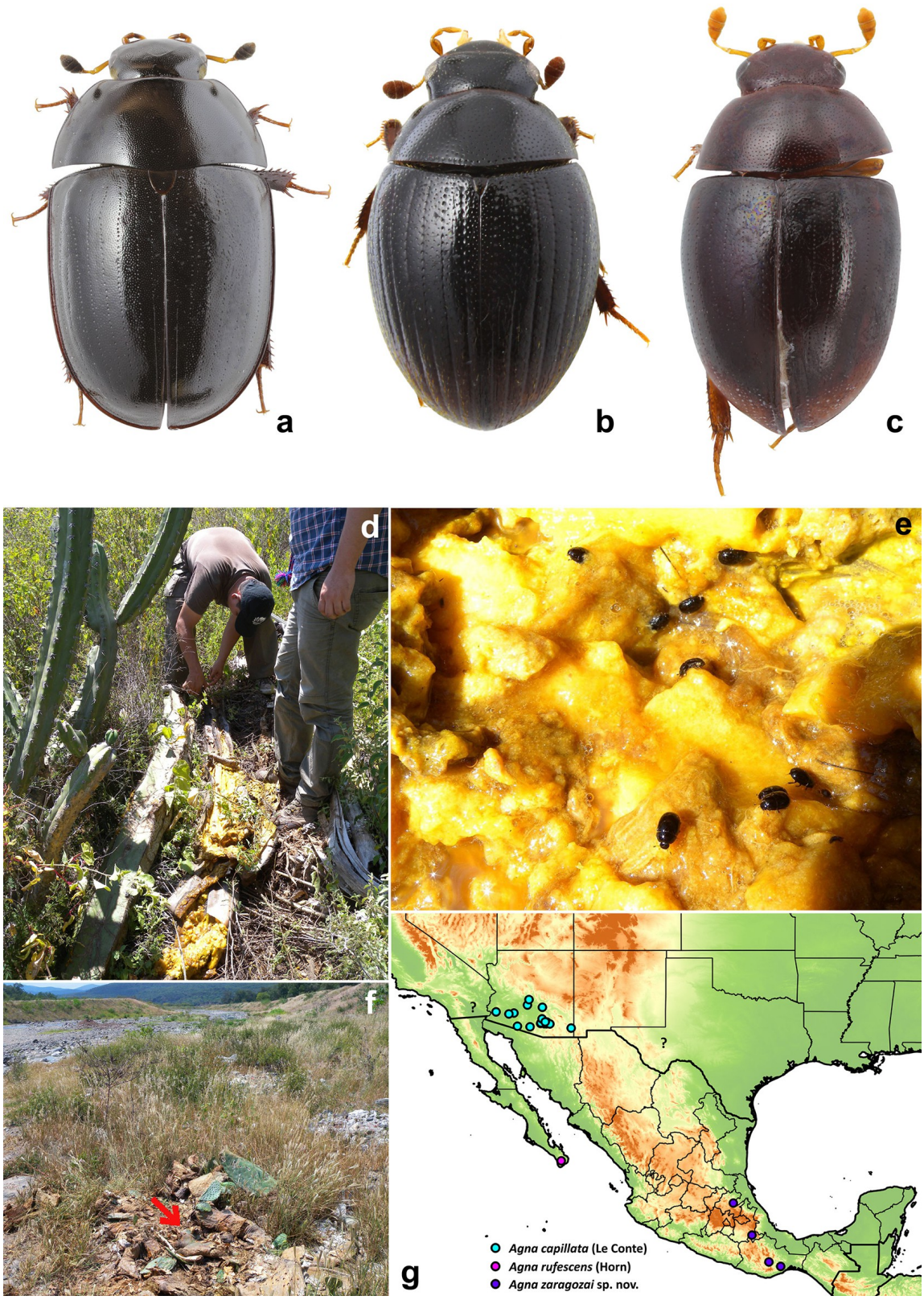

Figure 4. A-C, dorsal habiti of rotten-cacti associated hydrophilids; A, *Dactylosternum cacti* (Le Conte), length: 6.6 mm; B, *Cryptopleurum impressum* Sharp, length: 1.6 mm; C, Pelosoma sp., length: 2.6 mm; D-F, habitats of rotten-cacti associated hydrophilids; D, collecting *Agna zaragozai* sp. nov. and *Dactylosternum cacti* in rotten *Stenocereus* in Mezquititlán, Hidalgo; E, *Dactylosternum cacti* in rotten *Stenocereus*; F, locality at the river bank in Mezquititlán, Hidalgo were *Pelosoma* sp. specimens were collected in a pile of rotten *Opuntia ficus-indica* (indicated by red arrow); G, map with known distribution of *Agna* species, cyan circles: *A. capillata* (Le Conte), interrogation marks: imprecise localities of *A. capillata*; purple circle: *A. rufescens* (Horn), blue circles: *A. zaragozai* sp. nov.

Instituto de Biología UNAM

Revista Mexicana de Biodiversidad
Universidad Nacional Autónoma de México

Ciudad Universitaria, a 3 de mayo del 2019

Estimados Emmanuel Arriaga-Varela, Jesús Cortés-Aguilar y Martin Fikáček,

Después de revisar la versión corregida de su trabajo "Water scavenger beetles in rotten cacti: A review of *Agna* with the description of a new species from Mexico (Coleoptera: Hydrophilidae: Sphaeridiinae)", les informo que ha sido aceptado para su publicación en nuestra revista y aparecerá en el próximo número disponible. En cuanto tengamos listas las pruebas de galeras se las haremos llegar para una última revisión. Les reitero nuestra invitación a enviar fotografías relacionadas con su trabajo para la selección de imágenes que aparecerán en la portada correspondiente.

Sin más por el momento, reciban un saludo cordial.

Atentamente,

Dr. Juan J. Morrone Lupi

Editor Asociado

Chapter 5

Micro-CT reveals hidden morphology and clarifies the phylogenetic position of Baltic amber water scavenger beetles (Coleoptera: Hydrophilidae)

Arriaga-Varela, E., Brunke, A., Girón, J.C., Szawaryn, K., Bruthansová, J. and Fikácek, M. (*Submitted*). Micro-CT reveals hidden morphology and clarifies the phylogenetic position of Baltic amber water scavenger beetles (Coleoptera: Hydrophilidae). *Papers in Palaeontology.*

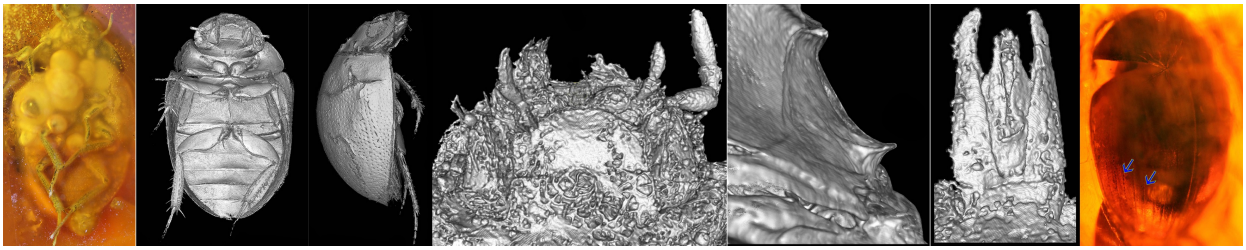

Micro-CT reveals hidden morphology and clarifies the phylogenetic position of Baltic amber water scavenger beetles (Coleoptera: Hydrophilidae)

EMMANUEL ARRIAGA-VARELA[1,2*], ADAM BRUNKE[3], JENNIFER C. GIRÓN[4,5], KAROL SZAWARYN[6], JANA BRUTHANSOVÁ[7] & MARTIN FIKÁČEK[2,1*]

[1]Department of Zoology, Faculty of Science, Charles University, Prague, Viničná 7, CZ-12843, Prague, Czech Republic; e-mails: arriagavarelae@natur.cuni.cz, biorbit@hotmail.com

[2]Department of Entomology, National Museum, Cirkusová 1740, CZ-19300 Prague, Czech Republic;

[3]Canadian National Collection of Insects, Arachnids and Nematodes, 960 Carling Avenue, K1A 0C6, Ottawa, Ontario, Canada; e-mail: adam.j.brunke@gmail.com

[4]Department of Ecology & Evolutionary Biology, and Division of Entomology, Biodiversity Institute, University of Kansas, Lawrence, KS 66045, USA; e-mail: jcgiron@ku.edu

[5]Natural Science Research Laboratory, Museum of Texas Tech University, Lubbock, TX 79409, USA;

[6]Museum and Institute of Zoology, Polish Academy of Science, Wilcza 64, 00-679, Warsaw, Poland; e-mail: k.szawaryn@gmail.com

[7]Department of Paleontology, National Museum, Cirkusová 1740, CZ-19300 Prague, Czech Republic; e-mail: jana_bruthansova@nm.cz

*Corresponding authors

ABSTRACT

Water scavenger beetles (Coleoptera: Hydrophilidae) are a broadly distributed group with high extant diversity. However, reliable records from Baltic amber (Eocene) are scarce and limited to two undescribed species previously reported in the literature. Here we study these two specimens plus four additional ones. All specimens were sub-optimal in terms of preservation and visibility of their morphology using traditional light microscopy. Opaque bubbles, cracks in the amber pieces and contracted appendages obscured most of the crucial characters, preventing their formal description and making them prone to misidentification. Here we used X-ray micro-computed tomography (μCT) to reconstruct the morphology of the embedded specimens and described three new species: *Anacaena morla* sp. nov., *Crenitis profechuyi* sp. nov. and *Helochares fog* sp. nov. Micro-CT reconstructions allowed us to visualize the morphology of the specimens to an extent where it was possible to hypothesize possible phylogenetic relations of the new taxa as well as the biogeographic implications of these relationships.
Key words: Eocene; Hydrophiloidea; Chaetarthriinae; Acidocerinae; X-ray μCT

Reconstructing the evolutionary history of any group of living organisms is increasingly based mostly on genetic data acquired and analysed by a rapidly developing set of techniques. In order to have a more precise insight of the tempo and mode of evolution of living organisms, it is crucial to integrate evidence from the fossil record (Quental & Marshall 2010). Studies of extinct taxa help us to strengthen hypotheses about phylogenetic relationships among organisms and the timing of evolutionary events (Grimaldi & Engel 2005; Penney 2008; Ho & Duchêne 2014; Hipsley & Müller 2014). Fossil species can be included as terminals in phylogenetic analyses with their morphological characters coded (so-called total evidence dating or tip dating) or their ages can be used to constrain the minimum ages of clades (node dating).

The quantity and quality of the information we can extract from fossil specimens is

inherently limited by the preservation process (Martínez-Delclòs *et al.* 2004; Labandeira 2014; McCoy *et al.* 2018). Organisms embedded in amber are amongst the best-preserved fossils as they often preserve a life-like fidelity that allows scientists to observe their morphology in detail. Unfortunately, not all amber pieces are perfect windows to the past; contracted limbs, clouds of opaque substances, bubbles and cracks in the amber piece might obscure the visibility of important characters and make them unsuitable for examination using conventional light microscopy (Judson 2003; Lak *et al.* 2008; Kypke & Solodovnikov 2018). Even in cases of well-preserved amber fossils, specialists can face challenges in the interpretation of characters that are not clearly observable or are distorted (Clarke et al. 2019). Non-invasive methods of visualization like X-ray micro-computed tomography (μCT) allow for the observation, manipulation and analysis of the fine morphological details of extant and extinct insects and other invertebrates (Dierick *et al.* 2007; Semple *et al.* 2018), including features of their internal anatomy (e.g. Perrau & Tafforeau 2011; Galinskaya *et al.* 2018; Jałoszyński *et al.* 2018; Kehlmaier *et al.* 2014). Methods for acquiring X-ray images of insects range from less accessible devices that generate high-resolution images like the Synchrotron particle accelerator (Perreau 2012; Soriano *et al.* 2014), to more affordable desktop models that are often associated with individual labs or departments, albeit with lower resolution (e.g. Iwan *et al.* 2015). In paleontology, μCT methods are a valuable tool to visualize the morphology of sub-optimal specimens in which many characters are not visible with traditional optics and are thus, otherwise impossible to unambiguously identify (Lak *et al.* 2008; Kypke & Solodovnikov 2018).

In the present contribution we examine the morphology of all available fossil water scavenger beetles (family Hydrophilidae) from Baltic amber. Theories on the temporal origin of Baltic amber vary from Lower Eocene to Lower Oligocene, with the most commonly accepted estimate at nearly 44 million years old (Ritzkowski 1997). It is by far

among the best known and diverse deposits of fossilized insects (Perkovsky *et al.* 2007; Alekseev 2013, 2017). More than 400 species of beetles in 290 genera have been described, allowing experts to have a basic understanding of the biogeographical relevance of Eocene insect communities in the Baltic region (Zanazzi *et al.* 2007; Liu *et al.* 2009; Bogri *et al.* 2018) and its significance for the reconstruction of paleoclimatic conditions. Nevertheless, water scavenger beetles from Baltic amber are rare among inclusions and only known from specimens with most relevant characters obscured, a situation that had led to misidentifications and prevented their identification beyond generic level (Kubisz 2000; Fikaček & Engel 2011; Bloom *et al.* 2014).

Hydrophilidae is a relatively diverse family of beetles, of which most members inhabit aquatic habitats. More than 3,000 extant species have been described (Hansen 1999b; Short 2018), while approximately 180 extinct species have been mentioned in the literature. Detailed studies of specimens from some deposits revealed that a large percentage of the fossil records attributed to Hydrophilidae is based on misidentifications (e.g., Fikáček & Schmied 2013; Fikáček *et al.* 2014). The majority of described fossil water scavenger beetles are compression fossils from the Mesozoic (Fikáček *et al.* 2014) or Eocene to Miocene deposits (e.g., Fikáček & Schmied 2013), and therefore many crucial morphological characters are not clearly visible. Amber inclusions of Hydrophilidae are very scarce (Fikáček & Engel 2011), with only two species formally described: *Cretocrenis burmanicus*, Fikáček *et al.* 2017 from Burmese amber (Cretaceous) and *Crenitulus paleodominicus* (Fikáček & Engel 2011) from Dominican amber (Early Miocene).

Nine records of Hydrophilidae from Baltic amber are found in the literature (Fikáček & Engel 2011), yet none of them have been formally described. Only two of these specimens can be found in museum collections and re-examined: *Cercyon* sp. (Sphaeridiinae: Megasternini), first reported by Kubisz (2000), and *Helochares* (*Hydrobaticus*) sp. reported in the supplementary material of Bloom *et al.* (2014). Both

these fossils have been used as calibration points for dating the Hydrophilidae phylogeny by Bloom *et al.* (2014) and Toussaint & Short (2018). In addition to these specimens, we have recently had access to four novel fossils, which are included in this study.

The visibility of all specimens studied is far from optimal: specimens are surrounded by opaque clouds or froth that prevents morphological study, as it is frequent for specimens from Baltic amber (Dierick *et al.* 2007; Kypke & Solodovnikov 2018). Additionally, some amber pieces possess cracks, or the appendages of inclusions are contracted, contributing to poor specimen visibility. We aim to exemplify here that µCT reconstructions, including those from accessible, lower-resolution devices, provide an effective solution for the morphological study of suboptimally preserved fossil specimens, to avoid misidentification, taxonomic inflation, and to provide more robustly identified candidate specimens for calibration points in phylogenetic divergence dating.

MATERIAL AND METHOD

Repository of the fossils

The six specimens studied are preserved inside the same number of Baltic amber pieces. Baltic amber from the Baltic Sea region and is among the best known fossiliferous deposits of the world (Perkovsky *et al.* 2007; Alekseev 2013, 2017).

Origin and age of the amber specimens

Six specimens embedded in pieces of Baltic amber were studied. The pieces are deposited in the following collections:

SDEI Senckenberg Deutsches Entomologisches Institut, Müncheberg, Germany (Stephan Blank, Lutz Behne);

MAIG Museum of Amber Inclusions, Gdańsk, Poland (Elżbieta Sontag)

ISEA Institute of Systematic and Evolution of Animals, Polish Academy of Sciences, Kraków, Poland (Daniel Kubisz).

In order to confirm the origin of the amber, Fourier Transformed Infrared Spectra (FT-IR) were obtained for the amber samples containing specimens of *Crenitis profechuy* sp. nov.; analysis was performed at the laboratory of the International Amber Association, Gdańsk, Poland with a Nicolet iS10 Spectrometer with an ATR (Attenuated Total Reflectance) accessory.

With the exception of the holotype of *Crenitis profechuyi* sp. nov., µCT imaging of amber inclusions studied was performed at the Department of Theoretical Biology, University of Vienna, using a Zeiss/Xradia MicroXCT-200 system with a tungsten X-ray source set at 60 kVp, with no beam filter and exposure time of 20 s per projection. The holotype of *Crenitis profechuyi* sp. nov. was scanned at the Paleontology Department, National Museum, Prague, using a Skyscan1172 Bruker system, voltage 80 kVp, with an aluminium filter (Al 0.5mm) and exposure time of 0.5s per projection. Tomographic sections were reconstructed with an isotropic voxel size of 2.2 µm (*Anacaena morla* sp. nov. and Phalacridae sp.), 2.3 µm (*Helochares fog* sp. nov., paratypes of *Crenitis profechuyi* sp. nov.) or 9.0 µm (holotype of *Crenitis profechuyi* sp. nov.). Segmentation and visualization were accomplished in AMIRA 6.0.1® (https://www.fei.com/software/amira-forlife-sciences/).

Volume renderings were constructed using either a cropped series of image files (Figs 4, 6, 10) or images with inverted values (Figs 2, 7, 11) to make the empty space inside the amber more visible. This method is useful when the external-most layer of chitin is only fragmentarily reconstructed (see Kypke and Solodovnikov 2018).

Colour photographs were taken using a Canon D-550 digital camera with attached

Canon MP-E65mm f/2.8 1–5 macro lens or a Canon D1100 digital camera attached to an Olympus BX41 compound microscope. Individual photos were stacked using Helicon Focus® software (https://www.heliconsoft.com/heliconsoft-products/helicon-focus/). The distribution map of extant species related to the examined fossils was made in Corel Draw®; distribution data were taken from Hansen (1999b), Ji & Komarek (2003) and Jia *et al.* (2016). Final plates were edited and composed using Adobe Photoshop CS6® (https://www.adobe.com/products/photoshop.html). All obtained images and the source files for the µCT scans of all specimens have been deposited in Zenodo (https://www.zenodo.org/) under DOI: -

SYSTEMATIC PALAEONTOLOGY

Family **Hydrophilidae** Latreille, 1802

Subfamily **Chaetarthriinae** Bedel, 1881

Tribe **Anacaenini** Hansen, 1991

Genus ***Anacaena*** Thomson, 1859

Type species: *Anacaena globulus* (Paykull, 1798)

†*Anacaena morla* Arriaga-Varela, Brunke & Fikáček sp. nov.

(Figs 1, 2)

Material examined. Holotype (male): specimen preserved in Baltic amber, preserved in a quasi-rectangular prism of amber (10 × 3 × 4 mm) encapsulated in a rectangular prism of artificial resin (14 × 5 × 5 mm) (Hoffeins collection #742-3 in SDEI #300621).

Visibility of specimen. The dorsum of the specimen is only partially visible because of cracks that obscure the visibility of the left half of the body (Fig. 1A). Ventral side is covered by an opaque cloud, with only the legs visible in detail (Fig. 1D). µCT allowed us to reconstruct the morphology of the thoracic surface as well as the mouthparts. Antennae were not found and may be broken off from the specimen.

Etymology. The species name is based on *Morla*, a character from Michael Ende's novel and homonymous movie *The Neverending Story*. Morla is a turtle as ancient as time, living in the Swamps of Sadness. Noun in apposition.

Description. *Body* 2.6 mm long, short-oval, 1.3× as long as wide, widest at basal sixth of elytra; markedly convex, 2.1× as long as high (Figs 1A–C, 2A–C). *Head.* Labrum fully exposed about 5.3× wider than long, anterior margin arcuate. Eyes small, interocular distance about 7× the width of an eye in dorsal view (Fig. 2D). Antenna not visible. Mentum about 2.1× wider than long, lateral margins parallel sided, anterior margin slightly projected, sub-rounded, not emarginate (Fig. 2E). Labial palpi with apical palpomere weakly arcuate and inflated at mid-length. Maxillary palpi rather stout; palpomere 2 inflated, widening apically, palpomere 4 twice as long as previous one, wider at mid-length, apex subtruncate, briefly rounded (Fig. 2E). *Thorax.* Pronotum transverse, 2.5× wider than long, 1.6× wider at base than at anterior margin, without any impressions. Prosternum nearly flat medially, intercoxal process acute, short (Fig. 2G). Scutellar shield rather small, 1.6× wider than long. Elytra widest at basal sixth, 0.85× as long as wide, 2.2× longer and 1.1× wider (at widest point) than the pronotum. Elytral punctation distinctly arranged in approximately ten longitudinal series on each elytron, punctures very fine (Fig. 2F). Anapleural sutures distinct, strongly converging mediad along posterior half, then weakly in anterior half, widely separated at anterior margin (Fig. 2H). Mesoventrite with a

projected, transverse and thick ridge almost as wide as the length of a mesocoxa, acute in lateral view (Fig. 2H). Metaventrite (Fig. 2B) without femoral lines, raised medial area moderately wide, weakly defined along posterior half; lateral areas of metaventrite without conspicuous sculpture in basal half. *Legs.* Femora with hydrofuge pubescence on ventral face not visible. Metatibia short and stout with comparatively short, strong spines along lateral margins (Fig. 1E), with the longest tibial spur extending to half the length of tarsomere 2. Tarsi short with dense, strong setae ventrally (Fig. 1E), metatarsus about 0.8× as long as metatibia. *Abdomen.* Ventrites 1–4 gradually getting very slightly shorter towards apex. Fifth ventrite about twice as long as ventrite 4 (Fig. 2B). Aedeagus partially exposed (Fig. 2C). Parameres widest at base (Fig. 2I), separated at base by half the width of a paramere, rather continuously narrowing towards apical third, then subparallel, weakly curved inwards, briefly rounded at apex. Median lobe 0.9× the length of parameres, broad at base, strongly narrowed at apical fourth, then subparallel, with a longitudinal slit along apical three fourths, apex narrow but obtusely rounded.

Diagnosis and discussion. The combination of abdomen with 5 ventrites, relatively short and stout labial palpi, labrum well sclerotized and exposed in front of clypeus, anapleural sutures not converging at anterior margin, and mesoventrite with transverse ridge assign the species to the genus *Anacaena* in the tribe Anacaenini (Chaetathriinae). This is also supported by the morphology of the male genitalia, with median lobe broad at base, strongly narrowing at apical fourth and then subparallel, closely resembling the aedeagus of some extant *Anacaena* from Africa and Asia (e.g. Figs 3–4 in Hansen 1999; Fig. 13 in Komarek 2012). *Anacaena morla* sp. nov. differs from other known species of the genus by the following combination of characters: markedly convex body (2.1× as long as high); mentum rather transverse, with lateral margins parallel and anterior margin distinctly rounded (Fig. 2E) (variable in extant *Anacaena* species but usually less transverse, with

lateral margins at least weakly rounded or convergent and anterior margin emarginate (e.g. Figs 38–51 in Komarek 2012)); elytra with approximately ten distinct rows of serial punctures (Fig. 2F); anapleural sutures widely separated at anterior margin (Fig. 2H); mesoventrite with a projected transverse ridge almost as wide as the length of mesocoxa; tarsi short with dense, stout setae ventrally (Fig. 1E), aedeagus with narrow parameres (Fig. 2I). *Anacaena morla* sp. nov. resembles the extant South African species *A. endroedyi* (Hansen) and *A. striata* (Hansen) by the subhemisphaerical body, the punctate-seriate elytra and the short tarsi. These two extant terrestrial species were originally assigned to a separate genus *Grodum* Hansen by Hansen (1999a), which was later synonymized with *Anacaena* by Komarek & Beutel (2007). *Anacaena morla* sp. nov. differs from the South African species by (a) the mentum with anterior margin rounded instead of almost straight, (b) mesoventrite with a broad transverse ridge (entirely flat in *A. endroedyi* and *A. striata*), (c) tarsi with dense setation ventrally, and (d) distinctly narrower parameres (Fig. 2I; compare to figs 3 and 4 in Hansen 1999a). The dense short setae on the ventral face of tarsi are not known known in any other *Anacaena* species; they are clearly not natatorial but resemble tarsal setation of many terrestrial Hydrophilidae, suggesting possible terrestrial habits of *A. morla* sp. nov.

Potential use in divergence dating. The good preservation of the examined specimen and visibility of most relevant characters except antennae reliably assigns this species to *Anacaena*. As this fossil contains a combination of characters not known in extant *Anacaena*, it may represent a stem or extinct lineage of the genus. *Anacaena morla* sp. nov. is suitable to calibrate the most recent common ancestor of *Anacaena* and its sister taxon at the moment and has the potential to calibrate the age of the crown group *Anacaena* or its subgroups if its phylogenetic position is further clarified in future studies of the extant *Anacaena*.

Genus ***Crenitis*** Bedel, 1888

Type species: *Crenitis punctatostriata* (Letzner, 1840)

†*Crenitis profechuyi* Arriaga-Varela, Brunke & Fikáček sp. nov.

(Figs 3–7)

Material examined. Holotype (male): specimen preserved in Baltic amber from Poland (MAIG #5954), preserved in a quasi-rectangular prism of amber (8 × 6 × 4 mm) (MAIG). Paratype no. 1 (male): specimen preserved in Baltic amber from Poland (MAIG #5950), preserved in a quasi-triangular prism of amber (17 × 9 × 3 mm) (MAIG). Paratype no. 2 (sex unknown): specimen preserved in Baltic amber from Poland (MAIG #5951), preserved in a quasi-rectangular prism of amber (19 × 9 × 4 mm) (MAIG).

Visibility of the specimens. *Holotype*. The dorsum and most of the ventral side are clearly visible; portions of labium, hypomeron, prosternum, mesoventrite and abdomen are covered by whitish clouds and bubbles (Fig. 3). *Paratype no.1*. The overall visibility of the specimen is very good and allows the observation of the body surface (Fig. 5); the genitalia is not visible, and the sex of the specimen cannot be determined. *Paratype no. 2.* Dorsal surface is visible including details of the punctation. A sagittal crack on the amber piece obscures the visibility of the lateral parts of pronotum and elytra (Fig. 7A); ventral surfaces, except legs are obscured by a whitish cloud (Fig. 7B–C).

Etymology. The first author dedicates this species to his father, José de Jesús Arriaga Sánchez “Profe Chuy” as a way to thank him for everything (in general) and for taking him to the cinema to watch the Jurassic Park movie when he was nine years old (in particular).

Description. *Holotype. Body* 2.6–2.7 (Holotype 2.6) mm long, moderately short-oval, 1.6×

as long as wide, widest at basal fourth of elytra; moderately convex, 2.5–2.6 (HT 2.5)× as long as high (Figs 3A–C, 4A–C, 5A–C, 6A–C). *Head.* Labrum fully exposed, about 4× wider than long, anterior margin weakly bisinuate, dorsal surface with fine punctation and a continuous transverse series of punctures bearing long setae (Figs 3D, 6E). Eyes rather large, interocular distance about 4.3× the width of an eye in dorsal view. Antenna with 9 antennomeres; scapus weakly curved, almost twice longer than pedicel; pedicel as long as antennomeres 3–4 combined; antennomere 3 1.5× longer than antennomere 4; antennal club slightly shorter than antennomeres 2–6 combined (Fig. 6D). Clypeus mesally weakly emarginate. Clypeus and frons sparsely punctured, punctures fine but sharply impressed; interstices without microsculpture (Fig. 3D). Labial palpi with apical palpomere weakly arcuate and inflated at mid-length (Fig. 6G). Maxillary palpi stout, palpomere 2 inflated, widening apically, apical palpomere twice as long as previous one, widening apically, apex subacuminate, narrowly rounded (Fig. 6F). *Thorax.* Pronotum transverse, 2.5× wider than long, 1.5× wider at base than at anterior margin, without any impressions. Pronotal punctation fine, evenly distributed, nearly as dense as on head; interstices without microsculpture (Figs 3A, 5A). Prosternum not bulging or carinate at mid-line, intercoxal process briefly acute, moderately long, portion anterior to procoxae nearly half as long as procoxal cavities (Fig. 6B). Scutellar shield rather large, 1.1× wider than long. Elytra widest at basal sixth, 1.2× longer than wide, 3.9× longer and 1.1× wider than pronotum. Elytral punctation slightly denser than on pronotum (Fig. 5A, C), punctures with distinct subserial arrangement anteriorly; elytral striae more conspicuous and deeper at posterior sixth; interstices without visible microsculpture (Figs 3C, 6K). Anapleural sutures distinct, converging anteromesally at an angle forming approximately 90 degrees if they were to touch (Figs 4E, 6H, 7E). Mesoventrite with moderately raised transverse posteromesal ridge; ridge acute in lateral view (Fig. 6H, I), almost as wide as the length of a mesocoxa. Metaventrite with weakly raised median area, moderately wide, weakly defined, about as

long as wide (Fig 6J); lateral areas of metaventrite homogeneously and rather sparsely covered by decumbent setae (Fig 3E). *Legs***.** Mesofemora with dense pubescence on ventral face reduced to basal half (Fig. 3E), metafemora with very sparse long setae and few denser setae near attachment of trochanter (Fig. 3E). Metatibia with long, strong spines along lateral margins; longest tibial spur extending to half-length of tarsomere 2 (Figs 6F, 7B). Metatarsus about 0.8× as long as metatibia, without long natatorial setae. Metatarsomere 1 shorter than tarsomere 2; tarsomere 5 as long as tarsomeres 3–4 combined. Claws small. *Abdomen* with 5 ventrites, all with fine microsculpture and dense pubescence all over (Figs 3B, 6B). Ventrites 1–4 gradually becoming narrower towards apex. Ventrite 5 about 1.3× longer than ventrite 4. Ventrite 5 with posterior margin entire (Fig. 3B, 4B). Aedeagus with broad parameres (Fig. 3F), preapically slightly curved inwards, widely rounded at apex; median lobe triangular, rounded at apex, apex nearly reaching midlength of parameres.

Diagnosis and discussion. The combination of short basal metatarsomere, abdomen with 5 ventrites, abdominal ventrite 5 with entire posterior margin, antenna with 9 antennomeres, labrum well sclerotized and exposed in front of clypeus, and the triangular mesoventrite with weak transverse ridge unambiguously assign this fossil to the genus *Crenitis* in the tribe Anacaenini (Chaetarthriinae). This is moreover supported by the morphology of the male genitalia, which corresponds well to the extant *Crenitis apicalis* species group distributed in China (*C. apicalis* (Reitter), *C. convexa* Ji & Komarek) and in North America (*C. morata* (Horn), *C. digesta* (LeConte), *C. rufiventris* (Horn), *C. paradigma* (Orchymont) and *C. snoqualmiae* Miller) (see Fig. 12) (Smetana 1978; Ji & Komarek 2003; Jia *et al.* 2016). Both Chinese species differ from *C. profechuyi* sp. nov.: *C. convexa* has deeply striate elytra and impressions on the pronotum (both absent in the fossil species); *C. apicalis* differs in having a more extended pubescent basal area of the

metafemur and a very sparse transverse row of setiferous setae on the labrum (*C. profechuyi* sp. nov. has a dense row of setae). Of the North American species, all except *C. rufiventris* and *C. paradigma* differ from the fossil in the metafemur with more extended basal dense pubescence and, in some species, the presence of a fine microsculpture on the head and pronotum. *Crenitis rufiventris* differs from the fossil species in the much narrower median lobe. The genitalia of *C. paradigma* looks very similar to that of the fossil, but the median lobe extends closer to the apices of the parameres.

Comments. The µCT reconstruction of the holotype, even when performed at a lower resolution, provided us with enough details to reconstruct the morphology of the antennae, mouthparts and the mesoventrite, which were otherwise not visible. These characters allowed us to unambiguously assign the fossil to the genus *Crenitis* and compare it with other specimens examined. The volume reconstruction of all specimens allowed us to assign them to the same species, despite artefactual 'differences' in proportion and shape. Since the aedeagus is clearly visible for most of its length in this specimen, it is selected as the holotype. The FT-IR spectra of all three amber pieces confirm their origin, showing the typical "Baltic shoulder" between 1190–1280 cm^{-1} (Ritkowski 1997) (Fig. 8).

Potential use in divergence dating. The good preservation of the specimens and visibility of their characters allows us to definitely assign them to a single species of *Crenitis.* Since the fossil taxon shares characters with the extant *Crenitis apicalis* species group, it can be assigned to crown *Crenitis*. In node-calibrated divergence dating, this fossil taxon could be used to calibrate the MRCA of *Crenitis* and *Crenitulus* (in Toussaint & Short 2018), replacing the much younger *Crenitulus paleodominicus* Fikáček & Engel from Dominican amber (early Miocene), which was used to calibrate that node previously. *Crenitis profechuyi* could be used to calibrate deeper nodes within *Crenitis* in future analyses, as it can be unambiguously assigned to the Chinese-North American species

group characterized by the wide parameres with broadly rounded apices, as discussed in the diagnosis.

Subfamily **Acidocerinae** Zaitzev, 1908

Genus ***Helochares*** Mulsant, 1844

Type species: *Helochares lividus* (Forster, 1771)

†***Helochares fog*** Arriaga-Varela, Brunke, Girón & Fikáček sp. nov.

(Figs 9–10)

Examined material. Holotype (sex unknown): specimen preserved in Baltic amber from Poland, in an irregular prism of amber (15 × 12 × 5 mm) (Andrzej Górski collection In #7352 in MAIG).

Visibility of the specimen. The entire body of the specimen is covered by a whitish cloud and surrounded by numerous bubbles that obscure the visibility of the surface except, to some degree, the legs (Fig 9). Few large bubbles completely obstruct the visibility of key ventral characters of the thorax and head. The μCT reconstruction allowed us to partially reconstruct the morphology of the labium, prosternum and mesoventrite.

Etymology. This species is dedicated to geologist Fernando Ortega Gutiérrez, emeritus researcher at the National Autonomous University of Mexico, as an homage to his scientific career that inspired the first author to pursue a career in science, and in gratitude to the Ortega Varela family. The name '*fog*' is taken from the initials of his name (F.O.G.), and also describes the white "foggy" substance obscuring much of the specimen. Noun in

apposition.

Description. *Body* 5.8 mm long, moderately short-oval, 1.7× longer than wide, widest at half-length of elytra; moderately convex, 2.6× longer than high (Figs 9A-B, 10A-C). *Head.* Eyes large, interocular distance about 3.5× the width of an eye in dorsal view. Antennae not visible. Mentum rather flat, with large and deep punctures (Fig. 10D). Labial palps with palpomere 3 weakly arcuate at base and widened at mid-length; palpomere 2 about as long as apical (Fig. 10F); maxila with palpomere 2 narrow, widening apically, 0.4× as long as width of head; palpomere 3 half as long as second, continuously widening apically, slightly wider than palpomere 2; palpomere 4 around 1.2× longer than previous one, wider at apical fourth, apex briefly rounded. Gular sutures distinctly marked and seemingly impressed, widely separated, converging anteriorly to be separated by half of the width of posterior margin of mentum (Fig. 10D). *Thorax*. Pronotum transverse, 2.2× wider than long, 1.8× wider at base than at anterior margin. Prosternum flat, not bulging or tectiform at mid-line (Fig. 10E), with anterior margin apparently straight, intercoxal process short, acute, the portion anterior of procoxae nearly as long as procoxal cavities. Scutellar shield not observed. Elytra widest at basal two fifths, 1.2× longer than wide, 3.4× longer and 1.3× wider than pronotum. Elytra with longitudinal striae composed of deep punctures separated by 1–2 puncture diameters; interstices slightly convex (Figs 9B,10I). Anapleural sutures distinct, converging mesally at acute angle at anterior margin of mesoventrite. Mesoventrite seemingly with a weak transverse ridge, slightly curved mesally (Fig. 10G). *Legs.* Tibiae of all legs slightly medially arched, with regularly distributed, moderately long spines; the longest metatibial spur extending near half-length of basal tarsomere. Metatarsus slightly shorter than metatibia, with a series of about 10 long natatorial setae (Fig. 9F). Claws not enlarged. *Abdomen* with five ventrites all densely covered by hydrofuge pubescence. Ventrites 1–4 approximately of the same length; ventrite 5 about half as long as ventrite 4 (Fig. 10H). Genitalia not visible.

Diagnosis and discussion. The overall body form, short basal tarsomeres, straight (as opposed to 'zig-zag' shaped, i.e. excluding subfamily Enochrinae; see Short & Fikáček 2013) and relatively long maxillary palpi (excluding the tribe Hydrobiusini in Hydrophilinae), allow us to place the fossil confidently in the subfamily Acidocerinae. The specimen was originally identified as *Helochares* (*Hydrobaticus*) sp. based on its body shape, relatively long maxillary palpi and elytra with impressed series of punctures (see supplementary material in Bloom *et al.* 2014). However, due to the presence of a whitish cloud and numerous bubbles reducing the visibility of the specimen, further details were not observed at the time. The µCT reconstruction revealed a series of additional characters, especially on the ventral surfaces, that question the originally proposed subgeneric placement of the fossil.

Within Acidocerinae, the fossil easily fits the diagnosis of *Helochares* provided by Hansen (1991). *Helochares fog* sp. nov. can be differentiated from all known *Helochares* species by the combination of the following characters: body 5.8 mm long, moderately convex in lateral view (2.6× longer than high), weakly flattened along anterior half of elytra; maxillary palpi slender, only slightly longer than maximum width of the head; mentum with large and deep punctures (Fig. 10D); elytra with slightly impressed longitudinal rows of large and deep serial punctures (Fig. 10C, I); mesoventrite with anapleural sutures converging anteriorly, forming a nearly right angle at anterior margin of mesoventrite (Fig. 10G); ventral surface of all tarsomeres (including tarsomere 5) densely covered by thick setae (Fig. 9C, E, F); metatarsi each with a series of about 10 long natatorial setae (Fig. 9F). The unique combination of the shape of the mesoventrite, the strongly punctured mentum, and the ventrally pubescent tarsi seems to contradict the assignment of the fossil to the *Helochares* subgenus *Hydrobaticus*. All known members of *Helochares* (*Hydrobaticus*) and the majority of *Helochares* (s. str.) have a bell-shaped mesoventrite, with anapleural

sutures widely separated and nearly parallel anteriorly. Of the other subgenera, species of *Helochares* (*Sindolus*) bear a sharp longitudinal carina on the mesoventrite which is absent in the fossil. On the other hand, the fossil resembles the Afrotropical species of *Helochares* (*Batochares*) Hansen and *Peltochares* Régimbart, in the elytra with longitudinal striae of punctures, although less deeply marked or slightly more irregular. *Helochares* (*Batochares*) (Fig. 12D) has the anapleural sutures slightly more separated at the anterior margin and bears anteriorly explanate elytra (compare to Fig. 10A), and *Peltochares* (Fig. 12G) differs from the fossil by the general habitus: it is much larger, proportionally wider, and distinctly more dorsoventrally compressed and with much longer maxillary palpi (compare with Fig. 10D). A similarly shaped mesoventrite (Fig. 12F) also occurs in the Australasian species *H.* (s. str.) *foveicollis* and *H.* (s.str.) *taprobanicus*, but in both cases the elytra lack the rows of serial punctures (Fig. 12E) and the mesoventrite has a more or less developed posterior longitudinal carina, as opposed to the transverse elevation observed in *Helochares fog* sp. nov. In all mentioned extant taxa, the surface of the mentum is only laterally punctate and mesally and anteriorly strigate, as opposed to strongly punctate as in *Helochares fog* sp. nov. In addition, in most of the observed species of *Helochares* and allies, the ventral surface of the tarsi usually bears only paired rows of denticles on tarsomeres 1–4, none on tarsomere 5, whereas the tarsi in *Helochares fog* sp. nov. are densely covered by setae. With nearly 180 species described worldwide, *Helochares* is currently the largest, most widespread and, arguably, in the biggest taxonomic disarray within acidocerine hydrophilids, requiring a thorough revision. As currently defined, and in accordance with Hansen (1991), *Helochares* is a heterogeneous group and most likely non-monophyletic. The combination of observed characters allows a placement of the fossil in the genus *Helochares* in its current understanding (i.e. *Helochares sensu lato*). However, it is not possible to unambiguously assign it to any of the existing subgenera.

Potential use in divergence dating. Despite the poor preservation of the fossil limiting the observation of some crucial characters (e.g., antennae, posterior margin of ventrite 5, genitalia), it can be placed within *Helochares*, supporting its previous use as a calibration point for the *Helochares+Helobata* clade by Toussaint & Short (2018). The results of an ongoing investigation of the phylogeny of Acidocerinae (Short *et al.* in prep.) would likely allow a better insight on the morphological evolution of the subfamily and potentially would confirm or reject a close relationship of the fossil with representatives of *Helochares* (*Batochares*) or *Peltochares*. When confirmed, the fossil would be suitable to calibrate more recent nodes within *Helochares*.

Family **Phalacridae** Leach, 1815

Phalacridae sp.

(Fig. 11)

Misidentified as *Cercyon* sp. (Hydrophilidae): Kubisz (2000); Bloom et al. 2014; Toussaint & Short (2018).

Examined material. Specimen preserved in Baltic amber from Poland, in an irregular prism of amber (19 × 9 × 4 mm) (ISEA #MP/3/187/1/00).

Visibility of the specimen.

The dorsal habitus is visible, showing the surface of pronotum and elytra (Fig. 11A). The ventral view as well as the anterior portion of the head including antennae is completely obstructed by multiple cracks in the amber piece. The µCT reconstruction allowed us to reconstruct the morphology of antennae, legs including tarsi, and of thoracic and

abdominal ventrites (Figs 12B–C).

Comment. This specimen was originally identified as *Cercyon* sp. (Hydrophilidae: Sphaeridiinae: Megasternini) by Kubisz (2000), on the basis of the body shape and elytra with longitudinal striae of fine punctation, and was used by Bloom *et al.* (2014) and Toussaint & Short (2018) to calibrate the most recent common ancestor of Megasternini + Sphaeridiinae. Our µCT reconstruction of the ventral side of the beetle revealed that it belongs to the family Phalacridae (Cucujoidea). This placement is supported mainly by the loose three-segmented antennal club not preceded by a cupule (Fig. 11B) and the widely lobate mesotarsomeres 2 and 3 (Fig. 11C). These characters are never found in Hydrophilidae but are characteristic of Phalacridae. The structure of the thoracic ventrites confirms the family assignment as well. This specimen is currently under description by Matthew Gimmel (Santa Barbara Museum of Natural History).

Discussion

Sub-optimal amber specimens and µCT. Sub-optimal specimens probably form the majority of existing amber inclusions and, for many groups, they may represent the only specimens available. Therefore, for many lineages the only information about their diversity and distribution in space and time remains ‘hidden’ within sub-optimal fossils. Unfortunately, these specimens are rarely studied, described or included into evolutionary analyses because many of their characters are obscured, making their phylogenetic position difficult to infer. These fossils may simply be ignored in favor of better-preserved inclusions with lower effort needed to produce publication-worthy results (Perkovsky *et al.* 2007). Here, this is illustrated by the beetle family Hydrophilidae. Despite being a diverse family of beetles, its extinct diversity was only known previously from nine records in literature from which only two sub-optimally preserved Baltic amber specimens were

available to study (Fikáček & Engel 2011; Bloom *et al.* 2014). One of us (MF) examined them using classic optical microscopy, on which some preliminary identifications were based (see Bloom *et al.* 2014). All of these conclusions are proven incorrect in this study, highlighting the high risk of misidentification in suboptimal specimens. Four additional Baltic amber specimens were discovered recently, all except one in sub-optimal state of preservation and visibility. Nonetheless, after rigorous study using X-ray μCT, in addition to light microscopy, all three species identified in this material are the oldest known representative of their respective clades and important for divergence dating of Hydrophilidae. However, they may be members of particular generic or subgeneric lineages that are extinct or are surviving in biogeographical regions far from northern Europe, such as China and North America. Sub-optimally preserved fossils are therefore crucial for understanding the evolutionary history of the water scavenger beetles and should not be neglected.

Micro-CT technology proved to be crucial in the study of these sub-optimal specimens, revealing phylogenetically informative characters that would otherwise have remained hidden (Dierick *et al.* 2007; Kypke & Solodovnikov 2018; Semple *et al*. 2018). It also helped us to distinguish true morphological details from artefacts caused by the optical properties of amber or visual obstruction due to cracks or bubbles. Characters revealed by μCT allowed us to place all examined fossils into a phylogenetic context. We were also able to demonstrate that three of the examined specimens are conspecific, despite our original estimate of three separate species from artefactual ‘differences’ in proportion and shape. In this way, μCT imaging has prevented us from over-estimating the species diversity of Eocene hydrophilids, a scenario that may be more frequent in fossil insects than currently known, especially in the case of sub-optimally preserved fossils where each specimen is often described or considered to represent a separate species (see Fikáček & Schmied 2013).

We illustrate here that medium resolution (2.2–2.3 µm voxel size) or even low resolution (9 µm voxel size) µCT devices are enough for morphological studies of amber-embedded insect specimens of c. 2.5–5.0 mm long. Even in the lower-resolution scans performed by us – the holotype of *Crenitis profechuyi* sp. nov. (Fig. 4) – it is possible to visualise key characters that corroborate its conspecificity with other specimens and place it in a systematic framework. Additionally, we show that volume rendering using a set of inverted images (Figs 2, 7, 11), or manual removal of froth and bubbles (e.g. the one seen on Fig. 3B) using segmentation tools in volume reconstruction software (e.g. as implemented by Kypke & Solodovnikov 2018) are useful strategies for obtaining satisfying datasets for the visualization and subsequent description of fossil taxa. Additionally, Amira software functions like Isosurface (Figs 4A-E; 10H) or Orthoslice can be used to either partially remove parts of the body obstructing the view of key characters (Fig. 10G) or to see the profile of the cuticle (Fig. 4F).

Water scavenger beetles in Baltic amber. All three species of Hydrophilidae recognized by us represent modern genera or a generic group, but seem to represent lineages that are not present in Europe today. *Crenitis profechuyi* sp. nov. may be reliably assigned to the extant *C. apicalis* species group (Smetana, 1978; Ji & Komarek, 2003; Jia *et al.* 2016). The other two species (*Anacaena morla* and *Helochares fog* spp. nov.) seem to differ from any modern species of their respective genera and may represent extinct lineages. *Helochares fog* shares some characters with groups now living in Africa (*Peltochares* and *Helochares* subgenus *Batochares*) and SE Asia and Australia *(Helochares taprobanicus* group). The *Crenitis apicalis* group, to which *Crenitis profechuyi* sp. nov. belongs, is currently distributed in Japan, southern China and North America. The presence of taxa in Baltic amber with a modern distribution confined to east Asia and North America has been also reported for diving beetles (Adephaga: Dytiscidae); Gómez & Daamgard (2014) and

Balke & Hendrich (2019) described Baltic amber species of Agabinae and Laccophilinae and assigned them to genera previously known only from extant species distributed in such regions. This present day Pacific intercontinental disjunct pattern is an example of a trans-Beringian distribution (Wen 1999, Sanmartín *et al*. 2001) which has been discussed for other hydradephagan beetles (Nilsson 2003). Even though the material examined by us only includes three species, the known faunistic composition seems to corroborate the results in other groups of insects. Baltic amber insect fauna consists of a mixture of groups today confined to the temperate zone and both new and old world tropical elements (e.g. Emeljanov & Shcherbakov 2011; Wu et al. 2015; Alekseev 2017; Bogri *et al*. 2017; Brunke *et al*. 2017, 2019). The mesophilous forests in southern China are often considered as the modern vegetation analogue of the Eocene forests of Europe (Kvaček 2007; Teodiris *et al.* 2012). It is therefore noteworthy that southern China is where most of the species of the *Crenitis apicalis* group occur today (Ji & Komarek 2003; Jia *et al.* 2016), suggesting that this pattern is not restricted to plant taxa but includes insect lineages.

Acknowledgements

We are grateful to collectors and museum curators for making specimens available for our study,

Christel and Hans Werner Hoffeins (Hoffeins collection), Andrzej Górski (Andrzej Górski collection), Elżbieta Sontag (MAIG), Daniel Kubisz (ISEA), and Stephan Blank and Lutz Behne (SDEI). Micro-CT imaging of amber inclusions was performed by Brian Metscher (University of Vienna) and Jana Bruthansová (National Museum, Prague). We are thankful to Andrew E.Z. Short (University of Kansas) for discussing with us the possible relations of *Helochares fog* sp. nov. within Acidocerinae. This work was supported by the European Union's Horizon 2020 research and innovation programme under the Marie Skłodowska-

Curie grant agreement No. 642241 to EAV, the A-base funding of AJB, and by the Ministry of Culture of the Czech Republic (DKRVO 2018/13 and 2018/06, National Museum, 00023272) to MF and JB. The work of EAV at the Department of Zoology, Charles University, Prague was partly supported by grant SVV260434/2018.

References

Alekseev, V. I. 2013. The beetles (Insecta: Coleoptera) of Baltic amber: the checklist of described species and preliminary analysis of biodiversity. *Zoology and Ecology*, **23**(1), 5–12. https://doi.org/10.1080/21658005.2013.769717

Alekseev, V. I. 2017. Coleoptera from the middle-upper Eocene European ambers: generic composition, zoogeography and climatic implications. *Zootaxa*, **4290**(3): 401–443. http://dx.doi.org/10.11646/zootaxa.4290.3.1

Balke, M. & Hendrich, L. 2019. †*Japanolaccophilus beatificus* sp. n. from Baltic amber and
a key to the Laccophilinae genera of the World (Coleoptera: Laccophilinae). *Zootaxa*, **4567**(1), 176–182. http://dx.doi.org/10.11646/zootaxa.4567.1.10

Bloom, D., Fikáček, M., Short, A. E. Z. 2014. Clade age and diversification rate variation explain disparity in species richness among water scavenger beetle (Hydrophilidae) lineages. *PLoS ONE*, **9**(6), e98430, 1–9. DOI: https://doi.org/10.1371/journal.pone.0098430

Bogri, A., Solodovnikov, A., Żyła, D. & Smith, A. 2018. Baltic amber impact on historical biogeography and palaeoclimate research: oriental rove beetle *Dysanabatium* found in the Eocene of Europe (Coleoptera, Staphylinidae, Paederinae). *Papers in Palaeontology*, **4**, 433–452. https://doi.org/10.1002/spp2.1113

Brunke, A. J., Chatzimanolis, S., Metscher, B. D., Wolf-Schwenninger, K. &

Solodovnikov, A. 2017. Dispersal of thermophilic beetles across the intercontinental Arctic forest belt during the early Eocene. *Scientific Reports*, 7, 1–8. https://doi.org/10.1038/s41598-017-13207-4

Brunke, A. J., Żyła, D., Yamamoto, S., & Solodovnikov, A. 2019. Baltic amber Staphylinini (Coleoptera: Staphylinidae: Staphylininae): a rove beetle fauna on the eve of our modern climate. *Zoological Journal of the Linnean Society*, zlz021, https://doi.org/10.1093/zoolinnean/zlz021

Clarke, D. J., Limaye, A., McKenna, D. D. & Oberprieler, R. G. 2018. The Weevil Fauna Preserved in Burmese Amber—Snapshot of a Unique, Extinct Lineage (Coleoptera: Curculionoidea). *Diversity*, **11**(1), 1–233. https://doi.org/10.3390/d11010001

Dierick, M., Cnudde, V., Masschaele, B., Vlassenbroeck, J., Van Hoorebeke, L. & Jacobs, P. 2007. Micro-CT of fossils preserved in amber. *Nuclear Instruments and Methods in Physics Research Section A: Accelerators, Spectrometers, Detectors and Associated Equipment*, **580**, 641–643. https://doi.org/10.1016/j.nima.2007.05.030

Emeljanov, A. F., & Shcherbakov, D. E. 2011. Anew genus and species of Dictyopharidae (Homoptera) from Rovno and Baltic amber based on nymphs. *Zookeys*, **130**, 175–184. https://doi.org/10.3897/zookeys.130.1775

Fikaček, M. & Engel, M. S. 2011. An aquatic water scavenger beetle in Early Miocene amber from the Dominican Republic (Coleoptera: Hydrophilidae). *Annales Zoologici* **61(4)**, 621–628. https://doi.org/10.3161/000345411X622462

Fikaček, M. & Schmied, H. 2013. Insect fauna of the Late Miocene locality of Öhningen (Germany) less diverse than reported: an example of the hydrophilid beetles (Coleoptera). *Journal of Paleontology*, 87(3), 427–443. https://doi.org/10.1666/12-101.1

Fikaček, M., Prokin, A., Yan, E., Yue, Y., Wang, B., Ren, D. & Beattie, R. 2014. Modern hydrophilid clades present and widespread in the Late Jurassic and Early Cretaceous (Coleoptera: Hydrophiloidea: Hydrophilidae). *Zoological Journal of the Linnean Society*,

170, 710–734. https://doi.org/10.1111/zoj.12114

Fikaček, M., Minoshima, Y. N., Komarek, A., Short, A. E. Z., Huang D. & Cai C. Y. 2017. *Cretocrenis burmanicus*, the first Mesozoic amber inclusion of a water scavenger beetle (Coleoptera: Hydrophilidae). *Cretaceous Research*, **77**, 49–55. https://doi.org/10.1016/j.cretres.2017.04.017

Galinskaya, T. V., Gafurova (Gilyazetdinova), D. & Ovtshinnikova, O. G. 2018. X-ray microtomography (microCT) of male genitalia of *Nothybus kuznetsovorum* (Nothybidae) and *Cothornobata* sp. (Micropezidae). *Zookeys,* **744**, 139–147. https://doi.org/10.3897/zookeys.744.22347

Gomez, R. A. & Damgaard, A. L. 2014. A rare diving beetle from Baltic Amber: *Hydrotrupes prometheus* new species reveals former widespread distribution of the genus (Coleoptera, Dytiscidae). *Journal of Paleontology,* **88**, 814–822. https://doi.org/10.1666/13-017

Grimaldi, D. & Engel, M. S. 2005. *Evolution of the Insects*. Cambridge Evolution Series 1. Cambridge University Press. Cambridge, 772 pp.

Hansen, M. 1991. *The Hydrophiloid beetles: phylogeny, classification and a revision of the genera (Coleoptera, Hydrophiloidea).* Kongelige Danske videnskabernes selskab, Copenhagen, 367 pp.

Hansen, M. 1999a. Fifteen new genera of Hydrophilidae (Coleoptera), with remarks on the generic classification of the family. *Insect Systematics & Evolution*, **30**(2), 121–172. https://doi.org/10.1163/187631200X00228

Hansen, M. 1999b. *World catalogue of insects, volume 2. Hydrophiloidea (s. str.) (Coleoptera)*. Apollo Books, Stenstrup, 416 pp.

Hipsley, C. A. & Müller, J. 2014. Beyond fossil calibrations: realities of molecular clock practices in evolutionary biology. *Frontiers in Genetics*, **5**(138), 1–11. https://doi.org/10.3389/fgene.2014.00138

Ho, S. Y. W. & Duchêne, S. 2014. Molecular-clock methods for estimating evolutionary rates and timescales. Molecular Ecology, **23**, 5947–5965. https://onlinelibrary.wiley.com/doi/full/10.1111/mec.12953

Iwan, D., Kamiński, M. J. & Raś, M. 2015. The Last Breath: A μCT-based method for investigating the tracheal system in Hexapoda. *Arthropod Structure & Development*, **44**(3), 218–227. https://doi.org/10.1016/j.asd.2015.02.002

Jałoszyński, P., Brunke, A. J., Yamamoto, S., & Takahashi, Y. 2018. Evolution of Mastigitae: Mesozoic and Cenozoic fossils crucial for reclassification of extant tribes (Coleoptera: Staphylinidae: Scydmaeninae). *Zoological Journal of the Linnean Society*, **184**(3), 623–652. https://doi.org/10.1093/zoolinnean/zly010

Ji, L. & Komarek, A. 2003. Hydrophilidae: II. The Chinese species of *Crenitis* Bedel, with descriptions of two new species. Pp. 397–409 In M. A. Jäch & L. Ji, (eds). *Water beetles of China, Vol. 3.* Zoologisch-Botanische Gesellschaft in Österreich and Wiener Coleopterologenverein. Wien. **Jia, F.-L., Tang, Y. & Minoshima, Y. N.** 2016. Description of three new species of *Crenitis* Bedel from China, with additional faunistic records for the genus (Coleoptera: Hydrophilidae: Chaetarthriinae). *Zootaxa*, **4208**(6): 561–576. http://dx.doi.org/10.11646/zootaxa.4208.6.4

Judson M. L. I. 2003. Baltic amber fossil of *Garypinus electri* Beier provides first evidence of phoresy in the pseudoscorpion family Garypnidae (Arachnida: chelonethi). Pp. 127–131 In D.V. Logunov & D. Penney (eds). *Proceedings of the 21st European colloquium of arachnology.* Arthropoda Selecta. St-Petersburg. http://www.european-arachnology.org/wdp/wp-content/uploads/2015/08/127_131_Judson.pdf

Kvaček, Z., 2007. Do extant nearest relatives of thermophile European Tertiary elements reliably reflect climatic signal?. *Palaeogeography, Palaeoclimatology, Palaeoecology*, **253**, 32–40. https://doi.org/10.1016/j.palaeo.2007.03.032

Kehlmaier, C. Dierick, M. & Skevington, J. H. 2014. Micro-CT studies of amber

inclusions reveal internal genitalic features of big-headed flies, enabling a systematic placement of *Metaphrocerus* Aczél, 1948 (Insecta: Diptera: Pipunculidae). *Arthropod Systematics and Phylogeny*, **72**, 23–36. http://www.senckenberg.de/files/content/forschung/publikationen/arthropodsystematics/asp_72_1/03_asp_72_1_kehlmaier_23-36.pdf

Komarek, A. 2012. Taxonomic revision of *Anacaena* Thomson, 1859 IX. The People's Republic of China (Coleoptera: Hydrophilidae). *Koleopterologische Rundschau,* **82**, 235−284.

Komarek, A. & Beutel, R. G. 2007. Phylogenetic analysis of Anacaenini (Coleoptera: Hydrophilidae: Hydrophilinae) based on morphological characters of adults. *Systematic Entomology,* **32**, 205–226. https://doi.org/10.1111/j.1365-3113.2006.00359.x

Kubisz, D. 2000. Fossil beetles from Baltic amber in the collection of the Museum of Natural History of ISEA in Krakow. *Polskie Pismo Entomologiczne*, **69**, 225–230.

Kypke, J. L. & Solodovnikov, A. 2018. Every cloud has a silver lining: X-ray micro-CT reveals Orsunius rove beetle in Rovno amber from a specimen inaccessible to light microscopy, Historical Biology, DOI: 10.1080/08912963.2018.1558222

Labandeira, C. C. 2014. Amber. In M. Laflamme, J.D. Schiffbauer, A.F. Simon Darroch (eds), Reading and Writing of the Fossil Record: Preservational Pathways to Exceptional Fossilization. *The Paleontological Society Papers*, **20**, 163–217.

Lak, M., Néraudeau, D., Nel, A., Cloetens, P., Perrichot, V. & Tafforeau, P. 2008. Phase contrast X-ray synchrotron imaging: opening access to fossil inclusions in opaque amber. *Microscopy and Microanalysis*, **14**, 251–259. https://doi.org/10.1017/S1431927608080264

Liu, Z., Pagani, M., Zinniker, D., DeConto, R., Huber, M., Brinkhuis, H., Shah, S. R., Leckie, R. M. & Pearson, A. 2009. Global cooling during the Eocene-Oligocene climate transition. *Science*, **323**, 1187–1190. https://doi.org/10.1126/science.1166368

Martínez-Delclòs, X, Briggs, D. E. G. & Peñalver, E. 2004. Taphonomy of insects in carbonates and amber. *Palaeogeography, Palaeoclimatology, Palaeoecology*, **203**, 19–64. https://doi.org/10.1016/S0031-0182(03)00643-6

McCoy, V. E., Soriano, C. & Gabbott, S.E. 2018. A review of preservational variation of fossil inclusions in amber of different chemical groups. *Earth and Environmental Science Transactions of the Royal Society of Edinburgh*, **107**, 203–211. https://doi.org/10.1017/S1755691017000391

Nilsson, A. N. 2003. Dytiscidae: XII. A new species of *Hydrotrupes* Sharp from China, an example of Pacific intercontinental disjunction (Coleoptera). Pp. 279–284 In M. A. Jäch & L. Ji, (eds). *Water beetles of China, Vol. 3.* Zoologisch-Botanische Gesellschaft in Österreich and Wiener Coleopterologenverein. Wien.

Penney, D. 2008. *Dominican Amber Spiders: a comparative palaeontological-neontological approach to identification, faunistics, ecology and biogeography*, Siri Scientific Press, Manchester,
178 pp.

Perkovsky, E. E., Rasnitsyn, A. P., Vlaskin A. P., & Taraschuk M. V. 2007. A comparative analysis of the Baltic and Rovno amber arthropod faunas: representative samples. *African Invertebrates*, **48**(1) 229 – 245. https://journals.co.za/docserver/fulltext/nmsa_ai/48/1/nmsa_ai_v48_n1_a20.pdf?expires=1558728855&id=id&accname=guest&checksum=3A3EF3A9B9734276BA94BC5027A8C453

Perreau, M. 2012. Description of a new genus and two new species of Leiodidae (Coleoptera) from Baltic amber using phase contrast synchrotron X-ray microtomography. *Zootaxa,* **3455**, 81–88. http://dx.doi.org/10.11646/zootaxa.3455.1.5

Perreau, M. & Tafforeau, P. 2011. Virtual dissection using phase-contrast X-ray synchrotron microtomography: reducing the gap between fossils and extant species.

Systematic Entomology, **36**, 573–580. https://doi.org/10.1111/j.1365-3113.2011.00573.x

Quental, T. B. & Marshall, C. R. 2010. Diversity dynamics: molecular phylogenies need the fossil record. Trends in Ecology & Evolution. *Trends in Ecology & Evolution*, **25**, 434–441. https://doi.org/10.1016/j.tree.2010.05.002

Ritzkowski, S. 1997. K-Ar-Altersbestimmung der bernsteinführenden Sedimente des Samlandes (Paläogen, Bezirk Kaliningrad). *Metalla, Bochum*, **66**, 19–23.

Sanmartín, I., Enghoff, E. & Ronquist, F. 2001. Patterns of animal dispersal, vicariance and diversification in the Holarctic. *Biological Journal of the Linnean Society*, **73,** 345–390. https://doi.org/10.1006/bijl.2001.0542

Semple, T. L., Peakall, R. & Tatarnic, N. J. 2018. A comprehensive and user-friendly framework for 3D-data visualisation in invertebrates and other organisms. *Journal of Morphology*, **280**, 223–231. https://doi.org/10.1002/jmor.20938

Short, A. E. Z. 2018. Systematics of aquatic beetles (Coleoptera): current state and future directions. *Systematic Entomology*, **43**(1), 1-18. https://doi.org/10.1111/syen.12270

Short, A. E. Z. & Fikáček, M. 2013. Molecular phylogeny, evolution and classification of the Hydrophilidae (Coleoptera). *Systematic Entomology*, **38**(4), 723–752. DOI: https://doi.org/10.1111/syen.12024

Smetana, A. 1978. Revision of the subfamily Sphaeridiinae of America north of Mexico (Coleoptera: Hydrophilidae). *Memoirs of the Entomological Society of Canada*, **105**. 1–292. https://doi.org/10.4039/Ent116555-4

Soriano, C., Pollock, D., Neraudeau, D., Nel, A. & Tafforeau, P. 2014. First fossil record of polypore fungus beetles from Lower Cretaceous amber of France. *Acta Palaeontologica Polonica*, **59**(4), 941–946. http://dx.doi.org/10.4202/app.2012.0074

Teodoridis, V., Kvaček, Z., Zhu, H. & Mazouch, P. 2012. Environmental analysis of the mid–latitudinal European Eocene sites of plant macrofossils and their possible analogues in East Asia. *Palaeogeography, Palaeoclimatology, Palaeoecology*, **333–334**, 40–58.

https://doi.org/10.1016/j.palaeo.2012.03.008

Toussaint, E. F. A. & Short, A. E. Z. 2018. Transoceanic stepping-stones between Cretaceous waterfalls? The enigmatic biogeography of pantropical Oocyclus cascade beetles. *Molecular*

Phylogenetics and Evolution, **127**, 416–428. DOI: https://doi.org/10.1016/j. Ympev.2018.04.023.

Wen, J. 1999. Evolution of eastern Asian and eastern North American disjunct distributions in flowering plants. *Annual Review of Ecology and Systematics*, **30,** 421–455. https://doi.org/10.1146/annurev.ecolsys.30.1.421

Wu, H., Coty, D. & Ding, M. 2015. First artematopodid beetle in Mexican amber and its biogeographic implications (Coleoptera, Artematopodidae). *Alcheringa: An Australasian Journal of Palaeontology*, **39**(4), 508–513, DOI: 10.1080/03115518.2015.1041306

Zanazzi, A., Kohn, M. J., MacFadden, B. J. & Terry, D. O. 2007. Large temperature drop across the Eocene–Oligocene transition in central North America. *Nature*, **445**, 639–642. https://doi.org/10.1038/nature05551

Figure captions

Figure 1. A–E, *Anacaena morla* sp. nov. holotype: **A,** dorsal habitus; **B,** ventral habitus; **C,** lateral view; **D,** ventral view of head and thorax; **E,** meso- and metatibia and tarsi. Blue arrows = setae on meso- and metatarsi; **F**, *Crenitis profechuyi* sp. nov. paratype metatibia and tarsi. Red arrow = setae on mesotarsus. Scale bars = 1mm.

Figure 2. A–I, *Anacaena morla* sp. nov, holotype, volume rendering: **A,** dorsal habitus; **B,**

ventral habitus; **C,** lateral view; **D,** frontal view of head and pronotum; **E,** ventral view of head. Yellow arrow = anterior margin of mentum; **F,** dorsolateral view of left elytron. Blue arrows = 4th and 5th elytral series of punctures; **G,** prosternum; **H,** mesoventrite. Red arrow = anapleural suture at anterior margin. Blue arrow = transverse projection of mesoventrite; **I,** aedeagus. Scale bars = 1mm.

Figure 3. A–E, *Crenitis profechuyi* sp. nov. holotype: **A,** dorsal habitus; **B,** ventral habitus; **C,** lateral view; **D,** frontral view of head and thorax; **E,** ventral view of metathorax and meso- and metalegs. Red arrow = surface of metaventrite. Green arrow = pubescence in mesofemur. Blue arrow = pubescence at base of metafemora; **F**, aedeagus. Scale bars = 1mm.

Figure 4. A–E, *Crenitis profechuyi* sp. nov. holotype, isosurface reconstruction: **A,** dorsal habitus; **B,** ventral habitus; **C,** lateral view; **D,** ventral view of head and prosternum; **E,** mesoventrite. Yellow arrow = anapleural suture at anterior margin. Green arrow = transverse projection of mesoventrite; **F,** orthoslice reconstruction of mesothorax in lateral view. Green arrow = transverse projection of mesoventrite. Scale bars = 1mm.

Figure 5. A–C, *Crenitis profechuyi* sp. nov. paratype 2: **A,** dorsal habitus; **B,** ventral habitus. Yellow arrow = surface of mesofemur; **C,** lateral view. Scale bars = 1mm.

Figure 6. A–K, *Crenitis profechuyi* sp. nov. paratype 1, volume rendering: **A,** dorsal habitus; **B,** ventral habitus; **C,** lateral view; **D,** antenna; **E,** frontal view of head; **F,** ventral view of head; **G,** labial palp; **H,** ventral view of mesoventrite. Green arrow = transverse projection of mesoventrite; **I,** lateral view of mesoventrite; Green arrow = transverse projection of mesoventrite **J,** ventral view of metaventrite. Red arrow = surface of

metaventrite; **K,** detail of right elytron. Scale bars = 1mm.

Figure 7. A–C, *Crenitis profechuyi* sp. nov. paratype 2: **A,** dorsal habitus; **B,** ventral habitus; **C,** ventral view of abdomen and hind legs; **D–F,** *Crenitis profechuyi* sp. nov. paratype 2, volume rendering reconstruction of inverse images: **D,** dorsal habitus; **E,** ventral view of mesoventrite. Yellow arrow = anapleural sutures at anterior margin. Blue arrow = transverse projection of mesoventrite; **F,** apex of abdomen showing partially exposed aedeagus. Red arrow = tip of paramere. Scale bars = 1mm.

Figure 8. A–C, Fourier transformed infrared spectra (FT-IR) of the amber pieces containing the three *Crenitis profechuyi* sp. nov. types: A, holotype; B, paratype 1; C, paratype 2. Blue arrow = “Baltic shoulder” between 1190–1280 cm^{-1}.

Figure 9. A–F, *Helochares fog* sp. nov. holotype: **A,** dorsal habitus; **B,** dorsolateral habitus. Green arrow = impressed elytral stria; **C,** ventral view; **D,** ventral view of head; **E,** ventral view of abdomen and metalegs; **F,** metatarsi. Blue arrow = natatorial setae. Scale bars = 1mm.

Figure 10. A–I, *Helochares fog* sp. nov. holotype 1, volume rendering: **A,** dorsal habitus; **B,** ventral habitus; **C,** lateral view; **D,** ventral view of head. Red arrow = punctures in mentum; **E,** ventral view of prosternum. Green arrow = anterior margin of prosternum; **F,** labial palp; **G,** Orthoslice showing mesoventrite with pro- and mesocoxae removed. Yellow arrow = anapleural sutures at anterior margin; blue arrow = possible position of transverse ridge of mesoventrite. **H,** Isosurface reconstruction of ventral view of abdomen and metalegs; **I,** detail of right elytron. Scale bars = 1mm.

Figure 11. A, Phalacridae sp. dorsal habitus. Blue arrow = longitudinal punctate striae; **B,** antennal club. Yellow arrows = antennomeres in club; green arrow = 8th antennomere not cupuliform; **C,** mesotarsus. Red arrows = mesotarsomeres 2 and 3.

Figure 12. A, Distribution of genera and species groups probably related to Baltic amber species; **B,** dorsal habitus of *Crenitis apicalis* group representative; **C,** aedeagus of *Crenitis apicalis* group; **D,** dorsal habitus of *Helochares* (*Batochares*) representative; **E,** dorsal habitus of *Helochares* (s. str.) with triangular mesoventrite; **F,** ventral habitus drawing of *Helochares* (s. str.) with triangular mesoventrite; **G,** dorsal habitus of *Peltochares* representative.

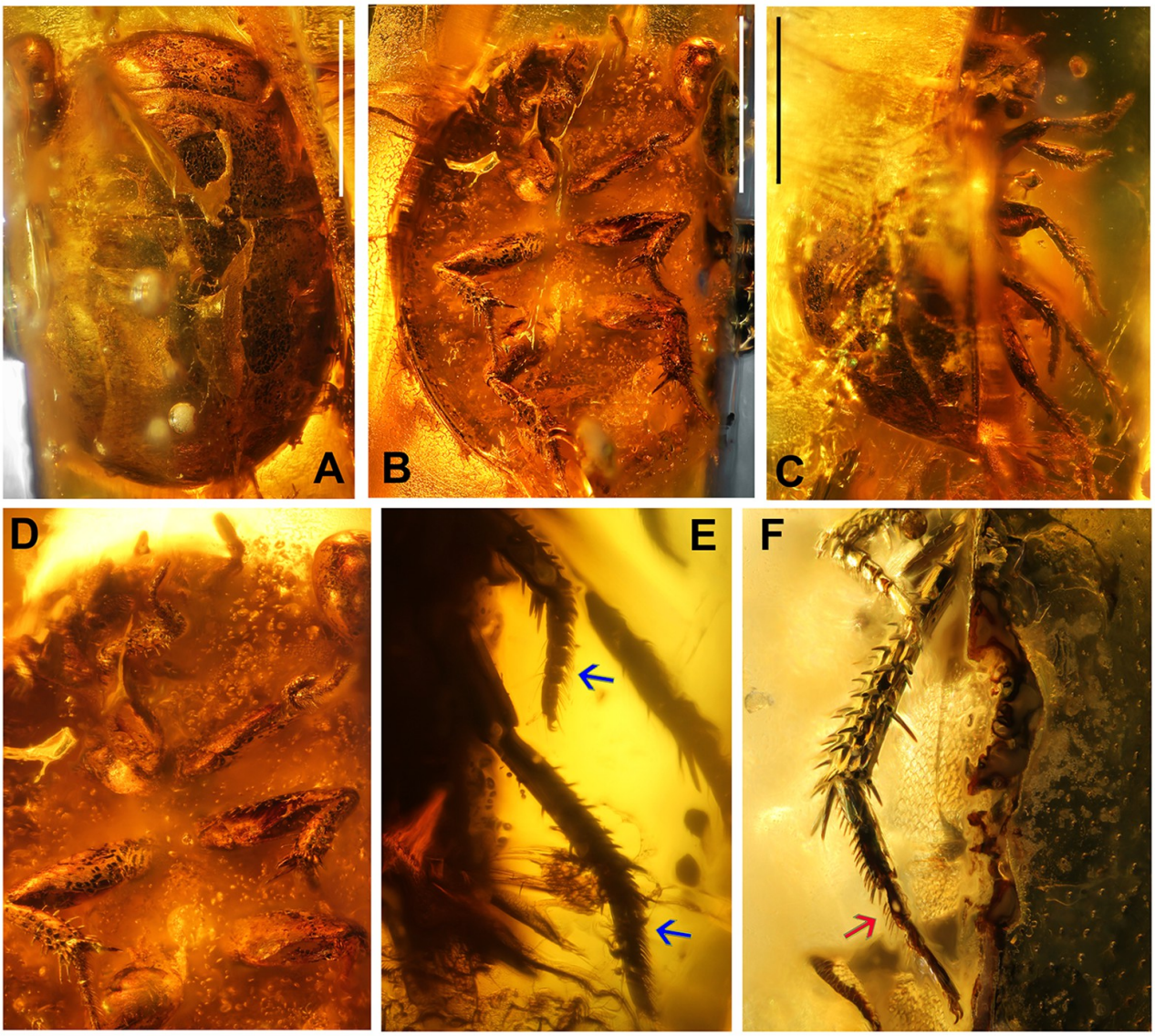

Figure 1. A–E, *Anacaena morla* sp. nov. holotype: **A,** dorsal habitus; **B,** ventral habitus; **C,** lateral view; **D,** ventral view of head and thorax; **E,** meso- and metatibia and tarsi. Blue arrows = setae on meso- and metatarsi; **F**, *Crenitis profechuyi* sp. nov. paratype metatibia and tarsi. Red arrow = setae on mesotarsus. Scale bars = 1mm.

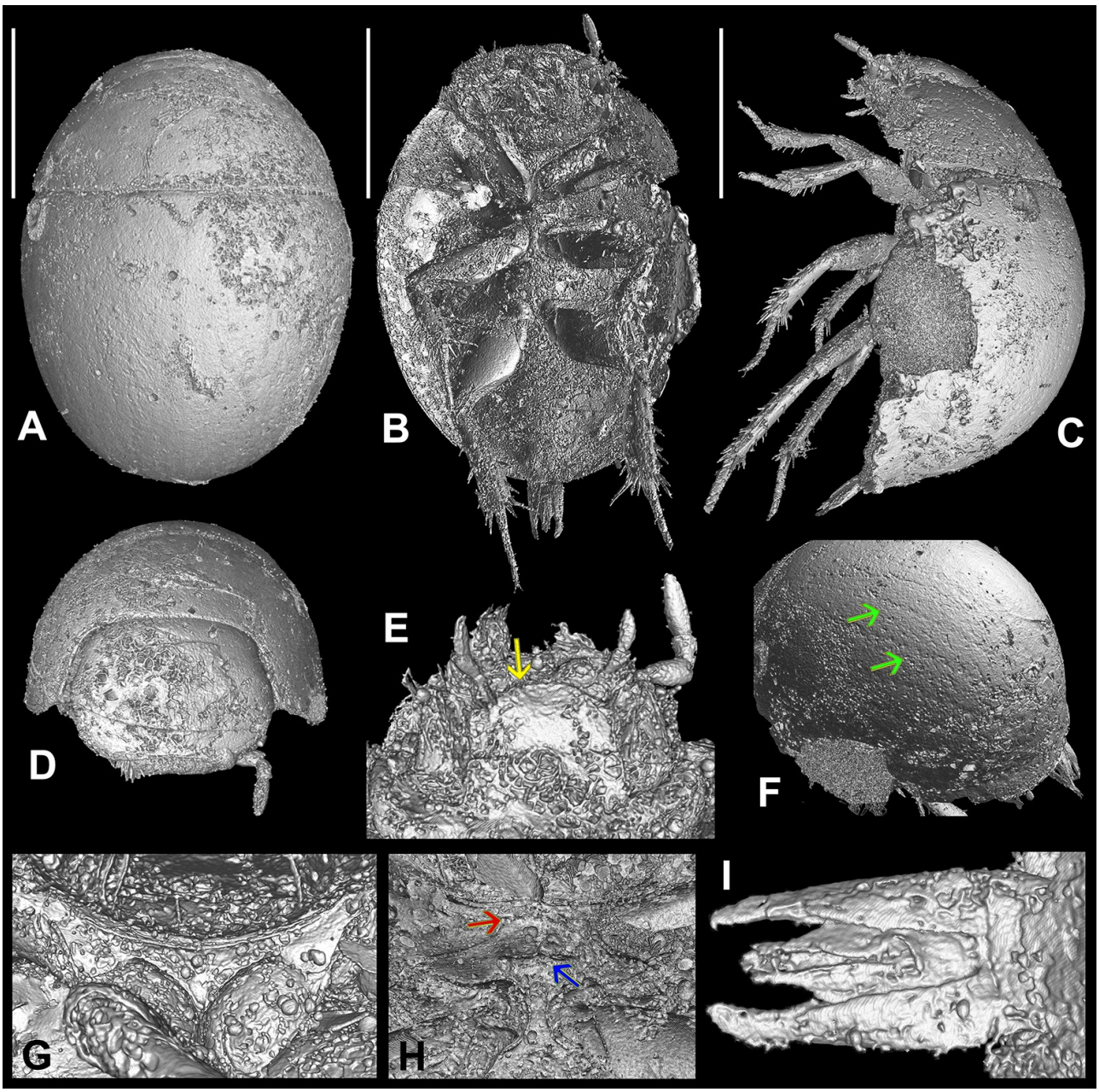

Figure 2. A–I, *Anacaena morla* sp. nov, holotype, volume rendering: **A,** dorsal habitus; **B,** ventral habitus; **C,** lateral view; **D,** frontal view of head and pronotum; **E,** ventral view of head. Yellow arrow = anterior margin of mentum; **F,** dorsolateral view of left elytron. Blue arrows = 4th and 5th elytral series of punctures; **G,** prosternum; **H,** mesoventrite. Red arrow = anapleural suture at anterior margin. Blue arrow = transverse projection of mesoventrite; **I,** aedeagus. Scale bars = 1mm.

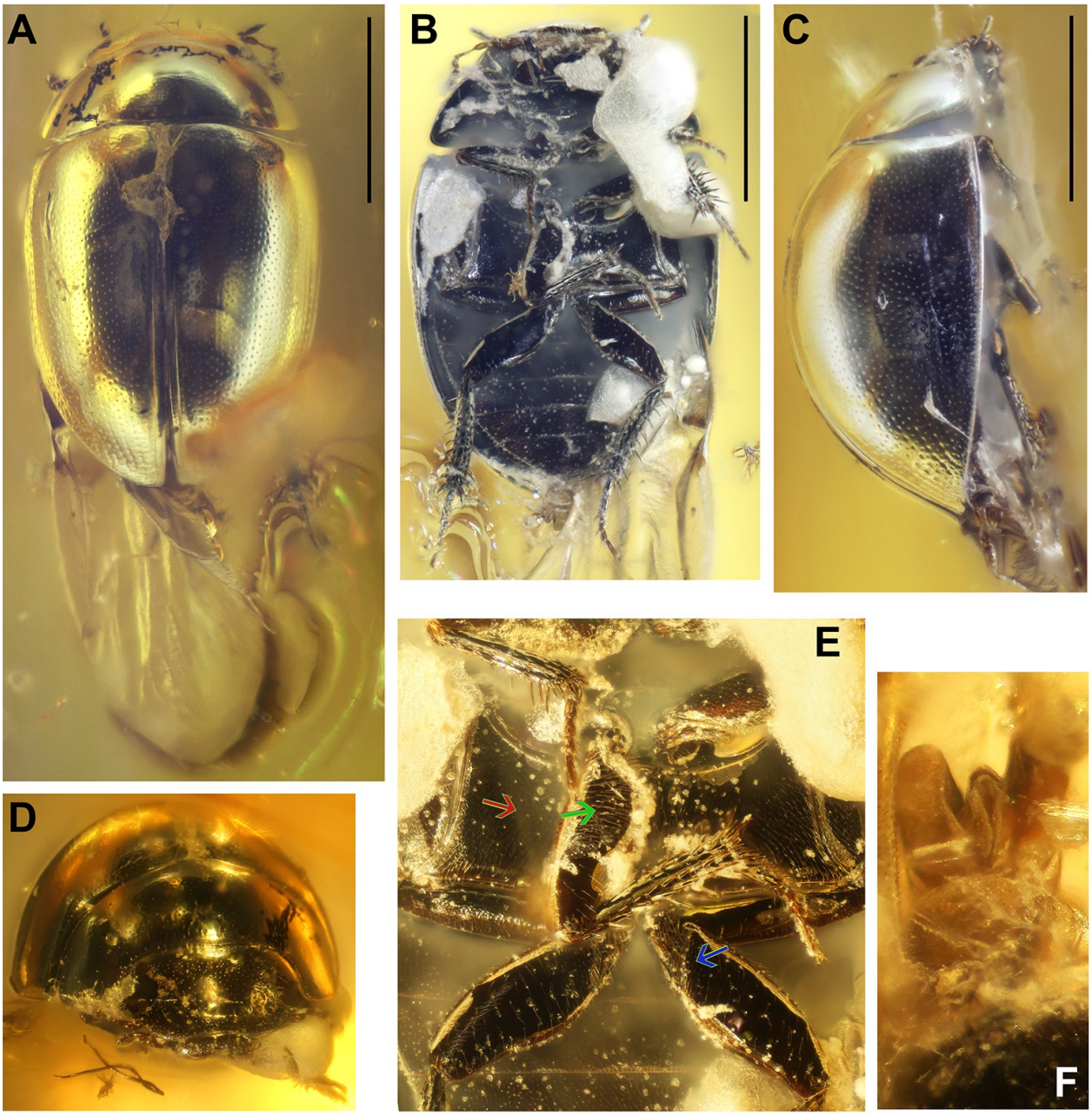

Figure 3. A–E, *Crenitis profechuyi* sp. nov. holotype: **A,** dorsal habitus; **B,** ventral habitus; **C,** lateral view; **D,** frontral view of head and thorax; **E,** ventral view of metathorax and meso- and metalegs. Red arrow = surface of metaventrite. Green arrow = pubescence in mesofemur. Blue arrow = pubescence at base of metafemora; **F**, aedeagus. Scale bars = 1mm.

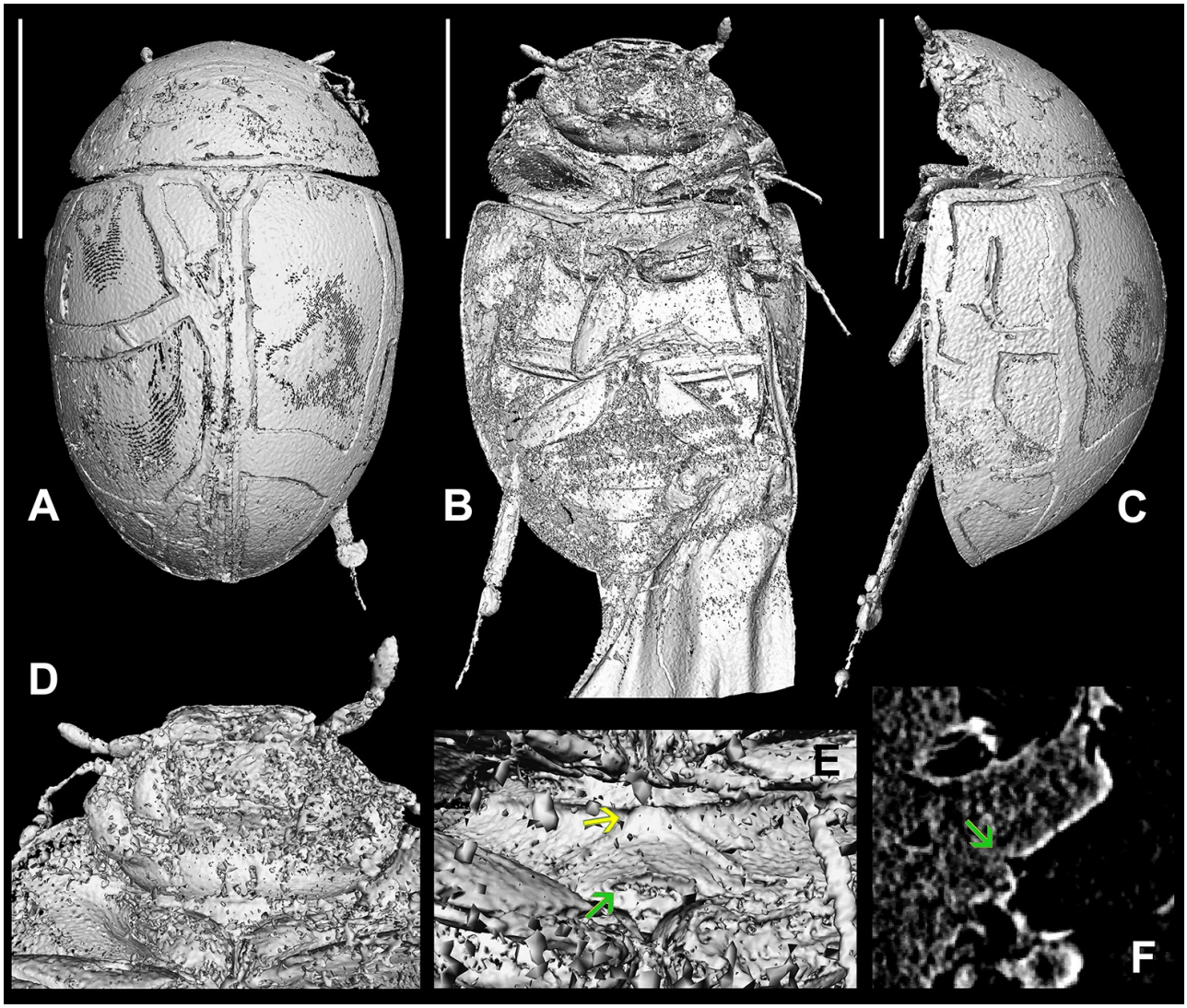

Figure 4. A–E, *Crenitis profechuyi* sp. nov. holotype, isosurface reconstruction: **A,** dorsal habitus; **B,** ventral habitus; **C,** lateral view; **D,** ventral view of head and prosternum; **E,** mesoventrite. Yellow arrow = anapleural suture at anterior margin. Green arrow = transverse projection of mesoventrite; **F,** orthoslice reconstruction of mesothorax in lateral view. Green arrow = transverse projection of mesoventrite. Scale bars = 1mm.

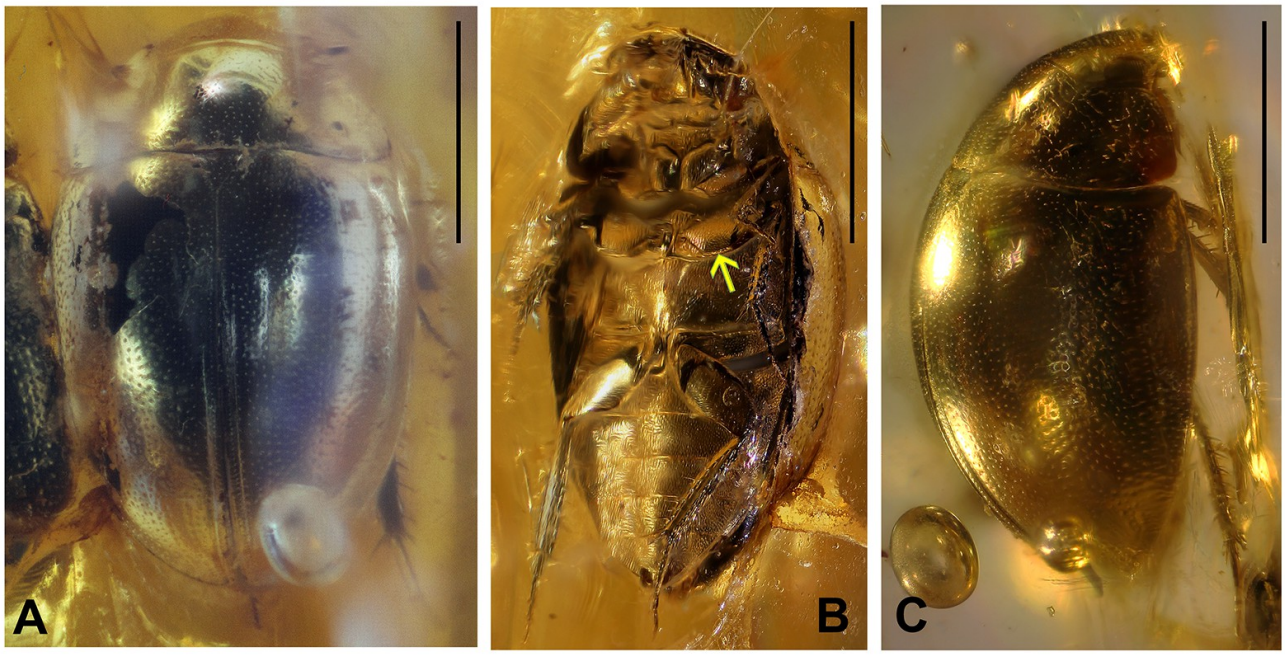

Figure 5. A–C, *Crenitis profechuyi* sp. nov. paratype 2: **A,** dorsal habitus; **B,** ventral habitus. Yellow arrow = surface of mesofemur; **C,** lateral view. Scale bars = 1mm.

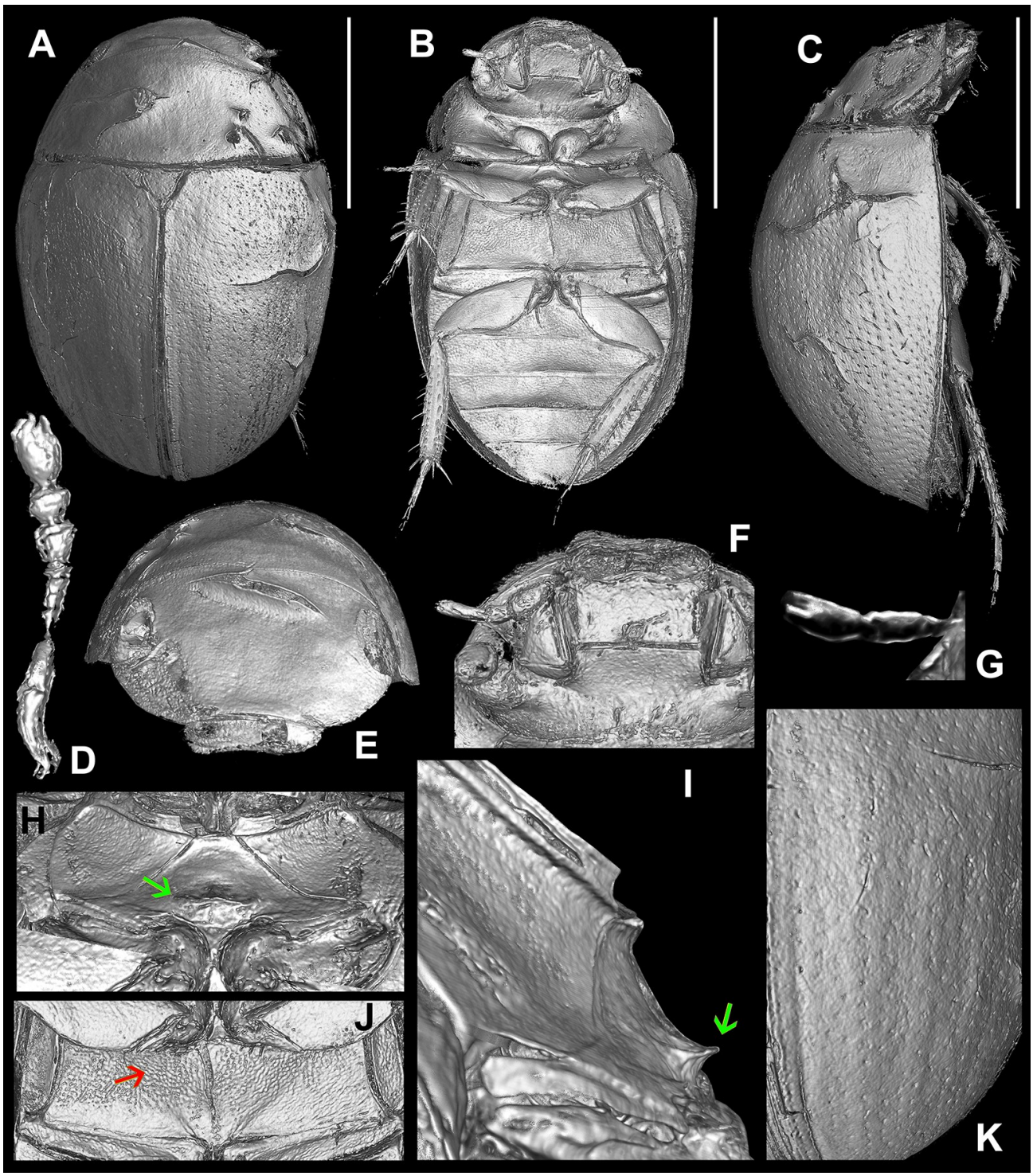

Figure 6. A–K, *Crenitis profechuyi* sp. nov. paratype 1, volume rendering: **A,** dorsal habitus; **B,** ventral habitus; **C,** lateral view; **D,** antenna; **E,** frontal view of head; **F,** ventral view of head; **G,** labial palp; **H,** ventral view of mesoventrite. Green arrow = transverse projection of mesoventrite; **I,** lateral view of mesoventrite; Green arrow = transverse projection of mesoventrite **J,** ventral view of metaventrite. Red arrow = surface of metaventrite; **K,** detail of right elytron. Scale bars = 1mm.

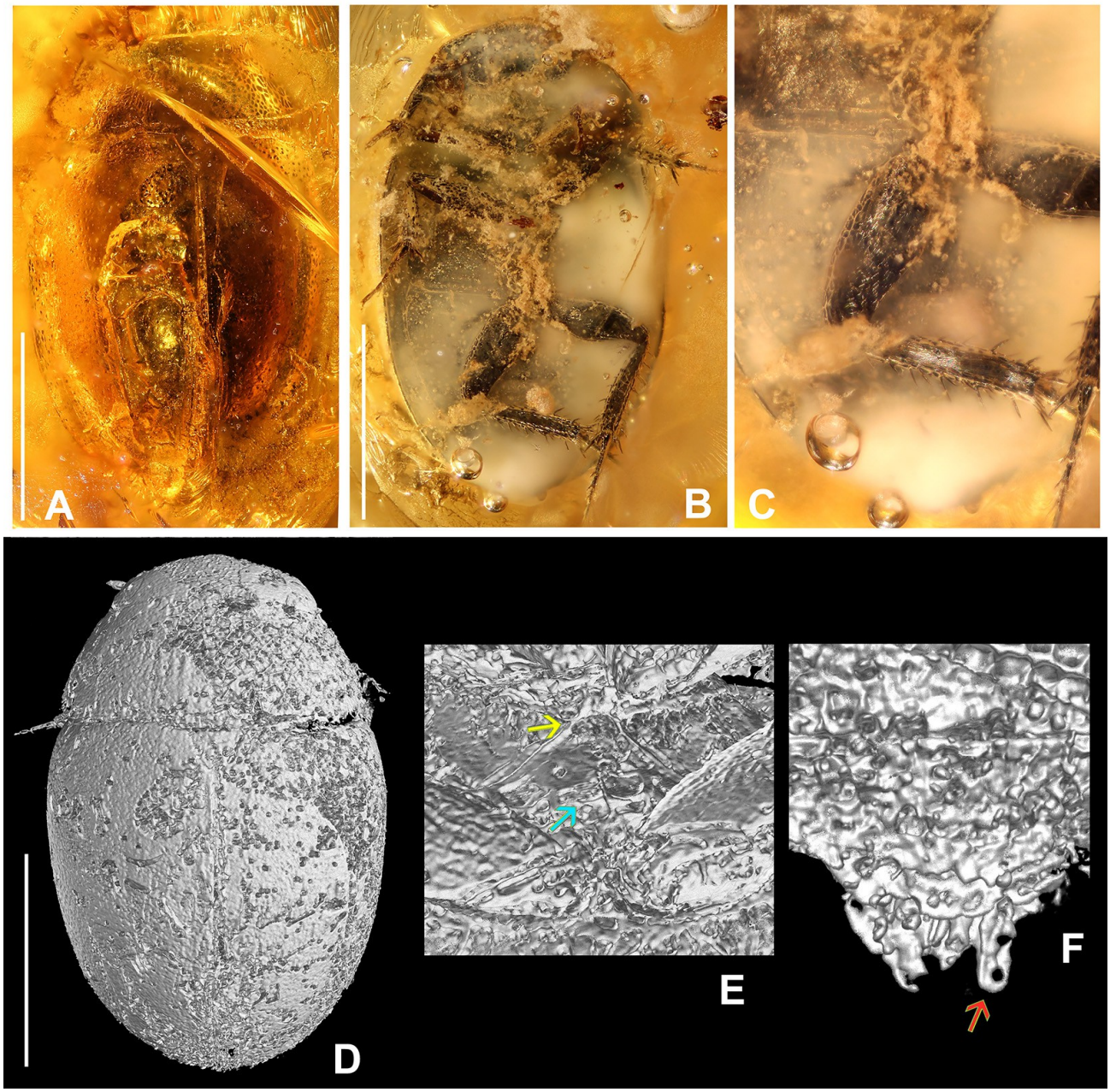

Figure 7. A–C, *Crenitis profechuyi* sp. nov. paratype 2: **A,** dorsal habitus; **B,** ventral habitus; **C,** ventral view of abdomen and hind legs; **D–F,** *Crenitis profechuyi* sp. nov. paratype 2, volume rendering reconstruction of inverse images: **D,** dorsal habitus; **E,** ventral view of mesoventrite. Yellow arrow = anapleural sutures at anterior margin. Blue arrow = transverse projection of mesoventrite; **F,** apex of abdomen showing partially exposed aedeagus. Red arrow = tip of paramere. Scale bars = 1mm.

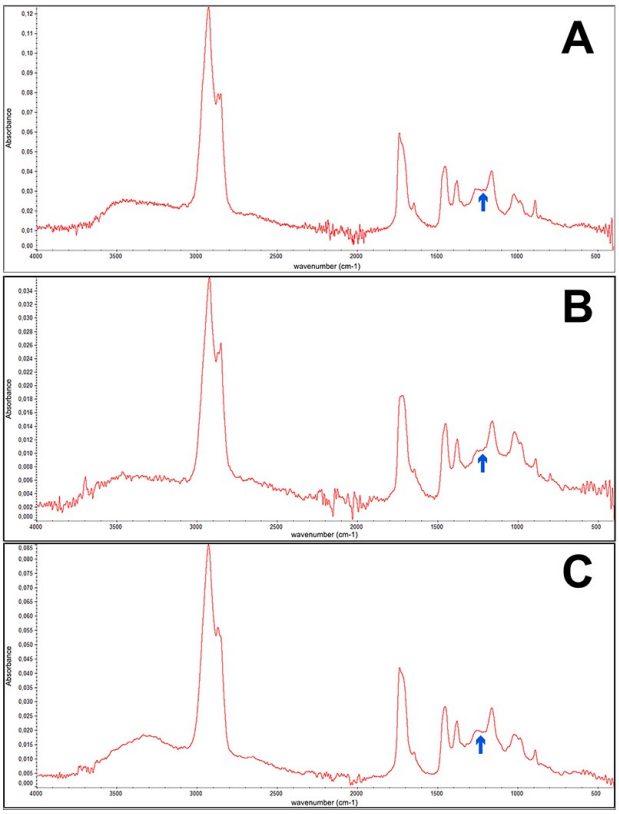

Figure 8. A–C, Fourier transformed infrared spectra (FT-IR) of the amber pieces containing the three *Crenitis profechuyi* sp. nov. types: A, holotype; B, paratype 1; C, paratype 2. Blue arrow = “Baltic shoulder” between 1190–1280 cm^{-1}.

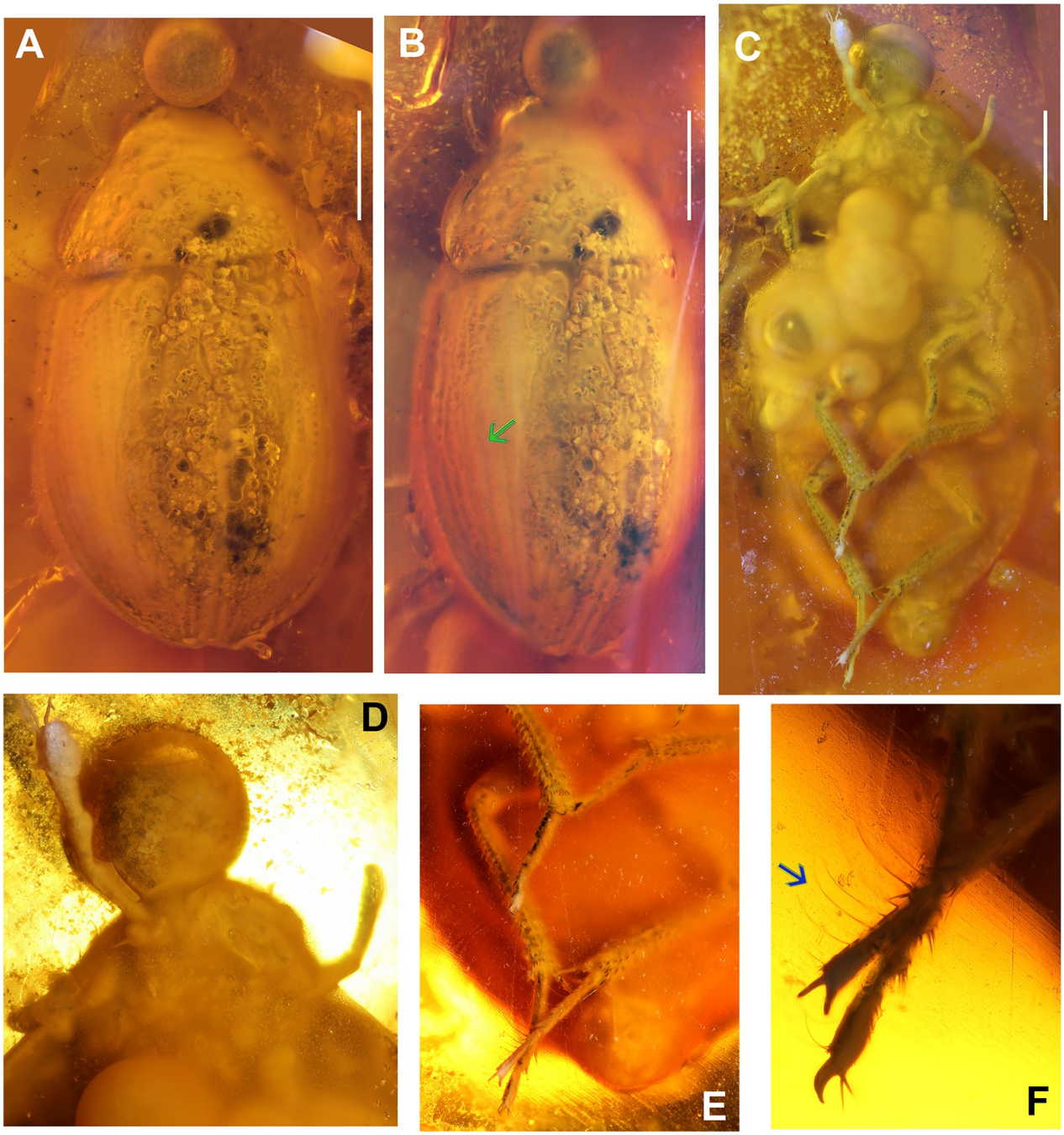

Figure 9. A–F, *Helochares fog* sp. nov. holotype: **A,** dorsal habitus; **B,** dorsolateral habitus. Green arrow = impressed elytral stria; **C,** ventral view; **D,** ventral view of head; **E,** ventral view of abdomen and metalegs; **F,** metatarsi. Blue arrow = natatorial setae. Scale bars = 1mm.

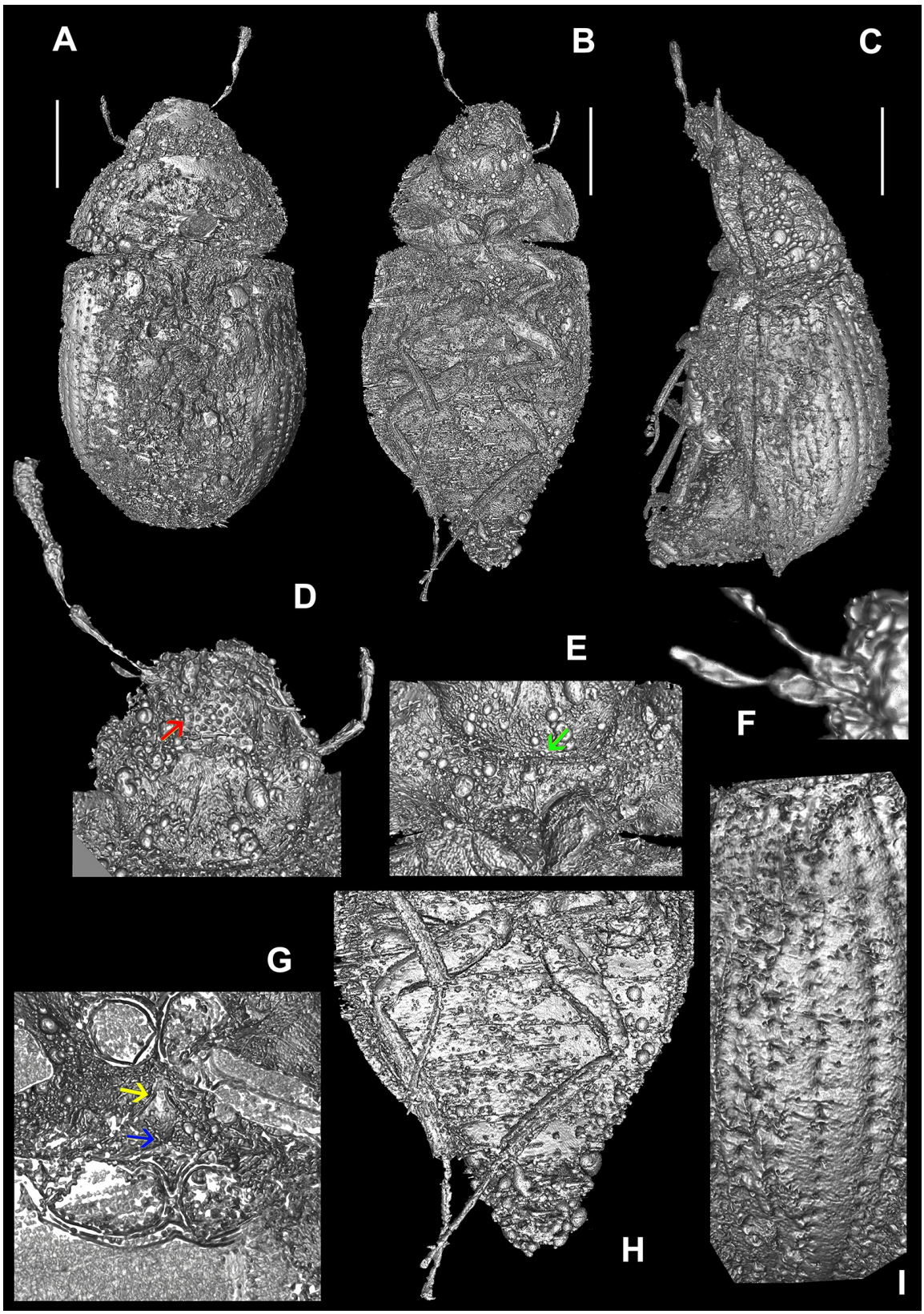

Figure 10. A–I, *Helochares fog* sp. nov. holotype 1, volume rendering: **A,** dorsal habitus; **B,** ventral habitus; **C,** lateral view; **D,** ventral view of head. Red arrow = punctures in mentum; **E,** ventral view of prosternum. Green arrow = anterior margin of prosternum; **F,** labial palp; **G,** Orthoslice showing mesoventrite with pro- and mesocoxae removed. Yellow arrow = anapleural sutures at anterior margin; blue arrow = possible position of transverse ridge of mesoventrite. **H,** Isosurface reconstruction of ventral view of abdomen and metalegs; **I,** detail of right elytron. Scale bars = 1mm.

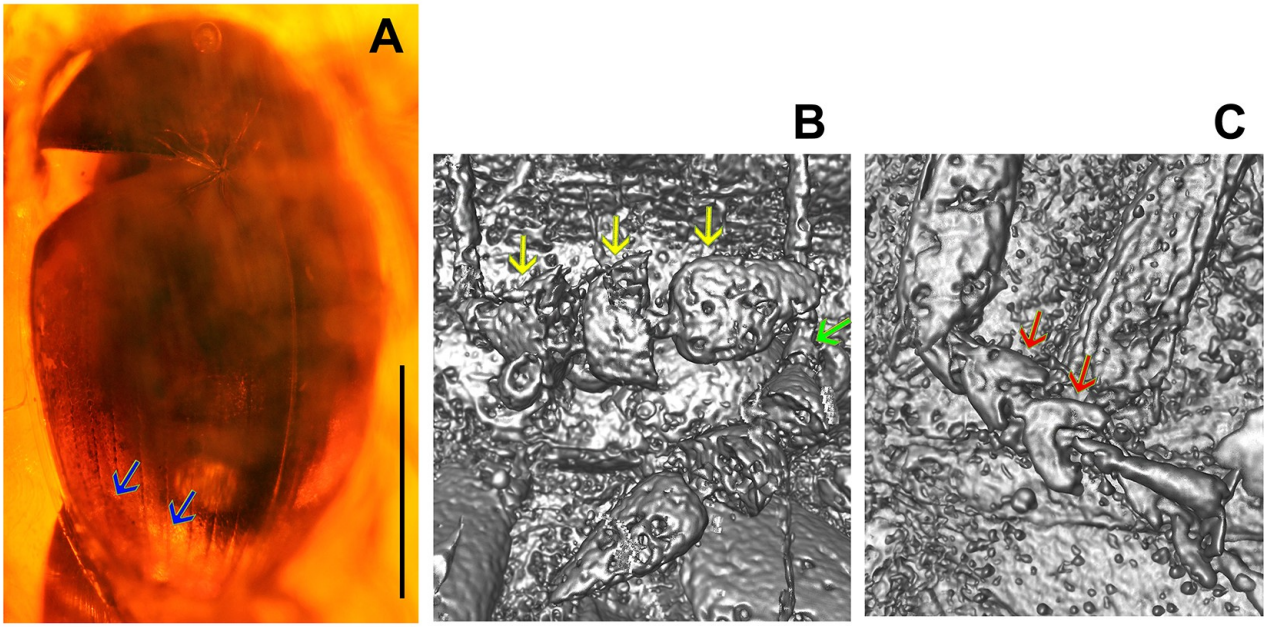

Figure 11. A, Phalacridae sp. dorsal habitus. Blue arrow = longitudinal punctate striae; **B,** antennal club. Yellow arrows = antennomeres in club; green arrow = 8th antennomere not cupuliform; **C,** mesotarsus. Red arrows = mesotarsomeres 2 and 3.

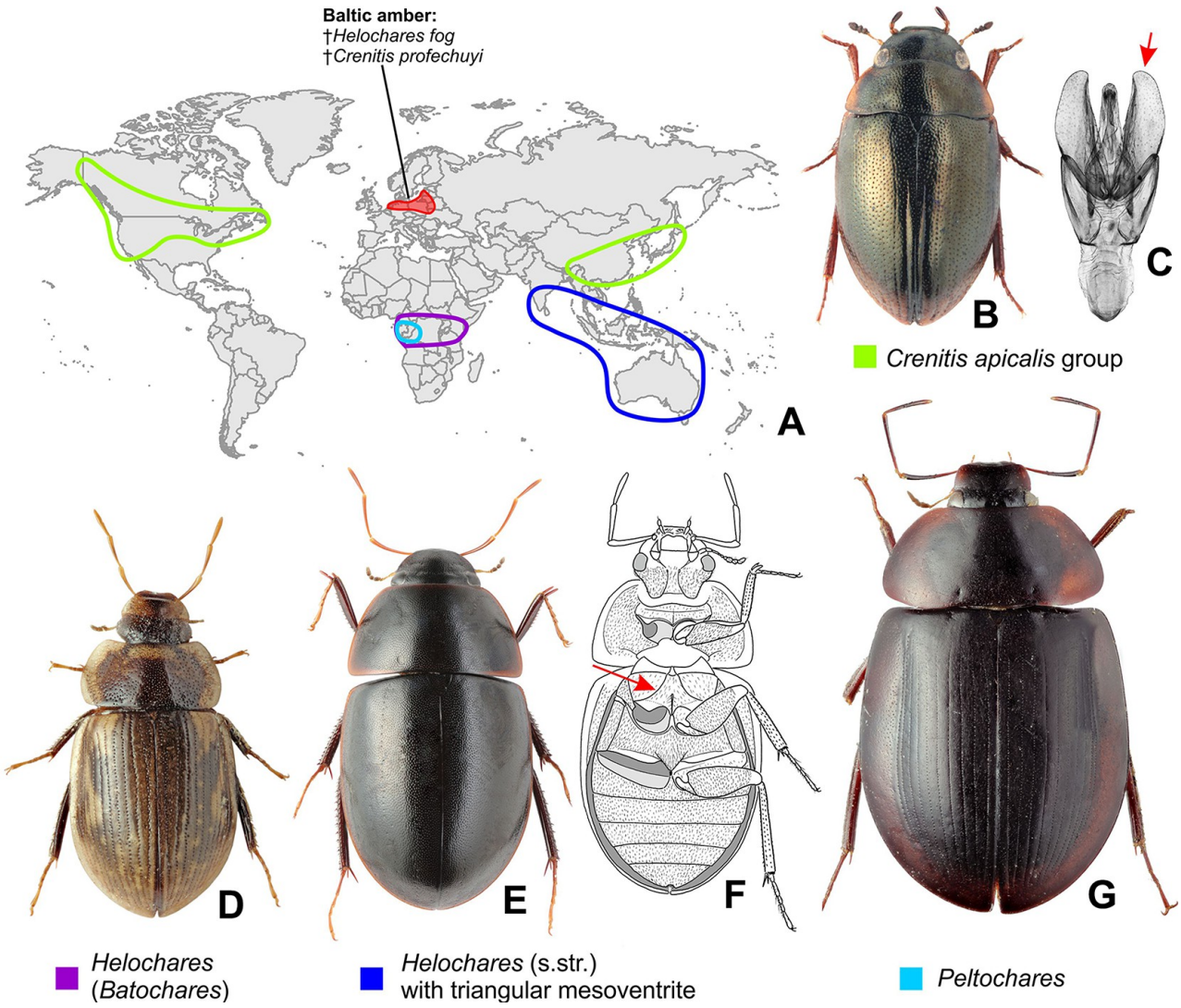

Figure 12. A, Distribution of genera and species groups probably related to Baltic amber species; **B,** dorsal habitus of *Crenitis apicalis* group representative; **C,** aedeagus of *Crenitis apicalis* group; **D,** dorsal habitus of *Helochares* (*Batochares*) representative; **E,** dorsal habitus of *Helochares* (s. str.) with triangular mesoventrite; **F,** ventral habitus drawing of *Helochares* (s. str.) with triangular mesoventrite; **G,** dorsal habitus of *Peltochares* representative.

Chapter 6

Phylogeny, habitat shifts and diversification of terrestrial water scavenger beetles (Hydrophiloidea: Hydrophilidae)

Arriaga-Varela, E. Sýkora, V., Ghanavi, H., Seidel, M. and Fikácek, M. (*Unpublished manuscript*).

Phylogeny, habitat shifts and diversification of terrestrial water scavenger beetles (Hydrophiloidea: Hydrophilidae)

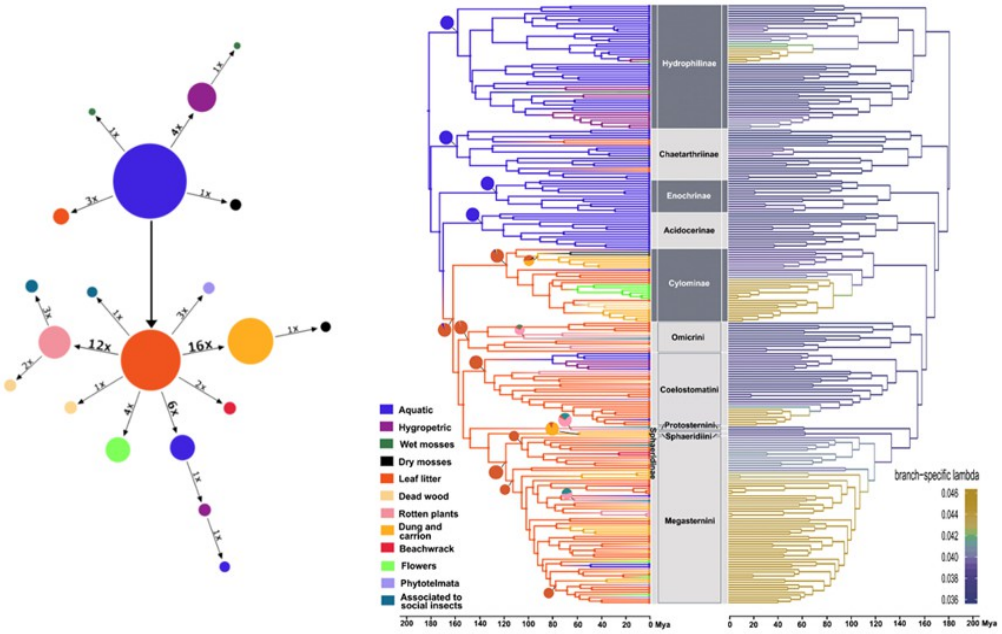

Phylogeny, habitat shifts and diversification of terrestrial water scavenger beetles (Hydrophiloidea: Hydrophilidae)

Emmanuel Arriaga-Varela[1,2], Vit Sykora[1,2], Hamid Ghanavi[3], Matthias Seidel[1,2] and Martin Fikáček[2,1]

[1] Department of Zoology, Faculty of Science, Charles University, Prague, Viničná 7, CZ-12843, Prague, Czech Republic; [2] Department of Entomology, National Museum, Cirkusová 1740, CZ-19300 Prague, Czech Republic; [3] Department of Biology, Lund University, Lund, Sweden

Abstract. Hydrophilidae or water scavenger beetles are a diverse family of ancestrally aquatic habits. However, about a third of species are found in terrestrial habitats, representing what is probably the most successful case of 'return to the land' in the whole Insecta. We present a multigene phylogeny and time estimates for the family with an emphasis on the ecologically and taxonomically diverse subfamilies Cylominae and Sphaeridiinae, and use the results to investigate the patterns of habitat transitions during their evolutionary history. Resulting topology agrees with the previous hypothesis of relations among main suprageneric taxa. Multiple transitions from aquatic to terrestrial and semiaquatic habitats were estimated. However, a single shift to terrestrial habitat, namely leaf litter, was reconstructed for the ancestor of the terrestrial lineages Cylominae and Sphaeridiinae. Leaf litter was recovered as the most flexible habitat, from which the majority of ecological secondary transitions were originated. Animal excrements and carrion was found to be the most common destination of those shifts. Nevertheless, tertiary or quaternary transitions were rare. The flexibility of inhabitants of leaf litter habitats is probably behind the success of terrestrial water scavenger beetles as a whole: it was recovered as ancestral for all principal terrestrial clades except the less diverse Sphaeridiinae and Protosternini. Megasternini was corroborated as showing the most extended increase in diversification in the family. This increase is, however, more accentuated in the *Cercyon* group of genera. Additional shifts were found in particular lineages in Hydrophylinae (*Limnoxenus*), Cylominae (genera *Cyloma, Adolopus* and *Rygmodus* from New Zealand) and Coelostomatini (*Phaenonotum*). These shifts can be explained by the colonization of insular environments that likely promoted their ecological and taxonomical diversification. The increase in diversification rate in Megasternini is likely linked to a wider array of colonized habitats and/or the faster pace of transitions facilitated by a relatively plastic morphology.

Keywords
Leaf litter, habitat transitions, branch spesific diversification, divergence dating, Hydrophiloidea

Introduction

The colonization of a new environment often brings new ecological opportunities that play a significant role in the diversification of the lineages (Gavrilets and Losos 2009; Roxo et al 2017). Colonizations of the terrestrial environment by the primarily aquatic organisms have been seminal in the evolutionary history of the most important and successful groups such plants (Rensing 2018; Davis 2019) vertebrates (Benton 2010; Ashley-Ross et al. 2013) and arthropods (Regier et al. 2005; Pisani et al. 2004).

Insects are the most successful group of animals in terms of diversity. Hexapods form are a lineage nested in what has been traditionally considered "Crustacea" (Regier et al. 2005; Hassanin 2006. Although with many exceptions, crustaceans are typically found in water bodies of all kind. Although it is a matter of debate whether first insects were aquatic or terrestrial (Pritchard et al. 1993) the extant species are predominantly terrestrial, with at least 90% of its species adapted to life in the land. Secondary shifts from a terrestrial habitat back to water occurred multiple times among insect lineages. Beetles (order Coleoptera) are one of the most successful secondary colonizers of water (Bilton et al. 2019). Aquatic beetles are found in 23 families, ca. 13,000 aquatic species have been described, and the estimated real number of aquatic species counts 20,000 species. Surprisingly, two beetle lineages contain 73% of this diversity: Hydradephaga and Hydrophiloidea. Hydrophiloid beetles are members of the Staphyliformia, a clade where two major shifts to water have occurred, in Hydrophiloidea and Hydraenidae. Leaf litter was hypothesized as the pivotal environment allowing the organisms that inhabit it to frequently colonize a variety of other microhabitats including the aquatic ones (McKenna et al. 2015). Within Hydrophiloidea, the shift to aquatic lifestyle was shown to have occurred in a single occasion (Bernhard et al. 2006; Bloom et al. 2014).

Family Hydrophilidae encompasses almost 80% of the species diversity of Hydrophiloidea and was shown to be ancestrally aquatic (Song et al. 2014). Nevertheless, approximately 150 million years ago, the common ancestor of subfamilies Cylominae and Sphaeridiinae returned to land (Toussaint and Short 2018). This major shift in life-style makes Hydrophilidae an interesting model group for studying evolutionary patterns and process and testing hypotheses on diversification, ecology, and biogeography (Bernhard et al. 2006; Bloom et al. 2014; Song et al. 2014; Toussaint and Short 2018). Hydrophilidae represent perhaps the most clear "return to land" example in insects, and

contradicts the idea that such reversion to terrestrial lifestyle has been never successful in aquatic insects (see Vršanský et al 2019).

The currently accepted classification for family Hydrophilidae was proposed by Short and Fikáček (2013) on the basis of a multigene phylogeny. It recognizes six subfamilies, four of them are mainly of aquatic habits: Hydrophilinae, Chaetarthriinae, Enochrinae and Acidocerinae; while two are mainly terrestrial: Cylominae and Sphaeridiinae. Members of Hydrophilinae family, like the giant water scavenger *Hydrophilus* beetles reach up to 10 cm of body length and show clear adaptations to natatorial locomotion, like paddle-like tarsi and keel-like thoracic ventrites (Short 2010). Nevertheless, most hydrophilids are well adapted to crawl. Most aquatic species can be seen crawling underwater, often in environment rich in organic material of mostly plant origin upon they feedi on. On the other hand, terrestrial hydrophilids can be found in a wide array of environments such as humid leaf litter (Fikáček and Short, 2006), vertebrate dung (Archangelsky 1997; Arriaga-Varela et al. 2018a), angiosperm inflorescences (Arriaga-Varela et al. 2018b, Minoshima et al., 2018) or debris accumulated by social insects (Spangler, 1962; Fikáček *et al.,* 2013).

The majority of the terrestrial species are classified in the five tribes of subfamily Sphaeridiinae. The most diverse tribe in number of species and ecology is Megasternini (Short and Fikáček 2011; Bloom et al. 2014), with 566 described species and probably up to one thousand in total including undescribed ones.

Bloom et al. (2014) dated the divergence events in the phylogeny using a set of eight fossils as calibration points on the basis of the molecular dataset used assembled by Short and Fikáček (2013). Under this framework, the general diversification patterns in the family were analyzed finding an increase in diversification rate on the root of Megasternini, the most recently diverging clade of the family. The increase on diversification rate did not coincide with any majob habitat shift and suggested a more complex explanation for the diversification patterns in terrestrial water scavenger beetles. The breadth of the ecological associations of terrestrial water scavenger beetles makes them an almost ideal candidate to explore the possibility of diversification increases driven by ecological opportunities.

Here we examine how the evolution of the habitat preferences have shaped the diversity in the family Hydrophilidae. For this we put together the most taxonomically representative dataset for the family with the most comprehensive sampling of terrestrial species in subfamilies Cylominae and Sphaeridiinae available at the moment, and recalibrate the Hydrophilidae time tree based on an updated set of fossils (Arriaga-Varela et al. Submitted; Fikaček et al. 2017). We aim, nevertheless, to obtain a sample representative enough that it can shade light on the pattern of ecological evolution and diversification in the family.

Material and Methods

Taxonomic and molecular sampling. We assembled a dataset for the Hydrophilidae aiming at taxon sampling more less proportional to known species diversity of the principal clades, and with an emphasis on covering the ecological and species diversity of the terrestrial clades, as this was underrepresented in previous studies. Our dataset is based on the family level dataset of Short and Fikaček (2013) with additional taxataken from Minoshima et al. (2018), Deler-Hernández et al. (2018), Toussaint and Short (2018) and Fikáček et al. (2018). Additionally, we performed an extensive *ex novo* sequencing focused on members of Cylominae and Sphaeridiini: Megasternini was performed. Total genomic DNA was extracted from entire beetles using QiaGen Blood and Tissue DNA extraction kit following the manufacturer's instructions. We did not attempt to amplify arginine kinase (ArgK) used by Short and Fikaček (2013) and Toussaint and Short (2018) for the newly sequenced samples. Instead, we obtained topoisomerase I (TopI) gene in order to provide topological resolution for the Megasternini.

Phylogenetic analyses. Sequences trace files were uploaded into Geneious (Kearse et al 2012) for inspection, assembly, and editing. All newly generated sequences are deposited in GenBank. Sequences were aligned in Geneious using ClustalW algorithm with default settings. Our dataset is composed of 8 genes: 18S (1,406 bp), 28S (1,101 bp), cytochrome oxidase I (COI) (753 bp), cytochrome oxidase II (COII) (659 bp), 16S (825 bp), histone 3 (290 bp), arginine kinase (ArgK) (705 bp) and topoisomerase I (TopI) (627 bp). The final concatenated alignment has the length of 6,366 bp. An independent partition was set for each ribosomal gene and for each codon position of the protein coding genes. Best-fitting models of substitution were selected using PartitionFinder 2 (Lanfear et al. 2016). The concatenate matrix was analysed using MrBayes 3.2.6 (Ronquist et al., 2012) implemented on the CIPRES Science Gateway 3.3 (Miller et al., 2010) using independent parameters for each partition. Four runs with six chains each were set to run for 25 million generations, with trees being sampled every 12,500 generations. The convergence of the runs and their parameters were assessed in Tracer 1.6 (Rambaut et al. 2014). A 25% burn-in fraction was applied to the data. Due to problems with alignment of the ribosomal genes when the non-hydrophilid taxa were included, we only included the representatives of the Hydrophilidae and used the earliest branching clade (Hydrophilinae) to root the tree, following the results of Short and Fikáček (2013) and Toussaint and Short (2018).

Divergence dating. The divergence dating analysis was carried out in BEAST 2.4.7.We linked substitution models in five partitions corresponding to mitochondrial ribosomal (16S), mitochondrial protein coding (COI, COII), nuclear protein coding (H3, Arginine Kinase,

Topoisomerase I), nuclear ribosomal 28S and nuclear ribosomal 18S genes. A lognormal relaxed clock model was applied to all five partitions, with clock rates left with uniform priors. The birth-death model was used for the tree prior. A set of 8 fossils was used for calibrations (Table 1). Calibration points largely agree with those used by Toussaint and Short (2018), but are modified to include the findings by Fikáček et al. (2017) and Arriaga-Varela et al. (submitted): *Cercyon* sp. used by Bloom et al (2014) and Toussaint and Short (2018) is removed, and *Crenitis profechuyi* Arriaga-Varela et al. and *Cretocrenis burmanicus* Fikáček et al. are included to date the minimum age of xthe MRCA of *Crenitulus* + *Horelophus* and xthe Stem of Anacaenini, respectively. We used exponential priors with minimum age of each fossil calibration based on the age of given fossil and maximum age based on the maximum age estimate of the Hydrophiloidea (273 Mya) by Toussaint and Short (2018) (Table 1). We ran pre-burnin for 100 million generations followed by the MCMC chain set to 250 million generations, logging parameters every 12,500 generations. The convergence of all parameters was checked in Tracer 1.6., and the consensus tree was obtained by Tree Annotator 2.4.7 and visualized in FigTree 1.4.3 (http://tree.bio.ed.ac.uk/software/figtree/).

Ancestral habitats reconstruction of habitats. In order to reconstruct the evolution of habitat preferences in Hydrophilidae we performed an ancestral character state reconstruction in BEAST 2.4.7 (Bouckaert et al., 2014), using a fixed topology as obtained in our BI analysis. Habitats were set as follows: (1) *Aquatic*: representing habitats of beetles fully associated to water bodies such streams, ponds and swamps; (2) *Hygropetric*: beetles living on rocks permanently covered by a thin layer of water, such as seepages and waterfall margins; (3) *Wet mosses:* beetles living in permanently wet mosses on sides of streams; (4) *Dry mosses*: beetles living in dry mosses on the forests floor; (5) *Leaf litter*: beetles living in leaf litter and other small pieces of decaying plant material on the forest floor; (6) *Dead wood*: beetles living among small to large pieces of dead rotten wood; (7) *Rotten plants*: beetles feeding on large integral pieces of rotting plants such bamboo or banana stems or cacti; (8) *Vertebrate excrements and carrion*: decaying material of animal origin (including organisms attracted to traps baited with different kinds of meat or dung); (9) *Beachwrack*: beetles inhabiting rotting seaweed or other plant material found at the shore of sea or other water body with high salinity; (10) *Flowers*: beetles living inside non water-filled flowers, either feeding on pollen or other decaying plant material; (11) *Phytotelmata*: beetles living in water-filled cavities of terrestrial plants; (12) *Associated to social insects*: beetles living in association with social insect such termites or ants. Each species was assigned to a category using the following information: (1) personal observation of the authors in the field, (2) the collecting information available on specimen labels, and (3)published data (Bloom et al. 2014; Boukal et al. 2008; Clarkson et al. 2014; Deler et al. 2017; Fikáček 2005, 2010, 2019; Fikáček and Vondráček 2014

Fikáček et al. 2012, 2013, 2014, 2015; Gustafson and Short 2010; Hansen 1990, 1999, 2003; Jia et al. 2014, 2015; Lea 1919; Minoshima and Hayashi 2012, Minoshima et al. 2015, 2018; Newton 1989; Ordish, 1974; d'Orchymont 1932, Ryndevich 2017; Seidel et al. 2018; Smetana 1978; Toussaint and Short 2018) (see Table 1 in Supplementary files for details). We ran pre-burnin for 100 million generations followed by the MCMC chain set to 250 million generations, logging parameters every 12,500 generations. The convergence of all parameters was checked in Tracer 1.6 (Rambaut et al., 2014). Consensus tree was obtained via Tree Annotator 2.4.7 and visualized in FigTree 1.4.3.

Diversification rates. We tested for potential speciation rate shifts in Hydrophilidae. The analysis was conducted in RevBayes (Höhna et al., 2016) using a Bayesian branch-specific diversification model on the time-calibrated phylogeny obtained in the divergence dating analysis. This approach uses pre-defined finite number of rate categories, instead of continuous distribution (as in BAMM (Rabosky 2014)), and draws changes in speciation and extinction rates from them. Because of the number of terminals in our tree, we used ten categories for our analysis. The total number of species follows the estimate made by Bloom et al. (2014). The RevBayes script used for the analysis is provided in Supplementary File 4. The results were visualized using the R package RevGadgets.

Fossil	Placement	Age (Ma)	Exp. offset	Exp. mean
Baissalarva hydrobioides	Stem of Hydrobiusini	135	133.81	45.06
Helochares sp.	Stem of Acidocerinae	44	42.23	69.87
Hydrobiomorpha eopalpalis	Stem of *Hydrobiomorpha*	47	45.25	69.07
Hydrobius titan	Stem of *Sperchopsis*	34	32.06	72.63
Hydrochara sp.	Stem of *Hydrochara*	47	45.25	69.07
Limnoxenus olenus	Stem of *Limnoxenus*	22.5	20.58	75.74
Crenitis profechuyi	MRCA of *Crenitulus* + *Horelophus*	44	42.23	69.87
Cretocrenis burmanicus	Stem of Anacaenini	99	97.6	55

Table 1. Fossil taxa used for time-calibration of nodes.

Results and discussion

Phylogeny. The resulting topology inferred under a BI agrees with those obtained by Short and Fikacek (2013) and Toussaint and Short (2018) in supporting the monophyly of all subfamilies and

tribes (see Supplementary File 3 for the complete tree). Posterior probability values (pp) for the basal bifurcations are 1.0, except for the position of Acidocerinae as sister of the terrestrial lineage (Cylominae+Sphaeridiinae) (pp = 0.75). The internal topology in Megasternini tribe supports the division of the clade in two groups: "*Oosternum*" and "*Cercyon*" group of genera (Fikaček 2010; Fikaček and Short 2010). The genus *Cercyon* Leach is found to be polyphyletic, appearing in the cladogram in more than 10 different positions. Parallely, *Oosternum*, the second most diverse genus in the tribe Megasternini was also found to be polyphyletic.

Divergence dating. The divergence dating results from our fossil-based calibration performed in BEAST resulted in a crown age for the family of 181.1 Mya (162.2–204.9) (Fig. 4). Our results stand between the crown-ages of the family given by Bloom et al. (2014) (205 My) and Toussaint and Short (2018) (170 My). We obtained similarly intermediate results for the crown-age of the terrestrial lineage (Cylominae + Sphaeridiinae), 162 Mya (143.8–183.4). Conversely, the age of the crown Sphaeridiinae 159.1 Mya (140.0–179.0) is in closer agreement with that of Bloom et al. (2013) (161 Mya) than to that of Toussaint and Short (2018) (137.4 Mya). The older age estimates for most divergence events in our tree as compared to those of Toussaint and Short (2018) may be related to the updates in the set of fossils used as calibration points, especially in the removal of the Baltic amber fossil identified previously as *Cercyon* sp. which age (44 Mya) is significantly younger than all available age estimates for the Megasternini. Similarly, the MRCA of *Crenitulus* and *Horelophus*, calibrated using †*Crenitulus palaeodomicus* from Dominican amber (Fikáček and Engel 2011) by Toussaint and Short (2018) and Bloom et al. (2014) was now dated using an older fossil, *Crenitis profechuyi*†, from Baltic amber (44 Mya). Our results correspond with the finding of Toussaint et al. (2016) that the age estimates are strongly influenced by the selection of fossils used for the calibration.

Ancestral state reconstruction of habitats. Our results (Figs 1–4) show that shifts from aquatic to terrestrial or semiaquatic habitats happened repeatedly in subfamilies Hydrophilinae and Chaetarthriinae, while all sampled members of Enochrinae and Acidocerinae are aquatic.
Shifts in Megasternini happened more recently than those in Cylominae or Omicrini. The terrestrial clade (Cylominae + Sphaeridiinae) share a common ancestor for which leaf litter was reconstructed as the most probable habitat (pp=0.9). Leaf litter was also found as the habitat for the MRCA of Cylominae (pp=0.9) and Sphaeridiinae (pp=1.0) (Fig. 4). Leaf litter was also recovered as the ancestral habitat for MRCA of all sphaeridiine tribes except Protosternini and Sphaeridiini. These two tribes turn out to be the least diverse lineages in Sphaeridiinae.
Of the 63 shifts reconstructed for our tree (Fig. 2), 45 were from leaf litter to a different

environment, most commonly to dung and carrion (16 shifts) and to rotten stems (12 shifts), back to water (6 shifts) and to flowers (4 shifts). These secondary habitats were the final ones in most cases (i.e. without subsequent shifts to other environments), and led to the colonization of yet another (tertiary or quarternary) habitats in eight cases only. The association with social insects like ants of termites is a highly specialized life style that have evolved at least four times in the family. Interestingly, in three cases, it evolved in clades inhabiting rotten plants (i.e. not leaf litter). The evolutionary ways leading to the association with social insects are still to be discussed.

Dung and carrion is the second most usual substrate for terrestrial hydrophilids, but in most cases also the final one, not leading to subsequent transitions. The only case of further transition reconstructed in our analysis is to the wet moss in *Cylomissus*+*Anticura*. However, the large ecological difference between both habitats questions such scenario: the MRCA of the wet moss genera and their dung-living sister clade may have lived in leaf litter, which was recovered as the second most probable habitat for that node.

Aquatic taxa most commonly shift to hygropetric habitats. This transition is common among water beetles (Hájek et al 2019). Although it probably does not involve any significant adaptation to a new food source, transitions to hygropetric habitats is sometimes linked to the locomotion adaptations (e.g. in *Limnoxenus*, Hydrophilinae: Short and Liebherr 2007; hydradephagan beetles: Ribera et al. 2002) or general flattening of the body .

Our taxon sampling allows to reconstruct the evolution of habitat preferences more accurately in groups in which most taxa and/or most taxa with contrasting habitat preferences were sampled (e.g., Cylominae). In such cases all shifts that have occurred in the lineage are represented in our analyses. The opposite situation is found in the Megasternini in which we certainly did not sample many transitions due to more limited taxon sampling. For example, the beach wrack is known to be inhabited by at least other five species belonging to two unrelated lineages; none of these lineages is sampled by us. Similarly, the preferences for flowers or rotten plant habitats likely evolved repeatedly in the Neotropical genus *Pelosoma* (Arriaga-Varela et al. in press). Some less frequent habitats, e.g. mushrooms and other macrofungi on which some megasternines feed on, are not included in our analyses.

The leaf litter environment can be taken as an umbrella category that encompasses a wide spectrum of habitats showing a large variation of ecological, physical or chemical conditions. In some of them, some kinds of leaf litter may resemble other habitats such as rotten integral parts of plants or animal carrion and excrements. The precise food source of leaf litter beetles is not known but it is probable that each taxon feeds on a slightly different combinations of decaying substrates of vegetal, fungal or animal origin

Branch specific diversification. Branch specific diversification analyses in RevBayes allowed us to infer the particular rates of species accumulation along the tree (Höhna et al. 2016) without the alleged problems of under- and overrepresentation of diversification rate shifts found in other platforms (May and Moore 2016; Meyer and Wiens 2018) and assuming an uniform extinction rate along the tree.

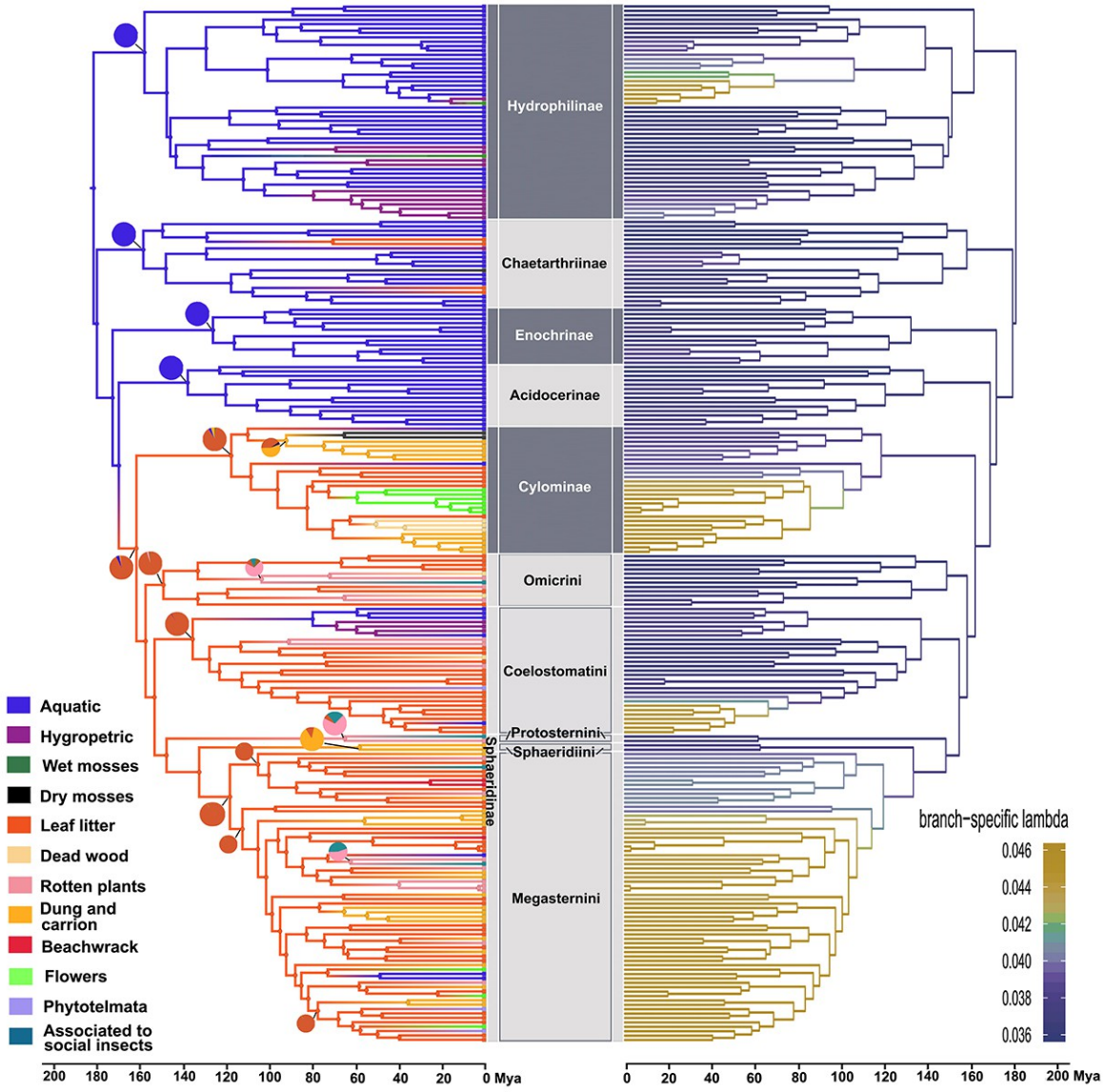

Figure 1. Ancestral reconstruction of habitats (left) and branch spedific diversification stimated in RevBayes (right). Ancestral reconstruction of habitats with color on branches and nodes according to reconstructed habitat (see code on inferior-left corner). Pie charts with proportion of probabilities for the reconstructed habitat in selected nodes.

Unfortunately, analyses of diversification taking into account branch-specific sampling proportion are still not implemented in methods for estimation branch-specific diversification in RevBayes.

Our results are hence likely biased by an uneven sampling along the tree. Four clades (Fig. 1) were revealed to have much higher values of lambda (speciation): *Limnoxenus* (Hydrophilinae), *Rygmodus+Adolopus+Cyloma* (Cylominae), *Phaenonotum* (Sphaeridiinae: Coelostomatini) and the "*Cercyon* group" (Sphaeridiinae: Megasternini).

Two of these groups are island groups which evolution shows signs of adaptive island radiation. *Limnoxenus* is the only aquatic lineage with high diversification rates. The genus includes few species with a disjunct distribution in the Palearctics, South Africa, and Australia+New Zealand, and seven species in Haiwaii. Hawaiian species form a monophylum which members colonized hygropetric habitats and dry mosses. This island clade shows an increased diversification rate. The subfamily Hydrophilinae is a rather well-sampled clade in our analysis. Within Cylominae, the most completely sampled clade in our analysis, the increased diversification was found in *Rygmodus, Adolopus* and *Cyloma* which are all New Zealand endemic genera with rather high number of species (10-30 per genus, compared to 1-3 species in other cylomine genera). The increase in diversification rate in these genera may hence correspond their within-New Zealand adaptive radiation likely driven by new opportunities present after the total or partial drowning of New Zealand in the Oligocene (Cooper and Cooper 1995). In Coelostomatini, the increase in diversification rate was found in the Neotropical genus *Phaenonotum* Sharp (Fig. 1); this is likely caused by a taxonomically biased sampling used by Deler et al. (2017) to investigated the biogeography of *Phaenonotum* species. Interestingly, no changes in the diversification rate were found in the *Coelostoma* clade, i.e. the only large clade of the terrestrial Hydrophilidae which returned to the aquatic environment.

The increase in the diversification rate in the Megasternini corresponds with the results of Bloom et al. (2014) who revealed Megasternini as the only clade of the Hydrophilidae with increased diversification rate. Our analysis, including much more comprehensive sampling of terrestrial representatives, recovered Megasternini as the only lineage with a faster accumulation of species in the whole family. Megasternini shows in our results a shift in diversification rate at its base to an intermediate level (0.041) compared to its sister lineage Sphaeridiini which shows the lowest lambda value (0.036). Within Megasternini we can see the most extended and significant rise situated at the base of a clade consistent with "*Cercyon* group" (Fikáček et al. 2010; Fikáček and Short 2010) furthering our understanding of the evolutionary dynamics and their differences among members of the tribe.

The asymmetry on the species accumulation rate in Megasternini is paired with a wider range of habitats and total number of transitions. With the evidence at hand, we are not able to draw a direct causal relation between these two patterns. However, it is worth analysing the possible causes of the stark asymmetry between Megasternini and is more closely related clades tribes Sphaeridiini and

Protosternini. Both these clades were reconstructed as having their common ancestors as present in dung and carrion and rotten plants stems respectively. On the other hand, Megasternini shows the highest proportion of species living in leaf litter (Fig. 3), a habitat that, according to our reconstruction, shows the higher proportion of shift to a different habitat (Fig. 2). The comparison of diversification patterns of Megastenini against those of Omicrini suggest that omicrines transitioned to specialized tertiary habitats earlier in their evolutionary history allowing speciation but probably restricting further transitions to new habitats.

The preliminary results on the phylogeny of megasternines point out to a escenario of morphological plasticity reflected, for example, in the notable polyphyly of genera such *Cercyon* or the presence of the highly modified myrmecophilous genus *Chimaerocyon* Fikáček et al. (2013) nested in lineages of usual looking *Cercyon.* We hypothethize that the species richness of Megasternini is at least partially related to being ancestrally adapted to leaf litter while at the same time being able to adapt its morphology at a probably faster pace than other lineages within the terrestrial lineages. Nevertheless, in order to understand the reasons behind the diferential diversification it is crucial to take into account the geographical factors that are not explored in the present contribution.

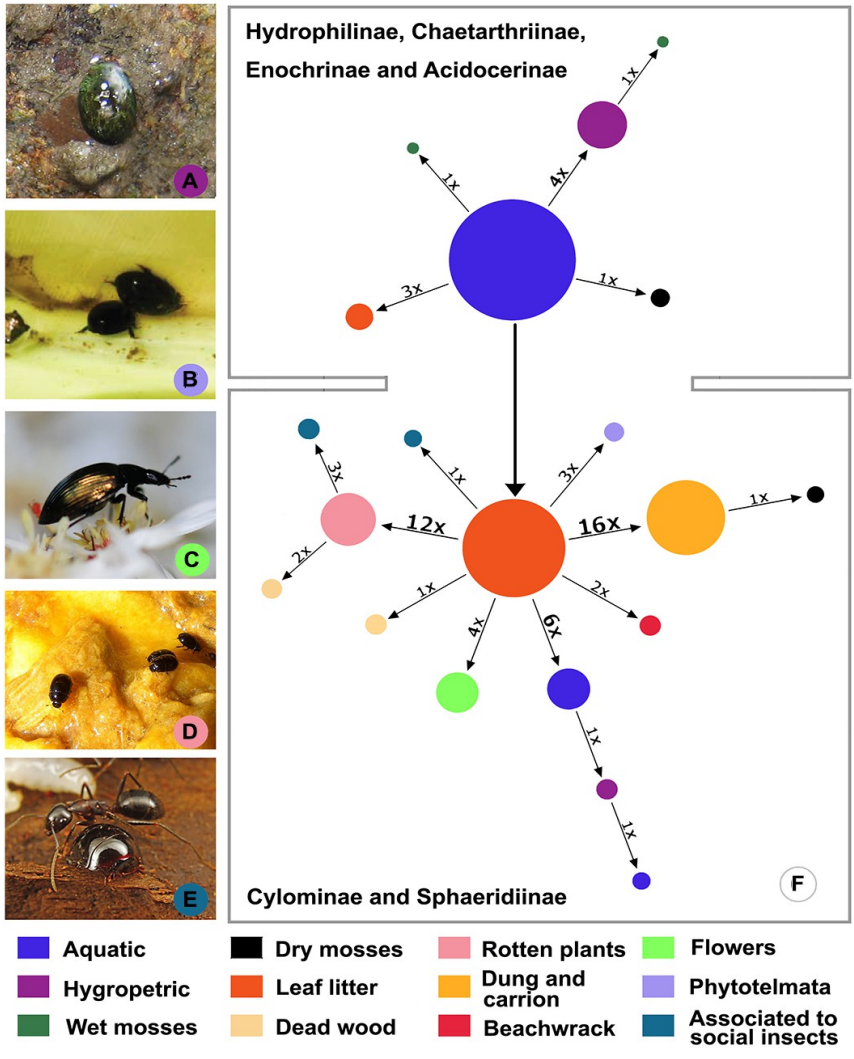

Figure 2. A - *Oocyclus* sp. (Hygropetric) image taken from Bloom et al. (2014); **B -** *Lachnodacnum luederwaldti* d'Orchymont (Phytotelmata) image taken from Clarkson et al. (2014); **C –** *Rygmodus modestus* White (Flowers) picture taken from Minoshima et al. (2018); D – *Dactylosternum cacti* LeConte (Rotten plants); **E –** *Sphaerocetum arboreum* Fikáček et al. (associated to social insects) picture taken from Fikáček et al. (2015); **F –** Scheme showing the evolution of habitat shifts in family Hydrophilidae as inferred in our recostruction of ancestral states. Size of circles is proportional of number of species sampled from each habitat. Numbers on arrows show the number of shifts reconstructed on the tree.

Conclusions

Water scavenger beetles probably represent the most succesful transition of an aquatic lineage back to terrestrial habitats among all insects. This is probably at least partially caused by the structural morphological characteristics of aquatic members of hydrophilidae that allowed them to conquer enviroments progressively more distant to water bodies. The likely escenario for the evolutionary sequence of the adaptation to terrestrial habitats is that the ancestors of cylomines and sphaeridiines probably went through a continuum between water bodies full with decaying organic material and habitats such humidity-saturated debris and leaf litter.

Leaf litter is corroborated, as a pivotal habitat from which organisms can reach a pletora of other habitats as found by McKenna et al. (2015). The common ancestor of hydrophiloid and histeroid beetles probably was a leaf litter inhabitant organism. Leaf litter has been proven again to be the key enviroment for a seminal event in the evolution of the ecological preferences of staphyliniform beetles. Although transitions to terrestriality in other groups of aquatic Coleoptera such hydradephagans have been seldom studied there are indications that colonization of forest litter as habitat could have been a key factor behind the radiation of genus *Paroster* Sharp in Australia (Toussaint et al. 2016). Conversely, it is corroborated that hygropetric habitats, such waterfall walls or permanetly wet stones on the sides of streams can lead radiations (Toussaint et al. 2018) it does not function as an intermediate step between fully aquatic and terrestrial microhabitats (Bloom et al. 2014).

Megasternini is proven to have suffered the most extensive and significant increase in diversification and that this increase is, however, not homogeneous along the whole tribe but accentuate in the *Cercyon* group of genera (sensu Fikácek 2010, Short and Fikáček 2013). Such increase is probably related to the ecological and morphological plasticity expressed in a wider range of habitats a faster pace in the transition among them and its likely coupled to a faster evolvability of its morphology.

Other shifts in diversification rate found in our results are probably a result of biased sampling and

their similar lambda values should not be taken as if these clades have accumulated species with the same pace in reality. However, these should not be regarded as artifactual results and must be considered into the context of their particular lineages. Possible explanations for these shifts are associated to the colonization of oceanic or other type of islands that open the door to divergent adaptation and smaller scale allopatric speciation.

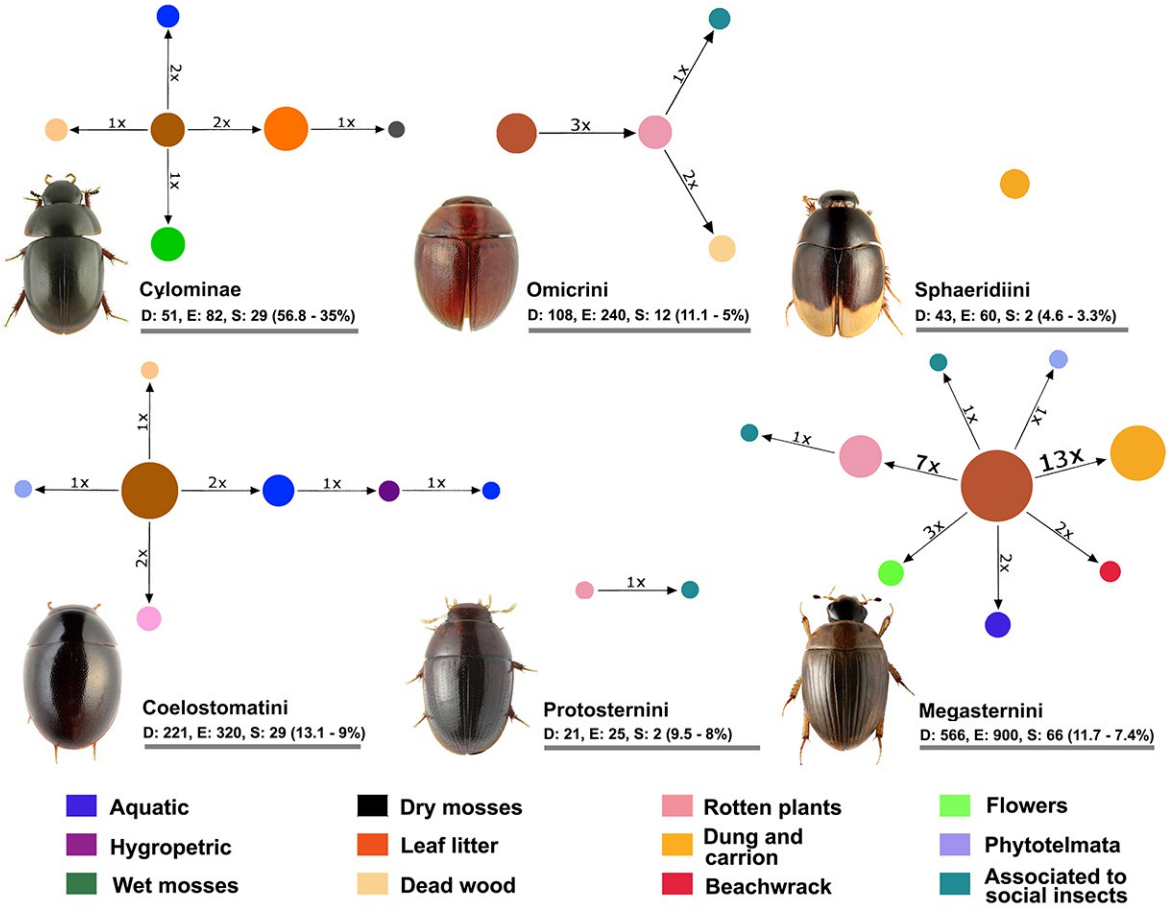

Figure 3. Scheme showing the evolution of habitat shifts in Cylominae and each tribe of Sphaeridiinae as inferred in our recostruction of ancestral states. Size of circles is proportional of number of species sampled from each habitat. Numbers on arrows show the number of shifts reconstructed on the tree. D - Number of described species; E – Estimated total number of species: S – Number of spacies sampled in our dataset (sampled percentage of described – and estimated number of species in parenthesis).

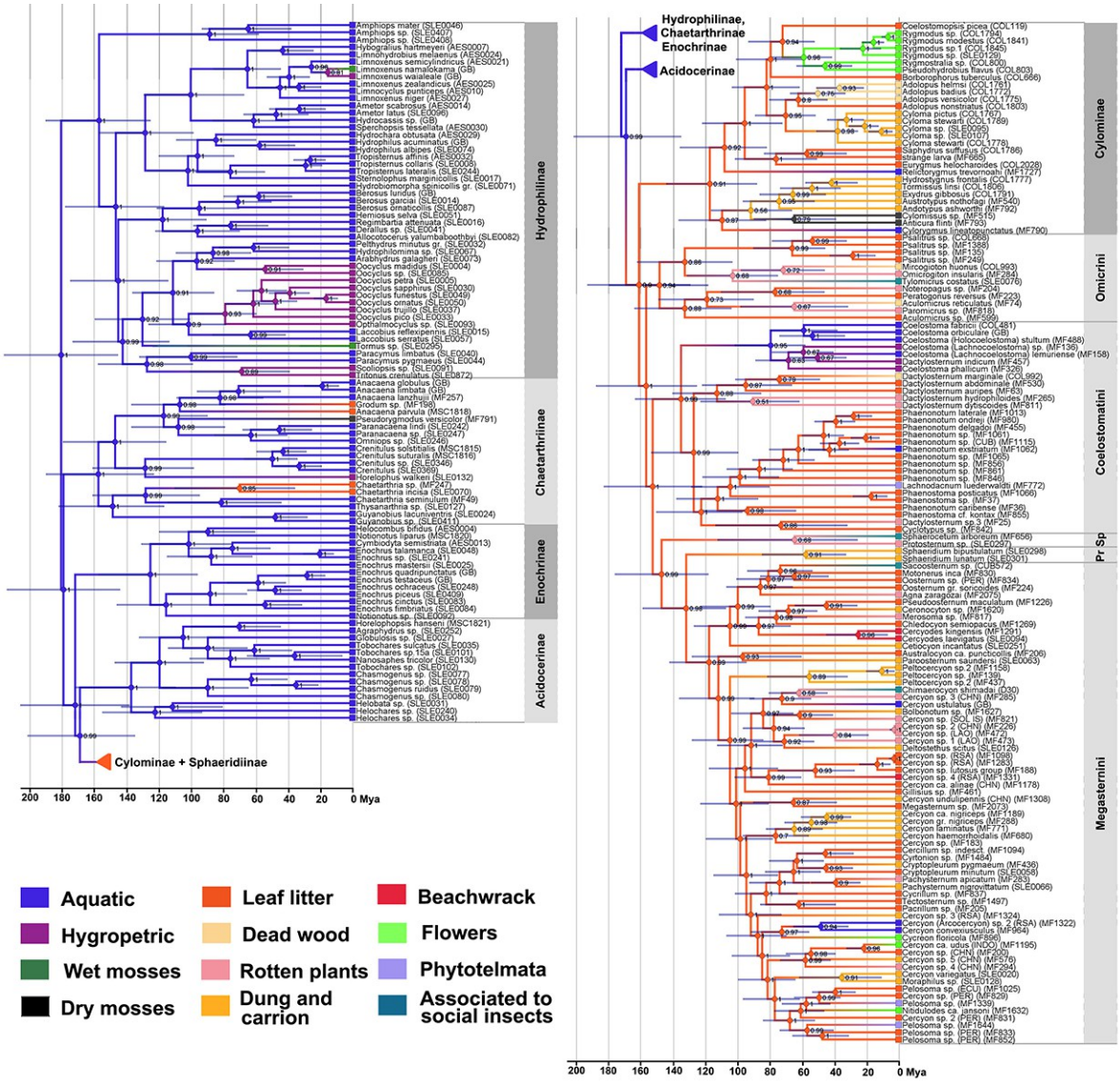

Figure 4. Time-calibrated phylogenetic tree of Hydrophilidae with reconstruction of ancestral state for habitats obtained in BEAST. Numbers on node correspond to Bayesian posterior probabilities of the character reconstruction. Horizontal blue bars show the 95% interval of confidence for the age.

Acknowledgments

We are thankful to the colleagues that provided us with specimens and observation on their natural history. Their names can be seen in Supplementary file 1 of chapter 7). Niklas Wahlberg (Lund University) is kindly acknowledged for the help during the secondment of EAV in Lund University. This work was supported by the European Union's Horizon 2020 research and innovation programme under the Marie Skłodowska-Curie grant agreement No. 642241 to EAV, and by the Ministry of Culture of the Czech Republic (DKRVO 2018/13, National Museum, 00023272) to MF. The work of EAV at the Department of Zoology, Charles University, Prague was partly supported by grant SVV260434/2018.

References

Arriaga-Varela, E., Seidel, M. and Fikáček, M. 2018a. A new genus of coprophagous water scavenger beetle from Africa (Coleoptera, Hydrophilidae, Sphaeridiinae, Megasternini) with a discussion on the *Cercyon* subgenus *Acycreon*. *African Invertebrates,* 59(1), 1–23. https://doi.org/10.3897/AfrInvertebr.59.14621

Arriaga-Varela, E., Cortés-Aguilar, J. and Fikáček, M. Accepted. Water scavenger beetles in rotten cacti: A review of *Agna* with the description of a new species from Mexico (Coleoptera: Hydrophilidae: Sphaeridiinae). Revista Mexicana de Biodiversidad.

Archangelsky, M. 1997. Studies on the biology, ecology, and systematics of the immature stages of New World Hydrophiloidea (Coleoptera: Staphyliniformia). *Bull. Ohio Biol. Surv*., (n. ser.), 12, 1-207.Ashley-Ross, M.A., Hsieh, S.T., Gibb, A.C., Blob, R.W. 2013. Vertebrate land invasions-past, present, and future: an introduction to the symposium. *Integrative and Comparative Biology,* 53(2), 192–196.

Benton, M.J. 2010. The origins of modern biodiversity on land. Philosophical Transactions of the Royal Society B: *Biological Sciences*, 365(1558), 3667-3679.

Bernhard, D., Schmidt, C., Korte, A., Fritzsch, G. and Beutel, R.G., 2006. From terrestrial to aquatic habitats and back again—molecular insights into the evolution and phylogeny of Hydrophiloidea (Coleoptera) using multigene analyses. *Zoologica Scripta*, 35(6), 597–606.

Bilton, D.T., Ribera, I. and Short, A.E.Z., 2019. Water beetles as models in ecology and evolution. *Annual Review of Entomology,* 64, pp.359-377.

Bloom, D., Fikáček, M., Short, A.E.Z. 2014. Clade age and diversification rate variation explain disparity in species richness among water scavenger beetle (Hydrophilidae) lineages. *PLoS ONE* 9(6), e98430. https://doi.org/10.1371/journal.pone.0098430

Bouckaert, R., Heled, J., Kühnert, D., Vaughan, T., Wu, C.H., Xie, D., Suchard, M.A., Rambaut, A. and Drummond, A.J., 2014. BEAST 2: a software platform for Bayesian evolutionary analysis. *PLoS Computational Biology*, 10(4), p.e1003537.

Boukal, D.S., Boukal, M., Fikáček, M., Hajek, J., Klečka, J., Skalický, S., Šťastný, J. and Trávníček, D. 2007. Katalog vodních brouků České republiky–Catalogue of water beetles of the Czech Republic (Coleoptera: Sphaeriusidae, Gyrinidae, Haliplidae, Noteridae, Hygrobiidae, Dytiscidae, Helophoridae, Georissidae, Hydrochidae, Spercheidae, Hydrophilidae, Hydraenidae, Scirtidae, Elmidae, Dryopidae, Limnichidae, Heteroceridae, Psephenidae). *Klapalekiana,* 43(suppl), 1-289.

Clarkson, B., Albertoni, F.F. and Fikáček, M. 2014. Taxonomy and biology of the bromeliad-inhabiting genus *Lachnodacnum* (Coleoptera: Hydrophilidae: Sphaeridiinae). *Acta Entomologica Musei Nationalis Pragae,* 54(1), 157-194.

Cooper, A. and Cooper, R.A. 1995. The Oligocene bottleneck and New Zealand biota: genetic record of a past environmental crisis. *Proceedings of the Royal Society of London. Series B: Biological Sciences,* 261(1362), 293-302.

Davis, C.C. and Matthews, S., 2019. *Evolution of Land Plants.* Oxford University Press.

Deler-Hernández, A., Sýkora, V., Seidel, M., Cala-Riquelme, F. and Fikáček, M. 2017. Multiple origins of the *Phaenonotum* beetles in the Greater Antilles (Coleoptera: Hydrophilidae): phylogeny, biogeography and systematics. *Zoological Journal of the Linnean Society,* 183(1), 97-120.

Fikáček, M. 2005. Taxonomic revision of the *Cercyon* (*Arcocercyon*) *dieganus* species group (Coleoptera: Hydrophilidae: Sphaeridiinae). *Bulletin de l´Institute Royal des Sciences Naturelles de Belgique, Entomologie*, 75, 79-102.

Fikáček, M. 2010. Hydrophilidae: The genus *Kanala* Balfour-Browne (Coleoptera). In: M.A. Jäch, and M. Balke, (Eds.) Water Beetles of New Caledonia, Vol. 1. *Monographs of Coleoptera*, 3, 365–394.

Fikáček, M. 2019. 20. Hydrophilidae Leach, 1815. pp. 271–337. In: Slipinski, A., and Lawrence, J. (eds). *Australian Beetles*. Volume 2. Archostemata, Myxophaga, Adephaga, Polyphaga (part). CSIRO Publishing, Clayton South, 765.

Fikáček, M. and Short, A.E.Z. 2010. A revision of the Neotropical genus *Sacosternum* Hansen (Coleoptera: Hydrophilidae: Sphaeridiinae). *Zootaxa*, 2538, 1–37.

Fikáček, M., Jia, F. L., and Prokin, A. 2012. A review of the Asian species of the genus Pachysternum (Coleoptera: Hydrophilidae: Sphaeridiinae). *Zootaxa*, 3219(1), 1-53.

Fikáček, M.., Maruyama, M., Vondráček, D. and Short, A.E. 2013. *Chimaerocyon* gen. nov., a morphologically aberrant myrmecophilous genus of water scavenger beetle (Coleoptera: Hydrophilidae: Sphaeridiinae). *Zootaxa*, 3716(2), 277-288.

Fikáček, M. and Vondráček, D. 2014. A review of *Pseudorygmodus* (Coleoptera: Hydrophilidae), with notes on the classification of the Anacaenini and on distribution of genera endemic to southern South America. *Acta Entomologica Musei Nationalis Pragae*, 54(2), 479-514.

Fikáček, M., Minoshima, Y. N. and A. F. Newton. 2014. A review of *Andotypus* and *Austrotypus* gen. nov., rygmodine genera with Austral disjuction (Hydrophilidae: Rygmodinae). *Annales Zoologici (Warszawa)*, 64(4), 557–596.

Fikáček, M., Maruyama, M., Komatsu, T., Von Beeren, C., Vondráček, D. and Short, A.E. 2015. Protosternini (Coleoptera: Hydrophilidae) corroborated as monophyletic and its larva described for the first time: a review of the myrmecophilous genus *Sphaerocetum*. *Invertebrate Systematics*, 29(1), 23-36.

Fikáček, M., Minoshima, Y.N., Komarek, A., Short, A.E., Huang, D. and Cai, C., 2017. Cretocrenis burmanicus, the first Mesozoic amber inclusion of a water scavenger beetle (Coleoptera: Hydrophilidae). *Cretaceous Research*, 77, pp.49-55.

Fikáček, M., Liang, W.-R., Hsiao Y., Jia F.-L. and Vondráček, D. 2018. Biology and morphology of immature stages of banana-associated Protosternum beetles, with comments on the status of Taiwanese endemic P. abnormale (Coleoptera: Hydrophilidae). *Zoologischer Anzeiger,* 277, 85-100.

Fikáček, M. and Short, A.E.Z. 2006. A revision of the Neotropical genus *Motonerus* Hansen (Coleoptera: Hydrophilidae: Sphaeridiinae). *Zootaxa*, 1268, 1–38.

Gavrilets, S. and Losos, J.B., 2009. Adaptive radiation: contrasting theory with data. *Science*, 323(5915), pp.732-737.

Gustafson, G.T. and Short, A.E., 2010. Redescription of the Neotropical water scavenger beetle genus *Phaenostoma* (Coleoptera: Hydrophilidae) with description of two new species. Acta *Entomologica Musei Nationalis Pragae*, 50(2), pp.459-469.

Hájek, J., Alarie, Y., Šťastný, J. and Vondráček, D. 2019. The first hygropetric Platynectes and its larva from eastern China (Coleoptera: Dytiscidae). *Acta Entomologica Musei Nationalis Pragae*, 59(1), 217-228.

Hansen, M., 1990. Australian Sphaeridiinae (Coleoptera: Hydrophilidae): a taxonomic outline with descriptions of new genera and species. *Invertebrate Systematics*, 4(2), 317-395.

Hansen, M. 1999. Fifteen new genera of Hydrophilidae (Coleoptera), with remarks on the generic classification of the family. *Insect Systematics & Evolution*, 30(2), 121-172.

Hansen, M. 2003. The discovery of *Australocyon* Hansen and *Pilocnema* Hansen (Coleoptera, Hydrophilidae) outside the Australian Region. pp. 53–84. In: Cuccodoro, G. and Leschen, R. A. B. (eds.): Systematics of Coleoptera: Papers celebrating the retirement of Ivan Löbl. *Memoirs of Entomology International*, 17, 1–968.

Hassanin, A. 2006. Phylogeny of Arthropoda inferred from mitochondrial sequences: strategies for limiting the misleading effects of multiple changes in pattern and rates of substitution. *Molecular Phylogenetics and Evolution,* 38(1), 100-116.

Höhna, S., Landis, M.J., Heath, T.A., Boussau, B., Lartillot, N., Moore, B.R., Huelsenbeck, J.P. and Ronquist, F., 2016. RevBayes: Bayesian phylogenetic inference using graphical models and an interactive model-specification language. *Systematic Biology*, 65(4), pp.726-736.

Jia, F.L., Aston, P. and Fikáček, M. 2014. Review of the Chinese species of the genus *Coelostoma* Brullé, 1835 (Coleoptera: Hydrophilidae: Sphaeridiinae). *Zootaxa,* 3887(3), 354-376.

Jia, F.L., Lin, R., Li, B. and Fikáček, M. 2015. A review of the omicrine genera Omicrogiton, *Mircogioton* and *Peratogonus* of China (Coleoptera, Hydrophilidae, Sphaeridiinae). *ZooKeys*, (511), 99.

Lanfear, R., Frandsen, P.B., Wright, A.M., Senfeld, T. and Calcott, B. 2016. PartitionFinder 2: new

methods for selecting partitioned models of evolution for molecular and morphological phylogenetic analyses. *Molecular biology and evolution*, 34(3), 772-773. http://dx.doi.org/10.1093/molbev/msw260

Lea, A.M. 1919. Notes on Some Miscellaneous Coleoptera, with Descriptions of New Species. - Part V. - *Transactions of the Royal Society of South Australia,* 43, 166-261, pl. xxv-xxvii.

May, M.R., and Moore, B.R. 2016. How well can we detect lineage-specific diversification-rate shifts? A simulation study of sequential AIC methods. *Systematic biology*, 65(6), 1076-1084.

Mckenna, D.D., Farrell, B.D., Caterino, M.S., Farnum, C.W., Hawks, D.C., Maddison, D.R., Seago, A.E., Short, A.E., Newton, A.F. and Thayer, M.K. 2015. Phylogeny and evolution of S taphyliniformia and S carabaeiformia: forest litter as a stepping stone for diversification of nonphytophagous beetles. *Systematic Entomology*, 40(1), 35-60.

Meyer, A.L. and Wiens, J.J. 2018, Estimating diversification rates for higher taxa: BAMM can give problematic estimates of rates and rate shifts. *Evolution*, 72, 39-53. http://doi:10.1111/evo.13378

Miller, M. A., Pfeiffer, W. and Schwartz, T. 2010. Creating the CIPRES Science Gateway for inference of large phylogenetic trees. Gateway Computing Environments Workshop. 1–8

Minoshima, Y. and Hayashi, M. 2012. Larval morphology of Amphiops mater mater Sharp (Coleoptera: Hydrophilidae: Chaetarthriini). *Zootaxa*, 3351, 47-59.

Minoshima, Y.N., Fikáček, M., Gunter, N. and Leschen, R.A. 2015. Larval Morphology and Biology of the New Zealand-Chilean Genera *Cylomissus* Broun and *Anticura* Spangler (Coleoptera: Hydrophilidae: Rygmodinae). *The Coleopterists Bulletin*, 69(4), 687-713.

Minoshima, Y.N., Seidel, M., Wood, J.R., Leschen, R.A., Gunter, N.L. and Fikáček, M. 2018. Morphology and biology of the flower-visiting water scavenger beetle genus *Rygmodus* (Coleoptera: Hydrophilidae). *Entomological science*, 21(4), 363-384.

Newton, A.F. 1989. Review of '*Dactylosternum'* Wollaston species of Australia and New Zealand (Coleoptera: Hydrophilidae). *The Australian Entomologist,* 16(3), 1-49.

d'Orchymont, A. 1932. Zur Kenntnis der Kolbenwasserkäfer (Palpicornia) von Sumatra, Java und Bali. *Archiv für Hydrobiologie, Supplement Band*, IX (Tropische Binnengewässer II): 623-714, pl. XIV-XVII.

Ordish, R.G. 1974. Anthropoda of the subantarctic islands of New Zealand (3) Coleoptera: Hydrophilidae. *Journal of the Royal Society of New Zealand*, 4(3), 307-314.

Pisani, D., Poling, L.L., Lyons-Weiler, M. and Hedges, S.B. 2004. The colonization of land by animals: molecular phylogeny and divergence times among arthropods. *BMC biology*, 2(1), 1.

Pritchard, G., McKee, M.H., Pike, E.M., Scrimgeour, G.J. and Zloty, J. 1993. Did the first insects live in water or in air?. *Biological Journal of the Linnean Society*, 49(1), 31-44.

Rabosky, D.L., Grundler, M., Anderson, C., Title, P., Shi, J.J., Brown, J.W., Huang, H. and Larson, J.G., 2014. BAMM tools: an R package for the analysis of evolutionary dynamics on phylogenetic trees. *Methods in Ecology and Evolution*, 5(7), pp.701-707.

Rambaut, A., Suchard, M.A., Xie, D. and Drummond, A.J., 2014. Tracer v1. 6. Computer program and documentation distributed by the author.

Regier, J.C., Shultz, J.W., Kambic, R.E., 2005. Pancrustacean phylogeny: hexapods are terrestrial crustaceans and maxillopods are not monophyletic. *Proceedings of the Royal Society of London B,* 272, 395–401.

Rensing, S.A. 2018. Great moments in evolution: the conquest of land by plants. *Current opinion in plant biology*, 42, 49-54.

Ribera, I., Beutel, R.G., Balke, M. and Vogler, A.P. 2002. Discovery of Aspidytidae, a new family of aquatic Coleoptera. *Proceedings of the Royal Society of London*. Series B: Biological Sciences, 269(1507), 2351-2356.

Ronquist, F., Teslenko, M., Van Der Mark, P., Ayres, D.L., Darling, A., Höhna, S., Larget, B., Liu, L., Suchard, M.A. and Huelsenbeck, J.P., 2012. MrBayes 3.2: efficient Bayesian phylogenetic inference and model choice across a large model space. *Systematic Biology*, 61(3), pp.539-542.

Roxo, F.F., Lujan, N.K., Tagliacollo, V.A., Waltz, B.T., Silva, G.S., Oliveira, C. and Albert, J.S., 2017. Shift from slow-to fast-water habitats accelerates lineage and phenotype evolution in a clade of Neotropical suckermouth catfishes (Loricariidae: Hypoptopomatinae). *PloS one,* 12(6), p.e0178240.

Ryndevich, S.K., Jia, F. and Fikáček, M., 2017. A review of the Asian species of the *Cercyon* unipunctatus group (Coleoptera: Hydrophilidae: Sphaeridiinae). *Acta Entomol Mus Natl Pragae* 57(2), 535-576.

Seidel, M., Minoshima, Y.N., Arriaga-Varela, E. and Fikáček, M. 2018, June. Breaking a disjunct distribution: a review of the Southern Hemisphere genera Cylorygmus and Relictorygmus gen. nov. (Hydrophilidae: Cylominae). *Annales zoologici*, 68(2), 375-403.

Short, A.E. 2010. Phylogeny, evolution and classification of the giant water scavenger beetles (Coleoptera: Hydrophilidae: Hydrophilini: Hydrophilina). *Systematics and Biodiversity*, 8(1), 17-37.

Short, A.E. and Liebherr, J.K., 2007. Systematics and biology of the endemic water scavenger beetles of Hawaii (Coleoptera: Hydrophilidae, Hydrophilini). *Systematic Entomology*, 32(4), pp.601-624.

Short A.E.Z. and Fikáček M. 2011 World catalogue of the Hydrophiloidea (Coleoptera): additions and corrections II (2006-2010). *Acta entomologica musei nationalis Pragae*, 51(1), 83-122.

Short, A.E.Z. and Fikáček, M. 2013. Molecular Phylogeny, Evolution, and Classification of the Hydrophilidae (Coleoptera). Systematic Entomology, 38, 723–752.

Smetana, A. 1978. Revision of the subfamily Sphaeridiinae of America north of Mexico (Coleoptera: Hydrophilidae). *Memoirs of the Entomological Society of Canada,* 105, 1-292.

Song, K.Q., Xue, H.J., Beutel, R.G., Bai, M., Bian, D.J., Liu, J., Ruan, Y.Y., Li, W.Z., Jia, F.L. and Yang, X.K. 2014. Habitat-dependent diversification and parallel molecular evolution: Water scavenger beetles as a case study. *Current Zoology*, 60(5), 561-570.

Spangler, P. J. 1962. A new species of the genus *Oosternum* and a key to the U. S. species (Coleoptera: Hydrophilidae). *Proceedings of the Biological Society of Washington,* 75, 97-100.

Toussaint, E.F., Hendrich, L., Escalona, H.E., Porch, N. and Balke, M. 2016. Evolutionary history of a secondary terrestrial Australian diving beetle (Coleoptera, Dytiscidae) reveals a lineage of high morphological and ecological plasticity. *Systematic entomology*, 41(3), 650-657.

Toussaint, E.F.A., Seidel, M., Arriaga-Varela, E., Hajek, J., Kral, D., Sekerka, L., Short, A.E.Z. and Fikáček, M. 2017. The peril of dating beetles. *Systematic Entomology*, 42(1), 1–10.

Toussaint, E. F., and Short, A. E. 2018. Transoceanic Stepping–stones between Cretaceous waterfalls? The enigmatic biogeography of pantropical Oocyclus cascade beetles. *Molecular Phylogenetics and Evolution,* 127, 416-428.

Vršanský, P., Sendi, H., Aristov, D., Bechly, G., Müller, P., Ellenberger, S., Azar, D., Ueda, K., Barna, P. and Garcia, T. 2019. Ancient roaches further exemplify 'no land return' in aquatic insects. *Gondwana Research*, 68, 22-33.

Supplementary files

Chapter

- **Supplementary file 1.** Specimen data on habitats and included gene regions.
- **Supplementary file 2.** Phylogenetic tree obtained in MrBayes.
- **Supplementary file 3.** Calibrated time-tree obtained in BEAST.
- **Supplementary file 4.** RevBayes script used for the branch-specific disversification analysis in RevBayes.

CODE	Genus	species	Habitat	COI	COII	16s	18s	28s	ArgK	H3	TOPO
AES0004	Helocombus	bifidus	A	KC935272	KC992475		KC935048	KC992576	KC935151		
AES0007	Hybogralius	hartmeyeri	A	KC935277			KC935054	KC992582	KC935157		
AES0013	Cymbiodyta	semistriata	A	KC935252			KC935029	KC992557	KC935136		
AES0014	Ametor	scabrosus	A	KC935213	KC992499		KC934988	KC992518	--		
AES0021	Limnoxenus	semicylindricus	A	KC935290	KC992496	KC992691	KC935070	KC992595	KC935172		
AES0024	Limnohydrobius	melaenus	A	KC935280	KC992495		KC935057	KC992585	--		
AES0025	Limnoxenus	zealandicus	A	KC935291	KC992494		KC935071	KC992596	KC935173		
AES0027	Limnoxenus	niger	A	KC935289	KC992493		KC935069	KC992594	KC935171		
AES0029	Hydrochara	obtusata	A	KC935281	-		KC935058	KC992586	KC935160		
AES0030	Sperchopsis	tessellata	A	KC935322	KC992421		KC935098	KC992631	KC935198		
AES0032	Tropisternus	affinis	A	KC935329	-		KC935105	KC992636	KC935205		
AES010	Limnocyclus	punticeps	A	***			***	***			
COL119	Coelostomopsis	picea	L	KC935245	KC992507		KC935022	KC992551	-		
COL1761	Adolopus	helmsi	W	***	***			***			
COL1767	Cyloma	pictus	D	***	***						
COL1772	Adolopus	badius	W	***	***			***			
COL1775	Adolopus	versicolor	W	***	***			***			
COL1777	Hydrostygnus	frontalis	D	***	***		***	***		***	
COL1778	Cyloma	stewarti	D	***	***			***			
COL1786	Saphydrus	suffusus	L	***	***			***		***	
COL1789	Cyloma	stewarti	D	***	***			***			
COL1791	Exydrus	gibbosus	D	***	***			***			
COL1794	Rygmodus	cyaneus	F	MG920289	***					MG920309	
COL1803	Adolopus	nonstriatus	L	***	***			***			
COL1806	Tormissus	linsi	D	***	***			***		***	
col1841	Rygmodus	modestus	F	MG920292	***		***	***		MG920315	
col1845	Rygmodus	tibialis	F	MG920294	***		***	***		MG920300	
Col2028	Eurygmus	helocharoides	L		***			***		***	
COL481	Coelostoma	fabrici	A	***			***	***			
COL666	Borborophorus	tuberculus	L	KC935232	KC992409		KC935009	-	-	-	
COL800	Rygmostralia	sp.	F	***	***			***		***	
COL803	Pseudohydrobius	flavus	F	***	***			***		***	
COL992	Dactylosternum	marginale	W	***			***	***			
COL993	Microgioton	huonus	W	***	***		***	***		***	
D30	Chimaerocyon	shimadai	I	***	***			***		***	***
GB Anacaena globulus			A	AM287086AM287086	AM287108AM287108	AM287064AM287064	AM287125AM287125	AM287133			
GB Anacaena limbata			A	DQ155734			AY745586AY745586	JX173143			
GB Berosus luridus			A	AM287087	AM287109	AM287065	AJ810721	AJ810756			
GB Cercyon ustulatus			A	DQ155947DQ155947	AM287115AM287115	AM287071AM287071	AM287129AM287129	AM287137AM287137			
GB Coelostoma orbiculare			A	AM287094AM287094	AM287116AM287116		EF213785EF213785	KC992549KC992549	KC935131KC935131		
GB Enochrus quadripunctatus			A	AM287090AM287090	AM287112AM287112	AM287068AM287068	AM287127AM287127	AM287135AM287135			
GB Enochrus testaceus			A	AM287089AM287089	AM287111AM287111	AM287067AM287067	AJ810719AJ810719	AJ810754AJ810754			
GB Hydrocassis sp.			A	KF128921	KF131553		KF131613	KF131633			
GB Hydrophilus acuminatus			A	KF128914	KF131546		KF131606	KF131626			
GB Limnoxenus namalokama			M	KY554445			KY554462	KY554471			
GB Limnoxenus waialeale			A	KY554448			KY554465	KY554473	***		
MF1013	Phaenonotum	laterale	L					MG208614			
MF1025	Pelosoma	sp. (ECU)	L	***	***		***	***		***	***
MF1061	Phaenonotum	sp.	L	MG208567	MG208592		MG208656	MG208615			
MF1062	Phaenonotum	exstriatum	A					MG208616			
MF1065	Phaenonotum	sp.	L	MG208570	MG208595						
MF1066	Phaenostoma	posticatus	L	MG208571	MG208596		MG208661	MG208619			
MF1094	Cercillum	sp. indesct.	L	***	***		***	***		***	***
MF1098	Cercyon	sp. (RSA)	L	***	***		***	***		***	***
MF1115	Phaenonotum	sp. (CUB)	L	MG208597	MG208572		MG208662	MG208620			
MF1158	Peltocercyon	sp. 2	D	***			***	***		***	***
MF1178	Cercyon	ca. alinae Ryndevich	L	***			***	***		***	***
MF1189_2	Cercyon	ca. nigriceps	D	***			***	***			***
MF1195	Cercyon	ca. udus D'Orchymo	L	***	***		***	***			***
MF1226	Pseudoosternum	maculatum	L	***	***	***	***	***			***
MF1269	Chledocyon	semiopacus	L	***	***		***	***		***	***
MF1283	Cercyon	sp. (AUS)	L	***			***	***		***	***
MF1291	Cercyodes	kingensis	B				***	***		***	***
MF1308	Cercyon	undulipennis Ryndev	D	***		***	***	***		***	
MF1322	Cercyon (Arcocercy	sp. 2 (RSA)	A	***	***		***	***		***	***
MF1324	Cercyon	sp. 3 (RSA)	D	***	***		***	***		***	
MF1331	Cercyon	sp. 4 (RSA)	B	***			***	***		***	***
MF135	Psalitrus	sp.	L	***			***	***			
MF136	Coelostoma (Lachn	sp.	K	***	***		***	***			
MF1388	Psalitrus	sp.	L	***			***	***		***	
MF139	Peltocercyon	sp.	D	***			***	***		***	
MF1484	Cyrtonion	sp.	L	***			***	***		***	***
MF1497	Tectosternum		L		***						
MF158	Coelostoma (Lachn	lemuriense	A	***	***		***	***			
MF1620	Ceronocyton	sp.	D				***	***		***	***
MF1627	Bolbonotum	sp.	D					***		***	***
MF1632	Nitidulodes	ca. jansoni Sharp	F		***			***		***	***
MF1727_2	Relictorygmus	trevornoahi	A	***	***		***	***			
MF183	Cercyon	sp. (femoral lines)	L	***			***	***			

Supplementary file 1 (1/3). Specimen data on habitats and included gene regions. Habitat codes: A – Aquatic; L – Leaf litter; D – Dung and carrion; F – Inflorescences; I – Inquiline of social insects; K – Hygropetric; B – Beachwrack; R – Rotten stems of plants; W – Dead wood; O – Wet mosses; M – Dry mosses; P – Phytotelmata; *** - Sequence obtained in this work.

CODE	Genus	species	Habitat	COI	COII	16s	18s	28s	ArgK	H3	TOPO
MF188	Cercyon (Arcocercy	sp. lutosus group	L				***			***	***
MF198	Grodum	sp.	L	***	***		***	***			
MF200	Cercyon	sp. (CHN)	L		***		***	***			***
MF204	Noteropagus	sp.	R	MH910640						***	
MF205	Pacrillum	sp.	L	KC935309KC93 5309	KC992489KC99 2489	--	KC935082KC93 5082	KC992615KC99 2615			
MF206	Australocyon	ca. puncticollis	L	KC935228	-	-	KC935004	KC992533		***	***
MF2073	Megasternum	sp.	L	***						***	
MF2075	Agna	zaragozai	R	***	***		***	***		***	
MF223	Peratogonus	reversus	L	KC935314KC93 5314	KC992408KC99 2408	--		KC992621KC99 2621			
MF224	Oosternum	gr. soricoides	L	KC935306	KC992513	-	KC935079	KC992612	-	***	
MF226	Cercyon	sp. 2 (CHN)	R	***			***	***		***	***
MF247	Chaetarthria	sp.	L	KC935237KC93 5237	KC992478KC99 2478	--	--	KC992543KC99 2543			
MF249	Psalitrus	sp.	L	KC935316KC93 5316	KC992410KC99 2410	--	KC935092KC93 5092	KC992625KC99 2625		***	
MF25	Dactylosternum	sp.3	R				***			***	
MF257	Anacaena	lanzhujii	A	KC935218KC93 5218	KC992455KC99 2455	--	KC935002KC93 5002	KC992523KC99 2523			
MF265	Dactylosternum	hydrophiloides	R	***	***		***				
MF283	Pachysternum	apicatum	R	***	***			***			***
MF284	Omicrogiton	insularis	R	KC935295KC93 5295	--	--		KC992602KC99 2602		***	
MF285	Cercyon	sp. 3 (CHN)	R	***	***		***	***		***	***
MF288	Cercyon	gr. nigriceps	D	***			***	***			***
MF294	Cercyon	sp. 4 (CHN)	R	***	***		***	***		***	***
MF326	Coelostoma	phallicum	K	KC935244KC93 5244	KC992398KC99 2398	--		KC992550KC99 2550			
MF36	Phaenonotum	caribense	L	KC935315KC93 5315	KC992399KC99 2399	--		KC992623KC99 2623			
MF37	Phaenostoma	sp.	L	MG208550			MG208639	MG208598			
MF436	Cryptopleurum	pygmaeum	D		***			***		***	***
MF437	Peltocercyon	sp. 2	D	***			***	***		***	***
MF455	Phaenonotum	delgadoi	L	MG208552	MG208583		MG208641	MG208600			
MF457	Dactylosternum	indicum	K	***	***		***	***			
MF461	Gillisius	sp.	L		***		***	***		***	***
MF472	Cercyon	sp. (LAO)	R	***			***	***		***	***
MF473	Cercyon	sp. 1 (LAO)	R	***	***		***				***
MF488	Coelostoma (Holocc	stultum	A	***			***	***			
MF49	Chaetarthria	seminulum	A	KC935238KC93 5238	KC992503KC99 2503	--	KC935015KC93 5015	KC992542KC99 2542			
MF515	Cylomissus	sp.	O		***			***		***	
MF530	Dactylosternum	abdominale	L	***	***		***				
MF540	Austrotypus	nothofagi	D	***	***			***		***	
MF576	Cercyon	sp. 5 (CHN)	D	***	***		***	***		***	***
MF599	Aculomicrus	sp.	L	***	***		***				
MF63	Dactylosternum	auripes	L	KC935253KC93 5253		--		KC992558KC99 2558			
MF656	Sphaerocetum	arboreum	I	KM874806			KM874807	KM874809			
MF665	Cyclominae	sp.	L	***							
MF668	Psalitrus	sp.	L	***	***		***	***			
MF680	Cercyon	haemorrhoidalis	D	***	***		***	***		***	***
MF74	Aculomicrus	reticulatus	W		KC992396KC99 2396			KC992514KC99 2514		***	
MF771	Cercyon	laminatus	D	***	***		***	***		***	***
MF772	Lachnodacnum	luederwaldti	P	MG208554			MG208643	MG208602			
MF790	Cylorygmus	lineatopunctatus	A	***	***			***		***	
MF791	Pseudorygmodus	versicolor	O	KM262052	KM262053		KM262050	KM262051			
MF792	Andotypus	ashworthi	D	***			***	***		***	
MF793	Anticura	flinti	O	KM262054			KT447582	***		***	
MF811	Dactylosternum	dytiscoides	R	***	***		***	***			
MF817	Merosoma	sp.	R	***	***		***	***		***	***
MF818	Paromicrus	sp.	R	***			***	***		***	
MF821	Cercyon	sp. (SOL IS)	R	***			***	***		***	***
MF829	Cercyon	sp. (PER)	L	***	***	***	***	***		***	
MF830	Motonerus	inca	L	***	***		***	***			***
MF831	Cercyon	sp. 2 (PER)	L	***	***	***	***	***		***	***
MF833	Pelosoma	sp. (PER)	L	***			***	***			
MF834	Oosternum	sp. (PER)	L	***			***	***		***	***
MF837	Cycrillum	sp.	L				***	***		***	***
MF842	Cyclotypus	sp.	L	MG208557	MG208585		MG208646	MG208605			
MF846	Phaenonotum	sp.	L	MG208560	MG208587		MG208649	MG208608			
MF852	Pelosoma	sp. (PER)	L	***	***	***	***	***		***	***
MF855	Phaenostoma	cf. kontax	L	***			***	***			
MF856	Phaenonotum	sp.	L	***	***		***	***			
MF861	Phaenonotum	sp.	L	***	***		***	***			
MF896	Cycreon	floricola	F	***	***		***	***		***	***
MF964	Cercyon	convexiusculus	A	***			***	***		***	***
MF980	Phaenonotum	ondreji	L					***			
MSC1815	Crenitulus	solstitialis	A	KC935223	-	KC992647	KC934998	KC992528	KC935119	-	
MSC1816	Crenitulus	suturalis	A	KC935226	-	KC992649	KC935001	KC992531	KC935120	-	
MSC1818	Anacaena	parvula	L	KC935222	-	-	KC934997	KC992527	KC935118	-	
MSC1820	Notionotus	liparus	A	KC935293KC93 5293	--	--	KC935073KC93 5073	KC992598KC99 2598	KC935174KC93 5174	--	
MSC1821	Horelophopsis	hanseni	A	KC935274KC93 5274	--	--	KC935051KC93 5051	KC992579KC99 2579	KC935154KC93 5154	--	
SLE0004	Oocyclus	madidus	K	KC935298	KC992435	-	KC935077	KC992604	KC935177		
SLE0005	Oocyclus	petra	K	KC935300	KC992442		KC935078	KC992606	KC935179		
SLE0008	Tropisternus	collaris	A	KC935330	KC992419	KC992714	KC935106	KC992637	KC935206		
SLE0014	Berosus	garciai	A	KC935231	KC992441	KC992652	KC935007	KC992536	-		
SLE0015	Laccobius	reflexipennis	A	KC935287KC93 5287	KC992439KC99 2439	KC992689KC99 2689	KC935067KC93 5067	KC992592KC99 2592	KC935169KC93 5169		

Supplementary file 1 (2/3). Specimen data on habitats and included gene regions. Habitat codes: A – Aquatic; L – Leaf litter; D – Dung and carrion; F – Inflorescences; I – Inquiline of social insects; K – Hygropetric; B – Beachwrack; R – Rotten stems of plants; W – Dead wood; O – Wet mosses; M – Dry mosses; P – Phytotelmata; *** - Sequence obtained in this work.

CODE	Genus	species	Habitat	COI	COII	16s	18s	28s	ArgK	H3	TOPO
SLE0016	Regimbartia	attenuata	A	KC935317KC935317	KC992423KC992423	KC992704KC992704	KC935093KC935093	KC992626KC992626	KC935192KC935192		
SLE0017	Sternolophus	marginicollis	A	KC935325	KC992416	KC992711	KC935101	KC992632	KC935202		
SLE0020	Cercyon	variegatus	D	KC935234KC935234	KC992484KC992484		KC935011KC935011	KC992539KC992539	--		
SLE0024	Guyanobius	lacuniventris	A	KC935267	KC992406	KC992676	KC935043	KC992571	KC935148		
SLE0025	Enochrus	mastersii	A	KC935259KC935259	KC992472KC992472	--	KC935035KC935035	--	--		
SLE0027	Globulosis	sp.	A	KC935266	KC992433		KC935042	KC992570	KC935147		
SLE0030	Oocyclus	sapphirus	K	KC935302	KC992444		-	KC992608	KC935181		
SLE0031	Helobata	sp.	A	KC935269	KC992453	KC992678	KC935045	KC992573	KC935149		
SLE0032	Pelthydrus	minutus gr.	A	KC935313KC935313	KC992422KC992422	--	KC935087KC935087	KC992620KC992620			
SLE0033	Oocyclus	pico	K	KC935301	KC992447		-	KC992607	KC935180		
SLE0034	Helochares	sp.	A	KC935270	KC992471	-	KC935046	KC992574	KC935150		
SLE0035	Tobochares	sulcatus	A	KC935327	KC992465	KC992713	KC935103	KC992634	KC935204		
SLE0037	Oocyclus	trujillo	K	KC935305	KC992448	KC992699	-	KC992611	KC935184		
SLE0040	Paracymus	limbatus	A	KC935310KC935310	KC992425KC992425	KC992701KC992701	KC935083KC935083	KC992616KC992616	KC935186KC935186		
SLE0041	Derallus	sp.	A	KC935256KC935256	KC992411KC992411	KC992666KC992666	KC935033KC935033	KC992561KC992561	KC935139KC935139		
SLE0044	Paracymus	pygmaeus	A	KC935311KC935311	KC992473KC992473	KC992702KC992702	KC935084KC935084	KC992617KC992617	KC935187KC935187		
SLE0046	Amphiops	mater	A	KC935214KC935214	KC992462KC992462	--	KC934989KC934989	KC992519KC992519	KC935113KC935113		
SLE0048	Enochrus	talamanca	A	KC935263KC935263	KC992486KC992486	KC992672KC992672	KC935039KC935039	KC992567KC992567	KC935144KC935144		
SLE0049	Oocyclus	funestus	K	KC935297KC935297	KC992445KC992445	KC992693KC992693	KC935076KC935076	KC992603KC992603	KC935176KC935176		
SLE0050	Oocyclus	ornatus	K	KC935299	KC992446	KC992694	-	KC992605	KC935178		
SLE0051	Hemiosus	selva	A	--	KC992412KC992412	KC992680KC992680	KC935049KC935049	KC992577KC992577	KC935152KC935152		
SLE0057	Laccobius	serratus	A	KC935288KC935288	KC992450KC992450	KC992690KC992690	KC935068KC935068	KC992593KC992593	KC935170KC935170		
SLE0058	Cryptopleurum	minutum	L	KC935248	KC992491	-	KC935024	KC992553	KC935132		
SLE0063	Paroosternum	saundersi	D	--	--	--	KC935086KC935086	KC992619KC992619	KC935189KC935189		
SLE0066	Pachysternum	nigrovittatum	D	KC935308	KC992492	-	KC935081	KC992614	-		
SLE0067	Hydrophilomima	sp.	A	-	KC992438	KC992686	KC935063	KC992589	KC935164		
SLE0070	Chaetarthria	incisa	L	--	KC992479KC992479	KC992655KC992655	KC935014KC935014	KC992541KC992541	KC935126KC935126		
SLE0071	Hydrobiomorpha	spinicollis gr.	A	KC992583	KC992418		KC935055	KC992583			
SLE0073	Arabhydrus	galagheri	A	***	***	***	***	***			
SLE0074	Hydrophilus	albipes	A				KC935064	KC992590			
SLE0076	Tylomicrus	costatus	I	KC935332	KC992426	-	-	KC992639	KC935208		
SLE0077	Chasmogenus	sp.	A	KC935241KC935241	KC992468KC992468	KC992658KC992658	--	KC992546KC992546	KC935128KC935128		
SLE0078	Chasmogenus	sp.	A	KC935242KC935242	KC992470KC992470	KC992659KC992659	KC935018KC935018	KC992547KC992547	KC935129KC935129		
SLE0079	Chasmogenus	ruidus	A	KC935240KC935240	KC992469KC992469	KC992657KC992657	KC935017KC935017	KC992545KC992545	KC935127KC935127		
SLE0080	Chasmogenus	sp.	A	KC935243KC935243	KC992466KC992466	--	KC935019KC935019	KC992548KC992548	KC935130KC935130		
SLE0082	Allocotocerus	yalumbaboothbyi	A	--	KC992402KC992402	KC992641KC992641	KC934986KC934986	KC992517KC992517	KC935111KC935111		
SLE0083	Enochrus	cinctus	A	KC935257KC935257	KC992464KC992464	KC992667KC992667	--	KC992562KC992562	KC935140KC935140		
SLE0084	Enochrus	fimbriatus	A	KC935258KC935258	KC992456KC992456	KC992668KC992668	KC935034KC935034	KC992563KC992563	KC935141KC935141		
SLE0085	Oocyclus	sp.	K	KC935303KC935303	KC992436KC992436	KC992698KC992698	--	KC992609KC992609	KC935182KC935182		
SLE0087	Berosus	ornaticollis	A	-	KC992424	KC992653	KC935008	KC992537	KC935123		
SLE0091	Scoliopsis	sp.	K	KC935321	KC992477	KC992708	KC935097	KC992630	KC935196		
SLE0092	Notionotus	sp.	A	KC935294KC935294	KC992508KC992508	KC992692KC992692	KC935074KC935074	KC992599KC992599	KC935175KC935175		
SLE0093	Opthalmocyclus	sp.	K	KC935307		KC992700	KC935080	KC992613	***	MH317831	
SLE0094	Cercyodes	laevigatus	B	KC935233KC935233	KC992504KC992504	--	KC935010KC935010	KC992538KC992538	KC935124KC935124		
SLE0095	Cyloma	sp.	D	KC935249	-	KC992661	KC935026	KC992554	KC935133		
SLE0096	Ametor	latus	A	KC935212KC935212	KC992498KC992498	--	KC934987KC934987	--	KC935112KC935112		
SLE0101	Tobochares	sp.15a	A	--	KC992474KC992474	KC992684KC992684	KC935061KC935061	KC992600KC992600	--		
SLE0102	Tobochares	sp. 10	A	KC935283	KC992487	KC992685	KC935060	KC992601	KC935162		
SLE0107	Cyloma	sp.	D	KC935250	KC992506	KC992662	KC935027	KC992555	KC935134		
SLE0126	Destostethus	scitus	D	KC935255KC935255	KC992480KC992480	KC992665KC992665	KC935032KC935032	KC992560KC992560	KC935138KC935138		
SLE0127	Thysanarthria	sp.	A	KC935326	KC992432	KC992712	KC935102	KC992633	KC935203		
SLE0128	Moraphilus	sp.	D	KC935292KC935292	KC992457KC992457	--	KC935072KC935072	KC992597KC992597	--		
SLE0129	Rygmodus	sp.	F	KC935318KC935318	KC992505KC992505	KC992705KC992705	KC935094KC935094	KC992627KC992627	KC935193KC935193		
SLE0130	Nanosaphes	tricolor	A	KC935282	KC992488	-	KC935062	KC992588	KC935163		
SLE0132	Horelophus	walkeri	K	KC935275	KC992430		KC935052	KC992580	KC935155		
SLE0240	Helochares	sp.	A	***	***		***		***		
SLE0241	Enochrus	sp.	A	***	***	***	***	***	***		
SLE0242	Paranacaena	lindi	A	***	***		***	***			
SLE0244	Tropisternus	lateralis	A	***	***	***	***	***	***		
SLE0246	Omniops	sp.	A		***		***	***	***		
SLE0247	Paranacaena	sp.	A	***		***	***		***		
SLE0248	Enochrus	ochraceus	A	***	***	***	***	***			
SLE0251	Cetiocyon	incantatus	D	***	***		***	***	***		
SLE0252	Agraphydrus	sp.	A	***		***	***		***		
SLE0295	Tormus	sp.	M	***			***	***			
SLE0297	Protosternum	sp.	R		***	***	***	***	***		
SLE0298	Sphaeridium	bipustulatum	D	***	***		***		***		
SLE0301	Sphaeridium	lunatum	D	***			***		***		
SLE0346	Crenitulus	sp.	A			***					
SLE0369	Crenitulus	hirsutus	A	***	***	***	***	***			
SLE0407	Amphiops	sp.	A	***	***	***	***	***			
SLE0408	Amphiops	sp.	A	***	***	***	***	***			
SLE0409	Enochrus	piceus	A	***	***	***	***	***			
SLE0411	Guyanobius	sp.	A	***	***	***	***	***			
SLE0872	Tritonus	crenulatus	K	***			***	***			
MF1644	Pelosoma	sp.	P		***		***	***		***	***
MF1339	Pelosoma	sp.	P	***			***	***		***	***
CUB572	Sacoosternum	sp.	I	***			***			***	

Supplementary file 1 (3/3). Specimen data on habitats and included gene regions. Habitat codes: A – Aquatic; L – Leaf litter; D – Dung and carrion; F – Inflorescences; I – Inquiline of social insects; K – Hygropetric; B – Beachwrack; R – Rotten stems of plants; W – Dead wood; O – Wet mosses; M – Dry mosses; P – Phytotelmata; *** - Sequence obtained in this work.

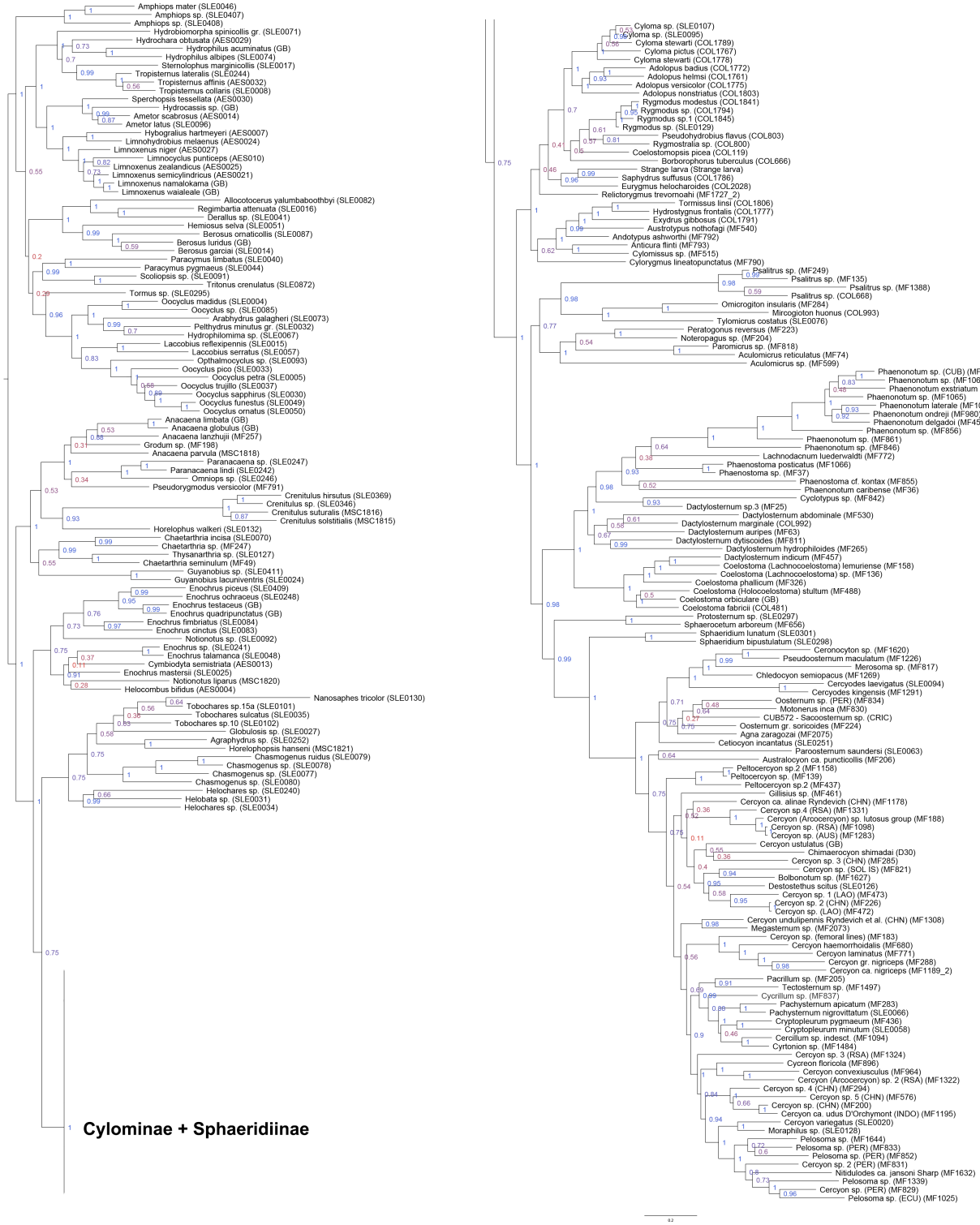

Supplementary file 2. Phylogenetic tree obtained in MrBayes. Posterior probability is shown on the nodes.

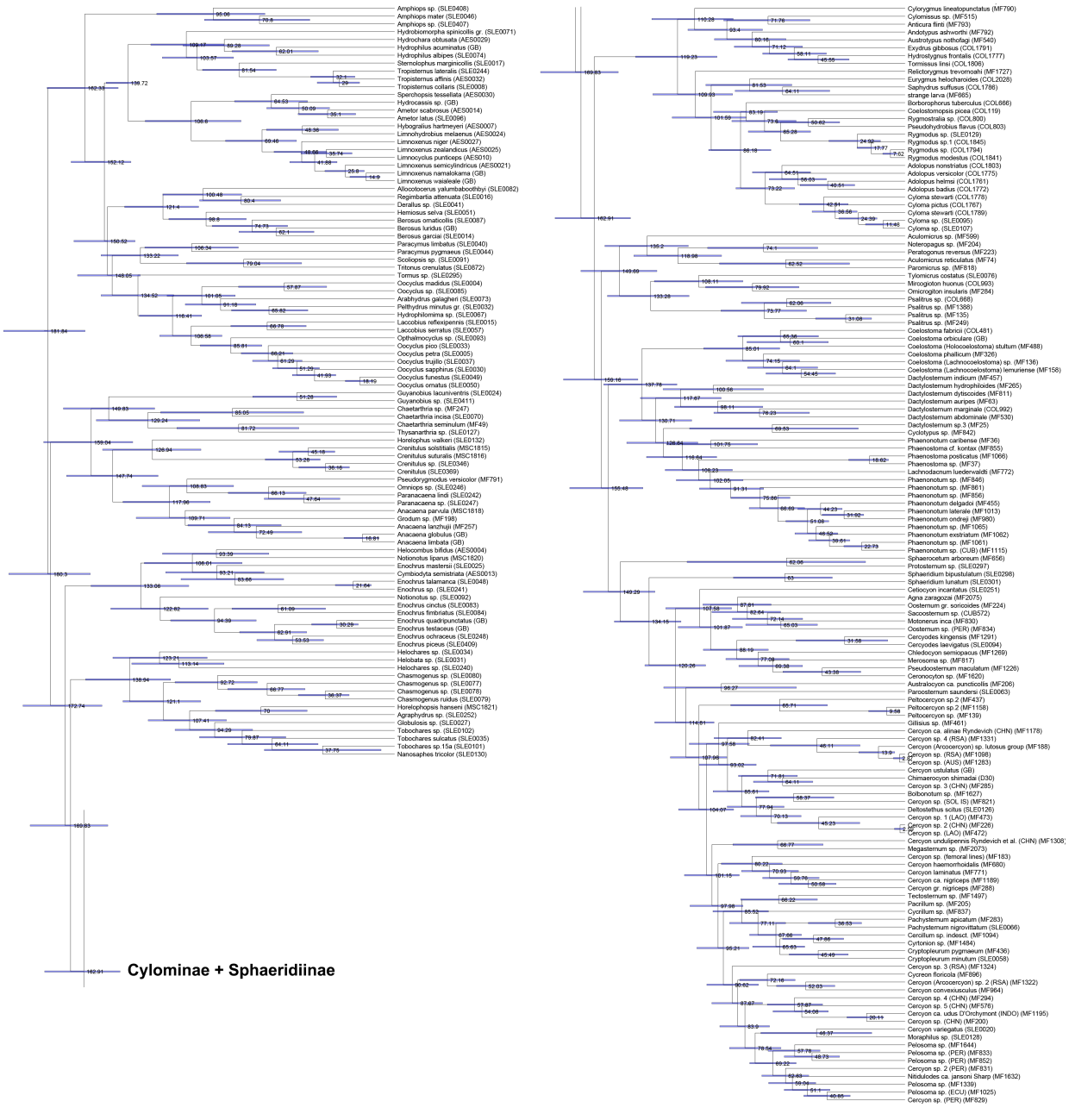

Supplementary file 3. Calibrated time-tree obtained in BEAST. Mean ages shown nn the nodes.

Supplementary file 4. RevBayes script used for the branch-specific disversification analysis in RevBayes.

```
################################################################################
#
# RevBayes Example: Bayesian inference of diversification rates under a
#                   conditioned birth-death-shift model
#
#
# authors: Sebastian Hoehna
#
################################################################################

########################
# Reading in the Data #
########################

# Read in the observed phylogeny
observed_phylogeny <- readTrees("data/hydrophilidae_tree.nex")[1]

# Get the names of the taxa in the tree and the age of the tree. We need these later on.
taxa <- observed_phylogeny.taxa()
root <- observed_phylogeny.rootAge()
tree_length <- observed_phylogeny.treeLength()


# Create some vector for the moves and monitors of this analysis
moves    = VectorMoves()
monitors = VectorMonitors()


# Global parameters for our analysis
NUM_TOTAL_SPECIES     = 4200
NUM_RATE_CATEGORIES   = 10
H = 0.587405

####################
# Create the rates #
####################

### Specify a prior on the speciation and extinction rates
rate_mean <- (NUM_TOTAL_SPECIES-2) / tree_length

### Create a lognormal distributed variable for the mean speciation rate
speciation_mean ~ dnLoguniform( 1E-6, 1E2)
speciation_mean.setValue( rate_mean )
moves.append( mvScale(speciation_mean, lambda=1, tune=true, weight=2.0) )

speciation_sd ~ dnExponential( 1.0 / H )
moves.append( mvScale(speciation_sd, lambda=1, tune=true, weight=2.0) )

### Create a deterministic variable for the speciation rate categories
### using a discretized lognormal distribution (the N-quantiles of it)
speciation := fnDiscretizeDistribution( dnLognormal(ln(speciation_mean), speciation_sd),
NUM_RATE_CATEGORIES )

### Create a lognormal distributed variable for the mean extinction rate
extinction_mean ~ dnLoguniform( 1E-6, 1E2)
extinction_mean.setValue( rate_mean / 2.0 )
moves.append( mvScale(extinction_mean, lambda=1, tune=true, weight=2.0) )

### Create a deterministic variable for the speciation rate categories
### Assume that all extinction rates are equal
extinction := rep(extinction_mean, NUM_RATE_CATEGORIES)

### Create a exponential distributed variable for the rate of rate-shift events
event_rate ~ dnUniform(0.0, 100.0/tree_length)
moves.append( mvScale(event_rate, lambda=1, tune=true, weight=2.0) )


### Create a uniformly distributed variable for the category at the root
rate_cat_probs <- simplex( rep(1, NUM_RATE_CATEGORIES) )


### rho is the probability of sampling species at the present
### fix this to 367/367, since there are ~367 described species of primates
### and we have sampled 367
rho <- observed_phylogeny.ntips() / NUM_TOTAL_SPECIES

#### construct a variable for the tree drawn from a birth death process
```

```
timetree ~ dnCDBDP( rootAge           = root,
                    speciationRates   = speciation,
                    extinctionRates   = extinction,
                    Q                 = fnJC(NUM_RATE_CATEGORIES),
                    delta             = event_rate,
                    pi                = rate_cat_probs,
                    rho               = rho,
                    condition         = "time" )

### clamp the model with the "observed" tree
timetree.clamp(observed_phylogeny)


##############
# The Model #
##############

### workspace model wrapper ###
mymodel = model(speciation)

### set up the monitors that will output parameter values to file and screen
monitors.append( mnScreen(printgen=10, event_rate, speciation_mean, speciation_mean) )
monitors.append( mnStochasticBranchRate(cdbdp=timetree, printgen=1,
filename="output/hydrophilidae_BDS_rates.log") )
monitors.append( mnModel(filename="output/hydrophilidae_BDS.log",printgen=1, separator = TAB) )


#################
# The Analysis #
#################

### workspace mcmc
mymcmc = mcmc(mymodel, monitors, moves, nruns=2, combine="mixed")

### pre-burnin to tune the proposals ###
mymcmc.burnin(generations=1000,tuningInterval=100)

### run the MCMC
mymcmc.run(generations=5000, tuningInterval=200)

## quit ##
q()
```

Chapter 7

Molecular phylogeny of terrestrial water scavenger beetle tribe Megasternini (Hydrophilidae: Sphaeridiinae) reveals repeated and bidirectional continental interchange during the Eocene

Arriaga-Varela, E. and Fikácek, M., (Manuscript). Molecular phylogeny of terrestrial water scavenger beetle tribe Megasternini (Hydrophilidae: Sphaeridiinae) reveals repeated and bidirectional continental interchange during the Eocene

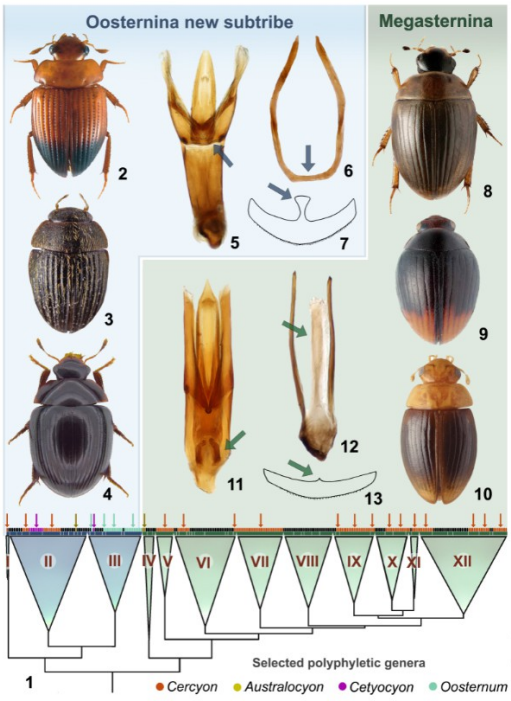

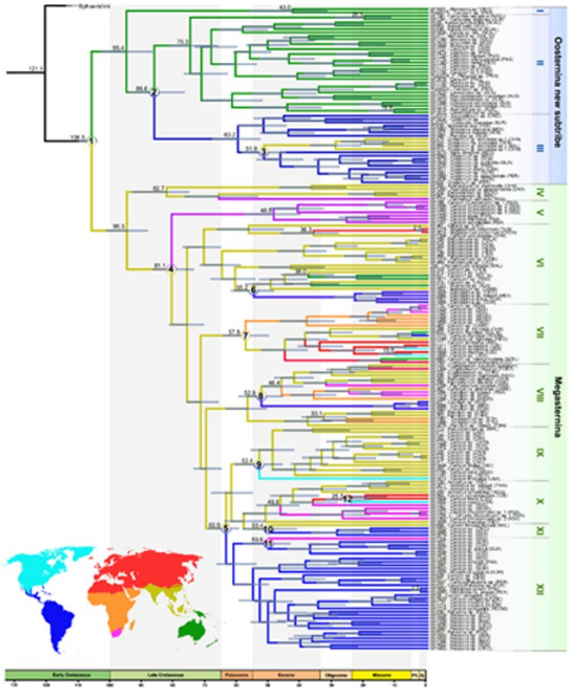

Molecular phylogeny of terrestrial water scavenger beetle tribe Megasternini (Hydrophilidae: Sphaeridiinae) reveals repeated and bidirectional continental interchange during the Eocene

EMMANUEL ARRIAGA-VARELA[1,2], and MARTIN FIKÁČEK[2,1]

[1] Department of Zoology, Faculty of Science, Charles University, Prague, Viničná 7, CZ-12843, Prague, Czech Republic; [2] Department of Entomology, National Museum, Cirkusová 1740, CZ-19300 Prague, Czech Republic

Abstract. Megasternini (Coleoptera: Hydrophilidae: Sphaeridiinae) is the most diverse tribe in the family with nearly 600 described saprophagous species distributed all over the globe. In this study we used sequences of eight gene regions, five nuclear (*histone 3*, *wingless*, *topoisomerase 1*, *18s*, *28s*) and three mitochondrial (*cytochrome oxidase I and II*, and *12S*), in order to investigate the phylogenetic relationships and historical biogeography of members of tribe Megasternini. Analyses employed are Maximum likelihood (ML) (IQtree), Bayesian inference (BI) including divergence dating based on a relaxed-clock model (MrBayes) and ancestral area estimation analyses (BioGeoBears). Results of the analyses of BI and ML resulted in similar tree topologies, although with low posterior probability support in basal divergences on the BI tree. The resulting topology from BI is adopted to revise the suprageneric classification and historical biogeography of the tribe. Our results support the division of the tribe in two main lineages that are defined by morphological characters: subtribes Megasternina and Oosternina **new subtribe**. We identify 12 clades, two in Oosternina and nine in Megasternina. The main morphological patterns among the members of these clades are discussed. Genera *Cercyon* Leach, *Oosternum* Sharp, *Cetiocyon* Hansen, *Australocyon* Hansen and *Pelosoma* were not recovered as monophyletic, with species of *Cercyon*, the most diverse genus in the tribe found all over the tree. Our results suggest that a taxonomical reorganization of the generic concepts in the tribe is needed. The ancestral area reconstruction estimation show a series parallel intercontinental dispersion events in diferent directions happening between 55-50 mya corresponding to the hyperthermal conditions of the early Eocene that allowed massive biotic interchange between landmasses. Interchange between the Oriental region and the New World happened in opposite directions during this period. The climatic changes that ocurred during the Eocene had a differential effect on the diversification patterns in both subtribes.

Keywords. Boreotropics, early Eocene climatic optimum, polyphyly, multigene phylogeny, saprophagous.

Introduction

With 3,000 species distributed worldwide, except polar areas, the family Hydrophilidae (water scavenger beetles) is the largest group of the polyphagan beetle superfamily Hydrophiloidea. As their common name suggests, hydrophilid beetles inhabit aquatic habitats like lakes, streams or waterfalls. Aquatic lifestyle is ancestral for the family, and likely also for the whole Hydrophiloidea. Nevertheless, about 150 million years ago (mya), the common ancestor of subfamilies Cylominae and Sphaeridiinae left the water in order to form the most successful lineages of aquatic insects which recolonized terrestrial ecosystems (Arriaga-Varela et al., in prep.). This terrestrial clade have colonized a wide spectrum of habitats, especially in the tropics, ranging from forest leaf litter (Fikáček & Short 2006) to ant nests (Fikáček et al. 2013) or flowers (Arriaga-Varela et al. 2018b; Minoshima et al. 2018), and a high species diversity. Approximately 570 species are described at the moment, but this number seems highly underestimated, as it is common for beetle groups highly diversified in the tropical regions (Bouchard et al. 2009).

At least a half of the terrestrial hydrophilid beetles are members of the tribe Megasternini in the subfamily Sphaeridiinae. Megasternini is the most diverse group of terrestrial Hydrophilidae in terms of ecological and species diversity, despite being the youngest group of the whole family, dating back to the Early Cretaceous (120 mya). This pattern was demonstrated to be a consequence of the increased diversification rate in the Megasternini clade compared to other hydrophilid lineages (Bloom et al., 2014; Arriaga-Varela et al. in prep.).

The real species richness of the clade is very likely higher than what is formally described. Total number of species was estimated to be around 850 species by Bloom et al. (2014), but the proportion of undescribed species found in museum collections (Arriaga-Varela, pers. observ.), as well as recent revisions exemplifying an unexpected species diversity in small tropical areas (e.g., Szczepanski et al., 2018; Arriaga-Varela et al., 2017), indicate that the real species diversity will be even higher. Representatives of the Megasternini can be found in a wide array of terrestrial habitats like humid leaf litter (Fikáček & Short, 2006), vertebrate dung or carrion (Archangelsky, 1997; Arriaga-Varela et al., 2018a), angiosperm inflorescences (Arriaga-Varela et al. 2018b), debris accumulated by social insects (Spangler, 1962; Fikáček et al., 2013), rotten succulent plants or fruits (Arriaga-Varela et al., in press) or beach wrack at the seashore (Arriaga-Varela et al. in prep).

Although they are small to rarely medium-sized beetles of compact ovoid body, they show a great diversity in morphology. Currently 51 genera and subgenera are recognized. The classification is largely based mainly on the shapes and proportions of the ventral parts of the thorax (Fig. A).

The first phylogenetic studies based on DNA sequences focused on the relationships among hydrophiloid families were performed by Bernhard et al. (2006, 2009) and Song et al. (2014). However, the megasternines were only represented by three or less species. Short & Fikáček (2013) assembled the first taxonomically comprehensive sampling for the family Hydrophilidae including 12 genera and 16 species of Megasternini. Their phylogenetic analyses of six gene fragments revealed two main clades within Megasternini: the *Cercyon* group of genera and the *Oosternum* group of genera (= 'Gondwanan genera' sensu Fikáček, 2007). Notoriously, the genus *Cercyon*, the most speciose in the tribe, was recovered as polyphyletic as the three species included in the analysis were found in different parts of the tree.

The global distribution of this clade makes it an excellent group to test hypotheses regarding the processes underlying tropical intercontinental disjunctions. The genus *Cercyon*, that comprises almost half of the species diversity in the tribe is distributed in all main biogeographical regions. Other genera like *Oosternum, Cryptopleurum, Pelosoma* and *Australocyon* show disjunct continental distributions that makes them an interesting target of phylogenetic adn biogeographical studies.

The goal of the present contribution is to propose a robust hypothesis on internal phylogenetic relationships within the tribe Megasternini using a multigene dataset obtained from an extensive taxonomic sampling at species and genus level. We discuss general patterns diversity, biogeography, classification and morphology based on the inferred phylogenetic hypothesis. This work is aimed to be a basis for understanding the evolution of morphological characters, and the first step towards a phylogeny-based classification below and above the generic level. Such rearrangements will be the focus of future contributions.

Materials and methods

Taxon sampling

We assembled a set of 193 specimens belonging to 189 species. This number represents around a third of the described species and nearly a fifth of the estimated total number of species of Megasternini including undescribed ones (Arriaga-Varela et al, in prep.). The species included in our dataset cover 38 of 49 described genera (i.e., 77 %) (Hansen, 1991; Hansen 1999; Fikáček & Short, 2010). The amount of described species classified in unsampled genera represents only 3.5 % of the described specific diversity of the Megasternini. The group is most diverse in the wet tropics

which is why our sampling mainly focused on tropical species from the Neotropical, Oriental and Australian regions. Our sample included multiple representatives of the speciose genera (e.g. *Cercyon*, *Oosternum*, *Pelosoma* and *Cryptopleurum*) in order to cover their morphological diversity and geographic range. In many cases, species were not identified beyond the genus level. We attempted to compare part of the species included in our dataset with the museum collections covering the vast majority of described species (Orchymont collection in Institute Royal des Sciences Naturelles in Brussels, and Sharp and Balfour-Browne collections in the Natural History Museum in London) but this revealed that the majority of species included are likely undescribed. Species-level identification (or an approximate one, indicated by cf. before species name) was only done for genera and species for which reliable identification tools exist. Table 1 lists all taxa used in the analysis.

All sequences were generated de novo, except those of *Cetiocyon incantatus* Fikáček & Short (obtained by Short & Fikáček, 2013) and *Cercyon melanocephalus* (obtained from Genbank) which were downloaded from GenBank. Eight species representing remaining tribes of the Spheridiinae were sequences and included as outgroups. The tree was rooted using *Agraphydrus* sp. (Acidocerinae). Voucher specimens are deposited at the National Museum, Prague, Czech Republic (NMPC). Localities and collecting data of vouchers are found in Supplementary file 1.

DNA extraction and amplification

Specimens were collected and kept in 95% ethanol and stored at -20ºC. Total genomic DNA was extracted from entire beetles using QiaGen Blood and Tissue DNA extraction kit following the manufacturer's instructions. Gene fragments were amplified using polymerase chain reaction (PCR). We included fragment of three nuclear protein-coding genes (histone 3 (*H3*), wingless (*Wg*) and toposimoerase 1 (*Top1*), two nuclear ribosomal genes (18S and 28S), two mitochondrial protein-coding genes (cytochrome oxidase I (*COI*), cytrochrome oxidase II (*COII*)) and one mitochondrial ribosomal (12S). *COI* and *18S* sequences were amplified as two or three fragments. Table 1 lists the primers used and the PCR protocol followed. New primers were designed for regions of the rDNA *28S* and cytochrome oxidase I (*COI*) genes, due to problems with the amplification using previously published primers. Amplification with standard primers for *28S* resulted in unspecific products from nematodes, probably present in the substrate from which the beetles were collected. Thus, we designed a forward primer to target a region of the 5' end of the gene with no variation within the family Hydrophilidae, using the sequence data of Toussaint & Short (2018) combined with part of our novel sequences: HYDR5F 5'-GTCMAAGTCCTTCTTGAACGGGGCCRYYTAC-3'. HYDR5F was coupled with the standard reverse primer LS1041R (Maddison 2008) to amplify a region of ca. 900 bp. In the case of *COI*,

amplification success was limited using primers LCO1490-HCO2198 (Folmer et al., 1994), hence a new primer pair amplifying a fragment of 625 bp in the 5' end of the *COI* gene (barcoding region) was designed using an alignment of 102 coleopteran sequences obtained from BOLD database (Ratnasingham & Hebert, 2007), with a few degenerated bases to cope with the variability found in the alignment. The primer sequences are Coleop_DMEAV5F 5'-HTGAKCWGGWATARTWGG-3' and Coleop_DMEAV5R 5'-RTAWACTTCWGGRTGDCC-3'; the forward primer region lies ~50 bp downstream from LCO primer, while the reverse overlaps with the 3' end of HCO primer.

Sequence editing and alignment

Sequences trace files were uploaded into Geneious (Kearse et al 2012) for inspection, assembly, and editing. All newly generated sequences will be deposited in GenBank. The list of vouchers, associated voucher data, and GenBank accession numbers of the sequences used in this study are listed in Table 1 of upplementary files. Sequences were aligned in Geneious using ClustalW algorithm with the default setting. Alignment of DNA sequences was trivial for *COI*, *COII*, *Top1*, *H3,* and *Wg*. Alignments for rDNA sequences were inspected by eye and corrected manually and with subsequent iterations of realignments of hypervariable zones using ClustalW or MUSCLE algorithms in Geneious. Concatenation of sequences was performed manually in Geneious software (Kearse et al. 2012).

Gene	Primer	Sequence (5'-3')	Annealing temperature (C°)	Reference
12s	12s ai	AAACTACGATTAGATACCCTATTAT	49	Simon et al. (1994)
	12s bi	AAGAGCGACGGGCGATGTGT	49	Simon et al. (1994)
18s	18S5end_F_18S5'1	GACAACCTGGTTGATCCTGCCAGT	50	Shull et al. 2001
	18S5end_R_18Sb05	TAACCGCAACAACTTTAAT	50	Shull et al. 2002
	18S5ce_F_18Sai	CTTGAGAAACGGCTACCACATC	50	Shull et al. 2003
	18S5ce_R_18Sb0.5	GTTTCAGCTTTGCAACCAT	50	Shull et al. 2004
	18S3_F_18Sa1.0	GGTGAAATTCTTGGACCGTC	50	Shull et al. 2005
	18S3_R_18S3'1	CACCTACGGAAACCTTGTTACGAC	50	Shull et al. 2006
28s	28S NLF184-21	ACCCGCTGAAYTTAAGCATAT	53	Van der Auwera et al. (1994)
	28S LS1041R	TACGGACRTCCATCAGGGTTTCCCCTGACTTC	53	Maddison 2008
	Hydr5f *	GTCMAAGTCCTTCTTGAACGGGGCCRYYTAC	53	This study
COI	LCO1490	GGTCAACAAATCATAAAGATATTGG	48	Folmer et al. 1994
	HCO2198	TAAACTTCAGGGTGACCAAAAAATCA	48	Folmer et al. 1995
	DMEAV5R *	HTGAKCWGGWATARTWGG	48	This study
	DMEAV5F *	RTAWACTTCWGGRTGDCC	48	This study
COII	COII TL2-J-3037	TAATATGGCAGATTAGTGCA	48	Simon et al. (1994)
	COIITK-N-3785	TTTAAGAGACCAGTACTT	48	Simon et al. (1994)
H3	H3aR	ATGGCTCGTACCAAGCAGACGGC	50	Colgan et al. (1998)
	H3aF	ATATCCTTGGGCATGATGGTGAC	50	Colgan et al. (1998)
TP	TP643F	GACGATTGGAARTCNAARGARATG	56	Wild and Maddison (2008)
	TP932R	GGWCCDGCATCDATDGCCCA	56	Wild and Maddison (2008)
	TP675F	GAGGACCAAGCNGAYACNGTDGGTTGTTG	56	Wild and Maddison (2008)
	TP919R	GTCTCTTTGCGTYTTRTTRTADATYTTYTC	56	Wild and Maddison (2008)
Wingless	Wg550F	ATGCGTCAGGARTGYAARTGYCAYGGYATGTC	56	Wild and Maddison (2008)
	WgABRZ	CACTTNACYTCRCARCACCARTG	56	Wild and Maddison (2008)
	Wg578F	TGCACNGTGAARACYTGCTGGATG	56	Ward and Downie (2005)
	WgABR	ACYTCGCAGCACCARTGGAA	56	Abouheif and Wray (2002)

Table 1. List of primers used in this study. Primers described in this study are indicated with a *.

Treatment of wild-card taxa

Despite our intention to include as many terminal taxa as possible, part of the taxa included originally revealed unstable in their position, resulting in largely unresolved larger clades. In most cases, these terminals were those which had a large amount of missing data; most of these taxa were excluded prior to the final set of analyses and are not listed among taxa examined. Of the final 193 taxa included in the analysis, five of them still showed the unstable "wild-card" behavior when analyzed using the Bayesian inference. For this reason, we assembled two datasets: *IN* (including wild-card taxa) and *EX* (excluding wild-card taxa). Species excluded from the *EX* dataset are *Cercyon melanocephalus* (Linnaeus), *Cercyon littoralis* (Gyllenhal), *Evanesternum pulsatum* (Orchymont), *Pyretus* sp. and a *Cercyon* sp (species with concave mesoventrite from Madagascar). The reasons for their wild-card behavior may be inferred only for *Cercyon melanocephalus* which had part of the data missing and was included as it is a type species of the genus *Cercyon*; the other four taxa had sequences of all gene fragments included.

Phylogenetic analyses

The concatenate alignments were used to infer the phylogenetic relationships using the Bayesian Inference (BI) and maximum Likelihood (ML). Protein-coding genes were partitioned by codon position and ribosomal genes were taken as a partition each. Best fitting models of substitution were selected using PartitionFinder 2 (Lanfear et al. 2016) with all models included and the greedy algorithm. The Akaike Information Criterion Corrected (AIC) was used to compare the likelihoods of the models. The ML analyses of both datasets (*IN* and *EX*) were carried out in W–IQ–TREE 1.5 (Nguyen et al. 2014; Trifinopoulos et al. 2016). An ultrafast bootstrap (UFB) with 1000 repetitions (Minh et al., 2013) was applied to estimatethe support for the hypothesized nodes.

The BI analyses of the *EX* dataset were performed using MrBayes 3.2.6 (Ronquist et al., 2012) implemented on the CIPRES Science Gateway 3.3 (Miller et al., 2010). Two simultaneous independent MCMC runs with six chains each and 100 million generations were used for the analysis, with a tree sampling every 12500 generations to calculate posterior probabilities (PP). The convergence of the runs and their parameters were assessed in TRACER 1.6 (Rambaut et al. 2014). A 50% burn-in fraction was applied to the data. The tree was summarized using the majority rule consensus for the general analysis, and using the *contype=allcompat* command for the purpose of the biogeography and diversification analyses which require fully bifurcating tree.

Divergence time estimation

Divergence dating was performed simultaneously to the phylogenetic inference. We used a relaxed clock method under the birth-dead model. Due to the absence of fossil members of tribe Megasternini .The only fossil megasternine reported by Kubisz 2000 as *Cercyon* sp. and used by Bloom et al. 2014, was revealed to not being part of Hydrophilidae, (Arriaga-Varela et al., submitted), we constrained the age of the basal nodes using the dates obtained by Arriaga-Varela et al. (in prep.) on the basis of the time tree for family Hydrophilidae generated using a comprehensive sampling for terrestrial hydrophilids and dated using a diverse and set of fossils including the corrected set of fossils (see Fikáček et al., 2017 and Arriaga-Varela et al (submitted)). The age of the following nodes was constrained using a truncated normal distribution as follows: MRCA of Sphaeridiinae (mean: 140 my; lower limit under 95% probability: 140 mya; SD: 9.5), MRCA of Sphaeridiini+Megasternini (134; 117.4; 8.9) and Megasternini (120.3; 104.5; 8.1).

Ancestral range estimation

To estimate the ancestral distribution at the nodes, we carried out the historical biogeography analyses in the R package BioGeoBEARS (Matzke, 2014). We used the fully resolved dated tree resulting from the divergence dating analysis as an input tree (outgroups were excluded). The distribution ranges were divided into the following seven areas following the main biogeographical realms plus a broadened concept of Cape Floristic Region South Africa: O – Oriental; U – Australian; E – Ethiopian; C - South Africa; P – Palaearctic; A – Nearctic; N – Neotropical. BioGeoBEARS implements three models in a maximum likelihood framework: DEC model (Ree & Smith 2008), DIVALIKE model (likelihood version of the DIVA model: Ronquist 1997) and BAYAREALIKE model (likelihood version of BayArea model: Landis et al., 2013). Founder event speciation can be added to any of the previously mentioned models and left as a free parameter estimated from the data, adding three extra models. Hence a total of six different models are available. We conducted non-time-stratified unconstrained analyses to estimate the ancestral range on the nodes, each with all six models. Unconstrained analyses were done using default parameter values. The performance of the different models was assessed using AIC scores.

Lineage through time.

We analyzed the divergence events along the tree by plotting the number of lineages through time (LTT) for the whole Megasternini and for each main clade (subtribe) separately. We used the logarithmic axis for the number of lineages, in order to infer the approximate diverfification rate as a slope of the resulting curve. The plots were constructed using the *ape* 1.8 package in R (Paradis et al. 2004).*Morphological studies.* The morphological studies and image documentation is based on the DNA vouchers used for the molecular analysis, and additional museum specimens. Habitus

photographs were taken using a Canon D-550 digital camera with attached Canon MP-E65mm f/2.8 1–5 macro lens. Pictures of genitalia were taken using a Canon D1100 digital camera attached to an Olympus BX41 compound microscope. In all cases, a series of photographs with a different focus was taken and combined with Helicon Focus software. Scanning electron micrographs were taken using Hitachi S-3700N environmental electron microscope at the Department of Paleontology, National Museum in Prague. Pictures used for plates were adapted in Adobe Photoshop CS6. Additional image documentation of voucher specimens not presented in this paper is included in the dataset submitted to the Zenodo archive under doi x/zenodo.x.

Results

Molecular dataset and selection of substitution models

The final concatenate alignment was composed of 6,587 bp divided in the next way: 12s (431 bp), 18s (1,841 bp), 28s (1,045 bp), Cytochrome oxidase I (COI) (1,413 bp), Cytochrome oxidase II (COII) (675 bp), 16s (825 bp), Histone 3 (234 bp); Wingless (Wg) (330 bp) and Topoisomerase I (TopI) (618 bp). Partition Finder analysis suggested GTR+I+G for all partitions except 28S, the second codon position of *H3*, second and third codon position of *Wg* and the first codon position of *Top1* for which the SYM+I+G model was suggested.

Phylogenetic analyses

Analyses of the *EX* dataset recovered similar topologies in Bayesian and maximum likelihood inference (ML tree can be seen in Supplementary file 4). The basal-most divergence within the tribe, the split of the *Oosternum* and *Cercyon* group of genera sensu Fikáček (2010) is recovered as strongly supported in ML (UFB = 100) and weakly supported in Bayesian analysis (PP = 0.65). Bootstrap values for all nodes were revealed above 80 % in the ML analysis. The resulting ML tree can be seen in Supplementary file 4. Bootstrap values in the BI analyses are generally above 90% within the first clade, referred herein as Oosternina subtribe nov. In the sister clade, refered herein as Megasternina subtribe nov., the support is low for some of the deepest nodes at the backbone of the tree, particularly in the clades VII and XII. For the subsequent analyses and discussion of the topology, we decided to follow the systematic hypothesis expressed in the fully bifurcating cladogram resulting from the *allcompat* tree reconstruction of BI analysis results of *EX* dataset, and its concomitant divergence dates estimated simultaneously, as it totally matches the resulting topology from ML analyses and it goes in concordance with the morphology and current distribution.

In order to better understand the morphology, biology and biogeography of tribe Megasternini we divide it into 12 clades, three of them in the new subtribe Oosternina (I-V) and nine in Megasternina (IV-XII). Internal relationships in Oosternina supports a scheme (I (II + III)). The support for this topology, as well for internal support of group II, is limited (pp = 0.65). While groups I and III have a internal support value of pp =1.0. Our BI results suggest a internal phylogenetic arrangement of clades in Megasternina as follows: (IV (V (VI (VIII ((IX (X + XI) + (XII))))))). The relationships among the clades VII, VIII, XII and IX+X+XI remain dubious due to the low support at the backbone of the Megasternina tree in BI analyses. Also the basal relationships within clades VIII and XII received low support in Bayesian analyses. The topology of these parts discussed here follows the *allcompat* one of the Bayesian analyses and corresponds with that received from maximum likelihood analysis. It is also supported by morphology and distribution of the terminal taxa.

Divergence dating

Time divergence estimates calculated simultaneously with the topology suggest a divergence of tribe Megasternini from Sphaeridiini at a mean of 121.1 mya (95% CI: 117.4–127.0) and a crown age for Megasternini at 106.5 (104.5–110.4) mya. The crown ages of both subtribes are recovered as approximately the same, 95.4 (87.0–103.6) mya for Oosternina and 95.3 (88.5–101.8) mya for Megasternina. The ages inferred by us for these basal divergence events are around 10–13 My younger than the dates recovered in the time tree by Arriaga-Varela et al. (in progress) from which the age constraints of the basal nodes were used here. We suppose that the difference is caused by the more complete taxon sampling in the current analysis, as the number of internal nodes generally has an impact on the results of dating analyses (cite Ronquist second Hymenoptera time tree). Our age estimates for these early splits are close to those reported by Bloom et al. (2014).

Taxonomy

Tribe Megasternini Mulsant, 1844

Tribe Megasternini is a group strongly supported as monophyletic based on molecular as well as morphological characters (Hansen 1991) (Fig. B). Our results corroborate the previously hypothesized subdivision of Megasternini tribe in two diagnosable clades corresponding to the *Cercyon* and *Oosternum* groups of Fikáček (2007, 2010), Fikáček & Short (2010b) and Short & Fikáček (2013) . This distinction corresponds to the morphology of male terminalia (Figs B5-7, 11-13). Both clades also show distict macroevolutionary and biogeographic patterns. To formalize

these two evolutionary different and morphologically diagnosable lineages, we describe them here as new subtribes: Oosternina Arriaga-Varela & Fikáček, new subtribe, and Megasternina Mulsant, new subtribe.

Oosternina Arriaga-Varela & Fikaček, new subtribe

Type genus: *Oosternum* Sharp, 1882

Diagnosis

With the diagnostic characters for tribe Megasternini. Members of Oosterninia can be differentiated from those of Megasternina by the morphology of the male genitalia and associated structures: the abdominal sternite 9 is crescent-like, with median portion not projecting anteriorly (Fig. B6), the sternite 8 has a medial projection at the anterior margin (Fig. B7), and the median lobe of the aedeagus does not reach deeply into phallobase and is firmly joint to the bases of parameres (Fig. B5).

Genera included in Oosternina

- *Clade I*: "Undescribed new genus": Undescribed new genus from Papua New Guinea (Fig. C2).
- *Clade II (Australian core): Kanala* Balfour-Browne (Fig. C3), *Merosoma* Balfour-Browne, *Platycyon* Hansen (Fig. C4), *Cercyon* Leach (part.), *Cetiocyon* Hansen (part.) (Fig. B2), *Cercyodes* Broun, *Ceronocyton* Hansen, *Pseudoosternum* Hansen (Fig. C5), *Chledocyon* Hansen, *Australocyon* Hansen (in part) (Fig. C6), *Cenebriophilus* Hansen (Fig. C7).
- *Clade III (Oosternum group sensu novo): Sacosternum* Hansen (Fig. C8), *Oosternum* Sharp (Figs A1, B3, C9-10), *Cetiocyon* Hansen (in part) (Figs B4, C2), *Motonerus* Hansen, *Agna* Smetana.

Genera included in Oosternina but not sampled for DNA

Notocercyon Blackburn, *Ercycodes* Hansen. On the basis of the morphology of male genitalia and associated structures, we preliminary classify these genera in Oosternina new subtribe. Both genera are very likely included in clade II. However, while the morphology of *Ercycodes* resembles that of *Cercyodes* on the nearly absent antennal grooves and on the shape of the meso- and metathoracical structures.

Megasternina Mulsant, 1844

Diagnosis

With the diagnostic characters for tribe Megasternini. Members of Megasternina can be

differentiated from those of Oosternina by the morphology of the male genitalia and associated structures: the abdominal sternite 9 is has a median portion developed as a tongue-like projection (Fig. B12), the sternite 8 lacks the anteromedial projection (Fig. B13), and the median lobe of the aedeagus reaches deeply into phallobase and is not firmly joint to the bases of parameres, being able to freely move in or out of the phallobase (Fig. B11).

Genera included in Megasternina

- *Clade IV (Paroosternum clade): Paroosternum* Scott, *Delimetrium* Hansen (Fig. D3), *Australocyon* Hansen (in part, *A. pilocnemoides* group) (Fig. D2).
- *Clade V (main South African clade): Cercyon* Leach (in part) (Figs 4-5).
- *Clade VI (Megasternum clade): Megasternum* Mulsant (Fig. D6), *Gillisius* Orchymont, *Peltocercyon* Orchymont (Fig. D7), *Chimaerocyon* Fikáček et al., *Pilocnema* Hansen, *Cercyon* Leach (in part) (Fig. D9), *Bolbonotum* Hansen, *Deltostethus* Sharp (Fig. D8).
- *Clade VII (Cercyon core): Cercyon* Leach, ?*Evanesternum* Arriaga-Varela et al. ?*Pyretus* Balfour-Browne. The assignment of the latter two genera into the clade is based on the ML analyses of the *IN* dataset, and needs to be confirmed in the future analyses (Fig. F).
- *Clade VIII (Cryptopleurum clade): Cryptopleurum* Mulsant (Fig. A3), *Pachysternum* Motschulsky, *Cyrtonion* Hansen, *Cercillum* Knisch, *Cycrillum* Knisch, *Pacrillum* D'Orchymont, *Tectosternum* Balfour-Browne.
- *Clade IX (Oriental clade): Pseudocercyon* d'Orchymont (Fig. E2), *Cercyon* Leach (in part),
- *Clade X (Armostus clade): Armostus* Sharp (Fig. A3), *Cercyon* Leach (in part) (Fig. E4-6).
- *Clade XI (Cycreon clade): Cycreon* d'Orchymont (E7-9), *Cercyon* Leach (in part).
- *Clade XII (Pelosoma clade): Pelosoma* Mulsant (Fig. E14), *Nitidulodes* Sharp (Fig. E11), *Moraphilus* d'Orchymont (Fig. E10), *Cercyon* Leach (in part) (Fig. 12-13).

Genera included in Oosternina but not sampled for DNA

Acaryon Hebauer, *Parastromus* Balfour-Browne, *Morastus* D'Orchymont, *Nipponocercyon* Satô, *Colerus* Hansen, *Oreocyon* Hebauer, *Pseucyon d*'Orchymont, *Pelocyon* Balfour-Browne, *Kahanga* Hansen, *Emmidolium* D'Orchymont, *Quadristernum* Balfour-Browne.

Comments

According to the ML analyses of the *IN* dataset, *Pyretus* is sister to the clade VII, while *Evanesternum* is nested inside of this clade (Fig. F). Of the genera not effectively sampled in our dataset, *Parastromus* might be a member of Clade VII on the basis of the broad central raised area of the metaventrite with its posterior margin concurrent with the position of femoral lines, and on

the convex anterior margin of the mentum. The shape of meso- and metaventrite of *Pelocyon* shows a strong resemblance to *Paroosternum* and *Delimetrium* from Clade IV (Fig. D3). *Acaryon* is very similar to *Cycreon* in Clade XI. All these hypotheses need to be corroborated by DNA data and the genera not sampled at the moment remain as Megasternina *incertae sedis*.

Internal relationships within Oosternina new subtribe

The support values of all internal nodes are above 0.9 (PP) and 90 (UFB) respectively for both BI and ML analyses. Three main clades may be recognized (Fig. C1). Clade I is a previously unknown lineage confined to New Guinea and represented by two undescribed species (i.e., much less diverse than its sister clade formed by Clades II+III). These two species were originally identified as *Cercyon* and *Merosoma* following current generic concepts. Despite the differences in dorsal sculpture (Fig. C2) and in the shape of the mesoventral plate, both species share a very short prosternum in front of the procoxae.

Clade II is a morphologically diverse group of genera. Its earliest branching lineage, *Cercyodes* Broun, is an atypically flattened genus missing antennal grooves on the prothorax and feeding on rotten beachwrack; it is the only megasternine lineage naturally occurring in New Zealand. Other members of this clade have been associated to animal excrements, leaf litter or rotten stems of plants (Arriaga-Varela et al. in prep).

Remaining members of clade II are the *Kanala*, *Cetiocyon* and *Australocyon* lineages. *Kanala* Balfour-Browne is a genus endemic to New Caledonia, with five described species (Fikáček 2010) relatively diversified morphologically but sharing the mesoventrite broadly connected to the mesoventrite (Fig. C3). *Cetiocyon* lineage includes a variety of species from New Guinea and northernmost Australia.This genus contains the largest known representatives of Megasternini (Szczepański et al. 2018). Other members of Clade II are species with ventral morphology forming a continuum in the degree of development of the ridge demarcating the anterolateral corners of the metaventrite (Fig. C4). The taxa with distinct ridge are at the moment classifed in *Platycyon* (Hansen 1999, Hebauer 2000, 2001), whereas those with less developed ridge are until today members of the broadly defined genus *Cercyon* and recently resurrected *Merosoma* (Balfour-Browne 1939; Fikáček 2019). None of these taxa are related to *Cercyon*; the similarity in morphology is caused by the convergent evolution and the genus-level classification of these taxa requires a revision. The *Australocyon* lineage consists of Australian genera (for details see Hansen 1999 and Fikáček 2019) and a group of small flattened New Guinean species assignable to *Platycyon* under the current the generic concept. The close proximity of *Australocyon* and *Cenebriophilus* indicating their very recent split (ca. 10.9 mya) is noteworthy since each of this genus is morphologically very characteristic (Fikáček 2019). Both genera share pores in the

anteromedial margin of the mesoventrite (Figs C6-7), a unique character within Megasternini, which support their sister relationship and suggests *Cenebriophilus* is a highly modified lineage within *Australocyon* with exaggerated dorsal and ventral sculptures and punctuation. A better taxonomic sampling, particularly the inclusion of *A. variegatus* Hansen (type species of the genus) and of the Neotropical representatives of the genus is needed to understand the relationship between both genera. Ecological observations are necessary to reveal the possible role of such modifications in these species.

Clade III (*Oosternum* clade) is the mainly Neotropical branch of the Oosternina. It split from the Australian Clade II at around 87 mya (76.9–94.5) and is formed by two subclades (Fig. C1). The first one groups *Motonerus*, *Sacoosternum* (Fig. C8)*, Pemelus* Horn (Fig. C10) (a genus merged under *Oosternum* by Hansen 1999), and a lineage formed by *Cetiocyon incantatus* Fikáček & Short (the only Neotropical species classified as *Cetiocyon*, Fikáček & Short 2010b) and species fitting the unpublished concept of '*Oosternum grandis* group' of M. Hansen and F. Hebauer. Our results indicate that both *Pemelus* and the species around *Cetiocyon incantatus* deserve a separate generic status from *Oosternum*. The second subclade is composed of core *Oosternum* species and *Agna*. *Agna* is a genus confined to the arid and semiarid zones in the southwestern USA and northern and central Mexico, specialized in rotten cacti (Arriaga-Varela et al. in press). It has a reduced dorsal and ventral sculpture when compared to *Oosternum*. The presence of *Agna* renders the core *Oosternum* paraphyletic, with the Oriental lineage of *Oosternum* being sister to *Agna* + Neotropical *Oosternum.* The dispersal of the MRCA of Oriental *Oosternum* from the New World is hypothesized to have happened ca. 52 mya (44.9–58.8) likely via the Beringia land bridge (see discussion on biogeography) (Fig. G, node 3).

Internal relationships within Megasternina (Clades IV – XII) Clade IV (*Paroosternum* group) is a collection of dissimilar and disjunct genera (Fig. D1): *Delimetrium* Hansen from South Africa (Fig. D3), *Paroosternum* Scott occurring in the Oriental and Ethiopian region, and the Asian species currently classified in *Australocyon pilocnemoides* species group (Hansen 2003). *Delimetrium* is revealed as sister to *Paroosternum*. Both genera share well-defined femoral lines on the metaventrite and the subpentagonal mesoventral plate broadly contacting the metaventrite. Members of the *Australocyon pilocnemoides* group need to be transferred to a new genus (Arriaga-Varela et al. in prep). Their separate status from *Australocyon* is supported by characters of male terminalia consistent with the subtribal diagnostics, and by loosely defined central part of the metaventrite (Fig. C2) (this is pentagonal and clearly defined in true *Australocyon*). Members of this clade have been found in leaf litter and dung.

Clade V (South African clade) is formed by two lineages of *Cercyon* species: a group of

closely similar species vaguely assignable to *C.* (*Clinocercyon*) (Balfour-Browne 1948) found on forest litter in Cape region oof South Africa and three species inhabiting the beach wrack (*C. aphodioides* Orchymont, *C. gigas* Orchymont, and *C. maritimus* Knisch). Both lineages show significant differences in the shape and proportions of the body. Additionally, the beachwrack species are characterized by comparatively flattened tibiae with thick spines on lateral marginsA. This morphological traits seem to have evolved independently in other non-related beachwrack species from other clades of Megasternini. All species in Clade V share the mesoventral plate with posterior apex not overlapping the anterior margin of the mesoventrite (Fig. D4-5).

Clade VI (*Megasternum* clade) is morphologically diverse and includes genera occurring mainly in the Oriental region. *Megasternum* (Fig. C6) is part of the earliest-diverging lineage, along with *Gillisius* and *Cercyon undulipenis* Ryndevich et al. *Megasternum* hence does not form a group with other genera with the wide mesoventral plate (see Clade VII, Figs D12-14) as it was suggested by Hansen (1991). The morphologically aberrant *Chimaerocyon* Fikáček et al., associated with *Pheidole* ants (Fikáček et al., 2013), is revealed as sister to typically looking species (specimen MF319, *Cercyon* cf. *madidus* Orchymont) from China. This situation is another example of high morphological plasticity of Megasternini species under divergent environmental selection. Clade VI also includes the Oriental genera *Peltocercyon* Orchymont (strongly supported as a monophylum) (Fig. D7) and *Bolbonotus* Hansen, Oriental/Australian *Pilocnema* Hansen, two lineages of *Cercyon* from Oriental and Australian regions (Solomon islands) including one lineage with vaguely defined antennal grooves (Fig. D9), and the American *Deltosthetus* Sharp. *Deltostethus* is estimated to have diverged from the Oriental ancestor ca. 55 mya (48.7-62.3) and its presence in America is probably a result of dispersion via the Beringian route.

The taxa recovered as part of the Clade VII (core *Cercyon*) are classified exclusively in *Cercyon.* The results of the ML analysis of the *IN* dataset indicates that this clade includes *C. melanocephalus* (Linnaeus), the type of the genus *Cercyon*, as a close relative of *Cercyon haemorrohidalis* (Fabricius) (Fig. F). Most specimens in this clades have distinct femoral lines on the metaventrite (Fig. A2), a character not present in *Cercyon* species in the following principal clades. Additionally, there is a tendency of the anterior margin of the mentum being rounded and not distinctly concave. The basal-most divergence in this clades is a split between African and Palaearctic+Nearctic+Oriental species which happened ca. 57 mya (50.3-64.9). The latter lineage is likely to contain the vast majority of Palearctic and Nearctic *Cercyon* species. A more extensive sampling of these species may help to elucidate the dispersal and diversification patterns in the northern hemisphere after the Eocene. The ML analysis of the *IN* dataset shows *Pyretus* Balfour-Browne as a sister clade of the whole Clade VII (Fig F). However, although some details like the shape of the mentum (Fig. Fb) the morphology of *Pyretus* points to a possible relationship to Clade

VIII (*Cryptopleurum* clade) and further analyses are necessary.

Clade VIII (*Cryptopleurum* clade) is formed by most genera with a compact convex body, strongly deflexed epipleura, very narrow metanspisterna, elevated and demarcate central part of the prosternum and a broad mesoventral plate; (Tthus it partially corresponds to the narrow concept of Megasternini of Horn (1890) except for *Megasternum*, whichis placed elsewhere (Clade VI). A potential synapomorphy for Clade VIII is the subangulate lateral edge of pronotum with a slight indentation in the anterior half caused by the wide antennal grooves (Figs A3, D11). The mentum is characteristic by the small rounded or pointed processes in anterolateral corners (Figs A3, D13), a shape is also found in *Megasternum.* Despite the wide set of shared morphological characters, the nodal support at suprageneric level is low (Fig. D1). The earliest-divergent group, *Pacrillum+Tectosternum*, show a narrow mesoventral plate and pentagonal central area of the mesoventrite (Fig. D12), Suggesting a transitional state between the *Cercyon* morphotype and the compact-body forms with broad mesoventral plate and metaventral medail region found in this clade (e.g., *Cryptopleurum,* Fig. XA3, and *Pachysternum*). The ancestor of the Neotropical genus *Cycrillum* split approximately 53 mya (45.9-60.0) from its sister clade composed by *Pachysternum, Cryptopleurum, Cercillum* and *Cyrtonion* (i.e. genera occurring in Oriental, Ethiopian, Palearctic and Nearctic regions). The topology revealed for *Pacrillum* + *Tectosternum* and *Cercillum* + *Cyrtonion* is partly supported by morphological characters and suggest the need to merge the genera in both these pairs.

Clade IX (*Pseudocercyon* group) is mainly formed by Oriental species of *Cercyon*, with *Pseudocercyon* Orchymont nested inside and *Cercyon fimbriatus* Mannerheim (a beachwrack species occurring on the Pacific coast of North America) as sister of all other members. The *Cercyon* species in this group lack femoral lines as is the case for *Cercyon* species in Clade XII classified as *Cercyon,* in contrast to members of Clade VII, "*Cercyon* core", where most species show femoral lines. Additionally, the mentum of most species has a straight or slightly concave anterior margin. Pseudocercyon differs from other members by the distinctly raised medial part of prosternum and mesoventral plate widely connected to the anterior margin of the mesoventrite (Fig. E2).

Clade X (*Armostus* group) is mainly formed by *Armostus* Sharp and *Cercyon* species currently classified in subgenera *Prostercyon* Smetana, *Arcocercyon* Hebauer and *Clinocercyon* Orchymont (Fig. E5). The specimens of this group are characterized by the following features: (1) the mesoventral plate is raised and separated from the central part of the mesoventrite by a gap of variable width (Figs E3, 4, 6), and (2) the anterolateral corners of the mesoventrite are delimited by a ridge (Fig. E3), which arereduced to a thickened anterior margin in some species classified as

Cercyon. Some species show a modified medial portion of the prosternum, with median carina strongly raised or anterior half raised (Fig. E5). This feature was the reason why Smetana (1978) established the subgenus *Prostercyon* for the Nearctic *Cercyon roseni*, but it is also present in the European *C. convexiusculus* group in which *C. roseni* is nested. *Cercyon* (*Clinocercyon*) *lineolatus* (Motschulsky) is an early diverging Oriental species of this clade sister to all remaining species, bearing a mesoventrite not separated by a gap from the metaventrite.

Clade XI (*Cycreon* group) is formed by the Oriental *Cycreon* d'Orchymont and a lineage of Neotropical species with *Cercyon* morphology lacking femoral lines. Cycreon is a genus of flattened flower-associated beetles with reduced antennal grooves (Fig. E8), very narrow mesoventral plate (Fig. E7), and deeply emarginate mentum (Fig. E9).The Neotropical lineage is estimated to have diverged from the Oriental *Cycreon* approximately 50 mya (41.5-58.6).

Clade XII (*Pelosoma* group) is composed almost exclusively of the Neotropical species classified at the moment in genera *Cercyon*, *Moraphilus*, *Nitidulodes* and *Pelosoma*. The only exception is a species from South Africa that separated from the Neotropical clades 50.6 mya (43.5–58.6). *Cercyon* species in this clade lack femoral lines. *Moraphilus* is nested in this group. This genus shows a basic *Cercyon* morphology with a flattened prosternum without distinct antennal grooves (Fig. E10) and subpentagonal mesoventral plate. On the other hand, *Pelosoma* species differ from *Cercyon* by a elongate mesoventral plate widely attached to the metaventrite in straight line (Fig. E14). *Nitidulodes* is a genus of large megasternines associated to large inflorescences of Araceae plants. So far only one *Nitidulodes* species have been described from Panama and Mexico. It shares with *Pelosoma*, to which it was recovered as sister (pp = 0.31), the shape of mesovantral plate. However, the mentum of Nitidulodes show a characteritic very deep emargination in the anterior margin (Fig. E11). Pelosoma species show a wide range of habitats, from phytotelmata, leaf litter, inflorescences, and rotten plant fleshy stems (see Arriaga-Varela et al. in press and Arriaga-Varela et al. in prep.). A group of Cercyon species was recovered as nested in *Pelosoma* lineage. These species are dung and carrion-feeding species mainly distributed in the Antilles (Fig. E12,13) (Arriaga-Varela et al. 2017) but they include a complex of species distributed throughout the Neotropics and USA, the *Cercyon variegatus* group, that includes simmilar looking *C. variegatus* Sharp, *C. insularis* Chevrolat, and a series of not described species only distinguished by the shape of male genitalia.

Historical biogeography of Megasternini

Our results of the unconstrained ancestral range estimation in BioGeoBears show DIVALIKE as the best-fitting model. This model minimizes the number of dispersal and extinction events using a three-dimensional cost matrix (Ronquist 1997) allowing changes in ancestral ranges to be a result of

vicariance. The resulting plot with the single most-probable ancestral range at each node is shown in a simplified way in Fig. 6. The Australian-Oriental vicariance was recovered for the basal-most divergence within Megasternini, separating Oosternina from Megasternina (node 1). This does not correspond to the position of these land masses in the Late Cretaceous. We suspect that the reconstruction of the MRCA of Megasternina as Oriental may be biased by our taxon sampling and that a Australian-African vicariance in the Late Cretaceous would be a more probable explanation (see below in Megasternina for details). This hypothesis needs to be tested by a expanded taxon sampling and the use of time-stratified biogeography analyses.

The Oosternina clade was recovered as ancestrally Australian with two major vicariant events: the colonization of the Neotropics in the Late Cretaceous to Paleocene (86.6–60.2 mya) (Fig. G node 2), and a subsequent dispersal of members of this Neotropical group into the Oriental region by the ancestors of the *Oosternum soricoides* group (Fikáček et al. 2009) during the Eocene-Oligocene (44.9-58.8 mya) (Fig. G node 3). The first vicariance event may be explained by the dispersal via Anctartica which connected to both Australia and South America and had tropical to subtropical vegetation with summer maximum temperature of nearly 20ºC in this time period (Pross et al., 2012). Similar patterns of dispersal between Australia and South America related to tropical climare in Antarctica have been found in plant taxa such orchids (Givnish et al. 2016a) and Liliales (Givnish et al 2016b). The dispersal of the MRCA of Oriental *Oosternum* from the New World was likely possible via the Beringia land bridge which was covered by boreotropical forests during the early Eocene climatic optimum (Archibald et al 2011, 2014).

The backbone of the Megasternina and all divergences during the Cretaceous have the Oriental region as ancestral state, with the exception of Clade V currently distributed in South Africa. As mentioned above, the Oriental origin of Megasternina should be regarded as provisional. Missing taxa may be crucial in this regard: tropical African genera *Pelocyon* Balfour-Brown and *Pseucyon* d'Orchymont are likely part of the early branching clade IV based on the morphology closely resembling *Paroosternum*, and *Paroosternum* is occurring both in Africa and Oriental Region (Hebauer 2002). This indicates that this clade may be mainly African, in contrast to our sampling which contains mostly Oriental taxa. In a similar way, we suspect that Clades VII and VIII also contain a significantly higher proportion of African taxa than we sampled at the moment. This indicates that Africa may have played a more significant role in the diversification and distribution of the Megasternina lineages through time. Irrespectively to the precise scenario, it is clear that the MRCA of the Megasternina was living in the Old World.

All our recognized main clades of Megasternina diverged from its sister lineage before the K-Pg boundary (65 mya). Soon after the end of the Cretaceous, the New World was colonized by the Megasternini for the second time by the ancestor of Clade XII around 63.9 mya (58.4-68.4).

During the Cenozoic, South America was isolated from the other continents, only having a non-permanent land connection with East Antarctica that lasted probably until the Late Paleocene (Reguero et al., 2014). The dispersal to South America via Antarctica would imply the historical presence of the group in Australia from where they are absent at the moment, implying the extinction of this lineage in Australia. An alternative explanation may be the colonization of South America from Africa by a long distance dispersal across the southern Atlantic Ocean, or via the land bridges connecting the land masses of the northern hemisphere during the Palaeocene (Brikiatis 2014). The long-distance dispersal across the Atlantic would imply the presence of this group Africa at the beginning of the Cenozoic. A more comprehensive taxon sampling is necessary to provide evidence for any of these scenarios and to understand the events that shaped the distribution of Clade XII in the Neotropical Region.

Our ancestral ranges reconstruction shows six intercontinental dispersals in the Early Eocene, between 55 and 50 mya (nodes 6-11 in Fig. G). Four of these events are dispersals of ancestrally Oriental lineages to the New World, giving rise to clades currently distributed in the Nearctics and Neotropics (nodes 6-11). Two dispersals went in the opposite direction, with Neotropical ancestors colonizing the Old World and giving rise to clades currently distributed in the Oriental region (node 3) and Africa (node 11). The time range in which these intercontinental dispersals took place coincides with the Palaeocene-Eocene Climatic optimum and the Early Eocene climatic optimum. This period (ca. 56–51 My) (Zachos et al. 2001; Gingerish 2006; Röhl et al. 2007; Huber and Caballero 2011) is characterized by high temperatures with mild winters in the northern hemisphere that allowed the existence of a boreotropical zone (Zachos et al. 2001; Brunke et al. 2017, Huang et al. 2019), a community of frost-intolerant organisms forming an Arctic rainforest that extended north to 76–78ºN of palaeolatitude (Basinger et al., 1994; Greenwood et al., 2010). The existence of meso- and megathermic biomes coupled with fluctuating sea levels that interconnected previously isolated land masses via four principal land bridges and straights (Beringian, De Geer, Thulean and Turgai Strait) that likely interrupted by 50 mya (Brikiatis 2014; Condamine et al., 2013; Praz and Packer 2014; Sanmartín et al., 2001; Woodburne 2010). The six Old World-New World dispersal events mentioned above were likely made possible via the Beringian route (Garrouste and Nel 2019). The Oriental *Oosternum soricoides* group derived from Neotropical ancestors is absent in the Palearctic, Ethiopian and Australian regions, rendering an alternative dispersal route via Europe unlikely. A similar scenario in the opposite direction is inferred for node 6 with the dispersal of the Oriental ancestor of *Deltostethus* dispersing into the New World ca. 55.2 (48.7–62.4). The genus is most diverse in central and northern South America at the moment, with one species present in North America reaching as far north as British Columbia, and small number of species in central parts of South America. The modern distribution is congruent with the dispersal of an ancestor of

Deltostethus from Asia via Beringia land bridge. Same is the case of *Cercyon fimbriatus* Mannerheim (node 9 in Fig G) currently inhabiting Pacific coast of North America, and of the Central American *Cercyon* species in clade XI (node 10 in Fig. G), as both these lineages are nested deeply in clades occurring in the Oriental region. The dispersal of the ancestrally Neotropical lineage into South Africa happening ca. 50.6 mya (43.5–58.6) mya in Clade XII is more difficult to explain: the dispersal via land bridges in the northern hemisphere would imply a subsequent extinction of this lineage in Asia, Europe, and North America. The long-distance dispersal from South America to Africa would be an alternative.

The genus *Cercyodes,* shows a divergence between the species from Australian and New Zealand of aproximately 20 mya. The presence of *Cercyodes,* a rotten beachwrack-feeding genus, in New Zealand, where no other megasternine is known to be distributed naturally can be explained by a long distance dispersal event. Such events can be likely caused by organisms using kelp accumulations as rafts transported by extreme weather conditions (Waters et al. 2018)

Younger colonizations events observed include the parallel colonizations of Australian Region from Asia ca. 38 mya in Clade VI (see the next chapter for details) or the colonization of North America by the European lineage of *Cercyon convexiusculus* group ca. 25.7 mya. Additional sampling at the species level is necessary to understand the historical biogeography of these clades. There are additional cases of disjunct distribution at intrageneric level not covered by our sampling which would be worthy to study in the future. These include *Megasternum* (Palearctic-Oriental-Nearctic), *Tectosternum+Pacrillum* (Ethiopian-Oriental-Nearctic), *Pelosoma* (Ethiopian-Neotropical-Nearctic), and *Australocyon* (Australian-Neotropical).

Diversification of the Megasternini through time

The lineage through time plot (LTT) (Fig. H) shows a steady accumulation of species in both subtribes happening from the beginning of the Paleocene approximate to the mid-Eocene. The early Eocene hyperthermal condition causing the presence of boreotropical forests in the northern hemisphere reached its end around 40 mya (Sluijs et al. 2009). Around this time (35-45 mya) we can see a contrasting pattern in the LTT plot between Megasternina and Oosternina. Fast accumulation of species continues in Megasternina even after the end of the climatic optimum, while the diversification rate decreases in the Oosternina. A possible explanation for this phenomenon is the retreat of the meso- and megathermal forests towards the equator when the climate started to cool down at the end of the Eocene (Wolfe 1975, Zachos 2001), as documented for many plant taxa (Smedmark and Anderberg 2007: Tiffney 1985; Tiffney and Manchester. 2001; Willard et al 2019). This process decreased drastically the range of the wet tropics and prompted the divergence of previously widespread tropical lineages. Many tropical taxa retreated to isolated

refuges: many boreotropical taxa found the refuge in Mexico and Central America, for example; Morley 2000, 2003. This 'crisis of tropics' was easier to cope for the Megasternina, which became world-wide in distribution by that time. In contrast, the Oosternina were confined mainly to megathermal forests in Australian Region and due to the isolation of Australia likely had a limited capacity to escape the cooling and later the massive aridification of the continent. On the other hand, the equator-wise contraction of tropical forests in the Late Eocene may have been responsible for the colonization of Australian Region by two independent lineages of the Oriental Clade VI. Such pattern has been found in riodinid butterflies which reached New Guinea from Southeast Asia ca. 40 mya (Espeland et al., 2015)

Conclusions

Taxonomy

We revealed 12 principal clades in the Megasternini grouped into two large clades which monophyly is strongly supported by molecular and morphological characters; these two clades are newly defined here as subtribes. - Morphological characters show a complex pattern of evolution probably driven by remarkable plasticity mirroring the biology rather than evolutionary relationships; the high amount of convergence complicates the diagnosability of the lineages.

The geographic distribution of clades often reflects their phylogenetic relationships better than morphological characters; on the other hand, frequent intercontinental dispersal events which may obscure this pattern are revealed especially in the Megasternina- Future attempts on creating a natural classification of Megasternini requires an integrative approach combining molecular data, morphology and distribution, and a subsequent reappraisal of morphological diagnostic characters.- The boundaries of the largely polyphyletic genera like *Cercyon, Oosternum, Cetiocyon,* and *Australocyon* need to be redrawn. The taxonomic rearrangement of *Cercyon* will be challenging because of a high degree of homoplasy among all unrelated clades currently classified in that genus; before the rearrangement is done we suggest to drop the use all subgeneric taxa in *Cercyon* as they clearly do not have any phylogenetic meaning.

Biogeography and diversification

Expected fast evolution and high extinction of lineages in the time window from the end of the Cretaceous to the beginning of the Eocene, and our failure to sample possible key taxa, complicates the resolution of the topology in clades VII-XII.- Early Eocene thermal conditions prompted range expansions and intercontinental dispersal in the Megasternini. We document complex biogeographical patterns with evidence of bi-directional faunal interchange between the New and

Old world likely through the Beringia land bridge with boreotropical forest during the Eocene climatic optimum 55-50 mya. Our results suggest that future studies should not only focus on distinguishing vicariance versus dispersal when interpreting biogeography pattern, but must take into account the effect of biome conservatism (Crisp et al 2009; Donoghue 2008).

Acknowledgments

We are thankful to the colleagues that provided us with specimens and observation on their natural history. Their names can be seen in Supplementary file 1). Matthias Seidel is kindly acknowledge for this help in the laboratory and field-work, Niklas Wahlberg and Hamid Ghanavi (Lund University) for their help during the secondment of EAV in Lund University. This work was supported by the European Union's Horizon 2020 research and innovation programme under the Marie Skłodowska-Curie grant agreement No. 642241 to EAV, and by the Ministry of Culture of the Czech Republic (DKRVO 2018/13, National Museum, 00023272) to MF. The work of EAV at the Department of Zoology, Charles University, Prague was partly supported by grant SVV260434/2018.

References

Abouheif, E. and Wray, G.A. 2002. Evolutionary lability of the regulatory gene network underlying the wing polyphenism in ants. *Science,* 297, 249–252.

Archangelsky, M. 1997. Studies on the biology, ecology, and systematics of the immature stages of New World Hvdronhiloidea (Coleoptera: Staphyliniformia). *Bull. Ohio Biol. Surv*.,(n. ser.), 12, 1-207.Ashley-Ross, M.A., Hsieh, S.T., Gibb, A.C., Blob, R.W. 2013. Vertebrate land invasions-past, present, and future: an introduction to the symposium. *Integrative and Comparative Biology,* 53(2), 192–196.

Archibald, S. B., Johnson, K. R., Mathewes, R. W. and Greenwood, D. R. 2011. Intercontinental dispersal of giant thermophilic ants across the Arctic during early Eocene hyperthermals. *Proceedings of the Royal Society of London B: Biological Sciences*, 278(1725), 3679-3686,

Archibald, S. B., Morse, G. E., Greenwood, D. R. and Mathewes, R. W. 2014. Fossil palm beetles refine upland winter temperatures in the Early Eocene Climatic Optimum. *Proceedings of the National Academy of Sciences*, 111, 8095–8100.

Arriaga-Varela, E., Seidel, M. and Fikáček, M. 2018a. A new genus of coprophagous water scavenger beetle from Africa (Coleoptera, Hydrophilidae, Sphaeridiinae, Megasternini) with a

discussion on the *Cercyon* subgenus *Acycreon*. *African Invertebrates,* 59(1), 1–23. https://doi.org/10.3897/AfrInvertebr.59.14621

Arriaga-Varela, E., Wong, S.Y., Kirejtshuk. A. and Fikáček, M. 2018b. Review of the flower-inhabiting water scavenger beetle genus *Cycreon* (Coleoptera, Hydrophilidae), with descriptions of new species and comments on its biology. *Deutsche Entomologische Zeitschrift,* 65(1), 99–115. https://doi.org/10.3897/dez.65.26261

Arriaga-Varela, E., Sykora, V. Ghanavi, H, Seidel, M. & Fikáček, M. (in prep.) Phylogeny, habitat shifts and diversification of terrestrial water scavenger beetles (Hydrophiloidea: Hydrophilidae). **(Chapter 6)**

Arriaga-Varela, E., Brunke, A., Girón, J.C., Szawaryn, K., Bruthansová, J. and Fikáček, M. (submitted) Micro-CT reveals hidden morphology and clarifies the phylogenetic position of Baltic amber water scavenger beetles (Coleoptera: Hydrophilidae). *Papers in Palaeontology* **(Chapter 5)**

Arriaga-Varela, E., Cortés-Aguilar, J. and Fikáček, M. (in press) Water scavenger beetles in rotten cacti: A review of *Agna* with the description of a new species from Mexico (Coleoptera: Hydrophilidae: Sphaeridiinae). *Revista Mexicana de Biodiversidad* **(Chapter 4)**

Balfour-Browne, J. 1939. LVII.—On the Aquatic Coleoptera of the New Hebrides and Banks Islands. Dytiscidse, Gyrinidæ, and Palpicornia. *Journal of Natural History*, 3(16), 459-479.

Balfour-Browne, J. 1948. New East African Palpicornia. *Annals and Magazine of Natural History* (11)14, 817-833.

Basinger, J. F., Greenwood, D. R. and Sweda, T. 1994. In: *Cenozoic plants and climates of the Arctic* (Eds. M.C. Boulter & H.C. Fisher), 127, 175-198. Springer-Verlag.

Bernhard, D., Komarek, A., Beutel, R., and Ribera, I. 2009. Phylogenetic analysis of Hydrophiloidea (Coleoptera: Polyphaga) based on molecular data and morphological characters of adults and immature stages. *Insect Systematics & Evolution*, 40(1), 3–41. http://doi:10.1163/187631209x416741

Bernhard, D., Schmidt, C., Korte, A., Fritzsch, G. and Beutel, R.G., 2006. From terrestrial to aquatic habitats and back again—molecular insights into the evolution and phylogeny of Hydrophiloidea (Coleoptera) using multigene analyses. *Zoologica Scripta*, 35(6), 597–606.

Bloom, D., Fikáček, M., Short, A.E.Z. 2014. Clade age and diversification rate variation explain disparity in species richness among water scavenger beetle (Hydrophilidae) lineages. *PLoS ONE* 9(6), e98430. https://doi.org/10.1371/journal.pone.0098430

Bouchard, P., Grebennikov, V.V., Smith, A.B. and Douglas, H., 2009. Biodiversity of Coleoptera. *Insect biodiversity: science and society*, pp.265-301.

Brikiatis, L. 2014. The De Geer, Thulean and Beringia routes: key concepts for understanding

early Cenozoic biogeography. *Journal of Biogeography*, 41, 1036–1054.

Brunke, A.J., Chatzimanolis, S., Metscher, B.D., Wolf-Schwenninger, K. and Solodovnikov, A. 2017. Dispersal of thermophilic beetles across the intercontinental Arctic forest belt during the early Eocene. *Scientific Reports*, 7(1), 12972.

Colgan, D.J., McLauchlan, A., Wilson, G.D.F., Livingston, S.P., Edgecombe, G.D., Macaranas, J., Cassis, G. and Gray, M.R. 1998. Histone H3 and U2 snRNA DNA sequences and arthropod molecular evolution. *Australian Journal of Zoology*, 46(5), 419-437.

Condamine, F.L., Sperling, F.A.H., Kergoat and G.J. 2013. Global biogeographical pattern of swallowtail diversification demonstrates alternative colonization routes in the Northern and Southern hemispheres. *Journal of Biogeography*, 40(1), 9-23

Crisp, M.D., Arroyo, M.T., Cook, L.G., Gandolfo, M.A., Jordan, G.J., McGlone, M.S., ... and Linder, H. P. 2009. Phylogenetic biome conservatism on a global scale. *Nature*, 458(7239), 754-756.

Donoghue, M.J. 2008. A phylogenetic perspective on the distribution of plant diversity. *Proceedings of the National Academy of Sciences*, 105(Supplement 1), 11549-11555.

Espeland, M., Hall, J.P., DeVries, P.J., Lees, D.C., Cornwall, M., Hsu, Y.F., Wu, L.W., Campbell, D.L., Talavera, G., Vila, R. and Salzman, S., 2015. Ancient Neotropical origin and recent recolonisation: Phylogeny, biogeography and diversification of the Riodinidae (Lepidoptera: Papilionoidea). *Molecular Phylogenetics and Evolution*, 93, 296-306.

Folmer, O., Black, M., Hoeh, W., Lutz, R. and Vrijenhoek, R. 1994. DNA primers for amplification of mitochondrial cytochrome c oxidase subunit I from diverse metazoan invertebrates. *Molecular Marine Biology and Biotechnology*, 3, 294–299.

Fikáček, M. 2010. Hydrophilidae: The genus *Kanala* Balfour-Browne (Coleoptera). In: M.A. Jäch, and M. Balke (Eds.). *Water Beetles of New Caledonia, Vol. 1. Monographs of Coleoptera, 3*, 365–394.

Fikáček, M. 2019. 20. Hydrophilidae Leach, 1815. pp. 271–337. In: Slipinski, A., and Lawrence, J. (Eds.). *Australian Beetles. Archostemata, Myxophaga, Adephaga, Polyphaga (part)*. CSIRO Publishing, Clayton South, 2, 765.

Fikáček, M. and Short, A.E.Z. 2006. A revision of the Neotropical genus *Motonerus* Hansen (Coleoptera: Hydrophilidae: Sphaeridiinae). *Zootaxa*, 1268, 1–38.

Fikáček, M. and Short, A.E.Z. 2010a. A revision of the Neotropical genus *Sacosternum* Hansen (Coleoptera: Hydrophilidae: Sphaeridiinae). *Zootaxa,* 2538, 1–37.

Fikáček, M. and Short, A.E., 2010. Taxonomic revision and phylogeny of the genus *Cetiocyon* and its discovery in the Neotropical region (Insecta: Coleoptera: Hydrophilidae). Arthropod Systematics & Phylogeny , 68(3), 309– 329.

Fikáček, M., Maruyama, M., Vondráček, D. and Short, A.E.Z. 2013. *Chimaerocyon* gen. nov., a morphologically aberrant myrmecophilous genus of water scavenger beetle (Coleoptera: Hydrophilidae: Sphaeridiinae). *Zootaxa*, 3716, 277–288.

Garrouste, R. and Nel, A., 2019. Alaskan Palaeogene insects: a challenge for a better knowledge of the Beringian 'route'(Odonata: Aeshnidae, Dysagrionidae). *Journal of Systematic Palaeontology*, 1-8.

Gingerich, P.D. 2006. Environment and evolution through the Paleocene–Eocene thermal maximum. *Trends in ecology and evolution*, 21(5), 246-253.

Givnish, T.J., Zuluaga, A., Lam, V.K.Y., Gomez, M.S., Iles, W.J.D., Spalink, D., Moeller, J.R., Lyon, S.P., Briggs, B.G., Zomlefer, W.B. and Graham, S.W. 2016a. Plastome phylogeny and historical biogeography of the monocot order Liliales: out of Australia and through Antarctica. *Cladistics*, 32. http://doi:10.1111/cla.12153

Givnish, T.J., Spalink, D., Ames, M., Lyon, S.P., Hunter, S.J., Zuluaga, A., Doucette, A., Caro, G.G., McDaniel, J., Clements, M.A. and Arroyo, M.T. 2016b. Orchid historical biogeography, diversification, Antarctica and the paradox of orchid dispersal. *Journal of Biogeography*, 43(10), 1905-1916.

Greenwood, D. R., Basinger, J. F. and Smith, R. Y. 2010. How wet was the Arctic Eocene rain forest? Estimates of precipitation from Paleogene Arctic macrofloras. *Geology* 38, 15–18.

Hansen, M. 1991. The Hydrophiloid Beetles. Phylogeny, Classification and a Revision of the Genera (Coleoptera, Hydrophiloidea). *Biologiske Skrifter, Det Kongelige Danske Videnskabernes Selskab*, 40, 1-368.

Hansen, M. 1999. Taxonomic changes in the genera *Oosternum* Sharp and *Paroosternum* Scott (Coleoptera: Hydrophilidae). *Entomologica Scandinavica,* 30, 241–242. http://doi:10.1163/187631200X00084

Hansen, M. 2003: Discovery of *Australocyon* Hansen and *Pilocnema* Hansen (Coleoptera; Hydrophilidae) outside the Australian region. In: Cuccodoro, G. and Leschen, R.A.B. (Eds.). *Systematics of Coleoptera: Papers Celebrating the Retirement of Ivan Löbl. Memoirs of entomology international*, Associated Publisher. 53–84.

Hebauer, F. 2000. The New Guinean species of the genus *Platycyon* Hansen, 1999 (Coleoptera, Hydrophilidae). *Acta Coleopterologica*, 16(1), 3-16.

Hebauer, F. 2001. Beitrag zur Kenntnis der Hydrophilidae von Neuguinea. Ergebnisse der

zoologischen Forschungsreisen von M. Balke und L. Hendrich nach West Neuguinea (Irian Jaya) in den Jahren 1990–1998 (Coleoptera: Hydrophilidae). *Acta Coleopterologica*, 17(1), 3-72.

Hebauer, F., 2002. New Hydrophilidae of the Old World (Coleoptera, Hydrophilidae). *Acta Coleopterologica*, 18(3), pp.3-24.

Horn, G.H. 1890. A revision of the Sphaeridiini inhabiting boreal America. *Transactions of the American Entomological Society*, 17 (3), 279–314, pl. 9. [Aug-Nov 1890 (footers); 28 Feb 1891 (recorded at CUL)]

Huang, X., Deng, T., Moore, M.J., Wang, H., Li, Z., Lin, N., Yusupov, Z., Tojibaev, K.S., Wang, Y. and Sun, H. 2019. Tropical Asian Origin, boreotropical migration and long-distance dispersal in Nettles (Urticeae, Urticaceae). *Molecular phylogenetics and evolution*, 137, 190-199.

Huber, M. and Caballero, R. 2011. The early Eocene equable climate problem revisited. *Climate of the Past*, 7, 603–633.

Kearse, M., Moir, R., Wilson, A., Stones-Havas, S., Cheung, M., Sturrock, S., Buxton, S., Cooper, A., Markowitz, S., Duran, C. and Thierer, T. 2012. Geneious Basic: an integrated and extendable desktop software platform for the organization and analysis of sequence data. *Bioinformatics*, 28(12), 1647-1649.

Kubisz, D. 2000. Fossil beetles from Baltic amber in the collection of the Museum of Natural History of ISEA in Krakow. *Polskie Pismo Entomologiczne*, 69, 225–230.

Landis, M.J., Matzke, N.J., Moore, B.R. and Huelsenbeck, J.P., 2013. Bayesian analysis of biogeography when the number of areas is large. *Systematic Biology*, 62(6), 789-804.

Lanfear, R., Frandsen, P. B., Wright, A. M., Senfeld, T. and Calcott, B. 2016. PartitionFinder 2: New methods for selecting partitioned models of evolution for molecular and morphological phylogenetic analyses. *Molecular biology and evolution*, 34(3), 772-773. https://doi.org/10.1093/molbev/msw260

Maddison, D.R. 2008. Systematics of the North American beetle subgenus *Pseudoperyphus* (Coleoptera: Carabidae: Bembidion) based upon morphological, chromosomal, and molecular data. *Annals of Carnegie Museum*, 77, 147–193.

Miller, M. A., Pfeiffer, W. and Schwartz, T. 2010. Creating the CIPRES Science Gateway for inference of large phylogenetic trees. *Gateway Computing Environments Workshop,* 1–8.

Minh, B.Q., Nguyen, M.A.T. and von Haeseler, A., 2013. Ultrafast approximation for phylogenetic bootstrap. *Molecular Biology and Evolution*, 30(5), 1188-1195.

Minoshima, Y.N., Seidel, M., Wood, J.R., Leschen, R.A., Gunter, N.L. and Fikáček, M. 2018. Morphology and biology of the flower-visiting water scavenger beetle genus *Rygmodus*

(Coleoptera: Hydrophilidae). *Entomological science*, 21(4), 363-384.

Morley, R.J. 2003. Interplate dispersal paths for megathermal angiosperms. *Perspectives in Plant Ecology, Evolution and Systematics*, 6(1-2), 5-20.

Morley, R.J. 2000. *Origin and evolution of tropical rainforests.* John Wiley and Sons. UK.

Nguyen, L.T., Schmidt, H.A., von Haeseler, A. and Minh, B.Q., 2014. IQ-TREE: a fast and effective stochastic algorithm for estimating maximum-likelihood phylogenies. Molecular biology and evolution, 32(1), pp.268-274.

Paradis E, Claude J. and Strimmer K. 2004. APE: Analyses of Phylogenetics and Evolution in R language. *Bioinformatics*, 20, 289-290.

Praz, C. J. and Packer, L. 2014. Phylogenetic position of the bee genera *Ancyla* and *Tarsalia* (Hymenoptera: Apidae): A remarkable base compositional bias and an early Paleogene geodispersal from North America to the Old World. *Molecular Biology and Evolution*, 81, 258–270.

Pross, J., Contreras, L., Bijl, P.K., Greenwood, D.R., Bohaty, S.M., Schouten, S., Bendle, J.A., Röhl, U., Tauxe, L., Raine, J.I. and Huck, C.E., 2012. Persistent near-tropical warmth on the Antarctic continent during the early Eocene epoch. *Nature*, 488(7409), 73.

Rambaut, A., Suchard, M.A., Xie, D. and Drummond, A.J., 2014. Tracer v1. 6. Computer program and documentation distributed by the author.

Ratnasingham, S. and Hebert, P.D. 2007. BOLD: The Barcode of Life Data System. *Molecular ecology notes*, 7(3), 355-364.

Ree, R.H. and Smith, S.A., 2008. Maximum likelihood inference of geographic range evolution by dispersal, local extinction, and cladogenesis. *Systematic Biology*, 57(1), 4-14,

Reguero, M.A., Gelfo, J.N., López, G.M., Bond, M., Abello, A., Santillana, S.N. and Marenssi, S.A., 2014. Final Gondwana breakup: the Paleogene South American native ungulates and the demise of the South America–Antarctica land connection. *Global and Planetary Change*, 123, 400-413.

Röhl, U., Westerhold, T., Bralower, T.J. and Zachos, J.C. 2007. On the duration of the Paleocene-Eocene thermal maximum (PETM). *Geochemistry, Geophysics, Geosystems*, 8(12).

Ronquist, F. 1997. Dispersal–vicariance analysis: a new approach to the quantification of historical biogeography. *Systematic Biology*, 46, 195–203.

Ronquist, F., Teslenko, M., Van Der Mark, P., Ayres, D.L., Darling, A., Höhna, S., Larget, B.,

Liu, L., Suchard, M.A. and Huelsenbeck, J.P., 2012. MrBayes 3.2: efficient Bayesian phylogenetic inference and model choice across a large model space. *Systematic Biology*, 61(3), 539-542.

Sanmartín, I., Enghoff, H. and Ronquist, F. 2001. Patterns of animal dispersal, vicariance and diversification in the Holarctic. *Biological Journal of the Linnean Society*, 73(4), 345-390.

Short, A.E.Z. and Fikáček, M. 2013. Molecular Phylogeny, Evolution, and Classification of the Hydrophilidae (Coleoptera). *Systematic Entomology*, 38, 723–752.

Shull, V.L., Vogler, A.P., Baker, M.D., Maddison, D.R., and Hammond, P.M. 2001. Sequence alignment of 18S ribosomal RNA and the basal relationships of Adephagan beetles: evidence for monophyly of aquatic families and the placement of Trachypachidae. Systematic Biology, 50(6), 945-969.

Simon, C., Frati, F., Beckenbach, A., Crespi, B., Liu, H., and Flook, P. 1994. Evolution, weighting, and phylogenetic utility of mitochondrial gene sequences and a compilation of conserved polymerase chain reaction primers. *Annals of the entomological Society of America*, 87(6), 651-701.

Smetana, A. 1978. Revision of the subfamily Sphaeridiinae of America north of Mexico (Coleoptera: Hydrophilidae). *Memoirs of the Entomological Society of Canada*, 105, 1–292.

Sluijs, A., Schouten, S., Donders, T.H., Schoon, P.L., Röhl, U., Reichart, G.J., Sangiorgi, F., Kim, J.H., Damsté, J.S.S. and Brinkhuis, H. 2009. Warm and wet conditions in the Arctic region during Eocene Thermal Maximum 2. *Nature Geoscience*, 2(11), 777.

Smedmark, J.E. and Anderberg, A.A. 2007. Boreotropical migration explains hybridization between geographically distant lineages in the pantropical clade Sideroxyleae (Sapotaceae). *American Journal of Botany*, 94(9), 1491-1505.

Song, K.Q., Xue, H.J., Beutel, R.G., Bai, M., Bian, D.J., Liu, J., Ruan, Y.Y., Li, W.Z., Jia, F.L. and Yang, X.K. 2014. Habitat-dependent diversification and parallel molecular evolution: Water scavenger beetles as a case study. *Current Zoology*, 60(5), 561-570.

Spangler, P. J. 1962. A new species of the genus *Oosternum* and a key to the U. S. species (Coleoptera: Hydrophilidae). *Proceedings of the Biological Society of Washington,* 75, 97-100.

Szczepański, W.T., Vondráček, D., Seidel, M., Wardhaugh, C. and Fikáček, M., 2018. High diversity of *Cetiocyon* beetles (Coleoptera: Hydrophilidae) along an elevational gradient on Mt. Wilhelm, New Guinea, with new records from the Bird's Head Peninsula. *Arthropod Systematics and Phylogeny*, 76, pp.323-347.

Tiffney, B.H. 1985. The Eocene North Atlantic land bridge: its importance in tertiary and

modern phytogeography of the Northern hemisphere. *Journal of the Arnold Arboretum*. 66(2), 243–273.

Tiffney, B.H.and Manchester, S.R. 2001. The use of geological and paleontological evidence in evaluating plant phylogeographic hypotheses in the Northern Hemisphere tertiary. *International Journal of Plant Sciences*, 162(S6), S3-S17.

Toussaint, E. F., and Short, A. E. 2018. Transoceanic Stepping–stones between Cretaceous waterfalls? The enigmatic biogeography of pantropical Oocyclus cascade beetles. *Molecular Phylogenetics and Evolution,* 127, 416-428.

Van der Auwera, G., Chapelle, S. and De Wachter, R. 1994. Structure of the large ribosomal subunit DNA of *Phytophthora megasperma*, and phylogeny of the oomycetes. *FEBS Letters,* 338, 133-136.

Waters, J.M., King, T.M., Fraser, C.I. and Craw, D. 2018. An integrated ecological, genetic and geological assessmentcet of long-distance dispersal by invertebrates on kelp rafts. *Frontiers of Biogeography*, 10(3-4).

Whidden, K.J., and Jones, R.W. 2012, Correlation of early Paleogene global diversity patterns of large benthic foraminifera with Paleocene and Eocene climatic events. *Palaios*, 27, 235–251, http://doi:10.2110/palo.2010.p10-109r

Willard, D.A., Donders, T.H., Reichgelt, T., Greenwood, D.R., Sangiorgi, F., Peterse, F., Nierop, K.G., Frieling, J., Schouten, S. and Sluijs, A. 2019. Arctic vegetation, temperature, and hydrology during Early Eocene transient global warming events. *Global and Planetary Change*, 178, 139-152.

Wolfe, J.A. 1975. Some aspects of plant geography of the northern hemisphere during the Late Cretaceous and Tertiary. *Annals of the Missouri Botanical Garden*. 62, 264–279.

Woodburne, M. 2010. The Great American Biotic Interchange: dispersals, tectonics, climate, sea level and holding pens. *Journal of mammalian evolution*. 17(4), 245–264.

Zachos, J., Pagani, M., Sloan, L., Thomas, E. and Billups, K. 2001. Trends, rhythms, and aberrations in global climate 65 Ma to present. *Science*, 292(5517), 686-693.

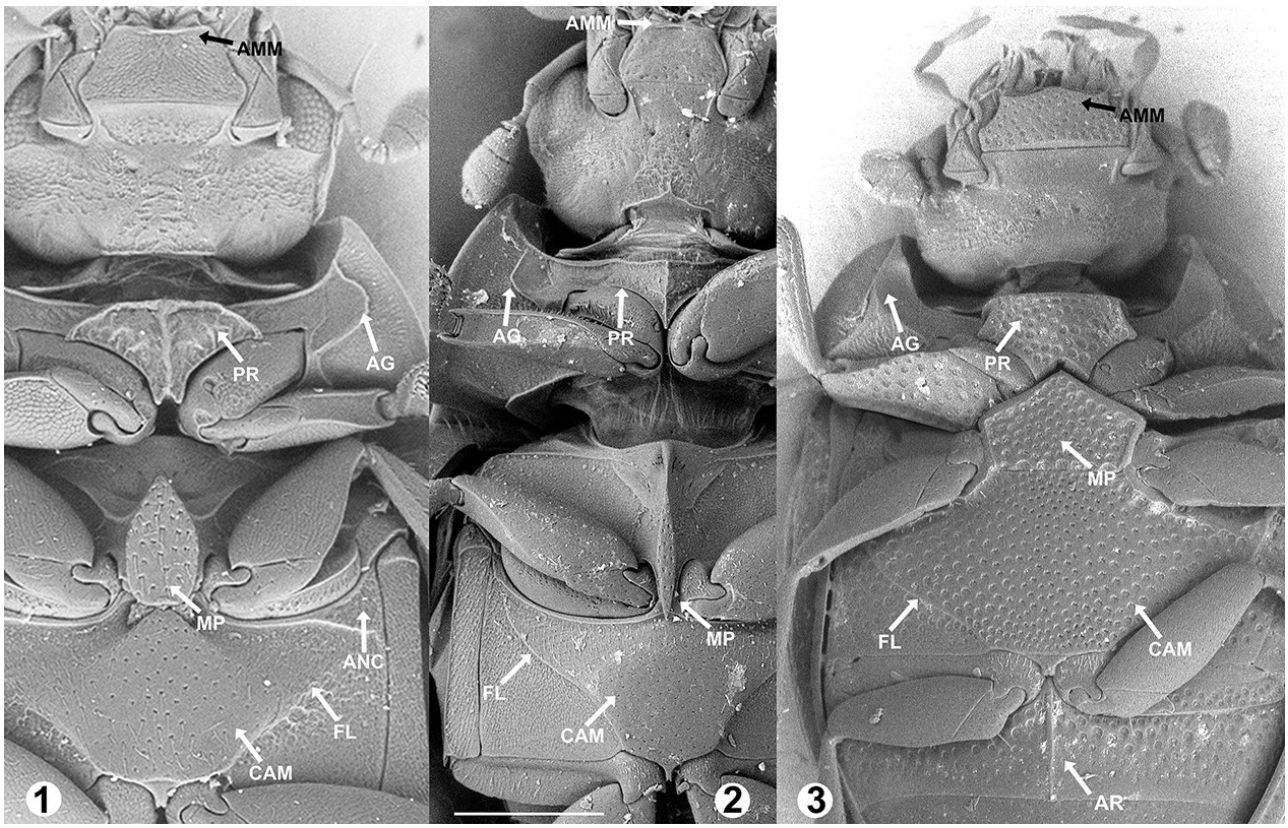

Figure A. Ventral morphology of Megasternini species. **1 –** *Oosternum* sp. (Guatemala; MF1679); **2 –** *Cercyon nigriceps* (Dominican Republic; MF1215); **3 -** *Cryptopleurum* sp. (China; MF332). AG – Antennal groove; AMM – Anterior margin of mentum; ANC – Anterolateral corner of metaventrite; AR – Ridge on first abdominal ventrite; CAM – Central area of metaventrite: FL – Femorla lines; MP – Mesoventral plate; PR – Prosternum.

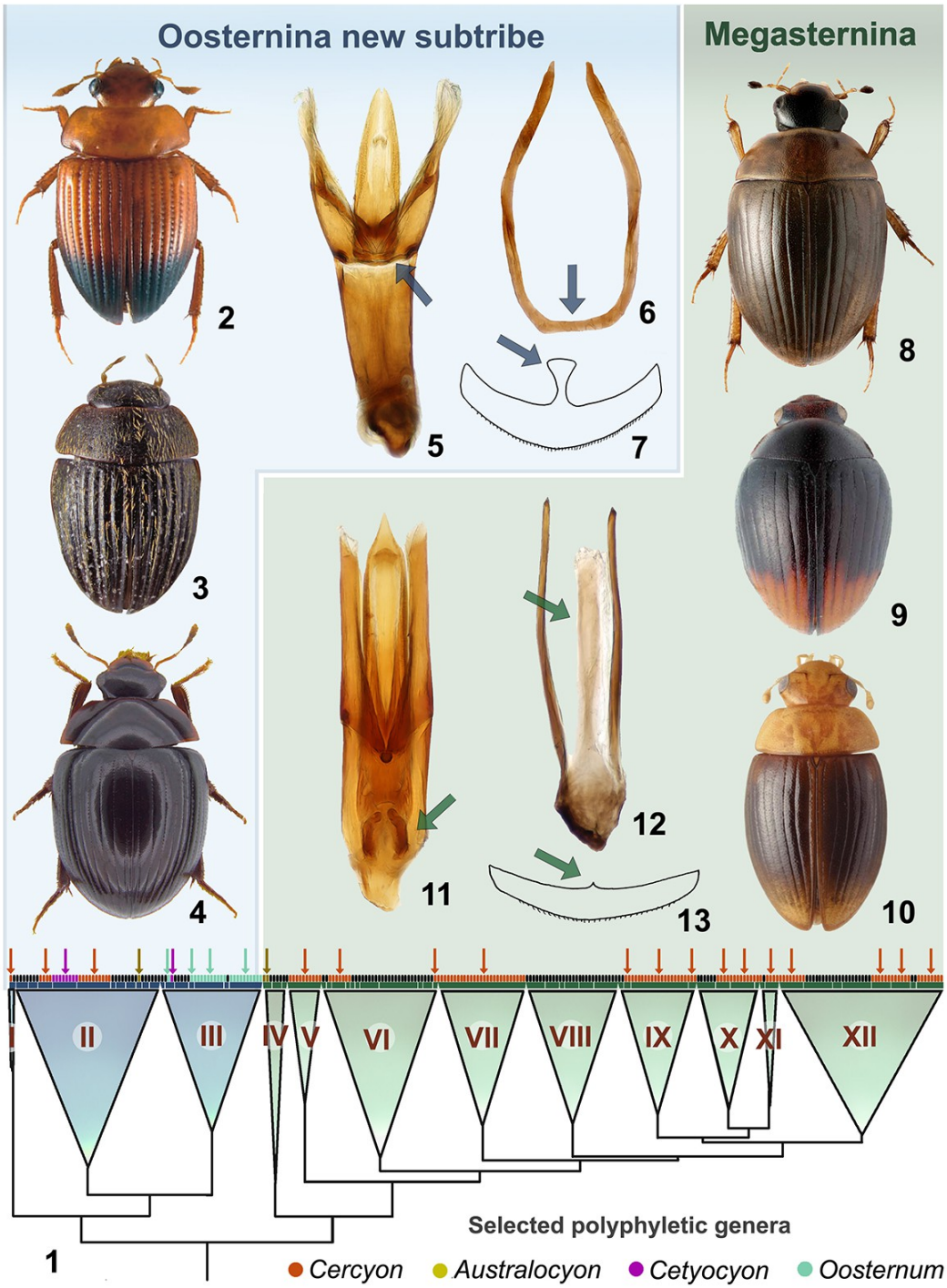

Figure B. 1 – Simplified resulting topology based on a time-calibrated tree obtained under Bayesian Inference with the proposed division of the tribe in two subtribes and 12 clades; **2 -** *Cetiocyon incantatus* Fikáček & Short dorsal habitus; **3 -** *Oosternum luciae* Deler et al. dorsal habitus; **4 -** *Cetiocyon augai* Szczepański et al. Dorsal habitus: **5 –** Aedeagus of *Cercyon* sp. (Papua New Guinea; MF1651); **6 -** 9th sternite of *Agna capillata* Horn; **7 -** 8th sternite of *Merosoma* sp. (Australia); *Cercyon spiniventris* Arriaga-Varela et al. dorsal habitus; **9 –** *Pachysternum apicatus* Motshulsky dorsal habitus; **10 -** *Cycreon floricola floricola* Arriaga-Varela et al. dorsal habitus; **11 –** Aedeagus of *Cycreon floricola floricola* Arriaga-Varela et al.; **6 -** 9th sternite of *Cycreon floricola floricola* Arriaga-Varela et al.; **7 -** 8th sternite of *Cercyon haemorrhoidalis* (Fabricius).

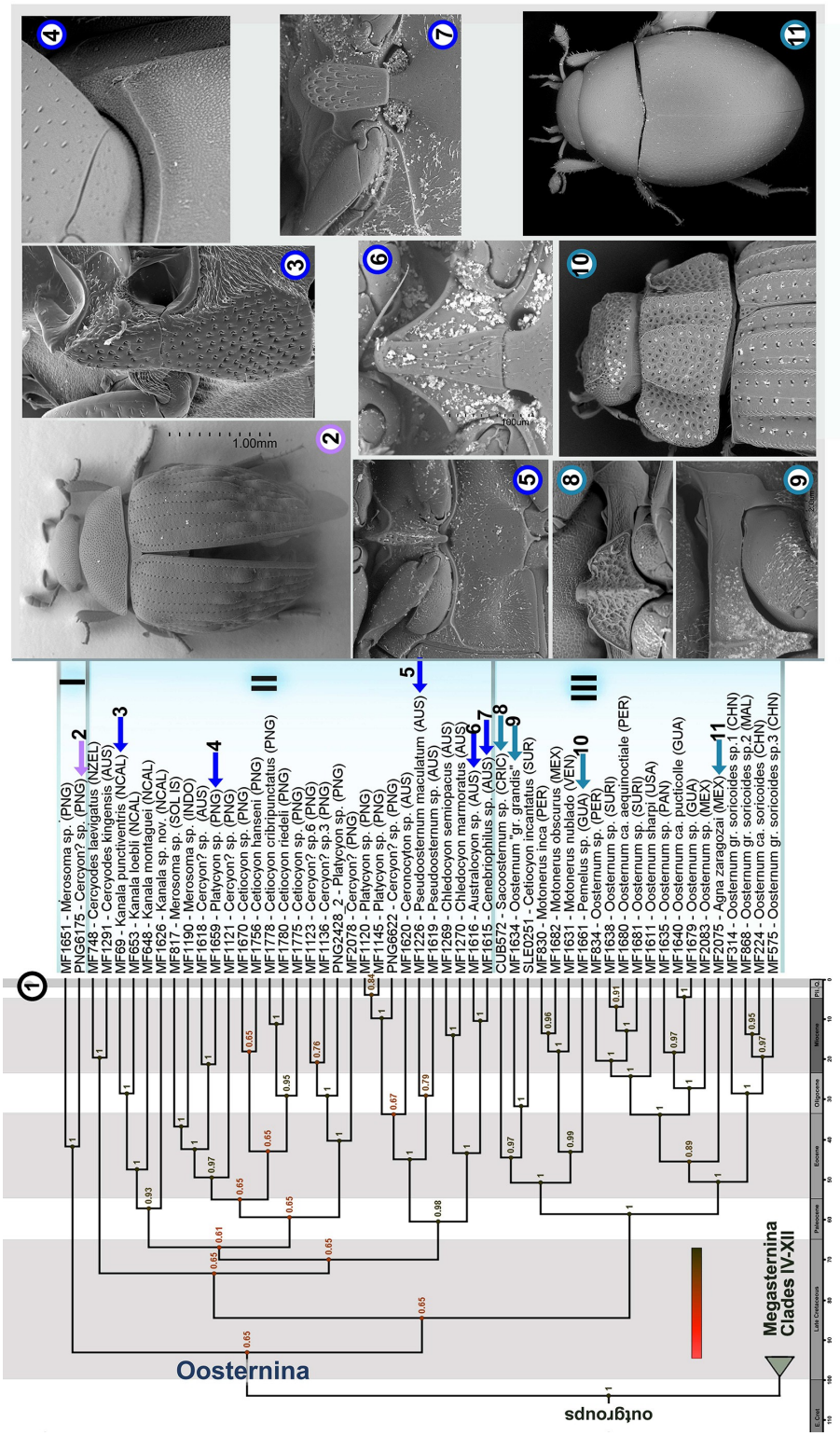

Figure C. 1 – Portion of time-calibrated phylogenetic tree obtained under Bayesian Inference showing Oosternina new subtribe (Clades I-III); **2 -** Dorsal habitus *Cercyon sp.* (PNG6175); **3** – Meso- and metaventrite *Kanala punctiventris* (MF69); **4** – Anterolateral corners of metaventrite of *Platycyon* sp. (MF1659); **5 -** Meso- and metaventrite of *Pseudoosternum maculatum* (MF1226); **6 -** Meso- and metaventrite of *Australocyon* sp. (MF1616); **7 -** Meso- and metaventrite of *Cenebriophilus* sp. (MF1615); **8 -** Prosternum of *Sacoosternum auribleps* Fikáček & Short (Brazil); **9** – prosternum of *Oosternum* '*grandis* group' sp. (MF1634); **10** – Laterodorsal habitus of *Oosternum* ('*Pemelus*') sp. (MF1661); **11 -** Dorsal habitus *Agna capillata* (USA).

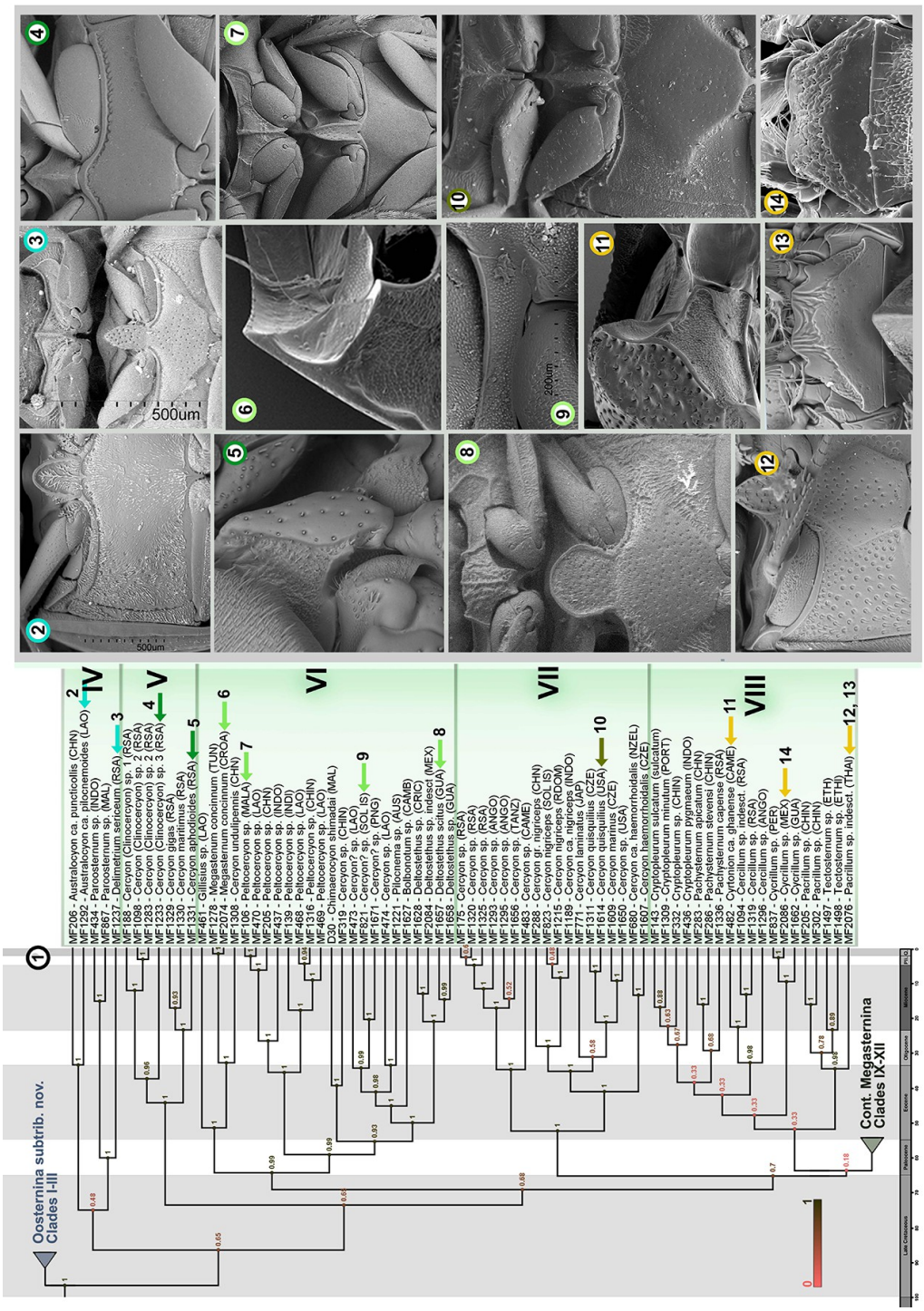

Figure D. 1 – Portion of time-calibrated phylogenetic tree obtained under Bayesian Inference showing Clades IV – VII of Megasternina; **2 -** Meso- and metaventrite of *Australocyon* gr. *pilocnemoides* (MF1292); **3** – Meso- and metaventrite *Delimetrium sericeum* Hansen (MF1237); **4** – Meso- and metaventrite of *Cercyon* sp. (MF1233); **5 -** Meso- and metaventrite of *Pseudoosternum maculatum* (MF1226); **6** – Mesosoventral plate of *Cercyon aphodioides* d'Orchymont (MF1331); **7** – Hipomeron and prosternum of *Megasternum concinnum* (Marsham) (MF1615); **8** – Thoracic ventrites of *Deltostethus scitulus* Spangler & Huajuca (MF1657); **9** – prosternum of *Cercyon* sp. (MF821); **10** – Thoracic ventrites of *Cercyon quisquillius* (Linnaeus) (MF1614); **11** – Pronotum and hipomeron of *Cyrtonion ca. ghanense* Hansen (MF482); **12** – Meso- and metaventrite of *Pacrillum* sp. indesct. (MF2076); **13 -** Mentum of *Pacrillum* sp. indesct. (MF2076); **14 -** Mentum of *Cycrillum* sp. (MF2086).

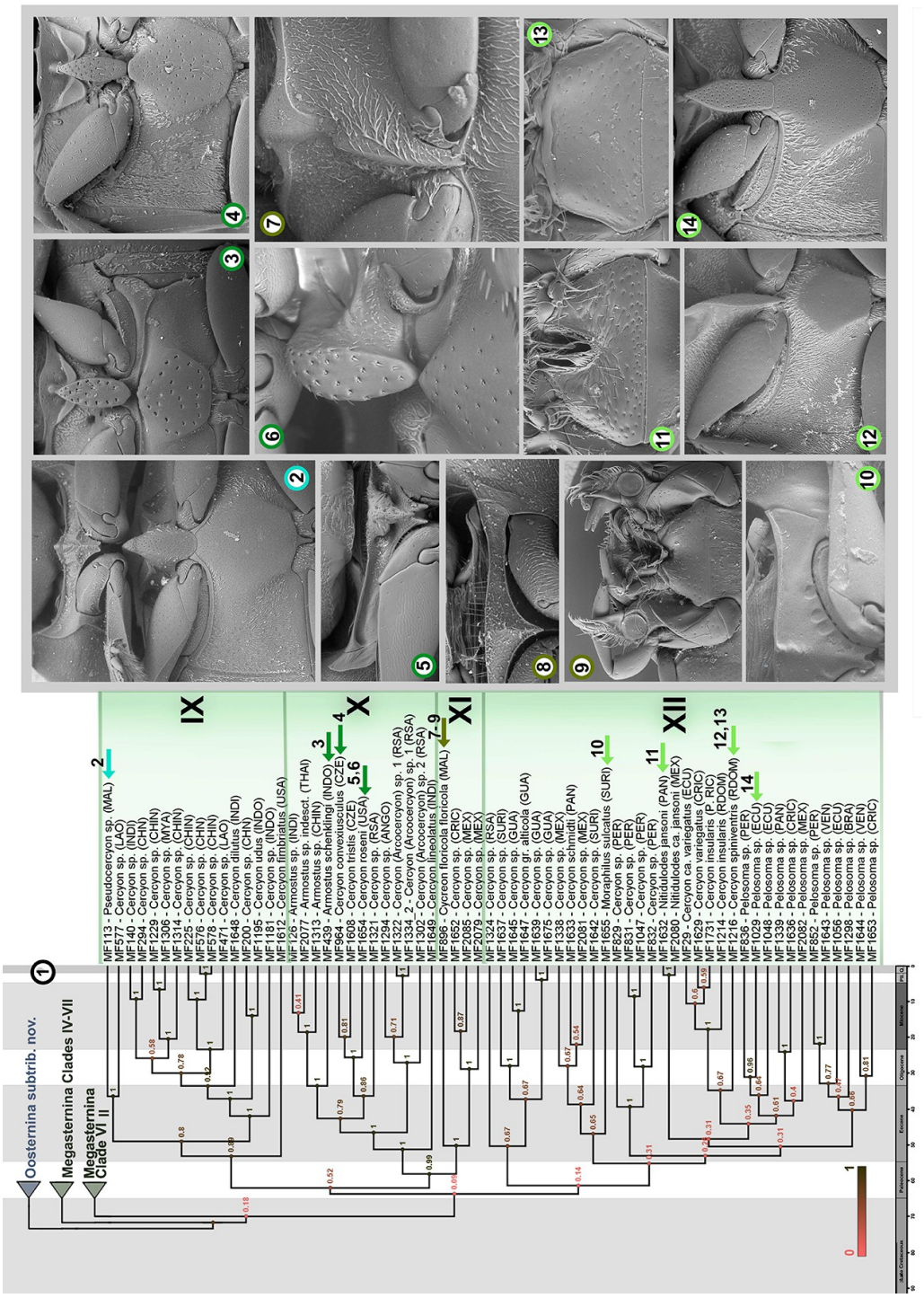

Figure E. 1 – Portion of time-calibrated phylogenetic tree obtained under Bayesian Inference showing Clades VI – XII of Megasternina; **2 –** Thoracic ventrites of *Pseudocercyon* sp. (MF113); **3 –** Meso- and metaventrite *Armostus schenklingi* d'Orchymont (MF439); **4 –** Meso- and metaventrite of *Cercyon convexiusculus* Stephens (MF964); **5 –** Prosternum of *Cercyon roseni* Knisch (MF1654); **6 –** Ventrolateral view of mesosoventral plate of *Cercyon roseni* Knisch (MF1654); **7 –** Mesoventrire *Cycreon floricola floricola* Arriaga-Varela et al. (MF896); **8 –** Prosternum of *Cycreon floricola floricola* Arriaga-Varela et al. (MF896); **9 –** Ventral view of mouth parts of *Cycreon floricola floricola* Arriaga-Varela et al. (MF896); **10 –** Prosternum of *Moraphilus sulcatus* d'Orchymont (MF1655); **11 –** Mentum of *Nitidulodes jansoni* Sharp (MF1632); **12 –** Meso- and metaventrite of *Cercyon spiniventris* Arriaga-Varela et al. (MF1216); **13 -** Mentum of *Cercyon spiniventris* Arriaga-Varela et al. (MF1216); **14 –** Meso and metaventrite of *Pelosoma* sp. (MF1029).

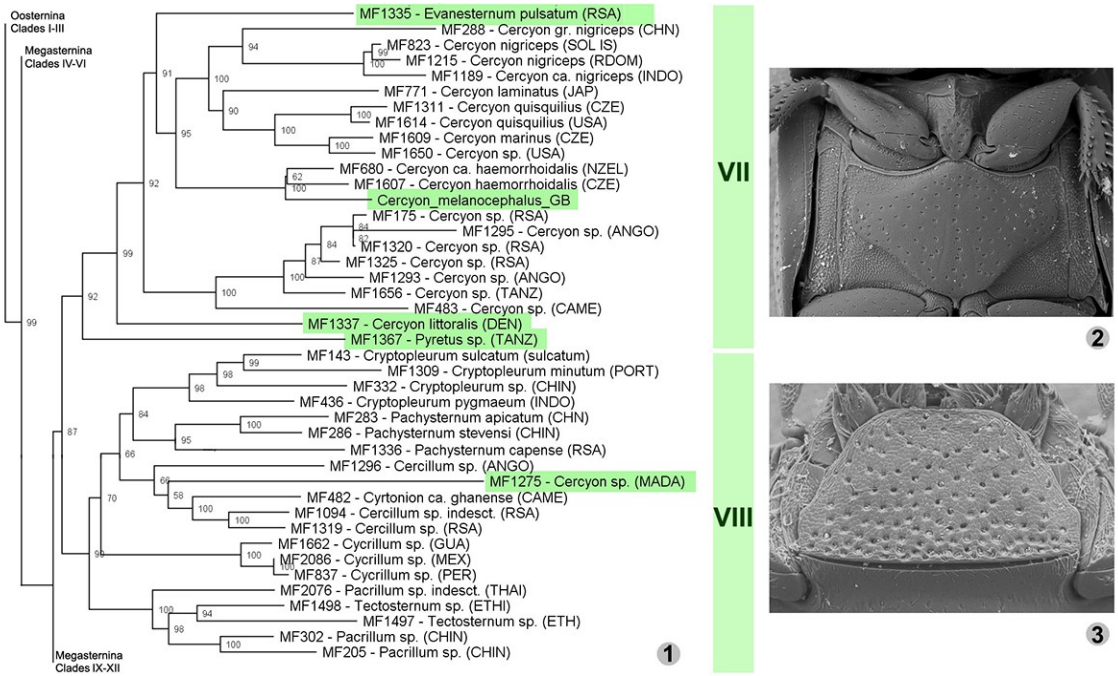

Figure F. 1 - Portion of the phylogenetic tree obtained by ML in IQtree of the *IN* dataset showing the position of '*wild-card*' taxa (marked in green); **2 –** Meso- and metaventrite Evanesternum pulsatum (d'Orchymont) (MF1335); **3 -** Mentum of *Pyretus* sp. (MF1367).

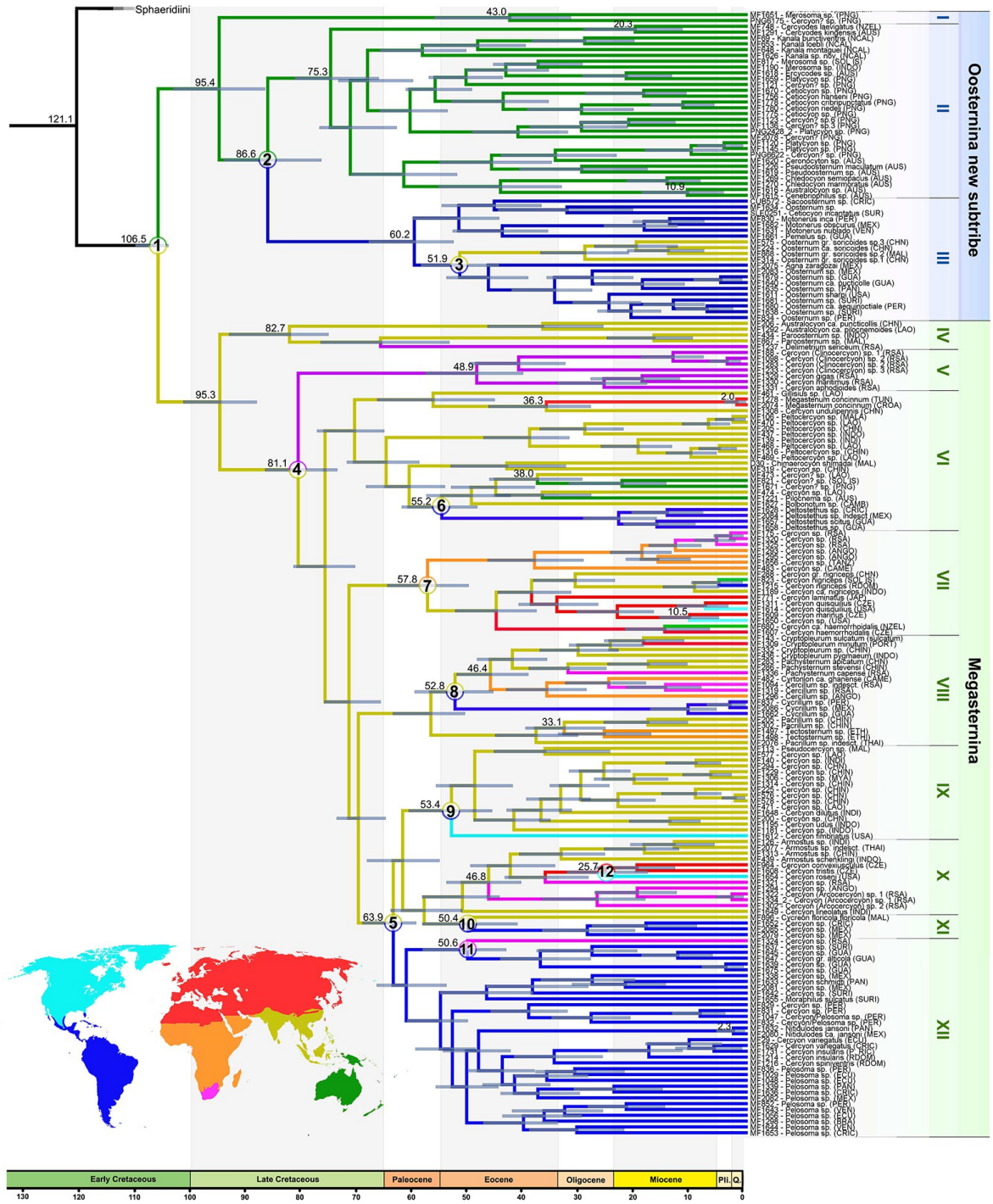

Figure G. Simplified scheme of the ancestral area estimation of the tribe Megasternini by BioGeoBears under DIVALIKE model. The seven regions used in the biogeographical analyses are as follows: Oriental (light green), Australian (dark green), Afrotropical (orange), South African (purple), Palearctic (red), Nearctic (light blue), Neotropical (dark blue). Nodes 1-12 are discussed in the text. Mean divergence ages shown fro selected nodes.

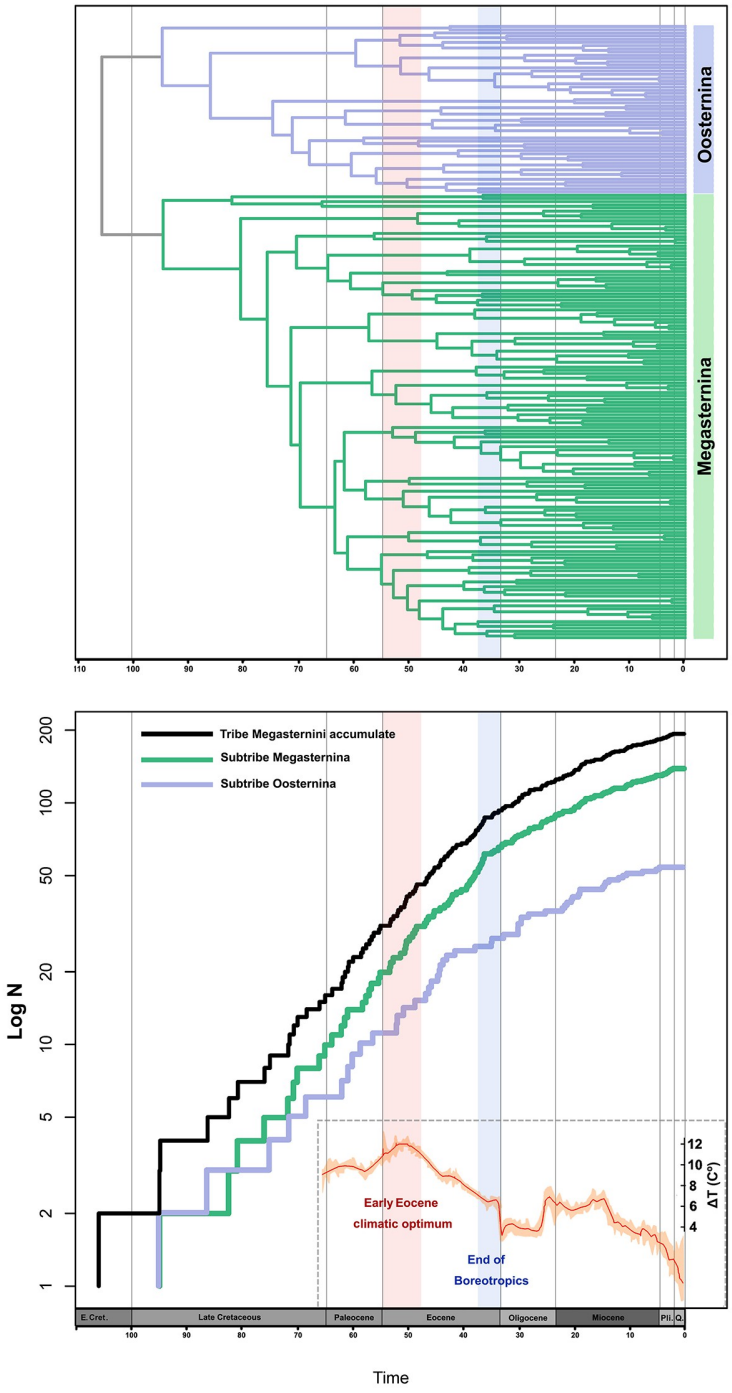

Figure H. Divergence through time in Megasternini. Upper recangle: Simplified dated topology of Megasternini. Lower rectangle: A lineage through time plot showing divergence time distribution of whole Megasternini tribe (black line), subtribe Megasternina (green line), new subtribe Oosternina (blue line). Global temperature curve over time is shown in lowe-lef corner. Data is estimated from oxygen isotopic patterns in deep-sea benthic foraminifera, which are proportional to temperature and total ice-sheet mass (adapted from Zachos et al. 2001). Red bar represents the Early Eocene climatic optimum and blue bar represents the decline of the boreotropical community due to lower temperatures.

Supplementary files
Chapter 7

- Supplementary file 1. Locality data for specimens used in this work

- Supplementary file 2. Succesfully amplified gene regions by specimen.

- Supplementary file 3. Resulting tree of *EX* dataset obtained in MrBayes. Estimated man age shown in nodes.

- Supplementary file 4. Resulting tree of *EX* dataset obtained in IQTree. Ultra Fast Bootstrap values shown in nodes.

- Supplementary file 5. Resulting tree of *IN* dataset obtained in IQTree. Ultra Fast Bootstrap values shown in nodes.

- Supplementary files 6. Resulting trees showing ancestral area estimation from BioGeoBears analyses.

MF CODE	Genus	Species	Country	Province	Locality	Elev	Date	Coordinates	Collector
29	Cercyon	variegatus group	Ecuador	Napo	4,4km NWW El Chaco, excrements	1690m	28-30.xi.2006		Fikáček & Skuhrovec
69	Kanala	punctiventris	New Caledonia	Prov. Nord	Mont Panié	200-500m	22.iii.2007	20°49'S/164°49'E	R. Leschen
106	Pellocercyon	sp.	W Malaysia		Ulu Gombak Field Studies Centre, in decaying Arthrocarpus fruit		25.viii.2007		D. Kovac
113	Pseudocercyon	sp. (wide mesoventr.)	W Malaysia		Ulu Gombak Field Studies Centre, felled young bamboo (G. Scortechinii) on ground		24.viii.2007		D. Kovac
126	Armostus	sp.	India	Meghalaya	E Khasi Hills, 11 km SW of Cherapunjee, Laitkynsew, secondary tropical rainforest with young trees + bamboo below village, thin layer of leaf litter	735m	25.iv.2008	25°12'48"N 91°39'48"E	25°12'48"N Fikáček, Podskalská, Šípek
139	Pellocercyon	sp.	India	Arunachal Pradebushes	1,5 km NE of Bomdila, nr. Bomdila pass, in cow excrements in dense evergreeen	2600m	2.-5.v.2008	27°16'34"N 92°25'49"E	27°16'34"N 92°25'49"E27°16'34"N Fikáček, Podskalská, Šípek
140	Cercyon	sp. 1	India	Arunachal Pradebushes	1,5 km NE of Bomdila, nr. Bomdila pass, in cow excrements in dense evergreeen	2600m	2.-5.v.2008	27°16'34"N 92°25'49"E	27°16'34"N 92°25'49"E27°16'34"N Fikáček, Podskalská, Šípek
143	Cryptopleurum	*sulcatum*	India	Assam	1,5 km S of Kohora (= Kaziranga village), cow + goat excrements	160m	16.-18.iv.2008	27°34'34"N 93°24'23"E	27°34'34"N 93°24'23"E27°34'34"N Fikáček, Podskalská, Šípek
175	Cercyon	sp.	RSA	KwaZulu-Natal	Mendeka Wilderness Area, Ngomi Forest		24-27.xi.2006	27°51'S 31°23'E	J. Janák
188	Cercyon	sp.	RSA		Mtumeni		2006		Bulirsch & Janák
200	Cercyon	sp. 1 (large, black)	China	Hainan	Bawangling Nat. Forest Park, 12,3 km SEE of Baotie	1050 m	8.v.2011	19°5,20'N 109°11,80'E,	Fikáček
202	Pellocercyon	sp. nov.	China	Hainan	Bawangling Nat. Forest Park, 12,3 km SEE of Baotie	1050 m	8.v.2011	19°5,20'N 109°11,80'E,	Fikáček
205	Pacrilium	sp. nov.	China	Hainan	Bawangling Nat. Forest Park, 12,3 km SEE of Baotie	1050 m	8.v.2011	19°5,20'N 109°11,80'E,	Fikáček
206	Australocyon	cf. Puncticollis	China	Hainan	Bawangling Nat. Forest Park, 12,3 km SEE of Baotie	1050 m	8.v.2011	19°5,20'N 109°11,80'E,	Fikáček
224	Oosternum	soricoides group	China	Jiangxi	Jinggangshan Mts, Xiangzhou, forested valley S of the villageú, cut and decaying tops of bamboo trunks	374 m	26.iv.2011	26°35,5'N, 114°16,0'E	Fikáček
225	Cercyon	sp.	China	Jiangxi	Jinggangshan Mts, Xiangzhou, forested valley S of the villageú, cut and decaying tops of bamboo trunks	374 m	26.iv.2011	26°35,5'N, 114°16,0'E	Fikáček
283	Pachysternum	apicatum	China	Hainan	Jianfengling Mts., Tiachi lake env., Bishu villa, rotten banana	950 m	9-11.v.2011	18°44,7'N 108°50,7'E	Fikáček
286	Pachysternum	stevensi	China	Jiangxi	Jinggangshan Mts., Jingzhushan, cow excrements	640 m	25.iv.2011	26°31,0'N, 114°05,9'E	Fikáček
288	Cercyon	sp. (migriceps group)	China	Jiangxi	Jinggangshan Mts., Jingzhushan, cow excrements	640 m	25.iv.2011	26°31,0'N, 114°05,9'E	Fikáček
294	Cercyon	sp.	China	Jiangxi	Jinggangshan Mts., Huyagla, rotting bamboo tops	1490 m	28.iv.2011	26°29,9'N, 114°07,3'E	Fikáček
302	Pacrilium	sp.	China	Jiangxi	Jinggangshan Mts., Songmuping, rotten bamboo tops	1280 m	27.iv.2011	26°34,7'N, 114°04,3'E	Fikáček, Hájek
312	Sphaeridium	sp.	China	Jiangxi	Jinggangshan Mts, Xiangzhou, forested valley S of the village, cow excrements	374 m	26.iv.2011	26°35,5'N, 114°16,0'E	Fikáček
314	Oosternum	sp.	China	Jiangxi	Jinggangshan Mts., Pingshuishan, sifting of dried-up fen and around	1590 m	28.iv.2011	26°30,4'N, 114°06,9'E	Fikáček
319	Cercyon	sp.	China	Hainan	Limushan Mts., along the road, rotting banana trunks	550-750 m	5.v.2011	19°9,1-8,2'N 109°45-46'E	Fikáček, Zhao
326	Coelostoma	phallicum	China	Hainan	Bawangling Mts., 2 km SEE of Baotie, exposed pools on horizontal rock shelves along the river	195 m	7.v.2011	19°6,63'N 109°6,10'E	Fikáček
332	Cryptopleurum	sp.	China	Jiangxi	Jinggangshan Mts, Xiangzhou, forested valley S of the village, rice fields	374 m	26.iv.2011	26°35,5'N, 114°16,0'E	Fikáček
434	Paroosternum	sp.	Indonesia	E Kalimantan	Muara Ritan, border of fields and rainforest in foothl near Belayan river	48m	5.xii.2011	00°24,0´N 116°03,1´E	Hájek, Schneider & Votruba
436	Cryptopleurum	pygmaeum	Indonesia	E Kalimantan	Muara Ritan, border of fields and rainforest in foothl near Belayan river	48m	5.xii.2011	00°24,0´N 116°03,1´E	Hájek, Schneider & Votruba
437	Pellocercyon	sp.	Indonesia	E Kalimantan	Muara Ritan, border of fields and rainforest in foothl near Belayan river	48m	5.xii.2011	00°24,0´N 116°03,1´E	Hájek, Schneider & Votruba
439	Armostus	sp.	Indonesia	E Kalimantan	Muara Ritan, border of fields and rainforest in foothl near Belayan river	48m	5.xii.2011	00°24,0´N 116°03,1´E	Hájek, Schneider & Votruba
461	Gillisius	sp.	Laos	Houa Phan	Phou Pane Mt., primary mountain forest, FIT	1480-1510m	2.-22.vi.2011	20°13´09-19´´N 103°59´54´´-104°V,	Kubáň
468	Pellocercyon	sp.	Laos	Houa Phan	Phou Pane Mt., primary mountain forest, FIT	1480-1510m	2.-22.vi.2011	20°13´09-19´´N 103°59´54´´-104°V,	Kubáň
469	Pellocercyon	sp.	Laos	Houa Phan	Phou Pane Mt., primary mountain forest, FIT	1480-1510m	2.-22.vi.2011	20°13´09-19´´N 103°59´54´´-104°V,	Kubáň
470	Pellocercyon	sp.	Laos	Houa Phan	Phou Pane Mt., primary mountain forest, FIT	1480-1510m	2.-22.vi.2011	20°13´09-19´´N 103°59´54´´-104°V,	Kubáň
471	Cercyon (s.str.)	sp.	Laos	Houa Phan	Phou Pane Mt., primary mountain forest, FIT	1480-1510m	2.-22.vi.2011	20°13´09-19´´N 103°59´54´´-104°V,	Kubáň
473	Cercyon (? Clinocercyon)	sp.	Laos	Houa Phan	Phou Pane Mt., primary mountain forest, FIT	1480-1510m	2.-22.vi.2011	20°13´09-19´´N 103°59´54´´-104°V,	Kubáň
474	Cercyon (s.str.)	sp.	Laos	Houa Phan	Phou Pane Mt., primary mountain forest, FIT	1480-1510m	2.-22.vi.2011	20°13´09-19´´N 103°59´54´´-104°V,	Kubáň
482	Cyrtonion	cf. ghanense	Cameroon	Northwest Provin	Big Babanki village env., 21 km NE of Bamenda, sifting along stream	2137m	25.i.2012	6°5´24,30´´N 10°17´56,36´´E	P. Janšta
483	Cercyon	sp.	Cameroon	Northwest Provin	Big Babanki village env., 21 km NE of Bamenda, sifting along stream	2137m	25.i.2012	6°5´24,30´´N 10°17´56,36´´E	P. Janšta
575	Oosternum	sp.	China	Guangdong	Danxia Shan NP, WoLongGang Forest Walkway, baited pitfall trap (pasti N)	100m	23.-26.iv.2013	25°01,3'N, 113°44,5'E	J.Hájek & J.Růžička leg.
576	Cercyon	sp.	China	Guangdong	Danxia Shan NP, WoLongGang Forest Walkway, baited pitfall trap (pasti N)	100m	23.-26.iv.2013	25°01,3'N, 113°44,5'E	J.Hájek & J.Růžička leg.
577	Cercyon	sp.	China	Guangdong	Danxia Shan NP, WoLongGang Forest Walkway, baited pitfall trap (pasti N)	100m	23.-26.iv.2013	25°01,3'N, 113°44,5'E	J.Hájek & J.Růžička leg.
578	Cercyon	sp.	China	Guangdong	Danxia Shan NP, WoLongGang Forest Walkway, baited pitfall trap (pasti L)	100m	23.-26.iv.2013	25°01,3'N, 113°44,5'E	J.Hájek & J.Růžička leg.
648	Kanala	montaguei	New Caledonia		Farino refuge	260m	3.xi.2010	-21,6488/165:7812	R. Ruta & M. Wanat
653	Kanala	boetii	New Caledonia		Pic du Pin (base)	280m	30.x.2010	-22,2484/166,8288	R. Ruta & M. Wanat
680	Cercyon	haemorrhoidalis	New Zealand	Gisborne	TeUrevera NP, Lake Waikaremoana Motorcamp, on roadside killed possum	600m	22.-26.xi.2012	38°45,3'S 177°9,4'E	Becker, Fikáček, Hájek
748	Cercyodes	laevigatus	New Zealand	Westland	Jackson Bay (at the end of Jackson Bay Rd.), in thick layer of accumulated seaweed on the beach at the inlet of a small stream	0m	12.xii.2012	43°58,3'S 168°36,9'E	Fikáček, Hájek & Leschen
771	Cercyon	laminatus	Japan	Kagoshima pref.	Tokunoshima island, Amagi-dake, primary forest, FIT		27.v-7.vi.2012		Lackner
817	Merosoma	sp.	Solomon Islands	Guadalcanal	ca. 8 km E of Honiara, Lungga river, gardens, in rotten Musa	45 m	20.xi.2013	9°25,5'S 160°1,6'E	J. Hájek
821	Cercyon	sp.	Solomon Islands	Guadalcanal	Mt. Austine, Barana env., gardens, in rotten Musa	280 m	23.xi.-8.xii.2013	9°28'S 159°58,4'E	J. Hájek
823	Cercyon (Paracycreon)	sp.	Solomon Islands	Guadalcanal	ca. 8 km E of Honiara, Lungga river, gardens, in rotten Musa	45 m	20.xi.2013	9°25,5'S 160°1,6'E	J. Hájek
829	Cercyon	sp. (big Cercyon)	Peru	Paucartambo	Wayqecha Biological Station, Winkler extraction, sifted cloud forest litter	2900m	16-18.x.2013	13°10'29,28"S 71°35'13,92"W	J. Parker
830	Motonerus	cf., inca sp. nov.)	Peru	Paucartambo	Wayqecha Biological Station, Winkler extraction, sifted cloud forest litter	2900m	16-18.x.2013	13°10'29,28"S 71°35'13,92"W	J. Parker
831	Cercyon	sp. (pale coloured)	Peru	Paucartambo	Wayqecha Biological Station, Winkler extraction, sifted cloud forest litter	2900m	16-18.x.2013	13°10'29,28"S 71°35'13,92"W	J. Parker
832	Cercyon	sp. (spotted elytra)	Peru	Paucartambo	Wayqecha Biological Station, Winkler extraction, sifted cloud forest litter	2900m	16-18.x.2013	13°10'29,28"S 71°35'13,92"W	J. Parker
834	Oosternum	sp. (maybe 2 species)	Peru	Paucartambo	Cock of the Rock Lodge, Winkler extraction, sifted cloud forest litter	1120m	12-16.x.2013	13°03'24,9"S 71°32'43,8"W	J. Parker
836	Pelosoma/Agna	sp. (colorful!)	Peru	Paucartambo	Cock of the Rock Lodge, Winkler extraction, sifted cloud forest litter	1120m	12-16.x.2013	13°03'24,9"S 71°32'43,8"W	J. Parker
837	Cycrilium	sp.	Peru	Paucartambo	Cock of the Rock Lodge, Winkler extraction, sifted cloud forest litter	1120m	12-16.x.2013	13°03'24,9"S 71°32'43,8"W	J. Parker
852	Pelosoma	sp. (flat bicolored)	Peru	Paucartambo	Cock of the Rock Lodge, sieving cloud forest litter	1120m	12-16.x.2013	13°03'24,9"S 71°32'43,8"W	J. Parker
863	Omicrus	sp.	Peru	Paucartambo	Cock of the Rock Lodge, sieving cloud forest litter, in Pheidole cf. Xanthogaster nest	1120m	12-16.x.2013	13°03'24,9"S 71°32'43,8"W	J. Parker
865	Psaltrus	sp.	Malaysia	Perak	Taiping, Bukit Laruk (Maxwell Hill)	90m	4.x.2011	4°51,499N 100°45,582E	J. Parker
867	Paroosternum	sp.	Malaysia	Perak	Taiping, Bukit Laruk (Maxwell Hill)	90m	4.x.2011	4°51,499N 100°45,582E	J. Parker
868	Oosternum	sp. (soricoides group)	Malaysia	Perak	Taiping, Bukit Laruk (Maxwell Hill)	90m	4.x.2011	4°51,499N 100°45,582E	J. Parker
896	Cycreon	sculpturatus	Malaysia	Kelantan	Gua Musang prov., Kuala Koh distr., Taman Negara, 700 m from entrance, Schismaglottis sp.	96m	11.i.2014	4°52,333N 102°26,872E	HY Chen
964	Cercyon	convexiusculus (cf.)	Czech Republic	Bohemia	Praha-Kunratice, Kunratický les, ca. 200 m downstream from Dolnokunratický pond	200m	5.vi.2014	50°1,1'N 14°28,6'E	Fikáček & Sýkora
1029	Cercyon	sp. (big Cercyon)	Ecuador		50 km SW of Quito, San Francisco de las Pampas, Otonga Reserve	1500 m	5-6.xii.2010	0°25´S 79°00W	Bolm
1047	Cercyon	sp. (small spotted)	Ecuador	Napo	Cosanga	1900-2100m	12-16.xii.2010	0°36´S 77°53´W	Bolm
1048	Cercyon	sp. (large, black)	Ecuador	Napo	Cosanga	1900-2100m	12-16.xii.2010	0°36´S 77°53´W	Bolm
1056	Pelosoma	sp.	Ecuador		6 km W of Zamora	900 m	24-25.xii.2010	4°08´S 78°55´W	Bolm

Supplementary file 1 (1/3). Locality data for specimens used in this work

MF CODE	Genus	Species	Country	Province	Locality	Elev	Date	Coordinates	Collector
1063	Phaenonotum	exstriatum	USA	Delaware					
1094	Cercillum	sp.	RSA	KwaZulu-Natal	Karkloof Forest, Bushwillow to waterfall trail, km. 1-3. Sifting.	1350-1500 m	8.xi.2013	-29,3017° S, 30,2976° E	M. Wanat
1098	Cercyon s. str.	sp.	RSA	KwaZulu-Natal	Karkloof Forest, Bushwillow to waterfall trail, km. 1-3. Sifting.	1350-1500 m	8.xi.2013	- 29,3017° S, 30,2976° E	M. Wanat
1120	Platycyon	sp.	Papua New Guinea						
1121	Cercyon	sp.	Papua New Guinea						
1123	Cercyon	sp.	Papua New Guinea						
1136	Cercyon	sp.	Papua New Guinea						
1145	Platycyon	sp.	Papua New Guinea						
1181	Cercyon	sp.	Indonesia	South Sulawesi	Gowa Distr., 6 km E Malino, Gn. Bawakaraeng Area, border of gardens and mixed forest (dominant Pinus) nr. Lembanna camp.	1520 m.	11-13.II.2015	05°15,4' S, 119°54,5' E	J. Hájek & J. Sumpich
1189	Cercyon	ca. nigriceps	Indonesia	Papua	Jayapura Distr., Sentani env., From Bos excrements	80-150 m.	28-29.II.2015	02°33-35' S, 140°31-32' E	J. Hájek & J. Sumpich
1190	Merosoma	sp.	Indonesia	Papua	Jayawijaya Distr. Baliem valley, 14 km NNE of Wamena wetland & gardens nr Jiwika (Kurulu)	1660 m.	6.II.2015	03°58,0-5' S, 138°55,8-56,3' E	J. Hájek & J. Sumpich
1192	Cryptopleurum?	sp.	Indonesia	Papua	Jayawijaya Distr. Baliem valley, 14 km NNE of Wamena wetland & gardens nr Jiwika (Kurulu)	1660 m.	6.II.2015	03°58,0-5' S, 138°55,8-56,3' E	J. Hájek & J. Sumpich
1195	Cercyon	sp.	Indonesia	Papua	Bali: Bedugang Distr. Tamblingan - Danau Tamblingan (lake) montane forest around lake	1250 m.	19-21.II.2015	08°16,1' S, 115°05,5-9' E	J. Hájek & J. Sumpich
1214	Cercyon	insularis	Dominican Republic	Monseñor Nouel	PN La Humeadora; ; 11,6km SSW of Piedra Blanca; in horse excrement in moist broad-leaf forest in a valley of small stony stream DR41	636 m.	8.iv.2014	13°44,92' N, 70°21,63' W	Delar, Fikáček, Gimmel
1215	Cercyon	nigriceps	Dominican Republic	Monseñor Nouel	PN La Humeadora; ; 11,6km SSW of Piedra Blanca; in horse excrement in moist broad-leaf forest in a valley of small stony stream DR41	636 m.	8.iv.2014	13°44,92' N, 70°21,63' W	Delar, Fikáček, Gimmel
1216	Cercyon	spiniventris	Dominican Republic	Monseñor Nouel	PN La Humeadora; ; 11,6km SSW of Piedra Blanca; in horse excrement in moist broad-leaf forest in a valley of small stony stream DR41	636 m.	8.iv.2014	13°44,92' N, 70°21,63' W	Delar, Fikáček, Gimmel
1221	Pilocnema	sp.	Australia	Queensland	Daintree National Park, Mt. Lewis, Brooklin Wildlife Sanctuary, 11 km up the Mt. Lewis Road, Sifted litter.	975 m.	19.ii.2012	16°35'46,0" S, 145°17'4,0" E	N. Scharff, J. Pedersen & G. Hormiga
1226	Pseudoosternum	maculatum	Australia	Queensland	Atherton Tablelands, Tully Falls National Park S. of Ravenshoe, Charmillin Creek, Wabunga Wayemba Rainforest Walkabout	931 m.	12.ii.2012	17°42'0,3" S, 145°31'20,8" E	N. Scharff, J. Pedersen & G. Hormiga
1229	Cercyon / Platycyon	sp.	China	Guangdong	PN La Humeadora; ; 11,6km SSW of Piedra Blanca; in horse excrement in moist broad-leaf forest in a valley of small stony stream DR41	100 m.	23-26.iv.2013	25°01,3' N, 113°44,5' E	J. Hájek & J. Ruzicka
1233	Cercyon	sp.	South Africa	Western Cape	Hottentots Holland NR borders, Mt. Rochelle-Perdekloof, nr. Franschhoek pass		26.x.2013	33°54,2' S, 19°9,8" E	P. Bulirsch
1237	Dellmetrium	sp.	South Africa	Western Cape	Table Mts. NP. Echo valley, indig. forest.		10.x.2013	34°7' S, 18°27' E	P. Bulirsch
1269	Chlaeocyon	semiopacus	Australia	Western Australia	Leeuwin Naturaliste N.P.		21.x.2007		C. Carlton & R. Leschen
1270	Chlaeocyon	marmoratus	Australia	Western Australia	Yalgorup National Park		24.x.2007		C. Carlton & R. Leschen
1278	Megasternum	sp.	Tunisia	Jendouba	2,6 km N from Ain Sebaa. Cork-oak old forest, sifting in wet depressions and forest		15.x.2014	36°58'35,6" N, 8°56'12,7"	A. Damaska, D. Benda, M. Mikát & K. Minarová
1283	Cercyon	sp.	South Africa	Eastern Cape	Kubusi State forest		31.i-1.ii.2012	32°32,5' S, 27°21,4' E	J. Janák
1291	Cercyodes	kingensis	Australia	Tasmania	Maria Island, Cape Boullanger, under wrack on stony beach			42.14467° S, 148°07980 E	JWE ?
1292	Australocyon	ca. pilocnemoides	Laos	Houa Phan	Phou Pane Mt. Primary mountain forest. Flight intercept trap.	1870 m	14-24.vi.2012	20°11'50" N, 104°01'04" E	Vit. Kubán. Laos 2012 Expedition National Museum Prag
1293	Cercyon	sp.	Angola		Catabola FIT				
1294	Cercyon	sp.	Angola		Catabola FIT				
1295	Cercyon	sp.	Angola		Catabola FIT				
1296	Cercillum	sp.	Angola		Catabola FIT				
1298	Pelosoma	sp.	Brazil	Sao Paulo	Salesópolis, env. Boracéia Biol. Station (MZSP). Fallen fruits		19.-22.2012	23°39'14" S, 45°53'22" W	Exp. Muz. Zool. Sao Paulo et Petr. Sipek
1302	Cercyon	sp.	South Africa	KwaZulu Natal	Pietermaritzburg, Acacia Loge, ad luc.	620 m	07.xii.2012	29,60870° S, 30,45761° E	P. Jałoszynski
1306	Cercyon	sp.	Burma	Shan State	Kalaw env.	1300-1600 m	6-9.x.2014	20°35' N, 96°31'E	Fouqué René
1308	Cercyon	sp.	China	Sichuan prov.	Leshan, Emeishan, Leidongping, parking lot, shops and hotels. Sweeping and indiv. Collect.	2400 m	9.vi.2014	29°32'25" N, 103°19'52"E	J. Hájek, J. Ružicka & M. Tkoc
1309	Cryptopleurum	sp.	Portugal	Alto Tras os mon	Peneda Gerês National Park, ca. 5km radius around: Castro Laboreiro		05-13.v.2015	42,028967° N, -8,155048°	M. Seidel
1311	Cercyon	quisquilius	Czech Republic	Prague	Natural History Museum, Horni Pocernice		10.vii.2015		
1313	Armostus ?	sp.	China	Guangxi	Pangxie Gou, 1,3 km S of Longsheng Hot Spring. Sifting of leaf litter and leaf accumulations along stony stream in evergreen lowland subtropical forest (sifting sample 13)	386 m	13.iv.2013	25°53,0' N, 110°12,6' E	Fikácek, Hájek & Ruzicka
1314	Cercyon	sp.	China	Guangxi	Shivandashan National Forest Park 28.75 km SSW of Shangsi. Baited pitfall traps (rotten cheese+fish) in secondary broad-leaf evergreen forest with sparse understory and rich in leaf litter	300 m	5-9.iv.2013	21°54,3' N, 107°54,2' E	Fikácek, Hájek & Ruzicka
1316	Peltocercyon	sp.	China	Guangxi	Shivandashan National Forest Park 28.75 km SSW of Shangsi. Baited pitfall traps (rotten cheese+fish) in secondary broad-leaf evergreen forest with sparse understory and rich in leaf litter	300 m	5-9.iv.2013	21°54,3' N, 107°54,2' E	Fikácek, Hájek & Ruzicka
1319	Cercillum?	sp.	South Africa	Mpumalanga	Mariepskop, bush pig trail.	1555 m	17.xi.2012	24,56651° S, 30,86382° E	P. Jałoszynski
1320	Cercyon	sp.	South Africa	KwaZulu Natal	Durban-Westville, along stream	270 m	06.xii.2012	29,81455° S, 30,90844° E	P. Jałoszynski
1321	Cercyon	sp.	South Africa	Western Cape	De Hoop Nature Reserve; De Hoop vlei at Tierhoek. Sifting of fine wet plant litter accumulations on the shore of the vlei in the area without plants and many animal footprints.	20 m	24.xi.2015	34°26,92' S, 20°24,650' E	Arriaga-Varela, Fikáček, Seidel & Vondráček
1322	Cercyon	sp.	South Africa	Western Cape	De Hoop Nature Reserve; De Hoop vlei at Tierhoek. Sifting of fine wet plant litter accumulations on the shore of the vlei in the area without plants and many animal footprints.	20 m	24.xi.2015	34°26,92' S, 20°24,650' E	Arriaga-Varela, Fikáček, Seidel & Vondráček
1324	Cercyon	sp.	South Africa	Western Cape	14,8 km NE of Knysna,Diepwalle Forest at Black Elefant Walk. Afrotemperate mixed forest with sparse podocarps and tree ferns: on excrements.	420 m	19.xi.2015	33°57,36' S, 23°10,49' E	Arriaga-Varela, Fikáček, Seidel & Vondráček
1325	Cercyon	sp.	South Africa	Western Cape	14,8 km NE of Knysna,Diepwalle Forest at Black Elefant Walk. Afrotemperate mixed forest with sparse podocarps and tree ferns: on excrements.	421 m	19.xi.2015	33°57,36' S, 23°10,49' E	Arriaga-Varela, Fikáček, Seidel & Vondráček
1329	Cercyon	sp.	South Africa	Western Cape	Onrus River Beach, In/under small dry pieces of beachwrack on the sandy beach	0 m	3.xii.2015	34°25,17' S, 19°10,70' E	Arriaga-Varela, Fikáček, Seidel & Vondráček
1330	Cercyon	sp.	South Africa	Western Cape	Onrus River Beach, In/under small dry pieces of beachwrack on the sandy beach	0 m	3.xii.2015	34°25,17' S, 19°10,70' E	Arriaga-Varela, Fikáček, Seidel & Vondráček
1331	Cercyon	sp.	South Africa	Western Cape	Onrus River Beach, In/under small dry pieces of beachwrack on the sandy beach	0 m	3.xii.2015	34°25,17' S, 19°10,70' E	Arriaga-Varela, Fikáček, Seidel & Vondráček
1334	Cercyon	sp.	South Africa	Western Cape	dung		26.x-2.xii.2015		
1336	Pachysternum	capense	South Africa	Western Cape	dung		26.xi-2.xii.2015		
1338	Cercyon	sp.	Mexico	Veracruz	Matlalapa, sifting leaf litter, extr. Winkler				F. Alvarado, E. Arriaga-Varela
1339	Pelosoma?	sp.	Panama	Chiriqui	La Fortuna-Cont Divide Trail. In costus sp. inflorescence	1170-1270 m	19.v.2015	08°47,069' N, 82°12,855' W	L. Sekerka & K. Stajerova
1497	Tectosternum	sp. (large)	Ethiopia		Bonga. Sift 30.	2247 m	11.x.2014	7,5056° S, 36,1068° E	Local collector
1498	Tectosternum	sp. (small)	Ethiopia		Bonga. Sift 30.	2247 m	11.x.2014	7,5056° S, 36,1068° E	Local collector
1607	Cercyon	haemorrhoidalis	Czech Republic	Moravia	Břeclav, Pools on meadow, decaying vegetation		23.iv.2016	48,720722°N, 16,899457° E	M. Seidel
1608	Cercyon	? tristis/granarius	Czech Republic	Moravia	Břeclav, Pools on meadow, decaying vegetation		23.iv.2016	48,720722°N, 16,899457° E	M. Seidel
1609	Cercyon	marinus	Czech Republic	Moravia	Břeclav, Pools on meadow, decaying vegetation		23.iv.2016	48,720722°N, 16,899457° E	M. Seidel
1611	Oosternum	sharpi (?)	USA	California	Santa Barbara, SBMNH grounds, sifting flood debris	100m	11.i.2016	34,44061° -119,71463°	M. Gimmel
1612	Cercyon	fimbriatus	USA	California	Santa Barbara, Jalama Beach, under seaweed		25.viii.2015	34.51282° -120.50408°	M. & L. Gimmel
1614	Cercyon	quisquilius	USA	Arizona	Pinal Co., 10 mi S of Florence on AZ-79, UV/MV light	600m	25.iv.2015	32,9019° -111,2805°	M. Gimmel & L. Indruchová
1615	Cenebriophilus	sp.	Australia	Queensland	Majors Mt summit, Mushroom trap.	1140 m	19.iv.2010	17,642° S, 145,534° E	G. Monteith
1616	Australocyon	sp.	Australia	Queensland	Majors Mt summit. Mushroom trap.	1140 m	19.iv.2010	17,642° S, 145,534° E	G. Monteith
1618	Ercycodes / Merosoma	sp.	Australia	Queensland	East Claude River. FIT traps, mushroom & banana bait	15 m	10-11.xii.2010	12,714° S, 143,287° E	Monteith & Aland
1619	Pseudoosternum	sp.	Australia	Queensland	Chilli Beach, Litter Berselate, 34795	5 m	11.xii.2010	12,630° S, 143,421° E	Monteith & Escalona
1620	Ceronocyton	sp.	Australia	New South Wales	Minamurra Rainforest. Pitfall trap.		20.xi.2010	34.633874°, 150.73668820° E	N. Gunter and B. Lessard
1626	Kanala	sp. nov.?	New Caledonia		Mt Humboldt, moss forest.	1300 m	13.11.2010	-0.1314836102	
1627	Bolbonotum	sp.	Cambodia		Kririrom NP. Disturbed tropical forest. Carrion (octopus) trap	369 m	8-17.12.2010	11° 18.652' N, 104°6.051' E	S.Tarasov
1628	Deltostethus	sp.	Costa Rica	Alajuela					

Supplementary file 1 (2/3). Locality data for specimens used in this work

MF CODE	Genus	Species	Country	Province	Locality	Elev	Date	Coordinates	Collector
1629	Cercyon	variegatus group	Costa Rica	Alajuela					
1631	Motonerus	cf. nutkaido	Venezuela	Trujillo	Laguna Agua Negra, margin of lagoon w/vegetation	1840 m	13.vii.2009	9°18.373 N, 70°10.516' W	Short et al. VZ09-0713-03A
1632	Nitidulodes	sp.	Panama	Coclé					
1633	Cercyon	schmidti	Panama	Chiriqui Prov.	Parque Internacional La Amistad. In rotten flowers.		17.vi.2008	8°53'37.3" N, 82°36'54.8" W	A.E.Z., Short
1634	"Oosternum grandis group"	sp.	Suriname	Sipaliwini	Camp 2, on Sipaliwini River. Dung trap	210 m	28-30.vii.2010	2°10.973' N, 56°47.235' W	Short
1635	Oosternum	sp.	Panama	Chiriqui Prov.	Parque Internacional La Amistad, Retoño trail: sifting litter		16-17.vi.2008	8°53'37.3" N, 82°36'54.8" W	A.E.Z., Short
1636	Pelosoma	sp.	Costa Rica	Cartago					
1637	Cercyon	sp.	Suriname	Sipaliwini					
1638	Oosternum	sp.	Suriname	Sipaliwini					
1639	Cercyon	sp.	Guatemala	Suchitepéquez	4 km S Vol. Atitlán. Cloud forest, ex sifted leaf litter.	1650 m	15.VI.2009	14,55008° N, 91,19374° W	LLAMA09 Wm-B-09-2-04
1640	Oosternum	sp.	Guatemala	Suchitepéquez	5 km S Vol. Atitlán. Cloud forest. ex sifted leaf litter.	1625 m	15.VI.2009	14,54915° N, 91,19055° W	LLAMA09 Wa-B-09-2-01-all
1642	Cercyon	sp.	Suriname	Sipaliwini	Camp 2, on Sipaliwini River. Dung trap	210 m	28-30.vii.2010	2°10.973' N, 56°47.235' W	
1643	Pelosoma	sp.	Venezuela	Tachira	El Tamá National Park. Heliconia inflorescences. VZ09-0716.06A	525 m	16.vii.2009	7°34.243' N, 72°12.134' W	Short & Gustafson
1644	Pelosoma	sp.	Venezuela	Tachira	El Tamá National Park. Heliconia inflorescences. VZ09-0716.06A	525 m	16.vii.2009	7°34.243' N, 72°12.134' W	Short & Gustafson
1645	Cercyon	sp.	Guatemala	Sacatepéquez	5km SE Antigua. Oak forest. Sifted litter	2455 m	10.vi.2009	14.52429° N, 9068846' W	LLAMA09 Wm-B-08-2-02
1647	Cercyon	silicola group	Guatemala	Jalapa	4km E Mataquescuintla. Cloud forest. Flight intercept trap	2615 m	1-4.vi.2009	14.52943° N, 90.14811° W	LLAMA09-FLB-07-1-01
1648	Cercyon	dilutus group	India	Maharashtra					
1649	Cercyon	lineolatus	India	Sanguem	nr. Bhagvan Mahaveer Sanct, 100 m E, Molem, Hg-vapor light	342 ft	24-25.ix.2005	15°22'43" N, 74°13'52" E	
1650	Cercyon	sp.	USA	Montana	Utah Co., E. Utah Lake, Lincoln Beach.		2.vii.2003		R.C. Mower
1651	Merosoma / Cercyon	sp.	Papua New Guinea	Chimbu					
1652	Cercyon	sp.	Costa Rica	Cartago					
1653	Pelosoma	sp.	Costa Rica	Puntarena	Las Alturas				
1654	Cercyon	roseni	USA	New York					
1655	Moraphilus	scitulus	Suriname	Sipaliwini					
1656	Cercyon	nigriceps group	Tanzania	Morogoro	Mikumi National Park guest house at Park HQ. UV pan trap	529 m	6.viii.2010	07°20,432' S, 37°07,048' E	R. Sites & A. Mbogho
1657	Dellostethus	scitus	Guatemala	El Progreso					
1658	Dellostethus	sp.	Guatemala	Sacatepequez					
1659	Platycyon	sp.	Papua New Guinea	Eastern Highland	Marnafu Village. Crater Mountain Research Area		8-11.vii.2001	06°30.36' S, 145°1.92' E	Whiting et al.
1661	Pemelus	sp.	Guatemala	Petén	13 km NW Machaquila. Ex. sifted leaf litter tropical moist for.	400 m	27.v.2009	16,445891 N, 89,54982° W	LLAMA09 Wa-B-06-1-all
1662	Cyrcillum	sp.	Guatemala	Petén	14 km NW Machaquila. Ex. sifted leaf litter tropical moist for.	400 m	27.v.2009	16,445891 N, 89,54982° W	
1670	Cetiocyon	sp.	Papua New Guinea	Eastern Highland	Herovana Village, Crater Mountain Research Area		15-19.vii.2001		Bradler, Jarvis, Svenson
1671	Cercyon	sp.	Papua New Guinea	East New Britain	Rabaul. Kulau Lodge Beach Resort		25-27.vii.2001	04°12,0' S, 152°5,98' E	Whiting et al.
1675	Cercyon	sp.	Guatemala	Jalapa	4km E Mataquescuintla. Cloud forest. Sifted leaf litter	2325 m	3.vi.2009	14,53409° N, 90,15290° W	LLAMA09 Wm-B-07-1-10
1679	Oosternum	sp.	Guatemala	Jalapa	4km E Mataquescuintla. Cloud forest. Sifted leaf litter	2600 m	1.vi.2009	14,5295° N, 90,14605° W	LLAMA09 Wm-B-07-1-03
1680	Oosternum	aequinoctiale group	Guatemala	Petén	13 km NW Machaquila. Ex. sifted leaf litter tropical moist for.	400 m	27.v.2009	16,44589° N, 89,54982° W	LLAMA09 Wa-B-06-1-All
1681	Oosternum	sp.	Suriname	Sipaliwini	Camp 2, on Sipaliwini River. Dung trap	210 m	28-30.viii.2010	2°10.973' N, 56°47.235' W	Short SR10-0828-01A 2010 CI-RAP Survey
1731	Cercyon	insularis	Puerto Rico	Naguabo	El Yunque National Forest, S part, 3.45 km N of Rio Blanco at rd. PR191, horse excrements	170 m	24.vi.2016	18°14.8N 65°47.9W	Deler, Fikáček, Seidel
1756	Cetiocyon	hanseni							
1775	Cetiocyon	sp.							
1778	Cetiocyon	cribripunctatus							
1780	Cetiocyon	riedeli							
2060	Sphaeridium	quinquemaculatum	Philippines	Mindanao	Bukidnon prov., CMU-dairy project, 5 km SW of Valencia City	308	14.ii.2017	7°51'54.22N 125°03'11.32E	Daniška, Hiřman, Šípek, Vondráček
2074	Megasternum	sp.	Croatia		Istra, Limski kanal, sifting in coastal forest	10	20.vi.2016		Hlavac
2075	Agna	sp.	Mexico	Hidalgo	4,5 km SSW of Cacalomé on rd.105, in rotten stems of Stenocereus cacti (partly fermented)	1785	13.ix.2016	20°25,0'N 98°41,3'W	Arriaga, Cortés, Fikáček & Seidel lgt.
2076	Pacrillum	sp. nov.	Thailand	Lampang	[illegible] Chae Son National Park, and near to rotten banana stems, and debris below bark of dead pigs,[illegible] of	675	26.ii.2017	18°59'46.2"N, 99°29'22.9"E	rriaga, Seidel, Suwannapong, Ployrat, Ponkit, Naree
2077	Oosternum	sp.	Thailand	Lampang	Chae Son National Park,	675	26.ii.2017	18°59'46.2"N, 99°29'22.9"E	rriaga, Seidel, Suwannapong, Ployrat, Ponkit, Naree
2078	Cercyon/Platycyon	sp.	Papua New Guinea		Teslega		3.v.2015		Shaverdo?
2079	Cercyon	sp.	Mexico	Hidalgo	La Mojonera 4,8 km SE Zacualtipan, upper part of Fagus forest, in rotten Boletus-like mushroom logs in relictual Fagus forest with intermixed Magnolia and tree ferns, with sparse to dense understory	2010	13-16.ix.2016	20°37.9'N 98°37.0'W	Arriaga, Cortés, Fikáček & Seidel lgt.
2080	Nitidulodes/Pelosoma	sp.	Mexico	Veracruz	Los Tuxtlas, Perla de San Martin, 16,7 km N of Catemaco, in rotten bases of Xanthosoma robustum plants at margins of pastures in tropical mesophilous forest	570	4.ix.2016	18° 34,3'N 95° 7,0'W	Arriaga-Varela, Fikáček, Ramirez & Seidel lgt.
2081	Cercyon	sp.	Mexico	Veracruz	Los Tuxtlas, Ruiz Cortinez, 14,2 km NNW of Catemaco, rotten Passiflora fruit, in mesophilous cloud forest	1120	3.ix.2016	18°32,7'N, 95°9,0'W	Arriaga-Varela, Fikáček, Ramirez & Seidel lgt
2082	Pelosoma	sp.	Mexico	Veracruz	Los Tuxtlas, Laguna Escondida 16,6 km N of Catemaco, in partly rotten ,sanding inflorescences of red Heliconia	135	7.ix.2016	18°35,4'N 95°5,3'W	& Seidel lgt. Arriaga, Fikáček & Seidel lgt.
2083	Oosternum	sp.	Mexico	Jalisco	Jalisco, Jocotepec, Cerro de los Agraciados, cañada de El Salto, Sifting thin layers of leaf-litter on a slope with tropical deciduos forest	1749	23,viii,2016	20,2964°N, 103,4300°W	Arriaga-Varela & Mölgora
2084	Dellostethus	sp.	Mexico	Jalisco	Jalisco, Talpa de Allende, Cumbre de Guadalupe, Parque Estatal Bosque de Arce, Sifting deep layers of leaf-litter and mushrooms in a cloud forest with abundant Acer and sparse Podocarpus, Quercus, and Pinus.	1713	26,viii,2016	20°13'6" N, 104°45'33"W	Arriaga-Varela & Mölgora
2085	Cercyon	sp. (big black)	Mexico	Veracruz	Los Tuxtlas, Ruiz Cortinez, 14,2 km NNW of Catemaco, sifting of small accummulations of leaf litter mixed with decaing fruits of Bielchmiebia at sides of road through mesophilous cloud forest [= sifting 2]	1120	3.ix.2016	18°32,7'N, 95°9,0'W	Arriaga-Varela, Fikáček, Ramirez & Seidel lgt.
2086	Cyrcillum	sp.	Mexico	Veracruz	[illegible] tree roots in lowland rainforest with sparse understory vegetation	150	4-7.ix.2016	18°34,9'N 95°4,6'W	Arriaga-Varela, Fikáček, Ramirez & Seidel lgt.
2088	Motonerus	sp.	Mexico	Hidalgo	La Mojonera 4,4 km SE Zacualtipan, lower part of Fagus forest; sifting of thin layer of very wet leaf litter among the hygrophilous vegetation at the sides of a stony stream in Fagus forest	1940	14-16.ix.2016	20°38.0'N 98°37.1'W	Cortés, Fikáček & Seidel lgt.
2221	Protosternum	abnormale	Taiwan	Taichung	Dongshi distr., Xiachuanglong above Shuangqi village	600m	6.i.2018	24.2779°N 120.89946°E	Fikáček, Liang & Hsiao
2387	Agraphydrus	sp. nov.	China	Macao	Siu Tam Hill		11.ix.2018	22,1608 113,5466	Chi-Man Leong

Supplementary file 1 (3/3). Locality data for specimens used in this work

MF CODE	CODE	Genus	species	Country of origin		12s	18S	28S	LCO-HCO	COII	H3	Wg	TP
29	MF29	*Cercyon*	variegatus	Ecuador	N	***	***	***			***	***	
69	MF69	*Kanala*	*punctiventris*	New Caledonia	U	***	***	***	***				***
106	MF106	*Peltocercyon*	sp.	Malaysia	O	***	***				***	***	
113	MF113	*Pseudocercyon*	abnormale	Malaysia	O	***	***	***	***		***	***	
126	MF126	*Armostus*	sp.	India	O	***	***						
139	MF139	*Peltocercyon*	sp.	India	O	***	***	***	***		***	***	***
140	MF140	*Cercyon*	sp. 1	India	O	***	***	***	***	***	***	***	
143	MF143	*Cryptopleurum*	cf. *sulcatum*	India	O	***	***	***		***		***	
175	MF175	*Cercyon*	sp.	R. South Africa	E	***	***		***	***	***		
188	MF188	*Cercyon* (Clinocercyon)	sp. (? lutosus group)	R. South Africa	E	***	***	***	***		***	***	***
200	MF200	*Cercyon*	sp. 1 (large, black)	China	O	***	***	***	***	***		***	***
202	MF202	*Peltocercyon*	sp. nov.	China	O	***	***	***	***	***	***		***
205	MF205	*Pacrillum*	sp. nov.	China	O	***	***	***	***		***	***	***
206	MF206	*Australocyon*	cl. Puncticollis	China	O	***	***	***			***	***	***
224	MF224	*Oosternum*	*soricoides* group	China	O		***	***			***		
225	MF225	*Cercyon*	sp.1 (pale)	China	O	***	***	***	***	***	***	***	***
283	MF283	*Pachysternum*	*apicatum*	China	O	***	***	***	***	***	***	***	***
286	MF286	*Pachysternum*	stevensi	China	O	***	***	***	***	***	***	***	***
288	MF288	*Cercyon*	nigriceps group	China	O	***	***	***	***				***
294	MF294	*Cercyon*	ca. incretus D'Orchymont (CHN)	China	O	***	***	***	***	***	***	***	***
302	MF302	*Pacrillum*	sp	China	O	***	***	***	***	***			***
312	MF312	Sphaeridium	sp. 2	China	o	***					***	***	***
314	MF314	*Oosternum*	sp.	China	O	***	***	***	***		***		
319	MF319	*Cercyon*	sp. (cf. Madidus)	China	O	***	***	***	***	***	***	***	***
326	MF326	Coelostoma	phallicum	China	o	***	***	***		***	***	***	
332	MF332	*Cryptopleurum*	sp	China	O	***	***	***		***	***		
434	MF434	*Paroosternum*	sp.	Indonesia	O		***	***				***	
436	MF436	*Cryptopleurum*	ferrugineum	Indonesia	O	***	***	***		***	***	***	***
437	MF437	*Peltocercyon*	ca. lunulatus (Gemminger & Harold)	Indonesia	O	***	***	***	***		***	***	***
439	MF439	*Armostus*	schenklingi (Orchymont, 1914)	Indonesia	O	***	***	***			***		***
461	MF461	*Gillisius*	sp. nov.	Laos	O	***	***	***	***	***	***	***	***
468	MF468	*Peltocercyon*	sp.	Laos	O	***	***	***			***	***	***
469	MF469	*Peltocercyon*	sp.	Laos	O	***	***	***	***		***	***	***
470	MF470	*Peltocercyon*	sp.	Laos	O	***	***	***	***		***	***	***
471	MF471	*Cercyon (s. str.)*	sp.	Laos	O	***	***	***	***	***	***	***	***
473	MF473	*Cercyon (Clinocercyon)*	sp.	Laos	O		***	***	***	***	***		***
474	MF474	*Cercyon (s. str.)*	sp. (ca. javanus)	Laos	O	***	***	***	***		***	***	***
482	MF482	*Cyrtonion*	cf. ghanense	Cameroon	E	***	***	***	***	***	***	***	***
483	MF483	*Cercyon*	sp.	Cameroon	E	***	***	***	***	***			***
575	MF575	*Oosternum*	sp.	China	O		***	***	***		***		
576	MF576	*Cercyon*	ca. incretus	China	O	***	***	***	***	***	***	***	***
577	MF577	*Cercyon*	sp.	China	O	***	***	***		***	***	***	***
578	MF578	*Cercyon*	sp.	China	O	***	***	***	***		***	***	***
648	MF648	*Kanala*	montaguei	New Caledonia	U		***	***				***	
653	MF653	*Kanala*	loebli	New Caledonia	U	***	***	***		***		***	***
680	MF680	*Cercyon*	haemorrhoidalis	New Zealand	P	***	***	***	***	***	***	***	***
748	MF748	*Cercyodes*	laevigatus	New Zealand	U	***	***	***	***	***	***	***	***
771	MF771	*Cercyon*	laminatus	Japan	P	***	***	***	***	***	***	***	***
817	MF817	*Merosoma*	cf. eremita Knisch	Solomon Islands	U	***	***	***	***	***	***	***	***
821	MF821	*Cercyon*	sp.	Solomon Islands	U	***	***	***	***		***	***	***
823	MF823	*Cercyon (Paracycreon)*	sp,	Solomon Islands	U	***	***	***					
829	MF829	*Cercyon*	sp.	Peru	N	***	***	***	***	***	***	***	
830	MF830	*Motonerus*	inca	Peru	N	***	***	***	***	***	***	***	***
831	MF831	*Cercyon*	sp.	Peru	N	***	***	***	***	***	***	***	***
832	MF832	*Cercyon*	sp.	Peru	N	***	***	***	***		***	***	***
834	MF834	*Oosternum*	sp.	Peru	N	***	***	***	***		***		***
836	MF836	*Pelosoma*	sp.	Peru	N	***	***	***	***	***	***	***	***
837	MF837	*Cycrillum*	sp.	Peru	N	***	***	***			***	***	***
852	MF852	*Pelosoma*	sp.	Peru	N	***	***	***	***	***	***	***	***
863	MF863	Omicrus	sp.	Peru	N	***	***	***	***		***	***	***
865	MF865	Psalitrus	sp.	Malaysia	o	***	***	***	***		***	***	***
867	MF867	*Paroosternum*	sp.	Malaysia	O	***	***	***			***	***	***
868	MF868	*Oosternum*	sp. (soricoides group)	Malaysia	O	***	***	***	***	***	***	***	
896	MF896	*Cycreon*	floricola floricola	Malaysia	O	***	***	***	***	***	***	***	***
964	MF964	*Cercyon*	convexiusculus	Czech Republic	P	***	***	***	***		***	***	***
1029	MF1029	*Pelosoma*	sp.	Ecuador	N	***	***	***	***	***	***	***	***
1047	MF1047	*Cercyon*	sp.	Ecuador	N	***	***	***	***	***		***	***
1048	MF1048	*Pelosoma*	sp.	Ecuador	N	***	***	***	***		***	***	***
1056	MF1056	*Pelosoma*	sp.	Ecuador	N	***	***	***	***	***	***	***	

Supplementary file 2. Succesfully amplified gene regions by specimen.

MF CODE	CODE	Genus	species	Country of origin		12s	18S	28S	LCO-HCO	COII	H3	Wg	TP
1063	MF1063	Phaenonotum	exstriatum	USA	N	***	***	***		***		***	***
1094	MF1094	*Cercillum*	sp. indescr.	South Africa	E	***	***	***	***	***	***	***	***
1098	MF1098	*Cercyon*	sp.	South Africa	E	***	***	***	***	***	***	***	***
1120	MF1120	Platycyon	1	Papua New Guinea	U		***				***		
1121	MF1121	*Cercyon*	sp. 2	Papua New Guinea	U	***	***	***	***		***		
1123	MF1123	*Cercyon*	sp. 6	Papua New Guinea	U	***	***	***		***	***		***
1136	MF1136	*Cercyon*	sp. 3	Papua New Guinea	U	***		***			***		
1145	MF1145	*Platycyon*	sp. 2	Papua New Guinea	U	***	***	***		***			***
1181	MF1181	*Cercyon*	sp.	Indonesia	U	***	***	***	***	***	***	***	***
1189	MF1189	*Cercyon*	nigriceps group	Indonesia	U	***	***	***				***	***
1190	MF1190	*Merosoma*	sp.	Indonesia	U	***	***	***	***	***	***	***	***
1192	MF1192	*Noteropagus*	sp.	Indonesia	o	***	***	***	***	***	***	***	***
1195	MF1195	*Cercyon*	ca. udus D'Orchymont (INDO)	Indonesia	U	***	***	***	***	***		***	***
1214	MF1214	*Cercyon*	insularis	República Dominicana	N	***	***		***	***	***		
1215	MF1215	*Cercyon*	nigriceps group	República Dominicana	N		***	***	***		***		
1216	MF1216	*Cercyon*	spiniventris n. sp.	República Dominicana	N		***		***	***	***		
1221	MF1221	*Pilocnema*	sp.	Australia	U	***	***	***	***		***		
1226	MF1226	*Pseudoosternum*	maculatum?	Australia	U	***	***	***	***	***		***	***
1229	MF1229	*Cercyon* *** *Platycyon*	sp.	China	O	***	***	***			***	***	***
1233	MF1233	*Cercyon*	sp.	Republic of South Africa	E	***	***	***	***		***	***	***
1237	MF1237	*Delimetrium*	sp.	South Africa	E	***	***	***	***			***	***
1269	MF1269	*Chledocyon*	semiopacus	Australia	U	***	***	***		***	***	***	***
1270	MF1270	*Chledocyon*	marmoratus	Australia	U	***	***	***	***	***	***	***	***
1275	MF1275	*Cercyon*	sp.	Madagascar	E	***	***	***	***				
1283	MF1283	*Cercyon*	sp. "small antennal grooves"	R. South Africa	E	***	***	***	***		***	***	***
1291	MF1291	*Cercyodes*	kingensis	Australia	U	***	***	***	***		***	***	***
1292	MF1292	*Australocyon*	ca. pilocnemoides	Laos	O	***	***	***	***	***	***	***	***
1293	MF1293	*Cercyon*	sp.	Angola	E	***	***	***	***	***	***	***	***
1294	MF1294	*Cercyon*	sp. "anterolateral corners, and wide me	Angola	E	***	***	***	***	***	***	***	***
1295	MF1295	*Cercyon*	sp.	Angola	E	***	***	***			***		
1296	MF1296	*Cercillum*	sp.	Angola	E	***	***		***	***	***	***	
1298	MF1298	*Pelosoma*	sp.	Brazil	N	***	***	***	***		***	***	***
1302	MF1302	*Cercyon*	sp.	Republic of South Africa	E	***	***	***					
1306	MF1306	*Cercyon*	sp.	Myanmar	O	***	***	***			***	***	***
1308	MF1308	*Cercyon*	undulipennis Ryndevich et al. (CHN)	China	O	***	***	***	***	***	***	***	
1309	MF1309	*Cryptopleurum*	minutum	Portugal	P	***	***	***	***	***	***		
1311	MF1311	*Cercyon*	quisquilius	Czech Republic	P	***	***	***	***	***	***		***
1313	MF1313	*PeltocercyonArmostus*	sp.	China	O	***	***	***	***	***	***	***	***
1314	MF1314	*Cercyon*	sp. (different from that above)	China	O	***	***	***			***		***
1316	MF1316	*Peltocercyon*	sp.	China	O		***	***				***	***
1319	MF1319	*Cercillum*	sp.	Republic of South Africa	E	***	***	***			***		
1320	MF1320	*Cercyon*	sp.	Republic of South Africa	E	***	***	***	***	***	***	***	***
1321	MF1321	*Cercyon*	sp.	Republic of South Africa	E	***	***	***		***	***	***	***
1322	MF1322	*Cercyon (Arcocercyon)*	dieganus group (R. South Africa)	Republic of South Africa	E	***	***	***	***	***	***	***	***
1324	MF1324	*Cercyon*	cf. oosternoides Knisch (R. South Afric	Republic of South Africa	E	***	***	***	***	***	***	***	***
1325	MF1325	*Cercyon*	sp.	Republic of South Africa	E	***	***	***	***		***	***	***
1329	MF1329	*Cercyon*	gigas	Republic of South Africa	E	***	***	***			***	***	***
1330	MF1330	*Cercyon*	maritimus	Republic of South Africa	E	***		***	***		***	***	***
1331	MF1331	*Cercyon*	aphodioides D'Orchymont (R. South Afr	Republic of South Africa	E	***	***	***	***		***	***	***
1334.2	MF1334.2	*Cercyon*	sp.	Republic of South Africa	E	***	***	***	***		***	***	
1336	MF1336	*Pachysternum*	capense	Republic of South Africa	E	***		***	***	***	***	***	***
1338	MF1338	*Cercyon*	sp.	Mexico	N	***	***	***	***		***	***	***
1339	MF1339	*Pelosoma*	sp.	Panama	N		***	***			***		***
1497	MF1497	*Tectosternum*	sp. (large)	Ethiopia	E	***	***	***		***	***	***	***
1498	MF1498	*Tectosternum*	sp. (small)	Ethiopia	E	***	***	***					
1607	MF1607	*Cercyon*	haemorrhoidalis	Czech Republic	P	***	***	***			***		
1608	MF1608	Cercyon	trsitis	Czech Republic	P		***	***				***	***
1609	MF1609	Cercyon	marinus	Czech Republic	P	***	***	***		***		***	***
1611	MF1611	Oosternum	sharpi (?)	USA	N						***		
1612	MF1612	Cercyon	fimbriatus	USA	a	***	***	***			***	***	
1614	MF1614	*Cercyon*	quisquilius	USA	P		***	***		***	***	***	***
1615	MF1615	Cenebriophilus	sp.	Australia	U			***			***		
1616	MF1616	Australocyon	sp.	Australia	U	***	***	***		***	***	***	
1618	MF1618	Ercycodes *** Mero	sp.	Australia	U	***	***	***		***	***	***	
1619	MF1619	*Pseudoosternum*	sp.	Australia	U	***	***	***					
1620	MF1620	Ceronocyton	sp.	Australia	U	***	***	***			***	***	***
1626	MF1626	Kanala	sp. nov.?	New Caledonia	U	***	***	***			***	***	
1627	MF1627	Bolbonotum	sp. indesct.	Cambodia	O	***	***	***	***		***	***	***
1628	MF1628	Deltostethus	sp.	Costa Rica	N	***	***	***	***	***	***	***	***

Supplementary file 2 (cont.). Succesfully amplified gene regions by specimen.

MF CODE	CODE	Genus	species	Country of origin		12s	18S	28S	LCO-HCO	COII	H3	Wg	TP
1629	MF1629	Cercyon	variegatus group	Costa Rica	N	***	***						
1631	MF1631	Motonerus	cf. nublado	Venezuela	N	***	***	***		***	***	***	***
1632	MF1632	Nitidulodes	jansoni Sharp	Panama	N	***	***	***	***	***	***		***
1633	MF1633	Cercyon	schmidti	Panama	N	***	***	***	***	***	***	***	
1634	MF1634	*Oosternum*	grandis group	Suriname	N	***	***	***			***	***	***
1635	MF1635	Oosternum	sp.	Panama	N	***	***	***					
1636	MF1636	*Pelosoma*	sp.	Costa Rica	N	***	***	***			***		***
1637	MF1637	Cercyon	sp.	Suriname	N	***	***	***			***	***	***
1638	MF1638	*Oosternum*	sharpi group?	Suriname	N	***	***	***			***		
1639	MF1639	*Cercyon*	sp.	Guatemala	N	***	***	***			***		
1640	MF1640	*Oosternum*	puncticolle group	Guatemala	N	***	***	***	***			***	***
1642	MF1642	*Cercyon*	sp.	Suriname	N	***	***	***			***	***	
1643	MF1643	*Pelosoma*	sp.	Venezuela	N	***	***	***	***			***	
1644	MF1644	*Pelosoma*	sp.	Venezuela	N	***	***	***		***	***	***	***
1645	MF1645	*Cercyon*	sp.	Guatemala	N	***	***	***		***	***	***	
1647	MF1647	Cercyon	alticola group	Guatemala	N	***	***	***		***	***		
1648	MF1648	*Cercyon*	dilutus	India	O	***	***	***	***	***	***		***
1649	MF1649	Cercyon	lineolatus	India	O		***	***		***	***		***
1650	MF1650	Cercyon	sp.	USA	a	***	***	***	***		***	***	***
1651	MF1651	Merosoma *** Cercy	sp.	Papua New Guinea	U	***	***	***		***	***		
1652	MF1652	Cercyon	sp.	Costa Rica	N		***	***	***	***	***	***	
1653	MF1653	*Pelosoma*	sp.	Costa Rica	N	***	***	***	***		***		
1654	MF1654	*Cercyon*	roseni	USA	a	***	***	***			***		***
1655	MF1655	Moraphillus	sulcatus Sharp	Suriname	N	***	***	***	***	***	***		
1656	MF1656	*Cercyon*	sp.	Tanzania	E	***	***	***	***	***		***	***
1657	MF1657	*Deltostethus*	scitus	Guatemala	N	***	***	***	***		***	***	***
1658	MF1658	*Deltostethus*	sp.	Guatemala	N	***	***	***		***	***	***	***
1659	MF1659	*Platycyon*	sp.	Papua New Guinea	U	***	***	***	***	***	***	***	***
1661	MF1661	*Pemelus*	sp.	Guatemala	N			***	***	***		***	***
1662	MF1662	*Cycrillum*	sp.	Guatemala	N	***	***	***	***		***	***	***
1670	MF1670	*Cetiocyon*	sp.	Papua New Guinea	U	***	***	***		***		***	
1671	MF1671	*Cercyon ? (no antennal*	sp.	Papua New Guinea	U	***	***	***	***	***	***	***	
1675	MF1675	*Cercyon*	sp. (black, spotted elytra)	Guatemala	N	***					***		
1679	MF1679	*Oosternum*	sp.	Guatemala	N	***	***	***					
1680	MF1680	*Oosternum*	aequinoctiale group	Guatemala	N	***	***	***		***	***		
1681	MF1681	*Oosternum*	sp.	Suriname	N	***	***	***	***		***		***
1731.1	MF1731.1	*Cercyon*	insularis	Puerto Rico (USA)	N		***				***		
1756	MF1756	Cetiocyon	hanseni	Papua New Guinea	u	***					***		
1775	MF1775	Cetiocyon	cribripunctatus	Papua New Guinea	u		***	***					
1778	MF1778	Cetiocyon	cribripunctatus	Papua New Guinea	u	***	***			***	***		***
1780	MF1780	Cetiocyon	riedeli	Papua New Guinea	u	***							***
2060	MF2060	Sphaeridium	quinquemaculatum	Philippines	o	***					***		***
2074	MF2074	*Megasternum*	sp.	Croatia	P	***	***	***	***		***		
2075	MF2075	*Agna*	sp.	Mexico	N	***	***	***	***	***	***		***
2076	MF2076	*Pacrillum*	sp. nov.	Thailand	o	***	***	***		***			***
2077	MF2077	*Armostus*	sp.	Thailand	o	***	***	***			***		***
2078	MF2078	*Cercyon***Platycyon*	sp.	Papua New Guinea	u	***	***	***					***
2079	MF2079	*Cercyon*	sp.	Mexico	N	***	***	***			***		
2080	MF2080	*Nitidulodes*	ca. jansoni Sharp	Mexico	N		***	***					***
2081	MF2081	*Cercyon*	sp.	Mexico	N	***	***	***					***
2082	MF2082	*Pelosoma*	sp.	Mexico	N	***	***				***		
2083	MF2083	*Oosternum*	sp.	Mexico	N	***	***	***		***	***		***
2084	MF2084	*Deltostethus*	sp. indescr.	Mexico	N		***	***			***		***
2085	MF2085	*Cercyon*	sp. (big black)	Mexico	N	***	***	***					***
2086	MF2086	*Cycrillum*	sp.	Mexico	N	***	***	***					
2088	MF2088	Motonerus	sp.	Mexico	N					***			
2221.1	MF2221.1	Protosternum	abnormale	Taiwan	o	***						***	***
2387	MF2387	Agraphydrus	sp.	China	o	***					***	***	***
CUB572	CUB572	Sacosternum	sp.	Costa Rica	N	***	***		***		***		
D30	D30	Chimaerocyon	shimadai	Malaysia	o	***	***				***		***
PNG 2428.2	PNG 2428.2	*Platycyon*	10	Papua New Guinea	u		***		***				
PNG 6175	PNG 6175	*Cercyon*	sp.	Papua New Guinea	u		***	***	***				
PNG 6622	PNG 6622	*Cercyon*	sp.	Papua New Guinea	u		***	***	***				
SLE0251	SLE0251	Cetiocyon	incantatus		N		***	***					

Supplementary file 2 (cont.). Succesfully amplified gene regions by specimen.

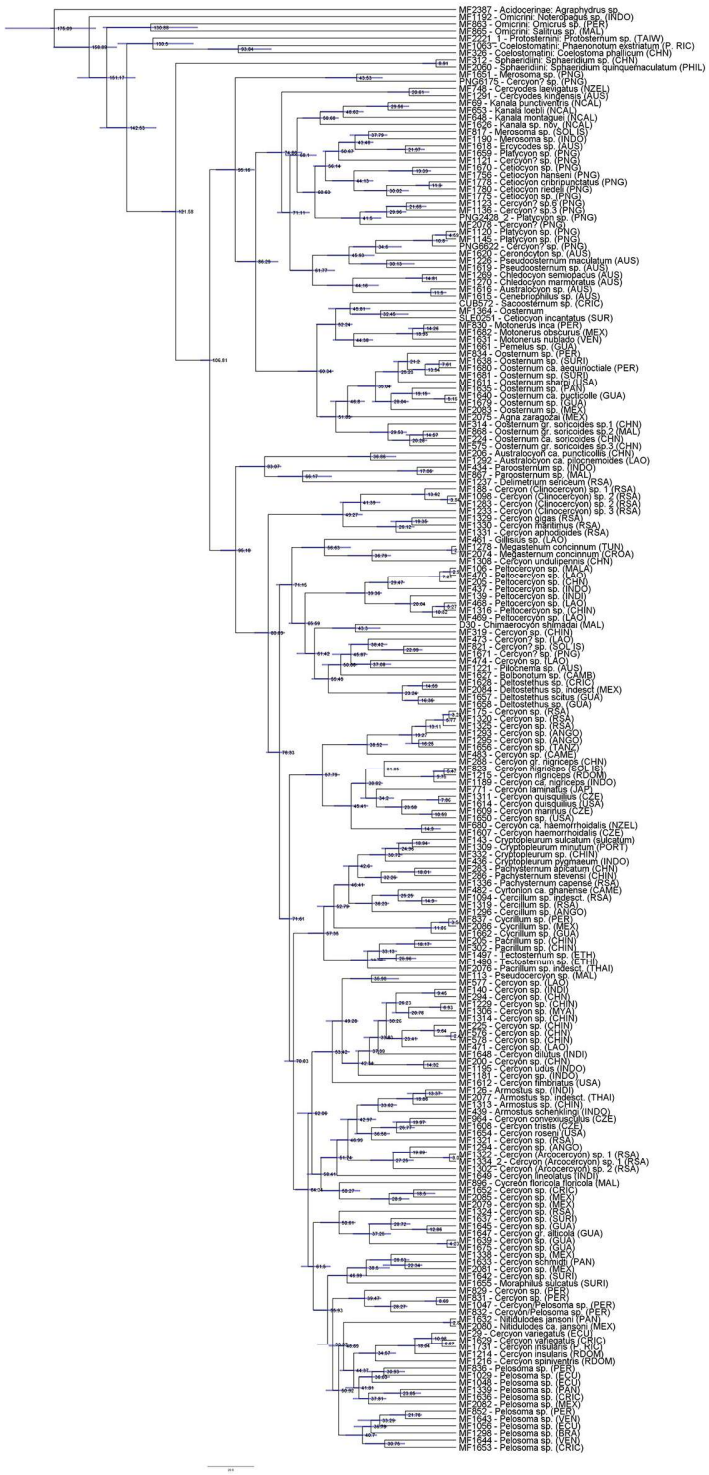

Supplementary file 3. Resulting tree of *EX* dataset obtained in MrBayes. Estimated mean age shown in nodes.

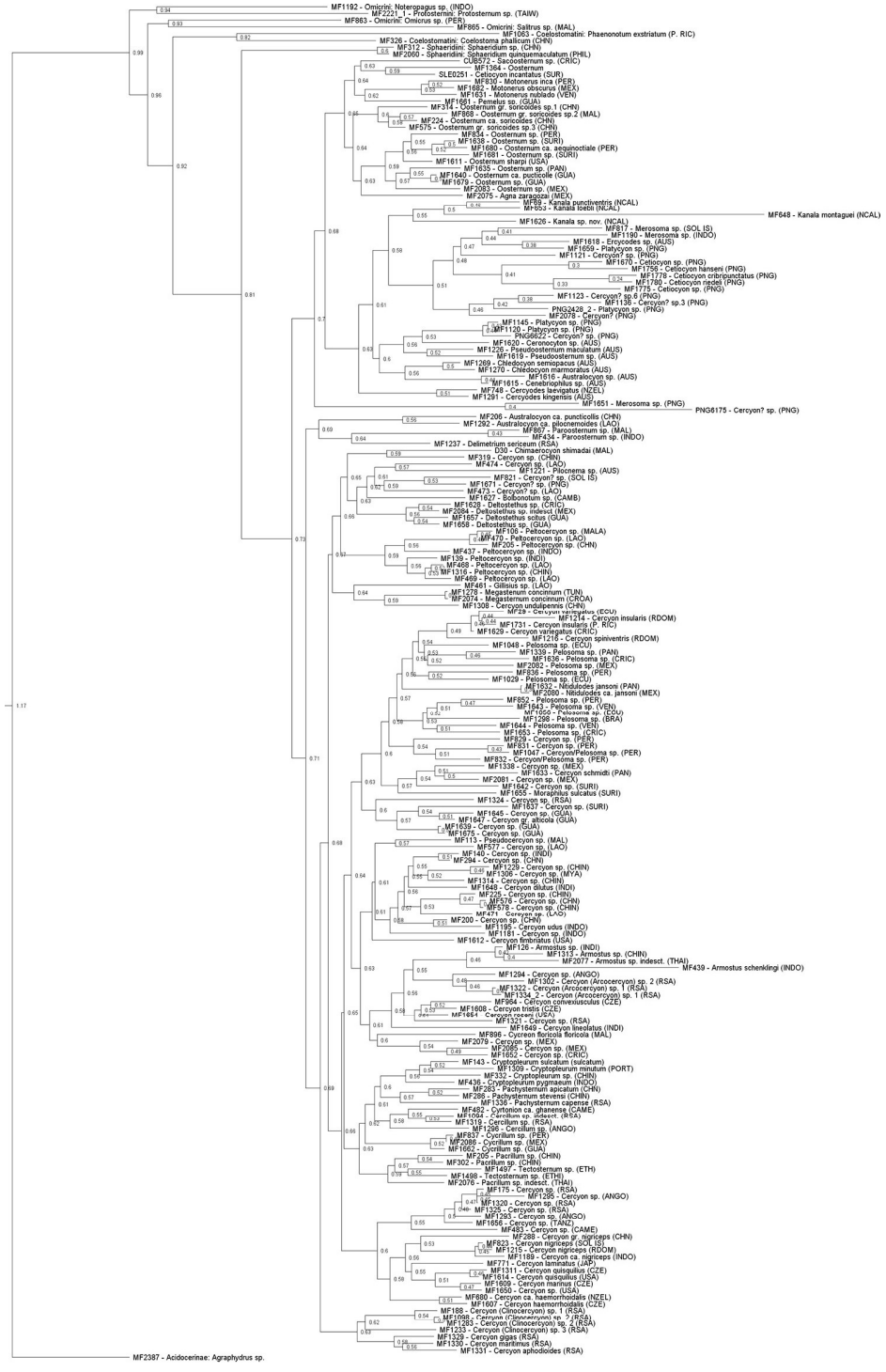

Supplementary file 4. Resulting tree of *EX* dataset obtained in IQTree. Ultra Fast Bootstrap values shown in nodes.

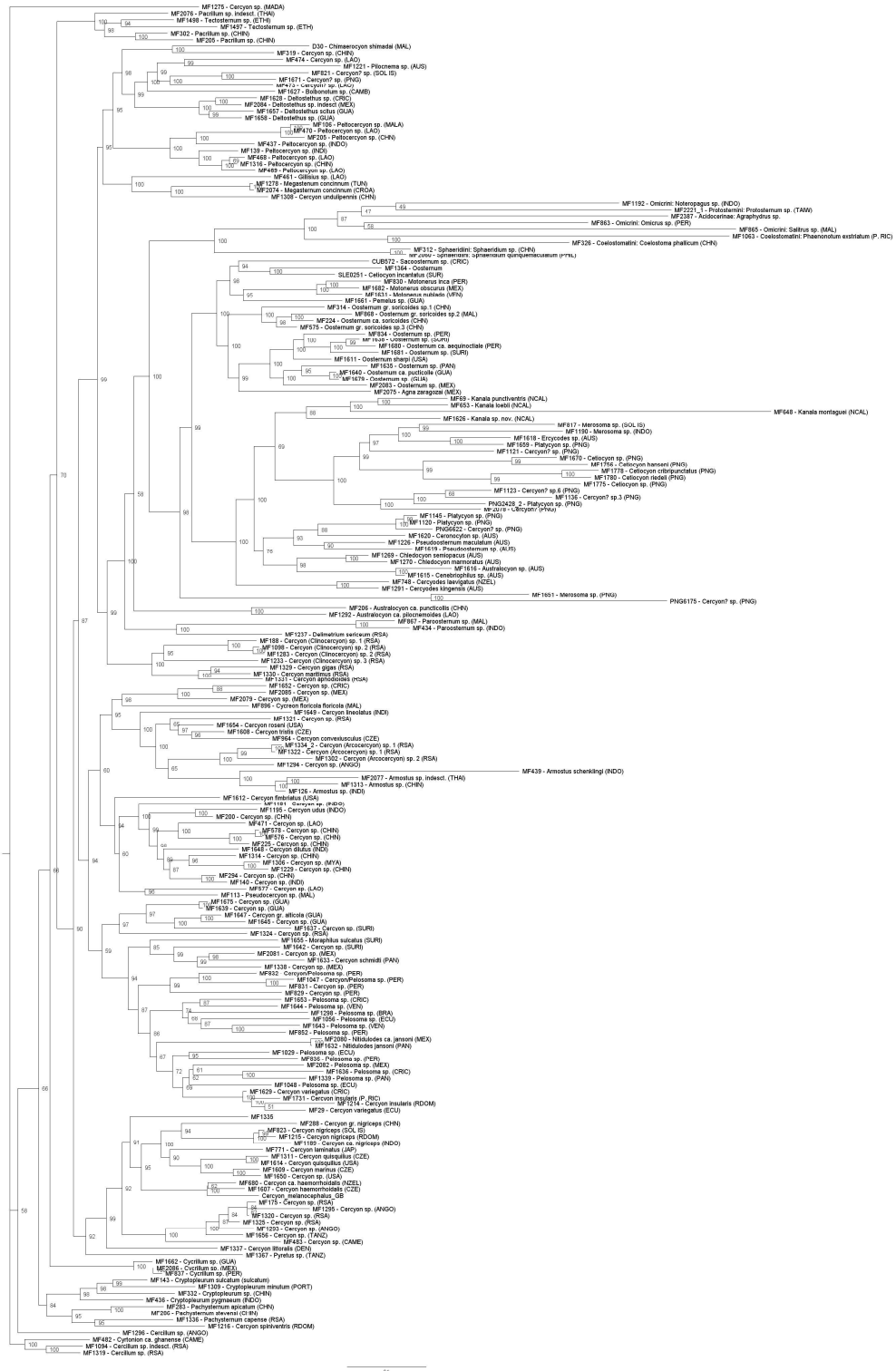

Supplementary file 5. Resulting tree of *IN* dataset obtained in IQTree. Ultra Fast Bootstrap values shown in nodes.

NEXT PAGES:
Supplementary files 6. Resulting trees showing ancestral area estimation from BioGeoBears analyses.

BioGeoBEARS BAYAREALIKE on Megasternini
ancstates: global optim, 7 areas max. d=7e−04; e=0.0078; j=0; LnL=−294.24

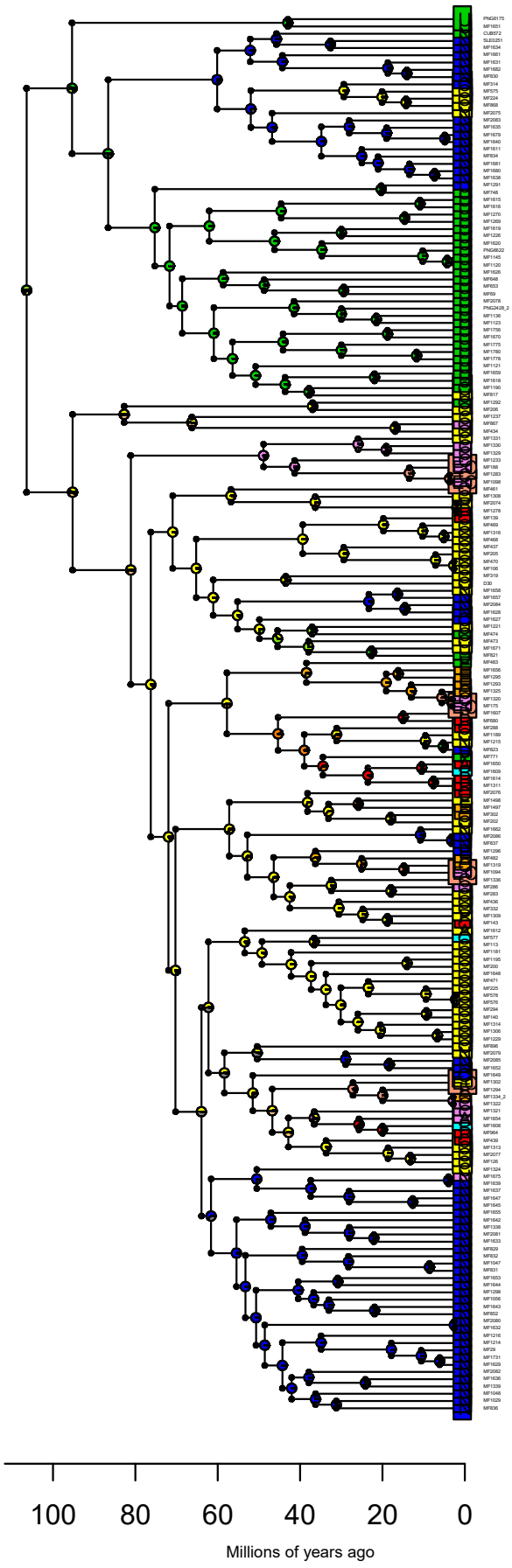

BioGeoBEARS BAYAREALIKE+J on Megasternini
ancstates: global optim, 7 areas max. d=1e−04; e=1e−04; j=0.0166; LnL=−198.30

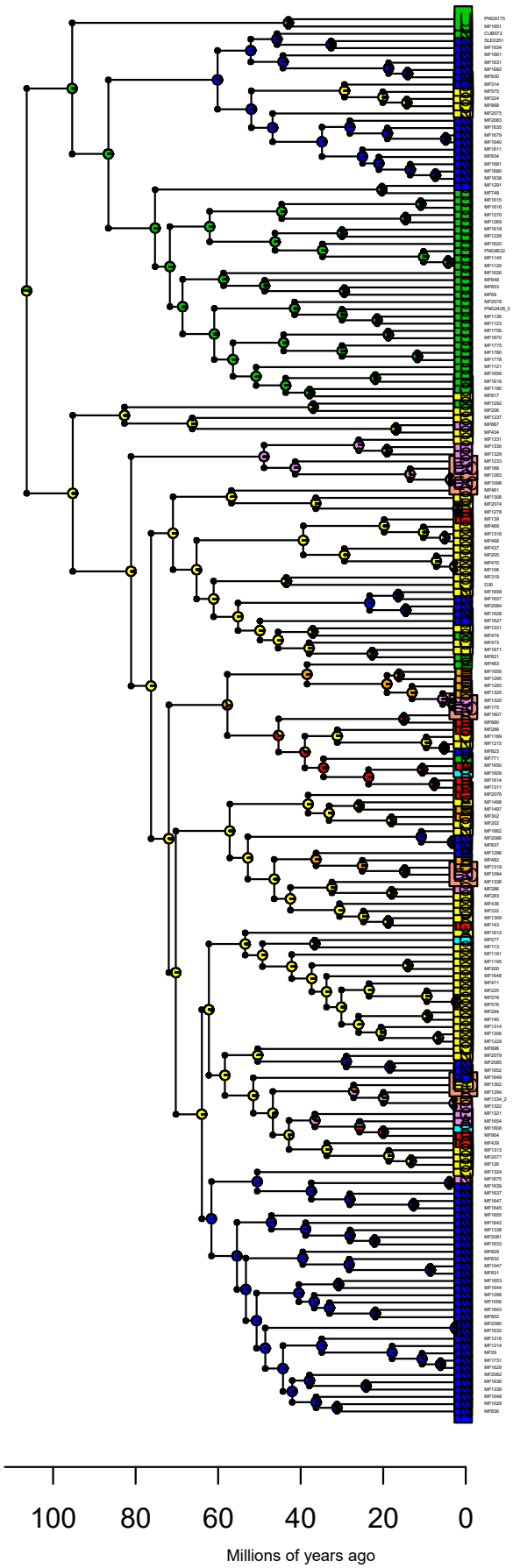

BioGeoBEARS DEC on Megasternini unconstrained
ancstates: global optim, 7 areas max. d=7e−04; e=1e−04; j=0; LnL=−230.07

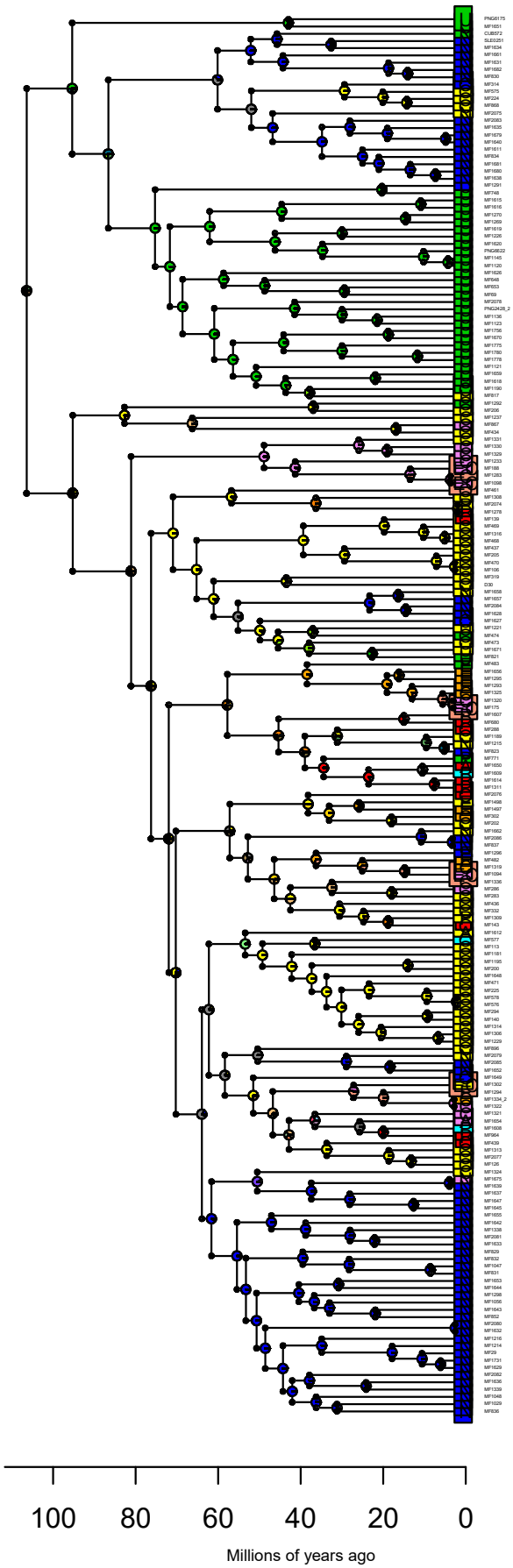

BioGeoBEARS DEC+J on Megasternini unconstrained
ancstates: global optim, 7 areas max. d=1e−04; e=0; j=0.0127; LnL=−189.09

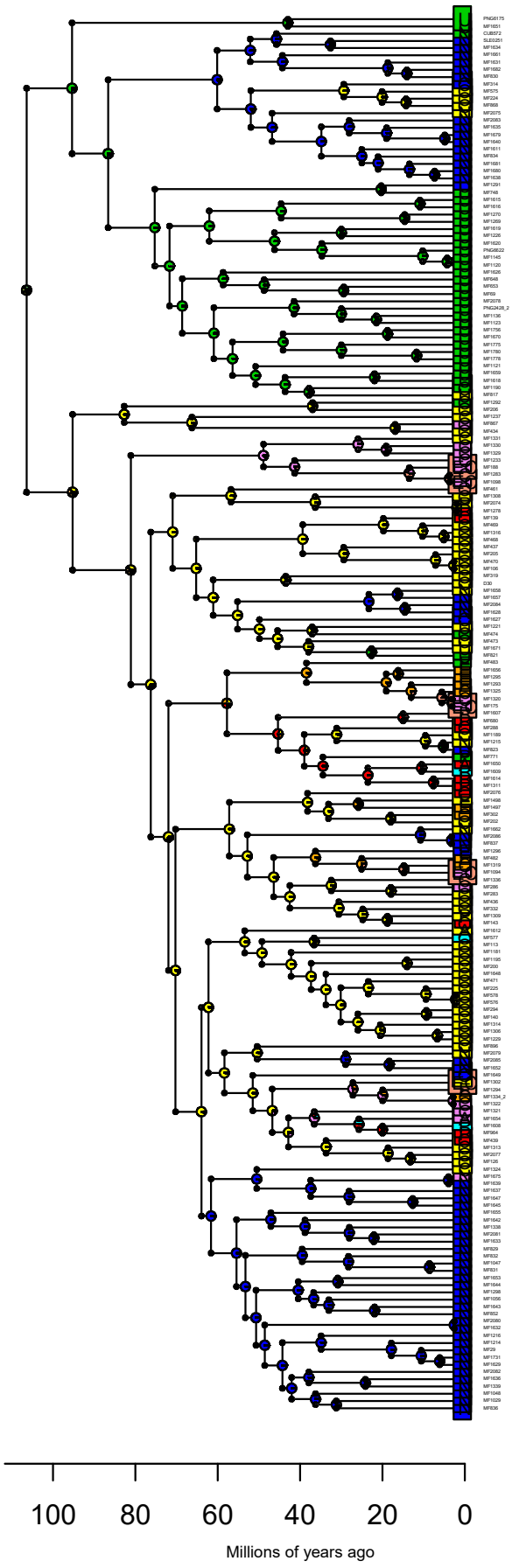

BioGeoBEARS DIVALIKE on Megasternini
ancstates: global optim, 7 areas max. d=9e−04; e=0; j=0; LnL=−227.01

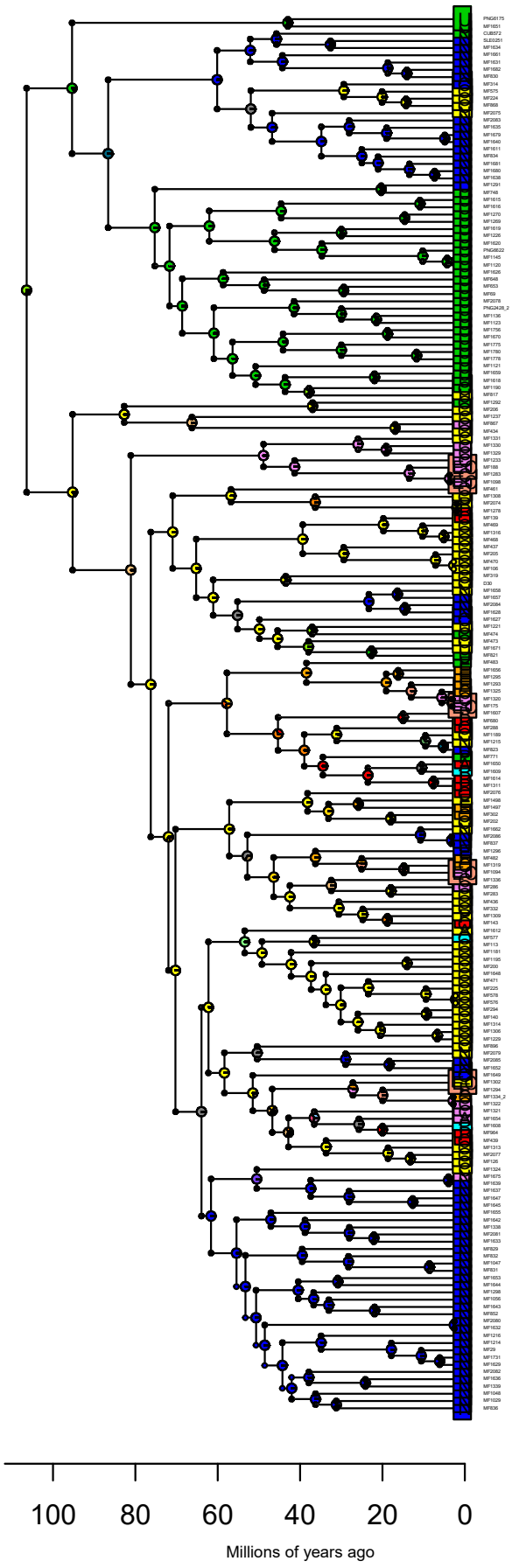

BioGeoBEARS DIVALIKE+J on Megasternini
ancstates: global optim, 7 areas max. d=2e−04; e=0; j=0.0155; LnL=−194.09